PART I. A PHOTOLABILE BACKBONE-AMIDE LINKER FOR SOLID-PHASE SYNTHESIS OF C-TERMINALLY MODIFIED PEPTIDES

PART II. CLASS-II HMG-COA REDUCTASE INHIBITORS FOR USE AS ANTIMICROBIALS

by

Mary L. Niedrauer

A Dissertation

Submitted to the Faculty of Purdue University

In Partial Fulfillment of the Requirements for the degree of

Doctor of Philosophy

Department of Chemistry

West Lafayette, Indiana

December 2020

THE PURDUE UNIVERSITY GRADUATE SCHOOL
STATEMENT OF COMMITTEE APPROVAL

Dr. Mark A. Lipton, Chair

Department of Chemistry

Dr. Elizabeth I. Parkinson

Department of Chemistry

Dr. Abram J. Axelrod

Department of Chemistry

Dr. Alexander Wei

Department of Chemistry

Approved by:

Dr. Christine Hrycyna

Dedicated to all the little girls who are told that science is a man's world,

and become scientists anyway.

ACKNOWLEDGMENTS

First and foremost, I'd like to thank my research advisor Professor Mark Lipton. His guidance and mentorship throughout graduate school have been crucial to my success. His philosophy is that graduate school is what you make of it, and he allows his students space to explore which areas of research they are most interested in. He places an emphasis on allowing his students the space to learn how to conduct research independently, but is always available to give advice about research or life in general. From taking us on ski trips, to group dinners, to hosting Christmas parties, he is always concerned about his student's well-being, and general quality of life. I could not have asked for a better research advisor and mentor.

Next, I'd like to thank my committee members Bram Axelrod, Betsy Parkinson, and Alex Wei for their guidance and support over the years. I would also like to recognize my lab members who have contributed to my survival of graduate school. My graduate student mentor, former group member Dr. Matthew Hostetler taught me everything I know about lab technique. Even after earning his PhD and leaving the group, Matt was always available to discuss research problems or just talk about life in general. I would also like to recognize my current lab mates Jordan, Adam, Allie, and Abi for their comradery and support through the endless hours spent in lab, and their willingness to wash my endless piles of glassware in exchange for a free lunch. I'd like to recognize Greg Eakins for his collaboration in the design and building of our photoreactor invention. Greg has always been willing to go the extra mile to ensure I could meet deadlines, even going to work on the weekend to 3D-print parts for me so I could collect data before my seminar.

Finally, I'd like to thank my (loosely defined) family members for their support and encouragement. Carlos and Lara have been my coaches, mentors, and pseudo step-parents throughout graduate school. Whether driving me to surgeries, inviting me to join their family for holiday celebrations, or just being there to listen, they have shown up for me countless times through the ups and downs. My sisters, Elizabeth, Chana, and Sarah for listening to my endless complaints while writing my dissertation, and every day for 25 years prior. And finally, Greg and Chrissy for being my COVID-19 lockdown buddies, gym partners, and general voices of reason through the crazy ups and downs of graduate school.

TABLE OF CONTENTS

LIST OF TABLES

LIST OF FIGURES

LIST OF SCHEMES

LIST OF ABBREVIATIONS

µL	microliter
AA	amino acid
Ac	acyl
Acm	acetamidomethyl
Ahx	aminohexanoic acid
aq	aqueous
BAIB	(diacetoxyiodo)benzene
BAL	backbone amide linker
Boc	t-butyloxycarbonyl
cat	catalytic
Cbz	benzyl chloroformate
CD_3OD	deuterated methanol
CDC	Center for Disease Control
$CDCl_3$	deuterated chloroform
CDI	carbonyldiimidazole
CH_2Cl_2	methylene chloride
CH_3CN	acetonitrile
d	doublet
DBU	1,8-diazabicyclo[5.4.0]undec-7-ene
DCC	n,n'-dicyclohexylcarbodiimide
dd	doublet of doublets

DEA	diethyl amine
DIEA	diisopropylethylamine
DIPA	diisopropylamine
DIPC	diisopropyl carbodiimide
DKP	diketopiperazine
DMA	dimethylallyl
DMAP	dimethyl aminopyridine
DMF	dimethyl formamide
DMS	dimethyl sulfide
DMSO	dimethyl sulfoxide
DPPA	diphenyl phosphoryl azide
e.f.	enterococcus faecalis
EA	ethyl acetate
EAS	electrophilic aromatic substitution
EDCI	1-ethyl-3-(3-dimethylaminopropyl)carbodiimide
eq	equivalents
ESI	electrospray ionization
FabF	β-ketoacyl-acp synthase ii
FDA	Food and Drug Administration
Fmoc	fluorenyl methoxycarbonyl
g	grams
h	hours
HATU	hexafluorophosphate azabenzotriazole tetramethyl uronium

Hcna	2-hydroxy-4-carboxy-6-nitrobenzaldehyde
Hcnb	2-hydroxy-4-carboxy-6-nitrobenzyl
Hex	hexanes
HF	hydrofluoric acid
Hmb	the 6-hydroxy-4-methoxybenzyl
Hnb	6-hydroxynitrobenzyl
HOAt	1-hydroxy-7-azabenzotriazole
HPLC	high-performance liquid chromatography
hv	light
Hz	hertz
IC_{50}	50% maximal inhibitory concentration
IDSA	Infectious Diseases Society of America
IR	infrared
J	coupling constant
LC-MS	liquid chromatography-mass spectrometry
LED	light-emitting diode
LiOH	lithium hydroxide
m	multiplet
M	molar
MBC	minimum bactericidal concentration
Me	methyl
MeCN	acetonitrile
MeOH	methanol

mg	milligrams
MIC	minimum inhibitory concentration
min	minutes
mL	milliliters
mmol	millimoles
MOM	methoxymethyl ether
MRSA	methicillin-resistance staphylococcus aureus
MS	mass spectrometry
NAD	nicotinamide adenine dinucleotide
NADP	nicotinamide adenine dinucleotide phosphate
NaOH	sodium hydroxide
nBuLi	*n*-butyl lithium
NCL	native chemical ligation
NHS	n-hydroxysuccinimide
nm	nanometers
NMR	nuclear magnetic resonance imaging
Nve	6-nitroveratryl
OTf	triflate
Pbf	2, 2, 4, 6, 7-pentamethyldihydrobenzofuran
PCB	printed circuit boards
PEG	polyethylene glycol
PG	protecting group
Ph	phenyl

ppm	parts per million
PS	polystyrene
PyAOP	7-azabenzotriazol-1-yloxy)tripyrrolidinophosphonium hexafluorophosphate
q	quartet
rt	room temperature
s	singlet
SFTI-1	sunflower trypsin inhibitor
SnAr	aromatic nucleophilic substitution
SPPS	solid-phase peptide synthesis
t	triplet
TBS	*tert*-butyldimethyl silyl
tBu	*tert*-butyl
TEA	triethyl amine
TEMPO	(2,2,6,6-tetramethylpiperidin-1-yl)oxyl
TES	triethyl silane
TFA	trifluoroacetic acid
TG	tentagel
THF	tetrahydrofuran
TIPS	triisopropyl silane
TLC	thin-layer chromatography
TMS	trimethyl silane
Trt	trityl
TS	transition state

UPLC	ultra-high performance liquid chromatography
UV	ultraviolet
VRE	vancomycin-resistant enterococci

ABSTRACT

Part I: Design of a Photolabile Backbone Amide Linker for the Synthesis of C-terminally Modified Peptides

A new photolabile backbone amide linker has been developed for the on-resin synthesis of cyclic and C-terminally modified peptides. The linker (Hcnb) is stable to strongly acidic conditions and instead releases the completed peptide through photolytic cleavage at 365 nm. Hcnb possesses four degrees of orthogonality and is amenable to the preparation of cyclic peptides, C-terminally modified peptides, and fully protected peptides due to its photolabile backbone amide linkage. The Hcnb precursor can be conveniently synthesized in 4 steps from commercially available 4-methyl-3,5-dinitrobenzoic acid. The C-terminal amino acid residue is loaded via reductive amination of the precursor followed by an O→N transacylation for the addition of the second residue in quantitative yields, even when employing sterically bulky residues. Standard Fmoc- or Boc-based synthesis can then be utilized to complete the desired peptide. Hcnb has been used to demonstrate the linear synthesis and subsequent on-resin cyclization of various cyclic peptides of interest, as well as synthesis of C-terminal thioesters on-resin.

Part II: Development of II-HMG CoA Reductase Inhibitors for use as Gram-Positive Selective Antimicrobials.

Bacterial resistance to antibiotic drugs is an issue that humans have faced since the first use of sulfa drugs in the 1930s. In recent years, the rate of production of new antimicrobial drugs has diminished, as they are no longer financially beneficial to pharmaceutical companies due to short term use and rapid resistance development. This places the burden of the development of new antimicrobial drug on the academic research field. In the work presented here, progress has been made toward the development of a novel class of antimicrobial compounds. These small molecule inhibitors target II-HMG CoA Reductase, a key enzyme involved in cell wall synthesis in gram-positive bacteria. Based on analysis of co-crystal structures obtained from first- and second- generation inhibitors, structural alterations were made to design a new generation of compounds. Efforts have also been made toward identification of a potential secondary target of these inhibitors.

PART I. A PHOTOLABILE BACKBONE-AMIDE LINKER FOR THE SOLID-PHASE SYNTHESIS OF C-TERMINALLY MODIFIED PEPTIDES

CHAPTER 1. DEVELOPMENT OF A PHOTOLABILE BACKBONE-AMIDE LINKER FOR USE IN SOLID-PHASE PEPTIDE SYNTHESIS

1.1 Introduction to Solid-Phase Peptide Synthesis

The synthesis of proteins and peptides has been of interest to chemists for over a century, as they play a crucial role in the survival of every living organism. Significant research has focused on elucidating the functions of various proteins and peptides, to assist in the development of drugs and other biological applications. Theodore Curtius successfully synthesized the first ever peptide bond between glycine and benzoylchloride in 1882, although the nomenclature had not yet been introduced.[1] Later in 1901, Emil Fischer and Ernest Forneau synthesized the first free dipeptide, Gly-Gly through hydrolysis of the diketopiperazine of glycine.[1] Following this synthesis, Fischer coined the term "peptides" which has been used ever since.[2] Fischer also developed the concept of activating the C-terminus to form amide bonds, using acyl chlorides to synthesize a simple octadecapeptide.[3] The early 20th century saw various developments in solution-phase peptide synthesis, including development of new activating reagents and the creation of new protecting groups, such as the benzyloxycarbobnyl (Cbz) group.[4] Use of this protecting group allowed for the first solid-phase total synthesis of oxytocin, a cyclic peptide hormone.[4]

Through most of its early stages, peptide synthesis was conducted in solution. Although some complex peptides can be accessed this way, the process tends to be tedious and requires extensive purification at deprotection and coupling steps. As the number of peptide bonds grows, the increasing polarity of the peptide makes the subsequent purifications more difficult. A solution to this problem was proposed in 1963 by Bruce Merrifield. He proposed anchoring the peptide to an insoluble support, allowing rapid and convenient isolation of the peptide away from reactants and side-products that are formed in the solution during synthesis.[5] Merrifield spent his life work improving the methods for solid-phase synthesis and was awarded the Nobel Prize in 1984 for his contributions to the field.[6,7] The general strategy for solid-phase synthesis involves linking the C-terminus of the first amino acid residue to a polymeric solid support through a reactive functional group, typically an amide or ester (Figure 1-1).[8]

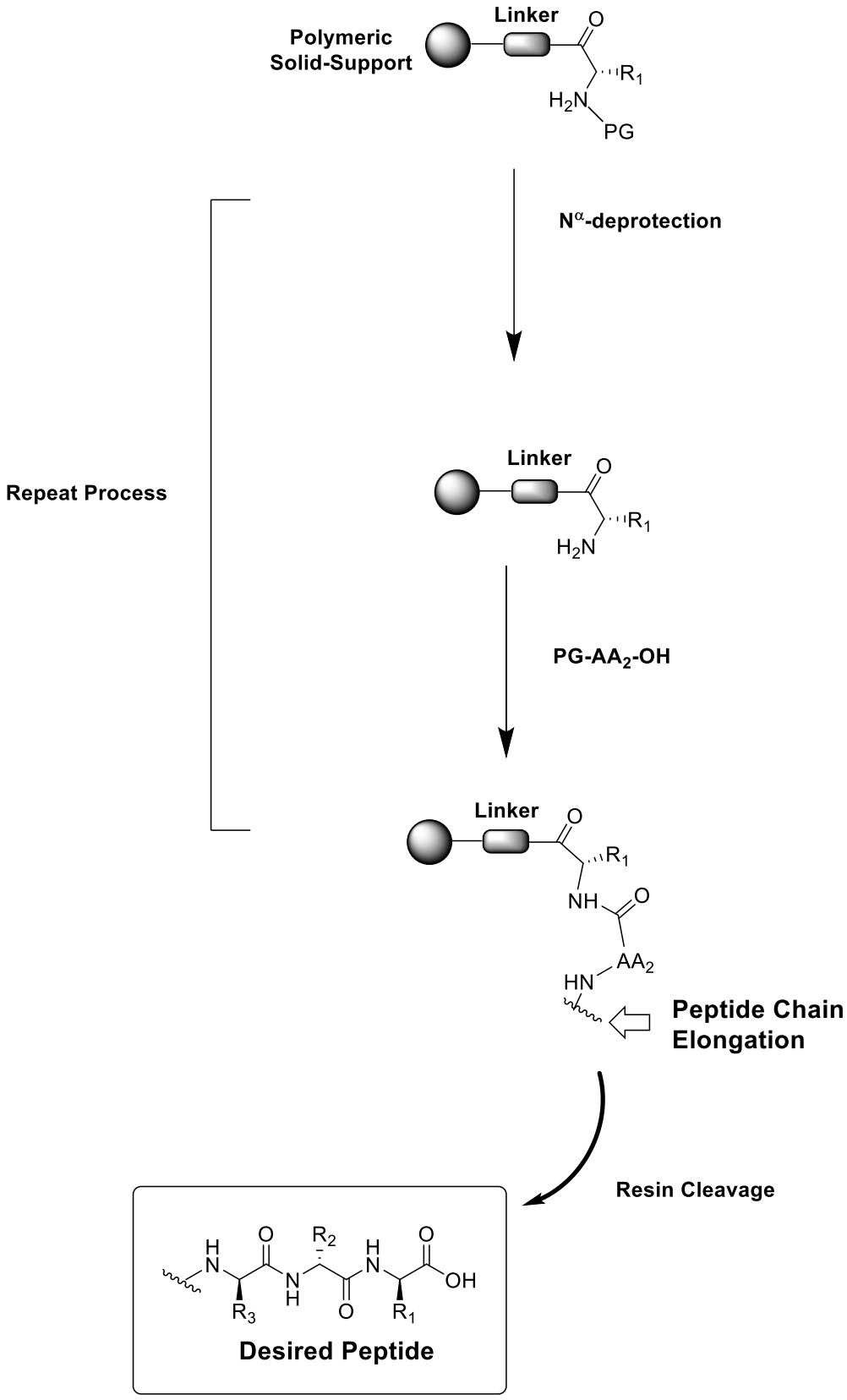

Figure 1-1: General approach to solid-phase synthesis

The N-terminus is typically protected with either the base-labile Fmoc or acid-labile Boc group. The synthesis proceeds by deprotecting the N-terminus and coupling the next amino acid residue with a protected N-terminus and an activated C-terminus. After each deprotection and coupling step, the excess reagents are removed by filtration, which leaves the resin-bound peptide behind. Orthogonality is the concept of using protecting groups that can be selectively removed in the presence of each other. The reactive side chains of the amino acids must also be protected with groups orthogonal to the N-terminal protecting group, to avoid side reactions from occurring.[8]

1.1.1 Linkers in Solid-Phase Synthesis

One of the key aspects of synthesis on a solid support is the use of a linker molecule to connect the insoluble polymeric support to the molecule that is being synthesized. A key feature of the linker is the ability to release the peptide upon completion of the synthesis, without damaging the functional groups present on the peptide. Additionally, it is essential to be able to conduct synthetic steps on the peptide without accidently cleaving the covalent linkage to the resin. The majority of available linkers use a strong acid such as TFA to release the completed peptide, leaving a terminal carboxylic acid or amide in its place.[9] Some commonly used linkers for Fmoc-based SPPS are shown in Figure 1-2. All the linkers shown link the C-terminus of the growing peptide through either an amide or ester bond. Acidic conditions are typically used for cleavage, ranging from concentrated HF to dilute TFA. The acidic cleavage conditions required pose a challenge for the synthesis of acid-sensitive peptides. Additionally, it can be a challenge to perform reactions under acidic conditions on these linkers without incidental cleavage of the peptide linkage.

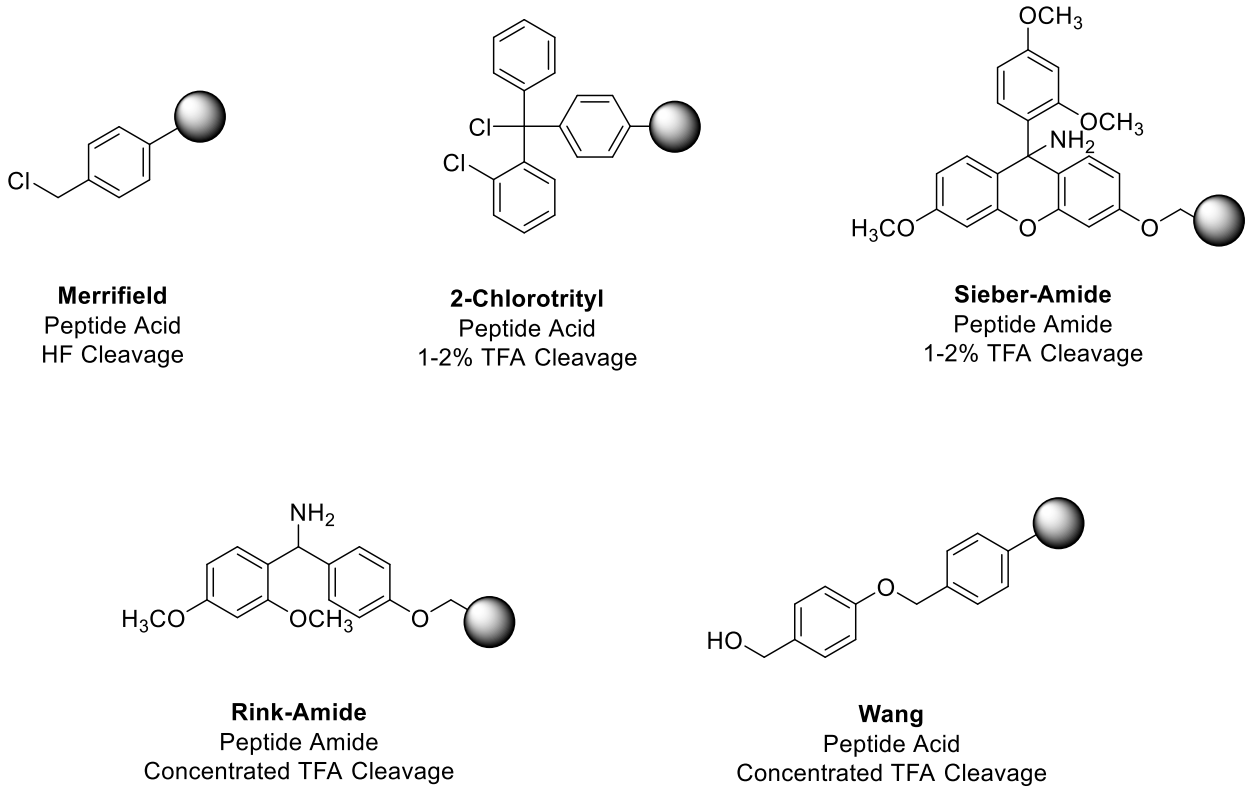

Figure 1-2: Common linkers used in SPPS[9, 10]

1.1.2 **Limitations of Standard Solid-Phase Peptide Synthesis**

In standard solid-phase synthesis, the peptide is linked to the solid support through the C-terminus. The peptide is then typically synthesized in the C→N direction. However, this method places a limitation on the synthetic transformations that are possible. Because the C-terminus is unavailable, no C-terminal modifications are possible without first cleaving the peptide from the solid support. Many different types of C-terminal modifications are highly desired. Cyclic peptides, which typically involve cyclizing the peptide in head-to-tail fashion cannot be formed on the resin through standard methods. Additionally, C-terminal thioesters are a synthetic target of interest for their use in the Native Chemical Ligation (NCL) technique that was developed by Kent and coworkers.[11] The ability to make these modifications on a solid support leads to a cleaner and more effective reaction, and allows the speed and convenience typically associated with solid-phase synthesis.

Cyclic peptides are a highly sought-after synthetic target. In medicinal therapeutics, cyclic peptides have many advantages over both small molecule- and linear peptide- based drugs.[12] Small

molecules often encounter problems *in vivo* due to their relative hydrophobicity. This limits the targets with which they can interact.[12] Small molecules also tend to be less selective and thus off-target effects are more like to be exhibited.[12] Use of larger macromolecules can improve many of these negative features. Heavier and less-rigid molecules are less likely to interact with enzyme active sites other than those for which they were designed leading to greater selectivity.[12, 13] Their larger size gives rise to a larger contact area, which can lead to tighter binding. Additionally, macromolecules therapeutics tend to be made primarily of amino acids or other biomolecules. This greatly reduces the effect of potentially toxic metabolites, since the building blocks of these macromolecules are already present in the biological system.[13]

There are many drawbacks associated with using linear peptides as drugs. Although the benefits over small molecule therapeutics exist as mentioned above, problems with cell permeability and metabolic instability greatly limit their usefulness.[12, 14] Macrocyclization of these peptides can greatly improve their cell permeability.[15] Additionally, the proteases that are responsible for rapidly metabolizing linear peptides often cannot recognize peptides in their cyclic form, as they require a free N- or C-terminus for recognition and subsequent binding.[15]

1.2 The Backbone-Amide Linker Approach

Fernando Albericio and George Barany developed a novel approach to the problem of C-terminus availability in SPPS. They proposed linking the peptide to the resin through the nitrogen of a backbone amide, thus freeing the C-terminus for modification on the resin. They developed the 5-(4-formyl-3,5-dimethoxyphenoxy)valeric acid linker moiety, which they called the Backbone Amide Linker (BAL, Scheme 1-1).[16] The precursor can be synthesized in solution and then loaded onto an aminomethyl resin through an amide coupling reaction with the terminal carboxylic acid. The first amino acid residue is then loaded by undergoing a reductive amination with the aldehyde of the linker precursor, followed by acylation with the second amino acid residue to form the dipeptide. Standard Fmoc-based synthesis can then be used to install the remainder of the desired peptide. By utilizing a palladium-labile C-terminal protecting group such as the allyl-ester, C-terminal modifications can be performed on the resin prior to cleaving the peptide. This effectively allows bidirectional synthesis to take place. The final peptide can be then released from the resin with 95% TFA.[16]

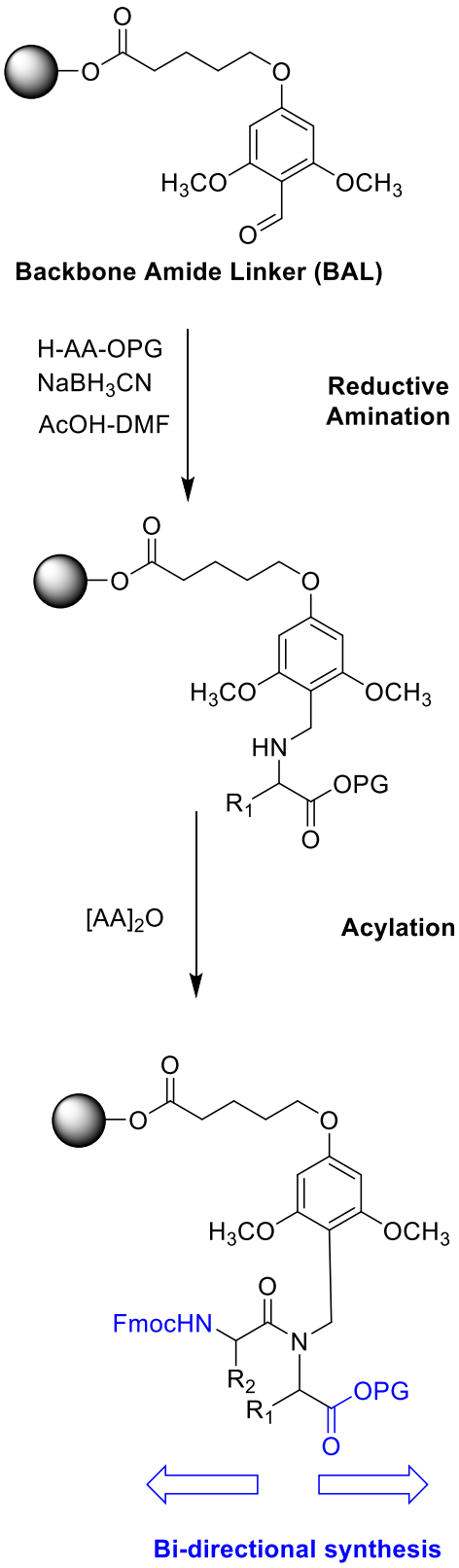

Scheme 1-1: The backbone-amide linker for solid-phase peptide synthesis of C-terminally modified peptides

1.3 Limitations of the BAL Strategy

The BAL strategy developed by Albericio and Barany has proved useful for the synthesis of cyclic peptides and other peptides with C-terminal modifications. However, the strategy comes with two major limitations. The peptide linkage is acid-labile, thus limiting the transformations that can be carried out on the resin without loss of the peptide. Additionally, formation of a diketopiperazine (DKP) byproduct at the dipeptide stage has proven a challenge to overcome [16].

1.3.1 Diketopiperazine Formation at the Dipeptide Stage

Quantitative formation of the DKP byproduct at the dipeptide stage with unhindered amino acids narrows the scope of substrates that can be used with the BAL linker. The authors address this problem extensively in the original paper.[16] Upon deprotection of the N-terminus of the dipeptide, rapid formation of the DKP product occurs, effectively halting the synthesis at that stage (Scheme 1-2, left). The formation of DKP is facilitated by the tertiary amide that links the dipeptide to BAL, which exists partially in the cis-conformation needed for cyclization to the DKP.[17] Additionally, the presence of a good leaving group such as allyl-alcohol furthers the preference of this side reaction. Finally, less sterically bulky amino acid side chains tend to favor DKP formation as well.

One method that has been used to overcome this problem is to employ a sterically bulky C-terminal protecting group such as a *t*-butyl ester. The steric hindrance slows the addition of the primary amine onto the C-terminus sufficiently to allow the deprotected dipeptide to be captured by coupling the next amino acid residue (Scheme 1-2, right).[16] However, the *t*-butyl ester is acid-labile. Use of this protecting group compromises the ability to selectively perform C-terminal modifications on the resin. Thus, the use of the BAL system is quite limited if used with this method.

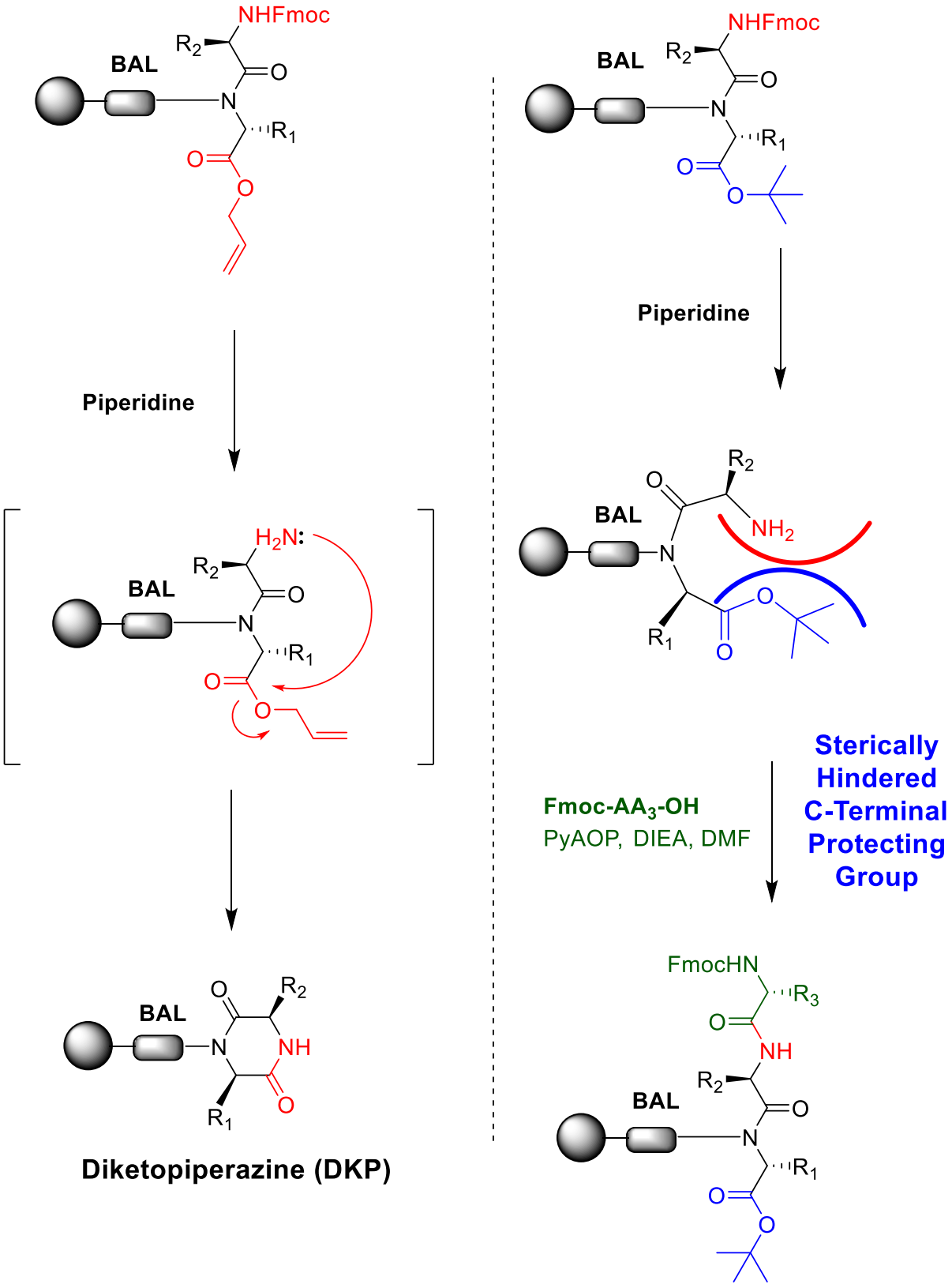

Scheme 1-2: Use of a sterically-hindered C-terminal protecting group to minimize DKP formation

The authors proposed another method for overcoming the problem of DKP formation at the dipeptide stage known as "*in situ* neutralization". The concept involves maintaining the primary amine of the N-terminus in the protonated state, thus minimizing its ability to act as a nucleophile on the C-terminus (Scheme 1-3). Because this method relies on a kinetic competition between an intermolecular acylation and an intramolecular cyclization, only relative success can be achieved. Up to 15% DKP formation is still seen using *in situ* neutralization, depending on sequence employed. Additionally, small quantities of the peptide are lost due to the acid- lability of the resin-linkage with the BAL system.[16]

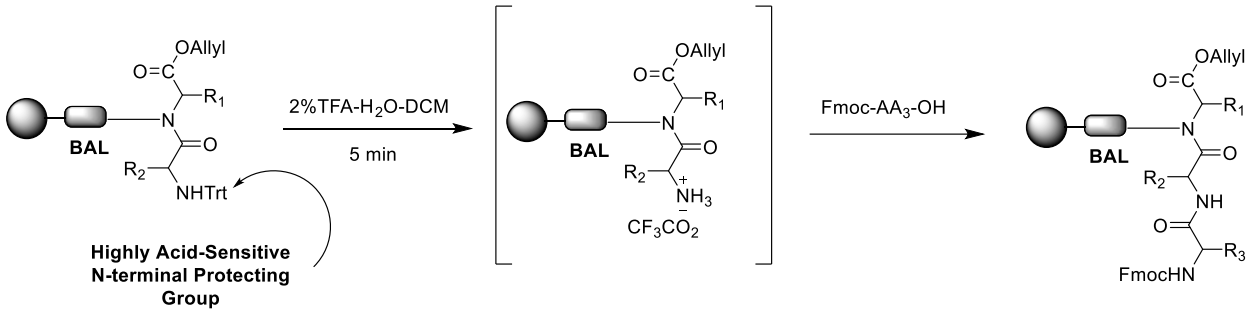

Scheme 1-3: In-situ neutralization to minimize formation of DKP

1.3.2 Lack of Orthogonality in the BAL System

The second limitation of the BAL concept is the acid lability of the peptide linkage. This feature makes Boc-chemistry and other acid-based transformations unable to be used on the resin. Although BAL requires concentrated TFA to achieve full release of the peptide, some loss of this linkage is seen even with stoichiometric amounts of TFA such as those used in *in-situ* neutralization.[16] As mentioned previously, use of the sterically bulky *t*-butyl ester protecting group to avoid DKP formation limits the ability to perform C-terminal modifications on the resin. The acid-labile side-chain protecting groups that are typically used in Fmoc-based SPPS cannot be deprotected on the resin without also cleaving the peptide. This effectively requires the peptide to be extensively purified following synthesis, as the protecting group byproducts cannot be washed away from the resin as other impurities can. Depending on the sequence, this can create a large quantity of impurities that must be separated away. Likewise, cleavage of the peptide from the resin removes most of the acid-labile side chain protecting groups, making it difficult or impossible to synthesize a fully protected peptide. This three-way lack of orthogonality between the C-

terminus, the side- chain protecting groups, and the resin linkage limits the transformations that can occur with this system (Figure 1-3). Introducing alternative methods for each of these features will help to differentiate them, allowing for more selective transformations to occur.

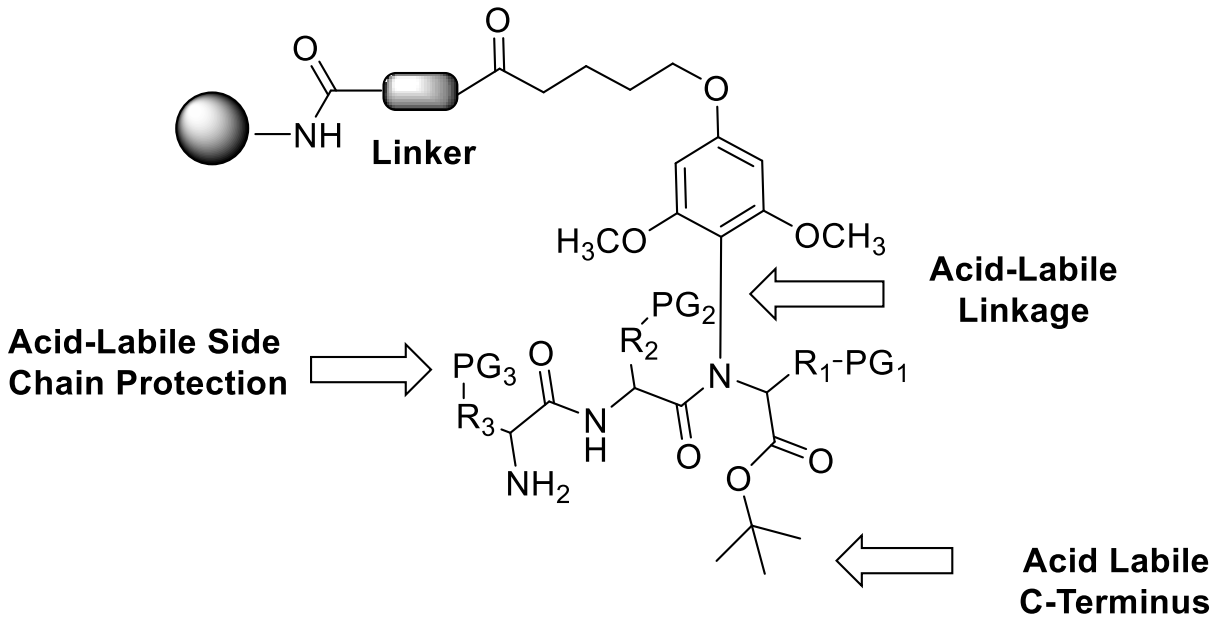

Figure 1-3: Acid-lability of BAL linkage limits the possible on-resin transformations

1.4 **Design of a Photolabile Backbone-Amide Linker**

The Lipton Lab at Purdue University has envisioned designing a new Backbone-Amide Linker that includes dual directionality of synthesis as in the original BAL, but that minimizes the challenges that are faced when using the standard BAL system. Replacing the acid-cleavable linkage with a bond that is cleavable only under UV irradiation would add a degree of orthogonality and solve the problem of acid-sensitivity.

1.4.1 **Selection of a Candidate for use as a Photolabile Backbone Amide Linker**

Former Lipton group member Dr. Soo Sung Kang began the mission of designing a new Backbone-Amide Linker with two primary features: (1) A resin linkage that is cleavable under UV light and (2) a resin linkage that is stable to strongly acidic conditions.[18] A series of known photoreactive functional groups were selected for testing for viability as a linker for SPPS (Figure

1-4). The two requirements for use as a linker candidate were (1) known UV reactivity and (2) the ability to covalently connect the primary amine of the first amino acid residue in a peptide sequence. The first candidates (1, 2, & 3) are categorized as the widely studied, photoreactive phenacyl group. Under 300-360 nm UV irradiation, this system releases an α-substituent. The *p*-alkoxy substituent is thought to stabilize the radical intermediates involved in the photolysis mechanism.[19] The α-substituents on candidates **2** and **3** further contribute stability of the radical intermediate, theoretically increasing the photoreactivity of these motifs.[20, 21]

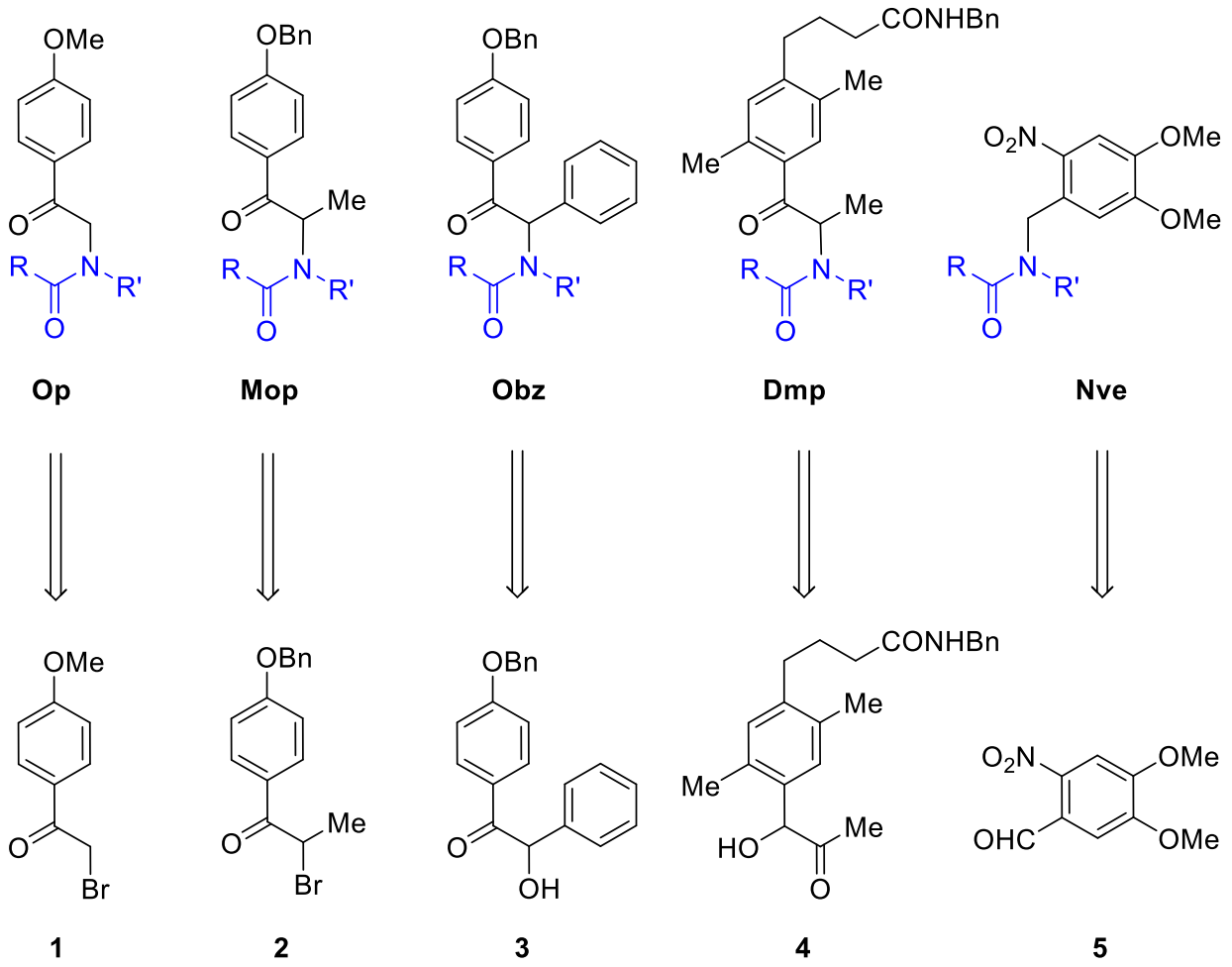

Figure 1-4: Modifications to make linker-like candidates [18]

These photoreactive skeletons were examined for their usefulness in the desired study. Key features considered were a) an anchoring point for connection of amino acids to the linker, b) the rate and efficiency of photo-cleavage, and c) the suppression of side reactions during photolytic

deprotection. To compare the 5 candidates, the dipeptide Boc-Phe-Gly-OMe was synthesized on each of the candidate precursors and subject to photolysis at 300 nm (Figure 1-5).

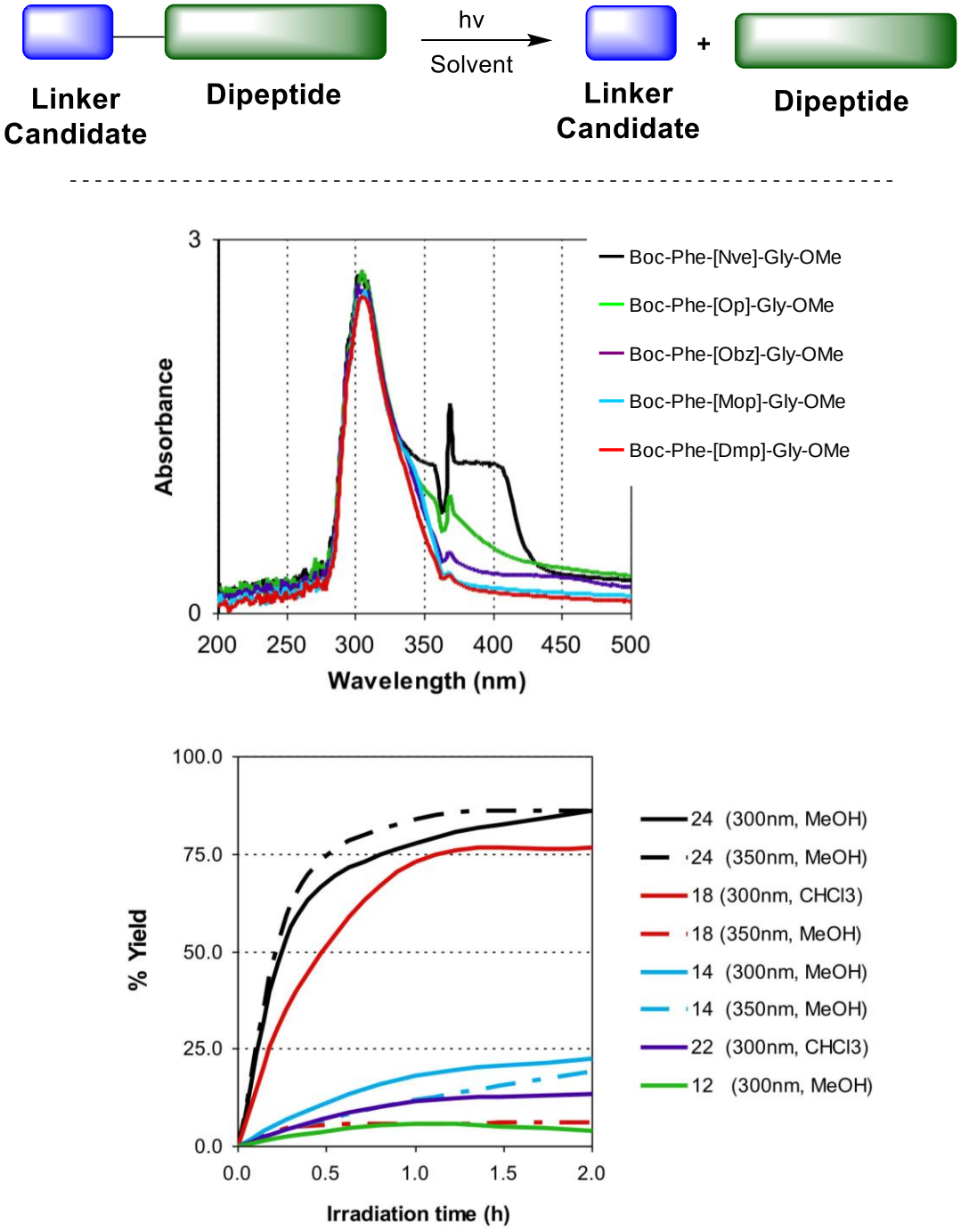

Figure 1-5: Linker candidate and wavelength selection [Figure taken from the thesis of Dr. Soo Sung Kang] [18]

On the basis of both acylation and photocleavage yields the nitrobenzyl motif of the Nve linker was chosen as the basic skeleton for a second-generation linker. Nve showed the most rapid and complete cleavage under UV irradiation at both 300 and 350 nm UV. The transacylation motif of the 6-hydroxy-4-methoxybenzyl (Hmb) and 6-hydroxynitrobenzyl (Hnb) auxiliaries was incorporated into the linker design to improve acylation efficiency of the sterically hindered secondary amine.[22] The acid-labile Hmb auxiliary was devised by Sheppard and coworkers for the protection of peptide amide backbones during the synthesis of 'difficult' peptide sequences. The related, photolabile Hnb auxiliary was developed by Smythe for the covalent modification of 'difficult' peptide sequences to facilitate their cyclization.[23] Both the Hmb and Hnb auxiliaries employ an *ortho*-hydroxyl group to acylate bulky amino acids via esterification and subsequent O-to-N transacylation (Figure 1-6).

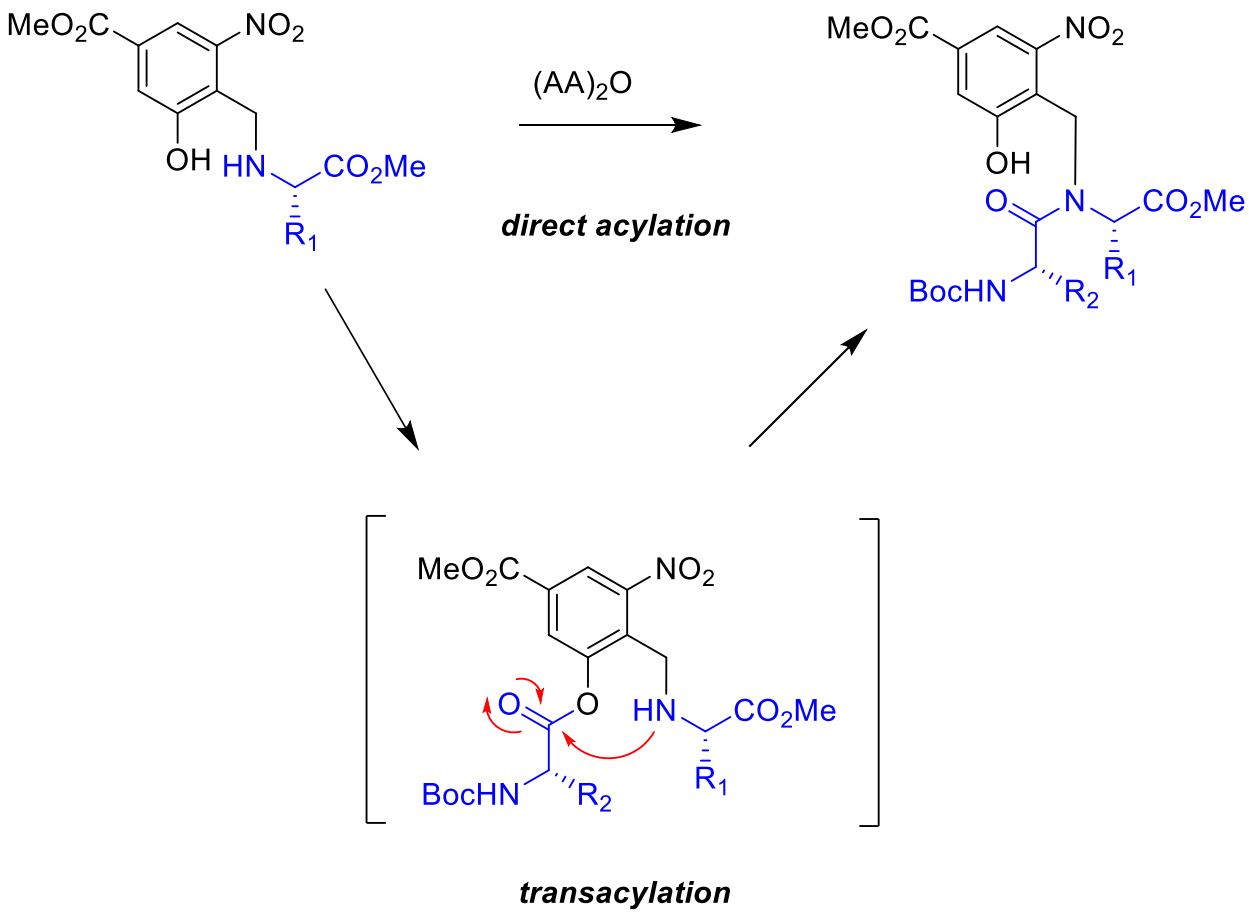

Figure 1-6: Ortho-hydroxyl assists in acylation of the secondary amine through transacylation

The presence of an *o*-phenol group improves the rate of the photolysis at a later stage. Installation of a carboxyl- group on the *o*-nitrobenzyl skeleton creates a site at which the linker can be attached to the resin. Additionally, this increases the electron-withdrawing nature of the ring, which improves the reactivity for several of the more difficult synthetic transformations. Thus, the 2-hydroxy-4-carboxy-6-nitrobenzyl (Hcnb) linker emerged as a second-generation candidate for a photolabile BAL linker. The UV absorbance spectrum of the proposed Hcnb linker was compared with the original Nve linker candidate (Figure 1-7). No significant difference was seen in the absorbance at 300-365 nm.

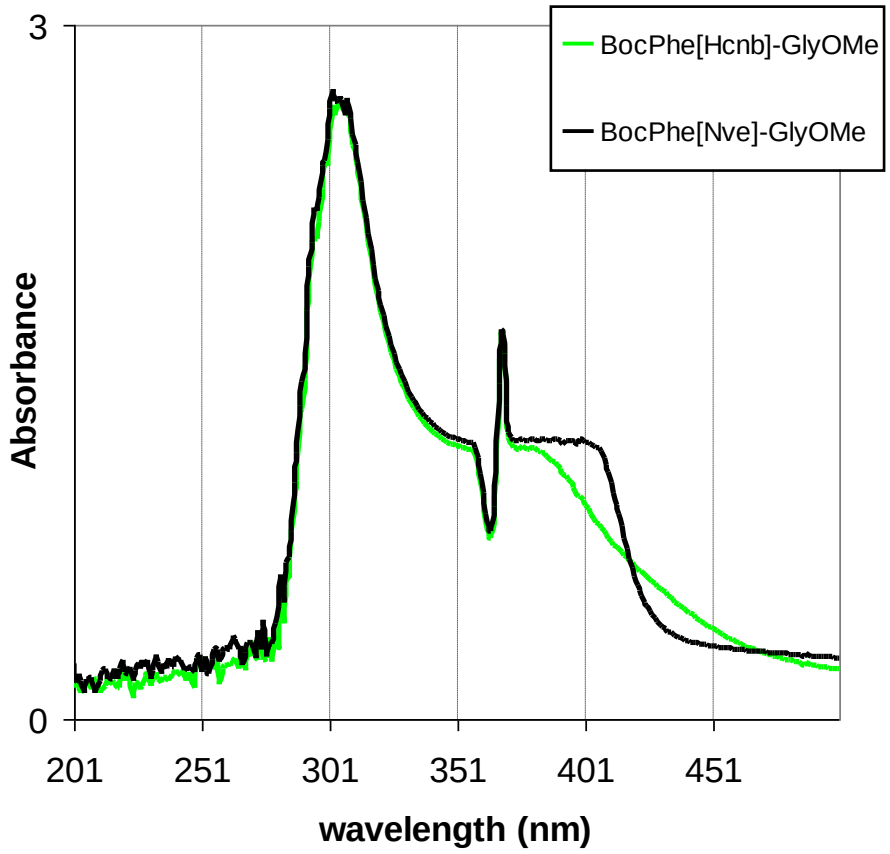

Figure 1-7: UV absorbance spectrum of Nve and Hcnb linker candidates [Figure taken from the thesis of Dr. Soo Sung Kang] [18]

The final proposed linker structure (Figure 1-8) provides 4 degrees of orthogonality for peptide synthesis on the solid support. With an acid- stable resin linkage (**1**), the system can be used for acid-based transformations. With the use of a palladium-labile C-terminal protecting group (**2**), C-terminal modifications can be made selectively. These features coupled with the

standard base-labile N-terminal Fmoc protecting group (**4**) and acid-labile side chain protecting groups (**4**) allow for differentiation in any exhaustive combination of the 3 modification points

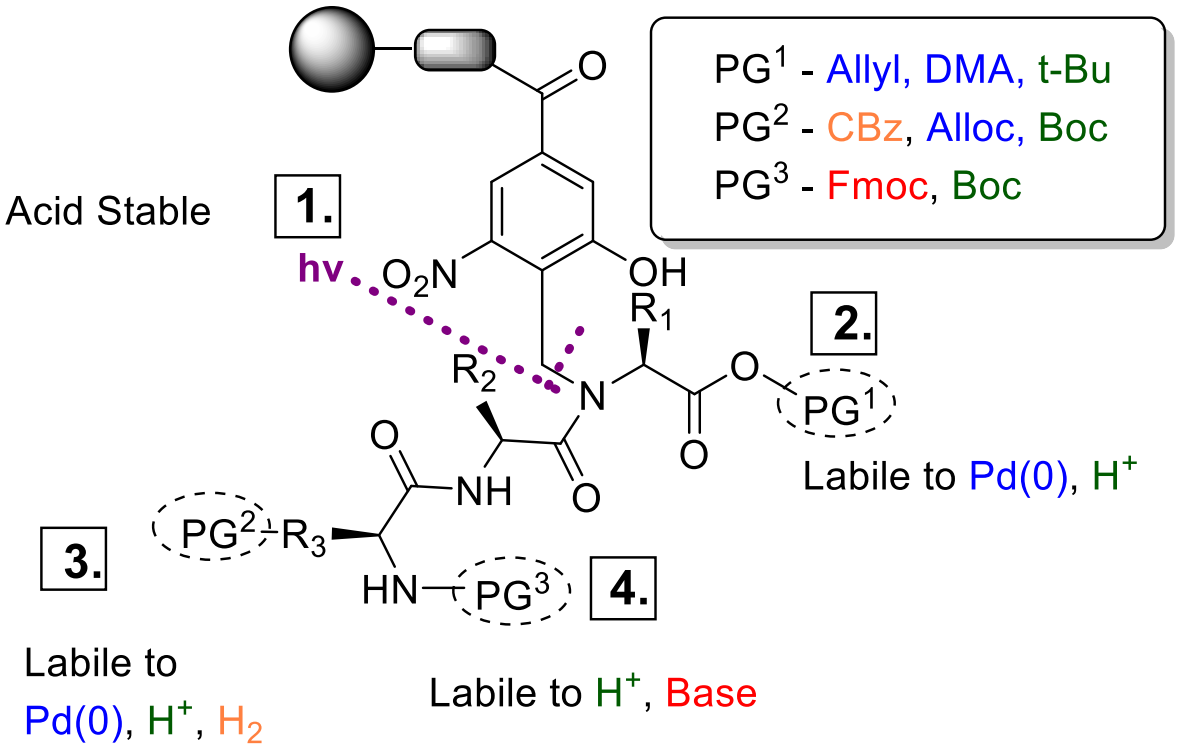

Figure 1-8: 4 Degrees of orthogonality for the proposed photolabile linker Hcnb

1.4.2 **Synthesis of A Second Generation Photolabile Linker**

The synthesis of the linker precursor 2-hydroxy-4-carboxy-6-nitrobenzaldehyde (Hcna) was designed and optimized by former group member Dr. Matthew Hostetler (Scheme 1-4).[24] Starting with commercially available 4-methyl-3,5-dinitrobenzoic acid, a condensation with DMF-DMA in toluene for 16 h yielded enamine **1.2** in 72% yield. Ruthenium- catalyzed oxidative cleavage of the enamine using sodium metaperiodate formed aldehyde **1.3** in 61% yield. A substitution reaction of acetaldoxime onto the ring generated the methyl- protected linker precursor **1.4**, used for all solution-phase linker studies. Saponification of the *para*-methyl ester generated **1.5** in 90% yield. The *para*-carboxyl group allows for connection of the linker to the solid support through an amide coupling reaction.

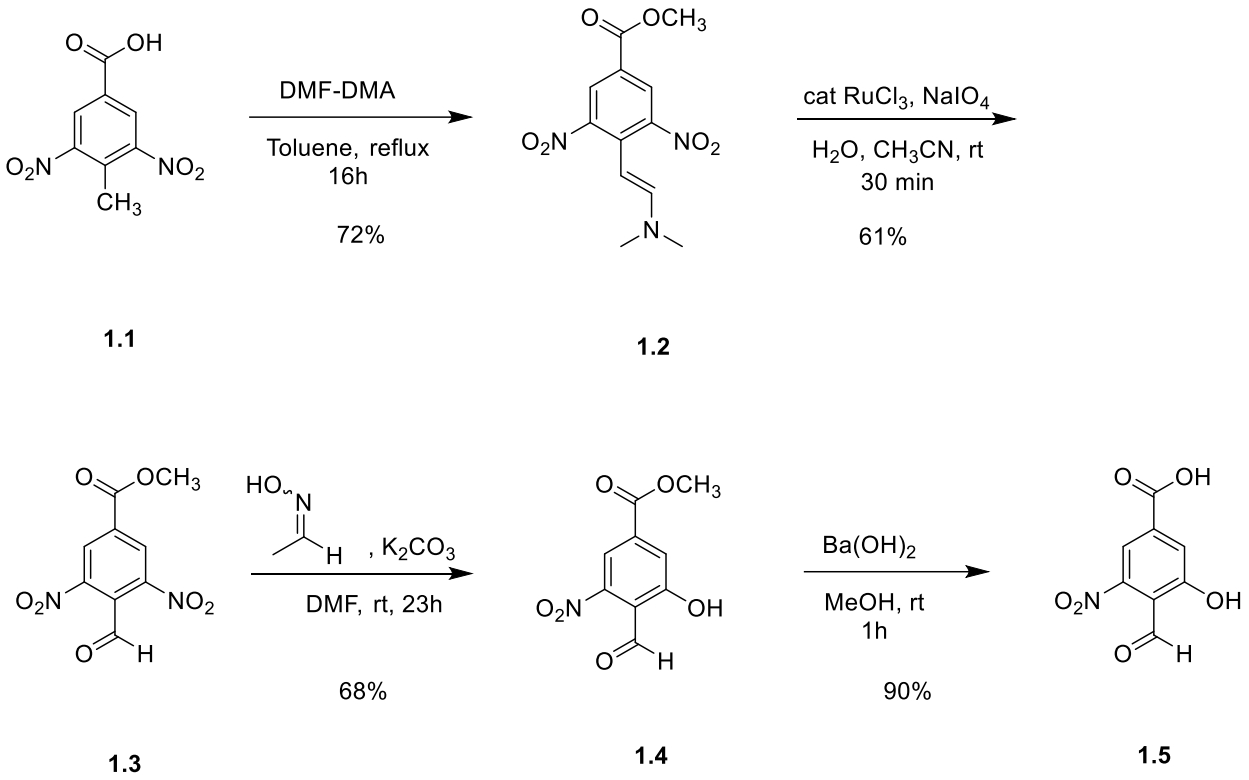

Scheme 1-4: Synthesis of the aldehyde precursor to the Hcnb linker[24]

1.5 **Conclusion**

Peptide synthesis has developed extensively over the previous 130 years. However, many challenges still remain unaddressed. C-terminal modifications pose a unique challenge to the solid-phase synthesis concept, since the peptide must be covalently linked to the solid support. Albericio and Barany proposed a new method for overcoming this challenge, the Backbone-Amide Linker strategy.[16] However, this approach faces several challenges that limit its usefulness. The formation of DKP at the dipeptide stage is a major drawback to the system and requires special steps to avoid termination of the peptide. The limits of orthogonality between resin linkage and various protecting groups also hinders the scope of possible synthetic targets that can be obtained from the system. A new, photolabile backbone amide linker was proposed that allows for the bidirectional manipulation of peptides on the solid support. This linker is stable to acid, base, and palladium, allowing for a wide range of chemical conversions to be carried out without cleavage of the resin linkage.

CHAPTER 2. THE DEVELOPMENT OF A PHOTOLABILE BACKBONE AMIDE LINKER FOR USE IN SOLID-PHASE SYNTHESIS

2.1 A Novel Photolabile Backbone Amide Linker

Former Lipton group member Dr. Soo Sung Kang selected a candidate to be adapted for use as a photocleavable Backbone-Amide Linker for use in solid-phase synthesis.[18] Former Lipton group member Dr. Matthew Hostetler developed a synthesis of the linker precursor, Hcna.[24] To continue with the development of the linker, we conducted solution-phase synthesis studies to establish the viability of creating peptides linked to Hcnb. Finally, several synthetic challenges needed to be addressed in the transition to conducting solid-phase synthesis with the linker, including inhibition of DKP formation and optimization of the photolytic cleavage to release the completed peptide.

2.2 Solution-Phase Synthesis of Dipeptides using Hcnb

We envisioned linking the peptide to the linker via a reductive amination between the primary amine of the first amino acid and the aldehyde precursor, in similar fashion to the loading protocol for the original BAL Linker.[16] The resulting secondary amine can then be acylated with the next amino acid in sequence, forming a tertiary amide linkage between the peptide and linker. The presence of the *ortho*-phenol in Hcnb is essential to completely acylating the secondary amine, especially when utilizing amino acids with bulky side chains. Finally, photolysis in the short-wave UV range should cause a clean release of the dipeptide from the linker.

A series of dipeptides were synthesized in solution on the methyl ester-protected Hcna linker precursor **1.4** (Scheme 2-1). In solution, addition of the desired C-terminally protected amino acid to the aldehyde handle in the presence of DIEA in MeCN forms the imine intermediate. Reduction of this intermediate by sodium borohydride in methanol yields the Hcnb-linked amino acids **2.1a-2.1d**. Acylation of this secondary amine with a pre-formed symmetric anhydride of the desired second amino acid resulted in acylation to give dipeptides **2.2a-d**, even in the case of bulky side-chains such as Thr. Photolysis at 365 nm in MeOH releases the desired dipeptides from the

linker to give **2.3a-d**. Due to rotomeric structures arising from peptides attached to Hcnb, yields were reported across 2 steps (Table 2-1).

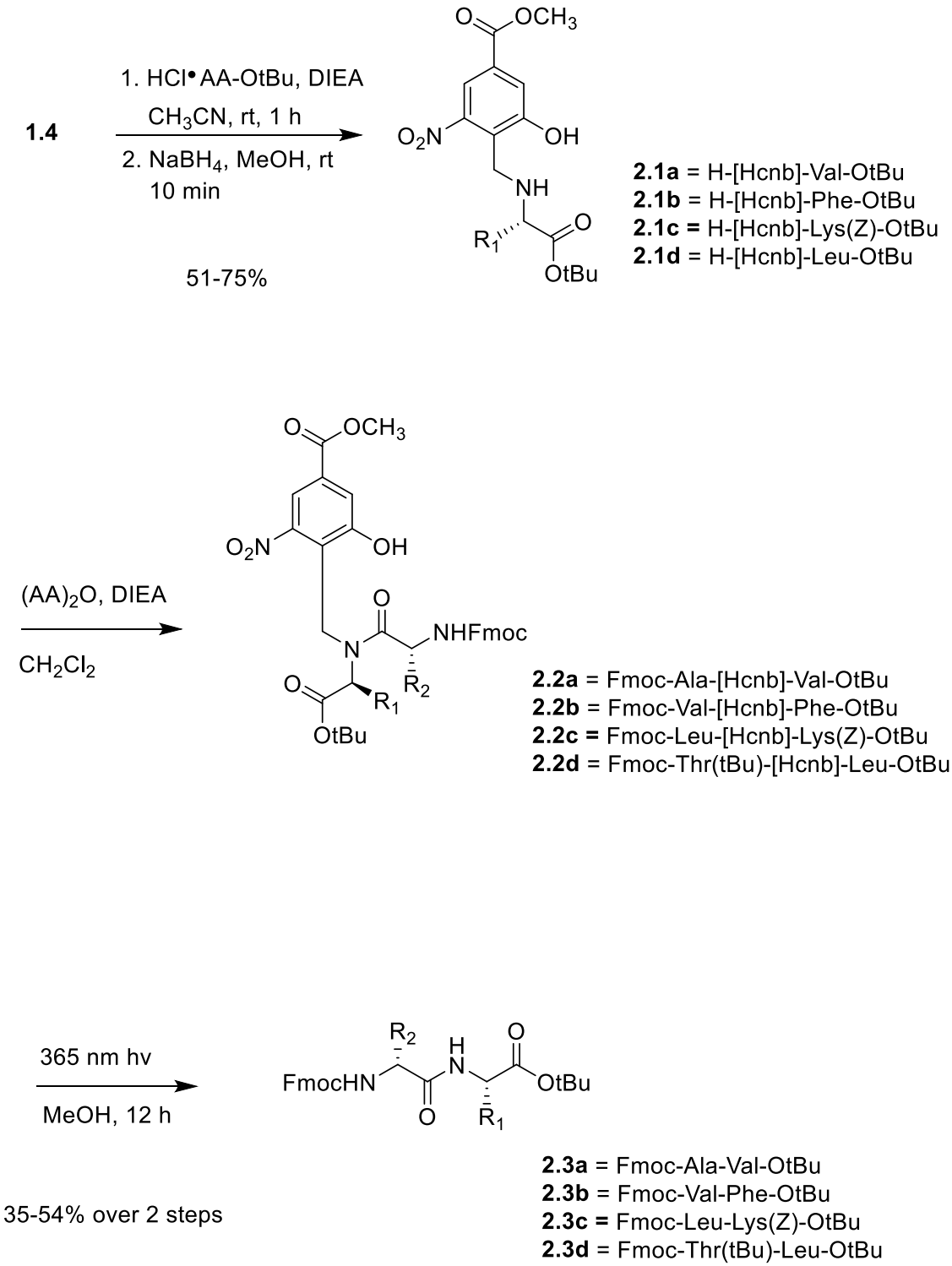

Scheme 2-1: Solution-phase synthesis of dipeptides using Hcna

Table 2-1: Solution-phase synthesis of dipeptides using Hcnb

Peptide	Reaction	Yield
H-[Hcnb]-Val-OtBu **(2.1a)**	Reductive Amination	51%
H-[Hcnb]-Phe-OtBu **(2.1b)**	Reductive Amination	63%
H-[Hcnb]-Lys(Z)-OtBu **(2.1c)**	Reductive Amination	69%
H-[Hcnb]-Leu-OtBu **(2.1d)**	Reductive Amination	75%
Fmoc-Ala-Val-OtBu **(2.3a)**	Photolysis	38%
Fmoc-Val-Phe-OtBu **(2.3b)**	Photolysis	35%
Fmoc-Leu-Lys(Z)-OtBu **(2.3c)**	Photolysis	54%
Fmoc-Thr(tBu)-Leu-OtBu **(2.3d)**	Photolysis	53%

2.2.1 **Acid Stability**

To confirm the stability of the linker in strongly acidic conditions, a simple dipeptide analogue, Ac-Ala-OMe, was synthesized on the linker in solution and exposed to 95% TFA in CH_2Cl_2 for 24 hours (Scheme 2-2). The reaction was monitored by TLC at various time intervals (30 minutes, 1 hour, 2 hours, 6 hours, 12 hours, and 24 hours). No change was observed by TLC at 24 hours of exposure time. Upon completion of the 24-hour time period, volatiles were evaporated from the reaction and a quantitative mass recovery was obtained. Additionally, no detectable change was observed by NMR spectroscopy. Based on this study it was concluded that the linker is indeed acid stable, at least under any reasonable conditions that would be desired for peptide synthesis.

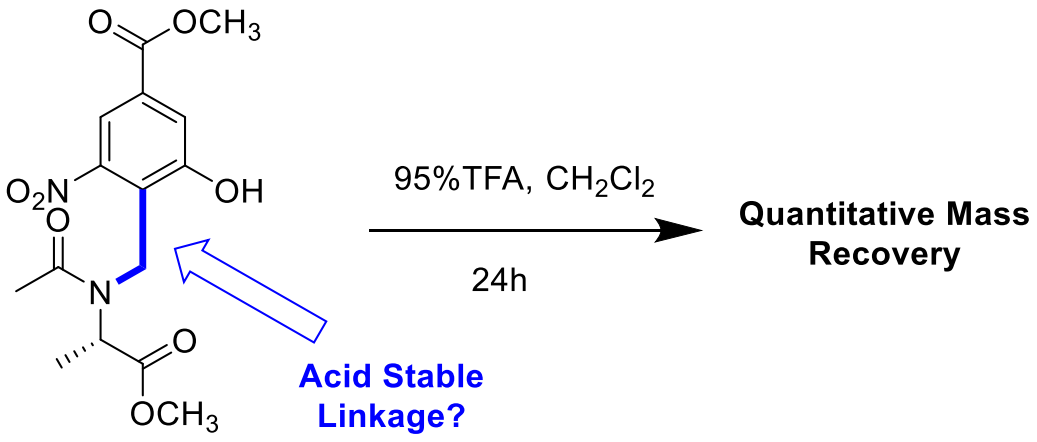

Scheme 2-2: Testing the acid-stability of a peptide- linked Hcnb

2.3 **Synthesis of 1,1 Dimethylallyl-Protected Amino Acids**

The Pd(0)-labile C-terminal protecting group 1,1-dimethylallyl (DMA) was previously developed by former Lipton group member Dr. Matthew Hostetler.[25, 24] DMA-protected amino acids can be simply prepared according to the procedure shown in Scheme 2-3. Starting from commercially available 3-methyl-2-buten-ol **2.7**, the sulfonium salt protecting group precursor **2.8** can be prepared using DMS and HBF_4. This sulfonium salt can then be coupled to the free C-terminus of a variety of Fmoc-protected amino acids (**2.4a-j**) to give the bi-directionally protected amino acids (**2.5a-j**) in 70-95% yields (Table 2-2). In-solution deprotection of the N-terminal Fmoc- group can be accomplished by using the volatile diethyl amine, which can be easily removed from the solution under reduced pressure following completion of the deprotection. 1-Octanethiol is employed as a nucleophile scavenger for the dibenzofulvene biproduct generated from the Fmoc- deprotection.

Table 2-2: Yield of dimethylallyl- protected amino acids

Dimethylallyl-Protected Amino Acid	**Yield**
Fmoc-Ala-ODMA (**2.5a**)	80%
Fmoc -Val-ODMA (**2.5b**)	80%
Fmoc -Gly-ODMA (**2.5c**)	77%
Fmoc -Leu-ODMA (**2.5d**)	85%
Fmoc -Glu(tBu)-ODMA (**2.5e**)	78%
Fmoc -Lys(Boc)-ODMA (**2.5f**)	75%
Fmoc -Thr(tBu)-ODMA (**2.5g**)	95%
Fmoc -Tyr(tBu)-ODMA (**2.5h**)	93%
Fmoc -Phe-ODMA (**2.5i**)	70%
Fmoc -Arg(Pbf)- ODMA (**2.5j**)	70%

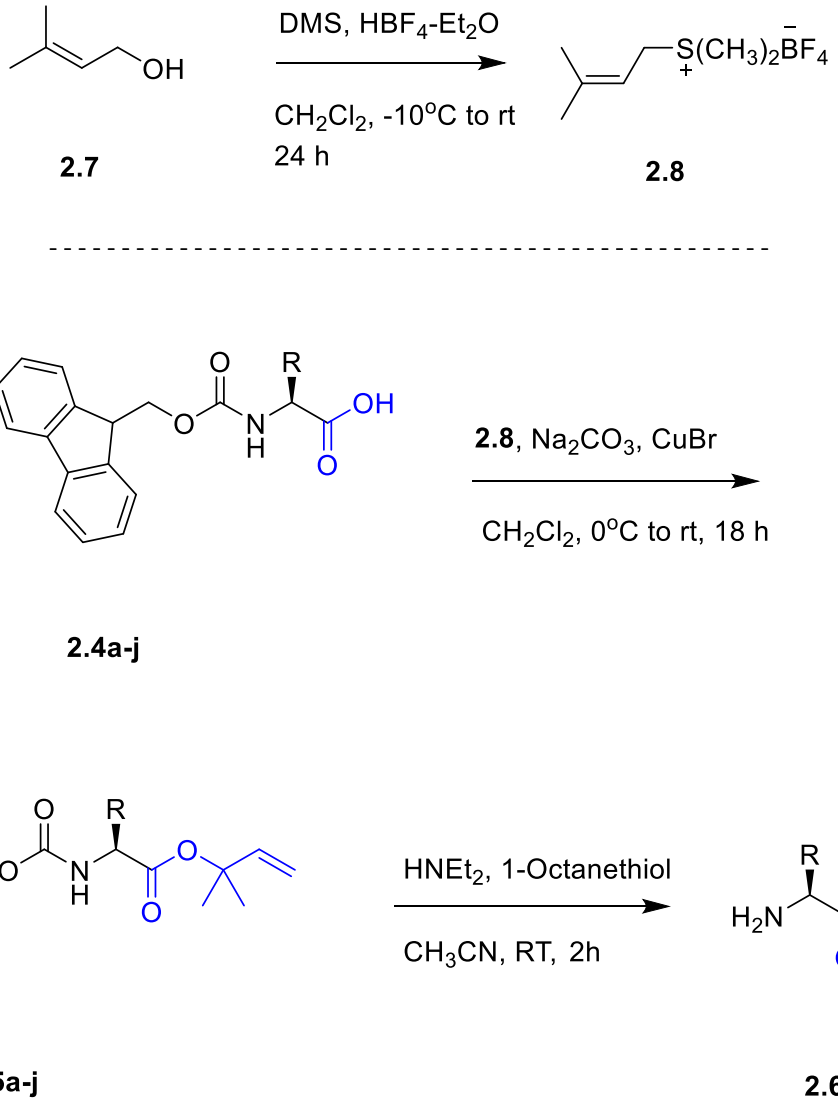

Scheme 2-3: Synthesis of 1,1-dimethylallyl protected amino acids[25]

2.4 **Adaptation of Hcnb to Solid-Phase Synthesis**

In order to prepare the linker for use on a solid support, a unit of aminohexanoic acid (Ahx) was installed on aminomethyl polyethylene glycol resin to serve as a spacer to create distance between the resin bead and the linker (**2.10**, Scheme 2-4). Attempts were made to load the Hcna handle (**1.5**) directly onto the Ahx- spacer unit. However, it was found that significant levels of cross-linking occurred between the free amine of the spacer moiety and the aldehyde group of Hcna. To avoid this side reaction, a proline residue was coupled to the Ahx- spacer (**2.11**). The secondary amine of proline was found to not generate any detectable quantities of cross-linked

product. Upon deprotection of Fmoc-Pro, Hcna can be introduced to the resin by coupling with PyBOP to achieve the prepared resin-loaded linker handle **2.13.**

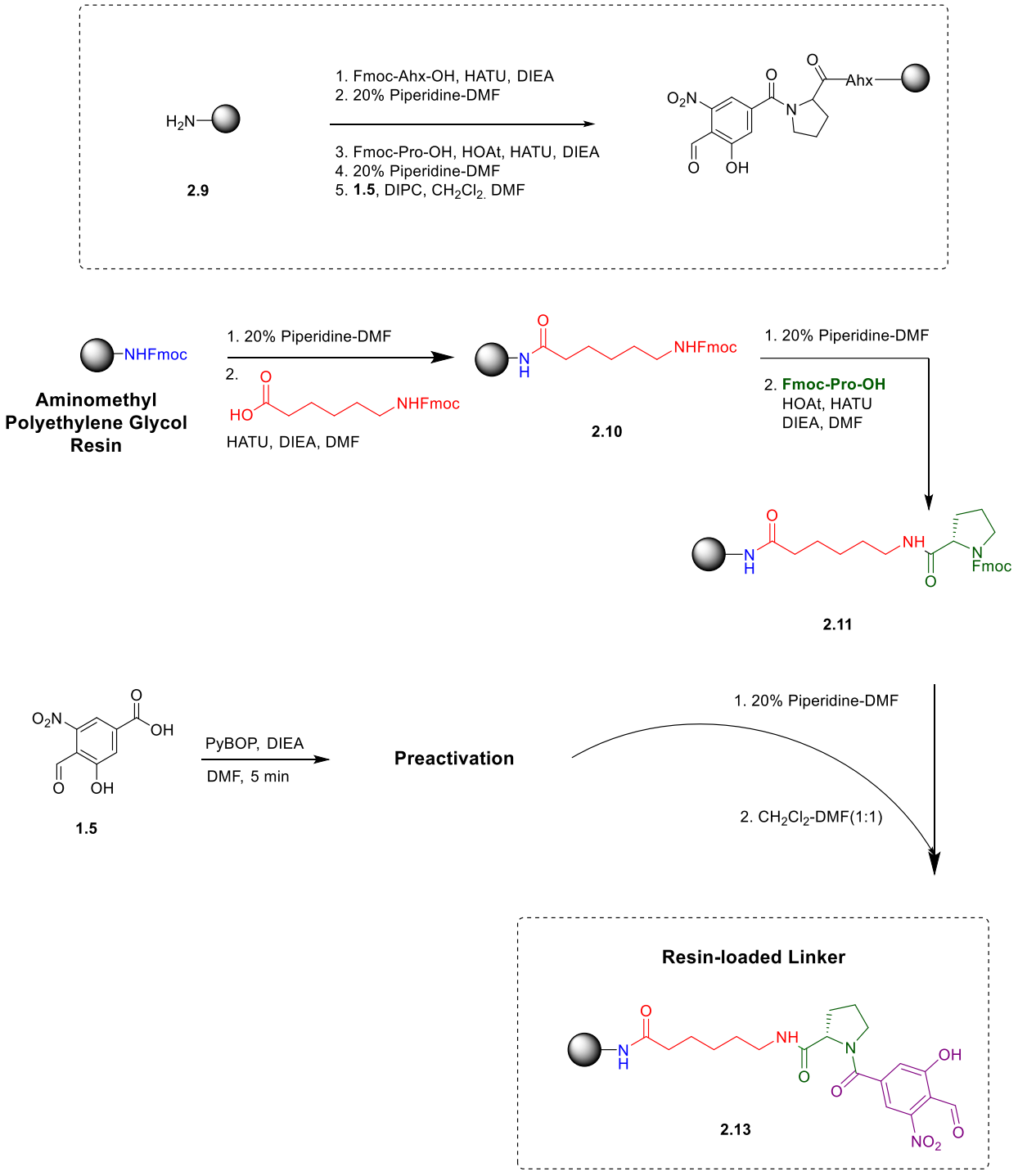

Scheme 2-4: Preparation of resin-loaded Hcna

For the purposes of optimization of synthetic procedures on the resin for Hcnb, a dual-linker system was implemented. A polystyrene resin pre-loaded with the Sieber Amide Linker was incorporated.[26] The rapid and mild cleavage conditions for this linker provide a convenient method for analysis following solid-phase reactions, to better optimize the photolabile linker and identify the cause of any problems encountered (Figure 2-1).

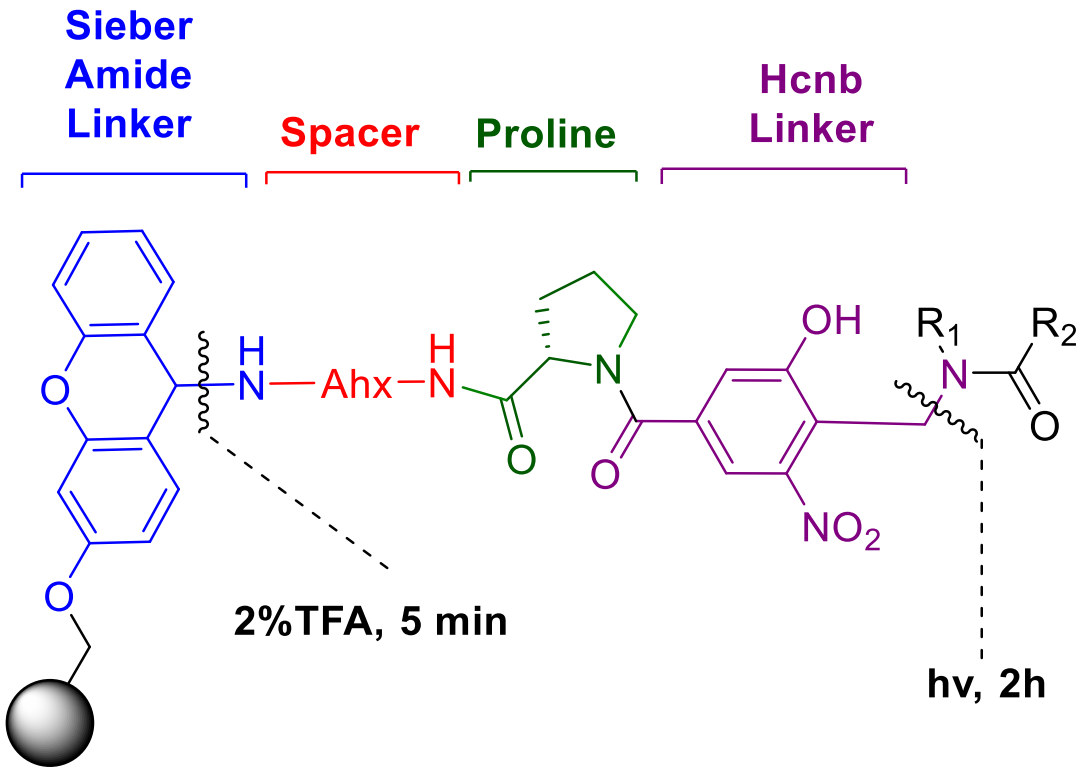

Figure 2-1: Dual-linker system for ease of analysis

2.5 **Optimization of On-Resin Reductive Amination Conditions**

Loading the first amino acid residue to Hcna in solution-phase studies resulted in high yields and complete transformation to the desired product. However, when the same conditions were employed to load amino acids on Hcna when connected to the solid-support, significant quantities of unreacted linker were detected (Scheme 2-5, bottom). The conditions were optimized and adapted to allow for near-complete conversion of the aldehyde handle to the desired benzyl amine.

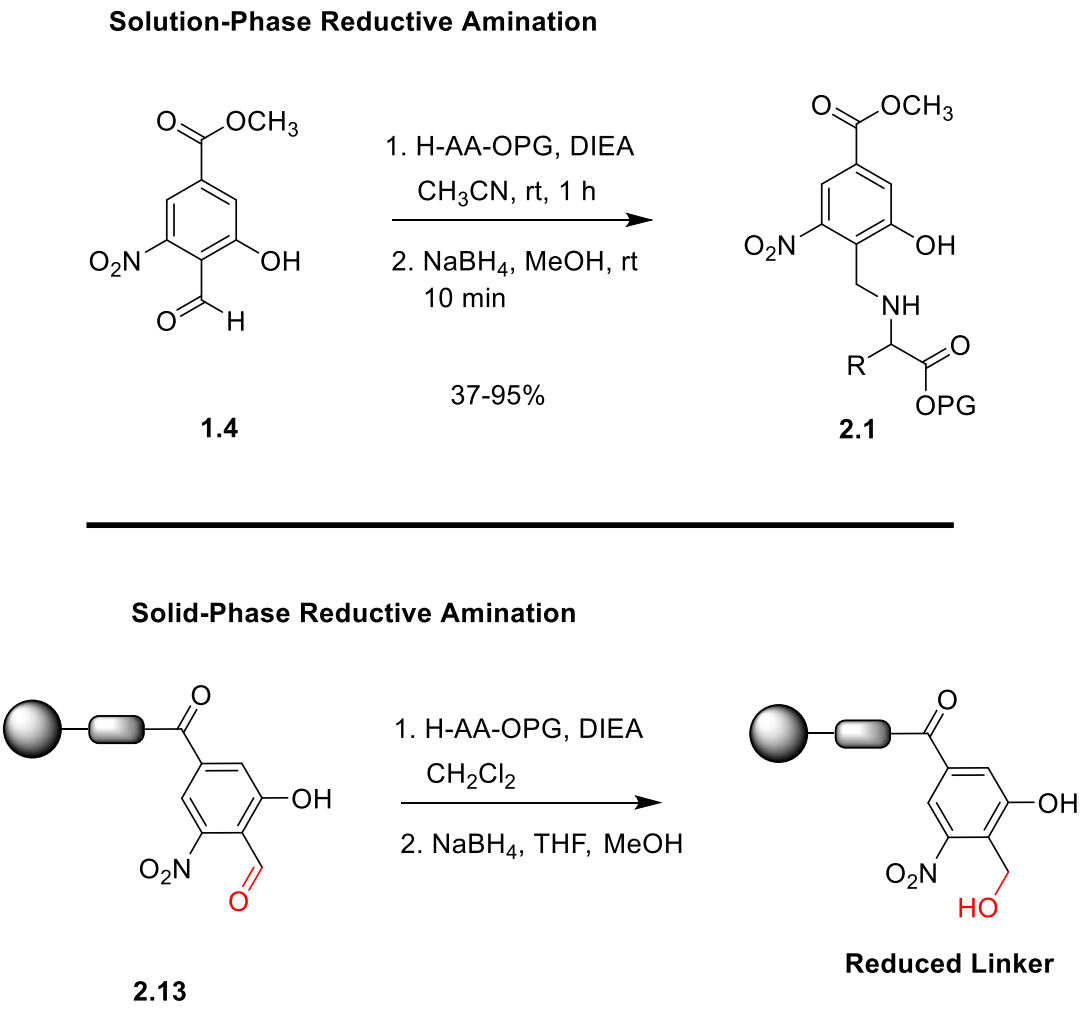

Scheme 2-5: Adaptation of reductive amination conditions to the resin-linked Hcna linker handle results in significant quantities of reduced linker

2.5.1 **Optimization of Reductive Amination Conditions**

The most likely problematic step is the formation of the imine, resulting in large quantities of benzyl alcohol forming in the reduction step. A variety of different conditions were tried to optimize the imine formation step (Table 2-3). Many conditions tried resulted in complex mixtures. Attempts to conduct the full reductive amination in a one-step reaction, as in the procedure for the original BAL linker,[16] did not give the desired product. A 2-step reductive amination conducted under basic conditions gave improved results, but a large quantity of benzyl alcohol remained on the resin with all conditions tried. An exhaustive combination of the conditions in Table 2-3 were tried. No significant difference was found between using a neutral amine or HCl salt form of the

amino acid. Additionally, the identity of the C-terminal protecting group made no noticeable difference in conversion %. Although DMF as a solvent worked slightly better than DCM, dry vs wet solvent was not found to make any difference. Finally, the *ortho*-phenol of the linker was silylated to test if the presence of the proton was inhibiting the formation of the imine. However, complex mixtures were obtained under these conditions. It was eventually discovered that conducting the imine formation step under acidic conditions, using molar equivalents of acetic acid, resulted in a significantly higher quantity of the product regardless of other conditions used.

Table 2-3: Screening of on-resin reductive aminations conditions

Amino Acid	**Additive**	**Solvent**	**Phenol**
HCl Salt	DIEA	DMF (Wet)	Free Phenol
Neutral Amine	DMAP	DCM(Wet	Silylated
- OtBu	AcOH	DMF (Dry)	-
- ODMA	-	DCM (Dry)	-
- OMe	-	-	-

The substrate scope was determined with a series of amino acids for the on-resin reductive amination under acidic conditions (Scheme 2-6). We found that most non-sterically hindered amino acids undergo near complete conversion to the imine under the optimized conditions (Table 2-4). Notably, we determined that glycine is highly incompatible with the reductive amination, resulting in only complex mixtures. When employing β-branched amino acids, complete reaction is still obtained except for extremely sterically bulky cases such as Thr (**2.14d**). This is likely due to the accentuated steric hindrance caused by the bulky t-butyl side-chain protecting group. Additionally, we found that Lys (**2.14c**) results in only ~90% conversion to the imine.

Table 2-4: Completion of on-resin reductive amination

Amino Acid	**% Reduced Linker Remaining**
H-Val-DMA **(2.14a)**	0%
H-Phe-DMA **(2.14b)**	8%
H-Lys-DMA **(2.14c)**	10%
H-Thr-DMA **(2.14d)**	14%
H-Glu-DMA **(2.14e)**	10%
H-Leu-DMA **(2.14f)**	0%
HCl·Leu-tBu **(2.14g)**	6%
HCl·Phe-tBu **(2.14h)**	0%
HCl·Val-tBu **(2.14i)**	3%

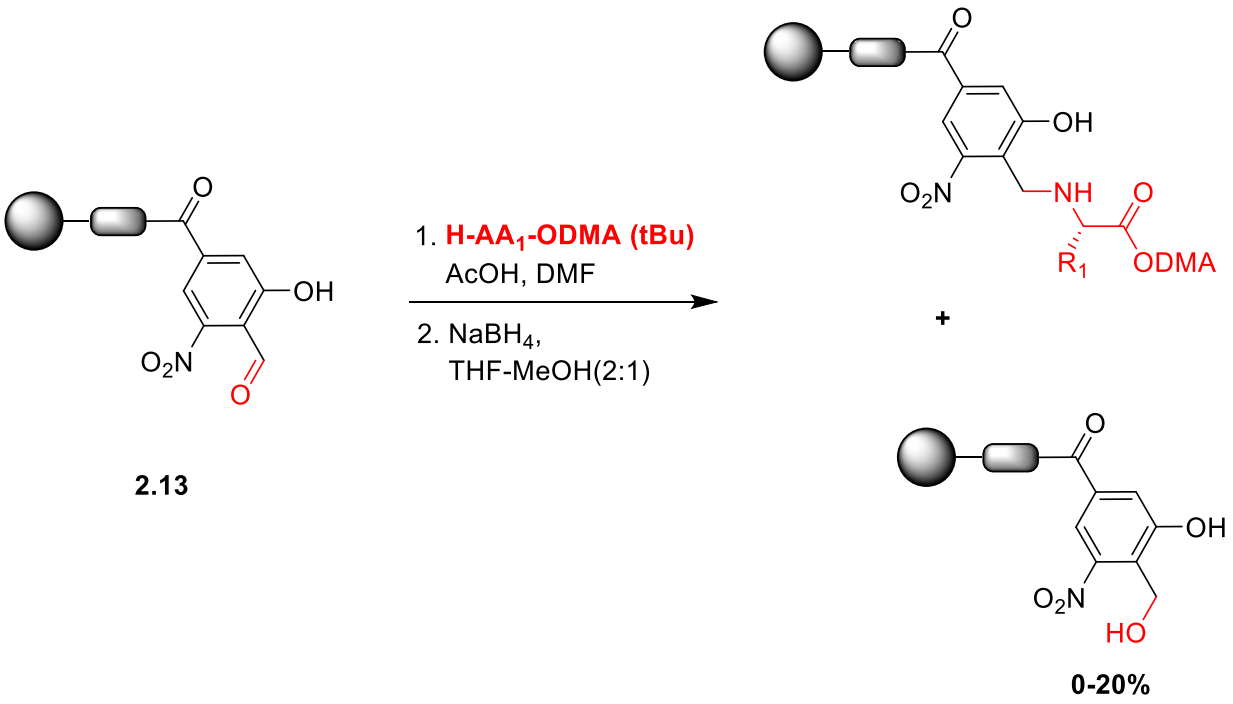

Scheme 2-6: Conditions for on-resin reductive amination

2.6 **Acylation of the Benzyl Amine**

Acylation of the secondary amine formed after the reductive amination step creates the tertiary amide- linkage between the peptide and Hcnb (Scheme 2-7). This coupling is best accomplished using a pre-formed symmetric anhydride form of the desired second amino acid. Obtaining complete acylation of sterically- hindered amines can cause challenges when employing amino acids with bulky side chains. To avoid problems with hindrance and slow reaction times, a method was employed that was developed by Sheppard and coworkers to utilize an *ortho*-phenol group to conduct an intramolecular acyl transfer to the secondary amine.[27] Nucleophilic attack by the phenol onto this symmetric anhydride, followed by a subsequent intramolecular acyl transfer yields the desired dipeptide (**2.15a-i**). Complete acylation of the secondary amine was obtained in all dipeptide sequences tested following 2 x 2 h couplings (Table 2-5).

Table 2-5: On-resin acylation of benzylamines to form dipeptides

Dipeptide Sequence	Uncoupled Benzylamine
Fmoc-Ala-[Hcnb]-Val-ODMA **(2.15a)**	0 %
Fmoc-Val-[Hcnb]-Phe-ODMA **(2.15b)**	0 %
Fmoc-Phe-[Hcnb]-Lys(Boc)-ODMA **(2.15c)**	0 %
Fmoc-Ala-[Hcnb]-Glu(tBu)-ODMA **(2.15d)**	0 %
Fmoc-Ala-[Hcnb]-Leu-ODMA **(2.15e)**	0 %
Fmoc-Val-[Hcnb]-Leu-OtBu **(2.15f)**	0 %
Fmoc-Ala-[Hcnb]-Phe-OtBu **(2.15g)**	0 %
Fmoc-Phe-[Hcnb]-Val-OtBu **(2.15h)**	0 %
Fmoc-Ala-[Hcnb]-Ala-OtBu **(2.15i)**	0 %

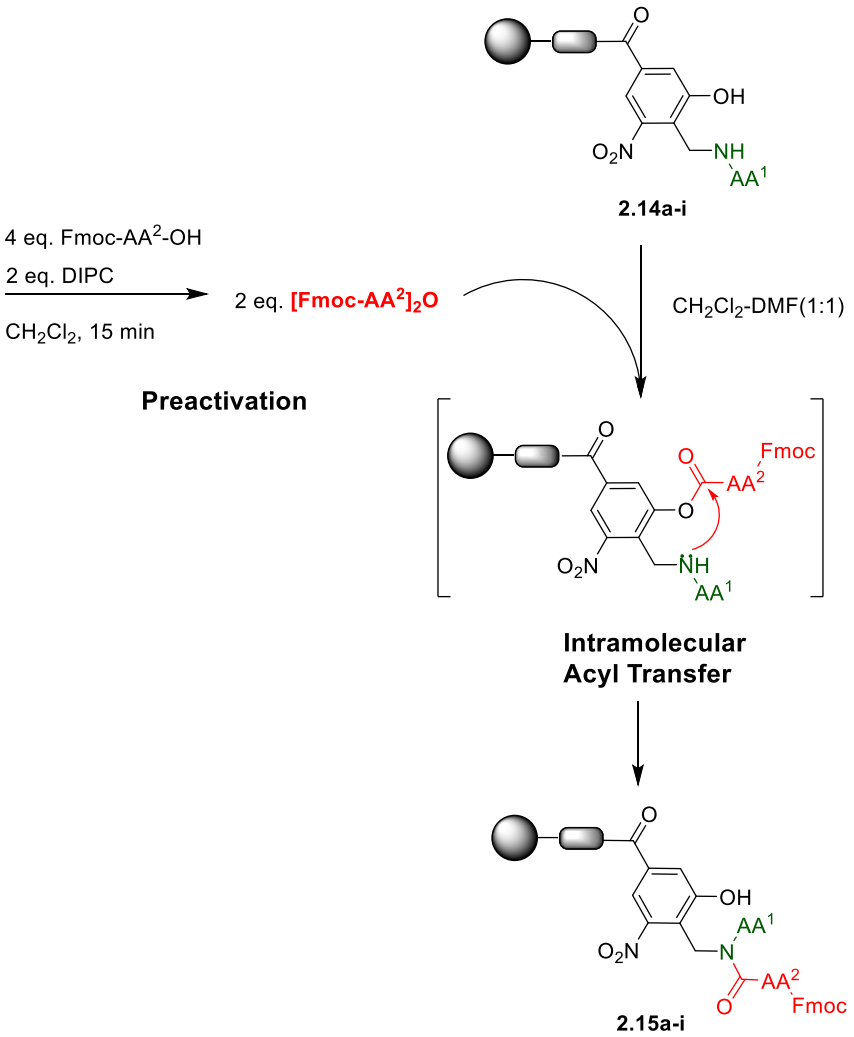

Scheme 2-7: On-resin acylation of benzylamines to form dipeptides

2.7 Diketopiperazine Formation at the Dipeptide Stage

One of the major challenges with the original BAL Linker is caused by the formation of a diketopiperazine (DKP) byproduct upon deprotection at the dipeptide stage.[16] The most effective method for overcoming this problem on the original BAL linker is to employ a sterically hindered C-terminal protecting group such as *t*-butyl- or 1,1-dimethylallyl- thereby reducing the likelihood of nucleophilic attack by the free N-terminus-, and thus reducing the formation of this undesired byproduct. However, it was found that near-quantitative DKP formation was obtained on Hcnb, regardless of the C-terminal protecting groups employed. The formation of DKP is facilitated by the tertiary amide that links the dipeptide to both BAL and Hcnb, which exists partially in the cis-conformation needed for cyclization to the DKP.[17] The enhanced DKP formation on Hcnb when compared to the BAL linker is likely explained by a possible Brønsted acid activation of the C-terminus by the nearby phenol proton, thereby catalyzing the formation of DKP (Scheme 2-8).

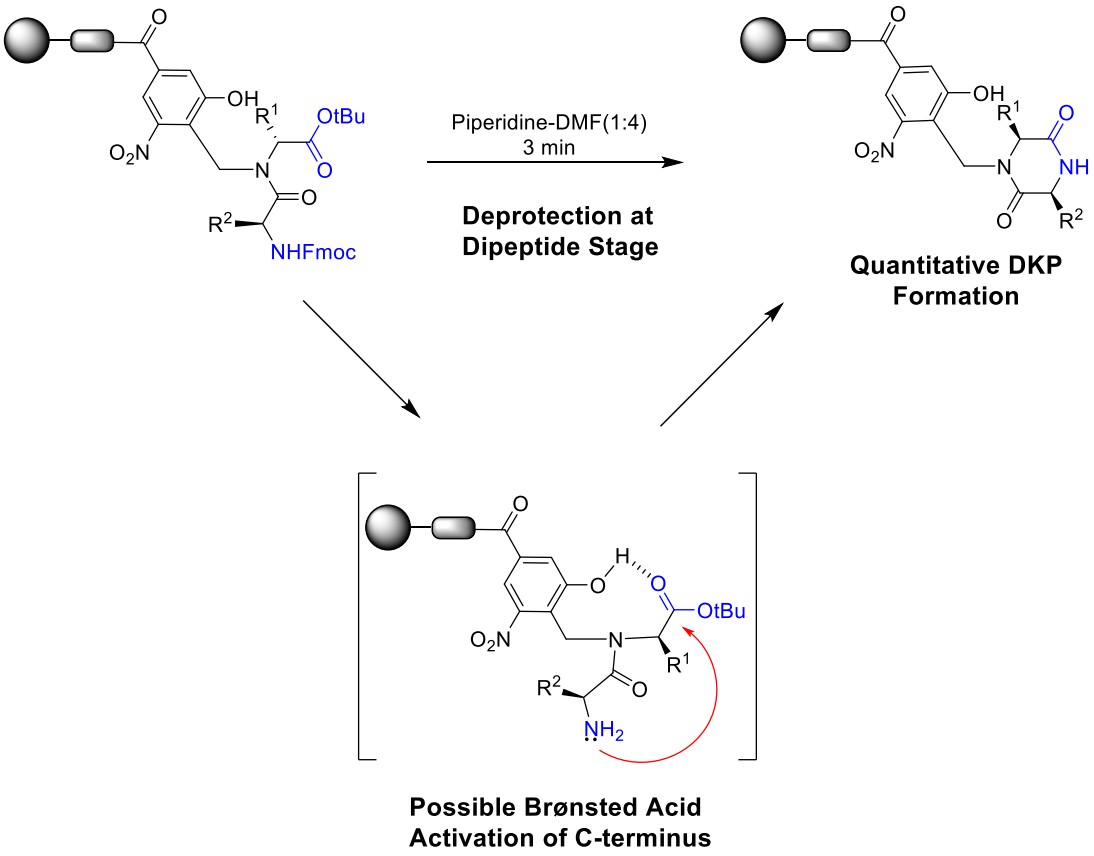

Scheme 2-8: Rapid, quantitative DKP formation upon deprotection of the dipeptide

We hypothesized that this effect could be minimized by removing the phenol proton from the system, thus avoiding activation of the C-terminus. The presence of the phenol group is required for efficient loading of the second amino acid residue as well as for photocleavage of the final product, and so a method is required to only temporarily block this group. Following the formation of the dipeptide, the phenol theoretically remains acylated with the excess of the amino acid anhydride. Exposure to the strongly nucleophilic piperidine for deprotection of the N-terminal Fmoc- group incidentally removed this acyl group as well. We theorized that replacing piperidine with DBU, a non-nucleophilic alternative for Fmoc-deprotection[28], would leave the acylated phenol intact and minimize formation of DKP. However, it was found that rapid, quantitative DKP formation was still obtained even when using DBU (Scheme 2-9). This is likely due to removal by the 1-octanethiol present in the deprotection cocktail. However, a nucleophile is needed to scavenge the dibenzofulvene byproduct generated during Fmoc- deprotection.

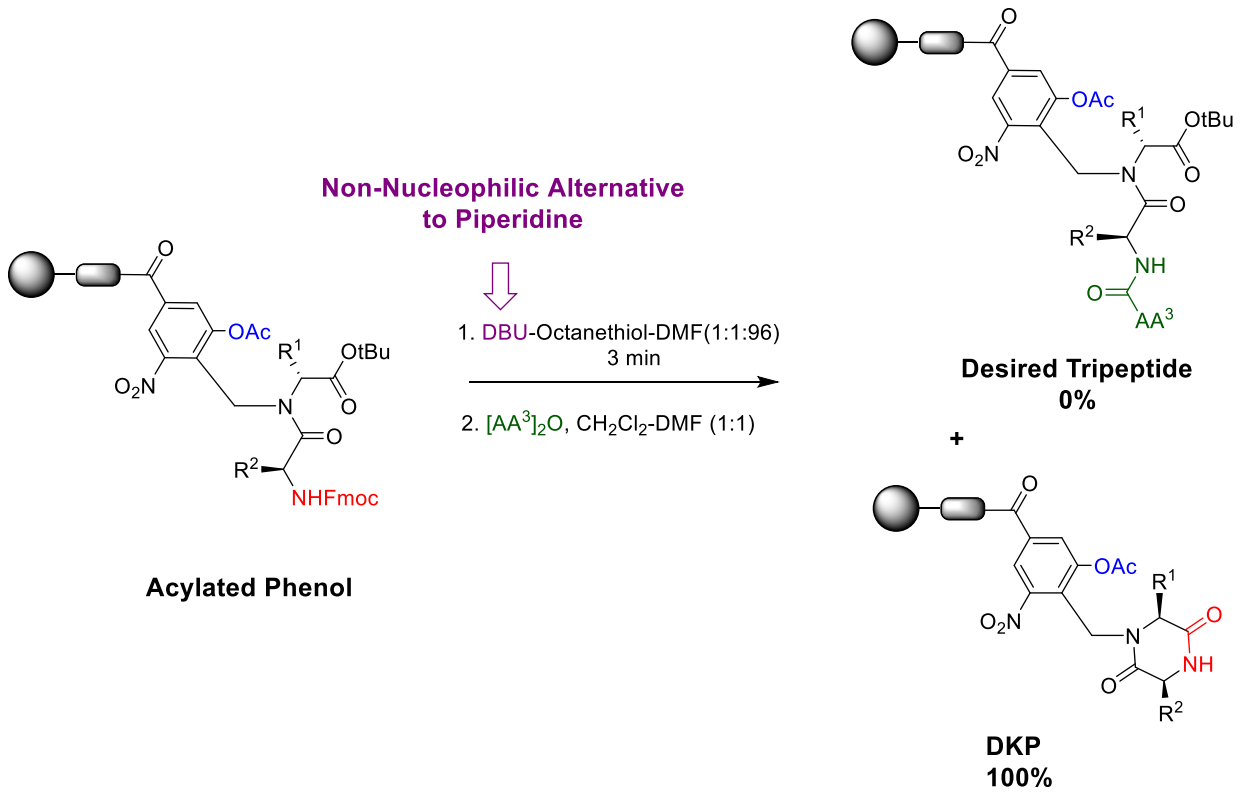

Scheme 2-9: Blocking C-terminal Brønsted acid activation through incidental acylation of the phenol group

We considered other more stable groups for blocking the phenol from interaction with the C terminus, including the use of silyl ethers. However, due to the electronics of the ring, attempts to silylate the phenol resulted in an exceedingly unstable transient product. Even attempts to observe the presence of a silyl group by LC-MS analysis were unsuccessful. Additionally, deprotection of the dipeptide with piperidine continued to result in rapid DKP byproduct formation, even immediately after phenol silylation. Finally, we conducted a solution-phase study and discovered that piperidine can remove a silyl group from the linker phenol, due to the extremely electron-deficient nature of the aromatic ring of the linker. The deprotection conditions were changed to the non-nucleophilic DBU and indeed, a detectable amount of tripeptide product was obtained. Various silylation conditions were screened for maximum efficacy (Table 2-6) using the tripeptide Fmoc-Gly-Ala-Ala-OtBu.

Table 2-6: Screening for silylation of the ortho-phenol group to minimize DKP formation for the tripeptide H-Gly-Ala-[Hcnb]-Ala-O*t*-Bu

Conditions	**DKP/Tripeptide**
TBS-Cl + Imidazole	50/50
TBS-Cl + 2,6-Lutidine	19/81
TIPS-Cl + Imidazole	25/75
TIPS-Cl + 2,6-Lutidine	28/78
TIPS-OTf + Imidazole	24/76
TES-Cl + Imidazole	19/81
TIPS-OTf + 2,6-Lutidine	12/88

To monitor the completion of silylation conditions, the phenol-protected dipeptide was Fmoc-deprotected for 3 min using a cocktail of 2% v/v DBU and 2% v/v 1-octanethiol in DMF, followed by immediate introduction of the third amino acid as a pre-formed symmetric anhydride (Scheme 2-10). The most successful conditions found were TIPS-OTf and 2,6-Lutidine for introduction of a TIPS-protected phenol on the linker. We theorize that the steric bulkiness of the TIPS group changes the conformation of the dipeptide sufficiently so that the resin-linked amide is forced out of the required cis-conformation. Even with delayed coupling of the 3rd amino acid residue, the N-terminally deprotected dipeptide was found to be transiently stable, only converting to DKP slowly over a period of several hours.

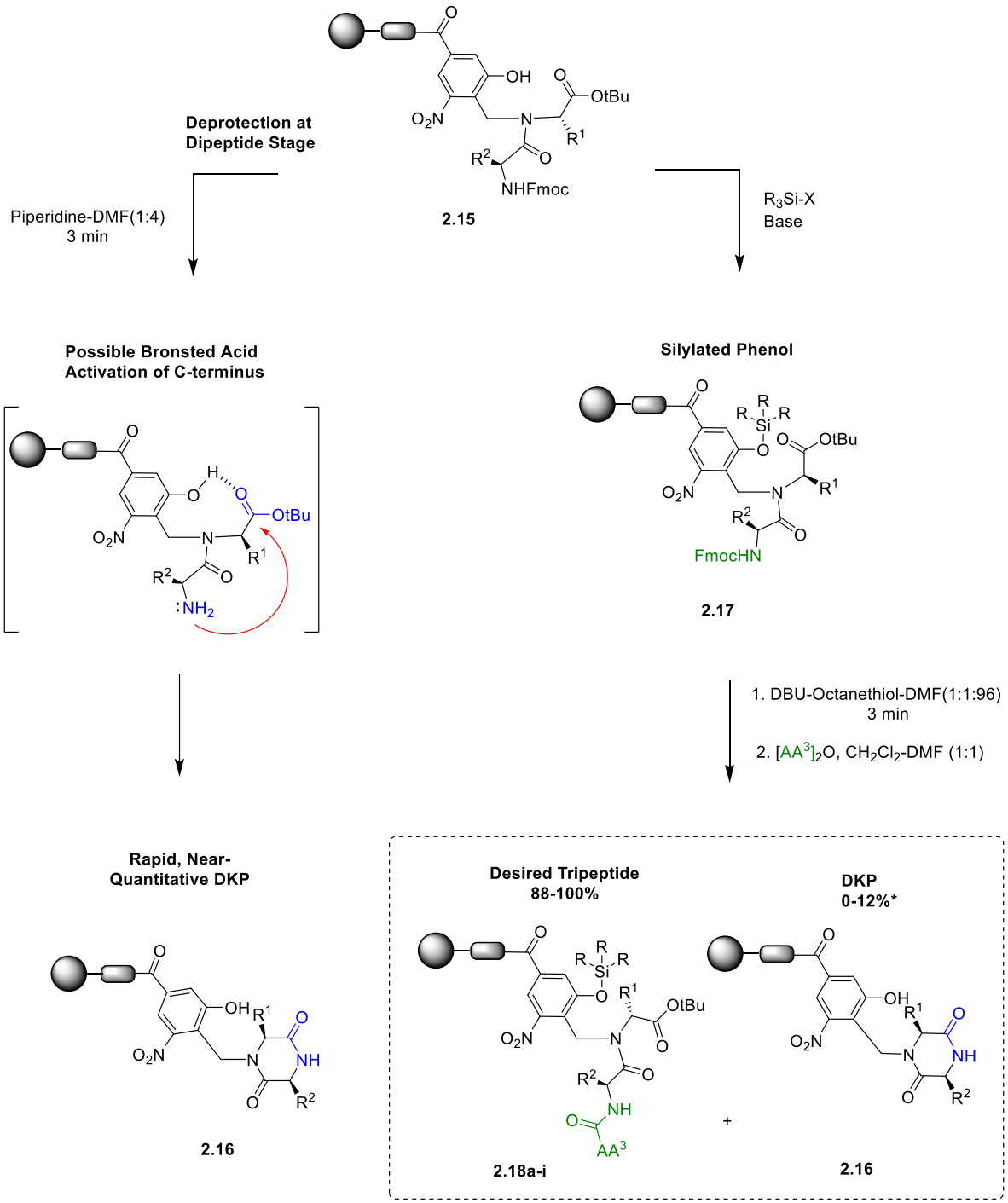

Scheme 2-10: Prevention of DKP byproduct formation

The substrate scope was examined using a variety of amino acid sequences (Table 2-7). It was found that in most cases, 0-4% DKP formation was observed en route to tripeptide formation. The most problematic sequence is the dipeptide Ala-Ala, which generates approximately 12%

DKP. Likely, the methyl sidechains allow the dipeptide to adopt the conformation needed for DKP formation, regardless of the presence of TIPS. However, all other sequences tested resulted in minimal formation of DKP, so that continued synthesis of the desired peptide is feasible.

Table 2-7: DKP/Tripeptide ratio for various amino acids

Tripeptide	DKP/Tripeptide
H-Gly-Ala-[Hcnb]-Val-ODMA **(2.18a)**	0/100
H-Phe-Val-[Hcnb]-Phe-ODMA **(2.18b)**	6/96
H-Val-Phe-[Hcnb]-Lys(Boc)-ODMA **(2.18c)**	0/100
H-Phe-Ala-[Hcnb]-Glu(tBu)-ODMA **(2.18d)**	2/98
H-Gly-Ala-[Hcnb]-Leu-ODMA **(2.18e)**	0/100
H-Gly-Val-[Hcnb]-Leu-OtBu **(2.18f)**	0/100
H-Phe-Ala-[Hcnb]-Phe-OtBu **(2.18g)**	0/100
H-Phe-Phe-[Hcnb]-Val-OtBu **(2.18h)**	0/100
H-Leu-Ala-[Hcnb]-Ala-OtBu **(2.18i)**	12/88

2.8 Conclusion

Following selection of a photolabile linker candidate, the features of the ring were optimized to enable peptide synthesis on the solid-phase. Solution-phase studies were conducted to synthesize dipeptides on Hcna. Additionally, efficient solution-phase photolysis of these dipeptides was confirmed. The acid-stability of the Hcnb-peptide linkage was tested for 24 hours in 95% TFA, with no detectable loss of the connected peptide. The procedure for use of the linker on the solid-phase was optimized, incorporating an aminohexanoic acid spacer unit and proline residue, before loading of the Hcna handle. The first amino acid residue can be loaded via a 2-step reductive amination, which was optimized to maximize the proportion of desired product obtained. The second amino- acid residue is introduced to the peptide via an intramolecular acyl transfer, allowing for efficient and complete acylation of the secondary amine even when utilizing amino acids with sterically bulky side chains. Finally, silylation of the linker phenol with TIPS-OTf was found to minimize the formation of the undesired by-product DKP, allowing for the installment of the 3rd amino acid residue. Following the synthesis of the first 3 residues of the peptide, the remaining amino acids can be coupled through standard peptide coupling conditions.

CHAPTER 3. THE INVENTION OF A HEAT-CONTROLLED LED UV-PHOTOREACTOR FOR USE IN SOLID-PHASE PHOTOCHEMICAL REACTIONS

3.1 Mechanism of Peptide Photolysis from Hcnb

The photolabile Backbone-Amide Linker discussed in Chapters 1 and 2 require photolysis to release the peptide upon completion of the final synthetic step. We believe that the *ortho*-nitro group allows the linker to undergo a Norrish Type-II mechanism to release the completed peptide (Scheme 3-1).[29]

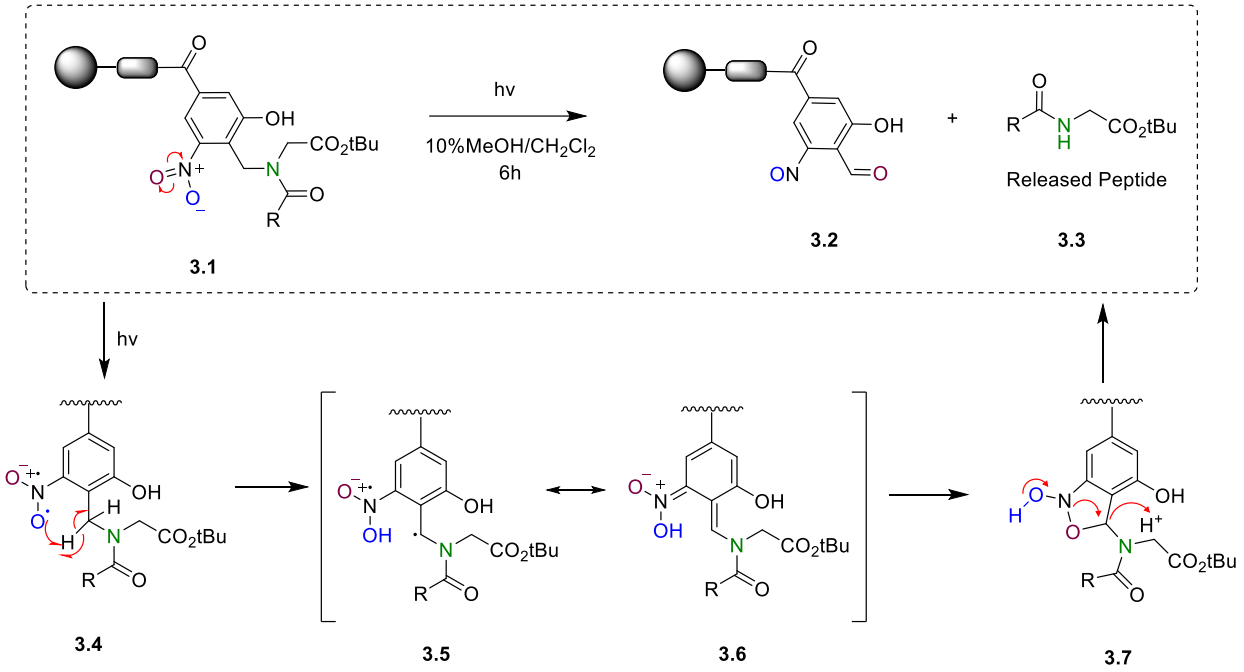

Scheme 3-1: Norrish type-II photolytic cleavage mechanism

Upon exposure to ultraviolet radiation at the correct wavelength, the O-N pi-bond undergoes photochemical excitation, forming a diradicaloid excited state **3.4**. The oxygen radical then performs a hydrogen atom abstraction from the benzylic carbon position leaving the free radical **3.5** stabilized in the benzylic position. This species can be shown in a non-radical alternate resonance form **3.6**. Attack of the free hydroxyl group at the benzylic sp^2 carbon forms cyclic intermediate **3.7**, driven by the re-aromatization of the linker aryl ring. Finally, the O-N pi-bond is reformed, expelling the peptide and reforming an aldehyde group on the linker. The backbone

amide at the linkage point is also protonated. The proton is likely provided by the hydroxyl group in the *ortho*-position on the linker, which is in the position to form a 6-membered ring transition state for the proton transfer. The photolysis is also performed in a protic solvent such as methanol. Upon completion of the reaction, the linker byproduct is generated as the original Hcna structure, but with an *ortho*-nitroso group. Future studies may be directed toward potential re-cycling of this photolysis byproduct.

3.2 Photochemical Cleavage Using Rayonet UV Photochemical Reactor

Initial attempts to complete photolysis of peptides from the Hcnb linker were carried out using a Rayonet Reactor equipped with 300 or 350 nm ultraviolet lamps. Although solution-phase studies suggested that the photocleavage should reach completion in methanol within 12 hours, attempts to recreate the reaction with on-resin peptides failed. We hypothesized that the problem stems from the insoluble nature of resin beads. Depending on the solvent of choice, all of the resin coagulates at either the top or bottom of the solvent resulting in poor dispersion of irradiation throughout the sample. We proposed inserting a vortex mixer into the reaction chamber to agitate the sample and create an improved distribution of light throughout the resin slurry. In collaboration with the Gregory Eakins in the Jonathan Amy Instrumentation Facility at Purdue University, a 3D-printed a sample holder was designed to suspend the sample in a quartz tube, fitted to the correct height to depress the vortex mixer in touch mode (Figure 3-1). The vortex mixer, fitted with the sample tube, can then be inserted directly into the reaction chamber.

Upon testing, it discovered that the reaction reached 50% completion in 24 hours with a 1:1 MeOH-CH_2Cl_2 solvent mixture. Various dual-linker systems were tested (Sieber[26] and Wang[30]) to determine if absorption of energy by the second linker was affecting the progress of the photolysis reaction. Additionally, an XV-RAM TG "Super-Swell" Resin[31] was tested and found to work significantly better when compared with the standard PS resins used previously. With use of this "super-swell" resin, switching from a 50% to 75% CH_2Cl_2 significantly increased the completion of the reaction. Based on this information, we determined that resin-swelling is essential for efficient photolysis to occur. Further optimization of both single and dual solvent systems (Table 3-1) suggested that a 1:9 MeOH:CH_2Cl_2 dual solvent mixture was ideal for the reaction. The cleavage times under these conditions were reduced to 6 h at 350 nm irradiation.

Figure 3-1: First prototype for a 3D printed photochemical reactor

Unfortunately, upon several uses of the 3D-printed plastic holder, we discovered that the high temperatures generated by the ultraviolent lamps (over 80 ◦C) resulted in melting and deformation of the plastic. Additionally, conducting the photolysis reactions in the volatile CH_2Cl_2-MeOH dual solvent system under the intense heat generated proved problematic, as any leak in the quartz reaction tubes resulted in rapid disappearance of the solvent. We proposed switching to a light-emitting diode (LED) ultraviolet light system instead, to reduce the

temperature variability that is typically experienced in the Rayonet reactor. Additionally, design of an LED UV reactor would allow for an increased intensity of light irradiation on the sample.

Table 3-1: Optimization of the solvent system for photochemical cleavage of the desired peptide from Hcnb on-resin

Resin	Solvent	Time	hv/H+
PS Sieber Resin	Acetone	6h	0/0*
PS Sieber Resin	Acetonitrile	24h	0/100
PS Sieber Resin	MeOH	24h	0/100
Solution	MeOH	24h	100/0
PS Wang Resin	MeOH	24h	10/90
PS Sieber Resin	MeOH-CH_2Cl_2 (3:7)	12h	64/36
PS Sieber Resin	MeOH-CH_2Cl_2 (1:1)	24h	50/50
TG XV-RAM	MeOH-CH_2Cl_2 (1:1)	12h	100/0
TG XV-RAM	MeOH-CH_2Cl_2 (1:4)	6h	100/0
Sieber	MeOH-CH_2Cl_2 (1:10)	6h	100/0

3.3 Initial Design of a 3D-printed LED UV Photochemical Reactor

The LED lights chosen were 365 nm LED strips from Waveform Lighting.[32] 12 LED strips were cut and wired together, then affixed to a 3D-printed chamber (Figure 3-2, bottom). The chamber was then placed over the vortex mixer containing the quartz sample vial, as was shown previously. We found that by using LEDs as the UV light source, the reaction times were reduced from 6 h to 2 h on average.

Although the amount of heat generated was significantly reduced compared with the Rayonet Reactor, the LED lights were also found to raise the temperature in the chamber significantly. Additionally, the plastic affixed directly to the UV-light strips began to melt and deform. Because plastic has a low melting point, we decided to re-design the reactor a final time with a 3D-printed metal reaction chamber. Additionally, we created a design to remove the heat generated by the lights and expel excess heat to the outside of the chamber, resulting in the ability to perform photochemical reactions at room temperature and with volatile solvents.

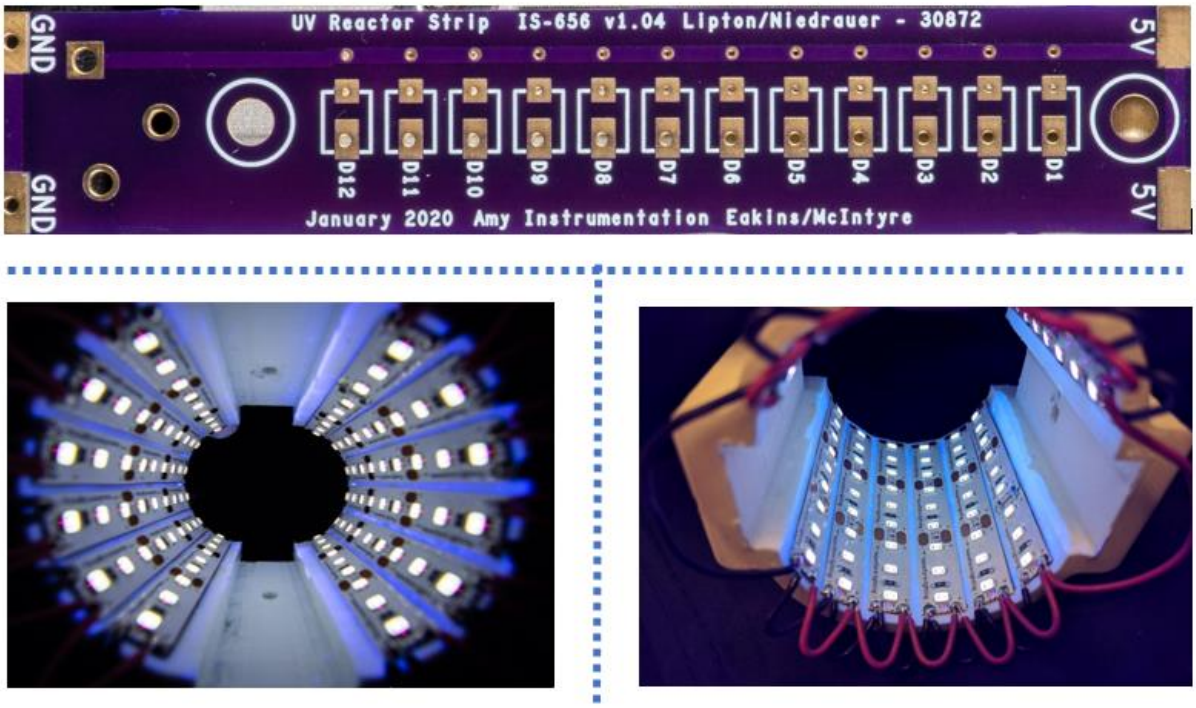

Figure 3-2: First attempt at a fully 3D-printed LED photochemical reactor

3.4 **Design of Final Prototype**

A final photoreactor was designed to improve upon prior methods. The prototype was 3D printed and assembled by Gregory Eakins at Purdue University (Patent Pending).[33] The exploded view of the photoreactor is shown below (Figure 3-3). The reactor **1** includes a vial holder which can hold a sealed vial **16** containing the reaction mixture. The vial is made of material that is optically transparent to the wavelength for the chemical reaction. The reactor includes Printed Circuit Boards (PCBs) **11** designed to mount LEDs selected to coincide with the required wavelength of the reaction. PCBs are designed to transport heat away from the inner chamber by conduction to prevent sample heating. The reactor also includes a chamber frame **12**. The PCBs are mounted to the chamber frame, which is constructed of a thermally conductive material such as copper, aluminum or steel to provide a thermal reservoir that sinks heat away from the PCBs and radiates it to the surrounding environment. A sample-holding frame **15** is mounted to a vortex-mixer **14**. A quartz sample vial **16** is inserted into the top of the frame **15** and held in place at the top with a cap **13**.

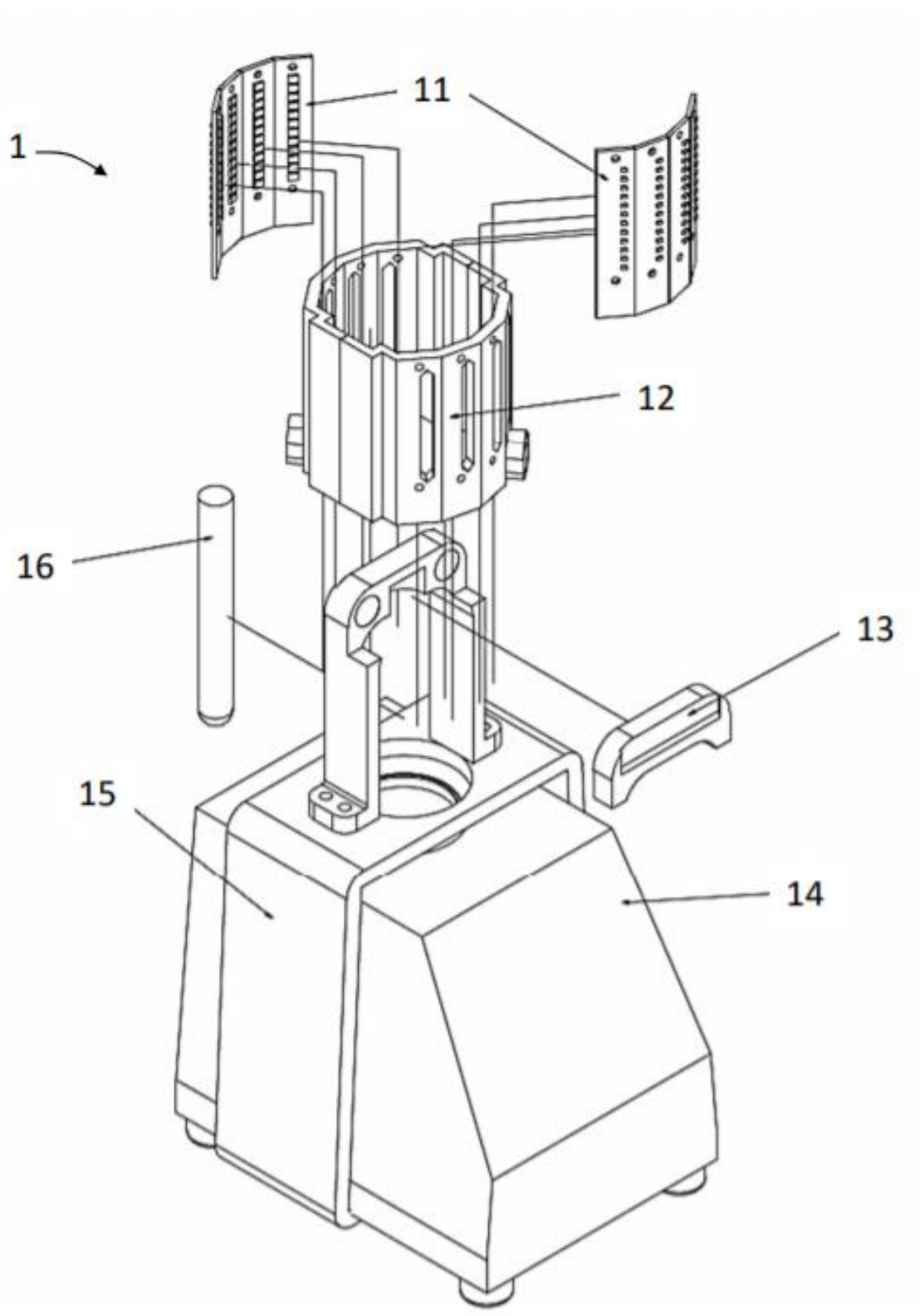

Figure 3-3: Exploded view of the instrument (Diagram created by Gregory Eakins)

With the heat-sink system incorporated, as well as the increased intensity of UV light emitted, the reaction time was reduced to 1 hour on average for the photolytic cleavage of a peptide from Hcnb. Additionally, the reaction could be performed in 90% CH_2Cl_2 with minimal evaporation of solvent during the necessary time. Photographs of the Metal 3D- printed reaction chamber are shown in Figure 3-4. The complete photoreactor setup is provided in Figure 3-5.

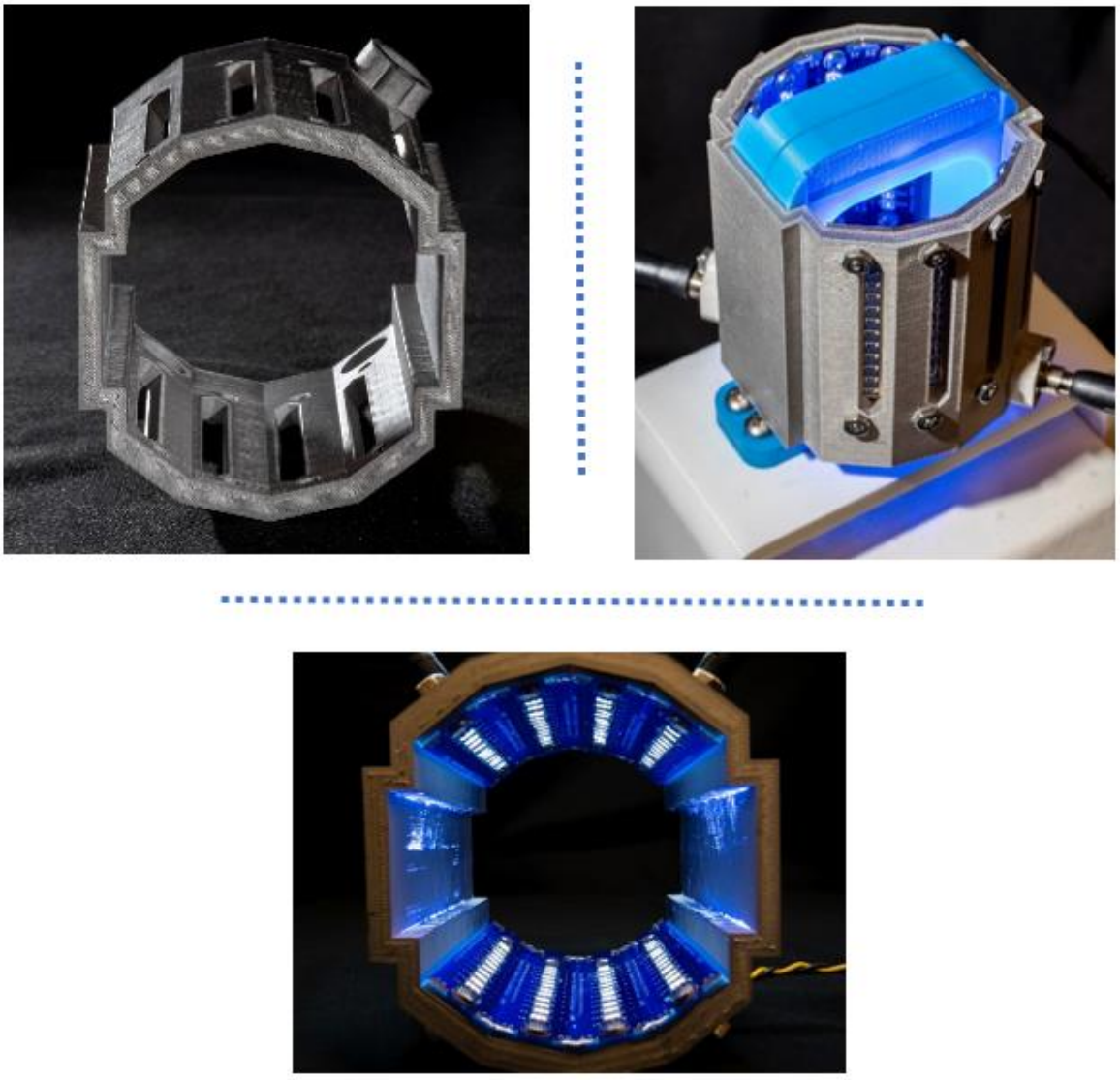

Figure 3-4: Metal 3D printed chamber for UV-LED Photoreactor

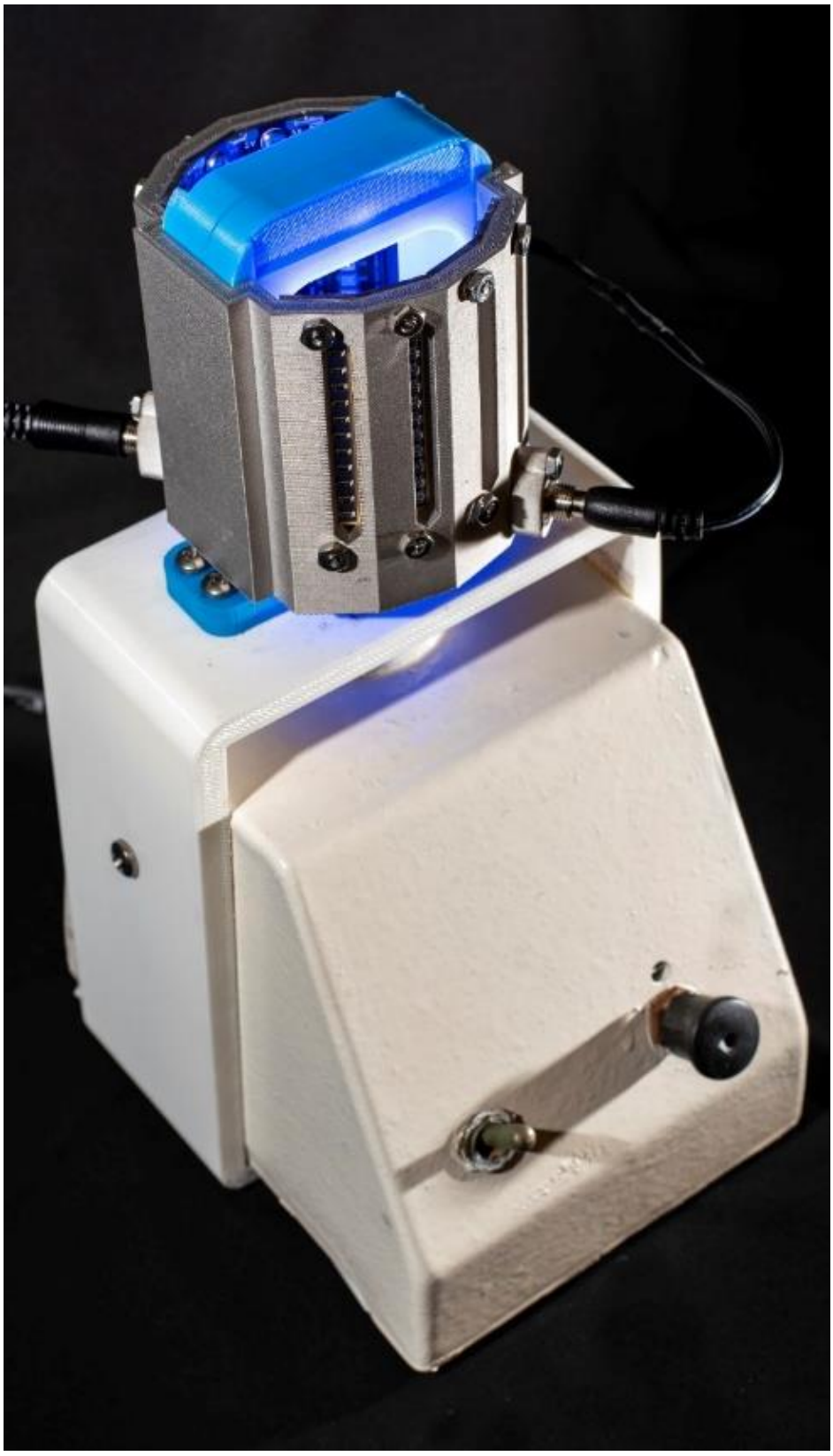

Figure 3-5: UV-LED Photoreactor

3.5 Comparison of the LED Reactor to Rayonet Photochemical Reactor

The conditions used were as follows: polyethylene glycol or polystyrene resin with 3-10 assorted amino acid residues attached, suspended in 5 mL of solvent consisting of 90% CH_2Cl_2 and 10% MeOH in a fused-quartz tube. The photochemical reactor used for comparison purposes was a Rayonet fitted with 350 nm lamps. Only trace quantities of product were detected following 24 hours of irradiation (Table 3-2). Additionally, measured reaction chamber temperatures reached up to 80°C, causing rapid evaporation of the solvent when a completely airtight system was not utilized. In contrast, 100% cleavage and 90% overall synthetic yield were achieved with up to 230 mg of resin (largest quantity tested) in under 1 hour with the LED-UV reactor design disclosed herein, fitted with 365 nm LEDs.

Table 3-2: Comparison of Hcnb photolysis times in different photochemical reactors

	Rayonet Reactor	**LED Reactor**	**LED Reactor**
Wavelength	350 nm	365 nm	365 nm
Irradiation Time	24 hours	1 h	1 h
Resin Quantity	70 mg	42 mg	230 mg
% Peptide Cleavage	Trace	100%	100%
Peptide	H-Phe-Ala-Ala-O*t*-Bu	H-Phe-Leu-Ala-O*t*-Bu	Cyclo[Arg-(D)-Phe-Pro-Glu-Asp-Asn-Tyr-Glu-Ala-Ala]

3.6 Conclusion

After recognizing that the currently available technology for conducting photochemical reactions on the solid-phase is limited, a new photoreactor was designed using a commercial laboratory vortex as a built-in agitator to create a resin slurry for better light penetration throughout the sample. UV-LEDs were employed to increase the light intensity output, leading to more efficient photochemical cleavages. A heat-sink was built in to reduce the heat generated by the high-energy output of the LED lights. The chamber of the final prototype remains close enough to ambient temperate to allow reactions to be conducted in CH_2Cl_2 with only minimal evaporation. Additionally, the time required for photochemical transformations on example peptides was reduced from only trace product after 24 hours to 100% peptide cleavage in under 1 hour.

CHAPTER 4. APPLICATIONS OF HCNA: THE ON-RESIN SYNTHESIS OF CYCLIC PEPTIDES AND C-TERMINAL THIOESTERS

4.1 Synthesis of Cyclic Peptides

Cyclic peptides have long been of interest in the field of medicinal chemistry. Many natural products drug candidates are cyclic peptides.[12, 15] These cyclic peptides often make superior drug candidates when compared with their linear peptide counterparts, for a number of functional reasons.[15] Conformational restriction of the cyclic peptide often increases the biological activity exhibited, as the peptide is restricted to the ideal confirmation for binding. In metabolism of peptides *in vivo*, the protease recognizes the peptide via the N- or C-termini.[12,15] Thus, by removing the recognized group, the cyclic peptide can no longer be recognized and exhibits increased metabolic stability. Finally, it has often been reported that cyclic peptides exhibit greater cell permeability when compared with linear peptides of the same sequence.[14] Cyclic peptides have been a target of interest in peptide synthesis for many years. Some methods exist to make them, however in standard peptide synthesis the C terminus is connected directly to the resin, and so the peptide must be cleaved from the solid support and cyclized in solution.

4.2 Use of Hcnb for the On-Resin Synthesis of Cyclic Peptides

To demonstrate the utility of Hcnb for the synthesis of cyclic peptides, three candidates were selected of varying chain sizes (5, 10, 14 residues) to compare the merits of Hcnb to available methods for synthesizing cyclic peptides.

4.2.1 Synthesis of a Cyclic Pentapeptide

The first peptide chosen was a short-chain analogue of the natural product Somatostatin, cyclo[(D)-Trp-Lys-Gly-(β)-Ala-Phe].[34] This pentapeptide was previously synthesized and cyclized on a modified BAL Linker, using Fmoc- based SPPS. The authors report a 34% cleavage yield and 87% purity by HPLC analysis.[34] The synthesis of cyclo[(D)-Trp-Lys-Gly-(β)-Ala-Phe] was carried out according to the procedures mentioned in Chapter 2 (Scheme 4-1). The first residue H-Phe-ODMA was loaded onto the prepared resin **2.4** via reductive amination. The

subsequent linear synthesis was then carried out as previously discussed. The head-to-tail cyclization was accomplished on the resin using PyAOP and 2, 4, 6-collidine. Global deprotection of the side chain protecting groups on-resin in 1% TIPS/49% CH_2Cl_2 /50% TFA for 1 h caused no detectable loss of the peptide-linker bond. Photocleavage from the resin at 365 nm for 1 h yielded the final cyclic decapeptide **4.2** in 50% purity and 96% cleavage yield.

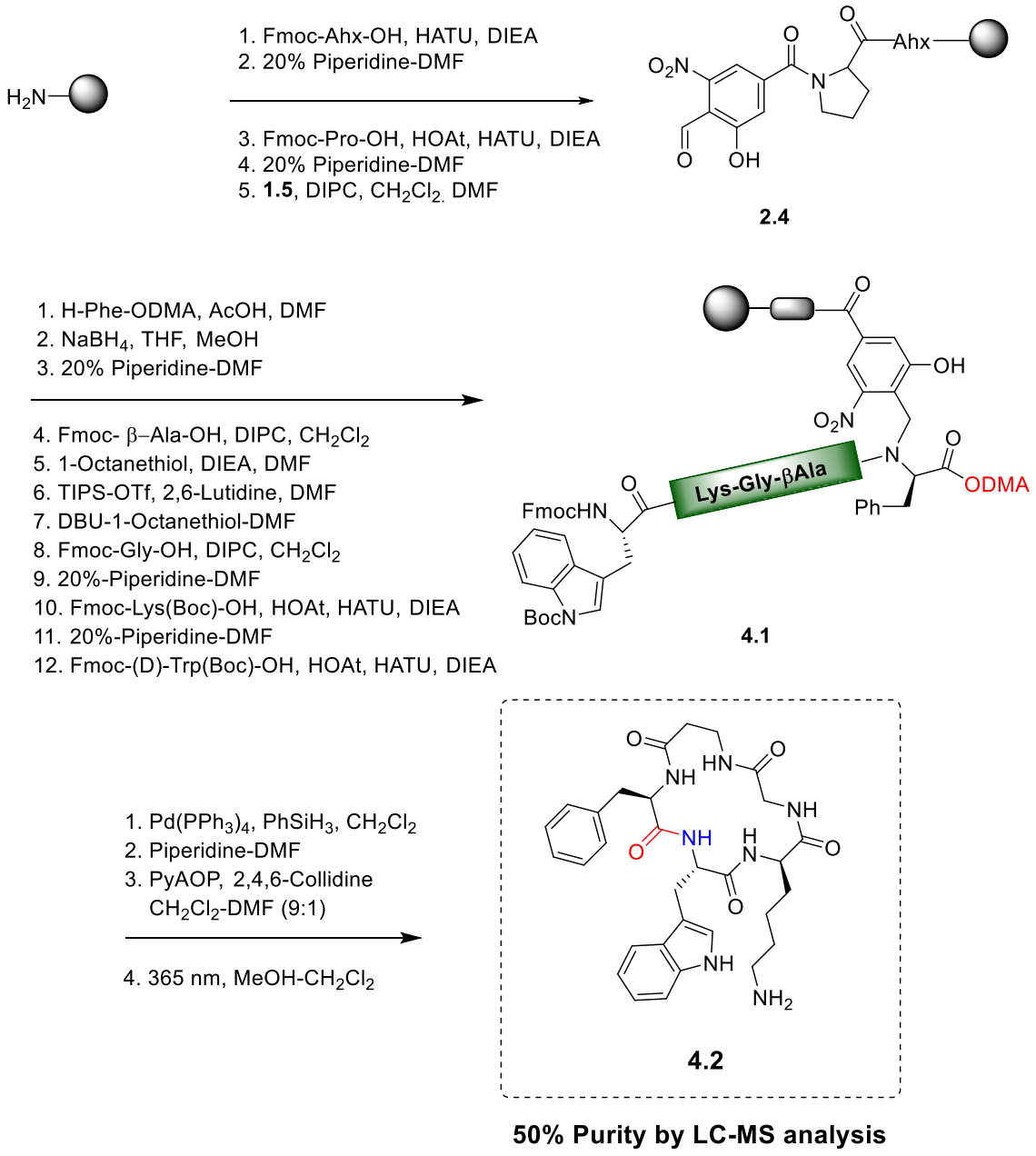

Scheme 4-1: Synthesis of a cyclic pentapeptide using Hcna

4.2.2 **Synthesis of a Cyclic Decapeptide**

The second cyclic peptide structure chosen was a cyclic decapeptide, cyclo[Arg-(D)-Phe-Pro-Glu-Asp-Asn-Tyr-Glu-Ala-Ala]. This peptide was synthesized by Albericio and coworkers to demonstrate the original BAL Linker.[16] The peptide was synthesized in 85% cleavage yield. ~12% was lost to DKP formation and 5% other impurities for a total purity of ~83%.[16] For the sake of consistency, this peptide was synthesized using the same cyclization point as in the originally published synthesis.

The synthesis of cyclo[Arg-(D)-Phe-Pro-Glu-Asp-Asn-Tyr-Glu-Ala-Ala] was carried out according to the procedures mentioned in Chapter 2 (Scheme 4-2). The first residue H-Ala-ODMA was loaded to the prepared resin **2.4** via reductive amination. The subsequent linear synthesis was then carried out as previously discussed. The head-to-tail cyclization was accomplished on the resin using HOAt and PyAOP. Global deprotection of the side chain protecting groups on-resin in 1% TIPS/49% CH_2Cl_2 /50% TFA for 4 hours caused no detectable loss of the peptide-linker bond. Photocleavage from the resin at 365 nm for 1 h yielded the final cyclic decapeptide **4.4** in 95% purity, 90% cleavage yield. Due to the initial sequence of amino acids (Ala-Ala), some of the peptide was likely lost due to DKP formation. However, this sequence is the worst case tested for DKP formation, and thus represents the theoretical limit to loss of peptide due to this side reaction.

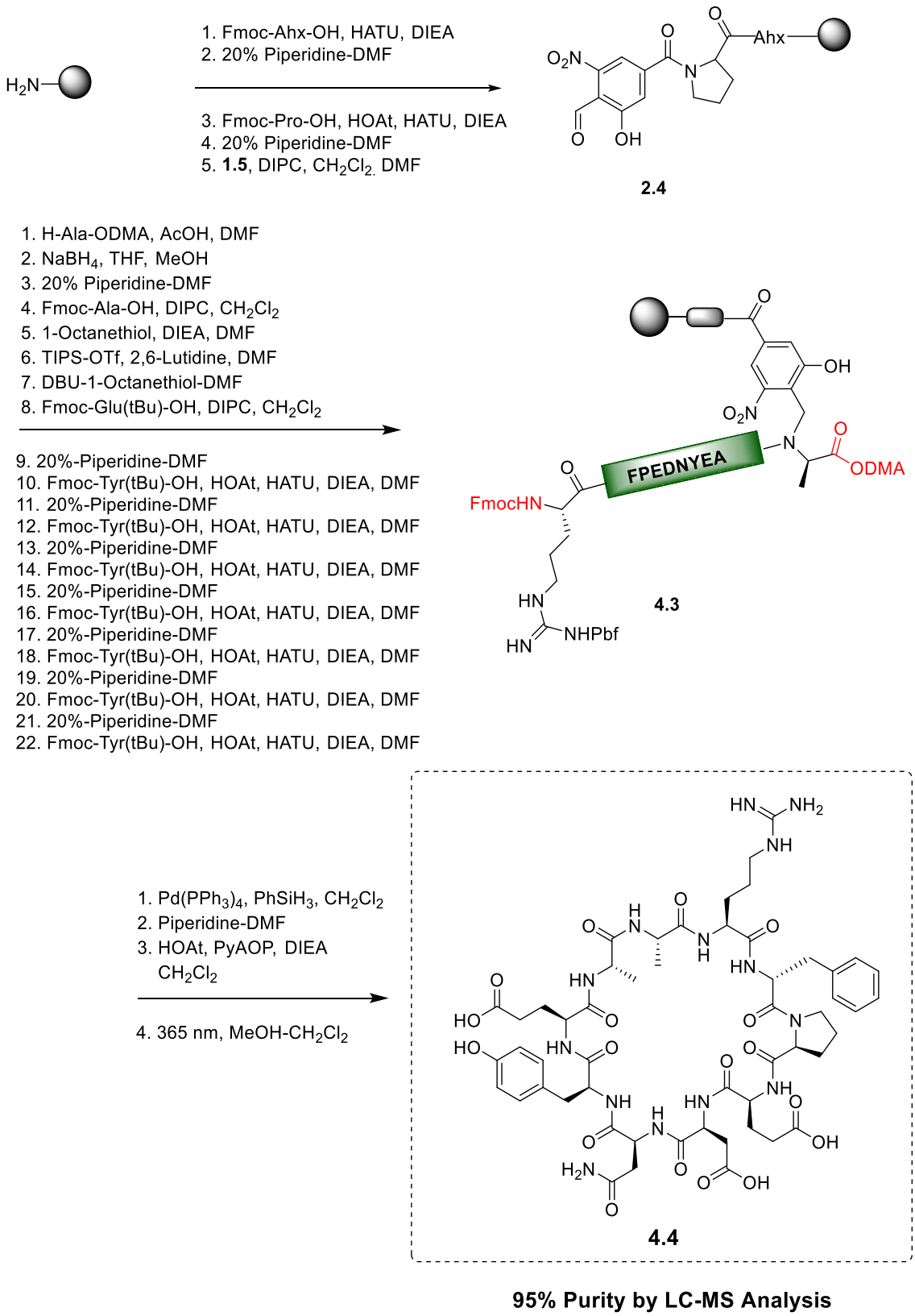

Scheme 4-2: Synthesis of a cyclic decapeptide using Hcna

4.2.3 **Synthesis of a Tetradecapeptide**

The final peptide chosen to demonstrate use of Hcna for cyclic peptide synthesis was the 14-residue natural product, Sunflower Trypsin Inhibitor (SFTI-1), a potent β-Trypsin and cathepsin inhibitor.[36] The sequence, cyclo[Pro-Asp-Gly-Arg-Cys-Thr-Lys-Ser-Ile-Pro-Pro-Ile-Cys-Phe], poses several challenges for synthesis. The high frequency of β-branched amino acids, as well as a common occurrence of proline residues, make choice of a cyclization point difficult. Additionally, prior syntheses have utilized Gly as the C-terminal residue for cyclization.[35] Unfortunately, glycine is incompatible with the reductive amination conditions required to load amino acids to Hcna (See Chapter 2). The prior reported synthesis utilized Fmoc- based SPPS on the Rink amide resin[37] to synthesize the linear peptide, then cyclized in solution.[35] No synthetic yields or purities were reported.

After several attempts to locate a viable cyclization point, it was found that Phe was the optimal choice for the resin-anchored residue (Scheme 4-3). H-Phe-ODMA was loaded to the prepared resin **2.4** via reductive amination. The subsequent linear synthesis was then carried out as previously discussed. The head-to-tail cyclization was accomplished on the resin using HOAt and PyAOP. Global deprotection of the side chain protecting groups on-resin in 1% TIPS/49% CH_2Cl_2/50% TFA for 4 hours caused no detectable loss of the peptide-linker bond. Photocleavage from the resin at 365 nm for 1 h yielded the final cyclic peptide **4.6** in 90% purity, 80% cleavage yield.

Table 4-1: Summary of cyclic peptides synthesized on Hcna

Cyclic Peptide	**Sequence Length**	**Cleavage Yield**	**Purity**
cyclo[(D)-Trp-Lys-Gly-(β)-Ala-Phe] **(4.2)**	5	96%	505
cyclo[Arg-(D)-Phe-Pro-Glu-Asp-Asn-Tyr-Glu-Ala-Ala] **(4.4)**	10	90%	95%
cyclo[Pro-Asp-Gly-Arg-Cys-Thr-Lys-Ser-Ile-Pro-Pro-Ile-Cys-Phe] **(4.6)**	14	80%	90%

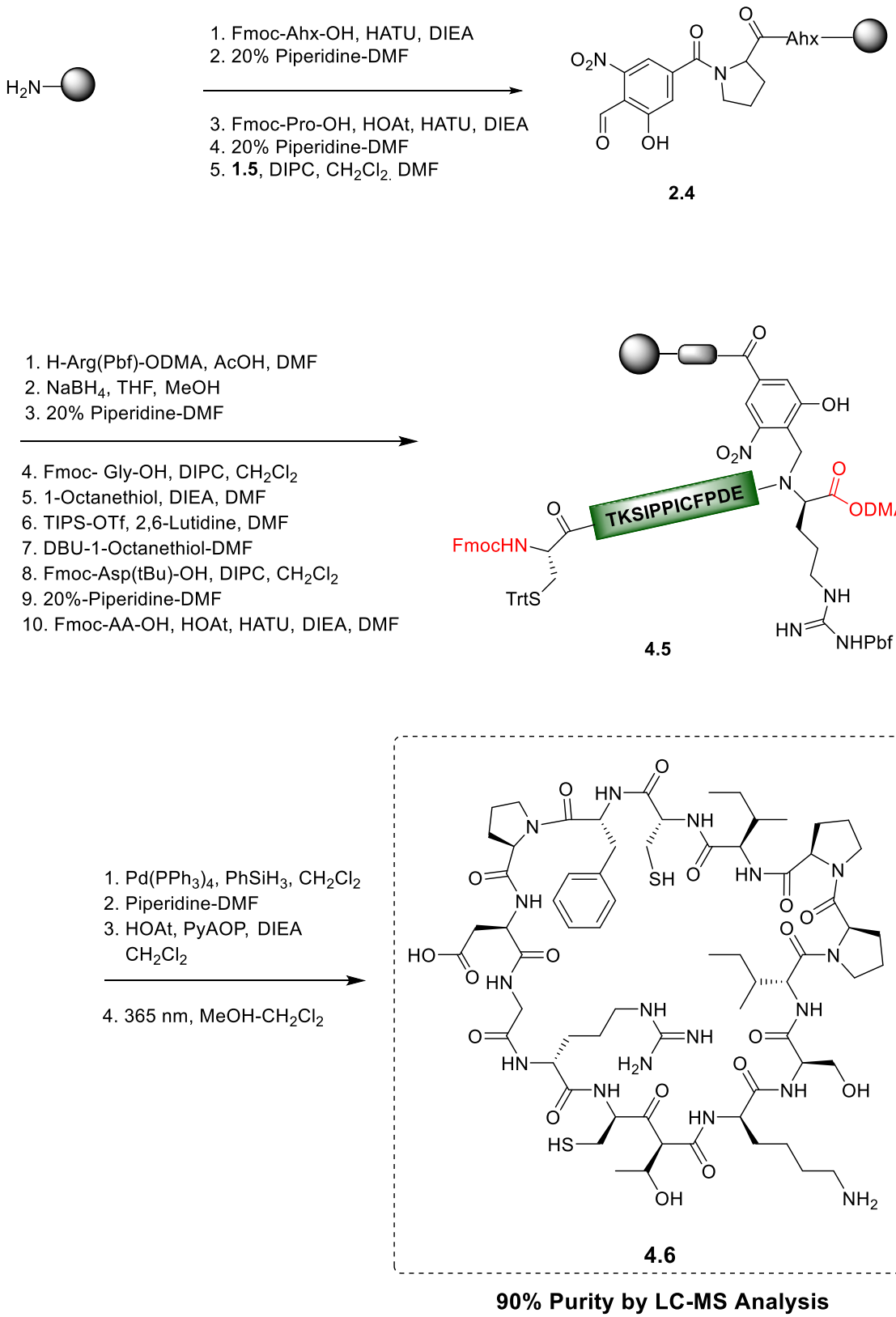

Scheme 4-3: Synthesis of a cyclic 14-residue peptide using Hcnb

4.3 Synthesis of C-Terminal Thioesters for use in Native Chemical Ligation (NCL)

The synthesis of large peptides and proteins (>50-70 residues) poses a problem by standard solid-phase synthesis methods. After a point, the growing chain begins to form secondary structures, limiting the access to the N-terminus for further coupling reactions. Additionally, larger peptides often begin to aggregate out of solution. Kent and coworkers developed a solution to this problem in the form of Native Chemical Ligation (NCL).[11]

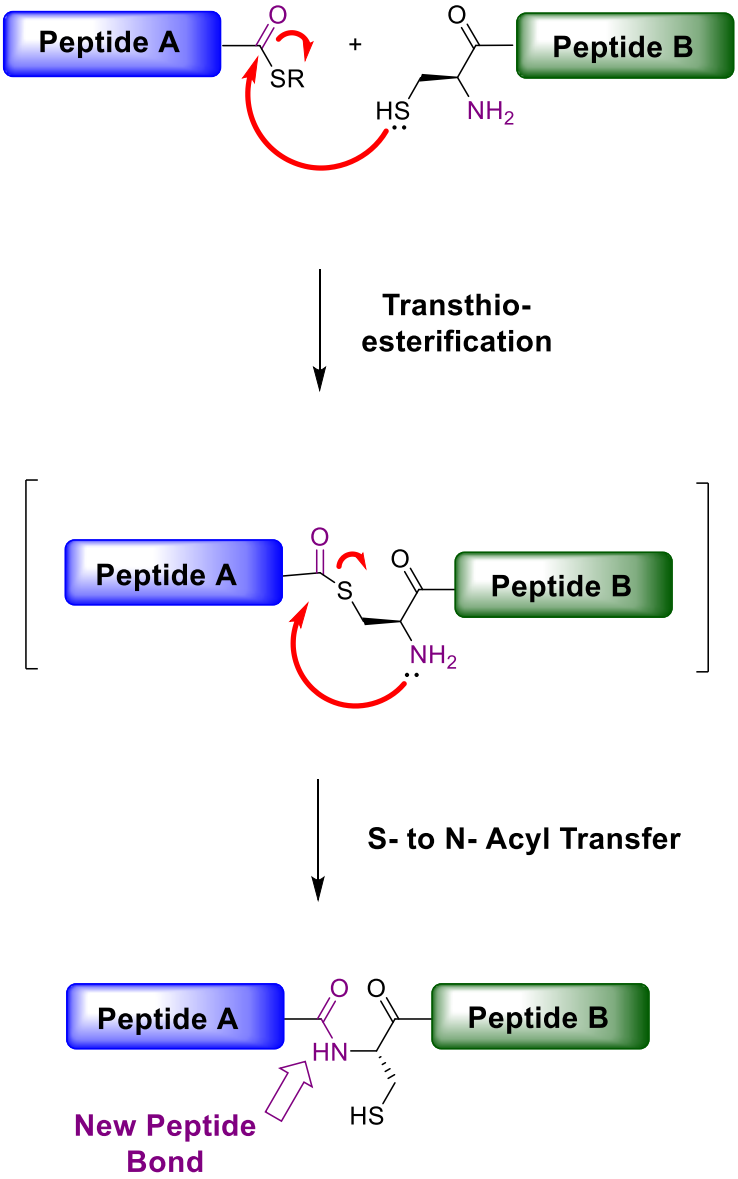

Scheme 4-4: Concept of Native Chemical Ligation

This method involves synthesizing a large peptide in two or more separate fragments with a cysteine residue on the N-terminus of one fragment. A thioester must then be installed on the C-terminus of the other fragment. Upon combining the two fragments (free of sidechain protection) in aqueous buffer, the cysteine sidechain undergoes a transthioesterification with the original thioester, followed by an S- to N- acyl transfer, forming the new, desired amide bond (Scheme 4-4). By this method, significantly larger peptides can be synthesized than can be obtained by standard methods linear or fragment based methods. One of the limiting factors in the use of NCL for the chemical synthesis of proteins is the need for routine production of peptide thioesters.[11]

4.4 Solution-Phase Synthesis of C-Terminal Thioesters

Initial attempts to synthesize C-terminal thioesters on an Hcnb-linked peptide were conducted in solution (Scheme 4-5). A simple Hcnb-linked dipeptide, Ac-[Hcnb]-Ala-OH **4.7** was synthesized in solution. Initially, attempts to directly install a thioester using DIPC were unsuccessful, resulting in recovery of the unreacted free acid **4.7**. However, it was found that protection of the *ortho*-phenol group resulted in the formation of detectable quantities of thioester. Introduction of a TIPS- protecting group onto the phenol prior to formation of the thioester resulted in the formation of the desired product, though in low yields. It was determined that further optimization of the conditions in solution would likely not prove useful, as most conditions are not optimal for both solution-phase and solid-phase synthesis.

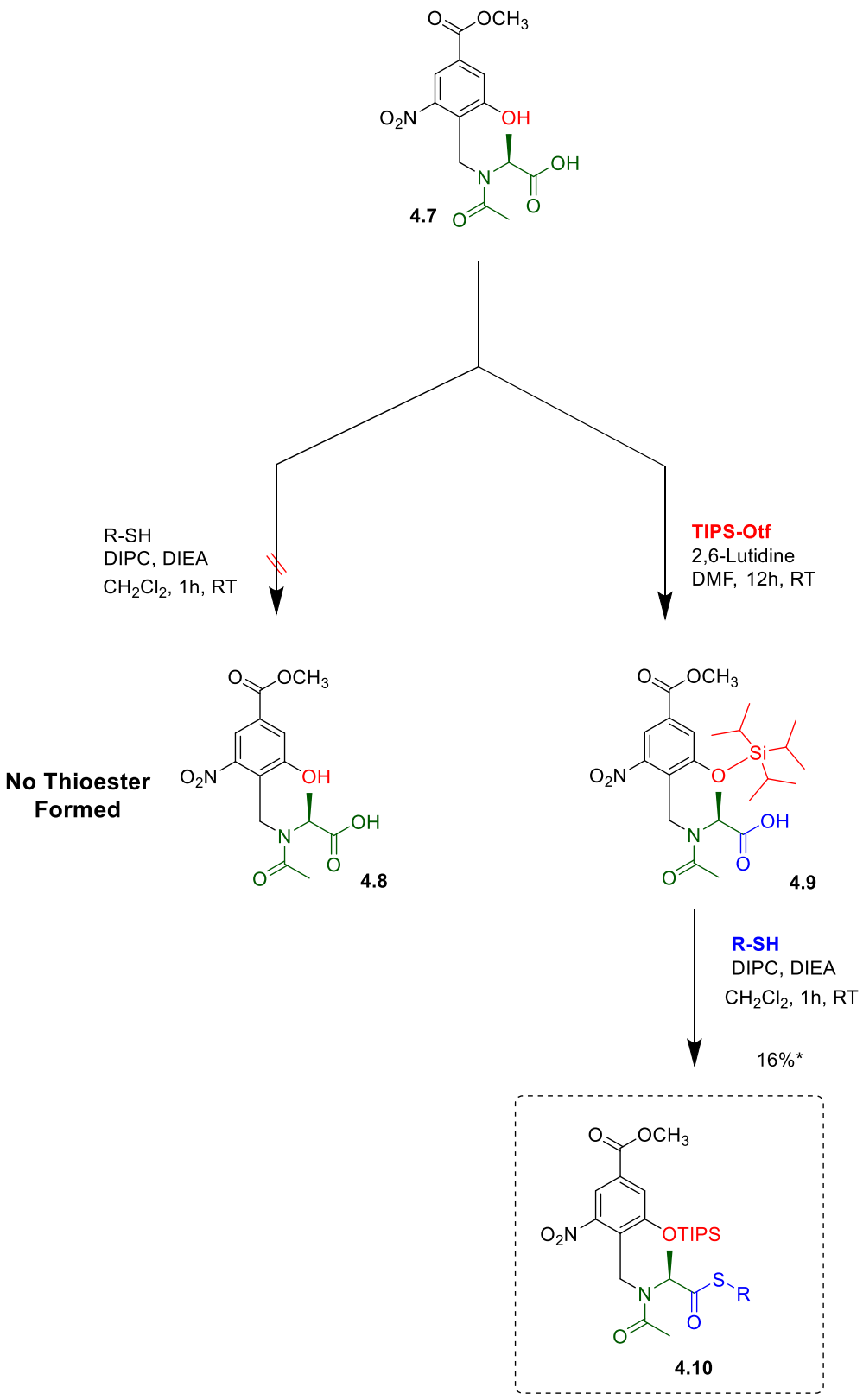

Scheme 4-5: Solution-phase synthesis of C-terminal thioesters

4.5 Adaptation of C-Terminal Thioester Synthesis to SPPS

A variety of coupling reagents were screened for the installation of C-terminal thioesters on the solid-phase (Table 11, Scheme 21). Conditions were screened using both thiophenol and benzyl mercaptan as the sulfur nucleophile. Solution-phase studies suggested that the presence of a free phenol on the linker was problematic. Introduction of a TIPS- protecting group prior to thioester formation was also found to be necessary on the resin. Use of carbodiimides as the coupling reagent yielded low conversions (0-30%). However, switching to HATU as a coupling reagent and pre-activating the carboxylic acid for 5 min prior to addition of the thiol yielded complete conversion to the desired thioester in 2 h.

Table 4-2: Screening conditions for thioester formation

Conditions	Solvent	% Conversion
RSH, DIPC, DIEA	DCM	30%
RSH, DIPC, DIEA	DMF	5%
RSH, CDI, DIEA	DMF	0%
RSH, DCC, DMAP	DMF	0%
1. DIPC, DIEA 2. RSH	DCM	0%
1. HATU, DIEA 2. RSH	DMF	100%

A series of pentapeptides were synthesized to examine the scope of C-terminal amino acid compatibility with thioester synthesis. It was found that the presence of β-branched amino acids as the C-terminal residue yield poor conversion to the thioester. However, it was reported by Kent and coworkers that bulky amino acids are not amenable to NCL due to the steric hindrance of the carbonyl required for the transthioesterification and subsequent acyl transfer.[11] Following reductive amination of the desired first amino acid residue, the linear sequence was synthesized as described previously (Scheme 4-6). The final amino acid in the sequence was coupled as the N-terminal Boc-protected structure. The C-terminal DMA protecting group was removed using Pd(0) and phenylsilane to give free acid **4.12**. Following TIPS- protection of the linker phenol, the C-terminus was pre-activated for 5 min with HATU and DIEA in DMF. Addition of thiophenol resulted in 95 - 100% conversion of carboxylic acid to thioester in 2h. The peptide thioester

sidechains were then globally deprotected using 5% H_2O in TFA for 1 h and the deprotected peptide was cleaved from the resin under 365 nm UV light for 1h. Depending on the identity of the first amino acid residue, peptide thioesters were obtained in 75-99% purity and 80-90% cleavage yield (Table 4-3). No epimerization of the C-terminal side chain was observed. Four pentapeptide sequences were synthesized with C-terminal thioester groups installed (Figure 4-1).

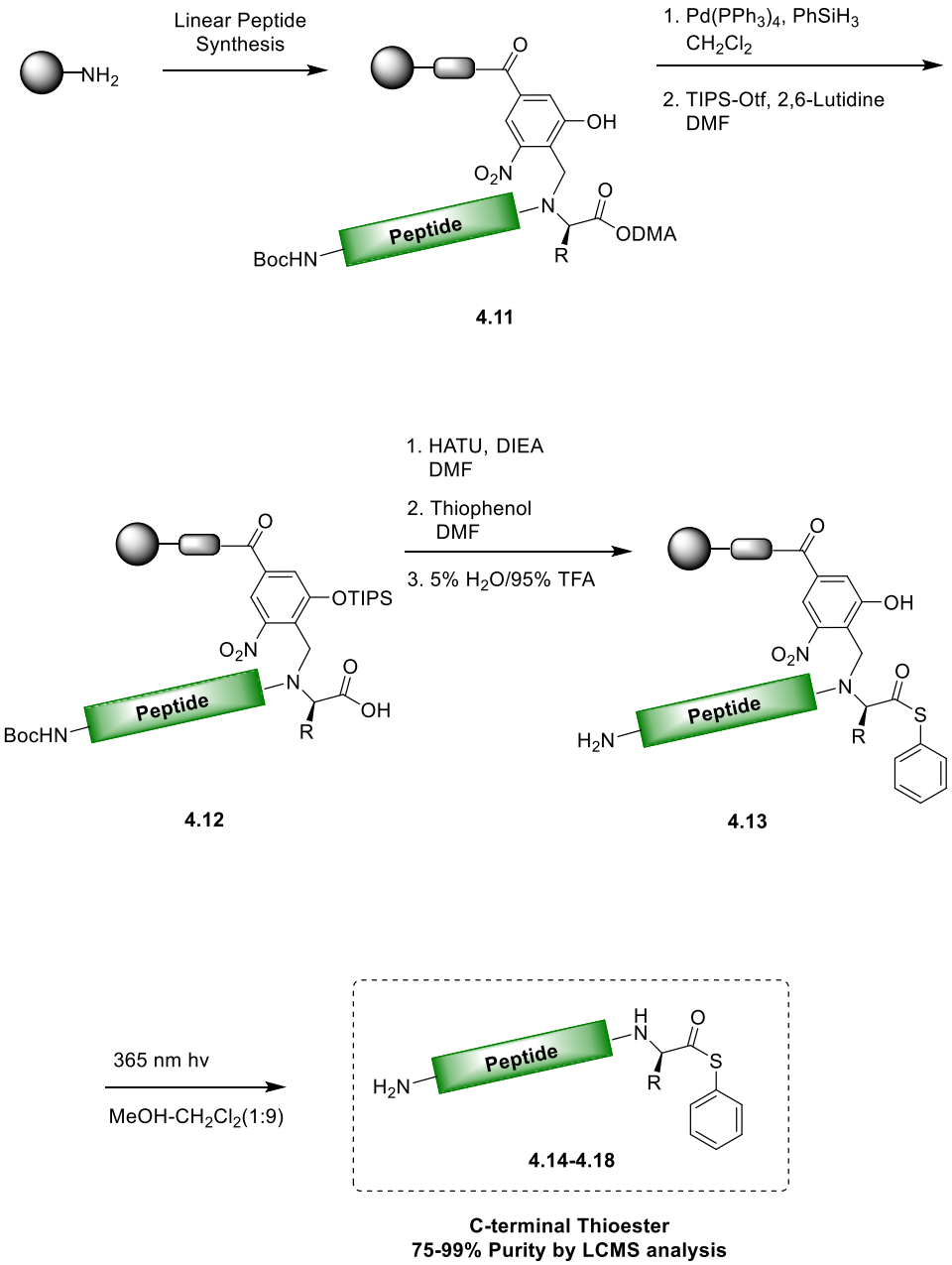

Scheme 4-6: On-resin synthesis of C-terminal thioesters

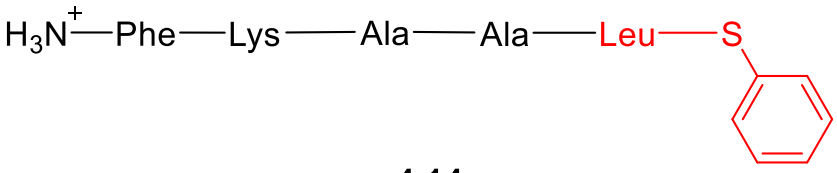

4.14

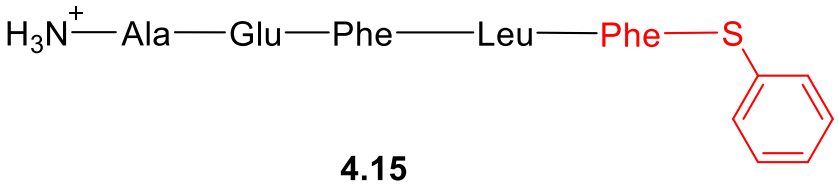

4.15

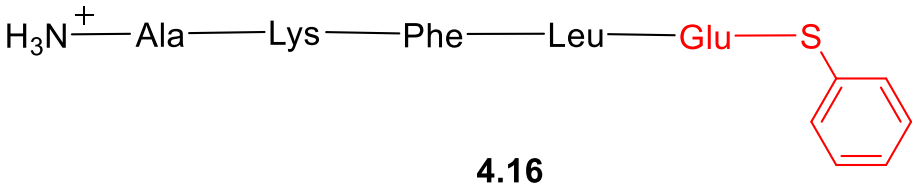

4.16

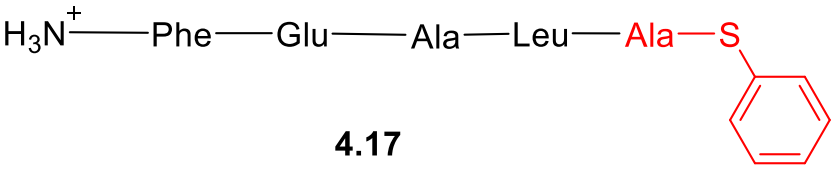

4.17

Figure 4-1: Pentapeptide thioesters synthesized using Hcnb

Table 4-3: Summary of thioester examples

Structure	Purity	Cleavage Yield
H-Phe-Lys-Ala-Ala-Leu-S-Ph (**4.14**)	99%	83%
H-Ala-Glu-Phe-Leu-Phe-S- Ph (**4.15**)	99%	66%
H-Ala-Lys-Phe-Leu-Glu-S- Ph (**4.16**)	75%	71%
H-Phe-Glu-Ala-Leu-Ala-S- Ph (**4.17**)	95%	92%

4.6 Conclusion

In searching for a photolabile backbone amide linker for the solid-phase synthesis of cyclic and C-terminally modified peptides, former group member Dr. Soo Sung Kang conducted a literature survey of various photolabile motifs. He established that the *o*-nitrobenzyl motif was the best candidate. Optimization of the functional groups on the linker candidate led to the development of the 2-hydroxy-4-carboxy-6-nitrobenzyl (Hcnb) linker. A convenient and scalable synthesis of a benzaldehyde precursor was developed by Dr. Matthew Hostetler. The linker tolerates the cleavage conditions for a variety of commonly used protecting groups, including acid, base, and palladium. Cleavage from the linker is then achieved via photolysis at 365 nm. The Hcnb linker can be conveniently attached to an aminoethyl TG resin using a 6-aminohexanoic acid spacer and proline residue, allowing for its use in solid phase peptide synthesis. The photolabile backbone amide linker was used to demonstrate the on-resin synthesis and cyclization of three cyclic peptides of varying chain sizes (5, 10, 14 residues). The cyclic peptides were obtained in 80-96% cleavage yield and 50-95% purity with no purification needed. The linker was also used to demonstrate the synthesis of thioesters on the original C-terminus for use in Native Chemical Ligation reactions. The thioesters were synthesized using a variety of amino acids, yielding 75-99% pure thioester peptides with no purification needed.

PART II. THE DESIGN AND SYNTHESIS OF SMALL-MOLECULE INHIBITORS OF CLASS-II HMG-COA REDUCTASE FOR USE AS ANTIMICROBIALS

CHAPTER 5. THE DESIGN AND SYNTHESIS OF SMALL MOLECULE INHIBITORS OF CLASS-II HMG-COA REDUCTASE

5.1 Overview

Before the discovery of sulfa drugs, and the influx of other antibiotics in the 1940s, death by bacterial infection posed a significant fear following injury, hospitalization, as well as infections such as bacterial meningitis. Sulfa drugs were stumbled upon as potent antibacterial compounds by Bayer, a German dye production company.[38] They noticed that attaching a sulfanilamide group to a dye molecule could save mice infected with certain bacterial infections. This led to the release of Prontosil, the first widely-used antibiotic.[39] Although the mechanism of action was not known, French chemists later performed structure-activity relationship studies and determined that the sulfanilamide group was the active portion of the molecule. This led to the development of improved sulfa-based drugs.[39] The side effects that accompany most sulfa drugs has led to a decrease in their use, but the discovery of this group started a revolution in the drug design industry.[39] Shortly after the discovery of Prontosil, Alexander Fleming mistakenly discovered a fungus, *Penicillium notatum*, which found its way into his laboratory and killed a sample of *Staphylococcus* while he was away on vacation.[40] Within a few years, penicillin was widely available as an FDA approved drug for the treatment of bacterial infections. However, bacterial resistance to penicillin began to appear two years before it was even approved as a drug by the FDA.[41] Antibiotic resistance arises through a number of different mechanisms, depending on the class of bacteria and the chemical structure of the antibiotics. Some common classes of antibiotics are show in Figure 5-1.

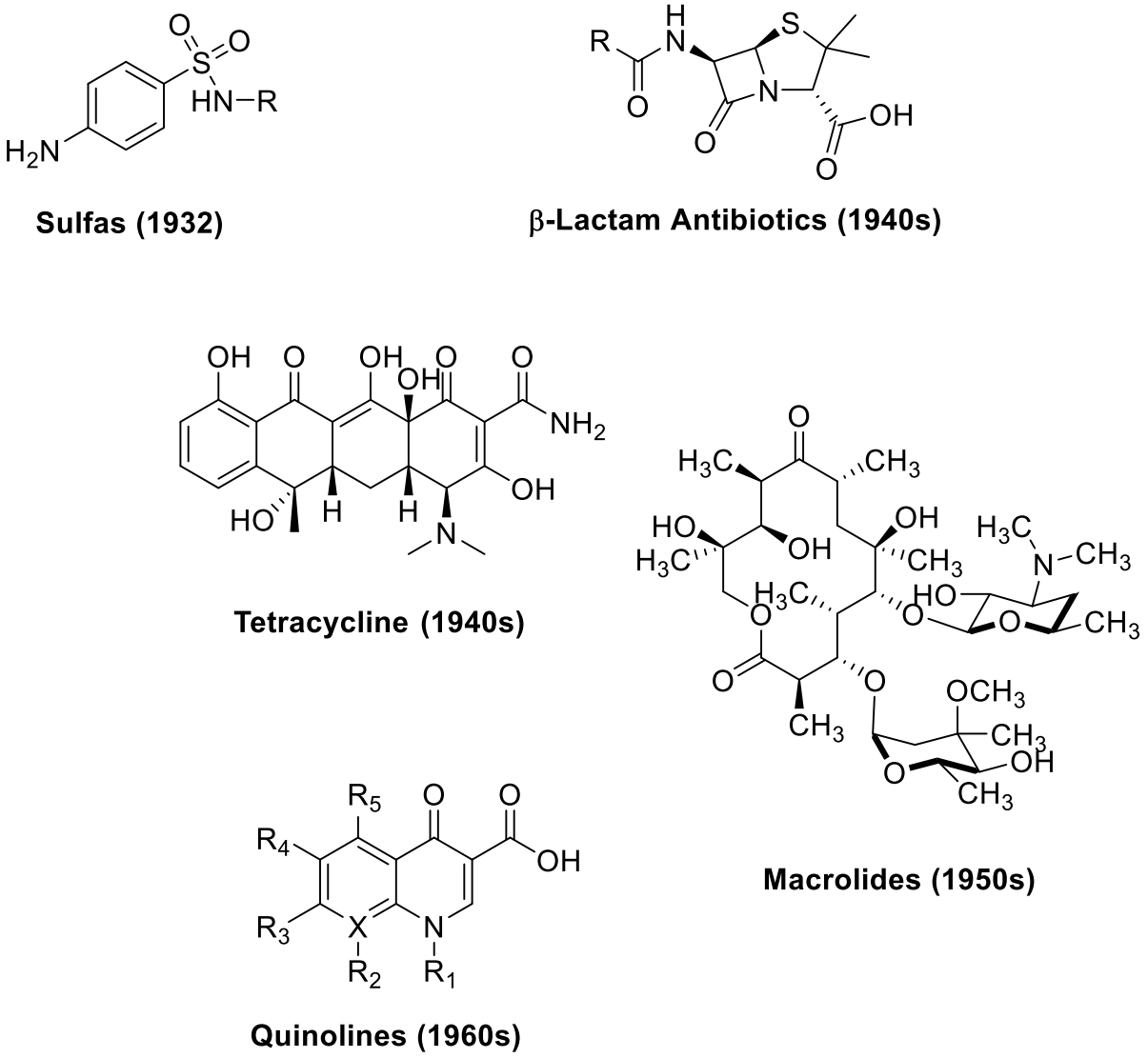

Figure 5-1: Common classes of antibiotics

5.2 Rise of Antibiotic Resistance

Since the 1940s, a plethora of different antimicrobial agents have become FDA-approved drugs. However, resistant strains continue to appear following the introduction of new drugs. For this reason, the production of new antimicrobials has declined in recent years, as it is less financially beneficial to pharmaceutical companies to devote resources toward a drug that is not only prescribed briefly for an acute infection, but that also may quickly be rendered ineffective within several years of its inception.[42] The Office of Health Economics in London, England estimates that the value of a new antibiotic drug is approximately $50 million, in contrast to a value

of over $1 billion for drugs that treat neuromuscular diseases.[43] Many factors contribute to the epidemic of resistant strains of bacteria, including careless prescription of antimicrobials for viral infections, patients failing to complete a prescribed regime of antibiotic, and the use of antimicrobial drugs for disease prevention and growth enhancement for animals in the food industry.[43] Thus, the impending crisis of untreatable bacterial infection looms ever closer.

In 2014, the Infections Diseases Society of America (IDSA) declared multiple drug resistant bacteria to be a "substantial threat to US public health and national security". [44] As a general trend, pathogenetic bacteria tend to be Gram-positive, while Gram-negative tend to be commensal. Currently, many drugs on the market target cell wall biosynthesis, inhibiting various enzymes involved in this process. This has proved to be an effective method for encouraging bacterial death.[45] However, many such drugs are non-specific. Broad spectrum antibiotics affect all types of bacteria non-selectively, including Gram-negative commensal bacteria.[46] Thus, a need exists for a new type target for antimicrobials that is selective to gram positive bacteria.[47] The Center for Disease Control publishes an annual report on the current biggest threats in the United States.[48] According to the 2019 report, 2.8 million antibiotic-resistant infections will occur this year and over 35,000 people are expected to die. Below is the list of bacterial threats that are currently considered to be "Urgent" or "Serious" by the CDC.

"Urgent" and "Serious" Bacterial Threats[48]

Carbapenem-resistant *Acinetobacter*

Clostridioides difficile

Carbapenem-resistant *Neisseria gonorrhoeae*

Drug-resistant *Campylobacter*

Vancomycin-resistant *Enterococci* (VRE)

Multidrug-resistant *Pseudomonas aeruginosa*

Drug-resistant *Salmonella* serotype Typhi

Methicillin-resistant *Staphylococcus aureus* (MRSA)

Drug-resistant *Streptococcus pneumoniae*

5.2.1 Hospital-Acquired Infections

The CDC estimates that over 2 million people are infected with preventable bacterial infections found in hospitals (nosocomial infections) leading to nearly 100,000 deaths annually.[49] These have become a major issue for hospitalized patients due to the prevalence of several risk factors. A high population of elderly patients and others with compromised immune systems cause these infections to run rampant. Additionally, surgical or implant procedures provide normal bacterial colonies access to bodily entry points that are otherwise protected by skin.[50] Nosocomial infections tend to arise from the list of urgent and serious bacterial threats outlined by the CDC. The most common species for these infections are Gram-positive MRSA and VRE.[51] To minimize the spread of hospital-acquired infections, it is common to frequently disinfect surfaces with antibacterial cleaners. This habit contributes to the rise in resistant strains of bacteria, furthering the challenges that hospitals face.

5.3 HMG-CoA Reductase

Previous efforts in the Lipton group have been made toward the design and synthesis of a new type of antimicrobial compound for the selective targeting of Gram-positive bacteria. The target selected for this project was the 3-hydroxy-3-methyl-glutaryl-CoA reductase enzyme (II-HMGR). It is responsible for catalyzing the reduction of HMG-CoA to mevalonate through a 4 electron oxidoreduction (Figure 5-3).[52] In humans, this is a key step in the biosynthesis of cholesterol, and has thus been the target of a class of cholesterol lowering drugs known as statins.[53] Mevalonate is a precursor to isopentenyl diphosphate (IPP), which is a component of undecaprenyl-phosphate, a lipid carrier. Undecaprenyl-phosphate is a requirement for bacterial cell wall synthesis. It is primarily responsible for the transport of N-acetylmuramic acid (NAM) and N-glucosamine (NAG) across the cytoplasmic membrane, where they polymerize and become

components of the peptidoglycan cell wall. The active site of II-HMGR consists of several different key residues compared to I-HMGR, making it feasible to design a molecule to selectively inhibit one in the presence of the other.[54] The mechanism of action for the conversion of HMG-CoA to mevalonate is shown in Figure 5-2.

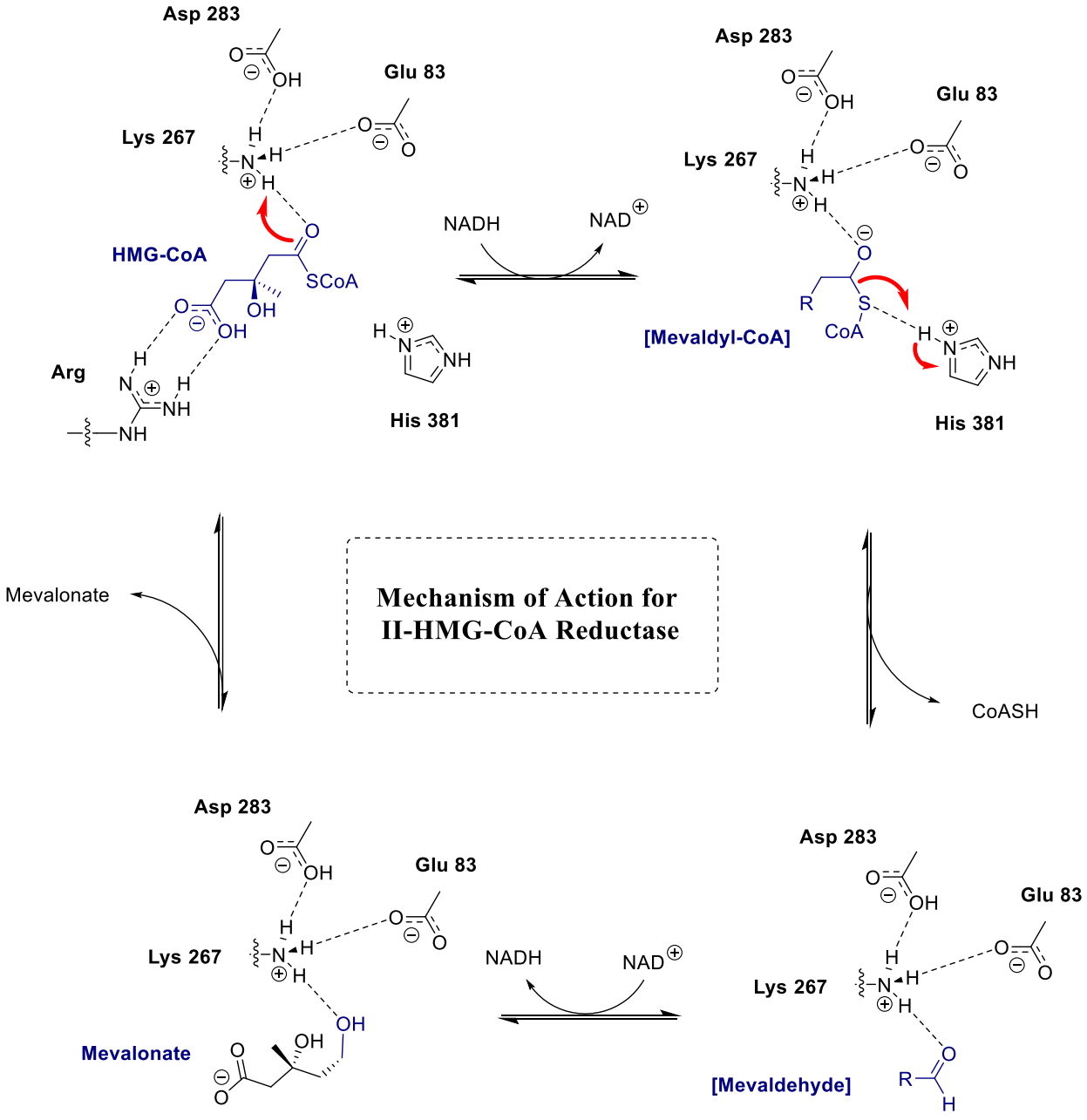

Figure 5-2: Mechanism of action for II-HMG-CoA Reductase

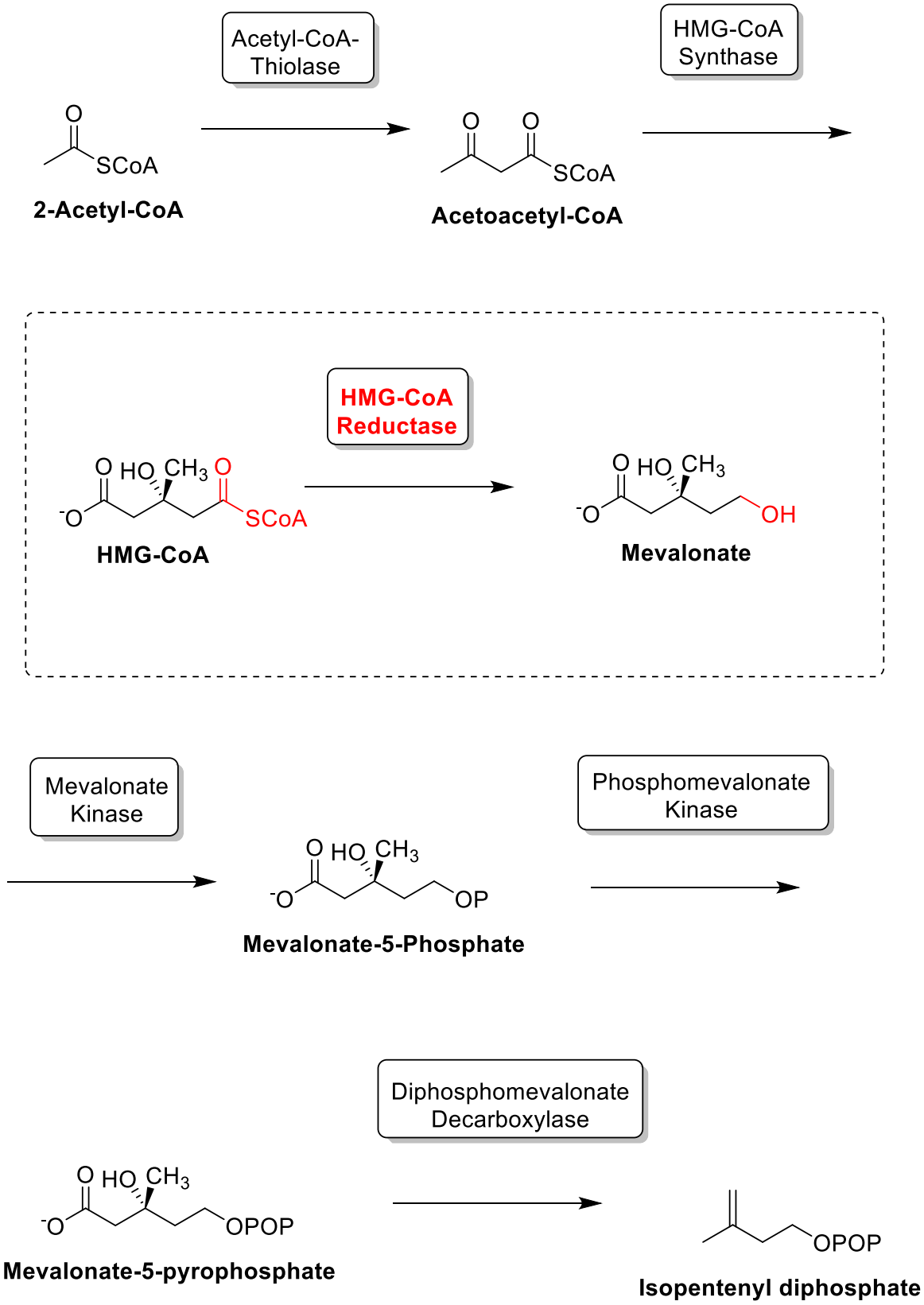

Figure 5-3: Biosynthetic pathway for the synthesis of IPP

5.4 **Previous Work – First Generation Inhibitors**

Dr. Cynthia Stauffacher's laboratory at Purdue University collaborated with the Southern Research Institute in Alabama to screen a library of 300,000 molecules for the inhibition of II-HMGR from *Enterococcus faecalis*. The best inhibitor found was 5-(N-(4-butylphenyl)sulfamoyl)-2-hydroxybenzoic acid **DL-3.1** (Figure 5-4) with and IC_{50} of 48 µM. Kinetic studies were conducted and determined that compound **DL-3.1** is a competitive inhibitor of *E. faecalis* II-HMGR. The Stauffacher group also obtained a crystal structure of **3.1** in the active site of II-HMGR and determined that it mimics the endogenous substrate HMG-CoA.[55] Former Lipton Lab member, Dr. Daneli Lopez-Perez worked to optimize the activity of this inhibitor. A small library of analogues was synthesized, and it was determined that the long aliphatic moiety on the *p*-aromatic ring was necessary to maintain activity.

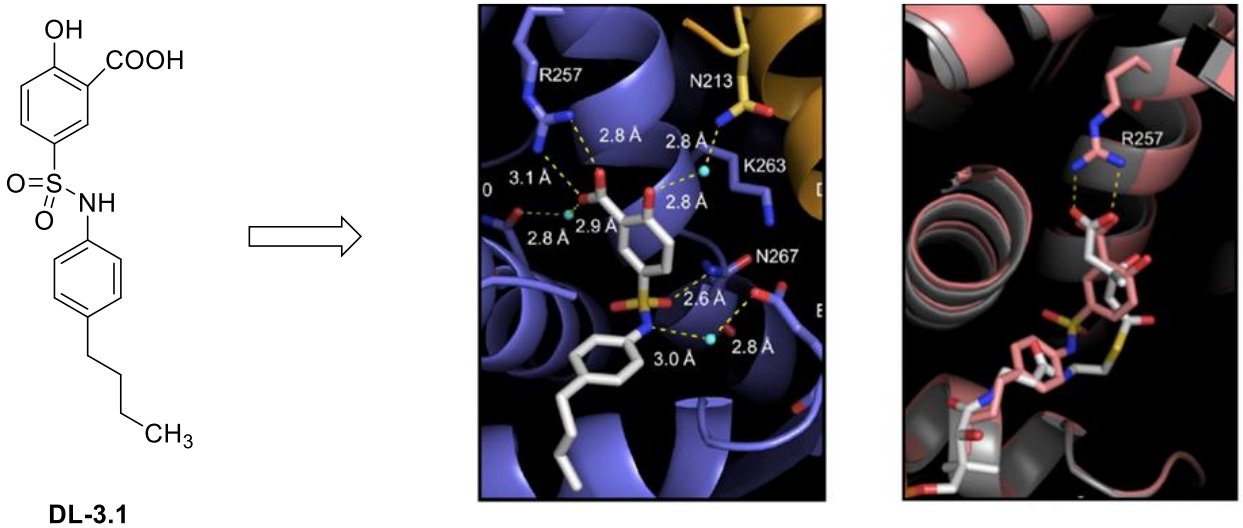

DL-3.1

Figure 5-4: Lead compound n-Bsha (**DL-3.1**) [Crystal Structure taken from the thesis of Dr. Daneli Lopez-Perez][55]

For the first generation of modifications, Dr. Lopez-Perez tested a variety of chain lengths, as well as two different headgroup structures (Figure 5-5). The enzymatic activity and antimicrobial activity of these compounds is show in Table 5-1. The best-in-class inhibitor was **DL-3.23** with an IC_{50} of 12 and 7 µM against *E. facaelis* and *S. aureus*, respectively, and an MIC/MBC of 32 and 16 µM when tested against VRE and MRSA, respectively. Enzymatic assays for the first generation inhibitors were conducted by our collaborator Nic Steussy in Cynthia

Stauffacher's laboratory at Purdue University. IC_{50} values were determined via spectrophotometric assays. The disappearance of NADPH was monitored at 340 nm to determine the catalytic activity of HMGR in the conversion of HMG-CoA to Mevalonate. These results are shown in Table 5-1. Bacterial assays were conducted by Dr. Mohammed Seleem in the Department of Pathobiology at Purdue University. The inhibitors were tested in concentrations ranging from 0.5 - 128 µM. Each inhibitor was incubated with bacteria in a 96-well plate at 37°C for 18 h. These results are shown in Table 5-1. Many of the compounds tested showed no inhibitory activity at all in bacterial assays, even those inhibitors with impressive IC_{50} values. This is likely due to a lack of cell-membrane permeability.

Table 5-1: IC_{50} and MIC/MBC for first generation HMGR inhibitors (all values are in µM)

Analogue	*S. aureus* IC_{50}	*e.f.* IC_{50}	VRE MIC/MBC	MRSA MIC/MBC
DL-3.1	121	91 ± 5	-	-
DL-3.2	x	x	-	-
DL-3.3	x	x	128/128	>128
DL-3.4	x	x	-	-
DL-3.5	167	130	-	-
DL-3.18	x	x	-	-
DL-3.19	265 ± 8	200 ± 37	-	-
DL-3.20	98 ± 3	65 ± 3	-	-
DL-3.21	77 ± 6	33 ± 4	>128	128/128
DL-3.22	28 ± 2	30 ± 2.7	-	-
DL-3.23	7.2 ± 0.6	12 ± 2	32/32	16/16
DL-3.24	5.9 ± 0.5	2.4 ± 0.07	128/128	128/>128
DL-3.25	1.9 ± 0.15	2 ± 0.015	-	-
DL-3.26	36 ± 4	22 ± 1.3	128/>128	128/>128
DL-3.27	22	18	128/128	64/64
DL-3.28	24.6 ± 5	32 ± 2	-	-
DL-3.29	63 ± 2	54 ± 2	128/128	>128
DL-3.30	105 ± 5	50 ± 2.7	-	-
DL-3.31	13.2 ± 0.3	16.9 ± 0.7	16/32	16/16
DL-3.32	16.2 ± 1	5.8 ± 0.5	64/64	32/32
DL-3.33	142 ± 7	200 ± 6	-	-
DL-3.34	x	x	-	-
DL-3.40	x	249 ± 5	-	-
DL-3.41	x	x	-	-

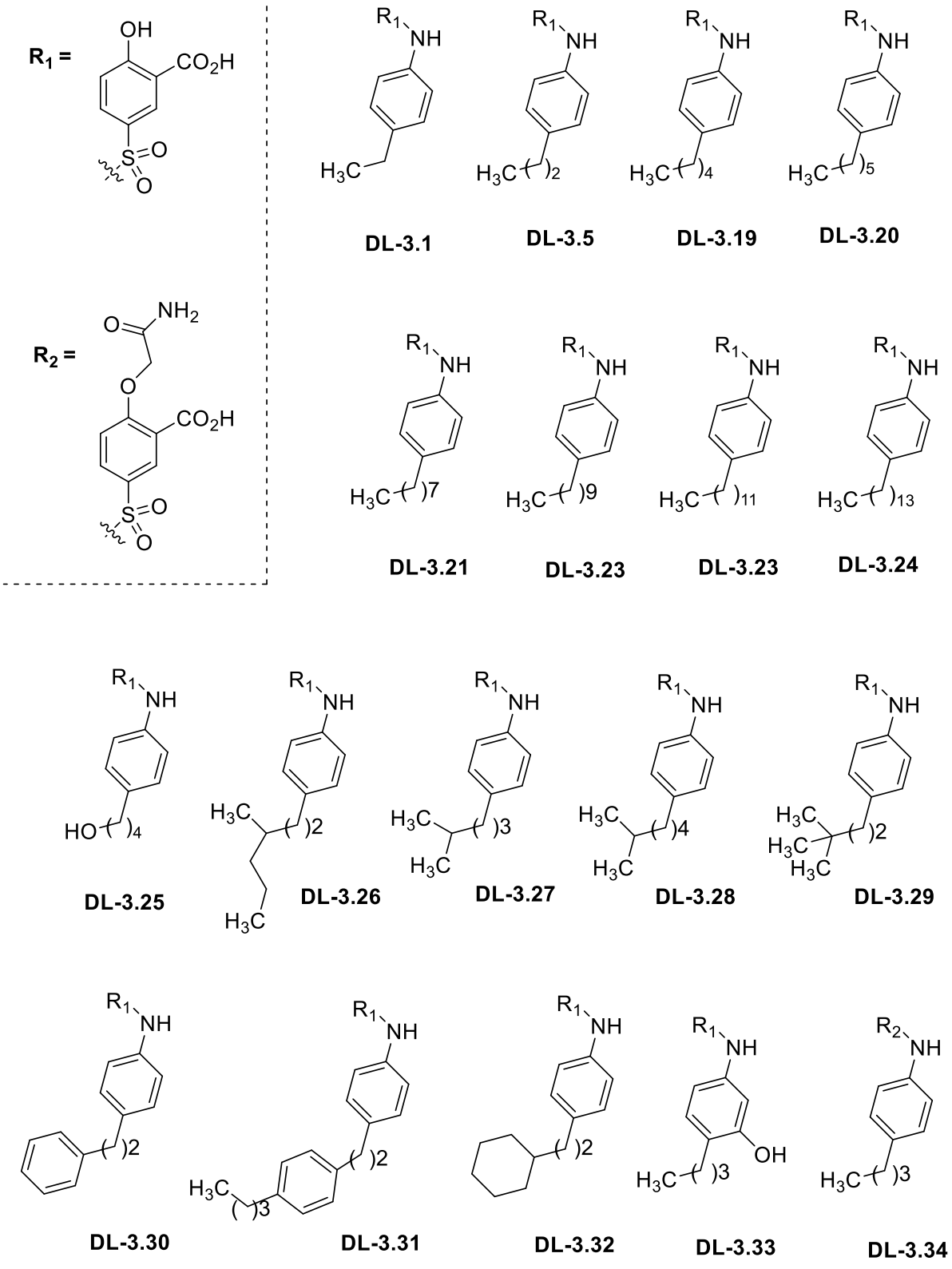

Figure 5-5: First generation of II-HMGR inhibitors

5.5 Second Generation Inhibitors

Current Lipton Lab member Matthew Hostetler synthesized a second and third generation of analogues, experimenting with various polar functionalities on the aliphatic chain concluding that compound **MH-2.3** had the highest activity with and IC_{50} of 5.4 µM, but with an MIC/MBC>256 µM (Figure 5-6).[24] A lack of correlation between IC_{50} and MIC/MBC (Table 5-2) suggests one of two possibilities: (1). The molecules are losing the ability to penetrate the cell membrane (2). The lead compound was inhibiting a secondary enzyme, in addition to II-HMGR. As the structure is optimized for the assumed primary target, activity toward the unidentified target is lost.

Table 5-2: IC_{50} and MIC/MBC date for second generation II-HMGR inhibitors

Analogue	***E. faecalis* IC_{50} (µM)**	**VRE MIC/MBC (µM)**	**MRSA MIC/MBC (µM)**
MH-2.1	13.3 ± 0.8	-	-
MH-2.2	9.6 ± 1.2	-	128/256
MH-2.3	5.4 ± 0.3	-	>256/>256
MH-2.4	12 ± 5	-	>256/>256
MH-2.5	30.4 ± 1.5	128/128	128/>512
MH-2.6	35.8 ± 1.5	128/256	128/>512
MH-2.7	38 ± 2	256/256	512/512
MH-2.8	-	-	-
MH-2.9	13.4 ± 0.9	8/16	16/32
MH-2.10	30.6 ± 2	64/128	64/128

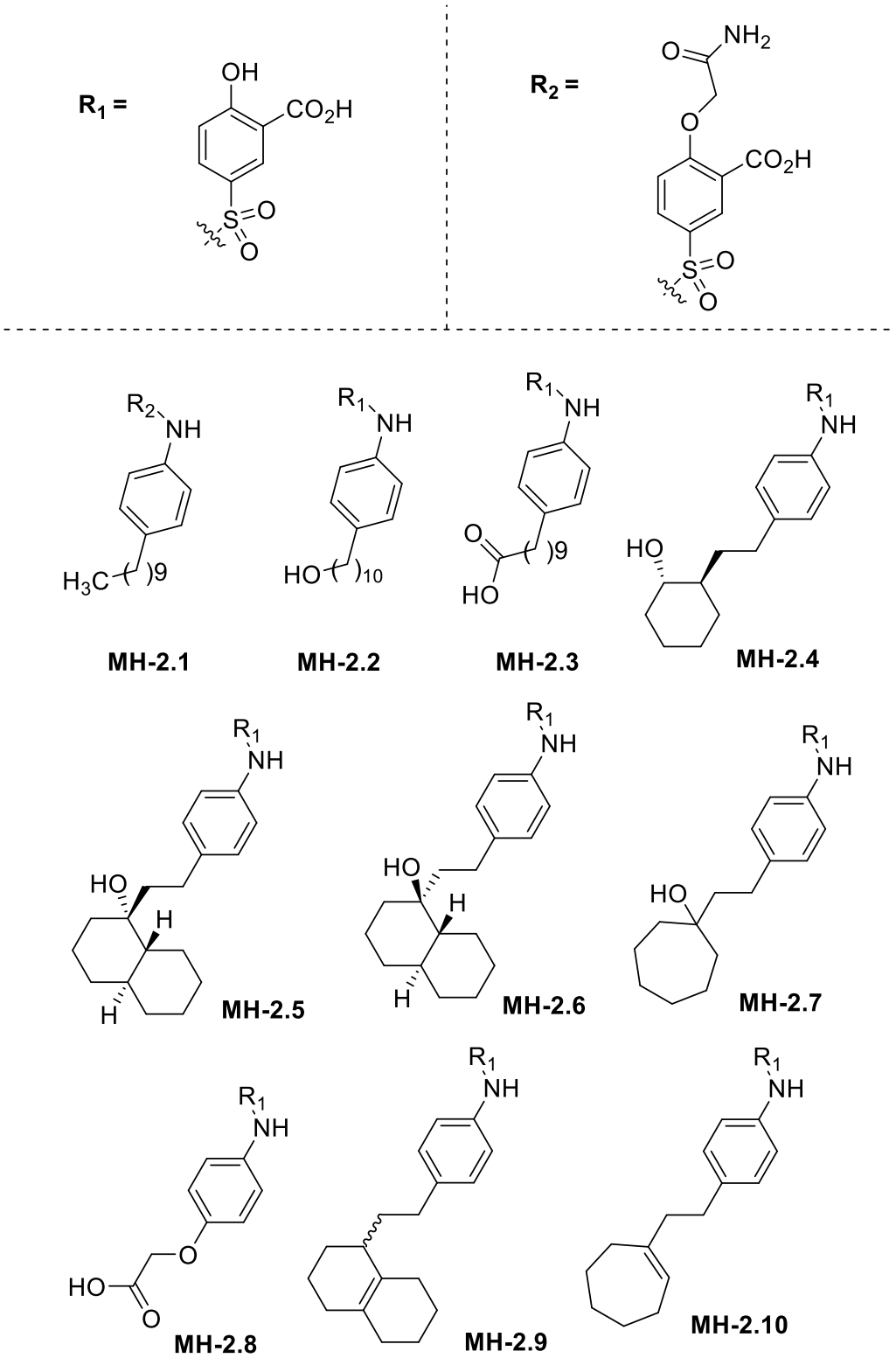

Figure 5-6: Second generation of II-HMGR inhibitors

5.6 **Conclusion**

Bacterial resistance to antibiotic drugs is an issue that mankind has faced since the first use of penicillin in the 1940s. In recent years, the rate of production of new antimicrobial drugs has diminished, as they are no longer financially auspicious to pharmaceutical companies. Gram-positive bacteria are particularly prevalent as nosocomial infections, targeting hospital patients with compromised immune systems. We have identified a potential antimicrobial target, II-HMG-CoA Reductase. Responsible for catalyzing a key step in cell-wall biosynthesis, this enzyme is found only in Gram-positive bacteria. Former group members Dr. Lopez-Perez and Dr. Hostetler synthesized a series of inhibitors to test against the enzyme. While several of these compounds show promising results in bacterial cell death assays, we are continuing the optimization process. Additionally, we believe that these compounds may interact with a second target as well, opening the door for potential dual-action therapeutics. The following 2 chapters will lay out the efforts that have been made toward achieving these two goals.

CHAPTER 6. THE DESIGN AND SYNTHESIS OF OPTIMIZED INHIBITORS OF CLASS-II HMG-COA REDUCTASE

6.1 Design of New II-HMGR Inhibitors

Former group members Dr. Daneli-Lopez Perez and Dr. Matthew Hostetler synthesized and tested a series of inhibitors for II-HMG CoA Reductase (II-HMGR) for use as selective anti-microbial therapies against gram-positive bacteria.[24,55] Co-crystal structures of the best-in-class compounds were examined to identify potential structural modifications. While the enzymatic activity of these inhibitors increased with structural optimization, the anti-bacterial activity showed no correlation (Figure 6-1). Several structural variations of the best in-class compounds were proposed to improve various polar contacts, to increase the structural rigidity of the inhibitor, or to improve cell membrane permeability (Figure 6-2). Due to the differing functionality when compared with previous inhibitors, original syntheses were developed for most of the transformations required to obtain these structures.

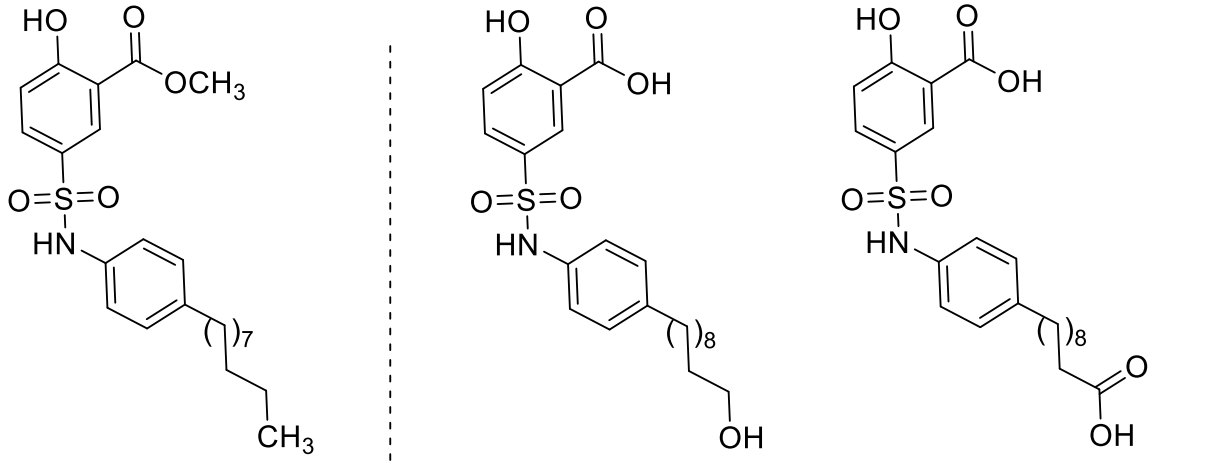

Figure 6-1: Top candidates from the first and second generation of II-HMGR inhibitors

.

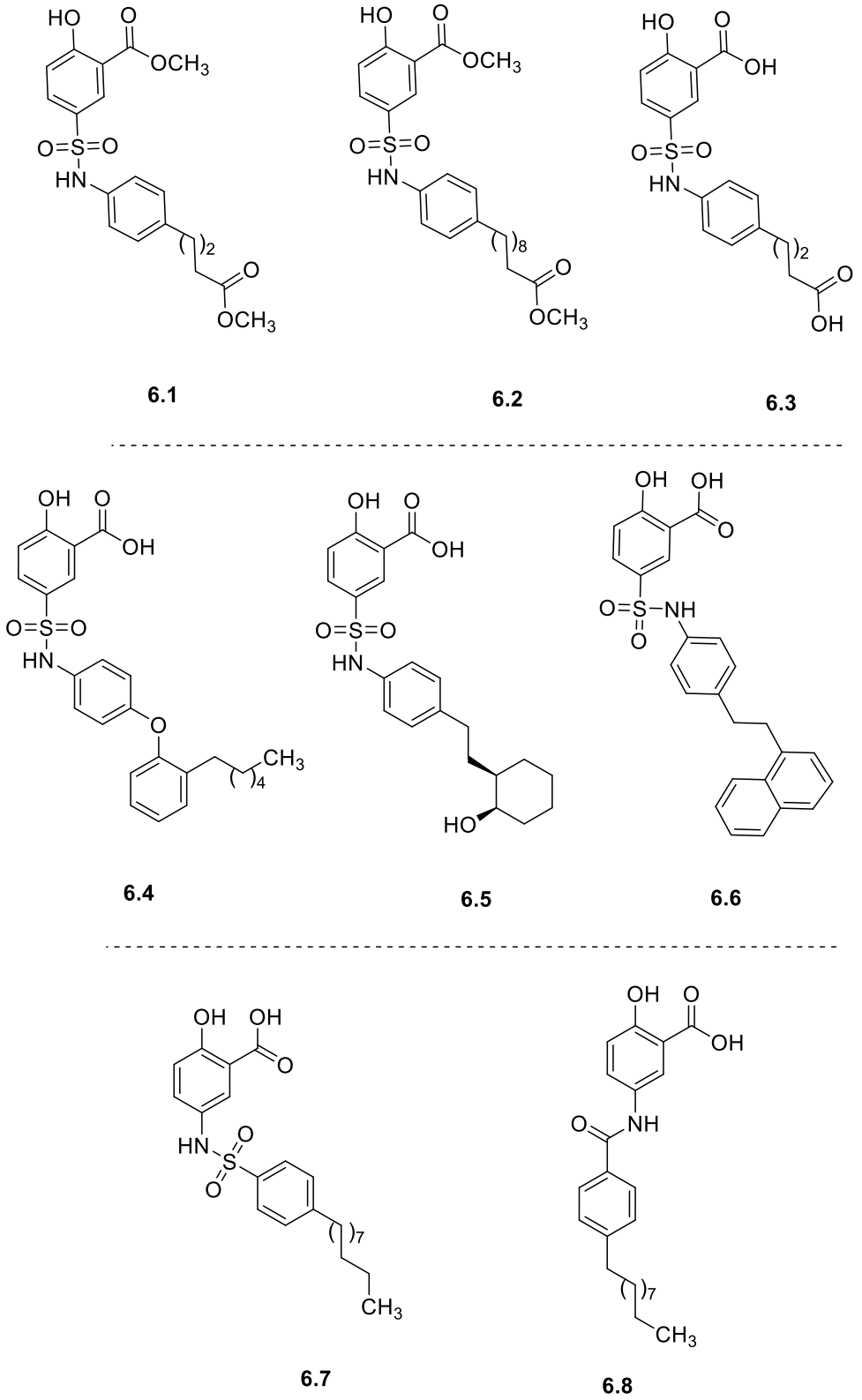

Figure 6-2: Structures of proposed new inhibitors for II-HMGR

6.2 Derivatives of Terminal Carboxylic Acid Inhibitor MH-2.3

When examining the crystal structure of **MH-2.3** (Figure 6-3), it was noted that the 10-carbon chain is forced to curl up in order to engage the polar residues with the terminal carboxylic acid group.[24] We proposed synthesis of compound **6.3**, with a shortened aliphatic chain, to avoid this effect and place the terminal carboxylic acid in the correct spot in 3-dimensional space for interaction with the polar residues of II-HMGR.

Additionally, while **MH-2.3** exhibited an impressive IC_{50} of 5 µM, little activity was shown in the subsequent anti-bacterial cell assays. We hypothesized that this was due to an inability of the compound to cross the cell- membrane, as the addition of a carboxylic acid on the end of the aliphatic tail increases the polarity of the inhibitor when compared with **DL-3.23**. To improve the membrane-permeability of the inhibitor, we proposed synthesizing and testing both the di-methyl ester version **6.2**, as well as the di-methyl ester version of the 4-carbon chain carboxylic acid derivative **6.1**.

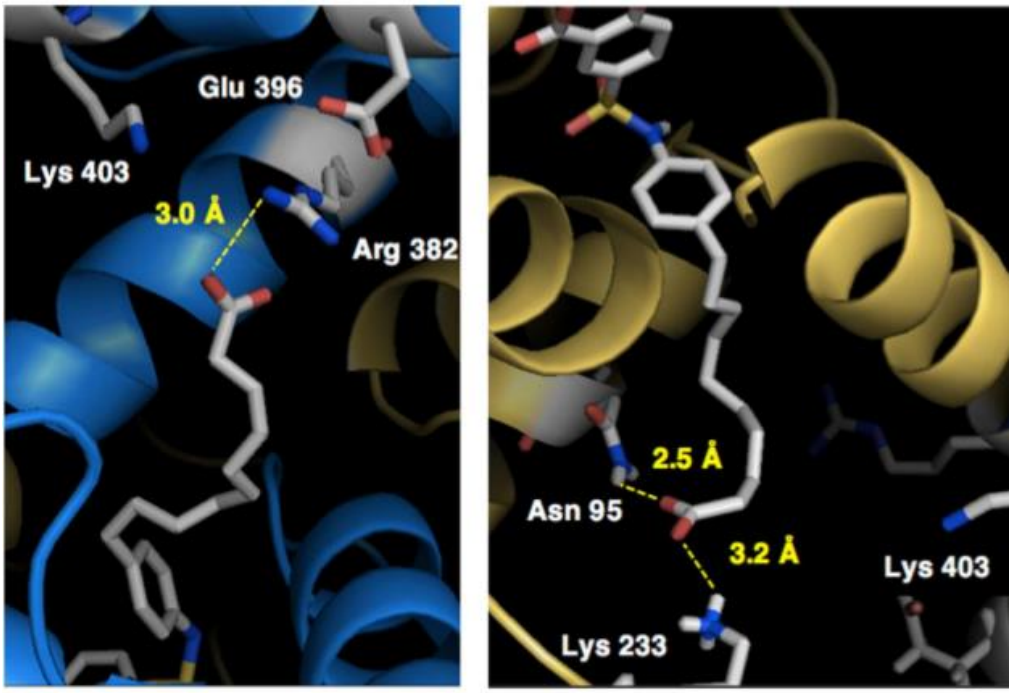

Figure 6-3: Co-crystal structure of **MH-2.3** bound in the active site of II-HMGR [Crystal structure taken from the thesis of Dr. Matthew Hostetler][24]

6.2.1 **Headgroup Synthesis**

The standard headgroup was synthesized according to the procedure developed by Dr. Daneli Lopez-Perez.[55] Beginning with commercially available methyl salicylate, an electrophilic aromatic substitution (EAS) reaction using chlorosulfonic acid and thionyl chloride from -10 ^{o}C to rt for 12 h gives the standardized head group (**6.9**) in 96% yield (Scheme 6-1).

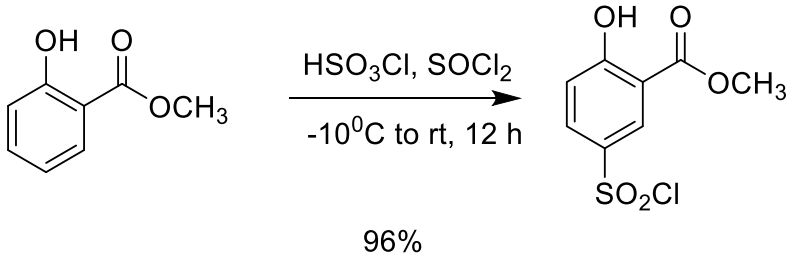

96%

6.9

Scheme 6-1: Synthesis of standard headgroup

6.2.2 **Synthesis of 6.1-6.3**

It was initially envisioned that the compounds **6.1-6.3** could be obtained in 6 steps from commercially available *p*-iodonitrobenzene and 3-butyn-1-ol or 9-butyn-1-ol, depending on the desired length of the carbon chain according to the synthetic procedure developed by Dr. Hostetler (Scheme 6-2).[24] First, a "copper-free Sonogashira coupling" (Heck alkynylation)[56] in H_2O/acetone between *p*-iodonitrobenzene and 9-decyn-1-ol or 3-butyn-1-ol yielded primary alcohols **6.10** and **6.11**, respectively. The alcohols were oxidized to carboxylic acids **6.12** and **6.13** using a TEMPO-catalyzed BAIB oxidation.[57] The terminal carboxylic acids were then methylated using thionyl chloride in methanol at reflux in 70% yield. The *para*-nitro group and alkynes were reduced in one step via platinum catalyzed hydrogenation in 98% yield. The resulting anilines **6.16** and **6.17** were then coupled with the previously prepared sulfonyl chloride headgroup **6.9** to yield **6.1** and **6.2** in 96% yield. **6.1** was hydrolyzed using aqueous NaOH at reflux to give the di-carboxylic acid **6.3.** However, it was found in the case of the 4 carbon chain, very low yields were obtained, particularly during the oxidation step. Thus, a revised synthesis was developed for the 4-carbon chain inhibitor.

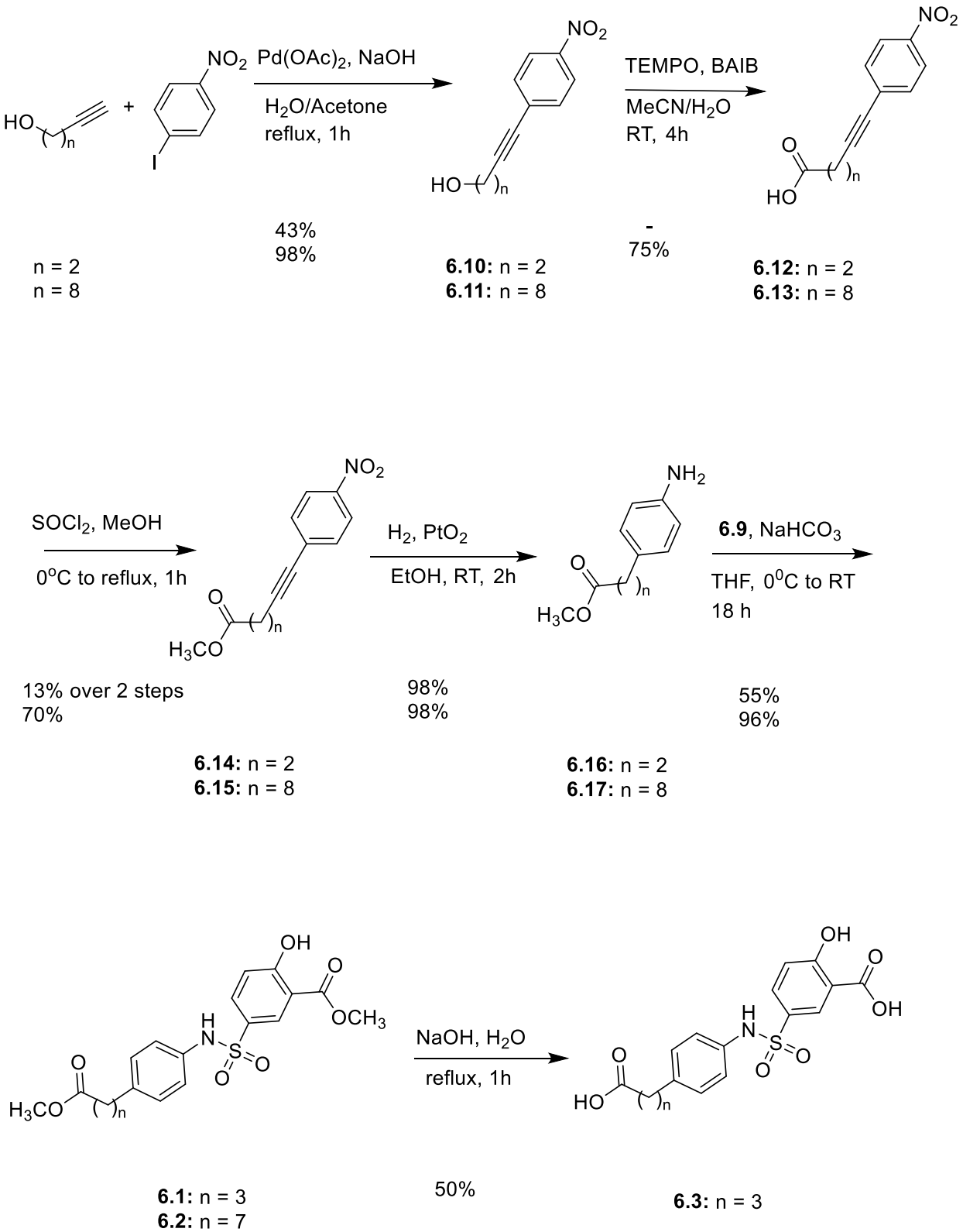

Scheme 6-2: First synthetic strategy for **6.1-6.3**

In the revised strategy (Scheme 6-3), commercially available 4-aminophenyl butyric acid **6.18** was protected as the methyl ester **6.16** using the same esterification conditions mentioned previously. This aniline was then coupled to **6.9** to give the desired dimethyl ester **6.2** in only 2 steps overall. Hydrolysis of both methyl esters in NaOH under reflux gave the carboxylic acid **6.3**. This shorter synthesis produced both compounds in significantly higher yield when compared with the 6-step synthesis necessary for making the structurally analogous **6.2**.

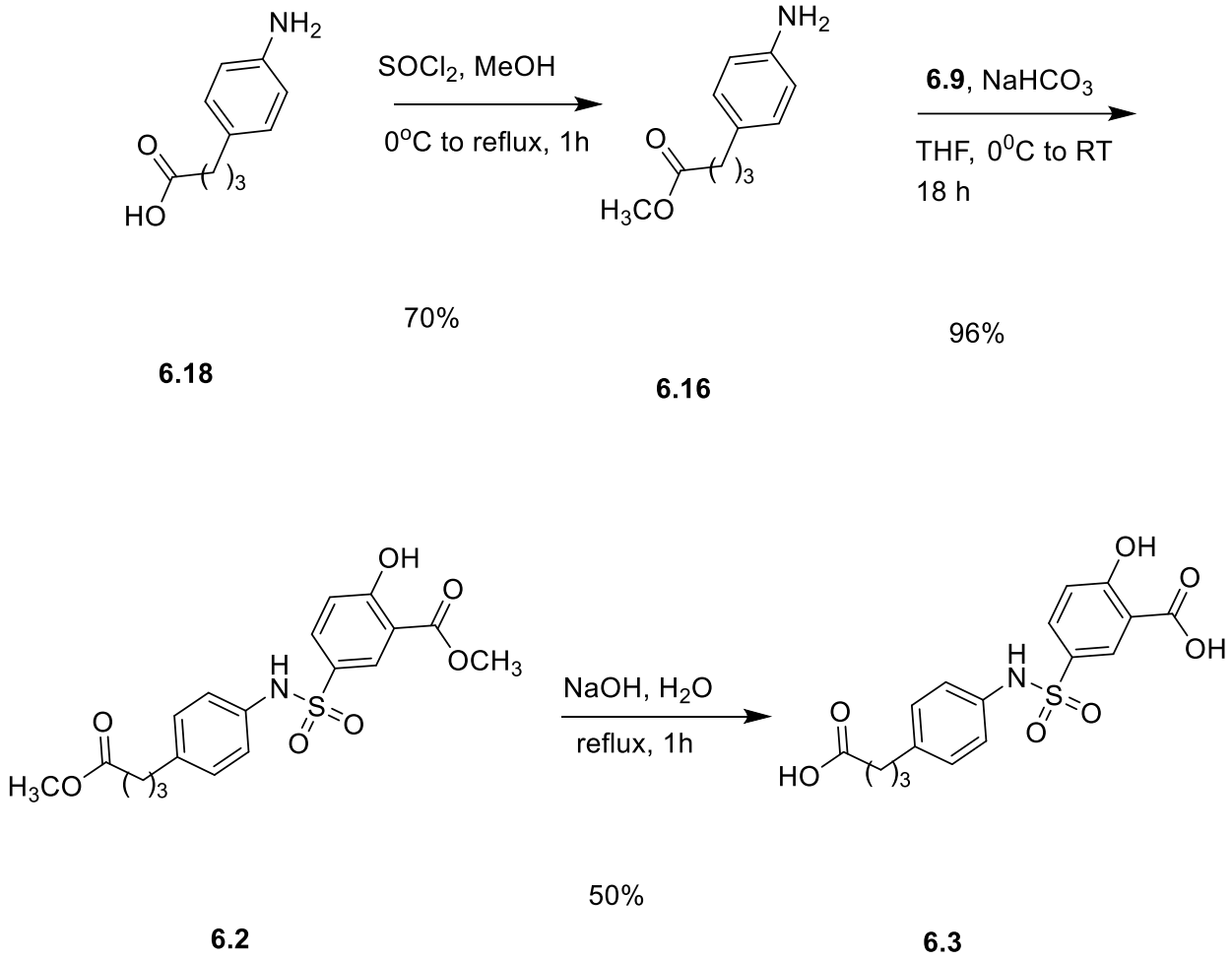

Scheme 6-3: A revised synthetic strategy for **6.1** and **6.3**

6.2.3 **Results for Inhibitors 6.1-6.3**

The methyl ester protected compounds **6.1** and **6.2** were tested against MRSA II-HMGR in an enzymatic assay (Table 6-1). Neither compound showed significant inhibition of the enzyme,

which is to be expected since the methyl protection of the carboxylic acids block interaction with the enzyme active site. The hope was that esterases in bacterial cells would hydrolyze these groups upon crossing of the cell membrane, thus allowing binding of the inhibitors to the active site of II-HMGR. However, both compounds showed an MIC/MBC >256 μM. The 4-carbon free carboxylic acid **6.3** was also tested in both assays. While it exhibited an IC_{50} of 58 μM, the MIC/MBC activity was once again >256 μM. Thus, it performed worse than the 10-carbon equivalent **MH-2.3**. We are awaiting the results of a co-crystal structure to examine the binding pose and determine the source of this reduced activity. These results suggest that membrane permeability was not the problem with **MH-2.3**, but rather the secondary target hypothesis appears more likely.

Table 6-1: Assay results for inhibitors **6.1-6.3**

Inhibitor	IC_{50} (μM)	MIC/MBC (μM)
6.1	>250	>256
6.2	-	>256
6.3	58	>256

6.3 Synthesis of Tail-Group Modified Inhibitors 6.4-6.5

Due to the broad nature of the hydrophobic pocket which engages the 10-carbon aliphatic chain in **DL-3.23**, several modifications to this tail group were chosen (Figure 6-2, **6.4-6.6)** to improve the interaction with the hydrophobic pocket, or to engage polar residues on the edges of this pocket.

6.3.1 Synthetic Approach to Proposed Inhibitor 6.4

One proposal to better engage the hydrophobic pocket of the II-HMGR active sight was to switch from the *para*-alkyl chain as in **DL-3.23** to an *ortho*- chain. Compound **6.4** was proposed as an option to test this theory. The synthetic approach taken is given in Scheme 6-4. Synthesis began with a substitution reaction to couple commercially available 2-iodophenol **6.19** and 4-fluoronitrobenzene **6.20**. After heating this mixture in DMSO in the presence of K_2CO_3 overnight, the di-aryl product **6.21** was obtained in good yield**.** A Pd(II)- and Cu(I)- catalyzed Sonogashira coupling with 1-heptyne gave compound **6.22** in 90% yield. Dual- reduction of the nitrobenzene

and alkyne via catalytic hydrogenation and subsequent coupling with sulfonyl chloride **6.9** gave the methyl ester-protected inhibitor **6.24** in 49% yield. Hydrolysis of this methyl ester with aqueous LiOH gave the final compound **6.4** in 50% yield.

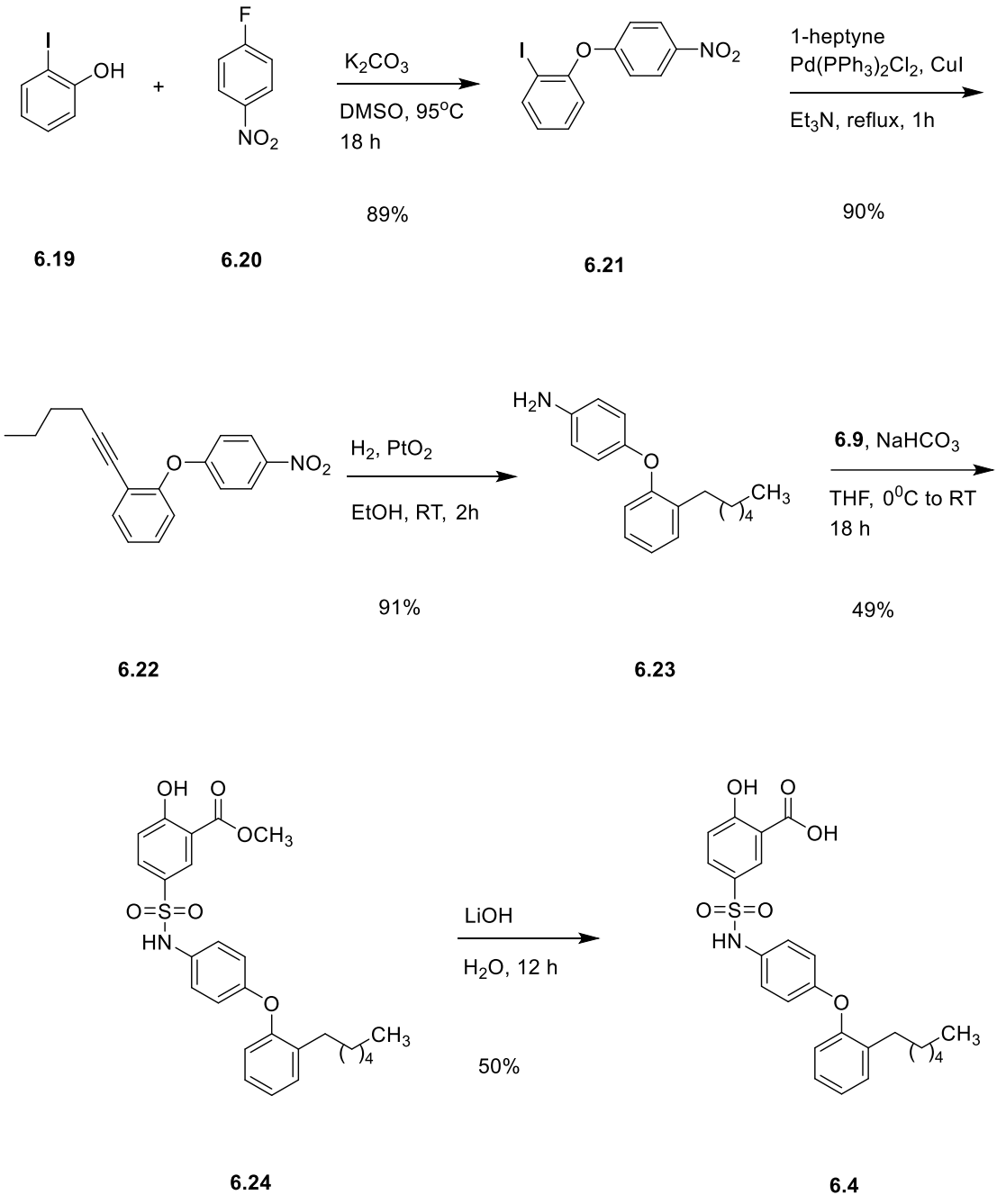

Scheme 6-4: Synthetic approach for **6.4**

6.3.2 **Synthetic Approach to Proposed Inhibitor 6.5**

In examination of the co-crystal structure of **MH-2.4** bound in the active site of II-HMGR, (Figure 6-4), the trans-hydroxyl group engages Asn 95 and Arg 365. However, the IC_{50} of 12 µM is significantly worse than the IC_{50} of 6 µM exhibited by the cyclohexane analogue. We proposed a modification of **MH-2.4** to incorporate a cis-cyclohexanol unit into the tail of the inhibitor to shorten the distance between the two engaged residues and improve the strength of these polar contacts.

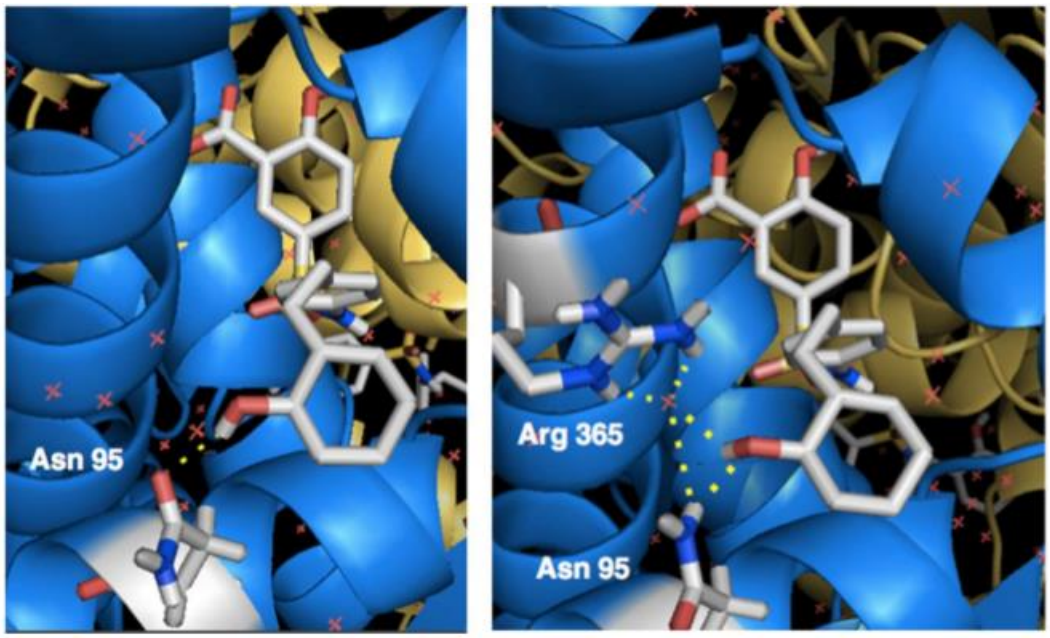

Figure 6-4: Crystal structure of **MH-2.4** bound in the active site of *ef* II-HMGR showing polar contacts [Crystal structure taken from the thesis of Dr. Matthew Hostetler] [24]

Compound **6.5** was proposed as an option to test this theory. This compound differs substantially from the previous II-HMGR inhibitors in that it is no longer flat. The presence of two stereogenic carbons requires a different synthetic approach, outlined in Scheme 6-5. Synthesis began with commercially available cyclohexene oxide **6.25**. Lewis acid activation of the epoxide with $BF_3 \cdot OEt_2$ followed by ring opening with deprotonated TMS-acetylene resulted in the trans-disubstituted cyclohexanol ring. Deprotection of the alkyne-TMS group with K_2CO_3 gave the functionalized cyclohexanol derivative **6.27.**

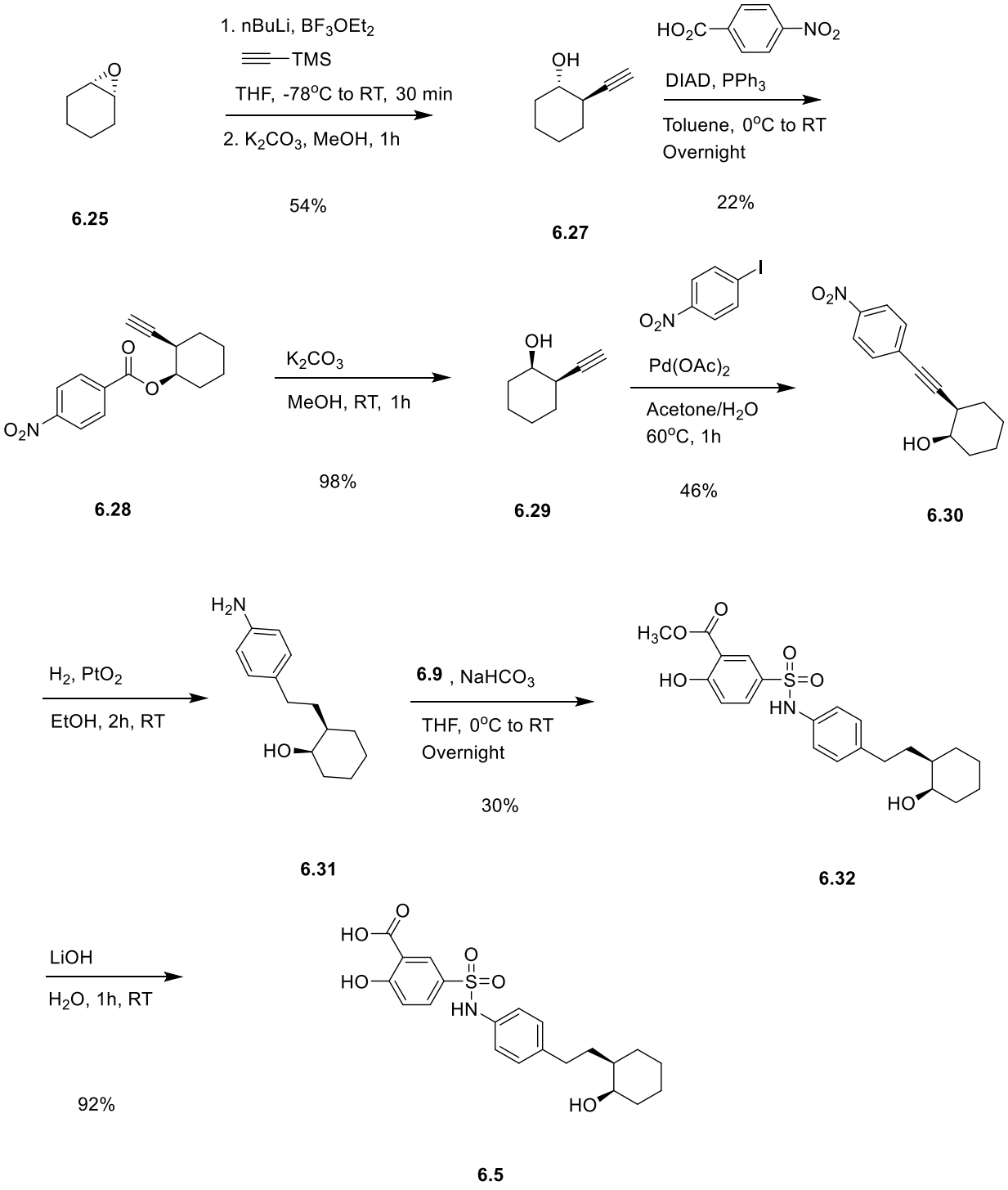

Scheme 6-5: Synthetic approach for **6.5**

To achieve the desired cis-stereochemistry, a Mitsunobu reaction using *para*-nitrobenzoic acid was used to invert the stereochemistry of the hydroxyl, giving the cis-cyclohexanol product **6.29**. A Pd(II)- and Cu(I)- catalyzed Sonogashira coupling with 4-iodonitrobenzene gave compound **6.30.** Simultaneous- reduction of the nitro- and alkyne groups via catalytic hydrogenation and subsequent coupling with **6.9** gave the methyl ester-protected inhibitor **6.32** in 30% yield. Hydrolysis of this methyl ester gave the final compound **6.5** with the desired cis-conformation.

*Assay Results for Proposed Inhibitor **6.5***

The enzyme assay results showed a slight improvement of 9.8 µM, compared with 12 µM from the *trans*-cyclohexanol product previously tested. The co-crystal structure shows the cis-hydroxyl group in closer proximity to the two polar residues, Arg 365 and Asn 95 (Figure 6-5). However, once again the MIC/MBC of >128 shows an inconsistency between the enzymatic and cell assays.

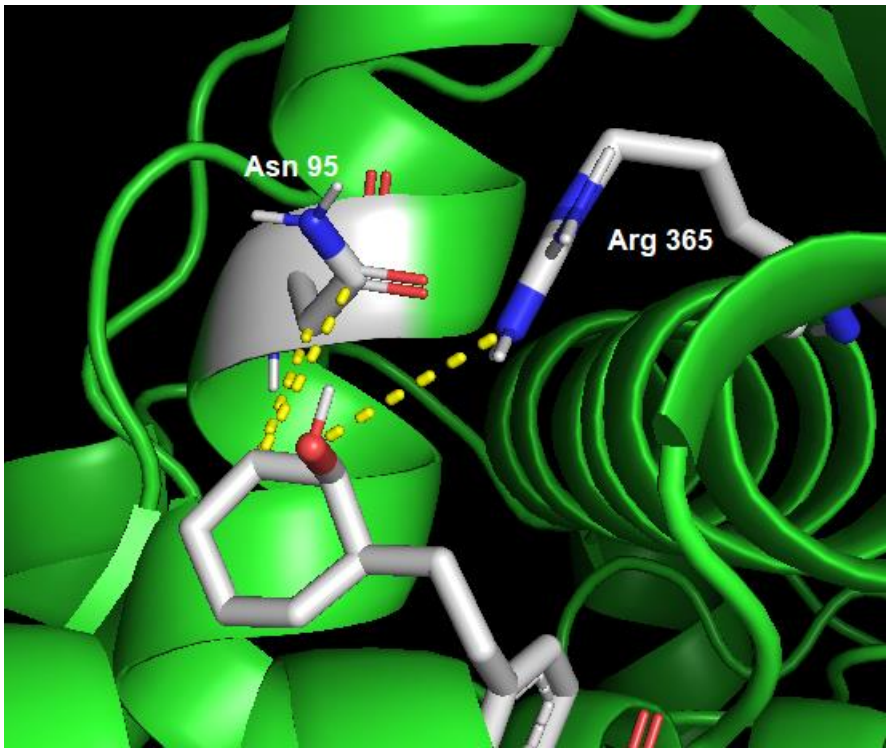

Figure 6-5: Co-crystal structure of **6.5** bound in the active site of *e.f.* II-HMGR

6.3.3 **Synthetic Approach to Proposed Inhibitor 6.6**

When examining a co-crystal structure of **DL-3.23** bound in the II-HMGR active site (Figure 6-6), it was observed that the 10- carbon chain was forced to wrap around itself to engage the hydrophobic pocket present in the active site. To optimize this engagement, **6.6** was proposed. Replacing the 10 carbon chain with a 10-carbon conformationally restricted naphthalene ring reduces the flexibility of the inhibitor, potentially increasing the binding affinity of the modified inhibitor. Synthesis for **6.6** is summarized in Scheme 6-6. Beginning with commercially available 1-iodonaphthalene, a Pd(II) and Cu(I) catalyzed Sonogashira coupling with TMS-Acetylene, followed by a TMS deprotection and a second Sonogashira coupling with 4-iodonitrobenzene gave compound **6.36**. Simultaneous-reduction of the nitro- and alkyne groups via catalytic hydrogenation and subsequent coupling with **6.9** gave the methyl ester protected inhibitor **6.38** in 57% yield. Hydrolysis of this methyl ester gave the final compound **6.6** in 94% yield.

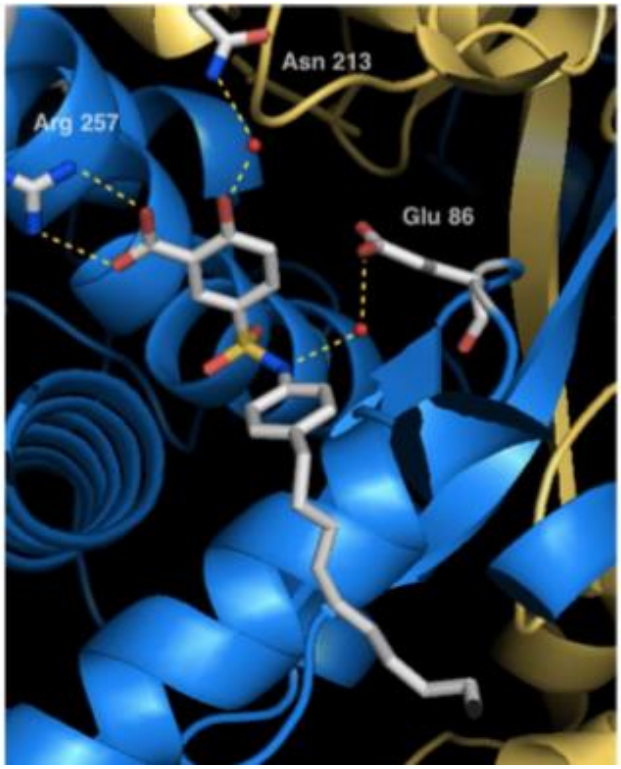

Figure 6-6: Co-crystal structure of DL-1.6f bound to *e.f.* II-HMGR [Crystal structure taken from the thesis of Dr. Daneli Lopez-Perez]

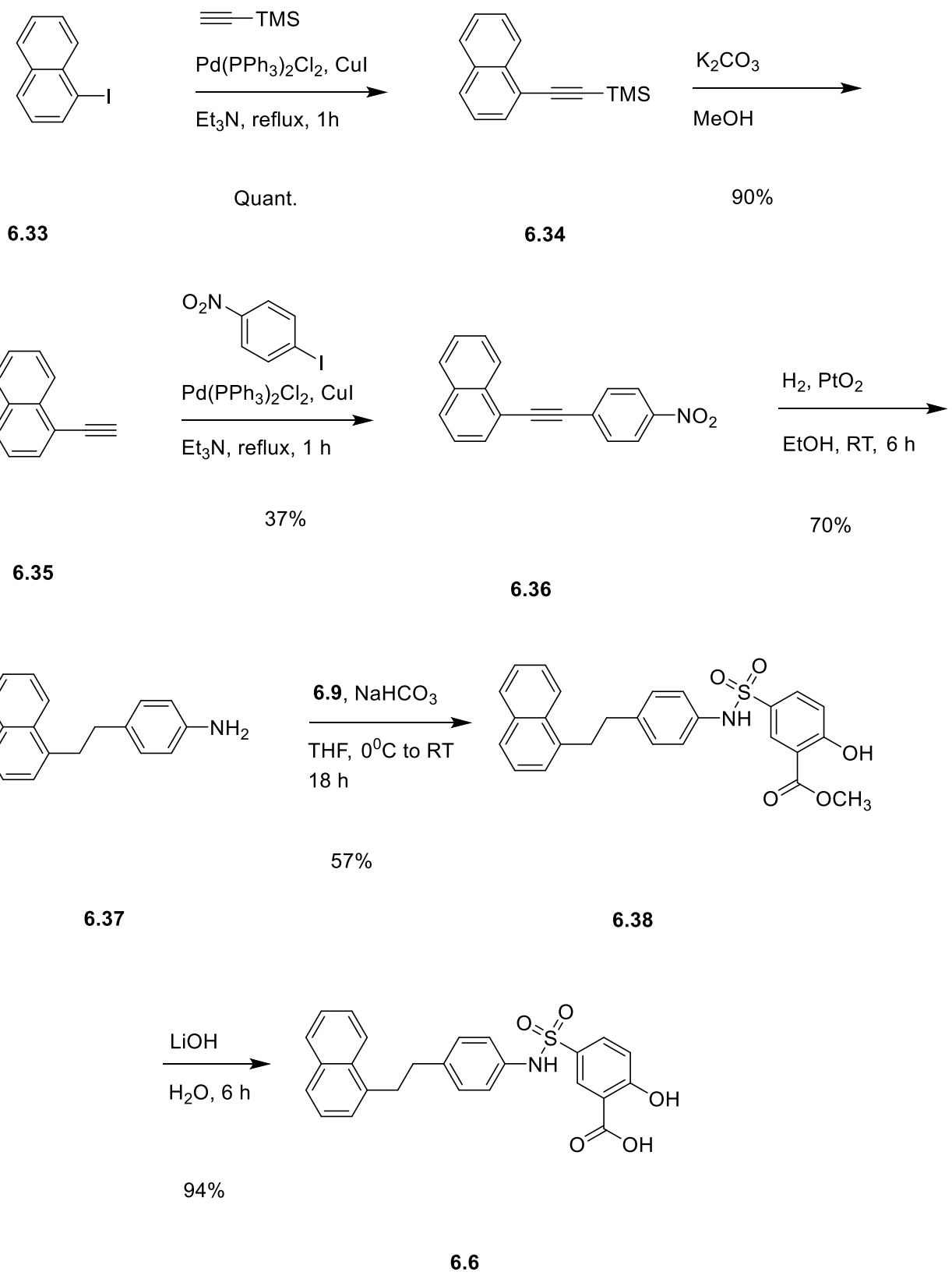

Scheme 6-6: Synthetic approach for **6.6**

6.3.4 **Assay Results for Proposed Inhibitors 6.4-6.6**

This series of inhibitors was tested against *e.f.* II-HMGR and MRSA cell lines. The results are shown in Table 6-2. The implications of **6.5** were discussed in section 6.3.2. The enzymatic and antimicrobial activity of **6.4** and **6.6** were both shown to be comparable to the best inhibitors synthesized thus far. We are awaiting co-crystal structures of these inhibitors bound in the active site of II-HMGR to better ascertain modifications to improve these values.

Table 6-2: Enzyme and cell assay results for proposed inhibitors **6.4-6.6**

Inhibitor	IC_{50} (µM)	MIC/MBC (µM)
6.4	23	16
6.5	9.7	>128
6.6	16	64

6.4 **Synthesis of Head-Group Modified Inhibitors 6.7 and 6.8**

The next structural modification tested was to alter the headgroup structure of the original inhibitor design. Two such proposals were made: to reverse the S- and N- portions of the sulfonamide (**6.7**) or replace the sulfonamide with an amide group (**6.8)**. Both could be achieved through synthesis of the same headgroup, **6.40** (Scheme 6-7)**.** Starting from commercially available methyl salicylate, an EAS Nitration reaction gave the desired nitro-substituted ring **6.39** in 30% of the desired regioisomer. Reduction of this nitro group via platinum-catalyzed hydrogenation gave the headgroup **6.40**, ready to be coupled to various inhibitor tail groups.

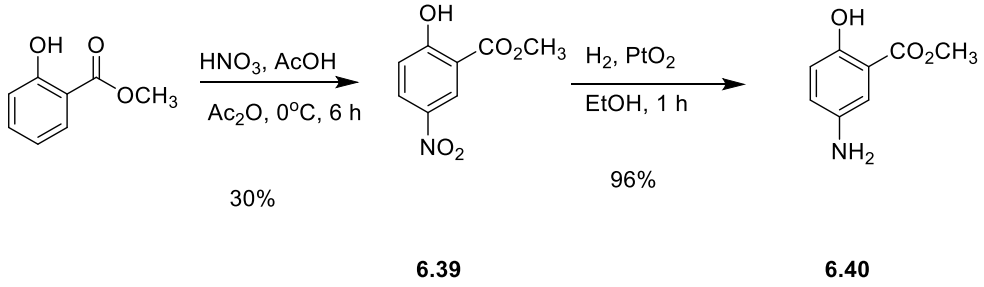

Scheme 6-7: Synthesis of alternate headgroup **6.40**

6.4.1 **Synthetic Approach to Proposed Inhibitor 6.7**

The first headgroup structural variation proposed was to reverse the orientation of the central sulfonamide group that is present in **DL-3.23** The synthesis for this proposed compound is outlined in Scheme 6-8. It was determined experimentally that the sulfonamide group must be formed early in the synthesis. Beginning with commercially available 4-bromobenzenesulfonyl chloride **6.46**, a sulfonamide coupling was conducted with amine **6.40** to yield the sulfonamide **6.47**. A Sonogashira coupling with 1-decyne followed by platinum-catalyzed hydrogenation gave compound **6.48**. The hydrogenation required 48 hours to reach completion, in stark contrast to the 2 hours required to reduce the analogous alkyne of **DL-3.23**. Use of a stronger catalyst such as Raney Ni may be employed to minimize the required reaction time. Hydrolysis of the methyl ester using aqueous LiOH produced the final proposed inhibitor **6.7**.

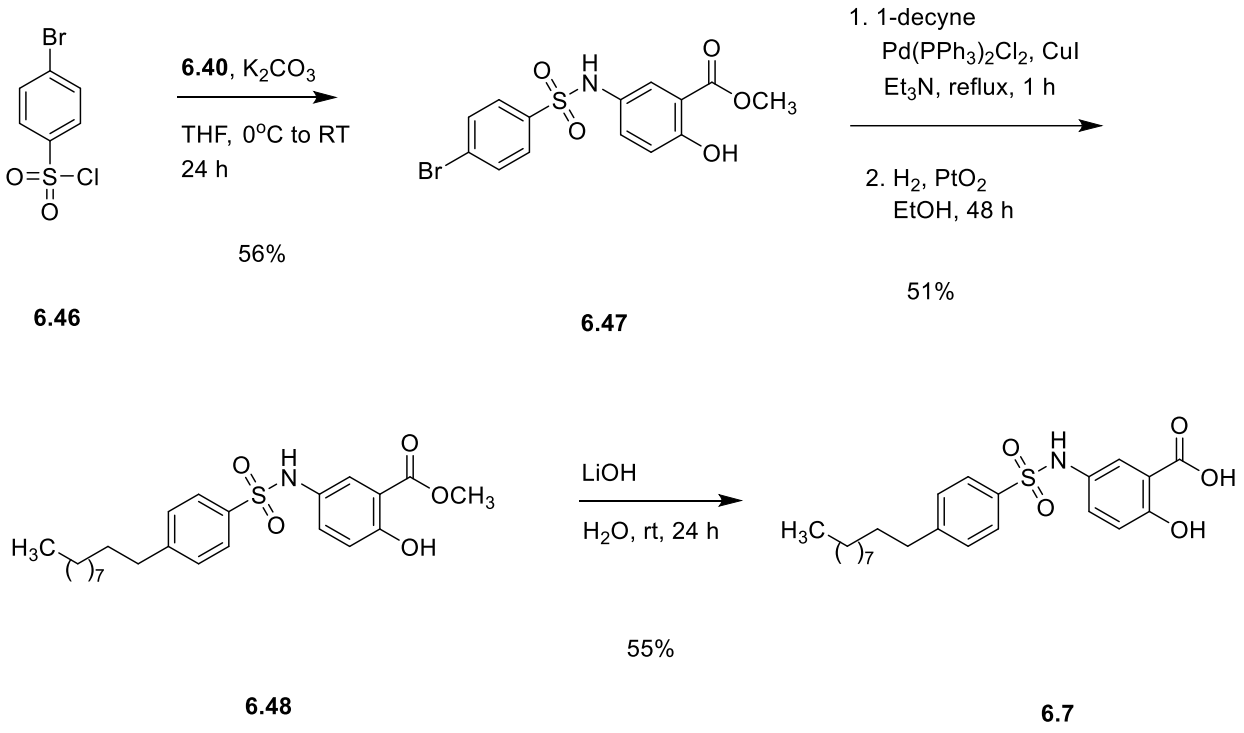

Scheme 6-8: Synthetic approach for inhibitor 6.42

6.4.2 **Synthetic Approach to Proposed Inhibitor 6.8**

An inhibitor was proposed that is structurally analogous to **DL-3.23**, except the sulfonamide group is replaced with an amide group. The key interactions shown between the phenol with Asn 213 and the carboxylic acid with Arg 257 will remain intact (Figure 6-7). However, the angle between the two aromatic rings should change significantly when switching from the tetrahedral 4-coordinate sulfur atom to the planar 3-coordinate sp^2 hybridized carbonyl carbon. This should result in the aromatic ring of the tail group occupying a slightly different space in 3-dimensions.

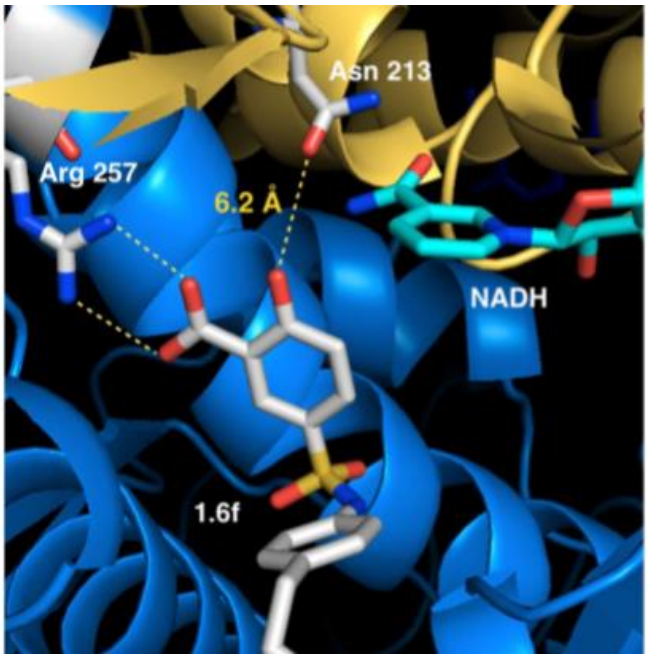

Figure 6-7: Co-crystal structure of **DL-3.23** in the active site of II-HMGR showing key headgroup interactions [Crystal structure taken from the thesis of Dr. Daneli Lopez-Perez]

The synthesis of this inhibitor is laid out in Scheme 6-9. Beginning with commercially available 4-iodobenzoate **6.42**, a Pd(II)- and Cu(I)- catalyzed Sonogashira coupling with 1-decyne gave **6.43** in 97% yield. Catalytic hydrogenation to reduce the alkyne, followed by hydrolysis of the methyl ester in NaOH yielded the free acid **6.44**. Formation of the acid chloride using oxalyl chloride, followed by coupling with amine **6.40** gave the amide **6.45** in 50% yield over 2 steps. Finally, hydrolysis of the headgroup methyl ester with NaOH gave the final amide-based inhibitor **6.41.**

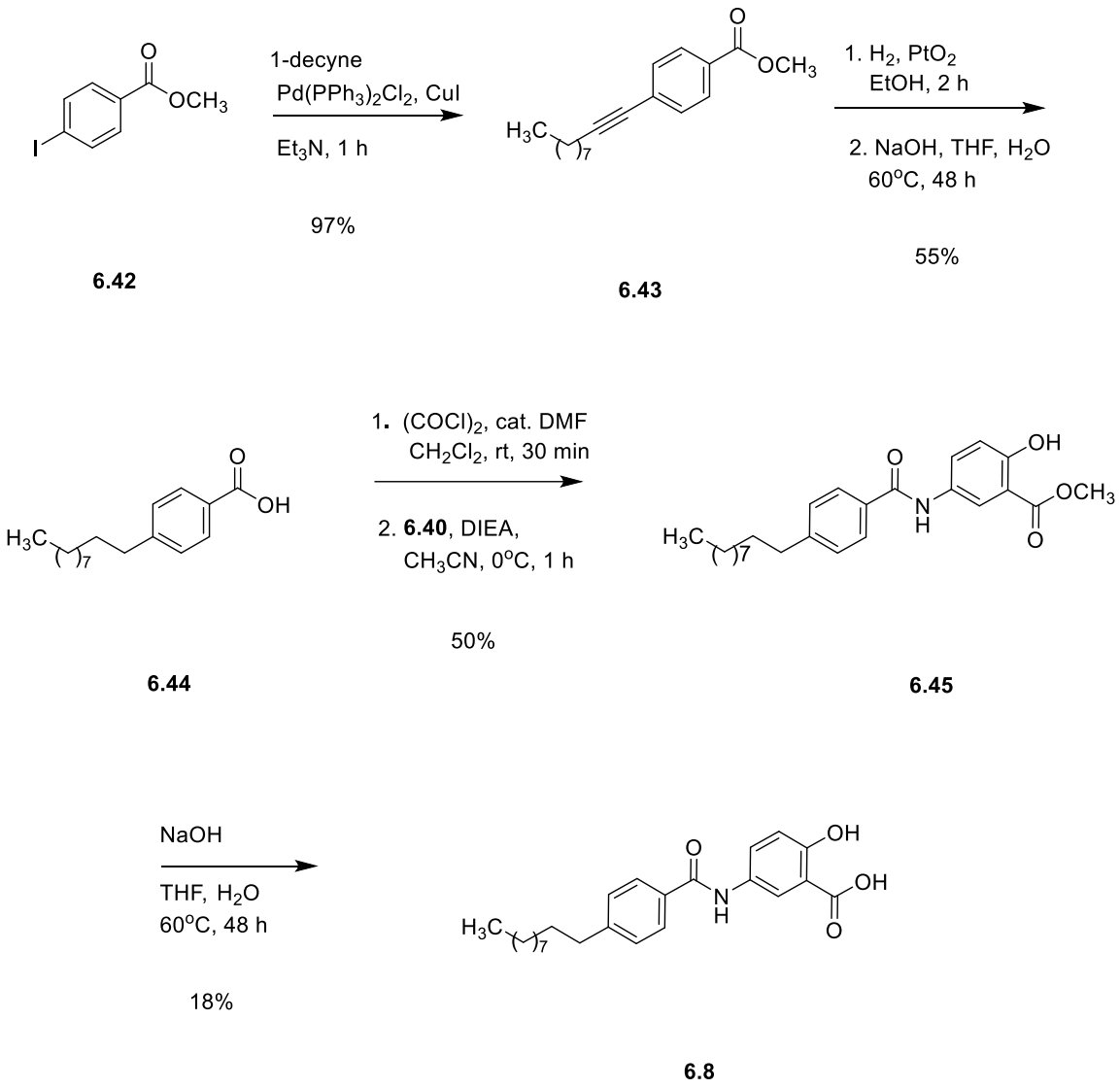

Scheme 6-9: Synthetic approach to inhibitor **6.41**

6.4.3 **Assay Results for Proposed Inhibitors 6.7 and 6.8**

Inhibitor **6.7**, reversed sulfonamide version of **DL-3.23** showed nearly identical activity to the original inhibitor in both enzymatic and cell-based assays (Table 6-3). We are awaiting results of a co-crystal structure of this inhibitor bound in the active site to determine if the interactions are identical to that of **DL-3.23**, or if this modification has engaged other residues that could potentially be combined with previous polar contacts to optimize the inhibitor structure. Inhibitor **6.8** also showed excellent enzyme activity with an IC_{50} of 6.8 µM. However, erosion of the MIC/MBC values suggest that perhaps the increased polarity of the amide group reduces cell-

membrane permeability. We are also awaiting a crystal structure of this inhibitor to determine if the amide group engages the same polar contacts as the sulfonamide, and if the 3-dimensional space occupied by the aliphatic chain is significantly altered.

Table 6-3: Assay results for proposed inhibitors **6.7** and **6.8**

Inhibitor	IC_{50} (µM)	MIC/MBC (µM)
6.7	15	16
6.8	30	>128

6.5 Penicillin Re-sensitization

Further evidence to support the secondary target hypothesis was found through a Penicillin Re-sensitization Assay of MRSA. MRSA utilizes the virulence factor *staphylloxanthin* in the maturation of penicillin binding protein PB2a, and it has shown to be critical to enzyme function.[58] Without PB2a, bacteria become susceptible to penicillin and other beta-lactam-containing. antibiotics. On the basis of a previously published study using statin drugs to inhibit the biosynthesis of *staphylloxanthin* and thus re-sensitizing MRSA to penicillin,[58] we tested several II-HMGR inhibitors that previously showed no antimicrobial activity. Incubation of *S. aureus* with penicillin and oxacillin in the presence of compounds **MH-2.2, MH-2.3,** and **6.2** resulted in a marked increase in MIC (Table 6-4).

Table 6-4: Penicillin re-sensitization assay

Drug	MRSA 300 MIC (uM)	MRSA 400 MIC (uM)
Penicillin	24	48
Oxacillin	20	20
MH-2.2	128	-
MH-2.3	>256	-
6.2	>256	-
Vancomycin	0.3	0.7
Linezolid	3	3
Penicillin + MH-2.2	<6	6
Oxacillin + MH-2.2	<1.2	<1.2
Penicillin + MH-2.3	24	24
Oxacillin + MH-2.3	10	10
Penicillin + 6.2	24	24
Oxacillin + 6.2	<1.2	<1.2

Vancomycin and linezolid were used as controls. Notably, **MH-2.2** administered in conjunction with oxacillin performed comparably to vancomycin, which is currently used as the last-resort antibiotic used for infections by multi-drug resistant-bacteria.[59] These results also suggest that the less polar compounds are able to cross the membrane, while the more polar compounds struggle to reach the interior of the cell. This is also supported by the fact that **6.2** performed significantly better than **MH-2.3,** suggesting that the dimethyl ester acts as a pro-drug and crosses the membrane as hoped, before esterases convert it back to the di-carboxylic acid **MH-2.3.**

6.6 Conclusion

Eight new inhibitors were synthesized in an effort toward improvement of the original II-HMGR inhibitors. These compounds included variations of **MH-2.3** (**6.1-6.3**), tail-group modifications of **DL-3.23** (**6.4-6.6**), and headgroup modifications of the same (**6.7-6.8**). While several of these modified inhibitors showed promising results in enzyme assays, a continued problem was the lack of correlation between IC_{50} and MIC/MBC values (Table 6-5). Our hypothesis to explain this phenomenon is the potential presence of a secondary target. As we optimized these inhibitors toward the active site of II-HMGR thus improving the IC_{50}, this unknown secondary target may be losing activity, resulting in decreased results when testing against bacteria. The success of these inhibitors to re-sensitize MRSA to penicillin suggest that membrane permeability is not the only explanation for the discrepancy between enzymatic inhibition and antimicrobial activity.

Table 6-5: Assay results for new II-HMGR inhibitors

Inhibitor	IC_{50} (µM)	MIC/MBC (µM)
6.1	>250	>256
6.2	-	>256
6.3	58	>256
6.4	23	16
6.5	9.7	>128
6.6	16	64
6.7	15	16
6.8	30	>128

CHAPTER 7. PROGRESS TOWARD THE IDENTIFICATION OF A SECONDARY TARGET OF KNOWN CLASS-II HMG-COA REDUCTASE INHIBITORS

7.1 Evidence for a Secondary Mode of Action

When comparing the IC_{50} values and MIC/MBC values for submitted inhibitors, it was found that there appeared to be little correlation between the two values. Our theories to explain this unexpected result were two-fold: 1). That insufficient membrane permeability was affecting the inhibitors ability to reach its target and 2). The presence of a secondary target. Hypothesis 1 was addressed by the synthesis of methyl ester protected inhibitors **6.1** and **6.2** to act as pro-drugs, discussed in the previous chapter. The second hypothesis could explain the observed phenomenon if the initial lead compounds **DL 3.23** was targeting another enzyme besides II-HMGR. However, as these inhibitors were optimized toward the active site of II-HMGR, the unidentified secondary target may be losing activity, thus resulting in poorer MIC/MBC values even when the IC_{50} improves.

To further support this hypothesis, some assays were performed in collaboration with the Seleem laboratory. Because II-HMGR is responsible for catalyzing the conversion of HMG-CoA to mevalonate, bacterial cell death should be prevented by addition of exogenous mevalonate. However, this study was conducted and it was found that after toxicity was induced by **DL-3.23** in both MRSA and VRE cells, addition of mevalonate made little difference in the survivability. [55] This supports the hypothesis that this class of II-HMGR inhibitors is acting through a secondary mode of action, thereby remaining effective even when the primary mode of action is blocked.

As a third piece of evidence for the existence of a secondary target, the II-HMGR inhibitors were tested for their ability to re-sensitize antibiotic-resistant bacteria. Although these inhibitors had excellent IC_{50} values when tested directly against II-HMGR, they were unable to kill bacteria on their own. However, they were able to successfully re-sensitize the bacteria to previously resistant antibiotics, suggesting that these compounds do indeed inhibit II-HMGR even within the bacteria. Thus, the presence of a secondary mode of action is a likely explanation for this occurrence.

To identify this potential secondary target, we took two approaches (Figure 7-1). First, a hybrid II-HMGR inhibitor **7.1b** was synthesized that mimics the structure of platensimycin, a known FabF/B inhibitor in gram-positive bacteria. Second, efforts were made toward synthesizing an inhibitor covalently linked to D-biotin, to conduct a streptavidin pull-down assay to hopefully confirm the identity of the elusive secondary target (**7.4** and **7.5**). Additionally, two nucleotide linked inhibitors **7.2** and **7.3** were synthesized to mimic the nucleotide portion of HMG-CoA.

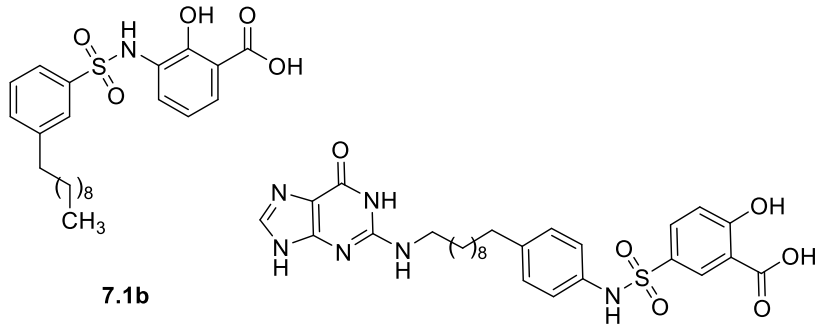

7.1b

7.2

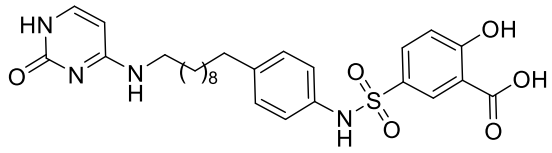

7.3

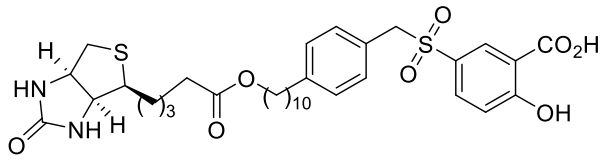

7.4

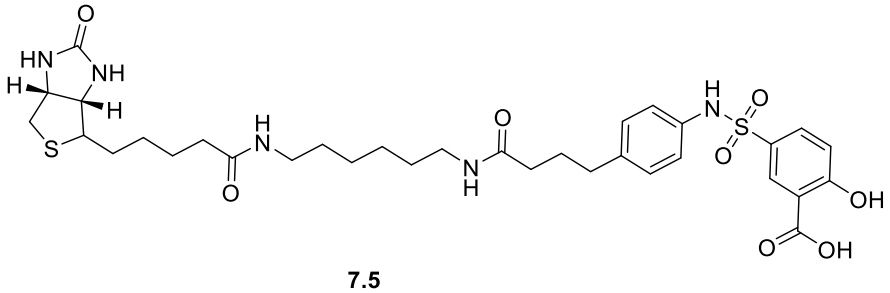

7.5

Figure 7-1: Compounds synthesized in pursuit of secondary-target identification

7.2 Synthesis of HMGR-FabF Inhibitor Hybrid 7.1b

Platensimycin is a well-known natural product that inhibits FabF/B, key enzymes in the biosynthesis of fatty acids in gram-positive bacteria.[60] There are several structural similarities between platensimycin and the inhibitors of II-HMGR discussed herein (Figure 7-2). We propose the synthesis of a hybrid inhibitor that is theoretically optimized toward the active sites of both enzymes, thereby greatly improving the antibacterial activity. Additionally, 2-target antimicrobial compounds will pose difficulties to the development of resistant bacteria, thus minimizing one of the key drawbacks that new antimicrobials often face.

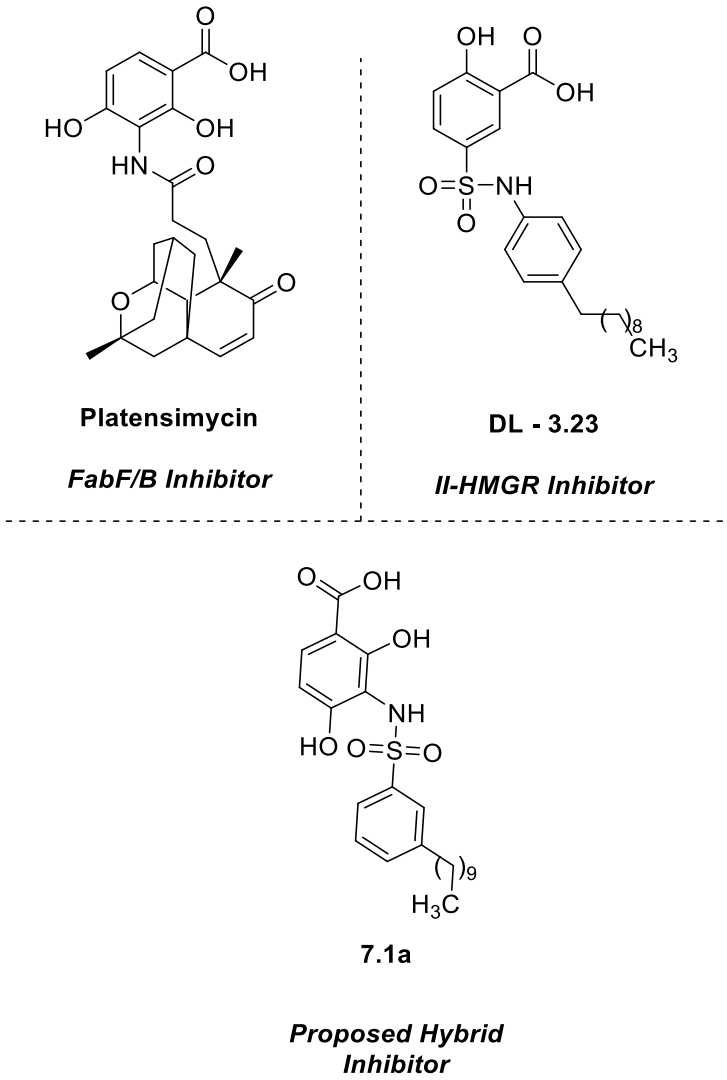

Figure 7-2: Proposal for an inhibitor hybrid betwen **3.23** and platencimycin

The platensimycin-mimicking headgroup for **7.1a** was synthesized according to literature procedure (Scheme 7-1). Beginning with commercially available 2,4-dihydroxybenzoic acid **7.6**, a Fisher esterification was used form methyl ester **7.7**. An electrophilic aromatic substitution nitration reaction resulted in **7.8** in 30% yield. The free phenol groups were then protected as either MOM **7.9** or methyl ethers **7.11**, followed by reduction of the nitro group with catalytic hydrogenation to yield **7.10** and **7.12**, respectively.

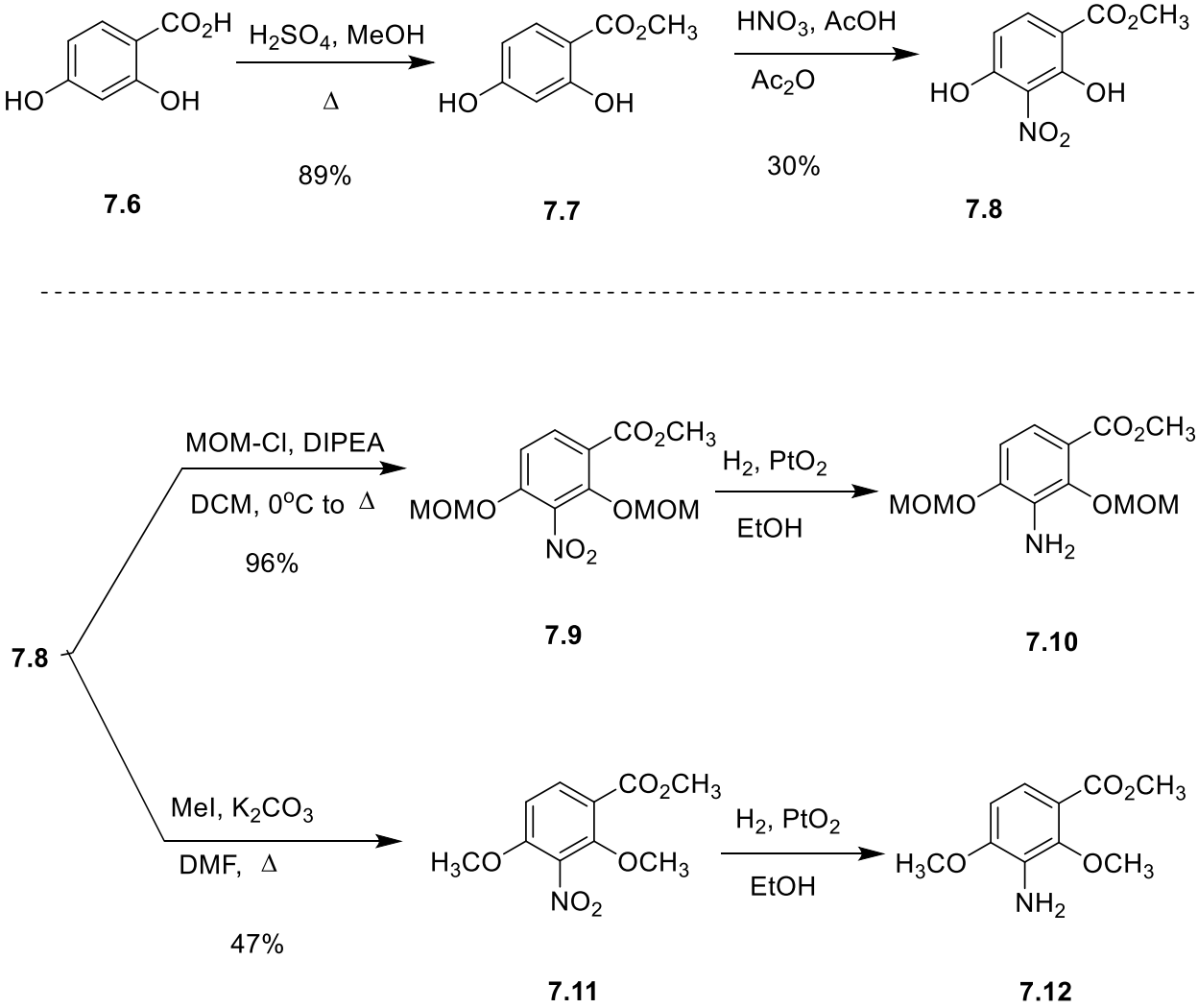

Scheme 7-1: Synthesis of platensimycin headgroup

7.2.1 Synthesis of 7.1a: First Synthetic Approach to the Proposed Hybrid-Inhibitor

The tail group designed to mimic previous II-HMGR inhibitors has proved more challenging to synthesize. The first approach was to transform commercially available 3-nitrosulfonic acid sodium salt **7.13** into the needed group **7.30** to then be coupled with previously prepared **7.10/7.12** to yield the desired inhibitor **7.1a** (Scheme 7-2).

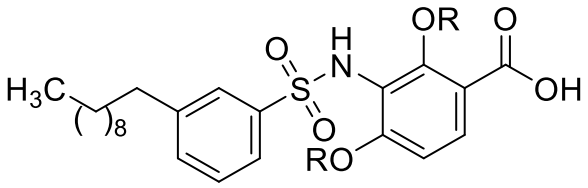

7.1a

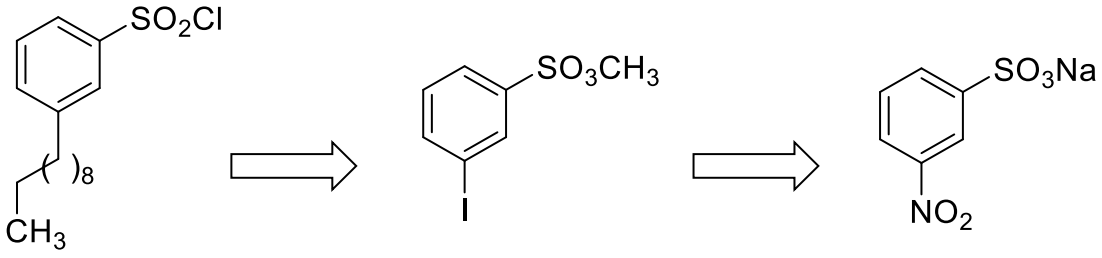

7.30 **7.15b** **7.13**

Scheme 7-2: First general approach to the synthesis of **7.1a**

Due to the highly polar nature of this reagent, it was determined that methylation of the sulfonic acid would make other synthetic transformations and subsequent purifications easier to accomplish. Six different conditions were tested to methylate the sulfonic acid **7.15** (Scheme 7-3), but none of the conditions tried resulted in formation of the desired product. Using the Sandmeyer reaction, we were able to successfully install a *meta*-iodo substituent, however the

subsequent Sonogashira coupling to yield **7.14** produced a complex mixture from which the desired product could not be extracted. Due to the difficult nature of working with and purifying the extremely polar sulfonic acid group, it was determined that a different synthetic approach was needed to bypass this functional group.

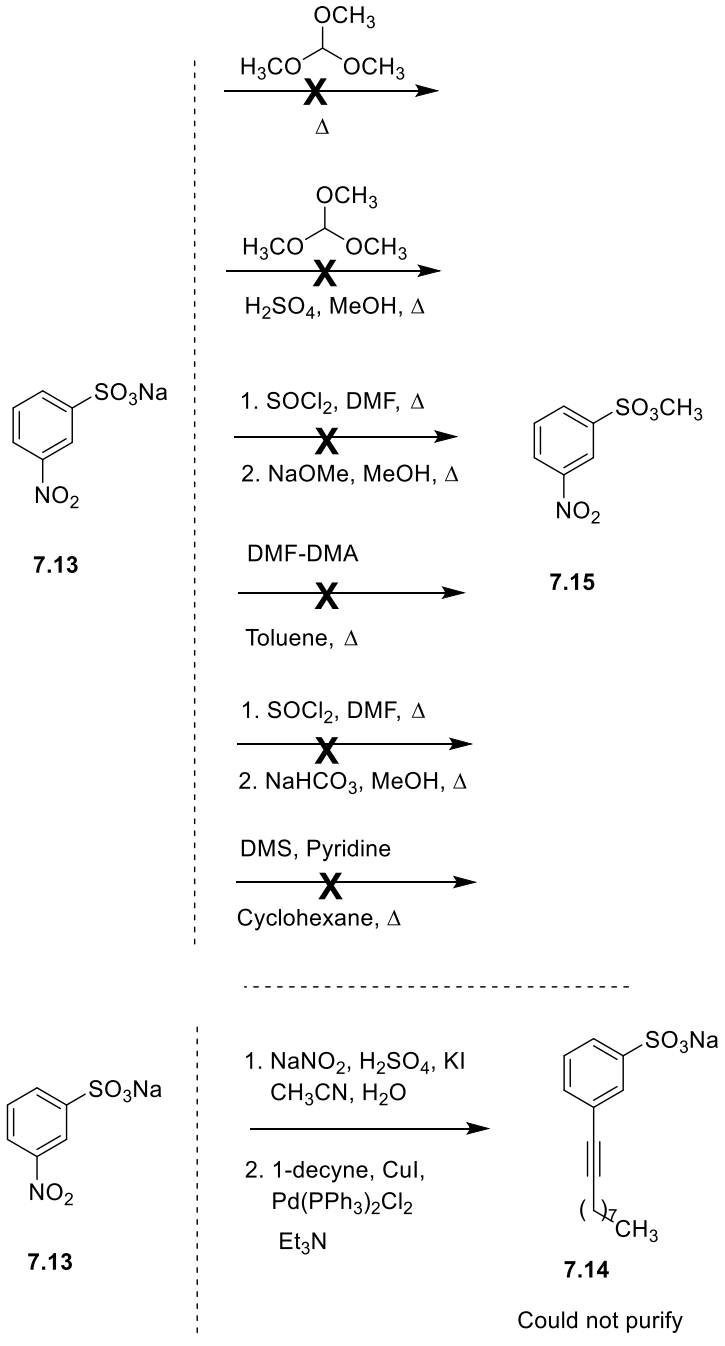

Scheme 7-3: Screening of conditions to methylate 3-nitrobenzene sulfonic acid

7.2.2 **Synthesis of 7.1a: Early Formation of Sulfonamide**

The proposed solution was to form the sulfonamide early in the synthesis, bypassing the presence of the sulfonic acid group later on (Scheme 7-4). This results in easier purification through standard methods, as the molecule would no longer be excessively polar.

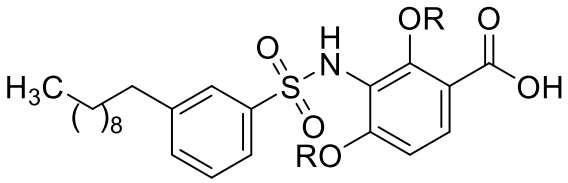

7.1a

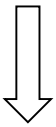

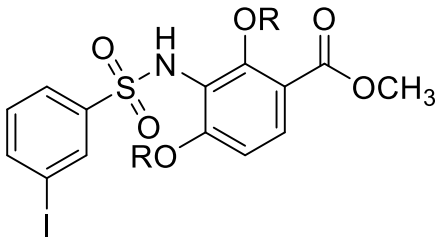

7.18b

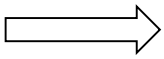

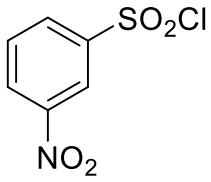

7.16

Scheme 7-4: Second synthetic approach to the synthesis of the proposed hybrid compound

Commercially available 3-nitrobenzenesulfonyl chloride **7.16** proved an excellent starting position for this strategy (Scheme 7.5). However, coupling conditions with the unprotected headgroup **7.17** and the MOM- ether-protected headgroup **7.10** resulted in rapid hydrolysis of the sulfonyl chloride **7.16**. Coupling with the methoxy-protected head group **7.12** produced the coupled product, but only in 10% yield. Due to the highly electron-withdrawing nature of the nitro substituent on **7.16** in combination with the sterically hindered aniline, hydrolysis of the sulfonyl chloride occurs too rapidly to form useful amounts of the sulfonamide product **7.18**. It seemed likely that removal of the nitro- group prior to sulfonamide coupling was necessary to obtain the desired product.

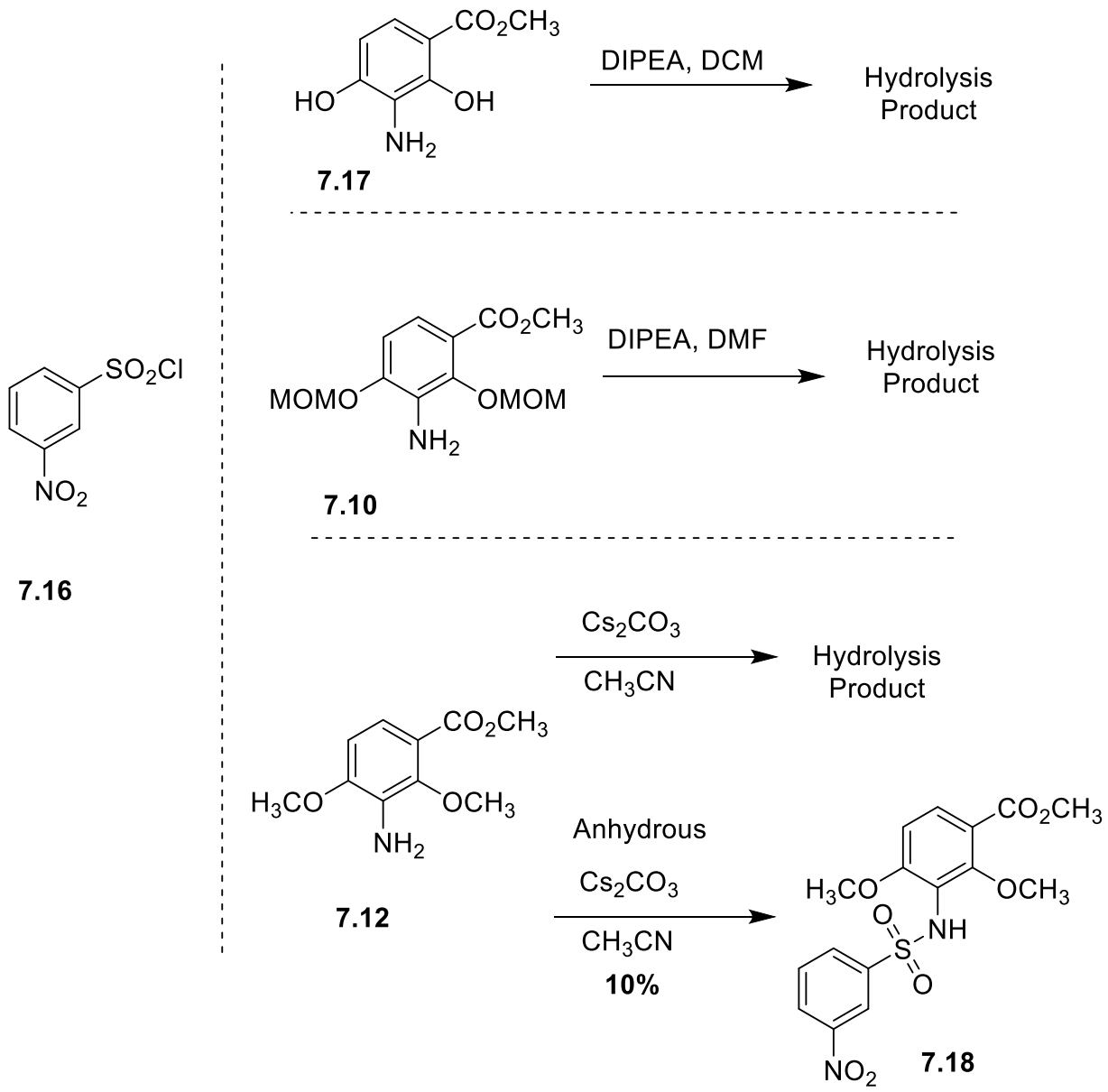

Scheme 7-5: Screening of conditions for sulfonamide couplings of *m*-nitrobenzene sulfonyl chloride with prepared headgroups

7.2.3 **Synthesis of 7.1a: Thiol Oxidation**

A new approach present itself in the form of 3-aminothiophenol **7.19** (Scheme 7-6). By this approach, the non-polar thiol functional group could be carried through the installation of the

alkyl chain, followed by subsequent oxidation of the thiol to install the sulfonyl chloride group needed for sulfonamide coupling.

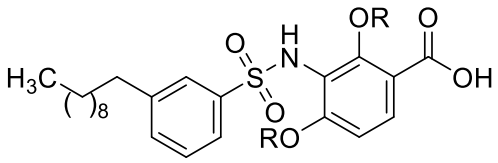

7.1a

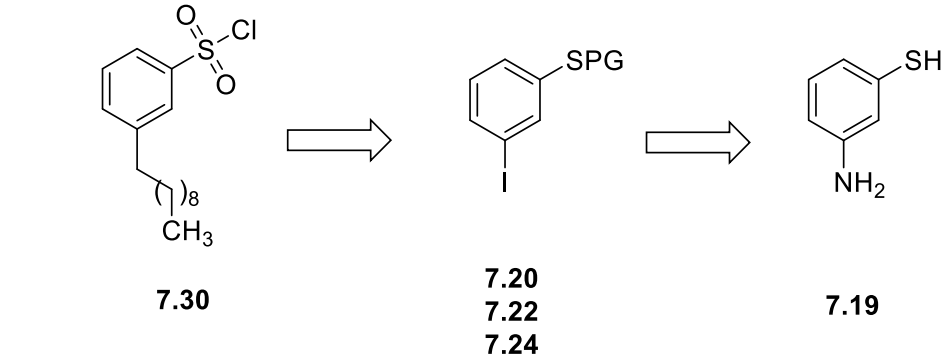

7.30 **7.20** **7.22** **7.24** **7.19**

Scheme 7-6: Oxidation of thiol group to access the proposed hybrid-inhibitor **7.1a**

Various thiol protecting conditions were attempted (Scheme 7-7). First, the disulfide **7.20** was formed by heating **7.19** in DMSO. However, the disulfide turned out to be incompatible with the harsh conditions of the Sandmeyer reaction applied at the next step to install the meta-iodo group for **7.21**. Next, an Acm-protecting group was installed on the thiol using acetamidomethyl hydroxide to yield **7.22**. However, it was discovered diazotization conditions can cause deprotection of the Acm-protected thiol. We hypothesize that this unwanted deprotection occurs through diazotization of the amide in the Acm-protecting group. This causes a deprotection, leaving a free thiol once again.

Finally, benzyl bromide was tested as a protecting group to form **7.24**. However, this protecting group also proved incompatible with the harsh conditions of the Sandmeyer reaction. This is most likely due to the due to the exceedingly electrophilic nature of the benzylic carbon, allowing nucleophilic attack at this position. Upon exhaustion of potential acid-stable thiol protecting groups, it was determined that a new approach was needed to access the desired functional groups.

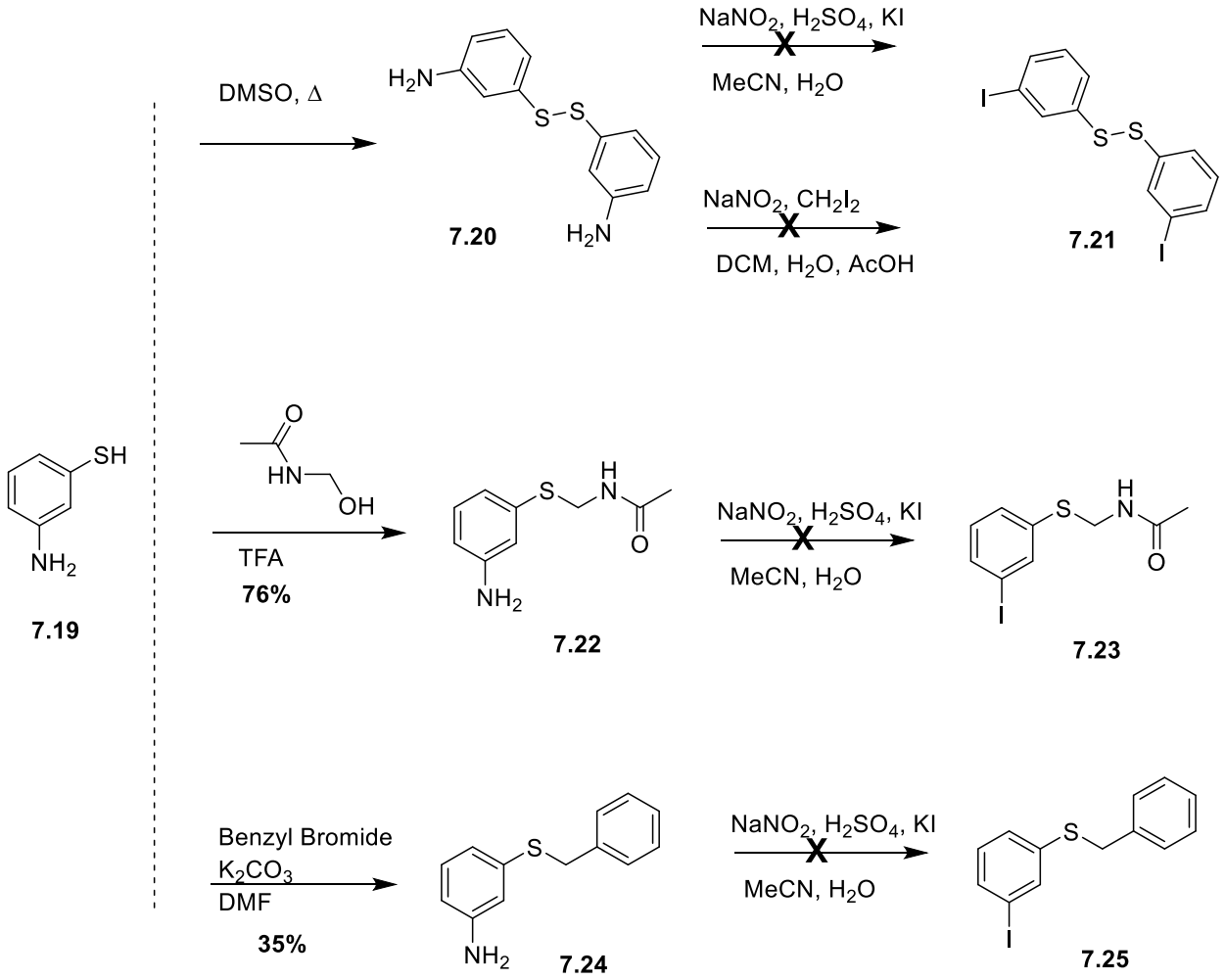

Scheme 7-7: Screening of conditions to protect the thiol group in **7.19**

7.2.4 **Synthesis of 7.1a: Late-Stage Thiol Installation**

Due to the harsh conditions of the Sandmeyer reaction needed to install the iodo- group for attaching the alkyl chain, it was determined that conducting this reaction early on in synthesis may

be a superior approach. The next strategy examined was to begin with 3-nitroaniline **7.26** and install the iodo- group first (Scheme 7-8). Upon alkylation, the amine **7.28** could then theoretically be oxidized to the needed sulfonyl chloride group in **7.30**.

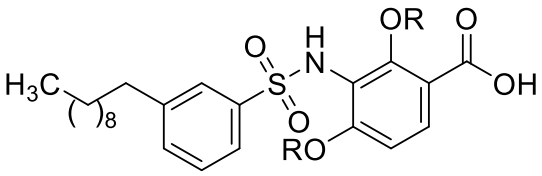

7.1a

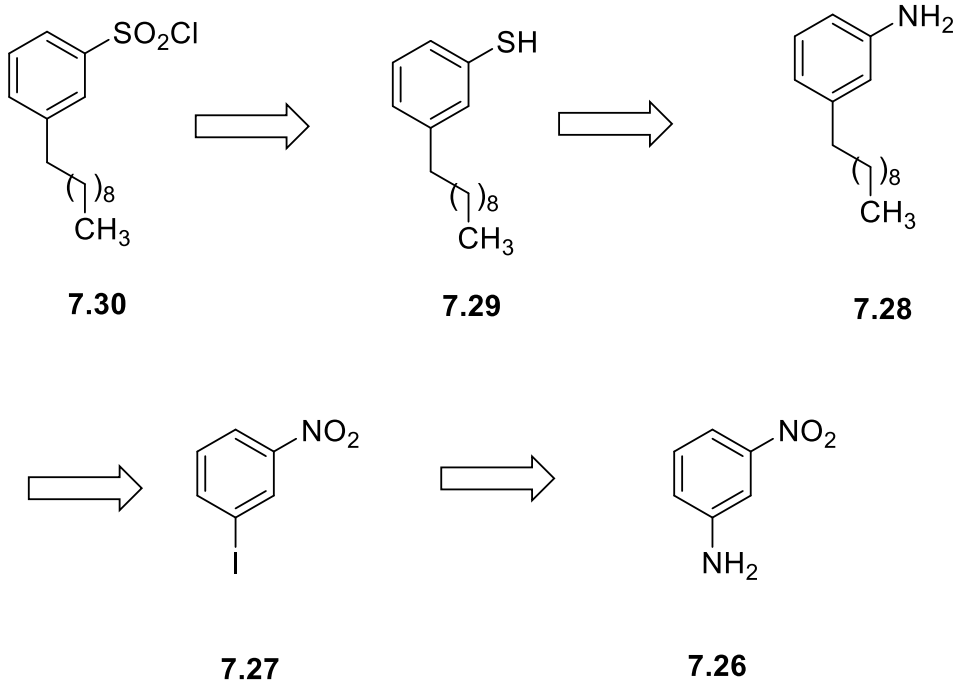

7.30 **7.29** **7.28**

7.27 **7.26**

Scheme 7-8: Synthetic access of **7.1a** through late-stage thiol installation

The synthetic steps to accomplish this transformation is shown in Scheme 7-9. Beginning from commercially available 3-nitroaniline **7.26,** conversion to 3-iodonitrobenzene **7.27** was

accomplished via the Sandmeyer reaction. Subsequent Sonogashira coupling with 1-decyne followed by simultaneous reduction of the alkyne and nitro group via catalytic hydrogenation yielded 3-decylaniline **7.28**. Diazotization of the aniline followed by exposure to ethyl xanthate did not yield the desired thiol group; however, exposure of the diazonium ion to thiourea followed by hydrolysis gave the desired 3-decylthiophenol **7.29**. Following successful installation of this thiol group, subsequent oxidation is required install the desired sulfonamide group.

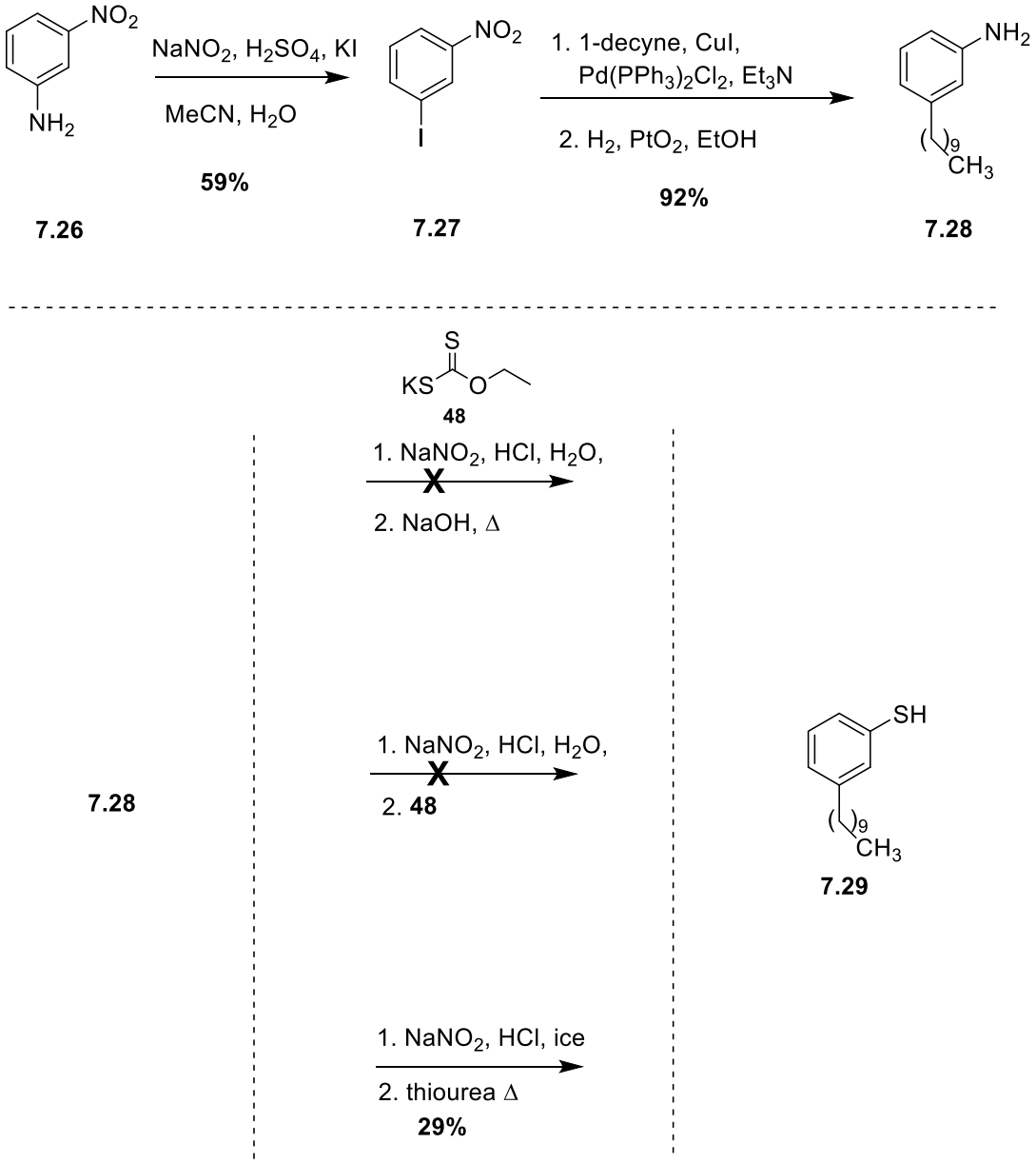

Scheme 7-9: Synthesis of 3-decylthiophenol

Numerous oxidation conditions were screened to transform the thiol **7.29** either directly to sulfonyl chloride **7.30**, or to first oxidize to sulfonic acid **7.31** (Scheme 7-10) However, none of these conditions proved successful. After exhaustion of all plausible oxidation conditions, it was determined that yet another approach may be necessary to successfully synthesize the desired inhibitor.

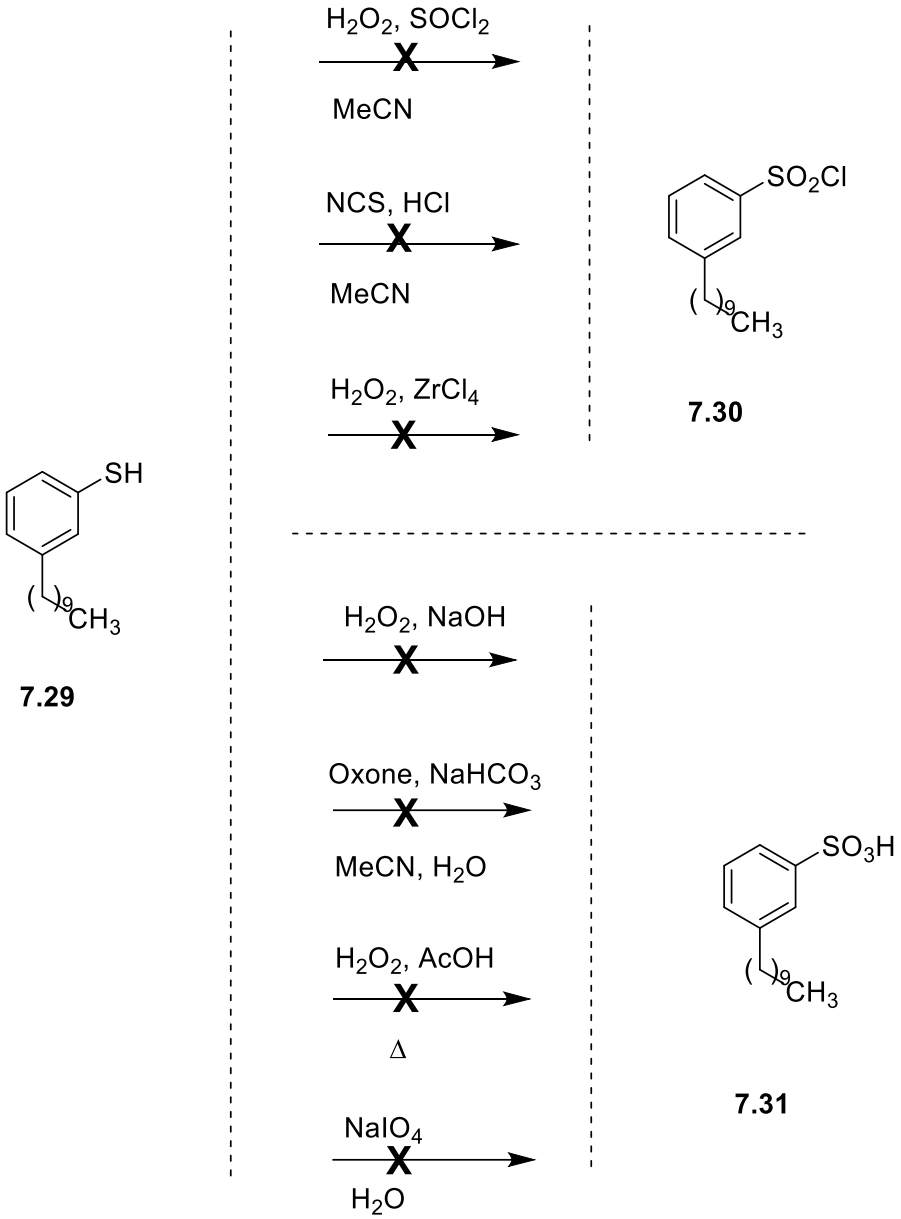

Scheme 7-10: Screening of conditions for thiol oxidation

7.2.5 **Synthesis of 7.1a: Access of Sulfur- Based Functional Groups via Carbon Nucleophile**

An alternative approach to accessing various sulfur- containing functional groups at the desired position was taken, starting from 3-bromoiodobenzene **7.32** (Scheme 7-11). We proposed the formation of a carbon nucleophile at the site of bromine in **7.33**, followed by addition of an electrophilic source of sulfur to directly install the needed functional group.

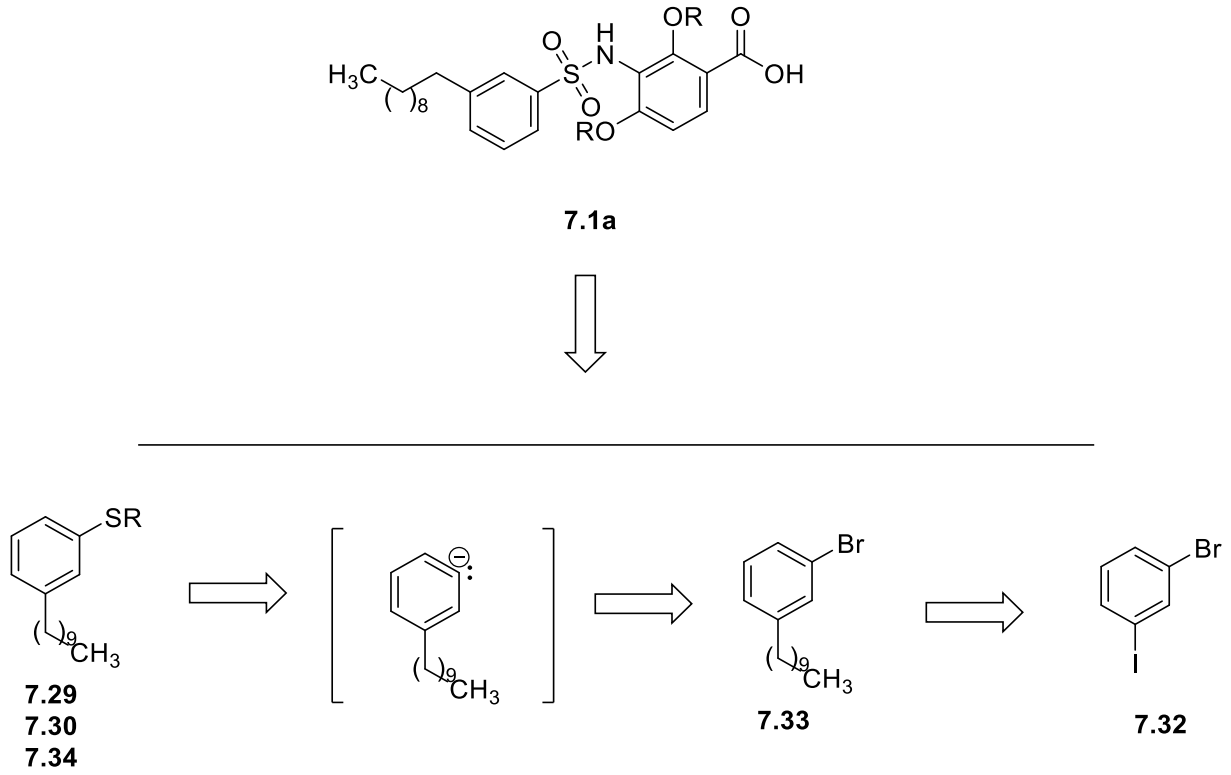

Scheme 7-11: Access of sulfur- group via formation of a carbon nucleophile

A regioselective Sonogashira coupling between the aryl iodide and 1-decyne was conducted, taking advantage of the faster reaction times of aryl iodides when compared with aryl bromides to obtain selectivity (Scheme 7-12). Reduction of the alkyne via catalytic hydrogenation yielded 3-decylbromobenzene **7.33**. Using nBuLi for a Li-Br exchange followed by exposure to S_8 as an electrophilic sulfur source yielded only a complex reaction mixture containing 4 different aromatic compounds, all of which were too non-polar to separate by flash column chromatography. Use of sulfur trioxide-pyridine as the electrophilic sulfur source also failed to produce a usable amount of the desired product.

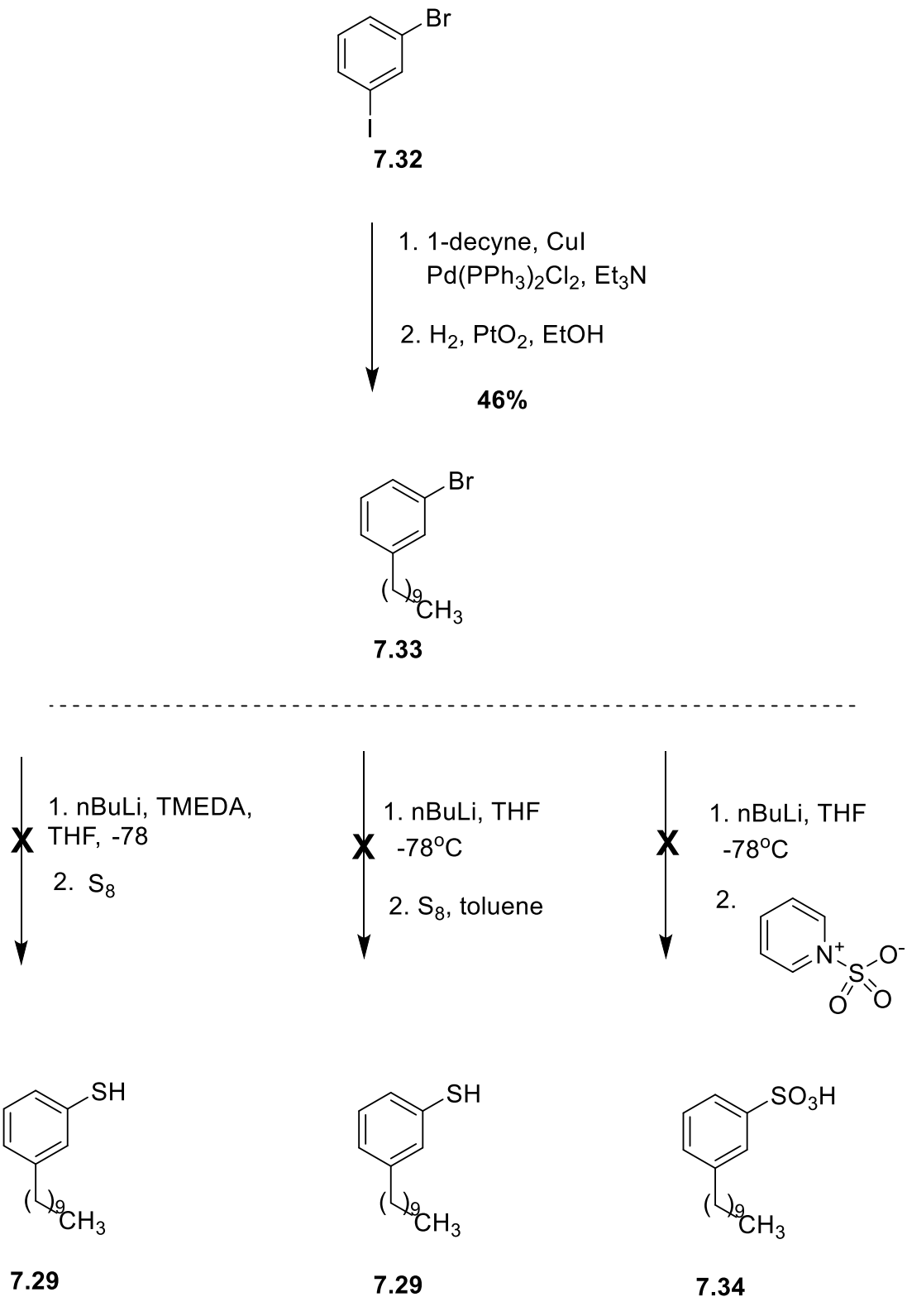

Scheme 7-12: Lithium-Halogen exchange to install sulfur- based functional groups

7.2.6 **Synthesis of 7.1a: Minimizing Synthetic Manipulations of Sulfur Groups**

Due to the repeated difficulties faced in late-stage access and manipulation of sulfur-based functional groups, it was determined that the starting material must contain the sulfonyl chloride group from the beginning, since the electronics of the ring system do not seem to allow for installation at a later point (Scheme 7-13).

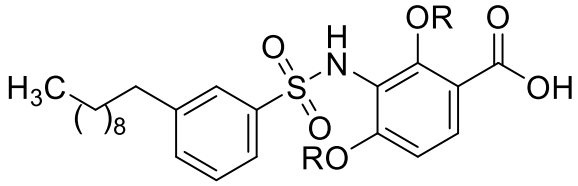

7.1a

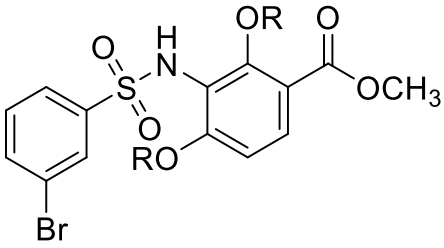

7.36

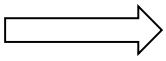

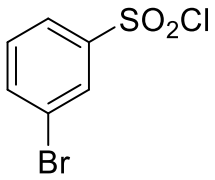

7.35

Scheme 7-13: Access of **7.1a** through minimal manipulation of sulfur functional groups

Beginning with commercially available 3-bromobenzene sulfonyl chloride **7.35**, the sulfonamide was installed in the first step (Scheme 7-14). Conditions were screened to optimize this coupling reaction. Initially, rapid hydrolysis of the sulfonyl chloride proved problematic, with

no detectable coupled product being produced. K_2CO_3/ THF produced the desired product in only 6% yield, while K_2CO_3/ DMF resulted in a significantly improved 27% yield.

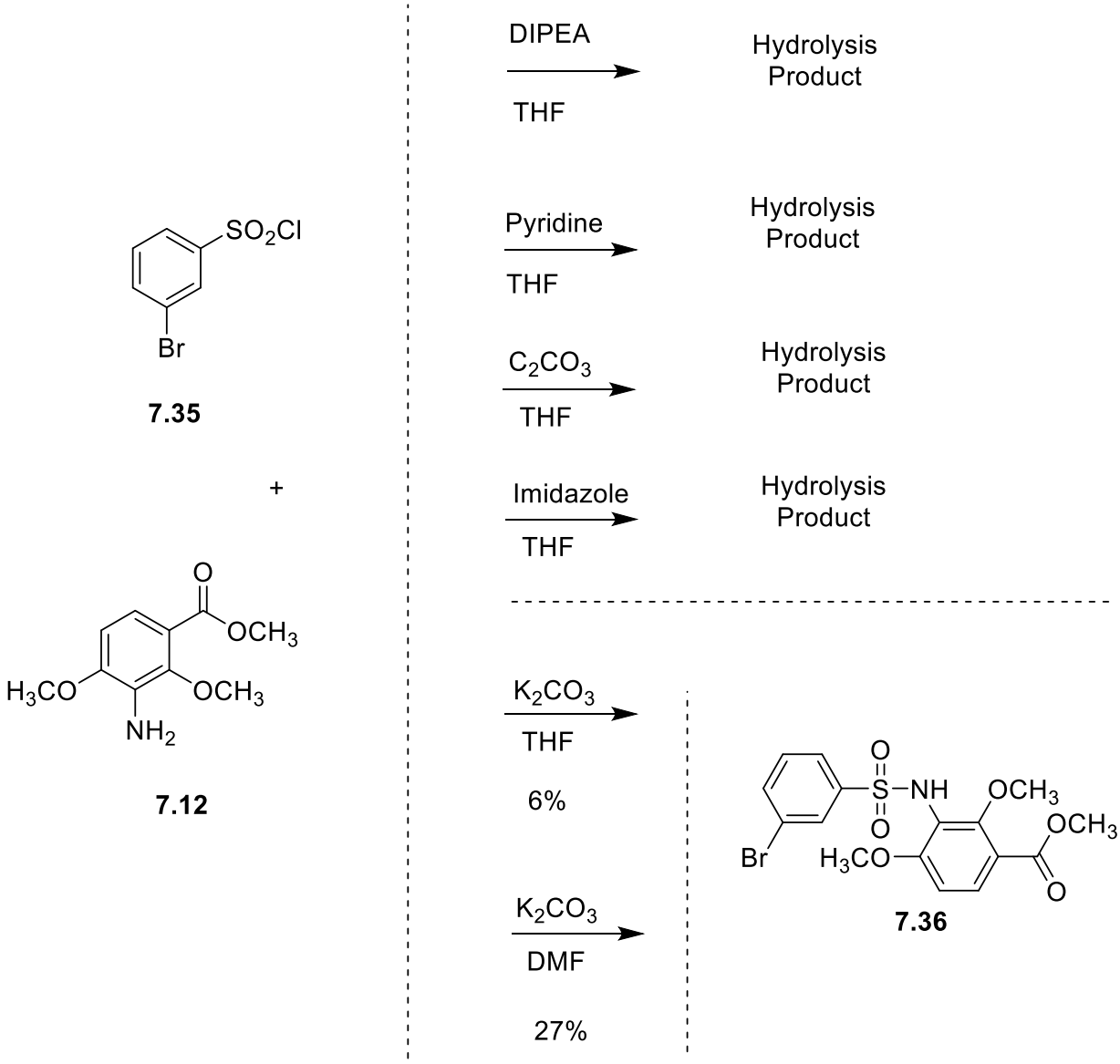

Scheme 7-14: Screening of coupling conditions for sulfonamide formation

Following successful installation of the sulfonamide group, a Sonogashira- coupling reaction was needed to install the alkyl chain to form **7.37**. However, the reduced reactivity of the aryl bromide group in **7.36** when compared to the aryl iodines typically used proved problematic.

Various conditions were screen for this coupling reaction (Scheme 7-15). Regardless of the catalyst used, no detectable product was formed.

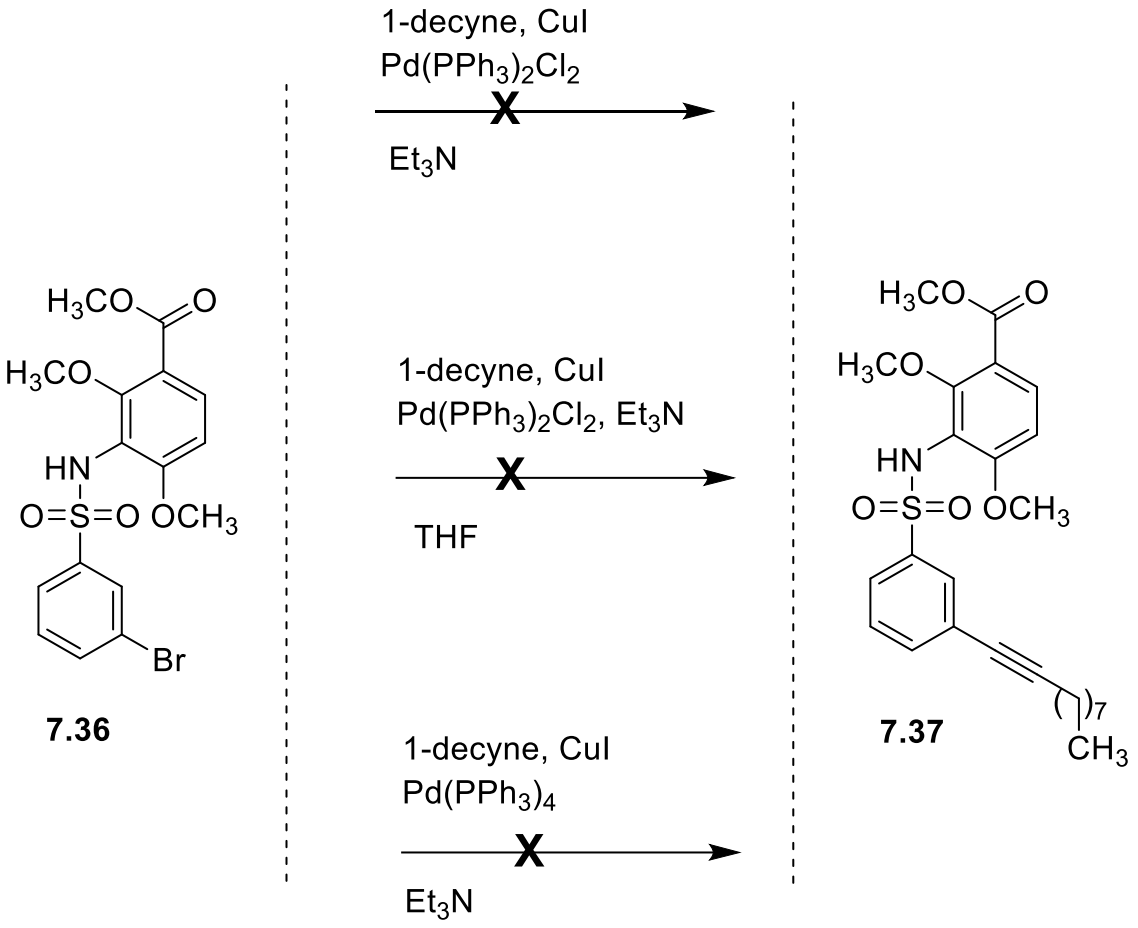

Scheme 7-15: Screening of conditions for Sonogashira coupling

7.3 **Synthesis of a Modified Hybrid-Inhibitor 7.1b**

Following repeated failed attempts to synthesize the originally designed **7.1a**, a structural modification was made to simplify the synthesis. We proposed deletion of the 4-hydroxyl group, leaving compound **7.1b** (Figure 7-3). Our hope in this modification was that by reducing the number of substituents on the headgroup, the steric hindrance of the 3- position would be reduced, allowing for coupling reactions to take place while simultaneously avoiding significant loss of activity of the inhibitor.

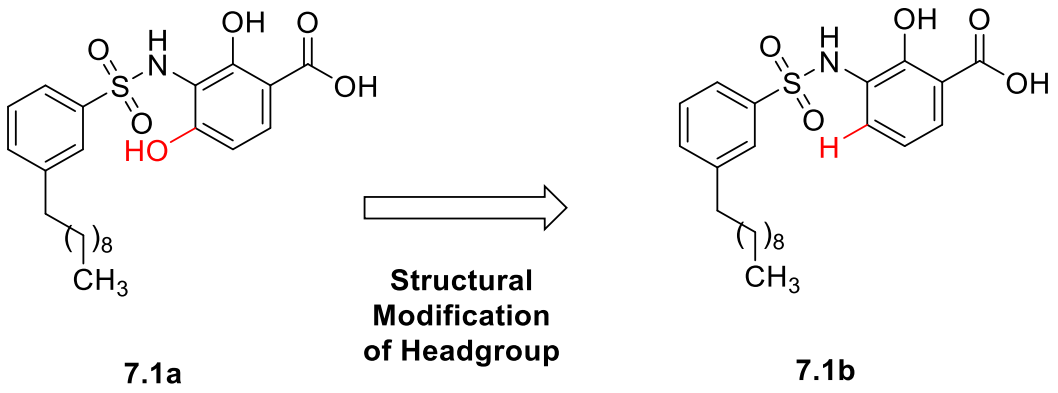

Figure 7-3: Modification of proposed hybrid-inhibitor **7.1a**

The new headgroup **7.50** was synthesized in a similar manner to those previously described (Scheme 7-16). Nitration of commercially available methyl salicylate followed by reduction via catalytic hydrogenation gave the modified headgroup **7.50.**

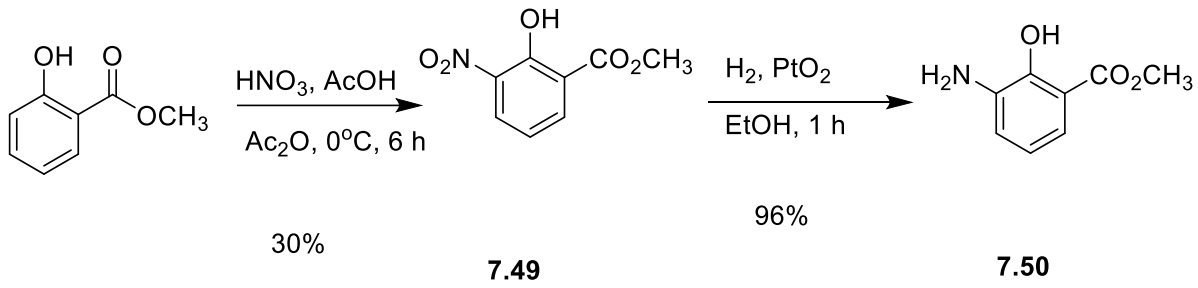

Scheme 7-16: Synthesis of modified headgroup **7.50**

Direct coupling with commercially available 3-bromobenzenesulfonyl chloride **7.35** gave the coupled product **7.51** (Scheme 7-17). The subsequent Sonogashira cross-coupling reaction followed by alkyne reduction to form **7.52** worked surprisingly well, considering the previous troubles faced when attempting this reaction with aryl bromide. In stark contrast to the case of **7.36** with both hydroxyl groups present on the headgroup structure, the Sonogashira coupling reaction to form **7.52** took place rapidly and in moderately-good yields. Finally, hydrolysis of the headgroup methyl ester gave **7.1b**, a slightly modified version of the initially envisioned HMGR-FabF-Hybrid inhibitor compound.

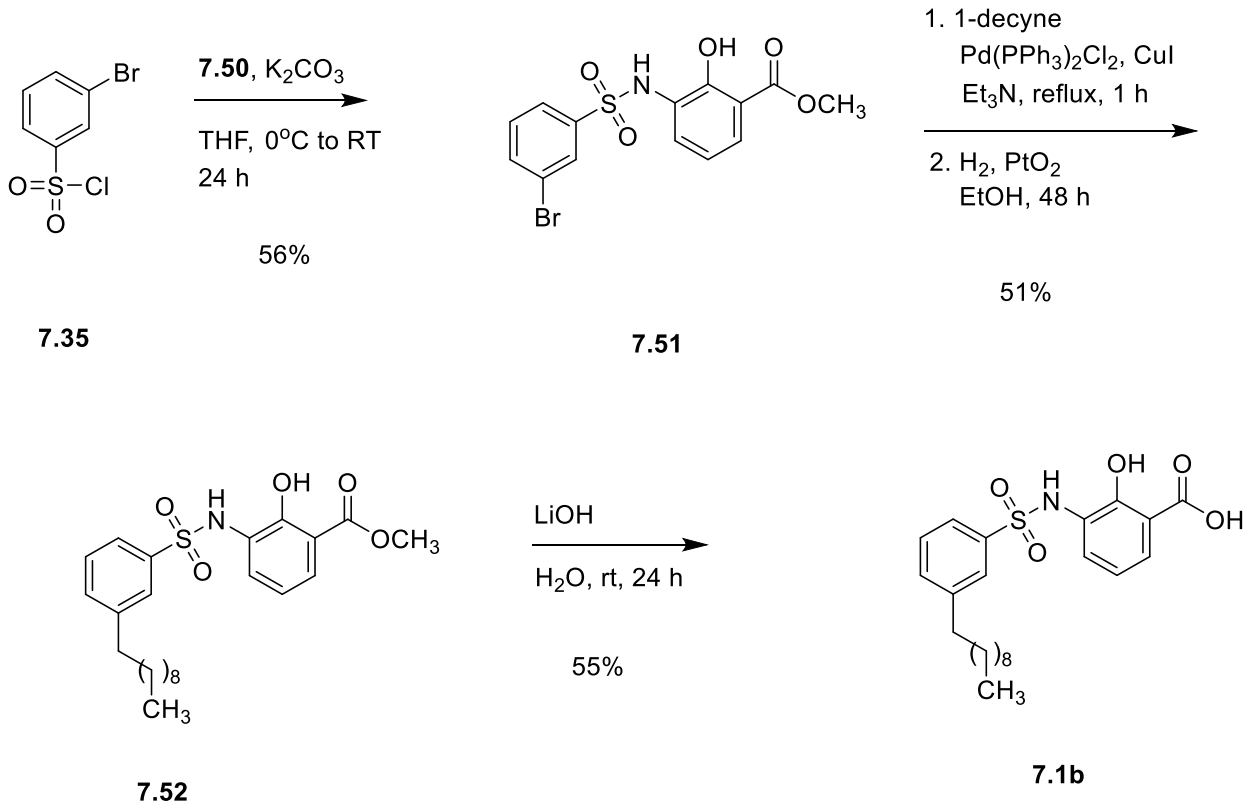

Scheme 7-17: Synthesis of **7.1b**

7.3.1 **Assay Results for 7.1b**

Compound **7.1b** was tested against *e.f.* II-HMGR and found to have an IC_{50} of 122 µM. However, the MIC/MBC was 64 µM, which is only a slight erosion from that of the original compound **DL-3.23**. This may support the hypothesis that FabF is a secondary target for this class of compounds. In the future, this compound will need to be tested directly with FabF to confirm secondary target inhibition.

7.4 **Synthesis of Nucleotide-linked Inhibitors**

We proposed linking nucleotide-structures to the core scaffold of the II-HMGR inhibitors, to determine if they would occupy the same chemical space in the active site as the adenine-portion of the endogenous ligand HMG-CoA. The structural similarities between HMG-CoA and proposed nucleotide-linked inhibitors **7.2** and **7.3** are shown in Figure 7-4.

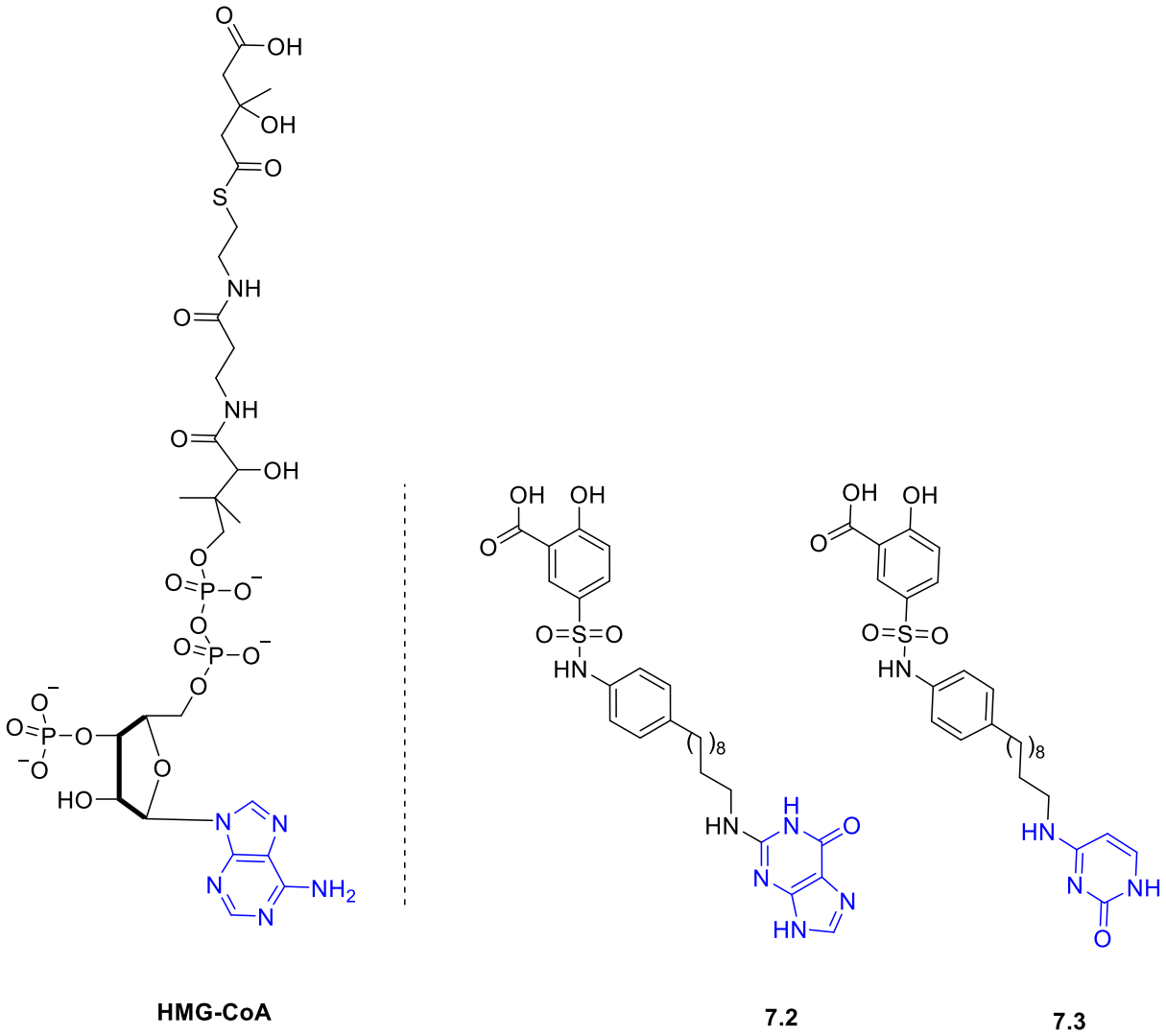

Figure 7-4: Structural comparison of HMG-CoA and nucleotide-linked inhibitors **7.2** and **7.3**

The proposed inhibitors involve linking of **7.54** (Scheme 7-18) to guanine and cytosine to form **7.2** and **7.3**, respectively. The synthesis of these nucleotide-linked inhibitors began from the common intermediate **6.11**, the synthesis of which was outlined in Chapter 6. Simultaneous reduction of the nitro-group and alkyne via catalytic hydrogenation yielded aniline **7.53**. Coupling with headgroup **6.9** gave sulfonamide **7.54** in excellent yield. Finally, a DMAP-catalyzed coupling reaction between **7.54** and tosyl chloride gave **7.55**.

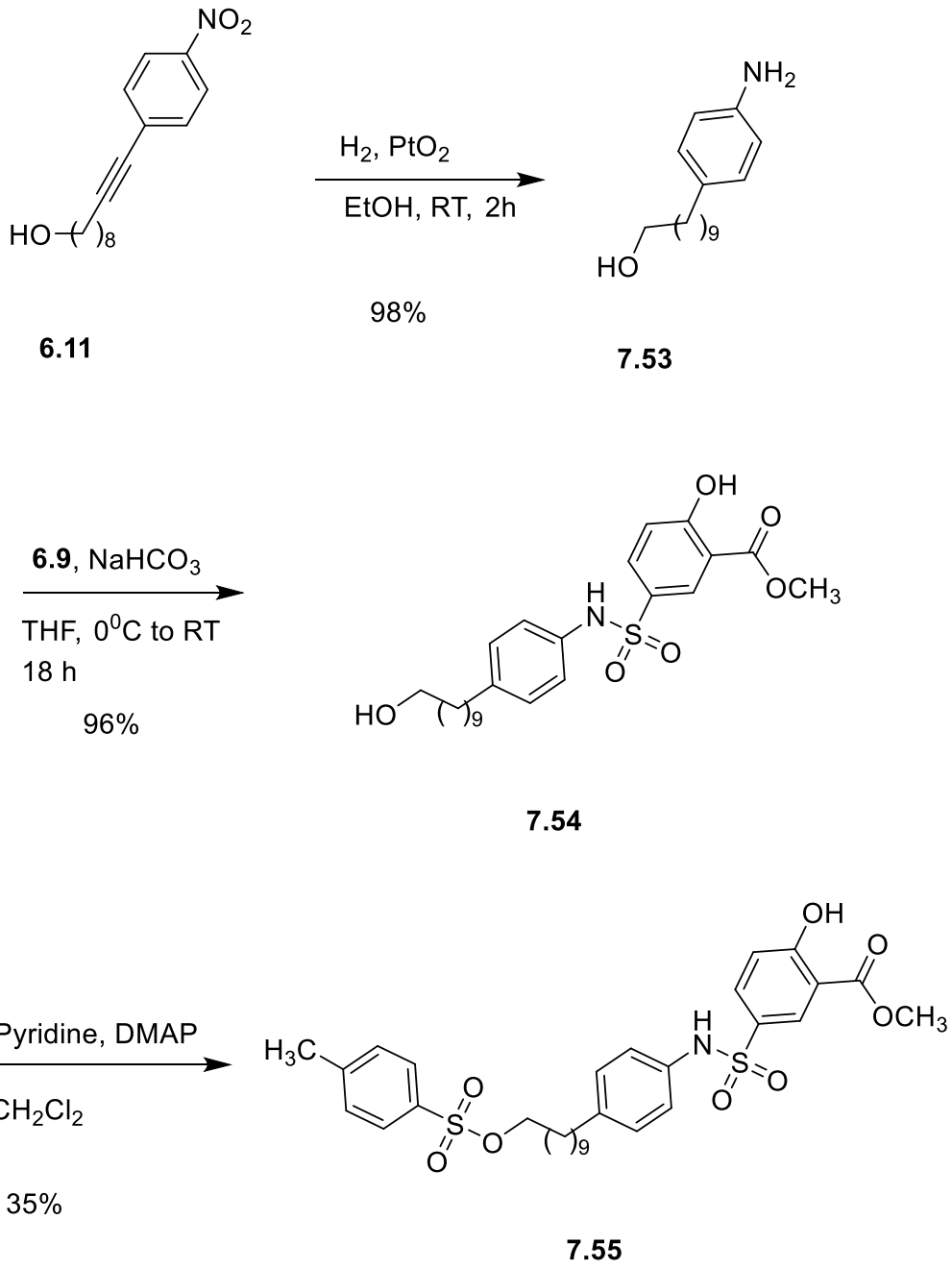

Scheme 7-18: Synthesis of **7.54**

With the terminal hydroxyl group now activated as a good leaving group, further coupling reactions could be conducted. Exposure to either guanine or cytosine in the presence of NaH, followed by hydrolysis of the headgroup methyl ester gave **7.2** and **7.3**, respectively (Scheme 7-19).

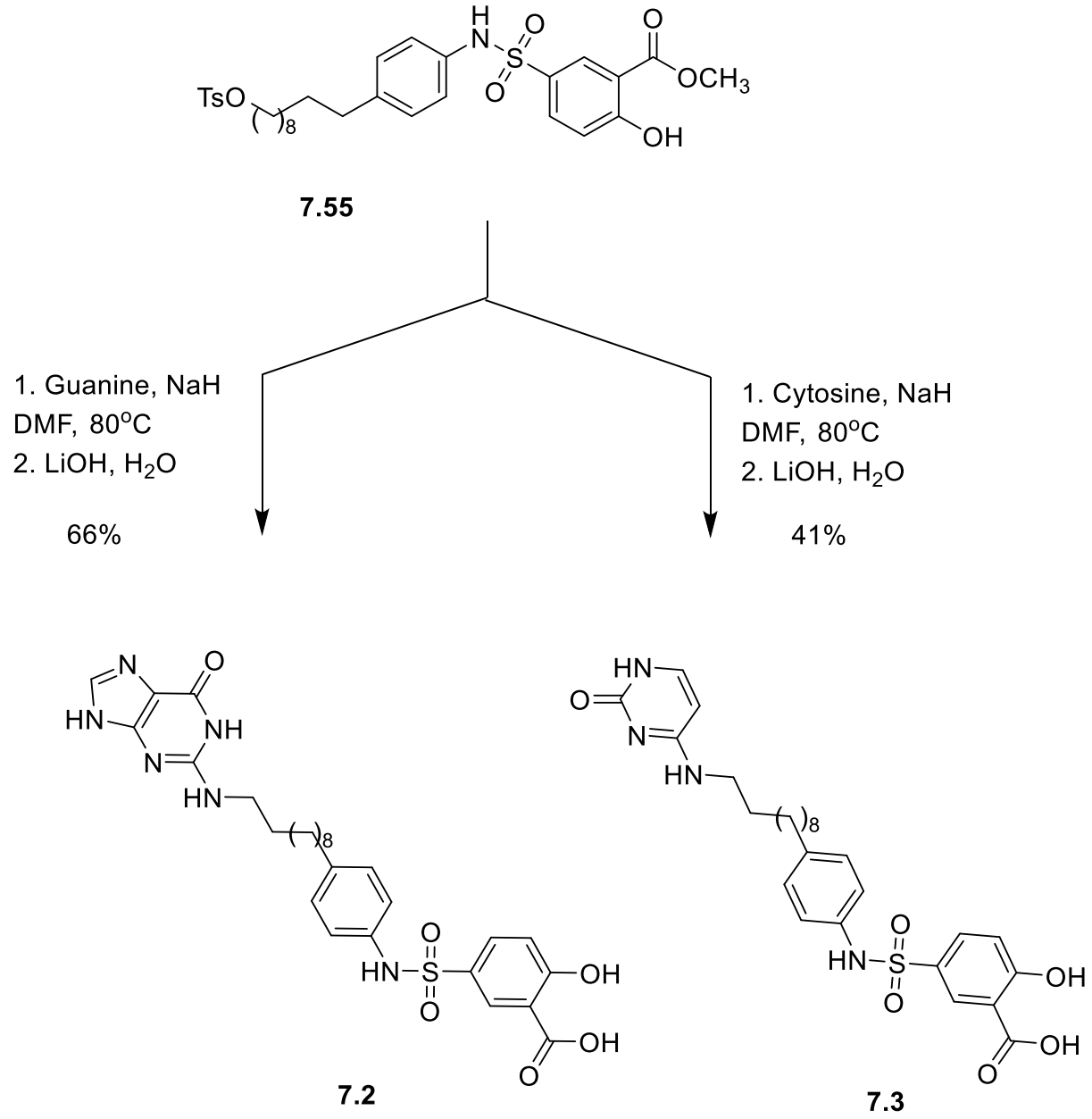

Scheme 7-19: Synthesis of cytosine- and guanine-linked inhibitors

The enzymatic activity followed the expected trend (Table 7-1). **7.2**, with a guanine-linked tail, showed an exceptional IC_{50} of 5.8 µM. The cytosine-linked analog **7.3** showed only a slight erosion in activity. This makes sense intuitively, as the guanine-group is most similar to the adenine moiety found in HMG-CoA that these inhibitors are designed to mimic. Unfortunately, neither compound performed well in bacterial assays. This is likely due to the ever-problematic membrane-permeability problem. As the structures become more polar through the addition of

biomolecule-type functional groups, the inhibitors lose the ability to cross the membrane into the cell.

Table 7-1: Assay data for nucleotide-linked inhibitors

Inhibitor	IC_{50} (μM)	MIC/MBC (μM)
7.2	5.8	>128
7.3	15.5	128

7.5 Synthesis of a Biotin-linked Inhibitor for use in a Protein Pulldown Assay

In order to identify the elusive secondary target of our inhibitors, we proposed linking one of the optimized II-HMGR inhibitors to a D-biotin molecule to perform a protein pulldown assay.[61] In the typical protocol, an agarose gel linked to streptavidin is incubated with the biotin-linked molecule, causing the biotin-moiety to bind to the gel (Figure 7-5). The remaining streptavidin sites are then filled with free biotin. This agarose gel is exposed to lysed bacteria, causing the inhibitor portion of the biotin-linked structure to bind any enzymes for which it has sufficient affinity. The biotin structures are then released from the agarose gel in a low pH buffer. Protein identification is then conducted to determine which proteins were extracted from the lysed bacteria.

The pull-down assays for this project were conducted in collaboration with the Chmielewski laboratory in the Purdue Department of Chemistry.

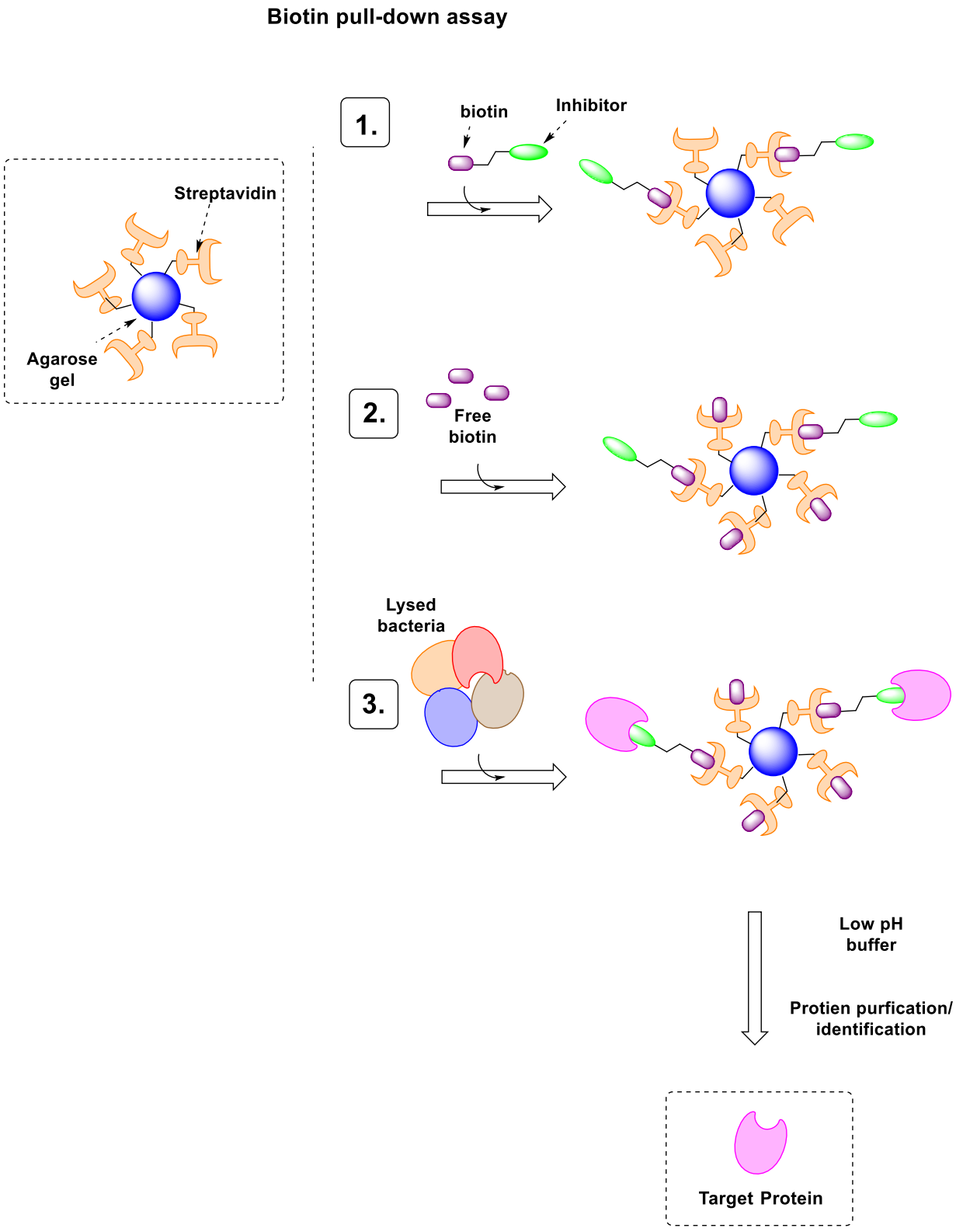

Figure 7-5: Streptavidin bead pull-down assay

7.5.1 **Progress Toward Synthesis of an Amide-Linked Biotinylated Inhibitor**

The inhibitor was prepared as previously reported to obtain carboxylic acid **6.13** (Scheme 7-20). The carboxylic acid was protected as a t-butyl ester **7.57** using Steglich Esterification conditions,[62] followed by simultaneous reduction of the alkyne and nitro group to yield aniline **7.58.** This was coupled with headgroup **6.9** to yield the fully-protected inhibitor **7.59**, with the two carboxylic acid groups differentiable by acidic vs basic deprotection conditions. The *t*-butyl ester was selectively deprotected using 30% TFA in DCM to yield **7.60**.

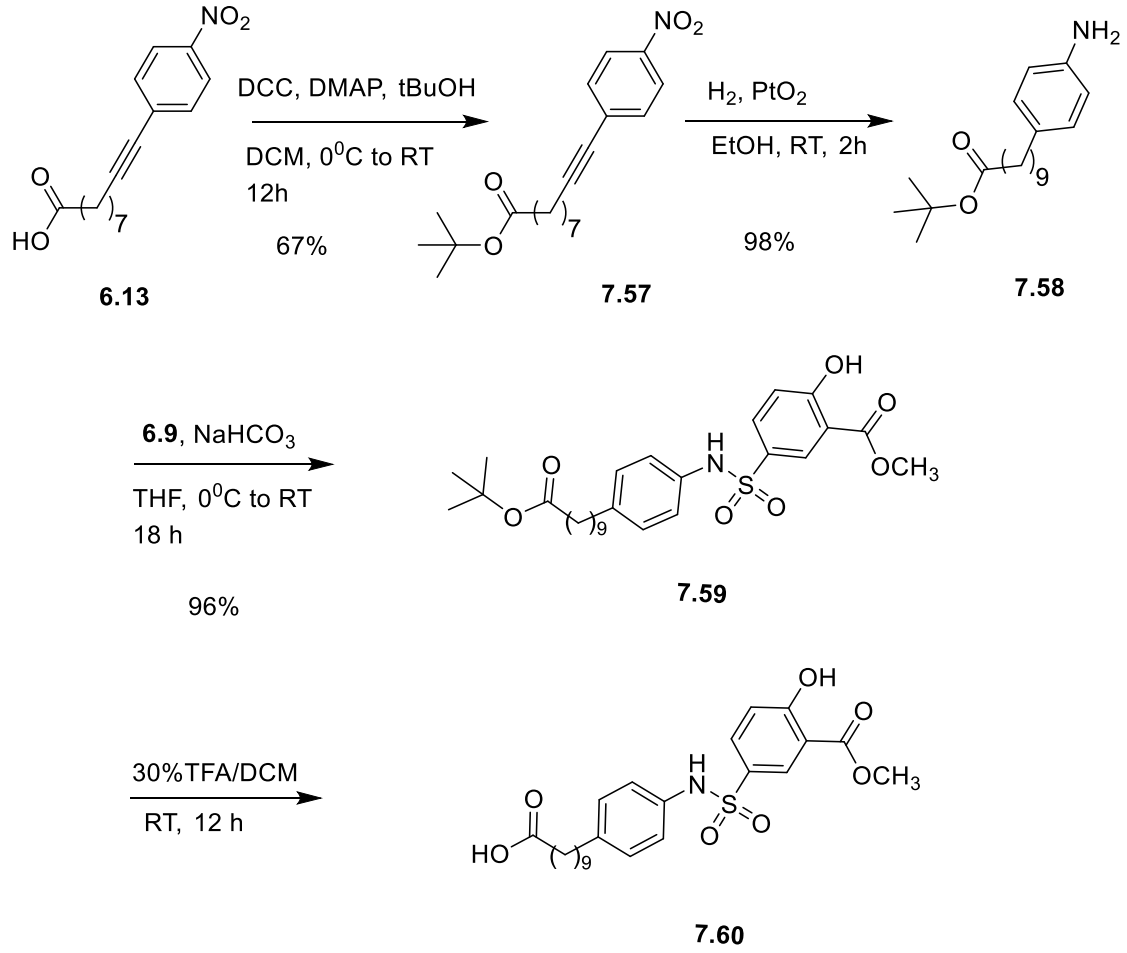

Scheme 7-20: Synthesis of HMGR-inhibitor moiety for protein pulldown assay

The carboxylic acid of biotin **7.55** was converted to primary amine via the Curtius rearrangement,[61] followed by deprotection of the resulting Boc-protected amine to form **7.56** in

50% yield over 2 steps (Scheme 7.21). However, attempts to couple **7.60** with this primary amine proved unsuccessful.

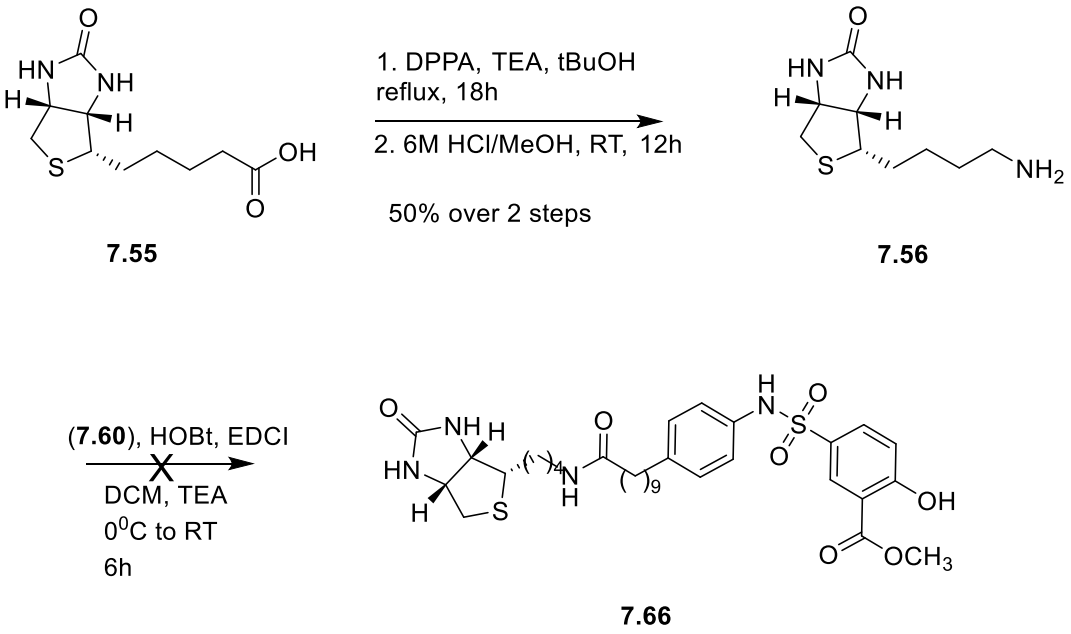

Scheme 7-21: First attempt to link biotin and inhibitor through an amide linkage

Because the formation of a linking-amide bond proved elusive, we proposed a reversal of the functional groups for this amide coupling, keeping the original carboxylic acid on Biotin and installing on amine on the inhibitor (Scheme 7-22). The extremely high polarity of Biotin creates difficulty in purification steps, so minimizing the synthetic transformations required with this moiety is advantageous. The carboxylic acid on biotin was coupled with N-hydroxysuccinimide to give activated biotin **7.62**. Compound **6.13** was converted to the Boc-amine **7.63** via the Curtius rearrangement, followed by deprotection to yield primary amine **7.64.** This was coupled with activated Biotin **7.62** followed by reduction of the nitro group through catalytic hydrogenation to yield the amide **7.65**. However, the coupling of **7.65** with the sulfonyl chloride of the headgroup **6.9** was unsuccessful for unknown reasons. It is likely due to a problem with the primary amine group. Several different approaches have been taken previously to synthesize a primary amine on this *p*-nitro ring for other purposes, to no avail. [24]

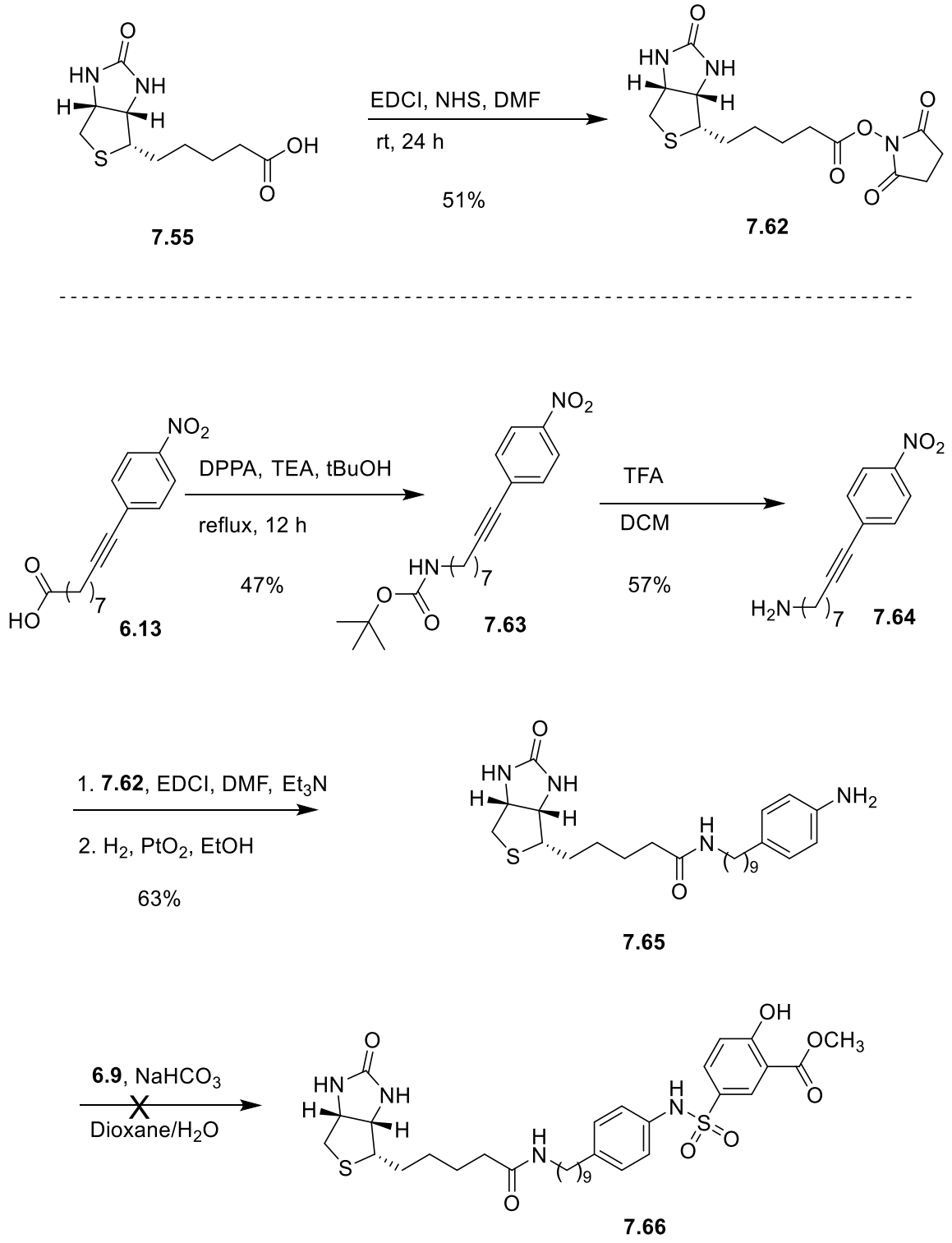

Scheme 7-22: Second approach to an amide linkage between biotin and inhibitor

Several alternate approaches were proposed to access the desired primary amine. Oxidation of 9-decyne-1-ol gave carboxylic acid **7.67** using a TEMPO-catalyzed BAIB oxidation (Scheme 7-23).[57] Attempts were then made to induce a Curtius rearrangement to form the Boc-protected amine **7.68**. However, upon exposure to DPPA and base in *t*-BuOH, the desired product was not obtained.

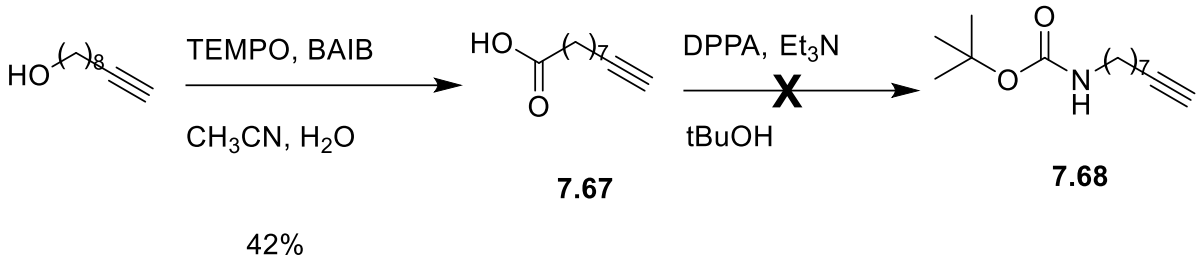

Scheme 7-23: Curtius rearrangement to form a primary amine

The next approach proposed to access the primary amine was through displacement of an activated hydroxyl group (Scheme 7-24). 9-decyn-1-ol could be activated with a tosyl group to yield **7.69**, followed by conversion to the primary azide. A Staundinger reduction could then be used to obtain the primary amine **7.70**. However, when this transformation was attempted, the desired product was not produced. An alternate approach to formation of the primary amine was to expose the activated alcohol **7.69** to 30% NH_4OH, but again, the desired product **7.70** was not produced by this method either.

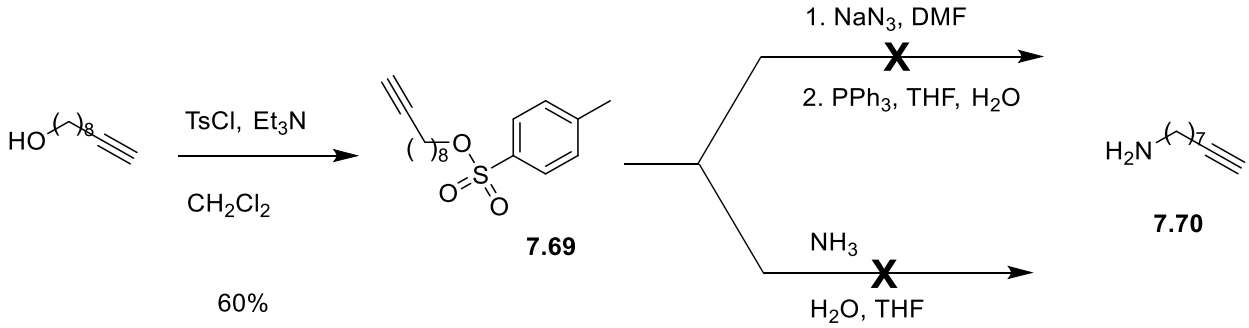

Scheme 7-24: Displacement of activated alcohol to form primary amine

We suspect that in all cases of the failed Curtius rearrangements and other azide-containing reactions, a click reaction is taking place between the azide and the alkyne (Scheme 7-25).[63]

Because there is no clear path to access of the amide linkage without use of an azide reagent, it was decided to switch the Biotin-inhibitor linkage to an ester group.

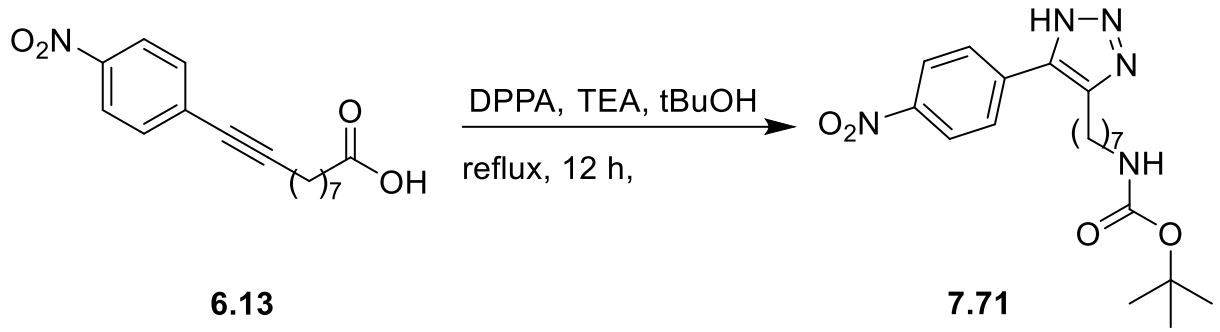

6.13 **7.71**

Scheme 7-25: Alkyne-azide Click reaction

7.5.2 **Synthesis of 7.4**

To link inhibitor **7.54** to D-Biotin through an ester linage, Steglich esterification were used (Scheme 7-26). Following successful formation of the ester linkage, the methyl ester group was hydrolyzed with aqueous LiOH to give the linked inhibitor **7.4**. This Biotin-inhibitor was tested against II-HMGR and interestingly, showed an IC_{50} of 56 µM. One theory to explain this observation is that the biotin moiety is mimicking the interaction of the adenine in the endogenous ligand, HMG-CoA. Unfortunately, it was determined post-synthesis that the esterases present in bacterial lysate would render a pull-down assay ineffective, since the biotin-inhibitor ester bond would likely be hydrolyzed.

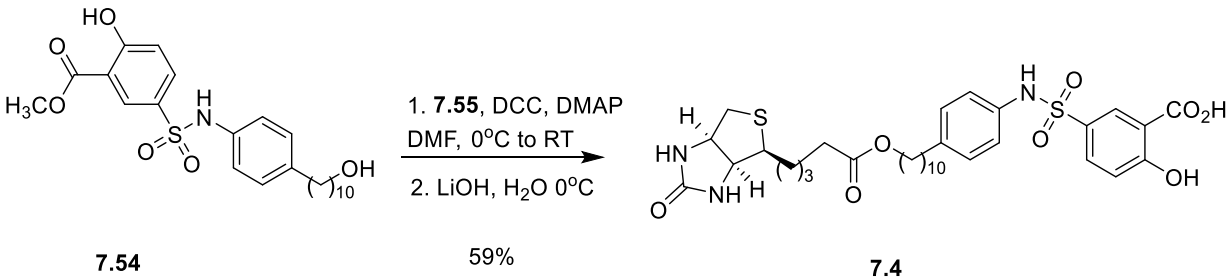

7.54 59% **7.4**

Scheme 7-26: Synthesis of biotin-linked inhibitor via an ester linkage

7.5.3 **Synthesis of 7.5**

As a final attempt obtain a biotin-linked inhibitor, we proposed linking the shortened inhibitor structure **7.72** to biotin through successive amide bonds, with a 6- carbon spacer molecule between (Scheme 7-27). Esterases would no longer pose a threat to the structural stability of the molecule, as all linkages would be secured through amide bonds. Additionally, the use of a di-amine spacer means that no synthetically novel functional groups would need to be installed on either biotin, or the inhibitor moiety beyond what has already been reported.

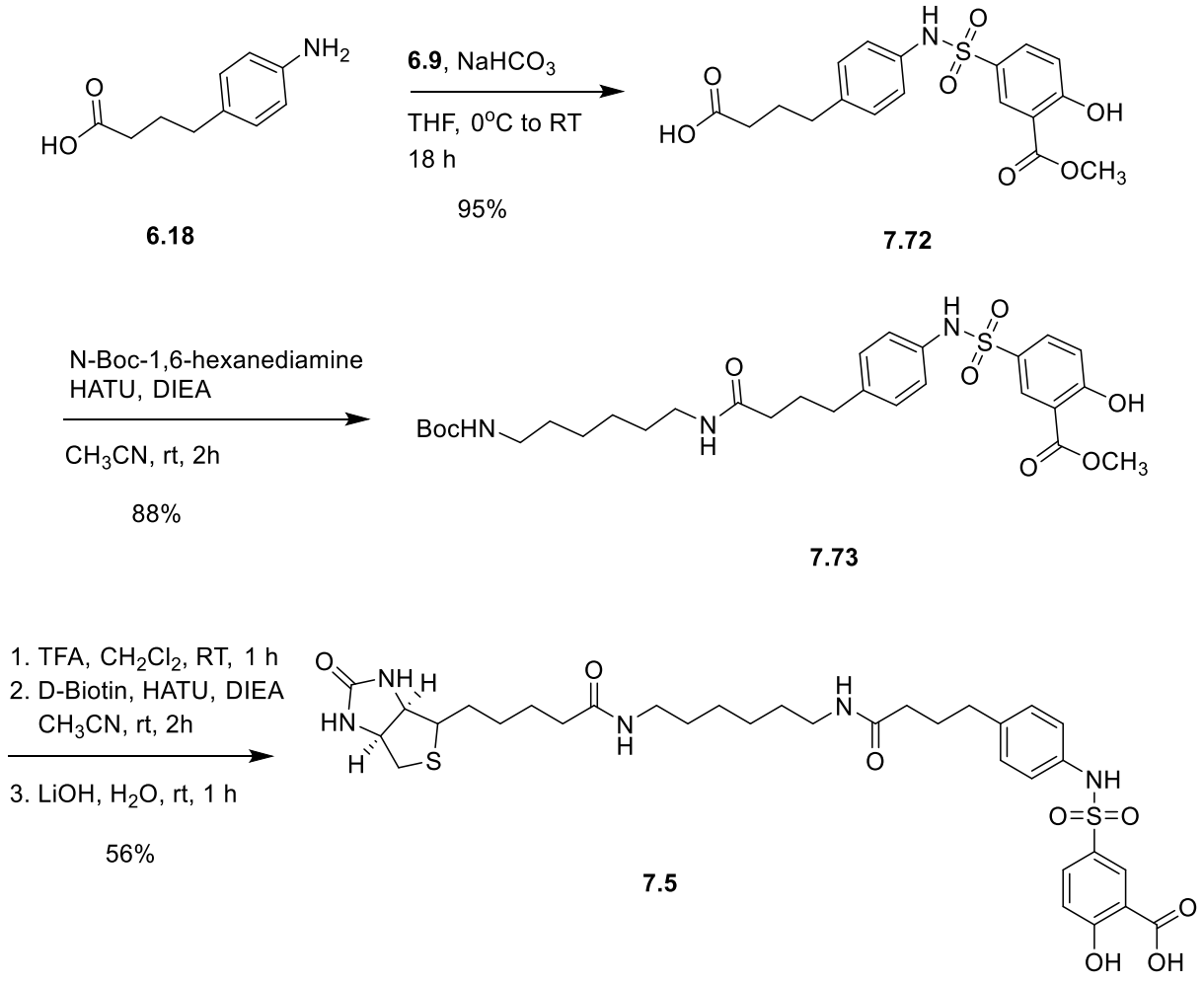

Scheme 7-27: Synthesis of a biotin-inhibitor hybrid linked through an amide bond

Synthesis began with commercially available aminophenylbutyric acid **6.18**. Coupling with the sulfonyl chloride of **6.9** gave **7.72**. This molecule was then coupling to a mono-protected N-

Boc-1,6-hexanediamine using HATU amide coupling conditions. Deprotection of the N-Boc group with TFA, followed by an additional HATU coupling formed the amide linkage with D-biotin. Finally, hydrolysis of the headgroup methyl ester with LiOH gave the final amide-linked biotinylated- inhibitor **7.5**. Due to insolubility in the buffer medium, an IC_{50} was not obtained.

7.6 Conclusion

Five new compounds were synthesized in pursuit of identification of a secondary target. The enzyme and cell assay results are summarized in Table 7-2. **7.1** was designed as a hybrid inhibitor for both II-HMGR and FabF, the target of Platensimycin. While the activity against II-HMGR fell off significantly, maintenance of the MIC/MBC suggests that we may be engaging the intended target with this hybrid-inhibitor. Crystal structures of this inhibitor bound in both active sites will be essential to determining future structural modifications.

Nucleotide linked inhibitors **7.2** and **7.3** showed excellent IC_{50} values when tested against II-HMGR. However, inhibitor polarity continues to pose a problem with membrane permeability. Due to the excessive polarity of the nucleotide moieties, the MIC/MBC values fell off significantly.

Finally, two biotinylated inhibitors were synthesized. Ester-linked **7.4** showed activity against the enzyme, but unfortunately, the ester moiety did not prove compatible with the esterases that are present in bacterial cells. **7.5** was insoluble in the buffer for enzyme assays, but will be used to conduct a biotin pull-down assay. We are currently awaiting the results of this assay.

Table 7-2: Summary of assay results

Inhibitor	IC_{50} (μM)	MIC/MBC (μM)
7.1	122	64
7.2	5.8	>128
7.3	15.5	>128
7.4	56	>256
7.5	-	-

APPENDIX A. EXPERIMENTAL PROCEDURES

EXPERIMENTAL PROCEDURES: PART 1

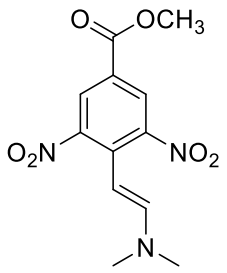

1.2

methyl (E)-4-(2-(dimethylamino)vinyl)-3,5-dinitrobenzoate (1.2).

To a solution of 4-methyl-3,5-dinitrobenzoic acid (4.00 g, 17.7 mmol) in anhydrous toluene (59.0 mL) was added DMF-DMA (7.1 mL, 47.7 mmol) dropwise at rt. The reaction was heated to reflux and stirred for 16 hours. The reaction was cooled to rt and the solvent was co-evaporated with MeOH. The crude product was recrystallized from hot EtOH to afford **1.2** (3.85g, 74%) as a shiny, green solid which turned red upon grinding. $\mathbf{R_f}$ = 0.36 (25% EA/Hex); **^{1}H NMR** (300 MHz, $CDCl_3$) δ 8.31 (s, 2H), 6.69 (d, *J* = 13.4 Hz, 1H), 5.49 (d, *J* = 13.4 Hz, 1H), 3.93 (s, 3H), 2.95 (s, 6H).

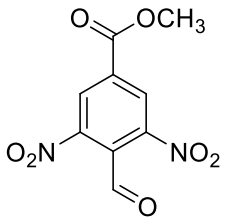

1.3

methyl 4-formyl-3,5-dinitrobenzoate (1.3).

To a mixture of **1.2** (3.85 g, 13.1 mmol) in CH_3CN-H_2O (6:1, 149.7 mL) was added a solution of 0.1 M aq. $RuCl_3$ (5.2 mL, 0.522 mmol), followed by $NaIO_4$ (6.98 g, 32.6 mmol). The reaction was stirred for 45 minutes, causing a color change from red to brown-green. After completion by TLC, the solids were removed by vacuum filtration and washed with CH_2Cl_2. The filtrate was extracted 3x with CH_2Cl_2. The combined organic extracts were washed with brine, then sat. aq. $Na_2S_2O_3$.

The resulting material was purified by flash column chromatography (30% EA/Hex) to afford **1.3** (2.03 g, 61%) as a light yellow solid. $\mathbf{R_f}$ = 0.33 (30% EA/Hex); **^{1}H NMR** (300 MHz, $CDCl_3$) δ 10.64 (s, 1H), 9.08 (s, 2H), 4.08 (s, 3H).

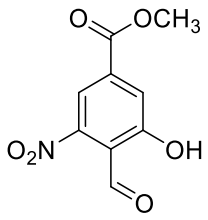

1.4

methyl 4-formyl-3-hydroxy-5-nitrobenzoate (1.4).

A solution of **1.3** (2.03 g, 10.0 mmol) in anhydrous DMF (20.0 mL) was added dropwise to a solution of acetaldoxime [mixture of isomers] (1.2 mL, 20.0 mmol) and K_2CO_3 (3.04 g, 2.20 mmol) in anhydrous DMF (20.0 mL). The reaction turned dark purple upon combination of all reagents. The reaction was stirred at RT for 18 h. The reaction was diluted with H_2O and extracted 5x Et_2O. The aqueous layer was acidified to pH = 2 with 6M HCl and extracted 4x with EA. The combined organic layers were washed 4x with brine and concentrated. Purification by flash column chromatography (25% EA/Hex) yielded **1.4** (1.53 g, 68%) as a bright yellow solid. $\mathbf{R_f}$ = 0.34 (25% EA/Hex); **^{1}H NMR** (300 MHz, $CDCl_3$) δ 12.05 (s, 1H), 10.37 (d, *J* = 0.6 Hz, 1H), 8.15 (d, *J* = 1.6 Hz, 1H), 7.93 (d, *J* = 1.7 Hz, 1H), 4.00 (s, 3H).

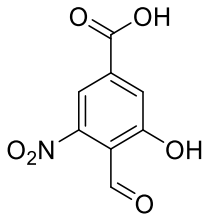

1.5

4-formyl-3-hydroxy-5-nitrobenzoic acid (1.5).

$Ba(OH)_2$ (3.50 g, 20.4 mmol) was added in portions to a solution of **1.4** (1.53 g, 6.80 mmol) in MeOH (68.0 mL) and stirred at rt for 4 h. Volatiles were removed and the residue was dissolved in H_2O and washed 3x with EA. The aqueous layer was acidified to pH = 2 with 6 M HCl and extracted 5x with EA. The combined organic extracts were washed with brine and concentrated to afford **1.5** (1.35 g, 94%) as an orange solid. **^{1}H** NMR (300 MHz, DMSO-d6) δ 11.73 (s, 1H), 10.28 (s, 1H), 7.77 (d, J = 1.3 Hz, 1H), 7.75 (s, 1H); **^{1}H NMR** (300 MHz, CD_3OD) δ 10.30 (s, 1H), 7.95 (d, J = 1.4 Hz, 1H), 7.83 (d, J = 1.4 Hz, 1H), 7.71 (d, J = 1.6 Hz, 1H), 7.63 (d, J = 1.6 Hz, 1H), 6.07 (s, 1H).

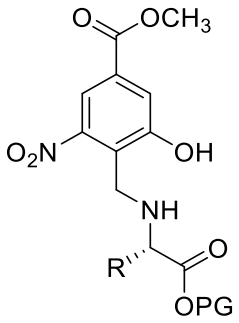

2.1a-d

General Procedure for Solution-Phase Reductive Amination

HCl-AA-OtBu (0.666 mmol) was added to a solution of **1.4** (200.0 mg, 0.666 mmol) and DIEA (244 µL, 1.40 mmol) in CH_3CN (9.5 mL). The reaction was stirred at rt for 45 min. Volatiles were removed and the residue was dissolved in MeOH (3.3 m). $NaBH_4$ (75.6 mg, 2.00 mmol) was added and the reaction was stirred for 15 min. Volatiles were removed and the residue was purified by flash column chromatography (20-45% EA/Hex) to yield **2.1a-d** in 51-75% yield.

General Procedure for Solution-Phase Acylation (2.2a-d)

A mixture of Fmoc-AA-OH (1.10 mmol) and DIPC (85 µL, 0.550 mmol) was preactivated in dry CH_2Cl_2 (0.88 mL) for 5 min. **2.1a-d** (0.500 mmol) as a solution in CH_2Cl_2 (0.85 mL) was added and the reaction was stirred for 2 h. 1-octanethiol (433 µL, 2.5 mmol) was added and the reaction was stirred overnight. Volatiles were removed and the residues were purified by flash column chromatography (20-45% EA/Hex) and used directly in the next reaction.

General Procedure for Solution-Phase Photolysis (2.3a-d)

A solution of Hcnb-linked dipeptides (**2.2a-d**) in MeOH (3 mL) were subject to 365 nm light for 12 h. Volatiles were removed and the residues were purified by flash column chromatography (15-35% EA/Hex) to give dipeptides **2.3a-d** in 35-53% yield.

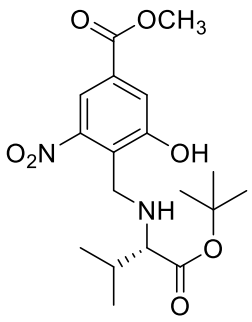

2.1a

H-[Hcnb]-Val-OtBu (2.1a).

Yellow Oil; **Yield** = 51%; $\mathbf{R_f}$ = 0.32 (20% EA/Hex); **^{1}H NMR** (400 MHz, $CDCl_3$) δ 7.91 (d, *J* = 1.6 Hz, 1H), 7.66 (d, *J* = 1.7 Hz, 1H), 4.25 (d, *J* = 15.6 Hz, 1H), 4.02 (d, *J* = 15.6 Hz, 1H), 3.92 (s, 3H), 2.98 (d, *J* = 5.5 Hz, 1H), 2.04 – 1.99 (m, 1H), 1.49 (s, 9H), 0.99 – 0.94 (m, 6H); **^{13}C NMR** (101 MHz, $CDCl_3$) δ 172.02, 164.91, 160.10, 150.15, 130.93, 121.69, 120.53, 115.64, 82.55, 66.36, 52.52, 46.30, 31.18, 27.95, 19.15, 18.04; **IR** (neat, cm-1) 2978, 2948, 2162, 1734, 1718, 1624, 1582, 1538, 1457, 1420, 1437, 1395, 1372, 1344, 1300, 1242, 1200, 1161, 1104, 1031, 1006, 982, 931, 902, 888, 837.

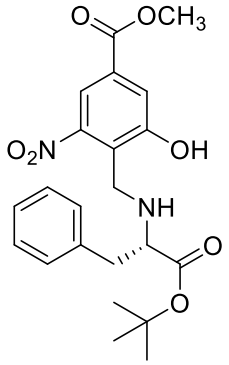

2.1b

H-[Hcnb]-Phe-OtBu (2.1b).

Yellow Oil; **Yield** = 63%; $\mathbf{R_f}$ = 0.26 (20% EA/Hex); **^{1}H NMR** (400 MHz, $CDCl_3$) δ 7.89 (d, *J* = 1.7 Hz, 1H), 7.62 (d, *J* = 1.7 Hz, 1H), 7.30 – 7.25 (m, 3H), 7.16 – 7.13 (m, 2H), 4.19 (d, *J* = 15.5 Hz, 1H), 4.02 (d, *J* = 15.6 Hz, 1H), 3.92 (s, 3H), 3.46 (dd, *J* = 7.7, 6.1 Hz, 1H), 3.07 – 3.02 (m, 1H), 2.94 – 2.89 (m, 1H), 1.43 (s, 9H); **^{13}C NMR** (101 MHz, $CDCl_3$) δ 171.73, 164.89, 159.99, 150.14, 135.76, 130.88, 129.10, 128.64, 127.16, 121.82, 120.32, 115.60, 82.79, 61.69, 52.52, 45.88, 39.09, 27.85; **IR** (neat, cm-1) 2986, 2257, 2096, 1721, 1620, 1580, 1532, 1458, 1448, 1430, 1395, 1370, 1314, 1258, 1240, 1196, 1156, 1131, 1099, 1065, 1034, 1010, 999, 900, 839.

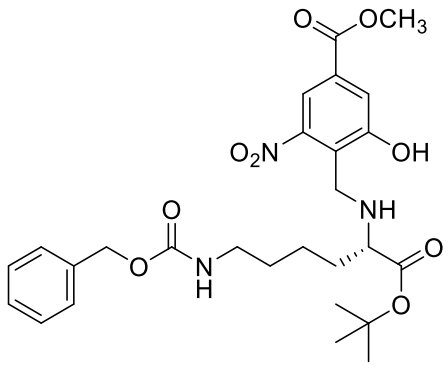

2.1c

H-[Hcnb]-Lys(Z)-OtBu (2.1c).

Yellow Oil; **Yield** = 69%; $\mathbf{R_f}$ = 0.23 (40% EA/Hex); **^{1}H NMR** (400 MHz, $CDCl_3$) δ 7.91 (d, *J* = 1.7 Hz, 1H), 7.66 (d, *J* = 1.7 Hz, 1H), 7.35 – 7.31 (m, 5H), 7.31 – 7.28 (m, 1H), 5.06 (s, 2H), 4.84 (s, 1H), 4.22 (d, *J* = 15.7 Hz, 1H), 4.06 (d, *J* = 15.9 Hz, 1H), 3.91 (s, 3H), 3.20 – 3.14 (m, 3H), 1.67 (dq, *J* = 14.1, 7.0, 6.3 Hz, 2H), 1.52 – 1.49 (m, 2H), 1.47 (d, *J* = 1.9 Hz, 9H), 1.42 (d, *J* = 3.1 Hz, 2H); **^{13}C NMR** (101 MHz, $CDCl_3$) δ 172.40, 171.05, 164.88, 160.04, 156.32, 150.18, 136.46, 130.95, 128.40, 127.98, 121.72, 120.34, 115.69, 82.69, 66.53, 60.29, 52.53, 45.94, 40.45, 32.42, 29.46, 27.91, 22.49, 20.94, 14.09; **IR** (neat, cm-1) 3371, 2943, 2162, 1979, 1722, 1684, 1621, 1586, 1531, 1457, 1435, 1396, 1365, 1316, 1290, 1236, 1262, 1212, 1196, 1152, 1116, 1098, 1063, 1028, 1010, 955, 912, 901, 854, 838.

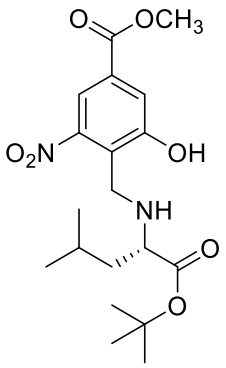

2.1d

H-[Hcnb]-Leu-OtBu (2.1d).

Yellow Oil; **Yield** = 75%; $\mathbf{R_f}$ = 0.40 (20% EA/Hex); **^{1}H NMR** (400 MHz, $CDCl_3$) δ 7.91 (d, *J* = 1.7 Hz, 1H), 7.66 (d, *J* = 1.7 Hz, 1H), 4.23 (d, *J* = 15.7 Hz, 1H), 4.06 (d, *J* = 15.7 Hz, 1H), 3.92 (s, 3H), 3.21 – 3.17 (m, 1H), 1.75 – 1.69 (m, 1H), 1.53 – 1.49 (m, 2H), 1.48 (s, 9H), 0.92 (d, *J* = 6.6 Hz, 3H), 0.87 (d, *J* = 6.6 Hz, 3H); **^{13}C NMR** (101 MHz, $CDCl_3$) δ 173.04, 164.90, 160.12, 150.13, 130.93, 121.71, 120.42, 115.66, 82.51, 59.12, 52.52, 45.92, 42.16, 27.90, 24.83, 22.60, 21.88; **IR** (neat, cm-1) 3295, 2958, 1724, 1656, 1574, 1531, 1435, 1391, 1366, 1298, 1231, 1145, 1096, 1017, 905, 843.

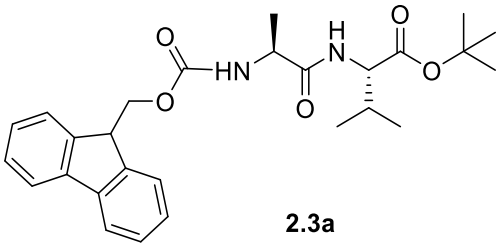

2.3a

Fmoc-Ala-Val-OtBu (2.3a)

Yellow Oil; **Yield** = 38%; **^{1}H NMR** (400 MHz, $CDCl_3$) δ 7.76 (dt, *J* = 7.6, 0.9 Hz, 2H), 7.59 (dd, *J* = 7.3, 2.9 Hz, 2H), 7.39 (tt, *J* = 7.5, 0.9 Hz, 2H), 7.30 (td, *J* = 7.5, 1.2 Hz, 2H), 6.44 (d, *J* = 8.8 Hz, 1H), 5.47 (d, *J* = 7.6 Hz, 1H), 4.46 – 4.41 (m, 1H), 4.41 – 4.37 (m, 2H), 4.30 (t, *J* = 7.1 Hz, 1H), 4.21 (t, *J* = 7.1 Hz, 1H), 2.20 – 2.12 (m, 1H), 1.48 – 1.43 (m, 9H), 1.43 – 1.39 (m, 3H), 0.93

– 0.86 (m, 6H); **^{13}C NMR** (101 MHz, $CDCl_3$) δ 171.94, 170.58, 155.62, 143.66, 141.19, 127.62, 126.98, 124.98, 119.88, 67.03, 57.41, 50.44, 47.01, 31.28, 27.92, 18.77, 18.55, 17.44; **IR** (neat, cm-1) 3292, 2968, 1727, 1688, 1655, 1530, 1477, 1449, 1390, 1367, 1292, 1243, 1149, 1103, 1079, 1029, 916, 844.

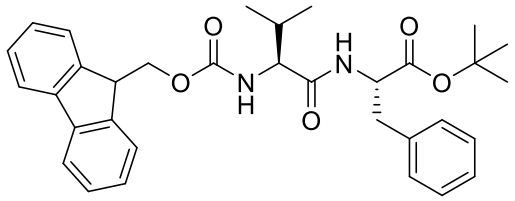

2.3b

Fmoc-Val-Phe-OtBu (2.3b)

Yellow Waxy Solid; **Yield** = 35%; **^{1}H NMR** (400 MHz, $CDCl_3$) δ 7.76 (ddt, *J* = 7.6, 2.2, 1.2 Hz, 2H), 7.59 (t, *J* = 7.7 Hz, 2H), 7.39 (td, *J* = 7.6, 6.7, 2.7 Hz, 2H), 7.31 (dddd, *J* = 8.4, 5.9, 2.9, 1.8 Hz, 2H), 7.25 – 7.08 (m, 5H), 6.34 (dd, *J* = 31.4, 7.9 Hz, 1H), 5.41 (t, *J* = 9.2 Hz, 1H), 4.80 – 4.71 (m, 1H), 4.46 – 4.38 (m, 1H), 4.34 (q, *J* = 6.4 Hz, 1H), 4.22 (q, *J* = 7.1 Hz, 1H), 4.03 (ddd, *J* = 20.3, 8.8, 5.9 Hz, 1H), 3.08 (d, *J* = 6.2 Hz, 2H), 2.06 (d, *J* = 15.9 Hz, 1H), 1.39 (s, 9H), 0.90 (ddd, *J* = 29.6, 18.2, 6.8 Hz, 6H); **^{13}C NMR** (101 MHz, $CDCl_3$) δ 170.51, 170.31, 170.14, 156.20, 143.69, 141.21, 135.95, 135.80, 129.36, 129.30, 128.33, 127.62, 127.00, 126.92, 125.01, 119.88, 82.36, 67.00, 60.16, 60.02, 53.46, 47.08, 38.19, 38.01, 31.16, 31.02, 27.82, 19.02, 17.73, 17.28; **IR** (neat, cm-1) 3290, 3064, 2956, 1729, 1688, 1650, 1531, 1498, 1477, 1449, 1390, 1465, 1367, 1293, 1244, 1151, 1101, 1080, 1028, 910, 845.

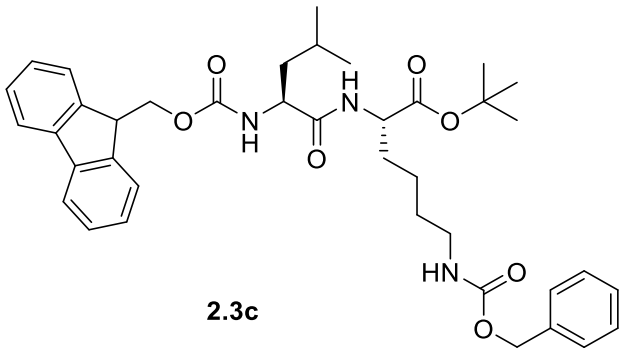

2.3c

Fmoc-Leu-Lys(Z)-OtBu (2.3c)

Yellow Oil; **Yield** = 54%; **^{1}H NMR** (400 MHz, $CDCl_3$) δ 7.75 (dq, *J* = 7.6, 1.3 Hz, 2H), 7.57 (d, *J* = 7.4 Hz, 2H), 7.41 – 7.27 (m, 10H), 6.67 (d, *J* = 7.6 Hz, 1H), 5.37 (dd, *J* = 56.8, 8.3 Hz, 1H), 5.15 (t, *J* = 5.7 Hz, 1H), 5.05 (dd, *J* = 11.1, 8.5 Hz, 2H), 4.45 – 4.38 (m, 2H), 4.23 (d, *J* = 3.8 Hz, 1H), 4.19 (d, *J* = 7.3 Hz, 1H), 3.11 (d, *J* = 14.9 Hz, 2H), 1.86 – 1.76 (m, 1H), 1.66 (s, 3H), 1.47 (s, 2H), 1.43 (d, *J* = 4.3 Hz, 9H), 1.35 – 1.25 (m, 3H), 0.96 – 0.90 (m, 6H); **^{13}C NMR** (101 MHz, $CDCl_3$) δ 172.05, 171.83, 171.14, 171.04, 156.40, 156.19, 143.75, 143.60, 141.20, 136.55, 136.51, 128.38, 127.98, 127.94, 127.62, 127.00, 124.95, 119.89, 82.20, 82.05, 66.91, 66.46, 53.41, 52.31, 47.05, 41.39, 40.50, 40.33, 31.92, 29.15, 27.98, 27.87, 24.67, 24.53, 22.89, 21.86, 21.74; **IR** (neat, cm-1) 3314, 2953, 1703, 1660, 1517, 1449, 1367, 1236, 1153, 1042, 910, 844.

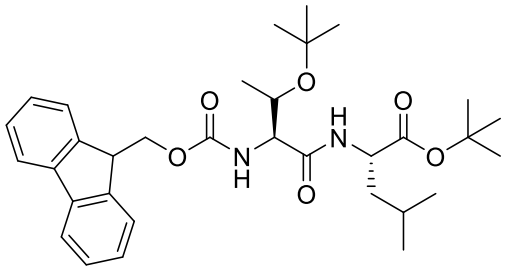

2.3d

Fmoc-Thr(tBu)-Leu-OtBu (2.3d)

Yellow Oil; **Yield** = 53%; **^{1}H NMR** (400 MHz, $CDCl_3$) δ 7.76 (dq, *J* = 7.6, 1.1 Hz, 2H), 7.61 (d, *J* = 7.5 Hz, 2H), 7.42 – 7.37 (m, 2H), 7.33 – 7.28 (m, 2H), 6.03 (dd, *J* = 5.1, 2.5 Hz, 1H), 4.50 – 4.41 (m, 1H), 4.41 – 4.34 (m, 2H), 4.26 – 4.15 (m, 3H), 1.68 – 1.59 (m, 2H), 1.58 – 1.52 (m, 1H), 1.47 (d, *J* = 1.4 Hz, 9H), 1.30 (d, *J* = 5.2 Hz, 9H), 1.13 (d, *J* = 6.3 Hz, 1H), 1.04 (d, *J* = 6.3 Hz, 2H), 0.96 (td, *J* = 6.4, 2.0 Hz, 6H); **^{13}C NMR** (101 MHz, $CDCl_3$) δ 171.60, 171.37, 169.05, 168.55, 155.89, 143.86, 143.63, 141.21, 127.59, 126.95, 125.09, 119.87, 81.62, 81.49, 66.83, 66.69, 66.38, 58.38, 58.22, 51.80, 51.53, 47.07, 41.60, 41.35, 28.07, 28.04, 27.92, 24.69, 22.67, 22.03, 21.75, 16.83, 16.36; **IR** (neat, cm-1) 3326, 2973, 1726, 1669, 1487, 1449, 1391, 1366, 1235, 1210, 1189, 1144, 1077, 1041, 990, 917, 868, 844.

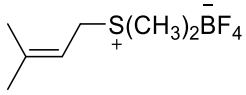

2.28

Prenyldimethylsulfonium tetrafluoroborate (2.8).

A solution of 3-methyl-2-buten-1-ol (2.4 mL, 23.0 mmol and dimethyl sulfide (5.2 mL, 71.0 mmol) in anhydrous CH_2Cl_2 (23.0 mL) under a N_2 atmosphere was cooled to -10◦C for 10 minutes. HBF_4 [55% in Et_2O by wt] (3.1 mL, 23.0 mmol) was added dropwise and the reaction mixture was slowly warmed to rt and stirred for 24 hours. Volatiles were removed and the residue was dissolved in Et_2O and cooled to 0◦C for 15 min. The solids were collected by vacuum filtration and washed with Et_2O to afford **2.8** (4.76 g, 94%) as a colorless solid.

General Procedure for Preparation of 1,1-dimethylallyl esters (2.5a-j).

A mixture of Fmoc-AA (1.00 mmol), Na_2CO_3 (116.6 mg, 1.10 mmol) in anhydrous CH_2Cl_2 (12.5 mL) was stirred at rt for 5 min. CuBr (14.4 mg, 0.100 mmol) was added, followed by **2.8** (240.5 mg, 1.10 mmol). The mixture was stirred at rt for 15-24 hours. Volatiles were removed and the residue was filtered through a thin pad of SiO_2 (15-30% EA/Hex) and concentrated to afford the pure 1,1-dimethylallyl esters **2.5a-j**.

General Procedure for Deprotection of 1,1-dimethylallyl esters (2.6a-j).

A solution of Fmoc-AA dimethylallyl ester **2.5a-j** (0.50 mmol), 1-octanethiol (434 µL, 2.50 mmol), and diethylamine (517 µL, 5.00 mmol) in CH_3CN (1.0 mL) was stirred at rt for 2 h. The volatiles were removed and co-evaporated twice with additional CH_3CN. The deprotected amino acids **2.6a-**j were used without purification.

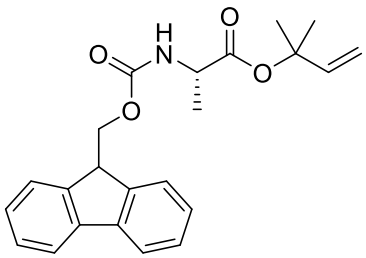

2.5a

Fmoc-Ala dimethylallyl ester (2.5a).

Colorless solid; **Yield** 80%; $\mathbf{R_f}$ = 0.35 (20% EA/Hex); **^{1}H NMR** (300 MHz, $CDCl_3$) δ 7.78 – 7.75 (m, 2H), 7.62 – 7.58 (m, 2H), 7.43 – 7.38 (m, 2H), 7.34 – 7.29 (m, 2H), 6.06 (dd, *J* = 17.5, 10.9 Hz, 1H), 5.42 – 5.32 (m, 1H), 5.21 (d, *J* = 17.4 Hz, 1H), 5.11 (d, *J* = 10.9 Hz, 1H), 4.38 (d, *J* = 8.0 Hz, 3H), 4.24 (d, *J* = 7.0 Hz, 1H), 1.55 (d, *J* = 2.5 Hz, 6H), 1.42 (d, *J* = 7.1 Hz, 3H).

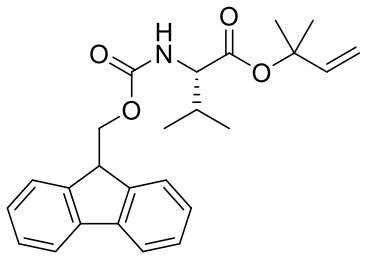

2.5b

Fmoc-Val dimethylallyl ester (2.5b).

Colorless glass; **Yield** 80%; $\mathbf{R_f}$ = 0.34 (15% EA/Hex); **^{1}H NMR** (300 MHz, $CDCl_3$) δ 7.77 (d, *J* = 7.4 Hz, 2H), 7.61 (d, *J* = 7.4 Hz, 2H), 7.40 (td, *J* = 7.4, 1.1 Hz, 2H), 7.35 – 7.29 (m, 2H), 6.08 (dd, *J* = 17.5, 10.9 Hz, 1H), 5.32 (d, *J* = 9.0 Hz, 1H), 5.22 (d, *J* = 17.5 Hz, 1H), 5.14 – 5.08 (m, 1H), 4.41 – 4.37 (m, 1H), 4.28 – 4.20 (m, 2H), 2.26 – 2.13 (m, 1H), 1.56 (s, 6H), 0.95 (dd, *J* = 19.5, 6.9 Hz, 6H).

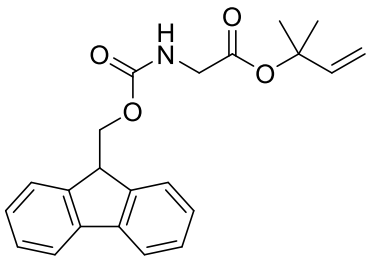

2.5c

Fmoc-Gly dimethylallyl ester (2.5c).

Colorless solid; **Yield** 77%; $\mathbf{R_f}$ = 0.4 (30% EA/Hex); **^{1}H NMR** (300 MHz, $CDCl_3$) δ 7.77 (dd, *J* = 7.5, 1.1 Hz, 2H), 7.60 (d, *J* = 7.4 Hz, 2H), 7.43 – 7.38 (m, 2H), 7.34 – 7.29 (m, 2H), 6.12 – 6.03 (m, 1H), 5.24 – 5.10 (m, 2H), 4.39 (d, *J* = 7.1 Hz, 2H), 4.24 (d, *J* = 7.1 Hz, 1H), 3.93 (d, *J* = 5.5 Hz, 2H), 1.56 (s, 6H).

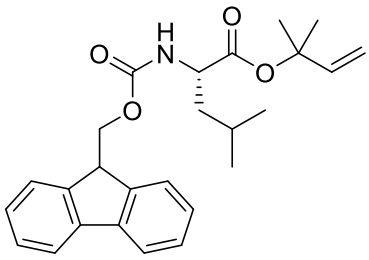

2.5d

Fmoc-Leu dimethylallyl ester (2.5d).

Colorless glass; **Yield** 85%; $\mathbf{R_f}$ = 0.36 (15% EA/Hex); **^{1}H NMR** (300 MHz, $CDCl_3$) δ 7.76 (d, *J* = 7.5 Hz, 2H), 7.60 (d, *J* = 7.4 Hz, 2H), 7.43 – 7.37 (m, 2H), 7.33 – 7.27 (m, 2H), 6.06 (dd, *J* = 17.5, 10.9 Hz, 1H), 5.17 (s, 1H), 5.15 (d, *J* = 2.3 Hz, 1H), 5.10 (d, *J* = 10.8 Hz, 1H), 4.39 (d, *J* = 7.1 Hz, 2H), 4.32 (d, *J* = 5.1 Hz, 1H), 4.22 (t, *J* = 7.0 Hz, 1H), 1.72 (s, 1H), 1.58 (d, *J* = 1.3 Hz, 1H), 1.54 (s, 6H), 0.97 (d, *J* = 6.3 Hz, 6H).

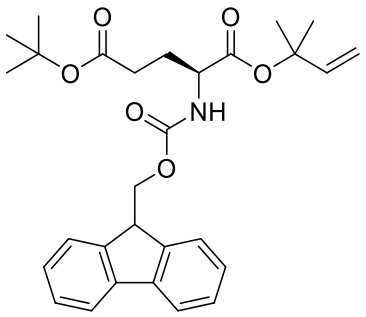

2.5e

Fmoc-Glu(tBu) dimethylallyl ester (2.5e).

Colorless glass; **Yield** 78%; $\mathbf{R_f}$ = 0.35 (20% EA/Hex); **^{1}H NMR** (300 MHz, $CDCl_3$) δ 7.76 (dd, *J* = 7.6, 1.1 Hz, 2H), 7.60 (d, *J* = 7.6 Hz, 2H), 7.40 (dddd, *J* = 8.2, 7.5, 1.3, 0.6 Hz, 2H), 7.31 (tt, *J* = 7.4, 1.0 Hz, 2H), 6.07 (dd, *J* = 17.5, 10.9 Hz, 1H), 5.43 (d, *J* = 8.2 Hz, 1H), 5.25 – 5.08 (m, 2H), 4.44 – 4.33 (m, 2H), 4.33 – 4.26 (m, 1H), 4.22 (t, *J* = 7.1 Hz, 1H), 2.42 – 2.23 (m, 2H), 2.23 – 2.14 (m, 1H), 1.94 (dt, *J* = 14.3, 7.2 Hz, 1H), 1.55 (s, 6H), 1.45 (d, *J* = 0.8 Hz, 9H).

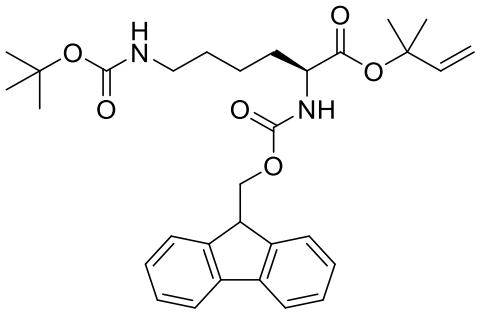

2.5f

Fmoc-Lys(Boc) dimethylallyl ester (2.5f).

Colorless Solid; **Yield** 75%; $\mathbf{R_f}$ **=** 0.36 (30% EA/Hex); ^{1}H NMR (300 MHz, $CDCl_3$) δ 7.76 (d, *J* = 7.5 Hz, 2H), 7.60 (d, *J* = 7.4 Hz, 2H), 7.40 (t, *J* = 7.4 Hz, 2H), 7.31 (t, *J* = 7.3 Hz, 2H), 6.06 (dd, *J* = 17.5, 10.9 Hz, 1H), 5.36 (d, *J* = 8.3 Hz, 1H), 5.20 (d, *J* = 17.5 Hz, 1H), 5.11 (d, *J* = 10.8 Hz, 1H), 4.56 (s, 1H), 4.38 (dd, *J* = 7.2, 2.2 Hz, 2H), 4.28 (d, *J* = 5.6 Hz, 1H), 4.22 (t, *J* = 7.0 Hz, 1H),

3.11 (d, *J* = 7.1 Hz, 2H), 1.96 – 1.74 (m, 1H), 1.68 (dd, *J* = 14.1, 6.4 Hz, 1H), 1.58 (s, 1H), 1.54 (s, 6H), 1.46 (s, 2H), 1.43 (s, 9H), 1.26 (t, *J* = 7.1 Hz, 1H).

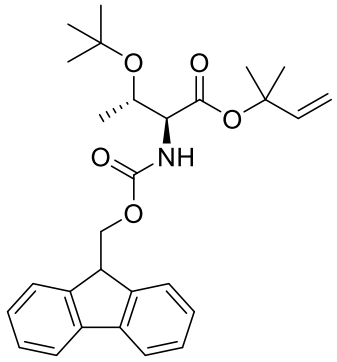

2.5g

Fmoc-Thr(tBu) dimethylallyl ester (2.5g).

Colorless glass; **Yield** 95%; **R_f =** 0.35 (15% EA/Hex); **^{1}H NM**R (400 MHz, $CDCl_3$) δ 7.76 (d, *J* = 7.5 Hz, 2H), 7.63 (dd, *J* = 7.7, 3.1 Hz, 2H), 7.40 (t, *J* = 7.5 Hz, 2H), 7.31 (t, *J* = 7.4 Hz, 2H), 6.09 (dd, *J* = 17.4, 10.9 Hz, 1H), 5.54 (d, *J* = 9.5 Hz, 1H), 5.21 (d, *J* = 17.5 Hz, 1H), 5.08 (d, *J* = 10.9 Hz, 1H), 4.38 (dd, *J* = 7.4, 3.8 Hz, 2H), 4.28 – 4.20 (m, 2H), 4.16 (dd, *J* = 9.4, 2.2 Hz, 1H), 1.22 (d, *J* = 6.1 Hz, 3H), 1.18 (s, 9H).

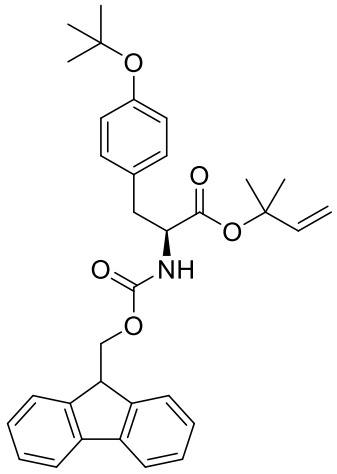

2.5h

Fmoc-Tyr(tBu) dimethylallyl ester (2.5h).

Colorless glassy solid; **Yield =** 93%; $\mathbf{R_f}$ = 0.33 (20% EA/Hex); **^{1}H NMR** (400 MHz, $CDCl_3$) δ 7.76 (d, *J* = 7.5 Hz, 2H), 7.58 (d, *J* = 7.4 Hz, 2H), 7.40 (t, *J* = 7.5 Hz, 2H), 7.31 (td, *J* = 6.2, 3.2 Hz, 2H), 7.06 (d, *J* = 7.9 Hz, 2H), 6.91 (d, *J* = 7.7 Hz, 2H), 5.99 (dd, *J* = 17.5, 10.9 Hz, 1H), 5.30 (d, *J* = 8.1 Hz, 1H), 5.15 (d, *J* = 17.5 Hz, 1H), 5.07 (d, *J* = 10.9 Hz, 1H), 4.55 (q, *J* = 6.6 Hz, 1H), 4.42 (dd, *J* = 10.6, 7.3 Hz, 1H), 4.34 (dd, *J* = 10.6, 7.0 Hz, 1H), 4.21 (t, *J* = 7.0 Hz, 1H), 3.06 (d, *J* = 6.1 Hz, 2H), 1.47 (s, 6H), 1.32 (s, 9H).

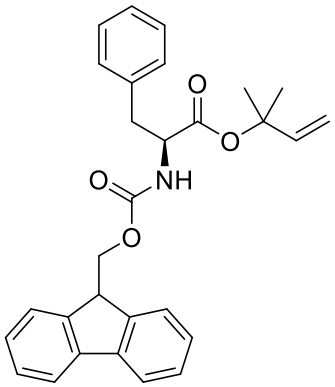

2.5i

Fmoc-Phe dimethylallyl ester (2.5i).

Colorless Solid; **Yield** 70%; **^{1}H NMR** (400 MHz, $CDCl_3$) δ 7.77 (d, *J* = 7.6 Hz, 2H), 7.58 (dd, *J* = 7.6, 4.3 Hz, 2H), 7.41 (t, *J* = 7.5 Hz, 2H), 7.30 (dt, *J* = 11.8, 6.0 Hz, 5H), 7.17 (d, *J* = 7.1 Hz, 2H), 6.02 (dd, *J* = 17.5, 10.9 Hz, 1H), 5.31 (d, *J* = 8.2 Hz, 1H), 5.18 (d, *J* = 17.4 Hz, 1H), 5.10 (d, *J* = 10.9 Hz, 1H), 4.60 (q, *J* = 6.6 Hz, 1H), 4.44 (dd, *J* = 10.6, 7.2 Hz, 1H), 4.33 (dd, *J* = 10.6, 7.0 Hz, 1H), 4.21 (t, *J* = 7.1 Hz, 1H), 3.12 (dd, *J* = 6.3, 3.2 Hz, 2H), 1.50 (s, 6H); **^{13}C NMR** (101 MHz, $CDCl_3$) δ 170.20, 155.45, 143.80, 143.73, 141.60, 141.22, 135.91, 129.49, 128.36, 127.62, 126.96, 125.09, 125.00, 119.89, 113.30, 82.53, 183.22 – 4.96 (m), 66.85, 54.96, 47.09, 38.30, 26.27, 26.03; **IR** (neat, cm^{-1}) 3334, 3064, 3029, 2980, 1713, 1209, 1123, 1046, 737.

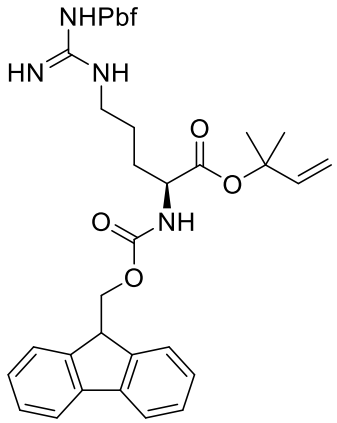

2.5j

Fmoc-Arg(Pbf) dimethylallyl ester (2.5j).

Colorless glassy solid; **Yield** 70%; $\mathbf{R_f}$ = 0.4 (60% EA/Hex); **^{1}H NMR** (300 MHz, $CDCl_3$) δ 7.74 – 7.71 (m, 2H), 7.55 (d, *J* = 7.4 Hz, 2H), 7.39 – 7.33 (m, 2H), 7.30 – 7.20 (m, 3H), 6.23 (s, 2H), 6.07 – 5.97 (m, 1H), 5.66 (d, *J* = 8.1 Hz, 1H), 5.16 (d, *J* = 17.5 Hz, 1H), 5.06 (d, *J* = 10.9 Hz, 1H), 4.32 (d, *J* = 7.3 Hz, 2H), 4.16 (d, *J* = 5.0 Hz, 1H), 3.20 (s, 2H), 2.89 (s, 2H), 2.58 (s, 3H), 2.50 (s, 3H), 2.04 (s, 4H), 1.82 (d, *J* = 5.9 Hz, 1H), 1.72 – 1.55 (m, 3H), 1.51 – 1.47 (m, 6H), 1.41 (s, 6H).

Solid-Phase Procedures

Cleavage condition A (Sieber Amide cleavage)

An aliquot (~1 mg) of resin-bound peptide was treated with 200 µL TFA/H_2O/CH_2Cl_2 (2:1:97) and the mixture agitated for 5 min at rt. Following this time period, volatiles were removed by N_2 stream. The resulting residue was dissolved in 200 µL MeOH-H_2O (1:1), filtered and analyzed by UPLC-MS. Note: Product / DKP ratio was determined by integrating 214 and 254 nm peaks and are reported as relative percentages.

Cleavage condition B (photocleavage)

The resin-bound peptide was suspended in a 5 mL solution of 1:10 MeOH:CH_2Cl_2 in a fused quartz tube and agitated under 365 nm UV light for 1 h. The solvent was filtered to remove the resin and removed under reduced pressure. The resulting residue was dissolved in MeOH-H2O (1:1), filtered and analyzed by UPLC-MS and HPLC.

Standard wash protocol

DMF (3 x 1 mL), CH_2Cl_2 (3 x 1 mL), MeOH (3 x 1 mL), CH_2Cl_2 (3 x 1 mL), then DMF (3 x 1 mL).

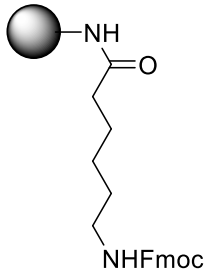

2.10

Loading of Ahx Spacer (2.10)

Fmoc-Sieber Amide PS Resin (0.6 mmol/g) or TentaGel S NH_2 (0.26 mmol/g) was swelled in DMF for 15 min, drained, and treated with piperidine-DMF (1:4, 1 x 2 mL, 30 min). The mixture was drained and washed with standard wash protocol to afford a positive Kaiser ninhydrin test. To

a mixture of Fmoc-Ahx-OH (4 eq) and HATU (3.9 eq) in DMF (0.03 M) was added DIEA (8 eq) and this mixture was added to the resin (pre-washed with DMF) after a 5 min preactivation period. After 2 h, the mixture was drained and washed with the standard wash protocol to afford a negative Kaiser ninhydrin test.

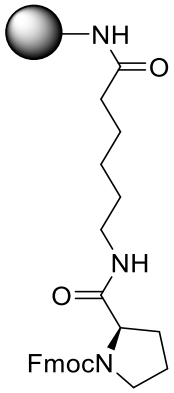

2.11

Loading of Proline Residue (2.11)

The prepared resin **2.10** was washed with DMF (3 x 2 mL) and agitated with piperidine-DMF (1:4, 1 x 2 mL, 30 min). The mixture was drained, and the resin washed with standard wash protocol to afford a positive Kaiser ninhydrin test. To a mixture of Fmoc-Pro-OH (4 eq), HATU (3.9 eq) and HOAt (4 eq) in DMF (0.03 M) was added DIEA (8 eq) and this mixture was added to the resin (pre-washed with DMF) after a 5 min preactivation period. After 2 h, the mixture was drained and washed with the standard wash protocol to afford a negative Kaiser ninhydrin test

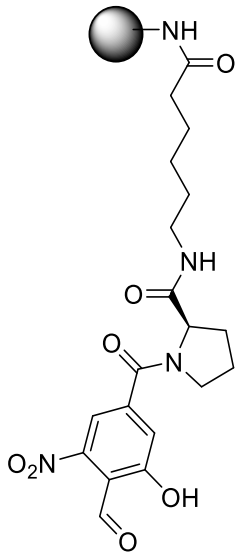

2.13

Loading of Hcna (2.13)

The prepared resin **2.11** was swelled in DMF for 15 min, drained, and treated with piperidine-DMF (1:4, 1 x 2 mL, 30 min). The mixture was drained, and resin washed with standard wash protocol to afford a positive chloranil test. To a mixture of **1.5** (3 eq) and PyBOP in DMF (0.03 M) was added DIEA (6 eq) and this mixture was added to the resin (pre-washed with DMF) after a 5 min preactivation period. After 2 h, the mixture was drained and washed with the standard wash protocol to afford a negative chloranil test.

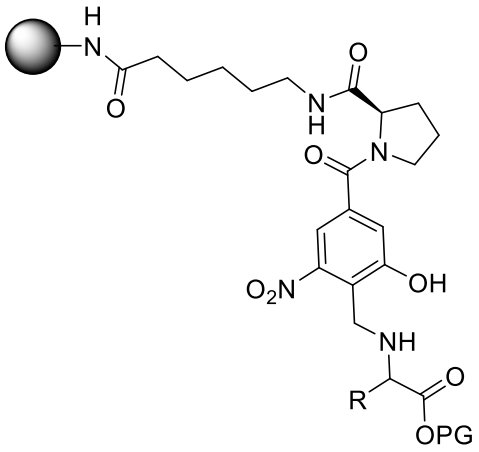

2.14a-j

Solid-Phase Reductive Amination (2.14a-j)

The prepared resin **2.13** was swelled in DMF for 15 min then treated with a mixture of H-AA-ODMA (**2.6a-j**) or HCl-AA-O*t*Bu (10 eq) and AcOH (10 eq) in CH_2Cl_2 (0.03 M). After 3 h, the mixture was drained and washed briefly with standard wash protocol then THF-MeOH (2:1). The resin was then taken up in THF-MeOH (2:1, 0.03 M) and treated with solid $NaBH_4$ (5 eq). After 2 h, the mixture was drained and washed with H_2O, standard wash protocol, then piperidine-DMF (1:4, 5 min). The resin was washed once more with standard wash protocol to afford a positive chloranil test.

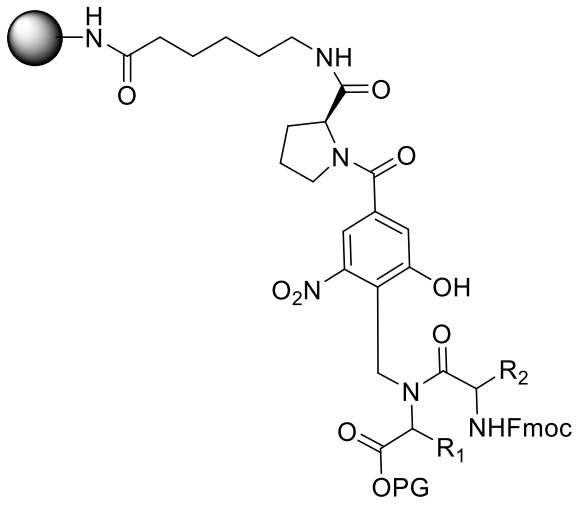

2.16

Acylation of Benzyl Amine (2.16).

A flame-dried flask was charged with the 2nd Amino Acid residue (4 eq) and dry CH_2Cl_2 (0.05 M), and symmetric anhydride formation was initiated by addition of DIPC (2 eq) dropwise at rt. The mixture was stirred at rt for 12 min and the resulting solution was solubilized by addition of DMF (0.05 M). This solution was added directly to prepared resin **2.14a-j** and mixture was agitated for 2 h, followed by standard wash protocol to afford a slightly positive chloranil test. This procedure was repeated once more to afford resin-bound dipeptide (and a negative chloranil test).

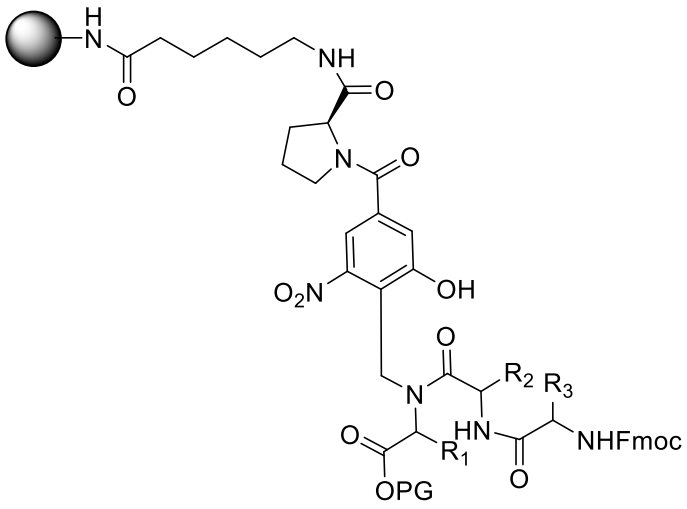

2.18a-i

General Procedure for Coupling of 3rd Amino Acid Residue (2.18a-i).

A solution of 1-octanthiol (10 eq), DIEA (10 eq), and DMF (0.03 M) was added to the prepared resin **2.16** and the mixture was agitated for 1 h, followed by the standard wash protocol. Next, a mixture of TIPS-OTf (10 eq), 2,6-Lutidine (10 eq), and DMF (0.03 M) was added to the resin and the mixture was agitated for 4 h, followed by the standard wash protocol. A flame-dried flask was charged with the 3rd Amino Acid residue (4 eq) and dry CH_2Cl_2 (0.05 M), and symmetric anhydride formation was initiated by addition of DIPC (2 eq) dropwise at rt. The mixture was stirred at rt for 12 min and the resulting solution was solubilized by addition of DMF (0.05 M).

The resin was agitated with a solution of DBU-1-Octanthiol-DMF (2:2:96, 1 x 2 mL, 3 min), washed with the standard wash protocol, and the pre-activated amino acid solution was added, taking care to minimize the time between deprotection and coupling. The mixture was agitated for 2 h, followed by standard wash protocol to afford a negative chloranil test. The resin was agitated with piperidine-DMF (1:4, 1 x 2 mL, 30 min). The mixture was drained, and the resin washed with standard wash protocol to afford a positive Kaiser ninhydrin test

General procedure for amino acid coupling

To a mixture of Fmoc-AA-OH (4 eq), HATU (3.9 eq) and HOAt (4 eq) in DMF (0.03 M) was added DIEA (8 eq) and this mixture was added to the resin after a 5 min preactivation period. After

2 h (3h following Proline), the mixture was drained and washed with the standard wash protocol to afford a negative Kaiser ninhydrin test. The resin was agitated with piperidine-DMF (1:4, 1 x 2 mL, 30 min). The mixture was drained, and the resin washed with standard wash protocol to afford a positive Kaiser ninhydrin test. The procedure was then repeated as needed.

Peptide Cyclization Condition A

After complete synthesis of the desired Fmoc or Boc-protected peptide, the C-terminal DMA protecting group was removed using $Pd(PPh_3)_4$ (1 eq) and Phenylsilane (20 eq) in CH_2Cl_2 under N2 for 2 h, after which the resin was drained and washed with DMF (3 x 1 min), sodium N,N-diethyldithiocarbamate (0.03 M in DMF, 3 x 1 min), and CH_2Cl_2 (3 x 1 min). The resin was agitated with piperidine-DMF (1:4, 1 x 2 mL, 30 min). The mixture was drained, and the resin washed with standard wash protocol to afford a positive Kaiser ninhydrin test. A mixture of PyAop (5 eq), HOAt (5 eq), and DIEA (10 eq) in DMF (0.03 M) was added directly to the resin. After 2 h, the mixture was drained and washed with the standard wash protocol to afford a negative Kaiser ninhydrin test.

Peptide Cyclization Condition B

After complete synthesis of the desired Fmoc or Boc-protected peptide, the C-terminal DMA protecting group was removed using $Pd(PPh_3)_4$ (1 eq) and Phenylsilane (20 eq) in CH_2Cl_2 under N2 for 2 h, after which the resin was drained and washed with DMF (3 x 1 min), sodium N,N-diethyldithiocarbamate (0.03 M in DMF, 3 x 1 min), and CH_2Cl_2 (3 x 1 min). The resin was agitated with piperidine-DMF (1:4, 1 x 2 mL, 30 min). The mixture was drained, and the resin washed with standard wash protocol to afford a positive Kaiser ninhydrin test. A mixture of PyAOP (3 eq), 2,4,6-collidine (6 eq), and DIEA (6 eq) in 9:1 CH_2Cl_2-DMF (0.03 M) was added directly to the resin. After 2 h, the mixture was drained and washed with the standard wash protocol to afford a negative Kaiser ninhydrin test.

General procedure for thioester synthesis

After complete synthesis of the desired Boc-protected peptide, the C-terminal DMA protecting group was removed using $Pd(PPh_3)_4$ (1 eq) and Phenylsilane (20 eq) in CH_2Cl_2 under N2 for 2 h, after which the resin was drained and washed with DMF (3 x 1 min), sodium N,N-diethyldithiocarbamate (0.03 M in DMF, 3 x 1 min), and CH_2Cl_2 (3 x 1 min). A mixture of PyAop

(5 eq), HOAt (5 eq), and DIEA (10 eq) in DMF (0.03 M) was added directly to the resin. After 2 h, the mixture was drained and washed with the standard wash protocol to afford a negative Kaiser ninhydrin test. A solution of 1-octanthiol (10 eq), DIEA (10 eq), and DMF (0.03 M) was added to the resin and the mixture was agitated for 1 h, followed by the standard wash protocol. Next, a mixture of TIPS-OTf (10 eq), 2,6-Lutidine (10 eq), and DMF (0.03 M) was added to the resin and the mixture was agitated for 4 h, followed by the standard wash protocol. A solution of HATU (5 eq) and DIEA (20 eq) in DMF (0.03 M) was added to the resin and agitated for a 5 min period. Without draining, thiophenol (10 eq) was added to the mixture. After 2 h, the mixture was drained and washed with the standard wash protocol to afford a negative Kaiser ninhydrin test

General procedure for global deprotection A

The resin was agitated with a solution of CH_2Cl_2-H_2O (95:5). After 2 h, the mixture was drained and washed with the standard wash protocol.

General procedure for global deprotection B

The resin was agitated with a solution of TFA-TIPS-CH_2Cl_2 (50:2:48). After 6 h, the mixture was drained and washed with the standard wash protocol.

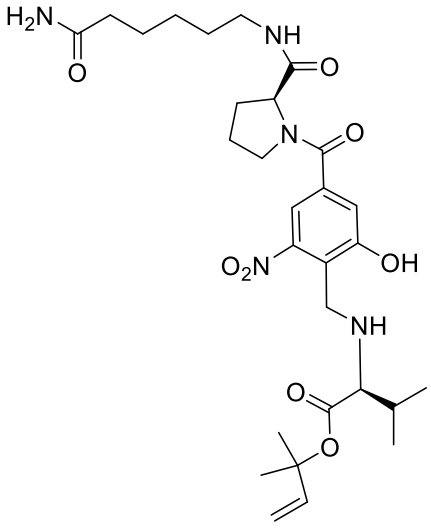

2.14a

Hcnb-Val-ODMA (2.14a).

Fmoc-Sieber Amide PS Resin (16.7 mg, 0.01 mmol) was prepared according to the *general procedure for reductive amination.* H-Val-ODMA was prepared according to the *general procedure for the preparation of 1,1-dimethylallyl esters.* Resin cleavage was achieved using *cleavage condition A* (Sieber Amide cleavage) to afford **2.14a**. **UPLC-MS** (5→60, CH_3CN-H_2O, 5 min gradient): $\mathbf{R_t}$ min, 0% reduced linker.

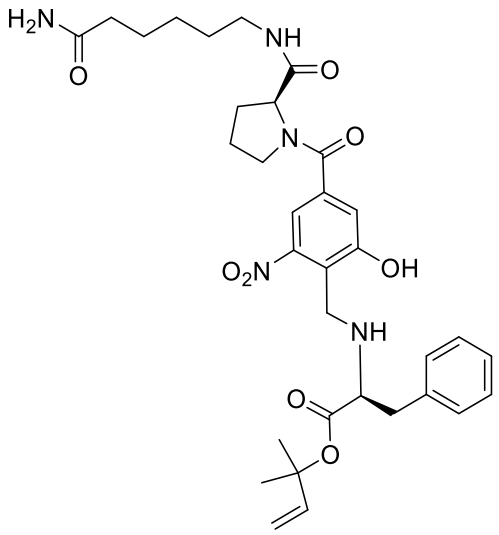

2.14b

Hcnb-Phe-ODMA (2.14b)

Fmoc-Sieber Amide PS Resin (16.7 mg, 0.01 mmol) was prepared according to the *general procedure for reductive amination.* H-Phe-ODMA was prepared according to the *general procedure for the preparation of 1,1-dimethylallyl esters.* Resin cleavage was achieved using *cleavage condition A* (Sieber Amide cleavage) to afford **2.14b**. **UPLC-MS** (5→60, CH_3CN-H_2O, 5 min gradient): $\mathbf{R_t}$ min, 8% reduced linker.

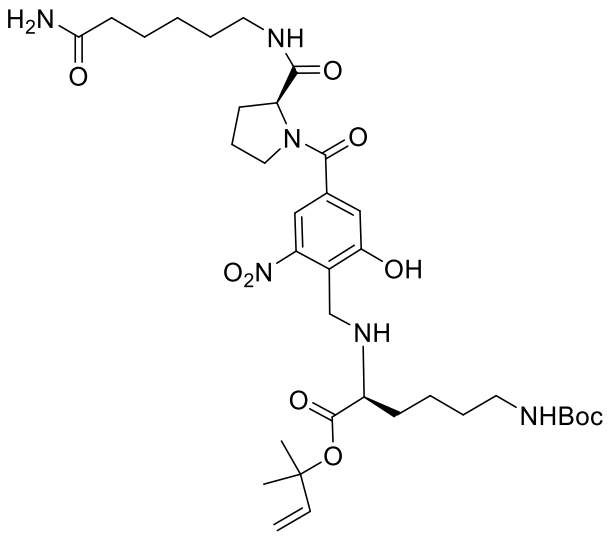

2.14c

Hcnb-Lys(Boc)-ODMA (2.14c)

Fmoc-Sieber Amide PS Resin (16.7 mg, 0.01 mmol) was prepared according to the *general procedure for reductive amination.* H-Lys(Boc)-ODMA was prepared according to the *general procedure for the preparation of 1,1-dimethylallyl esters.* Resin cleavage was achieved using *cleavage condition A* (Sieber Amide cleavage) to afford **2.14c**. **UPLC-MS** (5→60, CH_3CN-H_2O, 5 min gradient): $\mathbf{R_t}$ min, 10% reduced linker.

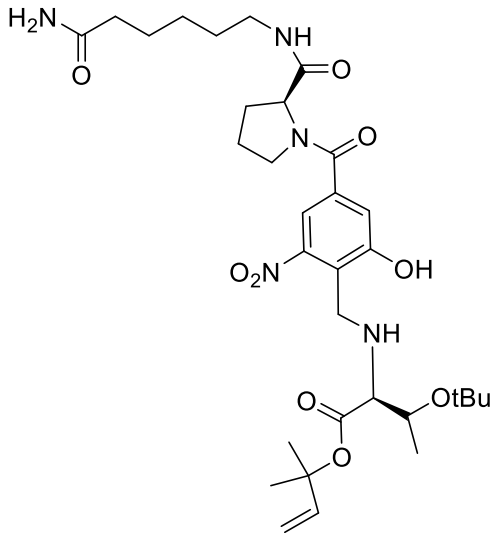

2.14d

Hcnb-Thr(tBu)-ODMA (2.14d).

Fmoc-Sieber Amide PS Resin (16.7 mg, 0.01 mmol) was prepared according to the *general procedure for reductive amination.* H-Thr(tBu)-ODMA was prepared according to the *general procedure for the preparation of 1,1-dimethylallyl esters.* Resin cleavage was achieved using *cleavage condition A* (Sieber Amide cleavage) to afford **2.14d**. **UPLC-MS** (5→60, CH_3CN-H_2O, 5 min gradient): $\mathbf{R_t}$ min, 14% reduced linker.

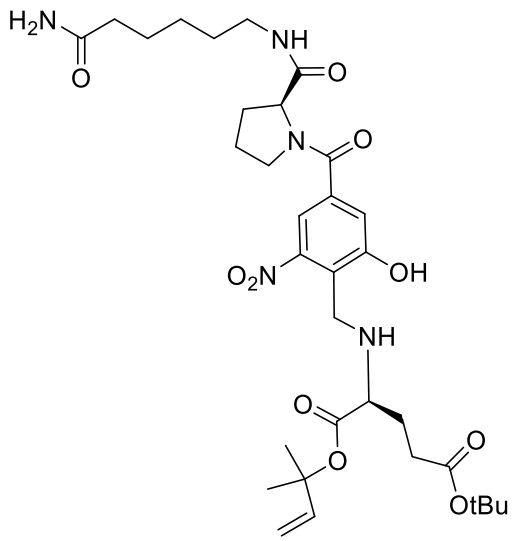

2.14e

Hcnb-Glu(tBu)-ODMA (2.14e).

Fmoc-Sieber Amide PS Resin (16.7 mg, 0.01 mmol) was prepared according to the *general procedure for reductive amination.* H-Glu(tBu)-ODMA was prepared according to the *general procedure for the preparation of 1,1-dimethylallyl esters.* Resin cleavage was achieved using *cleavage condition A* (Sieber Amide cleavage) to afford **2.14e**. **UPLC-MS** (5→60, CH_3CN-H_2O, 5 min gradient): $\mathbf{R_t}$ min, 10% reduced linker.

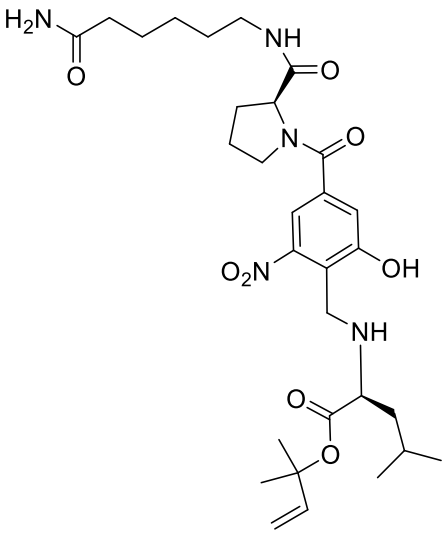

2.14f

Hcnb-Leu-ODMA (2.14f).

Fmoc-Sieber Amide PS Resin (16.7 mg, 0.01 mmol) was prepared according to the *general procedure for reductive amination.* H-Leu-ODMA was prepared according to the *general procedure for the preparation of 1,1-dimethylallyl esters.* Resin cleavage was achieved using *cleavage condition A* (Sieber Amide cleavage) to afford **2.14f**. **UPLC-MS** (5→60, CH_3CN-H_2O, 5 min gradient): $\mathbf{R_t}$ min, 0% reduced linker.

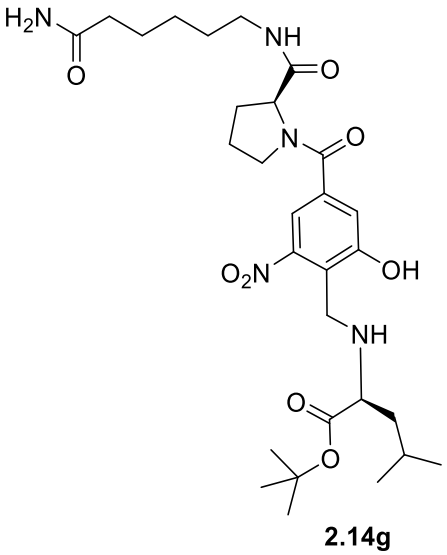

2.14g

Hcnb-Leu-OtBu (2.14g).

Fmoc-Sieber Amide PS Resin (16.7 mg, 0.01 mmol) was prepared according to the *general procedure for reductive amination* using commercially available HCl-Leu-OtBu. Resin cleavage was achieved using *cleavage condition A* (Sieber Amide cleavage) to afford **2.14g**. **UPLC-MS** (5→60, CH_3CN-H_2O, 5 min gradient): $\mathbf{R_t}$ min, 6% reduced linker.

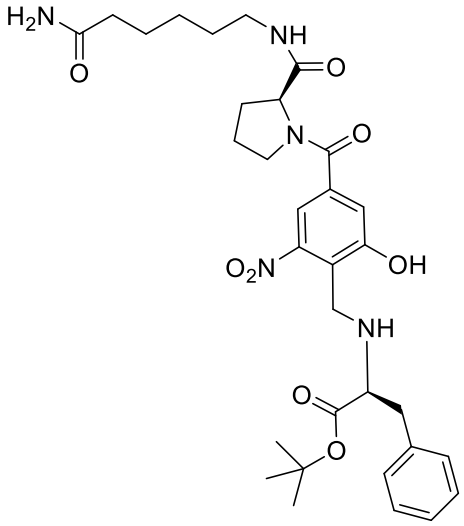

2.14h

Hcnb-Phe-OtBu (2.14h).

Fmoc-Sieber Amide PS Resin (16.7 mg, 0.01 mmol) was prepared according to the *general procedure for reductive amination* using commercially available HCl-Phe-OtBu. Resin cleavage was achieved using *cleavage condition A* (Sieber Amide cleavage) to afford **2.14h**. **UPLC-MS** (5→60, CH_3CN-H_2O, 5 min gradient): $\mathbf{R_t}$ min, 0% reduced linker.

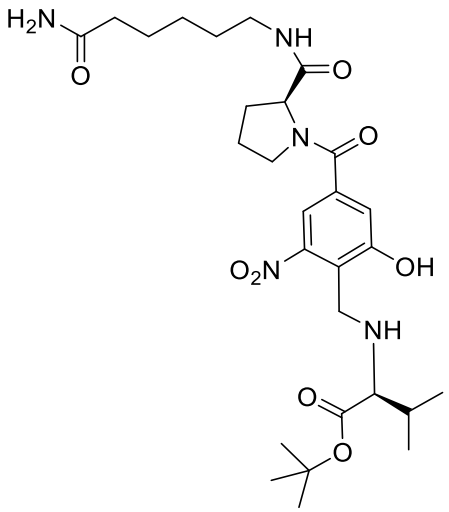

2.14i

Hcnb-Val-OtBu (2.14i)

Fmoc-Sieber Amide PS Resin (16.7 mg, 0.01 mmol) was prepared according to the *general procedure for reductive amination* using commercially available HCl-Val-OtBu. Resin cleavage was achieved using *cleavage condition A* (Sieber Amide cleavage) to afford **2.14i**. **UPLC-MS** (5→60, CH_3CN-H_2O, 5 min gradient): $\mathbf{R_t}$ min, 3% reduced linker.

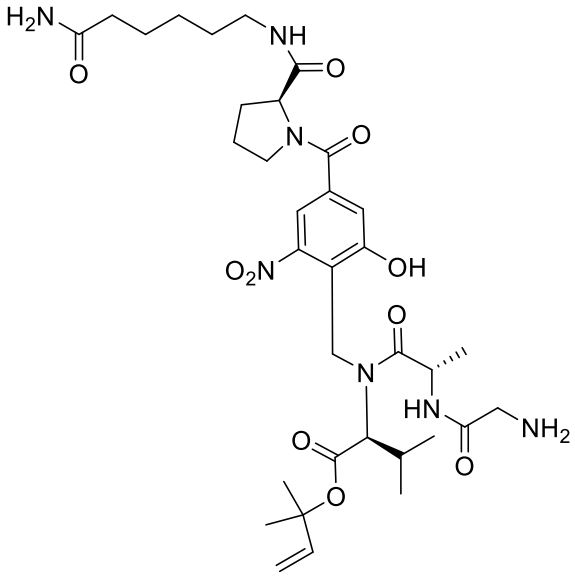

2.18a

H-Gly-Ala-Val-ODMA (2.18a).

Fmoc-Sieber Amide PS Resin (16.7 mg, 0.01 mmol) was prepared according to the *general procedure for preparation of resin-loaded tripeptide.* Resin cleavage was achieved using *cleavage condition A* (Sieber Amide cleavage) to afford **2.18a**. **UPLC-MS** (5→60, CH_3CN-H_2O, 5 min gradient): $\mathbf{R_t}$ 2.48 min, 0% DKP**.**

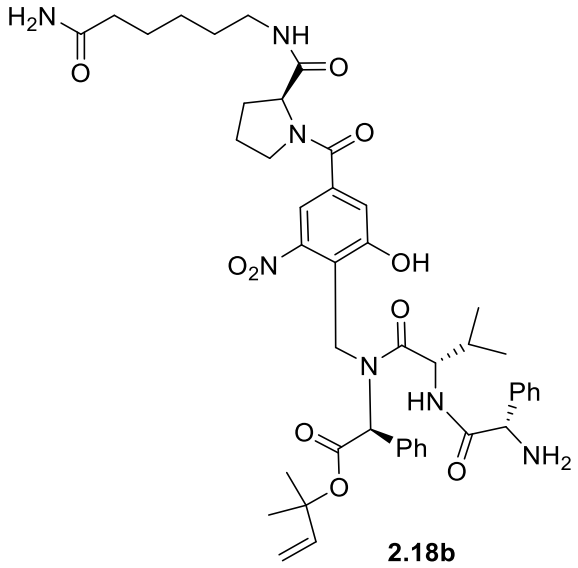

2.18b

H-Phe-Val-Phe-ODMA (2.18b).

Fmoc-Sieber Amide PS Resin (16.7 mg, 0.01 mmol) was prepared according to the *general procedure for preparation of resin-loaded tripeptide.* Resin cleavage was achieved using *cleavage condition A* (Sieber Amide cleavage) to afford **2.18b**. **UPLC-MS** (5→60, CH_3CN-H_2O, 5 min gradient): $\mathbf{R_t}$ 4.12 min, 6% DKP.

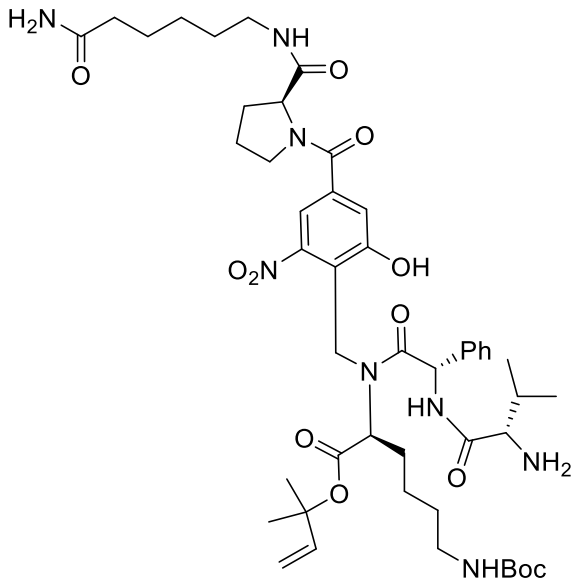

2.18c

H-Val-Phe-Lys(Boc)-ODMA (2.18c).

Fmoc-Sieber Amide PS Resin (16.7 mg, 0.01 mmol) was prepared according to the *general procedure for preparation of resin-loaded tripeptide.* Resin cleavage was achieved using *cleavage condition A* (Sieber Amide cleavage) to afford **2.18c**. **UPLC-MS** (5→60, CH_3CN-H_2O, 5 min gradient): $\mathbf{R_t}$ 3.32 min, 0% DKP.

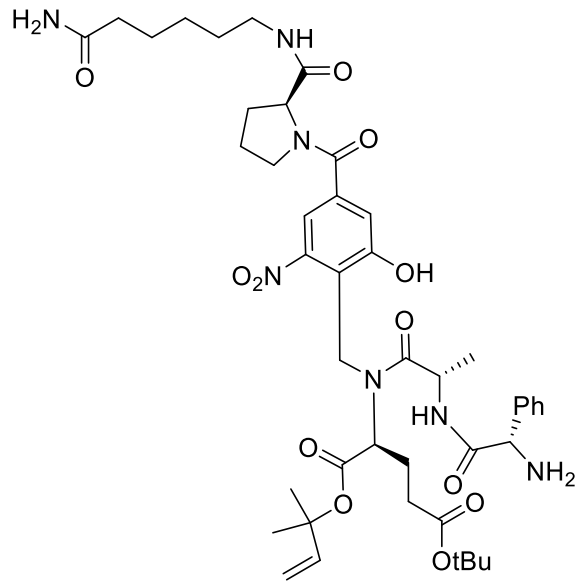

2.18d

H-Phe-Ala-Glu(tBu)-ODMA (2.18d).

Fmoc-Sieber Amide PS Resin (16.7 mg, 0.01 mmol) was prepared according to the *general procedure for preparation of resin-loaded tripeptide.* Resin cleavage was achieved using *cleavage condition A* (Sieber Amide cleavage) to afford **2.18d**. **UPLC-MS** (5→60, CH_3CN-H_2O, 5 min gradient): $\mathbf{R_t}$ 3.18 min, 3% DKP.

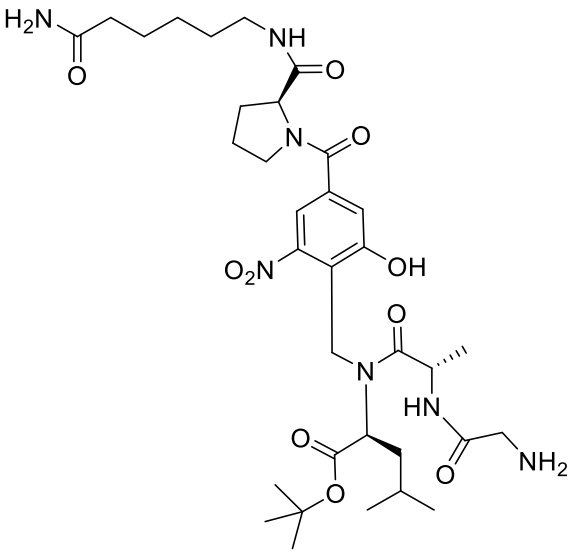

2.18e

H-Gly-Ala-Leu-O*t*Bu (2.18e).

Fmoc-Sieber Amide PS Resin (16.7 mg, 0.01 mmol) was prepared according to the *general procedure for preparation of resin-loaded tripeptide.* Resin cleavage was achieved using *cleavage condition A* (Sieber Amide cleavage) to afford **2.18e**. **UPLC-MS** (5→80, CH_3CN-H_2O, 5 min gradient): $\mathbf{R_t}$ 2.23 min, 0% DKP.

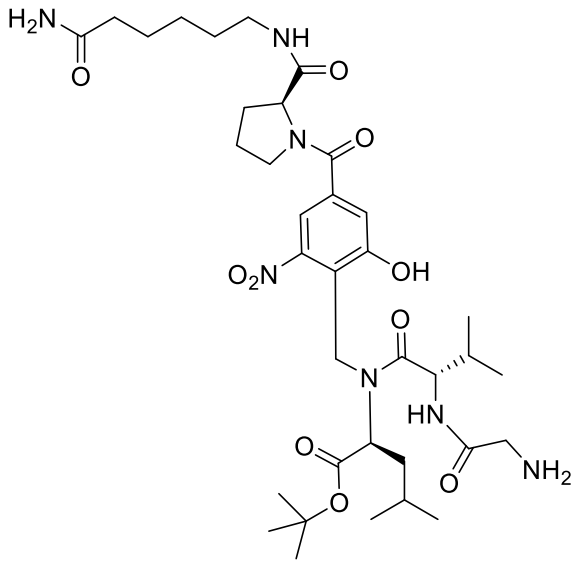

2.18f

H-Gly-Val-Leu-O*t*Bu (2.18f).

Fmoc-Sieber Amide PS Resin (16.7 mg, 0.01 mmol) was prepared according to the *general procedure for preparation of resin-loaded tripeptide.* Resin cleavage was achieved using *cleavage condition A* (Sieber Amide cleavage) to afford **2.18f**. **UPLC-MS** (5→60, CH_3CN-H_2O, 5 min gradient): $\mathbf{R_t}$ 2.70 min, 0% DKP.

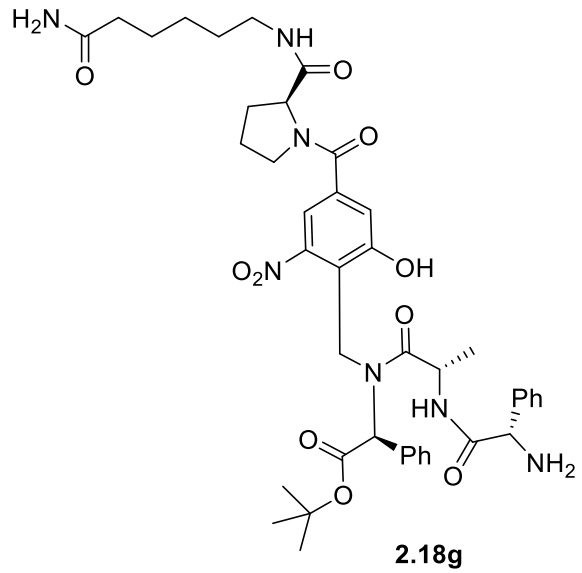

2.18g

H-Phe-Ala-Phe-O*t*Bu (2.18g).

Fmoc-Sieber Amide PS Resin (16.7 mg, 0.01 mmol) was prepared according to the *general procedure for preparation of resin-loaded tripeptide.* Resin cleavage was achieved using *cleavage condition A* (Sieber Amide cleavage) to afford **2.18g**. **UPLC-MS** (5→60, CH_3CN-H_2O, 5 min gradient): $\mathbf{R_t}$ 3.78 min, 0% DKP.

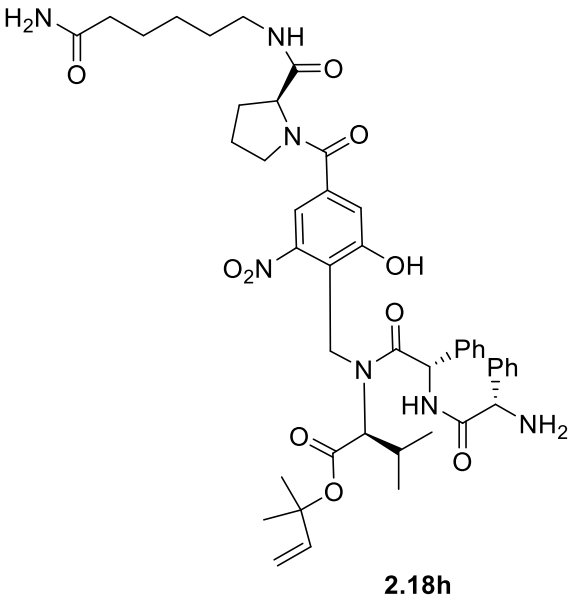

2.18h

H-Phe-Phe-Val-OtBu (2.18h).

Fmoc-Sieber Amide PS Resin (16.7 mg, 0.01 mmol) was prepared according to the *general procedure for preparation of resin-loaded tripeptide.* Resin cleavage was achieved using *cleavage condition A* (Sieber Amide cleavage) to afford **2.18h**. **UPLC-MS** (5→60, CH_3CN-H_2O, 5 min gradient): $\mathbf{R_t}$ 3.02 min, 0% DKP**.**

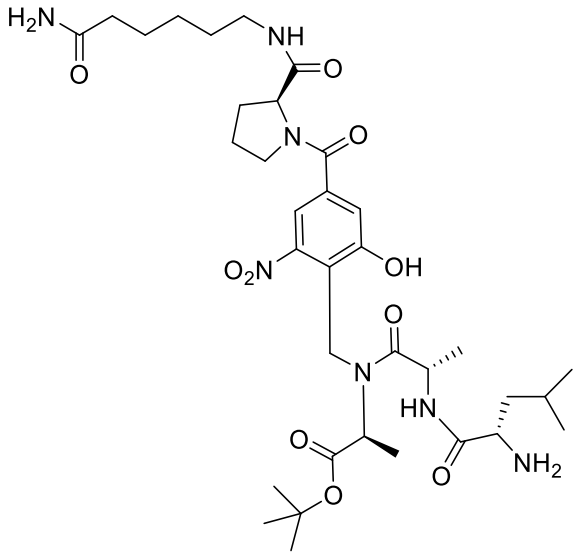

2.18i

H-Leu-Ala-Ala-O*t*Bu (2.18i)

Fmoc-Sieber Amide PS Resin (16.7 mg, 0.01 mmol) was prepared according to the *general procedure for preparation of resin-loaded tripeptide.* Resin cleavage was achieved using *cleavage condition A* (Sieber Amide cleavage) to afford **2.18i**. **UPLC-MS** (5→95, CH_3CN-H_2O, 5 min gradient): $\mathbf{R_t}$ 2.50 min, 12% DKP.

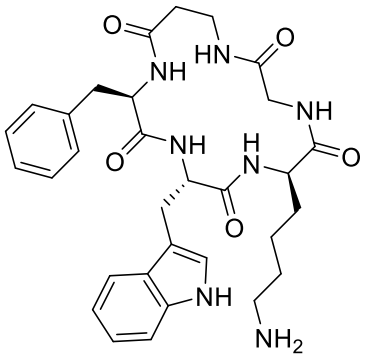

4.2

c-[(D)-Trp-Lys-Gly-(β)-Ala-Phe] (4.2)

TentaGel S NH_2 (230.8 mg, 0.06 mmol) was prepared according to the *general procedure for preparation of resin-loaded tripeptide.* The remaining amino acid residues were coupling using the *general procedure for amino acid coupling.* Cyclization of the peptide was achieved using the *peptide cyclization condition B* followed by *global deprotection condition A.* Resin cleavage was achieved using *cleavage condition B* (photocleavage) to afford **4.2**. **Cleavage yield** = 96% ; **HPLC** (5→50, CH_3CN-H_2O, 30 min gradient): $\mathbf{R_t}$ 22.3 min; 50% purity.

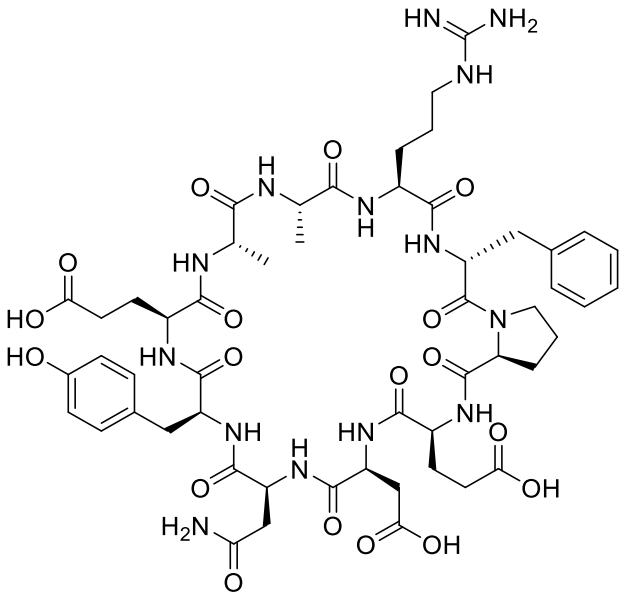

4.4

c-[Arg-(D)-Phe-Pro-Glu-Asp-Asn-Tyr-Glu-Ala-Ala] (4.4).

TentaGel S NH_2 (230.8 mg, 0.06 mmol) was prepared according to the *general procedure for preparation of resin-loaded tripeptide.* The remaining amino acid residues were coupling using the *general procedure for amino acid coupling.* Cyclization of the peptide was achieved using the *general procedure for peptide cyclization*, followed by *global deprotection condition B.* Resin cleavage was achieved using *cleavage condition B* (photocleavage) to afford **4.3**. **Cleavage yield** = 90%; **HPLC** (5→20 CH_3CN-H_2O, 30 min gradient): $\mathbf{R_t}$ 11 min; 95% purity.

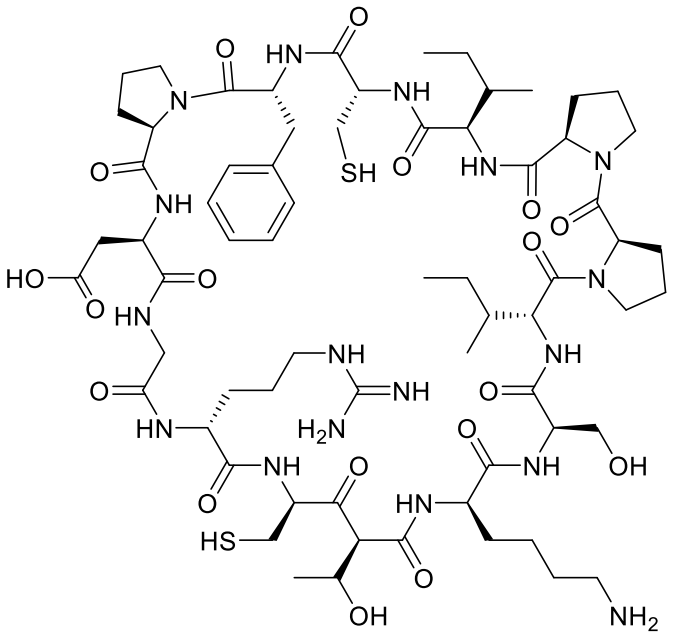

4.6

c-[Pro-Asp-Gly-Arg-Cys-Thr-Lys-Ser-Ile-Pro-Pro-Ile-Cys-Phe] (4.6).

TentaGel S NH_2 (230.8 mg, 0.06 mmol) was prepared according to the *general procedure for preparation of resin-loaded tripeptide.* The remaining amino acid residues were coupling using the *general procedure for amino acid coupling.* Cyclization of the peptide was achieved using the *general procedure for peptide cyclization*, followed by *global deprotection condition B.* Resin cleavage was achieved using *cleavage condition B* (photocleavage) to afford **4.6**. **Cleavage yield** = 80%; **HPLC** (5→15 CH_3CN-H_2O, 30 min gradient):$\mathbf{R_t}$ 14 min; 90% purity.

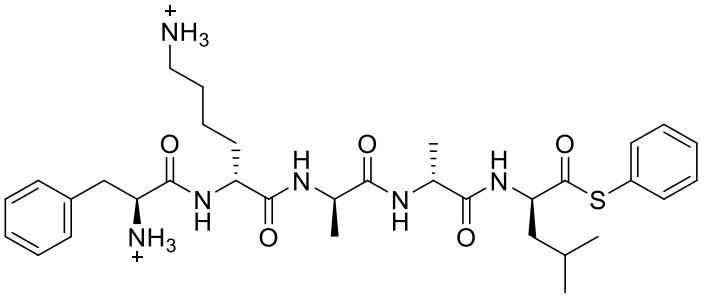

4.14

H-Phe-Lys-Ala-Ala-Leu-S-C_6H_5 (4.14).

TentaGel S NH_2 (115.4 mg, 0.03 mmol) was prepared according to the *general procedure for preparation of resin-loaded tripeptide.* The remaining amino acid residues were coupling using the *general procedure for amino acid coupling*, using a Boc-Phe-OH as the final residue. Thioester formation was achieved using the *general procedure for thioester synthesis*

followed by *global deprotection condition A.* Resin cleavage was achieved using *cleavage condition B* (photocleavage) to afford **4.14**. **Cleavage yield =** 83%; **HPLC** (30→50 CH_3CN-H_2O, 30 min gradient): $\mathbf{R_t}$ 18 min; 99% purity.

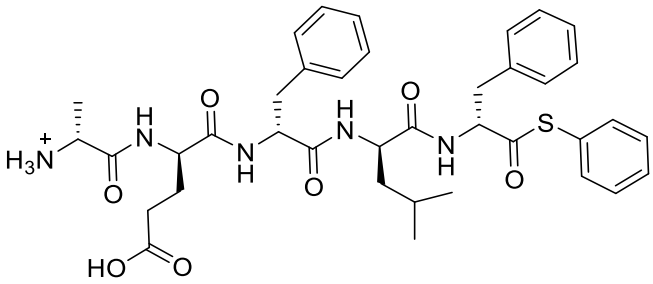

4.15

H-Ala-Glu-Phe-Leu-Phe-S-C_6H_5 (4.15).

TentaGel S NH_2 (115.4 mg, 0.03 mmol) was prepared according to the *general procedure for preparation of resin-loaded tripeptide.* The remaining amino acid residues were coupling using the *general procedure for amino acid coupling*, using a Boc-Ala-OH as the final residue. Thioester formation was achieved using the *general procedure for thioester synthesis*

followed by *global deprotection condition A.* Resin cleavage was achieved using *cleavage condition B* (photocleavage) to afford **4.15**. **Cleavage yield =** 66%; **HPLC** (30→50 CH_3CN-H_2O, 30 min gradient): $\mathbf{R_t}$ 17 min; 99% purity.

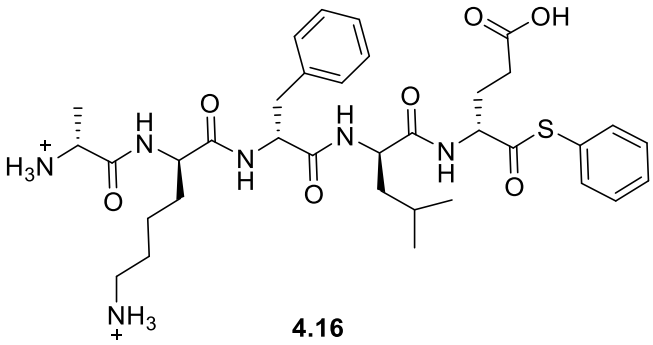

4.16

H-Ala-Lys-Phe-Leu-Glu-S-C_6H_5 (4.16).

TentaGel S NH_2 (115.4 mg, 0.03 mmol) was prepared according to the *general procedure for preparation of resin-loaded tripeptide.* The remaining amino acid residues were coupling using the *general procedure for amino acid coupling*, using a Boc-Ala-OH as the final residue. Thioester formation was achieved using the *general procedure for thioester synthesis*

followed by *global deprotection condition A.* Resin cleavage was achieved using *cleavage condition B* (photocleavage) to afford **4.16**. **Cleavage yield =** 71%; **HPLC** (50→75 CH_3CN-H_2O, 30 min gradient): $\mathbf{R_t}$ 23 min; 75% purity.

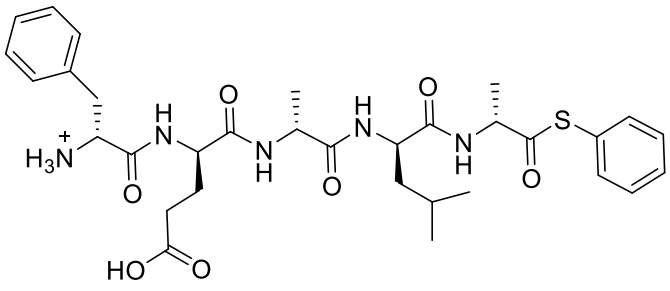

4.17

H-Phe-Glu-Ala-Leu-Ala-S-C_6H_5 (4.17).

TentaGel S NH_2 (115.4 mg, 0.03 mmol) was prepared according to the *general procedure for preparation of resin-loaded tripeptide.* The remaining amino acid residues were coupling using the *general procedure for amino acid coupling*, using a Boc-Ala-OH as the final residue. Thioester formation was achieved using the *general procedure for thioester synthesis* followed by *global deprotection condition A.* Resin cleavage was achieved using *cleavage condition B* (photocleavage) to afford **4.17**. **Cleavage yield =** 92%; **HPLC** (30→50 CH_3CN-H_2O, 30 min gradient): $\mathbf{R_t}$ 16 min; 95% purity.

EXPERIMENTAL PROCEDURES PART II

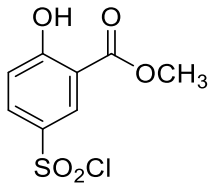

6.9

Methyl 5-(chlorosulfonyl)-2-hydroxybenzoate (6.9).

Methyl salicylate **6.8** (170 µL, 1.32 mmol) was added dropwise to a solution of chlorosulfonic acid (380 µL, 5.28 mmol) and thionyl chloride (100 µL, 1.32 mmol) at -10◦C. The reaction was brought to RT and stirred for 4 hours. The reaction mixture was poured over ice and collected by vacuum filtration to afford the **6.9** (269.0 mg, 96%) as a colorless solid. $\mathbf{R_f}$ = 0.35 (20% EA/Hex); **^{1}H NMR** (300 MHz, $CDCl_3$) δ 11.55 (s, 1H), 8.56 (d, *J* = 2.5 Hz, 1H), 8.08 (dd, *J* = 9.0, 2.5 Hz, 1H), 7.18 (d, *J* = 9.0 Hz, 1H), 4.04 (s, 3H).

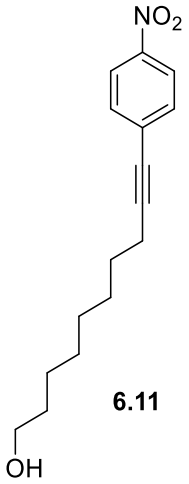

6.11

10-(4-nitrophenyl)dec-9-yn-1-ol (6.11).

Iodonitrobenzene (68.7 mg, 0.280 mmol) was added to a solution of decyn-1-ol (59 µL, 0.330 mmol), $Pd(OAc)_2$ (0.62 mg, 0.00330 mmol), and NaOH (22.4 mg, 0.560 mmol) in Acetone (1.1 mL) and H_2O (0.84 mL). The reaction was heated to 60◦C and stirred for 75 min. Upon completion, the reaction was warmed to RT and extracted 4x with CH_2Cl_2. Further purification

by flash column chromatography (40% EA/Hex) yielded **6.11** (70.5 mg, 93%) as an orange oil. $\mathbf{R_f}$ = 0.36 (40% EA/Hex); **^{1}H NMR** (300 MHz, $CDCl_3$) δ 8.11 (d, *J* = 8.4 Hz, 2H), 7.48 (d, *J* = 8.5 Hz, 2H), 3.60 (t, *J* = 6.6 Hz, 2H), 2.41 (t, *J* = 7.1 Hz, 2H), 1.65 – 1.52 (m, 4H), 1.39 (d, *J* = 36.3 Hz, 8H).

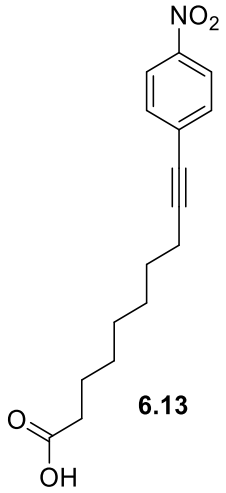

6.13

10-(4-nitrophenyl)dec-9-ynoic acid (6.13).

7.54 (25.1 mg, 0.0910 mmol), TEMPO (2.8 mg, 0.0179 mmol), and BAIB (64.6 mg, 0.201 mml) were combined in 1:1 CH_3CN:H_2O (1.0 mL), wrapped in foil, and stirred at RT overnight. 3M HCl was added, and product was extracted 3x with EA. Purification by flash column chromatography (50% EA/Hex) afforded **6.13** (22.1 mg, 84%) as a colorless solid. $\mathbf{R_f}$ = 0.30 (40% EA/Hex); **^{1}H NMR** (300 MHz, $CDCl_3$) δ 8.15 (d, *J* = 8.3 Hz, 2H), 7.51 (d, *J* = 8.3 Hz, 2H), 2.44 (t, *J* = 6.9 Hz, 2H), 2.36 (t, *J* = 7.5 Hz, 2H), 1.64 (q, *J* = 8.2, 7.5 Hz, 4H), 1.53 – 1.34 (m, 6H).

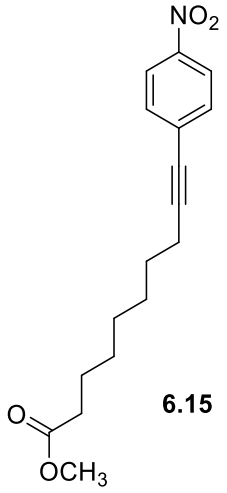

6.15

Methyl 10-(4-nitrophenyl)dec-9-ynoate (6.15).

$SOCl_2$ (8 µL, 0.104 mmol) was added dropwise to a solution of **6.13** (11.6 mg, 0.0400 mmol) in dry MeOH (0.10 mL) at 0◦C. Reaction was heated to reflux for 1 h. Volatiles were removed and the residue was washed with H_2O and extracted with CH_2Cl_2 to yield **6.15** (12.0 mg, 98%) as a yellow solid. $\mathbf{R_f}$ = 0.3 (15% EA/Hex); **^{1}H NMR** (400 MHz, $CDCl_3$) δ 8.14 – 8.10 (m, 2H), 7.51 – 7.45 (m, 2H), 3.65 (s, 3H), 2.42 (t, *J* = 7.1 Hz, 2H), 2.29 (t, *J* = 7.5 Hz, 2H), 1.64 – 1.56 (m, 4H), 1.47 – 1.40 (m, 2H), 1.33 (d, *J* = 3.8 Hz, 2H).

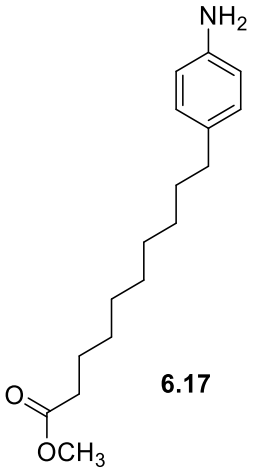

6.17

Methyl 10-(4-aminophenyl)decanoate (6.17).

PtO_2 (1.2 mg, 0.00515 mmol) was added to a solution of **6.15** (12.0 mg, 0.0396 mmol) in EtOH (0.2 mL) and stirred under an H_2 atmosphere for 2 h. The residue was filtered through a thin pad of Celite with EA yielding **6.17** (9.3 mg, 85%) as a brown oil. **R_f** = 0.35 (30% EA/Hex); **^{1}H NMR** (400 MHz, CDCl3) δ 6.96 (d, J = 8.3 Hz, 2H), 6.62 (d, J = 8.3 Hz, 2H), 3.66 (s, 3H), 2.53 – 2.44 (m, 2H), 2.29 (t, J = 7.6 Hz, 2H), 1.65 – 1.58 (m, 2H), 1.58 – 1.50 (m, 2H), 1.30 – 1.25 (m, 10H).

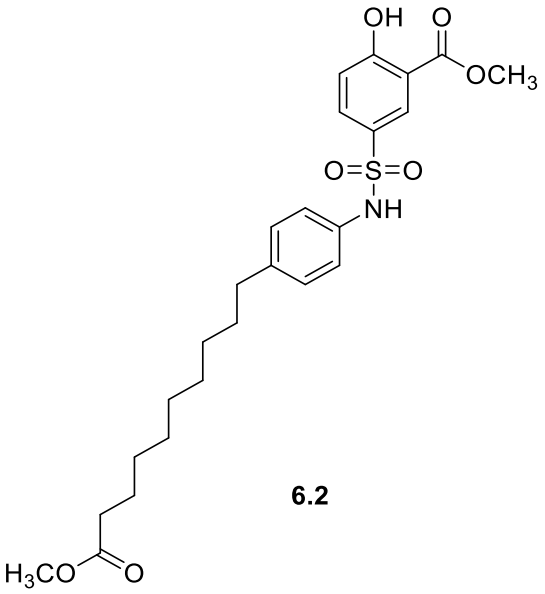

6.2

Methyl 2-hydroxy-5-(N-(4-(10-methoxy-10-oxodecyl)phenyl)sulfamoyl)benzoate (6.2).

$NaHCO_3$ (8.2 mg, 0.0972 mmol) was added to a solution of **6.17** (9.3 mg, 0.0335 mmol) in THF (0.05 mL) at 0^0C. **6.9** (18.5 mg, 0.0737 mmol) in THF (0.05 mL) was added dropwise. Reaction was brought to RT overnight. Reaction mixture was filtered through a short pad of silica gel with EA and purified by flash column chromatography (30% EA/Hex) to afford **6.2** (12.1 mg, 62%) as a brown oil. **R_f** = 0.32 (30% EA/Hex); **^{1}H NMR** (300 MHz, $CDCl_3$) δ 11.21 (s, 1H), 8.29 (d, *J* = 2.4 Hz, 1H), 7.72 (dd, *J* = 8.9, 2.4 Hz, 1H), 7.05 (d, *J* = 8.1 Hz, 2H), 7.00 – 6.93 (m, 3H), 6.41 (s, 1H), 3.95 (s, 3H), 3.66 (s, 3H), 2.51 (d, *J* = 7.8 Hz, 2H), 2.28 (d, *J* = 7.6 Hz, 2H), 1.57 (s, 6H), 1.26 (s, 8H).

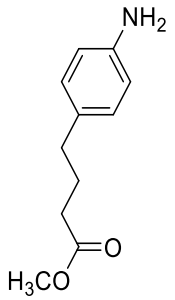

6.16

Methyl 4-(4-aminophenyl)butanoate (6.16)

4-(4-aminophenyl)butanoic acid (20.0 mg, 0.111 mmol) was dissolved in dry MeOH (0.25 mL) and brought to 0^0C. $SOCl_2$ (24 µL, 0.335 mmol) was added dropwise. The reaction mixture was slowly warmed to RT and then refluxed for 1 h. Volatiles were removed and residue was washed 3x with sat. aq. $NaHCO_3$, then brine, and extracted with CH_2Cl_2. **6.16** was brought forward without further purification as a brown oil (19.7 mg, 92%). $\mathbf{R_f}$ = 0.3 (80% EA/Hex); **^{1}H NMR** (400 MHz, $CDCl_3$) δ 6.97 – 6.94 (m, 2H), 6.62 (d, *J* = 8.3 Hz, 2H), 3.65 (s, 3H), 2.53 (t, *J* = 7.5 Hz, 2H), 2.31 (t, *J* = 7.5 Hz, 2H), 1.92 – 1.86 (m, 2H), 1.55 (s, 2H); **^{13}C NMR** (101 MHz, $CDCl_3$) δ 129.16, 115.16, 33.27; **IR** (neat, cm^{-1}) 2948, 2588, 1731, 1511, 1203, 1015.

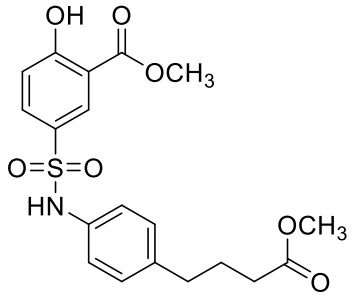

6.1

Methyl 2-hydroxy-5-(N-(4-(4-methoxy-4-oxobutyl)phenyl)sulfamoyl)benzoate (6.2).

$NaHCO_3$ (24.8 mg, 0.296 mmol) was added to a solution of **6.16** (19.7 mg, 0.102 mmol) in THF (0.12 ml) at 0^0C. A solution of **6.9** (56.2 mg, 0.224 mmol) in THF (0.12 mL) was added dropwise.

After 30 min, reaction was brought to RT and stirred overnight. Reaction mixture was filtered through a short pad of silica gel with EA and purified by flash column chromatography (35% EA/Hex) to afford the product (23.0 mg, 55%) as a brown oil. $\mathbf{R_f}$ = 0.32 (40% EA/Hex); **^{1}H NMR** (400 MHz, $CDCl_3$) δ 11.21 (s, 1H), 8.29 (d, *J* = 2.4 Hz, 1H), 7.75 (dd, *J* = 8.9, 2.4 Hz, 1H), 7.05 (d, *J* = 8.4 Hz, 2H), 7.00 – 6.95 (m, 3H), 6.59 (s, 1H), 3.95 (s, 3H), 3.65 (s, 3H), 2.57 (t, *J* = 7.6 Hz, 2H), 2.28 (t, *J* = 7.4 Hz, 2H), 1.91 – 1.85 (m, 2H); **^{13}C NMR** (101 MHz, $CDCl_3$) δ 164.74, 139.09, 133.93, 130.27, 129.33, 122.35, 118.50, 112.23, 52.75, 51.46, 34.31, 33.11, 26.22.

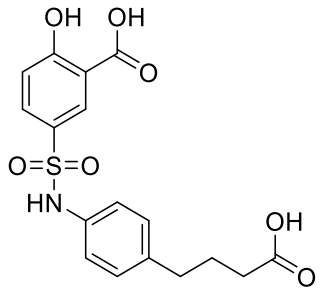

6.3

5-(N-(4-(3-carboxypropyl)phenyl)sulfamoyl)-2-hydroxybenzoic acid (6.3).

6.2 (23.0 mg, 0.0565 mmol) was added to aq. 1M NaOH (0.3mL) and stirred at RT for 15 min. 3M HCl was added, causing the pure product to crash out. Residual liquids were removed with a pipette and the residue was washed 3x with H_2O to afford the **6.3** as a colorless solid (17.5 mg, 82%). **mp** = 152 ^oC; **^{1}H NMR** (400 MHz, MeOD) δ 8.22 (d, *J* = 2.5 Hz, 1H), 7.67 (dd, *J* = 8.8, 2.4 Hz, 1H), 7.04 – 6.97 (m, 4H), 6.88 (d, *J* = 8.8 Hz, 1H), 2.53 (t, *J* = 7.7 Hz, 2H), 2.23 (t, *J* = 7.4 Hz, 2H), 1.81 (s, 2H); **^{13}C NMR** (101 MHz, MeOD) δ 176.08, 171.72, 165.03, 138.33, 135.20, 132.40, 130.21, 128.90, 128.69, 121.67, 117.05, 115.28, 47.36, 47.15, 46.94, 33.83, 32.68, 32.54, 26.22, 26.08; **IR** (neat, cm^{-1}) 3241, 2930, 1681, 1154, 562.

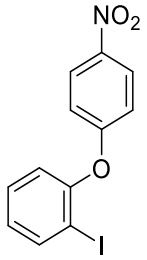

6.21

1-iodo-2-(4-nitrophenoxy)benzene (6.21).

1-fluoro-4-nitrobenzene (53µL, 0.500mmol) was added to a solution of 2-iodophenol (100.0 mg, 0.455 mmol) and K_2CO_3 (188.6 mg, 1.37 mmol) in DMSO (1.1 mL). The reaction was heated to 95^0C and stirred overnight. Upon completion, H_2O was added, and the product was extracted with EA. Further purification by flash column chromatography yielded **6.21** (138.9 mg, 89%) as a colorless solid. $\mathbf{R_f}$ = 0.3 (5% EA/Hex); **mp** = 100 ◦C; **^{1}H NMR** (400 MHz, $CDCl_3$) δ 8.23 – 8.17 (m, 2H), 7.91 (dd, *J* = 7.9, 1.5 Hz, 1H), 7.41 (ddd, *J* = 8.1, 7.4, 1.6 Hz, 1H), 7.09 (dd, *J* = 8.1, 1.5 Hz, 1H), 7.02 (td, *J* = 7.7, 1.5 Hz, 1H), 6.98 – 6.92 (m, 2H); **^{13}C NMR** (101 MHz, $CDCl_3$) δ 162.31, 154.14, 142.78, 140.35, 130.18, 127.41, 125.94, 121.79, 116.61, 89.96; **IR** (neat, cm^{-1}) 3108, 2928, 1589, 1500, 1334, 1232, 1160, 1106, 841, 745.

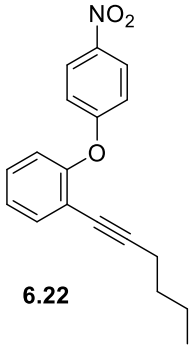

6.22

1-(hex-1-yn-1-yl)-2-(4-nitrophenoxy)benzene (6.22).

$Pd(PPh_3)_2Cl_2$ (28.8 mg, 0.0410 mmol) and CuI (15.6 mg, 0.0820 mmol) were combined in a round-bottom flask under N_2. Et_3N (1.0 mL) was added, followed by **6.21** (138.9 mg.0 mg, 0.410 mmol), then 1-heptyne (65 µL, 0.492 mmol). Reaction was heated at reflux for 1 h. Upon completion,

volatiles were removed, and the remaining residue was purified by flash column chromatography (5% EA/Hex) to yield **6.22** as a brown oil (113.5 mg, 90%). $\mathbf{R_f}$ = 0.35 (5% EA/Hex); **^{1}H NMR** (400 MHz, $CDCl_3$) δ 8.22 – 8.13 (m, 2H), 7.48 (dd, *J* = 7.7, 1.7 Hz, 1H), 7.33 (td, *J* = 7.8, 1.7 Hz, 1H), 7.20 (td, *J* = 7.6, 1.2 Hz, 1H), 7.08 (dd, *J* = 8.1, 1.3 Hz, 1H), 6.97 – 6.89 (m, 2H), 2.20 (t, *J* = 7.0 Hz, 2H), 1.32 (dq, *J* = 11.2, 6.9 Hz, 2H), 1.18 – 1.16 (m, 2H), 0.85 – 0.76 (m, 3H); **^{13}C NMR** (101 MHz, $CDCl_3$) δ 163.22, 154.44, 142.27, 133.85, 129.24, 125.65, 125.62, 121.50, 118.00, 116.18, 97.12, 75.24, 30.71, 27.91, 22.00, 19.26, 13.74; **IR** (neat, cm-1) 2928, 2857, 1611, 1588, 1567, 1513, 1482, 1443, 1339, 1252, 1231, 1191, 1162, 1108, 1034, 945, 873, 844.

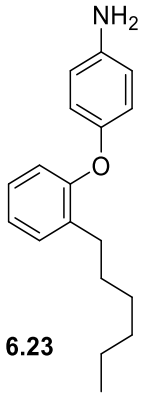

6.23

4-(2-hexylphenoxy)aniline (6.23).

PtO_2 (8.3 mg, 0.367 mmol) was added to a solution of **6.22** (113.5 mg, 0.367 mmol) in EtOH (1.2 mL) and stirred under an H_2 atmosphere for 5 h. The residue was filtered through a thin pad of Celite with EA yielding **6.23** (94.7 mg, 91%) as an orange oil. $\mathbf{R_f}$ = 0.1 (5% EA/Hex); **^{1}H NMR** (400 MHz, $CDCl_3$) δ 7.21 (dd, *J* = 7.5, 1.8 Hz, 1H), 7.08 (td, *J* = 7.7, 1.8 Hz, 1H), 6.98 (td, *J* = 7.4, 1.3 Hz, 1H), 6.87 – 6.78 (m, 2H), 6.75 (dd, *J* = 8.1, 1.3 Hz, 1H), 6.70 – 6.62 (m, 2H), 3.53 (s, 2H), 2.66 (dd, *J* = 8.9, 6.6 Hz, 2H), 1.62 (dd, *J* = 10.5, 4.7 Hz, 2H), 1.40 – 1.20 (m, 8H), 0.87 (t, *J* = 6.7 Hz, 3H); **^{13}C NMR** (101 MHz, $CDCl_3$) δ 155.99, 149.76, 141.81, 133.27, 130.21, 126.67, 122.44, 119.88, 117.36, 116.19, 31.74, 30.09, 30.05, 29.40, 29.07, 22.58, 14.02.

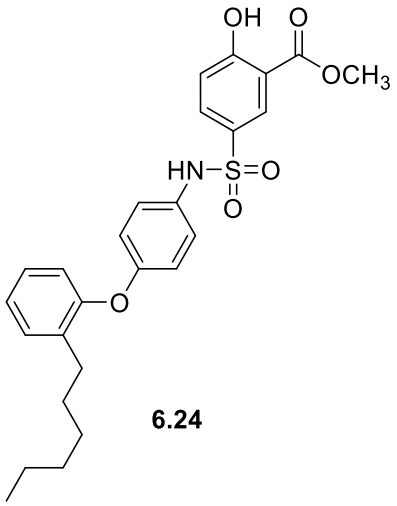

6.24

Methyl 5-(N-(4-(2-hexylphenoxy)phenyl)sulfamoyl)-2-hydroxybenzoate (6.24).

$NaHCO_3$ (81.4 mg, 0.735 mmol) was added to a solution of **6.23** (94.7 mg, 0.334 mmol) in THF (0.42 mL) at 0^0C. **6.9** (184.3 mg, 0.735 mmol) in THF (0.42 mL) was added dropwise. Reaction was brought to RT overnight. Reaction mixture was filtered through a short pad of silica gel with EA and purified by flash column chromotagraphy (25% EA/Hex) to afford **6.24** (79.4 mg, 49%) as an off-white solid. $\mathbf{R_f}$ = 0.33 (25% EA/Hex); **^{1}H NMR** (400 MHz, $CDCl_3$) δ 11.23 (s, 1H), 8.31 (d, *J* = 2.4 Hz, 1H), 7.78 (dd, *J* = 8.8, 2.4 Hz, 1H), 7.28 – 7.20 (m, 1H), 7.10 (dtd, *J* = 24.3, 7.5, 1.6 Hz, 2H), 7.01 (dd, *J* = 8.8, 1.6 Hz, 3H), 6.89 (s, 1H), 6.84 – 6.76 (m, 3H), 3.95 (s, 3H), 2.54 (dd, *J* = 8.9, 6.6 Hz, 2H), 1.68 – 1.43 (m, 2H), 1.36 – 1.17 (m, 8H), 0.85 (t, *J* = 6.7 Hz, 2H); **^{13}C NMR** (101 MHz, $CDCl_3$) δ 169.37, 164.76, 156.32, 153.95, 134.37, 134.00, 130.62, 130.33, 130.20, 129.55, 126.99, 124.84, 124.09, 119.42, 118.52, 118.17, 112.25, 52.77, 31.66, 29.97, 29.93, 29.26, 28.97, 22.53, 13.99.

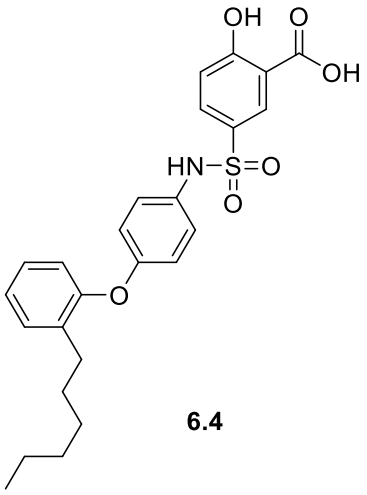

6.4

5-(N-(4-(2-hexylphenoxy)phenyl)sulfamoyl)-2-hydroxybenzoic acid (6.4).

6.24 (79.4 mg, 0.164 mmol) was added to aq. 3M LiOH (0.16 mL) and stirred at RT for 12 h. 3M HCl was added, causing a solid to crash out of solution. Residual liquids were removed with a pipette and the product was washed 3x with H_2O to yield **6.4** (35.1 mg, 50%) as a tan solid. **mp** = 249 ◦C; **^{1}H NMR** (400 MHz, MeOD) δ 8.16 (d, *J* = 2.4 Hz, 1H), 7.74 (dd, *J* = 8.8, 2.5 Hz, 1H), 7.23 (dd, *J* = 7.5, 1.8 Hz, 1H), 7.16 – 7.11 (m, 1H), 7.06 (dd, *J* = 7.4, 1.3 Hz, 1H), 7.00 (dd, *J* = 8.9, 2.2 Hz, 3H), 6.78 – 6.72 (m, 3H), 2.53 (d, *J* = 7.4 Hz, 2H), 1.53 – 1.49 (m, 2H), 1.25 – 1.19 (m, 8H), 0.83 (d, *J* = 7.1 Hz, 3H); **^{13}C NMR** (101 MHz, MeOD) δ 170.94, 164.84, 155.78, 154.04, 134.02, 133.30, 131.70, 130.41, 130.19, 129.56, 126.85, 124.02, 123.76, 119.29, 117.47, 117.34, 112.68, 31.36, 29.74, 29.57, 28.81, 28.59, 22.16, 12.92. **IR** (neat, cm^{-1}) = 3470, 3220, 2980, 2870, 1610, 1498.

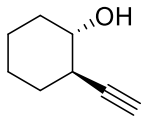

6.27

(1S,2R)-2-ethynylcyclohexan-1-ol (6.27).

To a solution of Ethynyltrimethylsilane (359 µL, 0.709 mmol) in dry THF (3.5 mL), nBuLi (1.6 M in Hex, 1.63 mL, 2.60 mmol) was added dropwise at -78^{0}C and stirred for 10 min. Cyclohexene

oxide (180 µL, 1.73 mmol) was added dropwise and reaction mixture was warmed to rt and stirred for 30 min. Upon completion, reaction was quenched with sat. aq. NH_4Cl, washed with brine, and extracted with EA. K_2CO_3 (478.2 mg, 3.46 mmol) was added to a solution of the residue in MeOH (3.5 mL) and stirred at RT overnight. Volatiles were removed and residue was washed with H_2O, Brine, and extracted with EA. Purification by flash column chromatography (25% EA/Hex) afforded **6.27** as a colorless oil (116.9 mg, 54%). $\mathbf{R_f}$ = 0.32 (25% EA/Hex); **^{1}H NMR** (300 MHz, $CDCl_3$) δ 3.47 (td, *J* = 9.7, 4.0 Hz, 1H), 2.27 – 2.16 (m, 2H), 2.09 – 1.92 (m, 2H), 1.81 – 1.56 (m, 3H), 1.48 – 1.34 (m, 1H), 1.31 – 1.18 (m, 2H); **^{13}C NMR** (101 MHz, $CDCl_3$) δ 85.72, 73.27, 70.11, 38.49, 33.07, 30.75, 24.63, 24.04; **IR** (neat, cm^{-1}) 3300, 2932, 2858, 2112, 1736, 1449, 1070, 1012, 625.

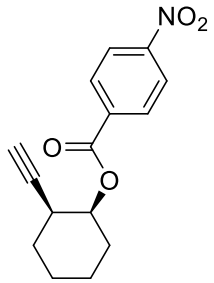

6.28

(1R,2R)-2-ethynylcyclohexyl 4-nitrobenzoate (6.28)

1-nitrobenzoic acid (236.1 mg, 1.41 mmol) and PPh_3 (369.8 mg, 1.41 mmol) were added to a solution of **6.27** (87.7 mg, 0.706 mmol) in dry toluene (1.4 mL) and cooled to 0^0C. DIAD (278 µL, 1.41 mmol) was added dropwise and reaction was brought to RT overnight. Volatiles were removed and residue was washed with sat. aq. $NaHCO_3$, brine, and extracted with EA. Further purification by flash column chromatography afforded **6.28** (42.6 mg, 22%) as a colorless oil. $\mathbf{R_f}$ = 0.33 (10% EA/Hex; **^{1}H NMR** (400 MHz, $CDCl_3$) δ 8.31 – 8.22 (m, 4H), 5.11 (dt, *J* = 9.4, 3.7 Hz, 1H), 3.08 – 3.02 (m, 1H), 2.09 (d, *J* = 2.5 Hz, 1H), 2.05 – 1.92 (m, 2H), 1.82 – 1.70 (m, 4H), 1.54 – 1.42 (m, 2H); **^{13}C NMR** (101 MHz, $CDCl_3$) δ 163.88, 150.43, 135.90, 130.70, 123.41, 83.34, 73.74, 70.84, 32.54, 29.17, 27.83, 22.83, 21.67); **IR** (neat, cm^{-1}) 3293, 2981, 2940, 2863, 1772, 1720, 1526, 1342, 1269, 1241, 1095, 718.

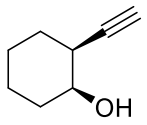

6.29

(1S,2S)-2-ethynylcyclohexan-1-ol (6.29).

K_2CO_3 (86.2 mg, 0.624 mmol) was added to a solution of **6.28** (42.6 mg, 0.156 mmol) in MeOH (0.52 mL) and stirred for 2 h. Volatiles were removed and residue was washed with H_2O, brine, and extracted with EA. Purification by flash column chromatography (25% EA/Hex) afforded **6.29** as a colorless oil (19.0 mg, 98%). $\mathbf{R_f}$ = 0.32 (25% EA/Hex); **^{1}H NMR** (400 MHz, $CDCl_3$) δ 3.68 (dt, *J* = 7.9, 4.0 Hz, 1H), 2.82 (h, *J* = 3.4 Hz, 1H), 2.15 (d, *J* = 2.5 Hz, 1H), 1.87 – 1.82 (m, 2H), 1.71 – 1.64 (m, 3H), 1.61 – 1.51 (m, 2H), 1.38 (ddq, *J* = 12.4, 6.1, 3.3 Hz, 1H), 1.33 – 1.24 (m, 1H); **^{13}C NMR** (101 MHz, $CDCl_3$) δ 84.27, 77.14, 71.67, 69.53, 35.53, 31.19, 28.51, 22.54, 22.04; **IR** (neat, cm^{-1}) 3307, 2923, 2852, 1681, 1446, 1071, 974.

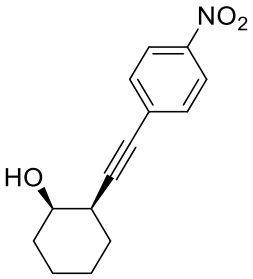

6.30

(1S,2S)-2-((4-nitrophenyl)ethynyl)cyclohexan-1-ol (6.30).

To a solution of $Pd(OAc)_2$ (2.1 mg, 0.00934 mmol) and NaOH (74.7 mg, 1.87 mmol) in Acetone (1.9 mL) and H_2O (1.9 mL) was added **6.29** (116.0 mg, 0.934 mmol) followed by addition of 1-iodo-4-nitrobenzene (255.9 mg, 1.03 mmol). Reaction was brought to 60^0C and stirred for 30 min. The product was extracted with CH_2Cl_2 and further purified by flash column chromatography (30% EA/Hex) to afford **6.30** as an orange solid (105.8 mg, 46%). $\mathbf{R_f}$ = 0.35 (30% EA/Hex); **mp** = ◦C; **^{1}H NMR** (300 MHz, $CDCl_3$) δ 8.20 – 8.14 (m, 2H), 7.59 – 7.53 (m, 2H), 3.80 (t, *J* = 5.3

Hz, 1H), 3.13 – 3.05 (m, 1H), 1.96 (dt, *J* = 11.6, 6.1 Hz, 1H), 1.84 – 1.71 (m, 4H), 1.65 (dd, *J* = 10.9, 4.7 Hz, 2H), 1.47 (s, 1H); **^{13}C NMR** (101 MHz, $CDCl_3$) δ 146.74, 132.38, 130.39, 123.42, 69.92, 53.67, 36.64, 31.55, 29.15, 28.65, 22.62, 22.23; **IR** (neat, cm^{-1}) 3408, 2931, 2858, 2225, 1509, 1335, 852.

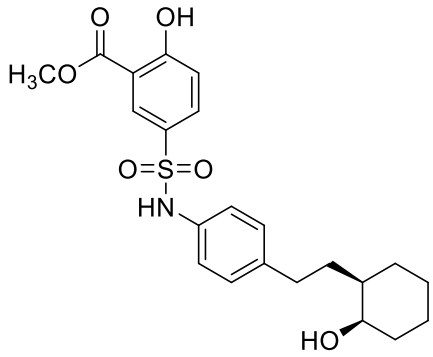

6.32

Methyl-2-hydroxy-5-(N-(4-(2-((1S,2S)-2-hydroxycyclohexyl)ethyl)phenyl)sulfamoyl) benzoate (6.32).

PtO_2 (9.8 mg, 0.0431 mmol) was added to a solution of **6.30** (105.8 mg, 0.431 mmol) in EtOH (1.1 mL) and stirred under an H_2 atmosphere for 2 h. The residue was filtered through a thin pad of Celite with EA. $NaHCO_3$ (105.0 mg, 1.25 mmol) was added to a solution of this residue (94.5 mg, 0.431 mmol) in THF (0.55 mL) at 0^0C. **6.9** (237.6 mg, 0.948 mmol) in THF (0.55 mL) was added dropwise. Reaction was brought to RT overnight. Reaction mixture was filtered through a short pad of silica gel with EA and purified by flash column chromotagraphy (40% EA/Hex) to afford **6.32** (56.3 mg, 30%) as a pinkish solid. **R_f** = 0.23 (30% EA/Hex); **mp** = 144 ◦C; **^{1}H NMR** (400 MHz, $CDCl_3$) δ 11.21 (s, 1H), 8.29 (d, *J* = 2.4 Hz, 1H), 7.73 (dd, *J* = 8.8, 2.4 Hz, 1H), 7.08 – 7.02 (m, 2H), 6.98 – 6.89 (m, 3H), 6.49 (s, 1H), 3.95 (s, 3H), 2.56 (dd, *J* = 9.0, 7.0 Hz, 2H), 1.80 – 1.73 (m, 1H), 1.68 – 1.62 (m, 2H), 1.52 – 1.39 (m, 7H), 1.29 – 1.17 (m, 2H); **^{13}C NMR** (101 MHz, $CDCl_3$) δ 169.38, 164.70, 140.65, 133.97, 133.47, 130.27, 129.68, 129.20, 122.47, 118.46, 112.22, 69.19, 52.77, 40.70, 33.54, 33.00, 32.60, 26.42, 24.93, 20.34; **IR** (neat, cm^{-1}) 3475, 3080, 2918, 2850, 1693, 1445, 1153, 588, 575, 557.

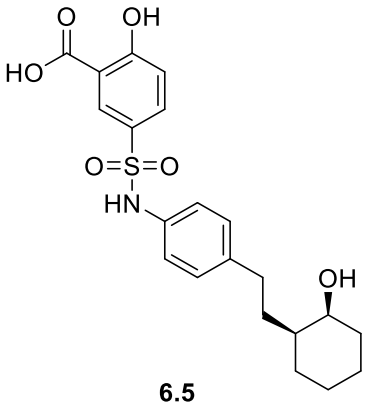

6.5

Methyl2-hydroxy-5-(N-(4-(2-((1S,2S)-2-hydroxycyclohexyl)ethyl) phenyl)sulfamoyl)benzoate (**6.5).**

6.32 (17.6 mg, 0.0402 mmol) was added to aq. 3M LiOH (0.04mL) and stirred at RT for 1 h. 3M HCl was added, causing the pure product to crash out. Residual liquids were removed with a pipette and the residue was washed 3x with H_2O to afford **6.5** as a colorless solid (15.6 mg, 92%). **mp** = 95 ◦C; **^{1}H NMR** (400 MHz, MeOD) δ 8.22 (d, *J* = 2.4 Hz, 1H), 7.67 (dd, *J* = 8.8, 2.4 Hz, 1H), 7.06 – 7.02 (m, 2H), 6.99 – 6.95 (m, 2H), 6.89 (d, *J* = 8.8 Hz, 1H), 3.83 – 3.79 (m, 1H), 2.53 (t, *J* = 8.0 Hz, 2H), 1.76 – 1.69 (m, 1H), 1.62 (ddd, *J* = 8.8, 5.5, 2.2 Hz, 2H), 1.50 – 1.15 (m, 8H); **^{13}C NMR** (101 MHz, MeOD) δ 132.66, 130.19, 128.52, 121.59, 117.04, 68.48, 48.13, 47.91, 47.70, 47.49, 47.28, 47.06, 46.85, 40.59, 33.14, 32.47, 32.13, 24.66, 20.26; **IR** (neat, cm^{-1}) 2924, 2853, 1584, 1160, 576, 559.

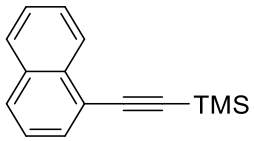

6.34

Trimethyl(naphthalen-1-ylethynyl)silane (6.34).

$Pd(PPh_3)_2Cl_2$ (77.9 mg, 0.111 mmol) and CuI (42.2 mg, 0.222 mmol) were combined in a round-bottom flask under N_2. Et_3N (2.8 mL) was added, followed by 1-iodonaphthalene (163 µL,

1.11mmol), then ethynyltrimethylsilane (185 µL, 1.33 mmol). Reaction was stirred at RT for 2 h. Upon completion, volatiles were removed, and the remaining residue was purified by flash column chromotagraphy (100% Hex) to yield **6.34** as a colorless oil (250.0 mg, Quantitative Yield). $\mathbf{R_f}$ = 0.5 (5% EA/Hex); **^{1}H NMR** (400 MHz, $CDCl_3$) δ 8.40 – 8.33 (m, 1H), 7.84 (td, *J* = 8.1, 1.4 Hz, 2H), 7.72 (dd, *J* = 7.1, 1.2 Hz, 1H), 7.60 (ddd, *J* = 8.3, 6.9, 1.4 Hz, 1H), 7.53 (ddd, *J* = 8.2, 6.8, 1.4 Hz, 1H), 7.42 (dd, *J* = 8.3, 7.1 Hz, 1H), 0.36 (s, 8H), 0.36 (s, 1H); **^{13}C NMR** (101 MHz, $CDCl_3$) δ 133.33, 133.00, 130.73, 128.89, 128.17, 126.74, 126.30, 126.12, 125.03, 120.67, 102.99, 99.36, 0.04; **IR** (neat, cm^{-1}) 3058, 2958, 2898, 2146, 1586, 1392, 1248, 837.

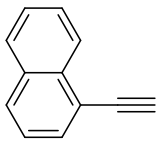

6.35

MN-34. 1-ethynylnaphthalene (6.35).

K_2CO_3 (1434 mg, 1.04 mmol) was added to a solution of **6.34** (211.6 mg, 0.943 mmol) in MeOH (1.3 mL). After 30 min, volatiles were removed. Residue was washed 3x with H_2O and extracted with 100% Hexanes to yield **6.35** (123.0mg, 86%) as a colorless oil. The product was carried forward without further purification. $\mathbf{R_f}$ = 0.5 (5% EA/Hex); **^{1}H NMR** (400 MHz, $CDCl_3$) δ 8.40 – 8.35 (m, 1H), 7.88 – 7.84 (m, 2H), 7.75 (dd, *J* = 7.1, 1.2 Hz, 1H), 7.56 (dddd, *J* = 23.8, 8.2, 6.8, 1.4 Hz, 2H), 7.43 (dd, *J* = 8.3, 7.1 Hz, 1H), 3.48 (s, 1H); **^{13}C NMR** (101 MHz, $CDCl_3$) δ 133.42, 132.99, 131.14, 129.18, 128.20, 126.85, 126.39, 125.95, 125.00, 119.67, 81.86, 81.66, 29.62); **IR** (neat, cm^{-1}) 3289, 3057, 2100, 1586, 1391, 797, 769.

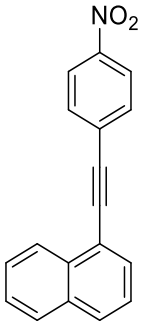

6.36

1-((4-nitrophenyl)ethynyl)naphthalene (6.36).

$Pd(PPh_3)_2Cl_2$ (56.7 mg, 0.0808 mmol) and CuI (30.7 mg, 0.162 mmol) were combined in a round-bottom flask under N_2. Et_3N (2.0 mL) was added, followed by 1-iodo-4-nitrobenzene (225.8 mg, 0.907 mmol), then **6.35** (151.8 mg, 0.997 mmol). Reaction was stirred at RT for 1.5 h. Upon completion, volatiles were removed, and the remaining residue was purified by flash column chromotagraphy (7% EA/Hex) to yield **6.36** as a Fluffy Yellow Solid (92.9 mg, 37%). $\mathbf{R_f}$ = 0.27 (5% EA/Hex); **mp** = 128 ◦C; **^{1}H NMR** (400 MHz, $CDCl_3$) δ 8.38 (dq, *J* = 8.4, 1.0 Hz, 1H), 8.27 – 8.23 (m, 2H), 7.93 – 7.88 (m, 2H), 7.81 (dd, *J* = 7.2, 1.2 Hz, 1H), 7.79 – 7.74 (m, 2H), 7.64 (ddd, *J* = 8.3, 6.8, 1.4 Hz, 1H), 7.60 – 7.55 (m, 1H), 7.49 (dd, *J* = 8.3, 7.1 Hz, 1H); **^{13}C NMR** (101 MHz, $CDCl_3$) δ 146.94, 133.10, 133.04, 132.19, 131.05, 130.23, 129.81, 128.43, 127.09, 126.61, 125.76, 125.19, 123.63, 119.60, 92.87, 92.27; **IR** (neat, cm^{-1}) 3050, 2980, 2925, 2440, 2209, 1931, 1591, 1504, 1333.

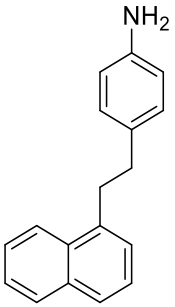

6.37

4-(2-(naphthalen-1-yl)ethyl)aniline (6.37).

A solution of **6.36** (92.9 mg, 0.340 mmol) in ethanol (1.1 mL) was placed under an H_2 atmosphere for 6 hours. The reaction mixture was passed through celite and purified by flash column chromatography (30% EA/Hex) to afford **6.37** (58.8 mg, 70%) as an orange oil. $\mathbf{R_f}$ = 0.5 (30% EA/Hex); **^{1}H NMR** (400 MHz, $CDCl_3$) δ 8.12 – 8.08 (m, 1H), 7.88 – 7.84 (m, 1H), 7.72 (d, *J* = 8.2 Hz, 1H), 7.55 – 7.46 (m, 2H), 7.38 (dd, *J* = 8.2, 7.0 Hz, 1H), 7.29 (dd, *J* = 7.0, 1.2 Hz, 1H), 7.06 – 7.02 (m, 2H), 6.67 – 6.63 (m, 2H), 3.35 – 3.30 (m, 2H), 2.97 – 2.93 (m, 2H); **^{13}C NMR** (101 MHz, $CDCl_3$) δ 144.25, 137.97, 133.78, 132.08, 131.70, 129.10, 128.70, 126.52, 125.90, 125.69, 125.45, 125.31, 123.63, 115.21, 36.18, 35.40; **IR** (neat, cm-1) 3360, 3034, 2921, 2851, 1679, 1618, 1596, 1514, 1441, 1394, 1274, 1178, 1162, 1077, 1017.

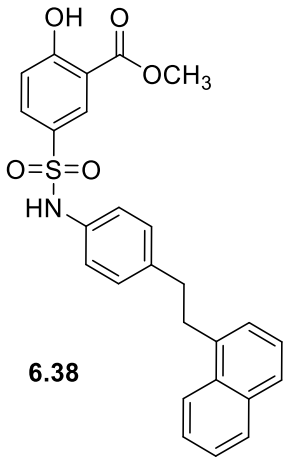

6.38

Methyl 2-hydroxy-5-(N-(4-(2-(naphthalen-1-yl)ethyl)phenyl)sulfamoyl)benzoate (6.38).

$NaHCO_3$ (25.1 mg, 0.299 mmol) was added to a solution of **6.37** (25.4 mg, 0.103 mmol) in THF (0.13 ml) at 0^0C. **6.9** (56.5 mg, 0.226 mmol) in THF (0.13 mL) was added dropwise. After 30 min, reaction was brought to RT and stirred overnight. Reaction mixture was filtered through a short pad of silica gel with EA and purified by flash column chromotagraphy (25% EA/Hex) to afford **6.38** (27.1 mg, 57%). $\mathbf{R_f}$ = 0.5 (40% EA/Hex); **^{1}H NMR** (400 MHz, $CDCl_3$) δ 11.23 (s, 1H), 8.36 – 8.29 (m, 1H), 8.03 (d, *J* = 8.0 Hz, 1H), 7.88 – 7.83 (m, 1H), 7.77 – 7.69 (m, 2H), 7.50 (t, *J* = 7.0 Hz, 2H), 7.34 (t, *J* = 7.7 Hz, 1H), 7.19 (d, *J* = 7.0 Hz, 1H), 7.09 (d, *J* = 8.0 Hz, 2H), 6.99 (t, *J* = 8.2 Hz, 3H), 6.52 (s, 1H), 3.95 (s, 3H), 3.30 (t, *J* = 8.1 Hz, 2H), 2.99 (t, *J* = 8.1 Hz, 2H); **^{13}C**

NMR (101 MHz, $CDCl_3$) δ 169.38, 164.75, 139.68, 137.16, 133.99, 133.83, 131.57, 130.28, 129.71, 129.35, 128.80, 126.78, 126.00, 125.82, 125.42, 125.34, 123.38, 122.42, 118.49, 112.25, 52.77, 36.26, 34.81; **IR** (neat, cm-1) 3243, 2920, 1676, 1609, 1580, 1509, 1475, 1440, 1392, 1330, 1295, 1249, 1210, 1153, 1106, 1075, 1018, 962.

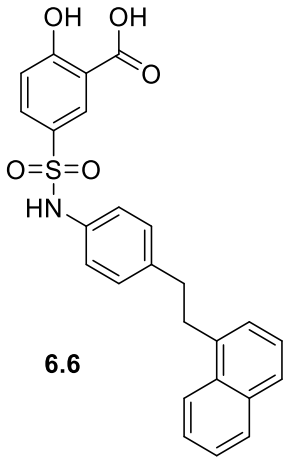

6.6

2-hydroxy-5-(N-(4-(2-(naphthalen-1-yl)ethyl)phenyl)sulfamoyl)benzoic acid (6.6).

6.38 (27.1 mg, 0.0587 mmol) was added to aq. 3M LiOH (0.06 mL) and stirred at RT for 6 h. 3M HCl was added, causing a solid to crash out. Residual liquids were removed with a pipette and the residue was washed 3x with H_2O to afford **6.6** as a colorless solid (24.7 mg, 94%). **mp** = 90 ◦C; **^{1}H NMR** (300 MHz, $CDCl_3$) δ 8.21 (d, *J* = 2.4 Hz, 1H), 8.03 (d, *J* = 7.4 Hz, 1H), 7.84 – 7.79 (m, 1H), 7.73 (dd, *J* = 8.8, 2.4 Hz, 1H), 7.66 (d, *J* = 8.2 Hz, 1H), 7.44 (ddd, *J* = 7.2, 5.1, 1.7 Hz, 2H), 7.26 (dd, *J* = 8.2, 7.0 Hz, 1H), 7.10 (d, *J* = 7.4 Hz, 1H), 6.99 – 6.96 (m, 4H), 6.94 (d, *J* = 2.2 Hz, 1H), 3.28 – 3.23 (m, 2H), 2.91 (dd, *J* = 9.0, 6.6 Hz, 2H); **^{13}C NMR** (100 MHz, CD_3OD) δ 170.87, 164.77, 138.65, 137.16, 135.13, 133.91, 133.43, 131.57, 130.18, 129.87, 128.78, 128.25, 126.20, 125.92, 125.33, 124.90, 123.16, 121.52, 117.53, 112.37, 36.07, 34.56; **IR** (neat, cm^{-1}) 3381, 2917, 1666, 1158.

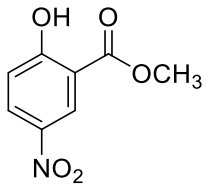

6.39

Methyl 2-hydroxy-5-nitrobenzoate (6.39).

A solution of nitric acid (197 µL, 4.73 mmol) in acetic acid (4.0 mL) was added dropwise to a solution of methyl salicylate **6.8** (420 µL, 3.94 mmol), acetic acid (4.0 mL), and acetic anhydride (2.4 mL) at 0◦C. The reaction was brought to RT over 6 hours. H_2O (15.0 mL) was added and stirred for an additional 30 minutes. The product was collected as a mixture of isomers by vacuum filtration. Further purification by flash column chromatography (15% EA/Hex to 30% EA/Hex) yielded **6.39** as a colorless solid (228.2 mg, 24%). **R_f** = 0.35 (15% EA/Hex); **mp** = 110 ◦C; **^{1}H NMR** (400 MHz, $CDCl_3$) δ 11.41 (s, 1H), 8.77 (d, *J* = 2.8 Hz, 1H), 8.32 (dd, *J* = 9.2, 2.9 Hz, 1H), 7.07 (d, *J* = 9.2 Hz, 1H), 4.02 (s, 3H); **^{13}C NMR** (101 MHz, $CDCl_3$) δ 169.20, 166.11, 139.92, 130.43, 126.54, 118.53, 112.02, 53.02; **IR** (neat, cm^{-1}) 3108, 2963, 1675, 1331.

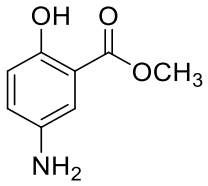

6.40

Methyl 5-amino-2-hydroxybenzoate (6.40).

PtO_2 (11.4 mg, 0.0.0502 mmol) was added to a solution of **6.39** (98.9 mg, 0.502 mmol) in EtOH (1.3 mL) and stirred under an H_2 atmosphere for 1 h. The residue was filtered through a thin pad of Celite with EA to afford **6.40** (80.1 mg, 96%). **R_f** = 0.17 (25% EA/Hex); **mp =** 85 ◦C; **^{1}H NMR** (400 MHz, $CDCl_3$) δ 10.18 (s, 1H), 7.14 (dd, *J* = 2.8, 0.5 Hz, 1H), 6.86 (dd, *J* = 8.8, 2.8 Hz, 1H), 6.81 (dd, *J* = 8.8, 0.6 Hz, 1H), 3.91 (s, 3H), 3.43 (s, 2H); **^{13}C NMR** (101 MHz, $CDCl_3$) δ 170.27,

154.70, 138.22, 124.22, 118.07, 114.60, 112.09, 52.09; **IR** (neat, cm^{-1}) 3409, 3327, 2963, 1671, 1440, 1231, 1209, 551.

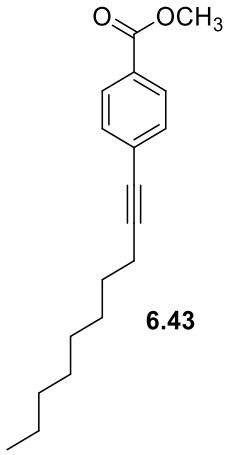

6.43

Methyl 4-(dec-1-yn-1-yl)benzoate (6.43).

$Pd(PPh_3)_2Cl_2$ (53.6 mg, 0.0763 mmol) and CuI (29.0 mg, 0.153 mmol) were combined in a round-bottom flask under N_2. Et_3N (1.9 mL) was added, followed by Methyl-4-iodobenzoate (200.0 mg, 0.763 mmol), then 1-decyne (165 µL, 0.916 mmol). Reaction was heated at reflux for 2 h. Upon completion, volatiles were removed, and the remaining residue was purified by flash column chromatography (5% EA/Hex) to yield **6.43** as a dark brown oil (201.3 mg, 97%). $\mathbf{R_f}$ = 0.28 (5% EA/Hex); **^{1}H NMR** (400 MHz, $CDCl_3$) δ 7.97 – 7.92 (m, 2H), 7.46 – 7.41 (m, 2H), 3.90 (s, 3H), 2.42 (t, *J* = 7.1 Hz, 2H), 1.65 – 1.58 (m, 2H), 1.48 – 1.40 (m, 2H), 1.33 – 1.27 (m, 8H), 0.87 (d, *J* = 7.0 Hz, 3H); **^{13}C NMR** (101 MHz, $CDCl_3$) δ 166.58, 131.35, 129.28, 128.86, 128.69, 93.94, 79.99, 52.03, 31.74, 29.08, 29.00, 28.83, 28.48, 22.55, 19.41, 14.00; **IR =** (neat, cm^{-1}) 2952, 9=2925, 2855, 2226, 1725, 1291, 1225, 752.

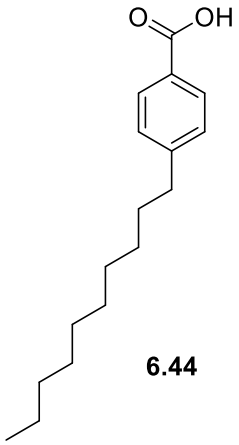

6.44

4-decylbenzoic acid (6.44).

PtO_2 (16.8 mg, 0.0739 mmol) was added to a solution of **6.43** (201.3 mg, 0.739 mmol) in EtOH (1.8 mL) and stirred under an H_2 atmosphere for 2 h. The residue was filtered through a thin pad of Celite with EA. The reside (170.7 mg, 0.618 mmol) was added to aq. 3M NaOH (0.6 mL) and THF (0.6 mL) and stirred at 60^0C for 48 h. 3M HCl was added, causing a solid to crash out. Residual liquids were removed with a pipette and reside was washed 3x with H_2O to afford **6.44** as an off-white solid (89.4 mg, 55%). $\mathbf{R_f}$ = 0.5 (40% EA/Hex); **mp** >300◦C; **^{1}H NMR** (400 MHz, MeOD) δ 7.91 (d, *J* = 8.0 Hz, 2H), 7.27 (d, *J* = 7.9 Hz, 2H), 2.67 (t, *J* = 7.7 Hz, 2H), 1.63 (t, *J* = 7.6 Hz, 2H), 1.33 – 1.27 (m, 14H), 0.89 (t, *J* = 6.7 Hz, 3H); **^{13}C NMR** (101 MHz, MeOD) δ 148.26, 129.37, 128.01, 48.12, 47.90, 47.69, 47.48, 47.27, 47.05, 46.84, 35.38, 31.56, 30.89, 29.18, 29.04, 28.93, 28.80, 22.22, 12.92; **IR** (cm^{-1}) 2953, 2917, 2847, 1678, 1099, 1063, 614.

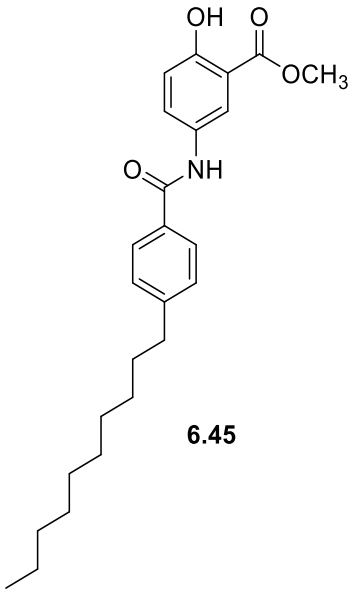

6.45

Methyl 5-(4-decylbenzamido)-2-hydroxybenzoate (6.45).

DMF (1 drop) and $(COCl)_2$ (44 µL, 0.511 mmol) were added to a solution of **6.44** (89.4 mg, 0.341 mmol) in dry CH_2Cl_2 (0.4 mL) and stirred under N_2 for 30 min. Volatiles were removed with a stream of N_2. A solution of **6.40** (62.7 mg, 0.375 mmol) and DIEA (178 µL, 1.02 mmol) in dry CH_3CN (0.8 mL) was added dropwise at 0^0C to pre-formed acid chloride and brought to RT. Reaction was stirred for 1 h. Volatiles were removed and purification by flash column chromatography (20% EA/Hex afforded **6.45** (69.2 mg, 50%) as an off-white solid. $\mathbf{R_f}$ = 0.33 (20% EA/Hex); **^{1}H NMR** (400 MHz, $CDCl_3$) δ 10.63 (s, 1H), 8.18 (d, *J* = 2.7 Hz, 1H), 7.77 (dd, *J* = 8.4, 2.0 Hz, 2H), 7.62 (dd, *J* = 8.9, 2.7 Hz, 1H), 7.27 (d, *J* = 8.0 Hz, 2H), 6.97 (d, *J* = 8.9 Hz, 1H), 3.94 (s, 3H), 2.66 (t, *J* = 7.7 Hz, 2H), 1.63 (p, *J* = 7.2 Hz, 2H), 1.29 (d, *J* = 22.7 Hz, 17H), 0.88 (t, *J* = 6.7 Hz, 3H); **^{13}C NMR** (101 MHz, $CDCl_3$) δ 170.12, 165.61, 158.46, 147.39, 131.77, 129.53, 128.83, 128.72, 126.90, 121.76, 117.92, 112.08, 52.31, 35.76, 31.79, 31.09, 29.50, 29.47, 29.36, 29.22, 29.15, 22.58, 14.01; **IR** (neat, cm^{-1}) 3266, 2955, 2918, 2849, 1675, 1637, 1537, 1490, 1443, 1202, 1084, 690.

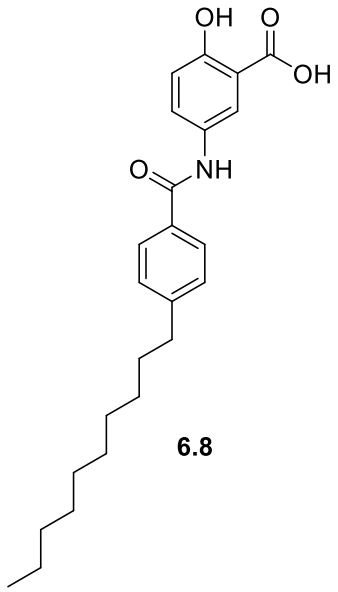

6.8

5-(4-decylbenzamido)-2-hydroxybenzoic acid (6.8).

6.45 (20.2 mg, 0.0491 mmol) was added to aq. 3M NaOH (0.05 mL) and THF (0.1 mL) and stirred at 60^0C for 48 h. 3M HCl was added, causing a solid to crash out of solution. The crude product was purified by flash column chromatography (10% MeOH/EA) to afford **6.8** as a colorless solid (3.5 mg, 18%). $\mathbf{R_f}$ = 0.32 (10% MeOH/EA); **mp** = 211◦C; **^{1}H NMR** (400 MHz, DMSO) δ 8.21 (t, *J* = 3.1 Hz, 1H), 7.83 (dd, *J* = 13.6, 8.5 Hz, 3H), 7.31 (d, *J* = 7.9 Hz, 2H), 6.89 (d, *J* = 8.9 Hz, 1H), 2.62 (t, *J* = 7.6 Hz, 2H), 1.57 (s, 2H), 1.23 (d, *J* = 13.5 Hz, 14H), 0.82 (d, *J* = 7.0 Hz, 3H); **^{13}C NMR** (101 MHz, DMSO) δ 171.99, 157.86, 146.61, 128.61, 127.95, 122.26, 117.15, 35.32, 31.64, 31.07, 29.34, 29.18, 29.04, 28.96, 22.45, 14.32; **IR** (2954, 2919, 2850, 2460, 2325, 1666, 1628, 1608, 1488, 1395, 1441, 827.

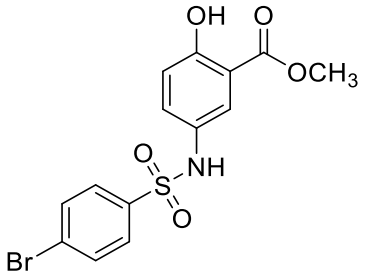

6.47

Methyl 5-((4-bromophenyl)sulfonamido)-2-hydroxybenzoate (6.47).

K_2CO_3 (461.6 mg, 3.34 mmol) was added to a solution of **6.40** (192.2 mg, 1.15 mmol) in THF (1.6 mL) at 0^0C. 4-bromobenzenesulfonyl chloride (300.0 mg, 1.17 mmol) in THF (1.5 mL) was added dropwise. After 30 min, reaction was brought to RT and stirred for 24 h. Reaction mixture was filtered through a short pad of silica gel with EA and purified by flash column chromatography (30% EA/Hex) to afford **6.47** (246.9 mg, 56%) as a yellow solid. $\mathbf{R_f}$ = 0.37 (30% EA/Hex); **mp =** 174 ◦C; **^{1}H NMR** (400 MHz, $CDCl_3$) δ 10.71 (s, 1H), 7.60 – 7.53 (m, 5H), 7.11 (dd, *J* = 8.9, 2.8 Hz, 1H), 6.88 (d, *J* = 8.9 Hz, 1H), 6.31 (s, 1H), 3.93 (s, 3H); **^{13}C NMR** (101 MHz, $CDCl_3$) δ 169.62, 160.28, 137.68, 132.28, 128.71, 128.10, 126.65, 126.03, 118.64, 52.53; **IR** = 3242, 3151, 3070, 2962, 1668, 1330.

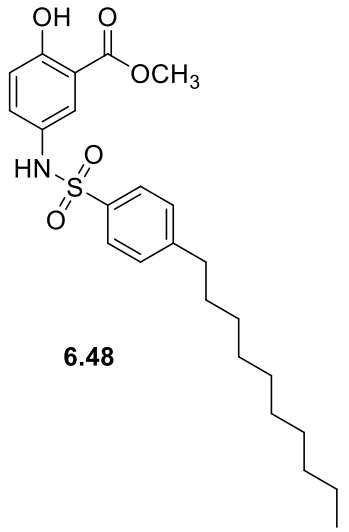

6.48

Methyl 5-((4-(dec-1-yn-1-yl)phenyl)sulfonamido)-2-hydroxybenzoate (6.48).

$Pd(PPh_3)_2Cl_2$ (18.2 mg, 0.0259 mmol), PPh_3 (20.4 mg, 0.0777 mmol), and CuI (4.9 mg, 0.0259 mmol) were combined in a round-bottom flask under N_2. Et_3N (0.3 mL) and MeCN (1.0 mL) were added, followed by **6.47** (100.0 mg, 0.259 mmol), then 1-decyne (56 µL, 0.311 mmol). Reaction was heated at reflux for 1 h. Upon completion, volatiles were removed. PtO_2 (5.8 mg, 0.0254 mmol) was added to a solution of this residue (113.5 mg, 0.254 mmol) in EtOH (0.64 mL) and stirred under an H_2 atmosphere for 48 h. The residue was filtered through a thin pad of Celite with EA. The remaining residue was purified by flash column chromatography (20% Hex) to yield

6.48 as a yellow waxy solid (63.1 mg, 51%). $\mathbf{R_f}$ = 0.45 (30% EA/Hex); **^{1}H NMR** (400 MHz, $CDCl_3$) δ 10.68 (s, 1H), 7.62 – 7.59 (m, 2H), 7.56 (d, *J* = 2.7 Hz, 1H), 7.42 – 7.40 (m, 2H), 7.11 (dd, *J* = 8.8, 2.8 Hz, 1H), 6.89 (s, 1H), 6.84 (d, *J* = 8.9 Hz, 1H), 3.91 (s, 3H), 2.40 (t, *J* = 7.1 Hz, 2H), 1.61 – 1.56 (m, 2H), 1.44 – 1.39 (m, 2H), 1.37 – 1.22 (m, 12H), 0.88 – 0.85 (m, 3H); **^{13}C NMR** (101 MHz, $CDCl_3$) δ 169.73, 159.96, 136.90, 131.94, 131.91, 129.28, 127.10, 127.07, 125.57, 118.46, 112.48, 95.07, 79.20, 60.38, 52.47, 31.73, 29.07, 28.98, 28.83, 28.35, 22.55, 19.37, 14.09, 14.01; **IR** (neat, cm^{-1}) 3236, 2960, 2925, 2847, 1674, 1489, 1222, 1159, 664.

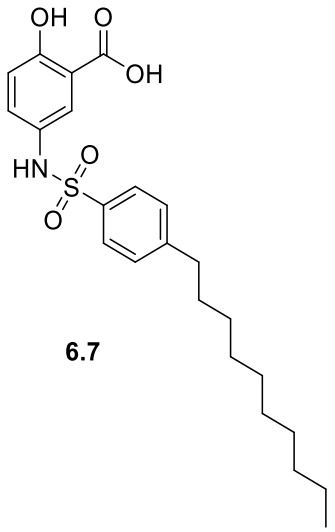

6.7

5-((4-decylphenyl)sulfonamido)-2-hydroxybenzoic acid (6.7).

6.48 (58.4 mg, 0.130 mmol) was added to aq. 3M LiOH (0.13 mL) and stirred at RT for 24 h. 3M HCl was added, causing a solid to crash out of solution. Residual liquids were removed with a pipette and the residue was washed 3x with H_2O to afford **6.7** (5.6 mg, 10%) as a colorless solid. **^{1}H NMR** (400 MHz, MeOD) δ 7.60 – 7.57 (m, 2H), 7.51 (d, *J* = 2.7 Hz, 1H), 7.44 – 7.41 (m, 2H), 7.16 (dd, *J* = 8.9, 2.7 Hz, 1H), 6.83 (d, *J* = 8.9 Hz, 1H), 2.40 (d, *J* = 7.1 Hz, 2H), 1.60 – 1.56 (m, 2H), 1.44 (d, *J* = 7.6 Hz, 2H), 1.38 – 1.23 (m, 12H), 0.88 (d, *J* = 7.0 Hz, 3H); **^{13}C NMR** (101 MHz, MeOD) δ 137.83, 131.32, 131.19, 129.44, 126.80, 124.03, 117.53, 117.33, 51.55, 31.46, 28.78, 28.65, 28.44, 28.08, 22.17, 19.48, 12.91; **IR** (neat, cm^{-1}) 3384, 3267, 2921, 2851, 2508, 2431, 1667, 1154.

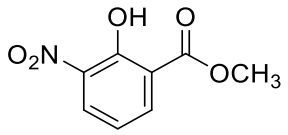

7.49

Methyl 2-hydroxy-3-nitrobenzoate (7.49).

A solution of nitric acid (197 µL, 4.73 mmol) in acetic acid (4.0 mL) was added dropwise to a solution of methyl salicylate (420 µL, 3.94 mmol), acetic acid (4.0 mL), and acetic anhydride (2.4 mL) at 0◦C. The reaction was brought to RT over 6 hours. H_2O (15.0 mL) was added and stirred for an additional 30 minutes. The product was collected as a mixture of isomers by vacuum filtration. Further purification by flash column chromatography (15% EA/Hex to 30% EA/Hex) yielded light **7.49** as a yellow solid (225.3 mg, 35%). $\mathbf{R_f}$ = 0.22 (15% EA/Hex); **mp** = 127 ◦C; **^{1}H NMR** (400 MHz, $CDCl_3$) δ 11.97 (s, 1H), 8.15 – 8.08 (m, 2H), 6.99 (t, *J* = 8.0 Hz, 1H), 4.00 (s, 3H); **^{13}C NMR** (101 MHz, $CDCl_3$) δ 169.12, 155.56, 137.91, 135.64, 131.29, 118.30, 115.69, 53.07; **IR** (neat, cm^{-1}) 3095, 2895, 1673, 1339.

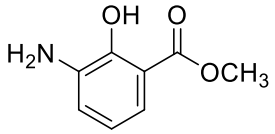

7.50

Methyl 3-amino-2-hydroxybenzoate (7.50).

PtO_2 (15.0 mg, 0.0.0668 mmol) was added to a solution of **7.49** (101.4 mg, 0.514 mmol) in EtOH (2.3 mL) and stirred under an H_2 atmosphere for 4 h. The residue was filtered through a thin pad of Celite with EA to afford the **7.50** (80.1 mg, 96%) as a brown solid. $\mathbf{R_f}$ = 0.5 (25% EA/Hex); **mp** = 78 ◦C; **^{1}H NMR** (400 MHz, $CDCl_3$) δ 10.89 (s, 1H), 7.23 (dd, *J* = 8.0, 1.6 Hz, 1H), 6.87 (dd, *J* = 7.7, 1.5 Hz, 1H), 6.70 (t, *J* = 7.9 Hz, 1H), 3.92 (s, 3H), 3.81 (s, 2H); **^{13}C NMR** (101 MHz, $CDCl_3$) δ 171.06, 149.57, 135.72, 119.52, 118.93, 118.60, 111.67, 52.15; **IR** (neat, cm^{-1}) 3399, 3302, 3102, 2964, 1673, 1434, 1302, 1290, 744.

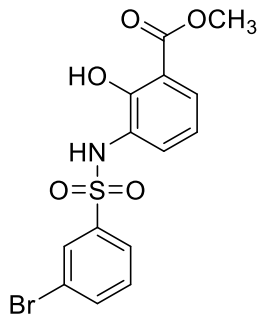

7.51

Methyl 3-((3-bromophenyl)sulfonamido)-2-hydroxybenzoate (7.51).

K_2CO_3 (464.4 mg, 3.36 mmol) was added to a solution of **7.50** (193.9 mg, 1.16 mmol) in THF (1.4 mL) at 0^0C. 3-bromobenzenesulfonyl chloride (367 µL, 2.55 mmol) in THF (1.5 mL) was added dropwise. After 30 min, reaction was brought to RT and stirred for 24 h. Reaction mixture was filtered through a short pad of silica gel with EA and purified by flash column chromatography (35% EA/Hex) to afford **7.51** (294.1 mg, 66%) as a yellow oil. $\mathbf{R_f}$ = 0.25 (30% EA/Hex); **^{1}H NMR** (400 MHz, $CDCl_3$) δ 8.11 (t, *J* = 1.8 Hz, 1H), 8.08 (t, *J* = 1.8 Hz, 1H), 7.90 (dd, *J* = 3.4, 1.5 Hz, 1H), 7.89 – 7.87 (m, 1H), 7.87 (t, *J* = 1.8 Hz, 1H), 7.82 – 7.77 (m, 2H), 7.71 – 7.59 (m, 2H), 7.49 (t, *J* = 8.0 Hz, 1H), 7.42 (t, *J* = 8.0 Hz, 1H), 7.36 (t, *J* = 8.0 Hz, 1H), 7.28 – 7.23 (m, 1H), 7.21 (dd, *J* = 7.7, 1.7 Hz, 1H), 7.11 (t, *J* = 7.9 Hz, 1H), 6.93 (dd, *J* = 8.0, 1.7 Hz, 1H), 3.75 (d, *J* = 0.7 Hz, 5H); **^{13}C NMR** (101 MHz, $CDCl_3$) δ 165.44, 163.96, 140.62, 138.43, 138.07, 137.51, 137.33, 136.28, 135.99, 134.08, 131.29, 131.23, 131.07, 130.84, 130.56, 130.48, 130.02, 128.64, 128.16, 128.04, 127.62, 127.06, 127.00, 126.72, 125.61, 123.20, 122.98, 122.90, 121.04, 120.91, 52.51, 52.22; **IR** (neat, cm^{-1}) 3484, 3386, 3087, 2951, 1722, 1292, 1190, 1164.

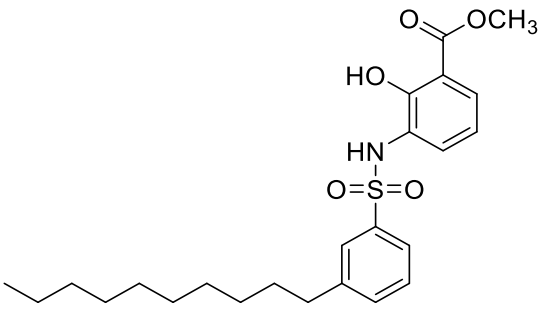

7.52

Methyl 3-((3-(dec-1-yn-1-yl)phenyl)sulfonamido)-2-hydroxybenzoate (7.52).

$Pd(PPh_3)_2Cl_2$ (13.8 mg, 0.0197 mmol) and CuI (3.7 mg, 0.0197 mmol) were combined in a round-bottom flask under N_2. Et_3N (0.26 mL) and MeCN (0.79 mL) were added, followed by **7.51** (76.1 mg, 0.197 mmol), then 1-decyne (43 µL, 0.236 mmol). Reaction was heated at reflux for 1 h. Upon completion, volatiles were removed. Raney Ni (5.2 mg, 10% wt/wt) was added to a solution of this residue (52.2 mg, 0.118 mmol) in EtOH (0.30 mL) and THF (0.3 mL) and stirred under an H_2 atmosphere for 3 h. The residue was filtered through a thin pad of Celite with EA. was purified by flash column chromatography (20% EA/Hex) to yield **7.52** as a colorless oil (65.3 mg, 75%). **R_f** = 0.5 (30% EA/Hex); **^{1}H NMR** (400 MHz, $CDCl_3$) δ 7.77 (dt, *J* = 2.5, 1.3 Hz, 1H), 7.75 (q, *J* = 1.7 Hz, 1H), 7.73 (d, *J* = 1.9 Hz, 1H), 8.24 – 6.02 (m, 4H), 7.51 – 7.46 (m, 1H), 7.39 (dd, *J* = 6.6, 1.5 Hz, 1H), 7.19 (dd, *J* = 7.7, 1.6 Hz, 1H), 7.10 (t, *J* = 7.8 Hz, 1H), 6.89 (dd, *J* = 7.9, 1.7 Hz, 1H), 3.73 (d, *J* = 3.1 Hz, 3H), 2.72 – 2.64 (m, 2H), 1.61 (dt, *J* = 13.2, 3.9 Hz, 2H), 1.32 – 1.20 (m, 14H), 0.90 – 0.83 (m, 3H); **^{13}C NMR** (101 MHz, $CDCl_3$) δ 165.69, 144.98, 144.52, 140.61, 138.78, 138.53, 136.21, 135.64, 135.20, 134.46, 133.20, 131.48, 130.44, 130.05, 129.32, 129.01, 128.97, 128.35, 128.05, 127.64, 127.52, 127.30, 127.14, 127.02, 126.53, 125.70, 125.61, 120.80, 52.33, 52.08, 35.60, 35.56, 31.79, 31.02, 30.98, 29.50, 29.44, 29.31, 29.21, 29.11, 29.06, 22.58, 14.01; **IR** (neat, cm^{-1}) 3238, 2924, 2852, 1728, 1290, 1161, 757, 718, 552.

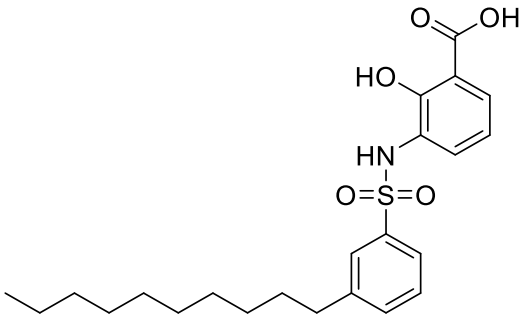

7.1b

3-((3-decylphenyl)sulfonamido)-2-hydroxybenzoic acid (7.1b).

7.52 (33.5 mg, 0.0748 mmol) was added to aq. 3M LiOH (0.07 mL) and THF (0.19 mL) and stirred at RT for 24 h. 3M HCl was added, causing a solid to crash out of solution. Residual liquids were removed with a pipette and the product was washed 3x with H_2O, then further purified by flash column chromatography (1% AcOH/10% MeOH/EA) to yield **7.1b** as an off-white solid. $\mathbf{R_f}$ = 0.2 (10% MeOH/EA); **mp** >320 ◦C. **^{1}H NMR** (400 MHz, MeOD) δ 7.76 (d, *J* = 1.8 Hz, 1H), 7.73 – 7.61 (m, 2H), 7.43 – 7.24 (m, 3H), 6.43 (dt, *J* = 11.5, 1.9 Hz, 1H), 5.72 (dt, *J* = 11.7, 7.4 Hz, 1H), 2.33 (qd, *J* = 7.3, 1.8 Hz, 2H), 1.46 (dd, *J* = 10.2, 4.8 Hz, 2H), 1.34 – 1.26 (m, 14H), 0.88 (td, *J* = 4.0, 1.9 Hz, 3H); **^{13}C NMR** (101 MHz, MeOD) δ 144.51, 137.79, 133.65, 130.11, 127.64, 127.36, 125.64, 125.33, 123.54, 122.76 (d, *J* = 16.1 Hz), 48.13, 47.92, 47.71, 47.49, 47.28, 47.07, 46.85, 31.52, 29.47, 29.22, 29.07, 28.89, 28.02, 22.20, 12.92; **IR** (neat, cm^{-1}) 3393, 2955, 2918, 2872, 2850, 1185, 627.

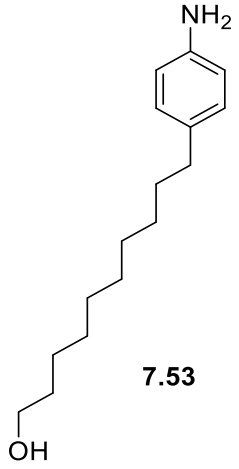

7.53

10-(4-aminophenyl)decan-1-ol (7.53).

PtO_2 (8.0 mg, 0.0352 mmol) was added to a solution of **6.11** (74.6 mg, 0.271 mmol) in EtOH (1.2 mL) and stirred under an H_2 atmosphere for 3 h. The residue was filtered through a thin pad of Celite with EA yielding **7.53** (48.7 mg, 72%) as a colorless solid. $\mathbf{R_f}$ = 0.3 (55% EA/Hex); **^{1}H NMR** (300 MHz, $CDCl_3$) δ 7.00 – 6.94 (m, 2H), 6.65 – 6.60 (m, 2H), 3.64 (d, *J* = 6.6 Hz, 2H), 3.54 (s, 2H), 2.52 – 2.46 (m, 2H), 1.55 (t, *J* = 6.5 Hz, 4H), 1.28 (d, *J* = 4.8 Hz, 12H).

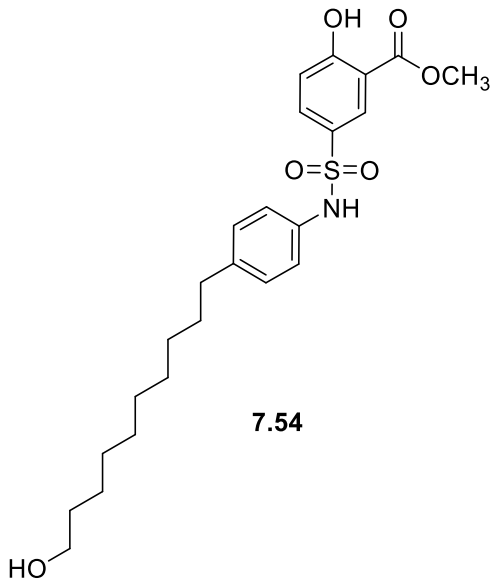

7.54

Methyl 2-hydroxy-5-(N-(4-(10-hydroxydecyl)phenyl)sulfamoyl)benzoate (7.54).

$NaHCO_3$ (26.0 mg, 0.310 mmol) was added to a solution of **MN-1-61** (26.6 mg, 0.107 mmol) in THF (0.12 mL) at 0^0C. **6.9** (58.8 mg, 0.235 mmol) in THF (0.12 mL) was added dropwise. The reaction was brought to RT overnight. The reaction mixture was filtered through a short pad of silica gel with EA and purified by flash column chromotagraphy (55% EA/Hex) to afford **7.54** (44.5 mg, 90%) as an off-white solid. $\mathbf{R_f}$ = 0.35 (55% EA/Hex); **^{1}H NMR** (300 MHz, $CDCl_3$) δ 11.19 (s, 1H), 8.30 (d, *J* = 2.5 Hz, 1H), 7.76 (dd, *J* = 8.8, 2.4 Hz, 1H), 7.04 – 6.94 (m, 5H), 3.91 (s, 3H), 3.63 (t, *J* = 6.6 Hz, 2H), 2.50 (t, *J* = 7.6 Hz, 2H), 1.53 (q, *J* = 7.2, 6.4 Hz, 4H), 1.26 (d, *J* = 10.4 Hz, 12H).

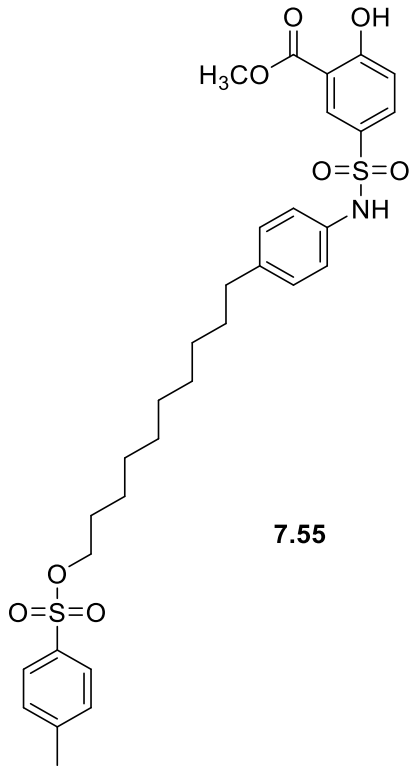

7.55

Methyl 2-hydroxy-5-(N-(4-(10-(tosyloxy)decyl)phenyl)sulfamoyl)benzoate (7.55).

Pyridine (33 µL, 0.403 mmol) was added dropwise to a solution of **7.54** (88.9 mg, 0.192 mmol), tosyl chloride (40.2 mg, 0.211 mmol), and DMAP (2.3 mg, 0.0192 mmol) in dry CH_2Cl_2 (0.38 mL) and dry THF (0.38 mL) at 0◦C. Reaction was heated to reflux overnight. Volatiles were removed and purification by flash column chromatography (25% EA/Hex) afforded **7.55** (42.1 mg, 35%) as a colorless oil. $\mathbf{R_f}$ = 0.29 (25% EA/Hex; **^{1}H NMR** (300 MHz, $CDCl_3$) δ 11.21 (d, *J* = 1.0 Hz, 1H), 8.29 (dd, *J* = 2.4, 1.0 Hz, 1H), 7.81 – 7.75 (m, 2H), 7.74 – 7.70 (m, 1H), 7.34 (dt, *J* = 7.3, 1.0 Hz, 2H), 7.08 – 7.04 (m, 2H), 6.99 – 6.93 (m, 3H), 6.40 (s, 1H), 3.95 (d, *J* = 1.1 Hz, 3H), 2.52 (t, *J* = 7.7 Hz, 2H), 1.67 – 1.57 (m, 2H), 1.53 (s, 2H), 1.32 – 1.14 (m, 14H); **^{13}C NMR** (101 MHz, $CDCl_3$) δ 163.40, 150.78, 146.00, 137.68, 136.00, 133.85, 133.70, 132.62, 131.90, 131.75, 131.09, 129.82, 129.74, 129.32, 128.48, 127.43, 126.80, 126.19, 124.63, 122.79, 122.62, 121.94, 121.65, 52.71, 45.10, 32.89, 32.50, 29.73, 29.31, 29.20, 29.14, 29.00, 28.70, 28.53, 26.75, 21.68); **IR** (neat, cm^{-1}) 2924, 2853, 1680, 1337, 1161, 661, 553.

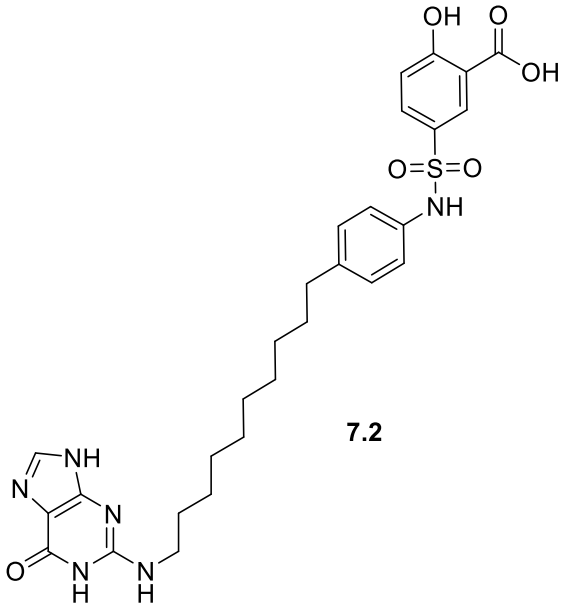

7.2

2-hydroxy-5-(N-(4-(10-((6-oxo-6,9-dihydro-1H-purin-2-yl)amino)decyl)phenyl) sulfamoyl)benzoic acid (7.2).

Guanine (6.1 mg, 0.0403 mmol), **7.55** (27.4 mg, 0.0444 mmol), and NaH (60% w/w, 2.9 mg, 0.121 mmol) were heated to 80◦C in dry DMF (0.080 mL) overnight. Reaction was cooled to RT and 3M LiOH (0.04 mL) was added and stirred for 1 h. 3M HCl was added, causing a solid to crash out of solution. After washing 4x H_2O, **7.2** (15.5 mg, 66%) was obtained as an off-white solid.; **mp** = 180°C; **^{1}H NMR** (400 MHz, MeOD) δ 8.22 (dd, *J* = 3.6, 2.4 Hz, 1H), 7.67 (ddd, *J* = 8.9, 5.1, 2.4 Hz, 1H), 6.96 (tdd, *J* = 22.6, 9.7, 3.7 Hz, 6H), 4.06 (dt, *J* = 16.5, 7.1 Hz, 2H), 3.52 (t, *J* = 6.6 Hz, 1H), 3.12 – 3.05 (m, 1H), 2.50 (dt, *J* = 7.8, 3.8 Hz, 2H), 1.99 (d, *J* = 8.9 Hz, 2H), 1.81 (s, 1H), 1.52 (s, 2H), 1.29 – 1.19 (m, 12H); **^{13}C NMR** (101 MHz, DMSO) δ 162.75, 149.91, 137.23, 133.67, 130.58, 130.25, 129.61, 128.48, 126.82, 125.85, 118.56, 48.10, 47.89, 47.68, 44.94, 36.17, 34.18, 34.10, 32.70, 31.13, 29.52, 29.04, 28.74, 26.01, 21.11, 14.30; **IR** (neat, cm^{-1}) 3374, 2923, 2852, 1631, 1160, 574.

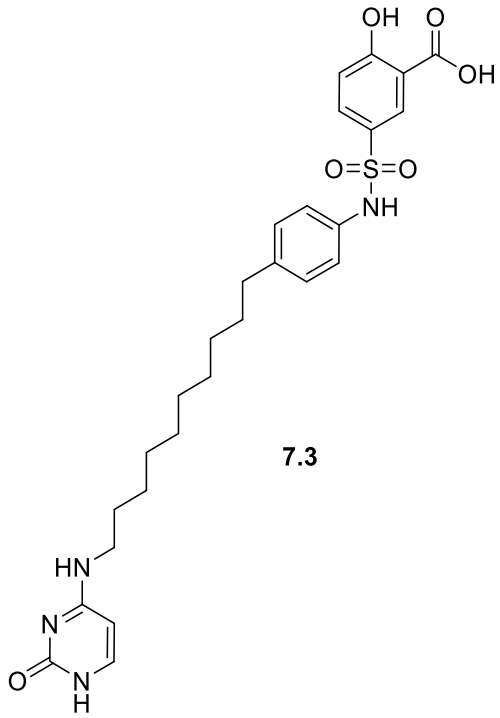

7.3

2-hydroxy-5-(N-(4-(10-((2-oxo-1,2-dihydropyrimidin-4-yl)amino)decyl)phenyl) sulfamoyl)benzoic acid (7.3).

Cytosine (8.9 mg, 0.0800 mmol), **7.55** (59.3 mg, 0.0960 mmol), and NaH (60% w/w, 9.6 mg, 0.240 mmol) were heated to 80◦C in dry DMF (0.16 mL) overnight. The reaction was cooled to RT and 3M LiOH (0.08 mL) was added and stirred for 1 h. 3M HCl was added, causing a solid to crash out of solution. After washing 4x H_2O, **7.3** (17.9 mg, 41%) was obtained as a tan solid. **mp** = 75°C; **^{1}H NMR** (300 MHz, $CDCl_3$) δ 8.24 (d, *J* = 2.5 Hz, 1H), 7.61 – 7.57 (m, 1H), 6.97 (d, *J* = 1.1 Hz, 5H), 6.79 (d, *J* = 8.7 Hz, 2H), 3.08 (s, 2H), 2.50 (s, 2H), 1.67 (s, 2H), 1.53 (d, *J* = 7.2 Hz, 2H), 1.31 (s, 6H), 1.24 – 1.21 (m, 6H); **^{13}C NMR** (101 MHz, MeOD) δ 131.20, 128.53, 121.24, 116.36, 57.48, 48.13, 47.92, 47.71, 47.49, 47.28, 47.07, 46.85, 41.82, 28.75, 28.54, 24.15; **IR** (neat, cm^{-1}) 2924, 2853, 1582, 1160, 661, 556.

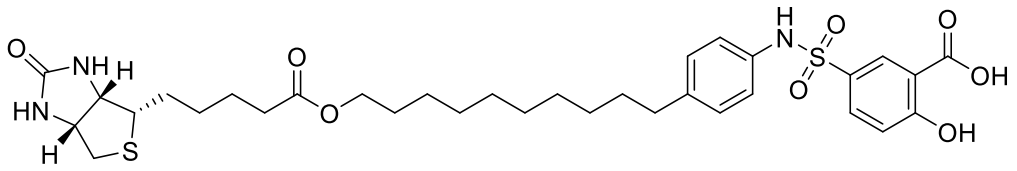

7.4

2-hydroxy-5-(N-(4-(10-((5-((3aS,4S,6aR)-2-oxohexahydro-1H-thieno[3,4-d]imidazol-4-yl)pentanoyl)oxy)decyl)phenyl)sulfamoyl)benzoic acid (7.4).

7.54 (108.1 mg, 0.256 mmol) and DMAP (2.8 mg, 0.0233 mmol) were added to a solution of D-Biotin (62.7 mg, 0.256 mmol) in DMF. The reaction was cooled to 0◦C and DCC (52.8 mg, 0.256 mmol) was added. After 5 min, the reaction was brought to RT and stirred for 3 h. 1M LiOH (0.75 mL) was added and stirred for 20 min. After addition of 3M HCl (0.75 mL), the reaction was placed in an ice bath for 10 min. The resulting slurry vacuum filtered, washed 3x Et_2O and 3x H_2O to afford **7.4** (94.5 mg, 59%) as a colorless solid. **mp** = 175 ◦C; **^{1}H NMR** (800 MHz, DMSO) δ 11.97 (s, 1H), 11.00 (d, *J* = 3.1 Hz, 1H), 10.02 (d, *J* = 3.1 Hz, 1H), 8.07 (d, *J* = 2.6 Hz, 1H), 7.73 (dt, *J* = 8.8, 2.6 Hz, 1H), 7.07 (dd, *J* = 8.9, 2.7 Hz, 1H), 7.02 (dd, *J* = 8.5, 2.6 Hz, 2H), 6.94 (dd, *J* = 8.5, 2.6 Hz, 2H), 6.41 (s, 1H), 6.33 (s, 1H), 5.56 (d, *J* = 8.0 Hz, 2H), 4.28 (d, *J* = 3.5 Hz, 1H), 4.12 – 4.11 (m, 1H), 3.85 (s, 1H), 3.85 (s, 1H), 3.34 (q, *J* = 4.0 Hz, 2H), 3.09 – 3.08 (m, 1H), 2.81 – 2.80 (m, 1H), 2.57 – 2.55 (m, 1H), 2.44 – 2.41 (m, 2H), 2.20 – 2.18 (m, 2H), 1.70 (dd, *J* = 8.9, 4.0 Hz, 4H), 1.61 – 1.58 (m, 5H), 1.49 (t, *J* = 7.8 Hz, 4H), 1.45 – 1.43 (m, 2H), 1.38 – 1.35 (m, 2H), 1.32 – 1.29 (m, 2H), 1.22 – 1.19 (m, 12H), 1.11 (dt, *J* = 12.3, 6.0 Hz, 2H), 1.02 (d, *J* = 11.6 Hz, 4H); **^{13}C NMR** (201 MHz, DMSO) δ 174.86, 167.49, 163.13, 162.68, 157.05, 139.00, 135.46, 133.45, 130.52, 130.24, 129.36, 121.34, 118.80, 114.78, 61.49, 61.15, 59.62, 55.84, 53.13, 47.95, 34.83, 33.93, 33.80, 32.98, 31.29, 29.50, 29.37, 29.25, 29.02, 28.56, 28.49, 25.93, 25.77, 24.98, 24.91; **IR** (neat, cm^{-1}) 3321, 2927, 2850, 1681, 1624, 1573, 1159, 640, 562.

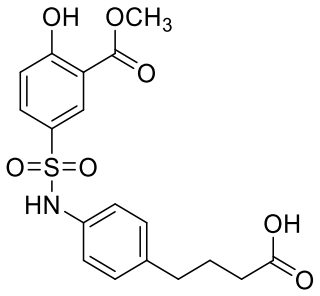

7.72

4-(4-((4-hydroxy-3-(methoxycarbonyl)phenyl)sulfonamido)phenyl)butanoic acid (7.72).

A solution of **6.9** (123.1 mg, 0.491 mmol) in THF (0.25 mL) was added dropwise to a solution of 4-(4-aminophenyl)butanoic acid **6.18** (40.0 mg, 0.223 mmol) and $NaHCO_3$ (56.2 mg, 0.669 mmol) in THF (0.25 mL) at 0◦C. The reaction was warmed to RT and stirred overnight. Volatiles were removed and the resulting residue was washed with 3x Et_2O, extracted with H_2O, acidified to pH=2 with 6M HCl, and extracted 3x with EA. Further purification by flash column chromatography (65% EA/Hex) yielded the **7.72** (83.3 mg, 95%) as a colorless oil. $\mathbf{R_f}$ = 0.3 (60% EA/Hex); **^{1}H NMR** (300 MHz, $CDCl_3$) δ 8.30 (dd, *J* = 2.4, 0.9 Hz, 1H), 7.77 (ddd, *J* = 8.8, 2.5, 0.9 Hz, 1H), 7.34 (s, 1H), 7.05 – 6.95 (m, 5H), 3.91 (d, *J* = 0.9 Hz, 3H), 2.58 (t, *J* = 7.6 Hz, 2H), 2.32 (t, *J* = 7.4 Hz, 2H), 1.88 (t, *J* = 7.6 Hz, 2H); **^{13}C NMR** (101 MHz, MeOD) δ 175.74, 169.01, 164.06, 138.53, 135.10, 133.49, 130.25, 129.68, 128.71, 121.74, 117.81, 112.05, 51.90, 48.14, 47.93, 47.71, 47.50, 47.29, 47.08, 46.86, 33.82, 32.56, 26.26; **IR** (neat, cm^{-1}) 1680, 1158, 562.

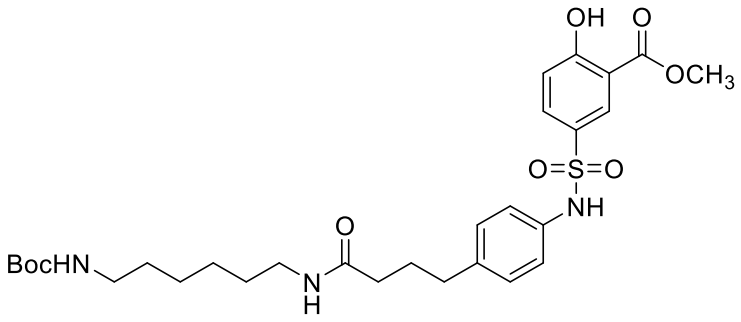

7.73

Methyl 5-(N-(4-(4-((6-((tert-butoxycarbonyl)amino)hexyl)amino)-4-oxobutyl)phenyl) sulfamoyl) -2-hydroxybenzoate (**7.73).**

7.72 (83.3 mg, 0.212 mmol), HATU (88.7 mg, 0.233 mmol), and DIEA (111 µL, 0.636 mmol) were stirred at RT in CH_3CN (0.42 mL) for 15 min. N-Boc-1,6-hexanediamine (57 µL, 0.254 mmol) was added and reaction was stirred at RT for 2 h. Volatiles were removed and resulting residue was washed with H_2O, extracted 4x EA, and purified by flash column chromatography (80% EA/Hex) to afford **7.73** (110.9 mg, 88%) as a colorless solid. $\mathbf{R_f}$ = 0.32 (80% EA/Hex); **mp** = 95 ◦C; **^{1}H NMR** (300 MHz, $CDCl_3$) δ 8.17 (dd, *J* = 4.5, 2.3 Hz, 1H), 7.85 – 7.72 (m, 2H), 7.05 – 6.94 (m, 5H), 3.92 (d, *J* = 6.7 Hz, 3H), 3.16 – 3.07 (m, 2H), 3.00 (t, *J* = 6.9 Hz, 2H), 2.51 (t, *J* = 7.6 Hz, 2H), 2.12 (d, *J* = 7.4 Hz, 2H), 1.81 (t, *J* = 7.3 Hz, 2H), 1.45 (d, *J* = 7.0 Hz, 4H), 1.40 (d, *J* = 6.2 Hz, 9H), 1.30 (p, *J* = 3.3 Hz, 4H). **^{13}C NMR** (101 MHz, $CDCl_3$) δ 172.86, 171.11, 169.39, 164.55, 156.17, 138.79, 134.34, 133.94, 131.90, 131.12, 130.19, 130.00, 129.17, 122.47, 122.01, 118.95, 118.38, 112.14, 60.30, 52.71, 40.10, 39.07, 35.67, 34.39, 29.79, 29.22, 28.31, 26.95, 26.03, 25.89, 20.93, 14.07; **IR** (neat, cm^{-1}) 2932, 2860, 1680, 1159, 839, 558.

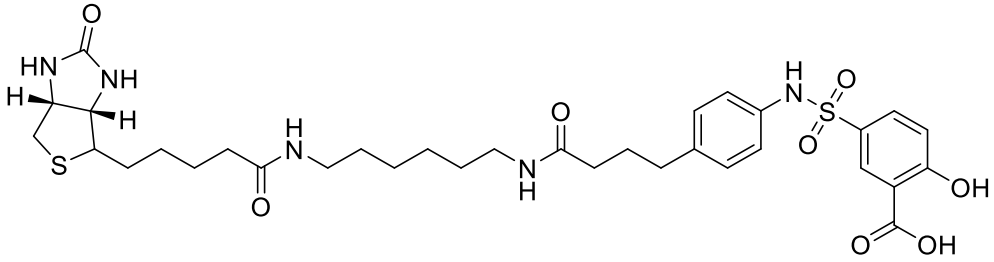

7.5

2-hydroxy-5-(N-(4-(4-oxo-4-((6-(5-((3aS,6aR)-2-oxohexahydro-1H-thieno[3,4-d]imidazol-4-yl)pentanamido)hexyl)amino)butyl)phenyl)sulfamoyl)benzoic acid (7.5).

7.73 (110.9 mg, 0.187 mmol) was stirred in a solution of 30% TFA/CH_2Cl_2 (0.60 mL) for 2 h. Volatiles were removed, and the resulting free-amine was added to a solution of D-Biotin (38.1 mg, 0.156 mmol), HATU (65.2 mg, 0.172 mmol), and DIEA (82 µL, 0.468 mmol) that had been pre-activated for 15 min in CH_3CN (0.31 mL) at RT. After 3 h, the volatiles were removed and 3M LiOH (0.16 mL) was added. After 1 h, the reaction mixture was washed 5x EA, and acidified

to pH = 2 with 6 M HCl, collected by vacuum filtration, and washed 3x with H_2O to afford **7.5** (61.6 mg, 56%) as an off-white solid. **mp** = 90 ◦C; **^{1}H NMR** (400 MHz, DMSO) δ 10.04 (d, *J* = 2.4 Hz, 1H), 8.11 (d, *J* = 2.5 Hz, 1H), 7.75 – 7.69 (m, 3H), 7.05 – 7.00 (m, 3H), 6.97 – 6.94 (m, 2H), 4.29 – 4.26 (m, 1H), 4.11 – 4.08 (m, 1H), 3.85 (s, 1H), 3.06 (dt, *J* = 4.3, 2.0 Hz, 1H), 2.97 (dt, *J* = 7.0, 3.3 Hz, 4H), 2.81 – 2.77 (m, 1H), 2.55 (d, *J* = 12.5 Hz, 1H), 2.40 (d, *J* = 7.7 Hz, 2H), 2.02 – 1.97 (m, 4H), 1.69 – 1.65 (m, 2H), 1.58 (dd, *J* = 6.9, 3.9 Hz, 1H), 1.49 – 1.42 (m, 3H), 1.33 – 1.20 (m, 10H); **^{13}C NMR** (101 MHz, DMSO) δ 172.15, 171.92, 164.11, 163.06, 133.65, 130.11, 129.36, 121.18, 61.40, 59.55, 55.79, 38.66, 35.57, 35.14, 34.29, 29.48, 28.57, 28.39, 27.34, 26.47, 25.70; **IR** (neat, cm^{-1}) 3241, 2930, 1681, 1154, 1105, 562.

APPENDIX B. NMR AND LC-MS DATA

NMR AND LC-MS DATA: PART 1

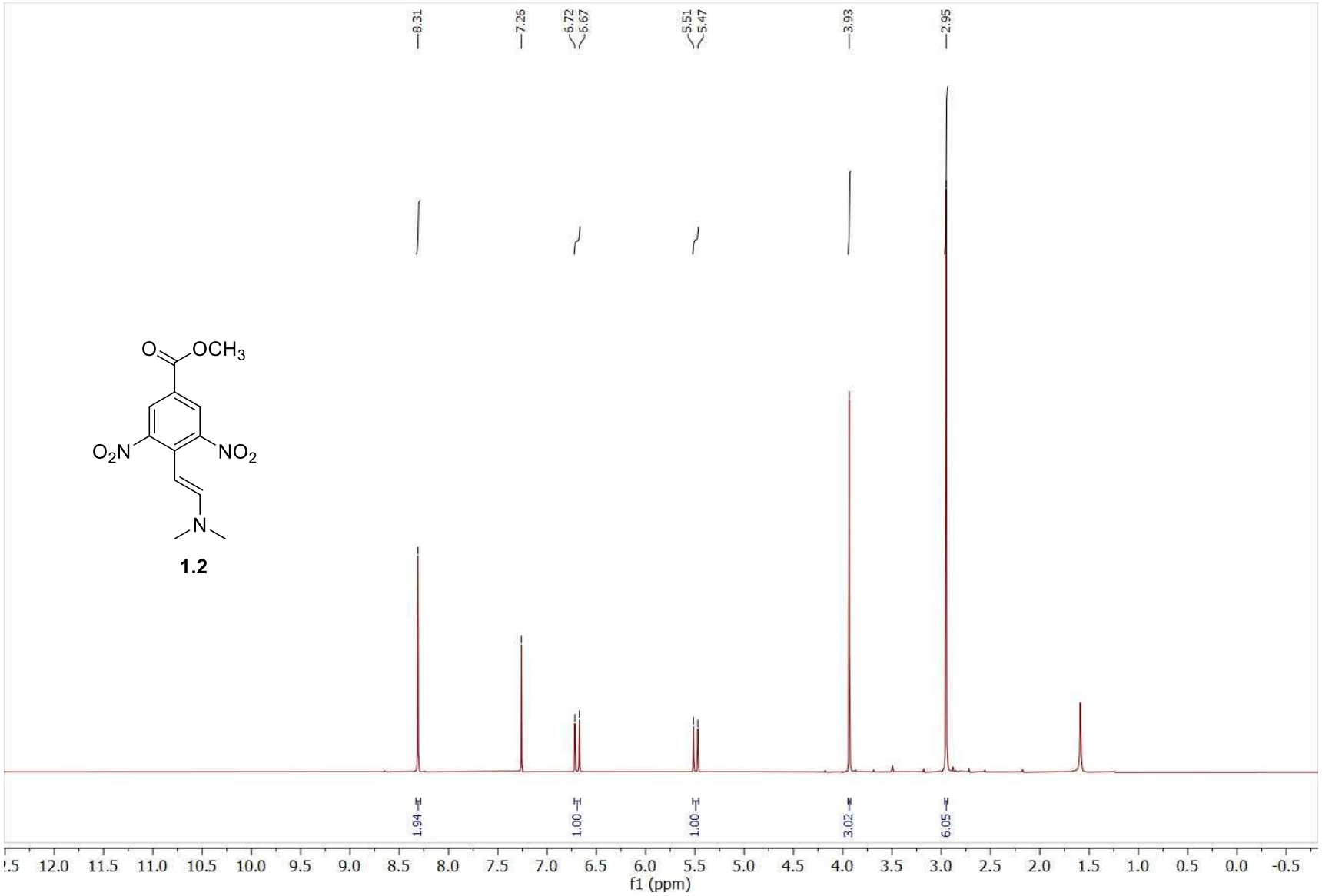

Figure B1: ^{1}H NMR of compound **1.2**.

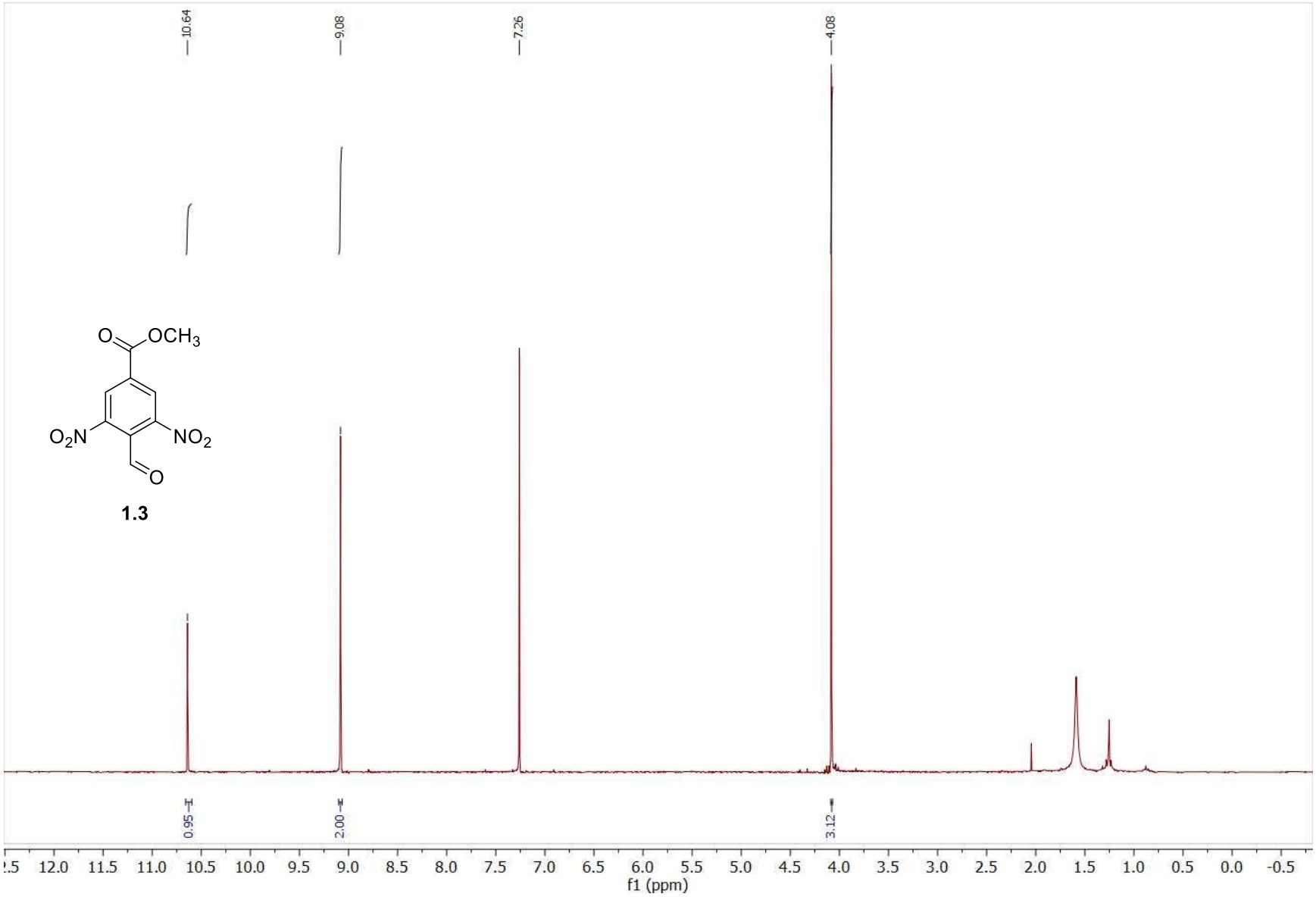

Figure B2: ^{1}H NMR of compound **1.3**.

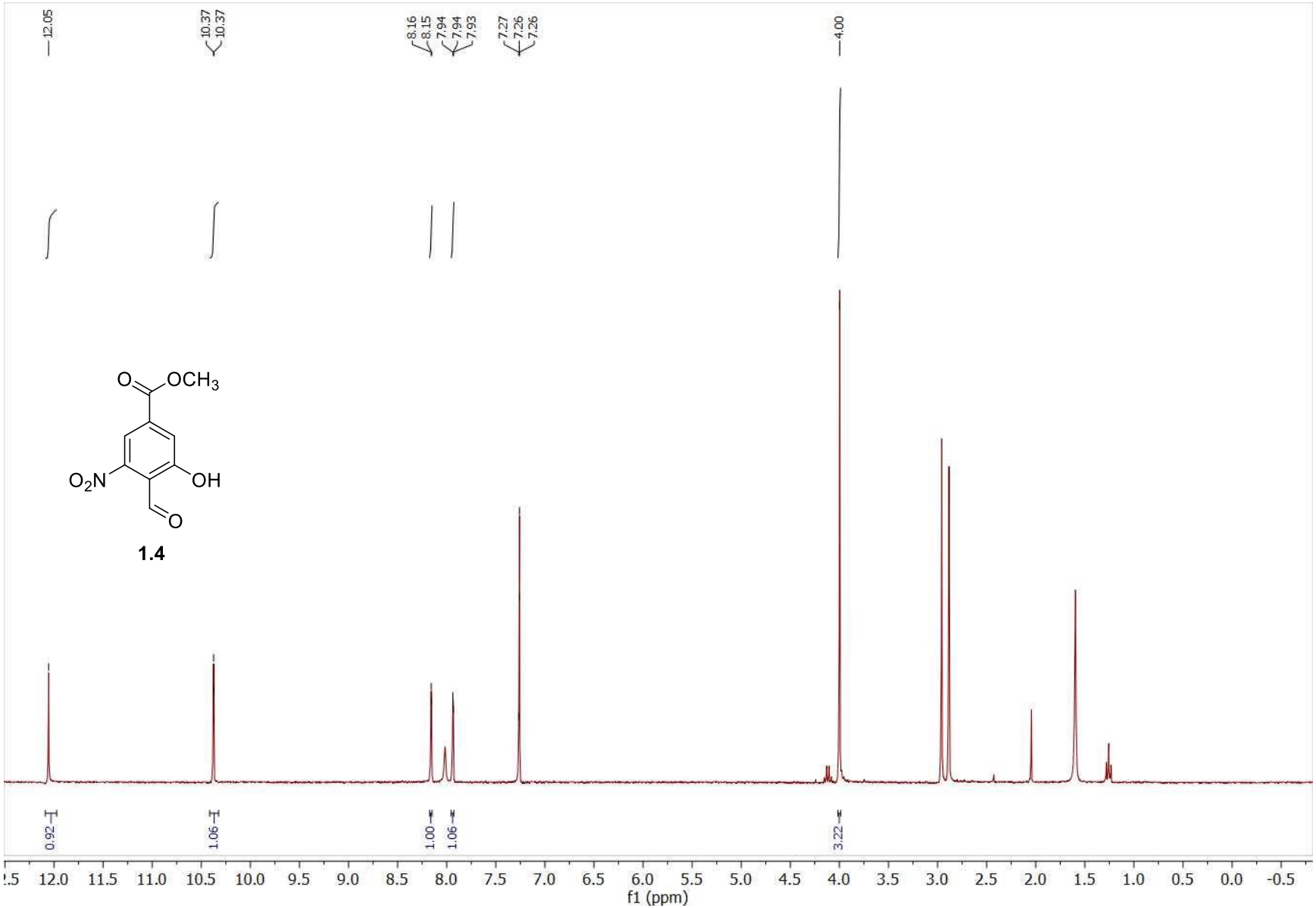

Figure B3: ^{1}H NMR of compound **1.4**.

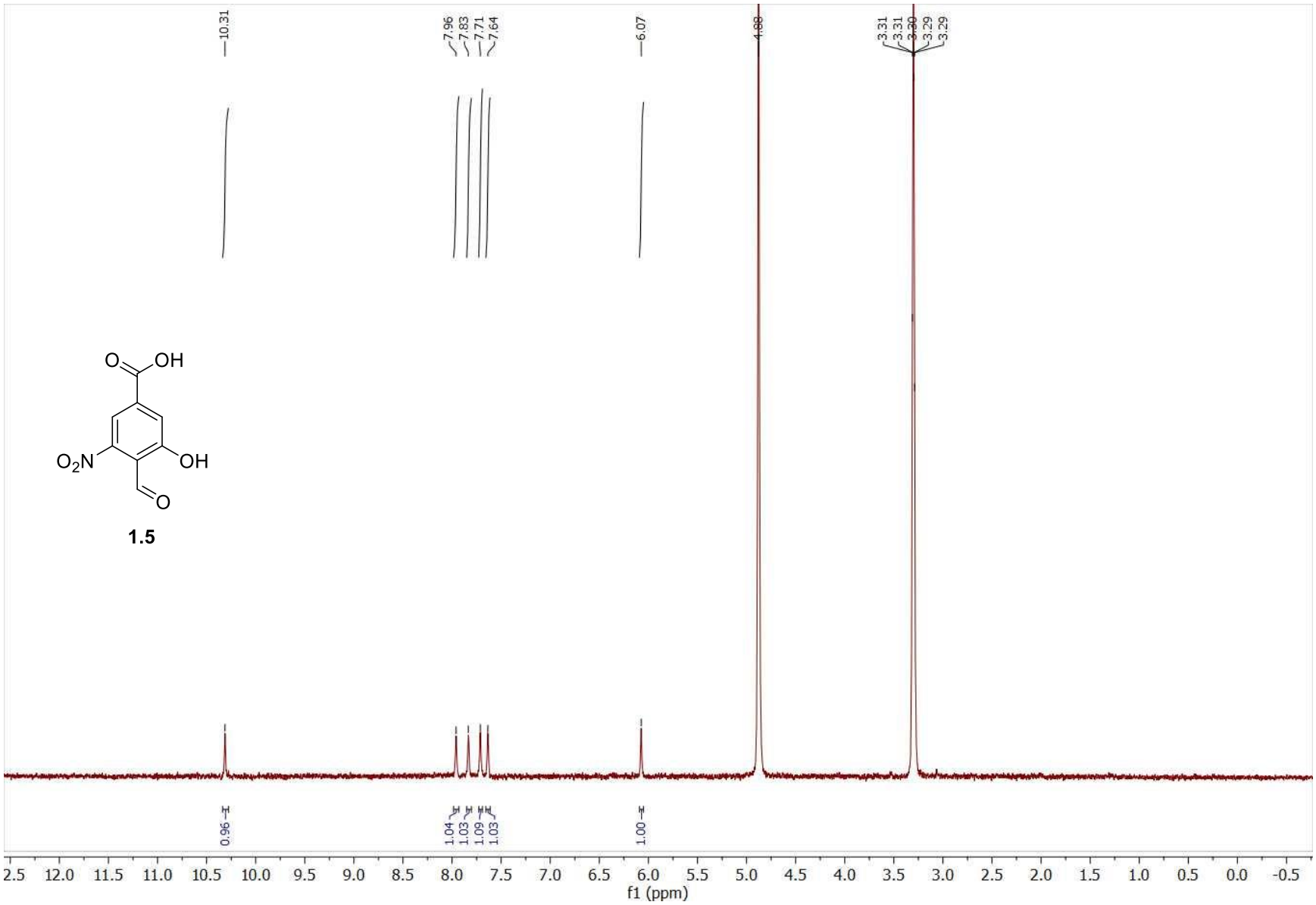

Figure B4: ^{1}H NMR of compound **1.5**.

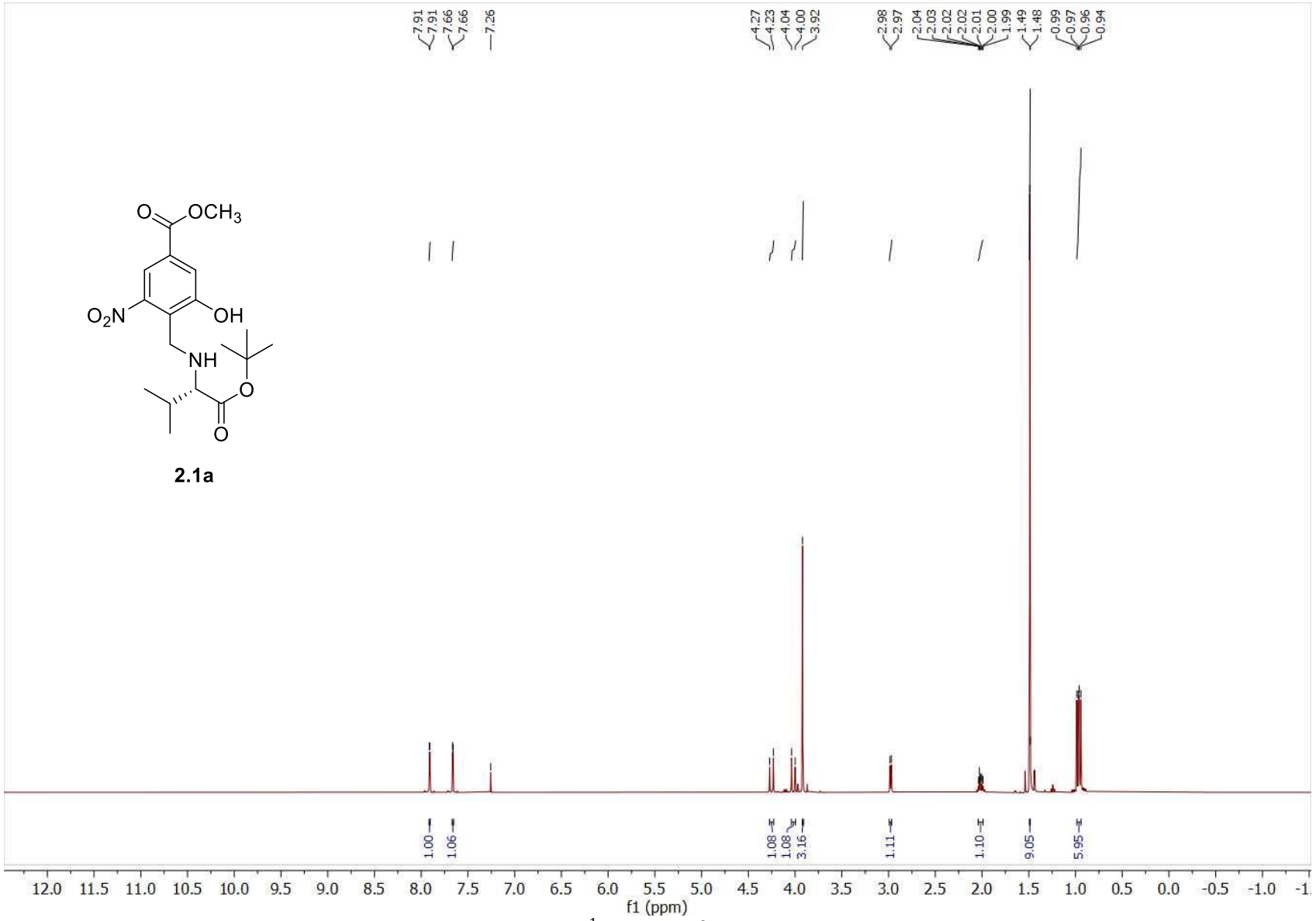

Figure B5: ^{1}H NMR of compound **2.1a**.

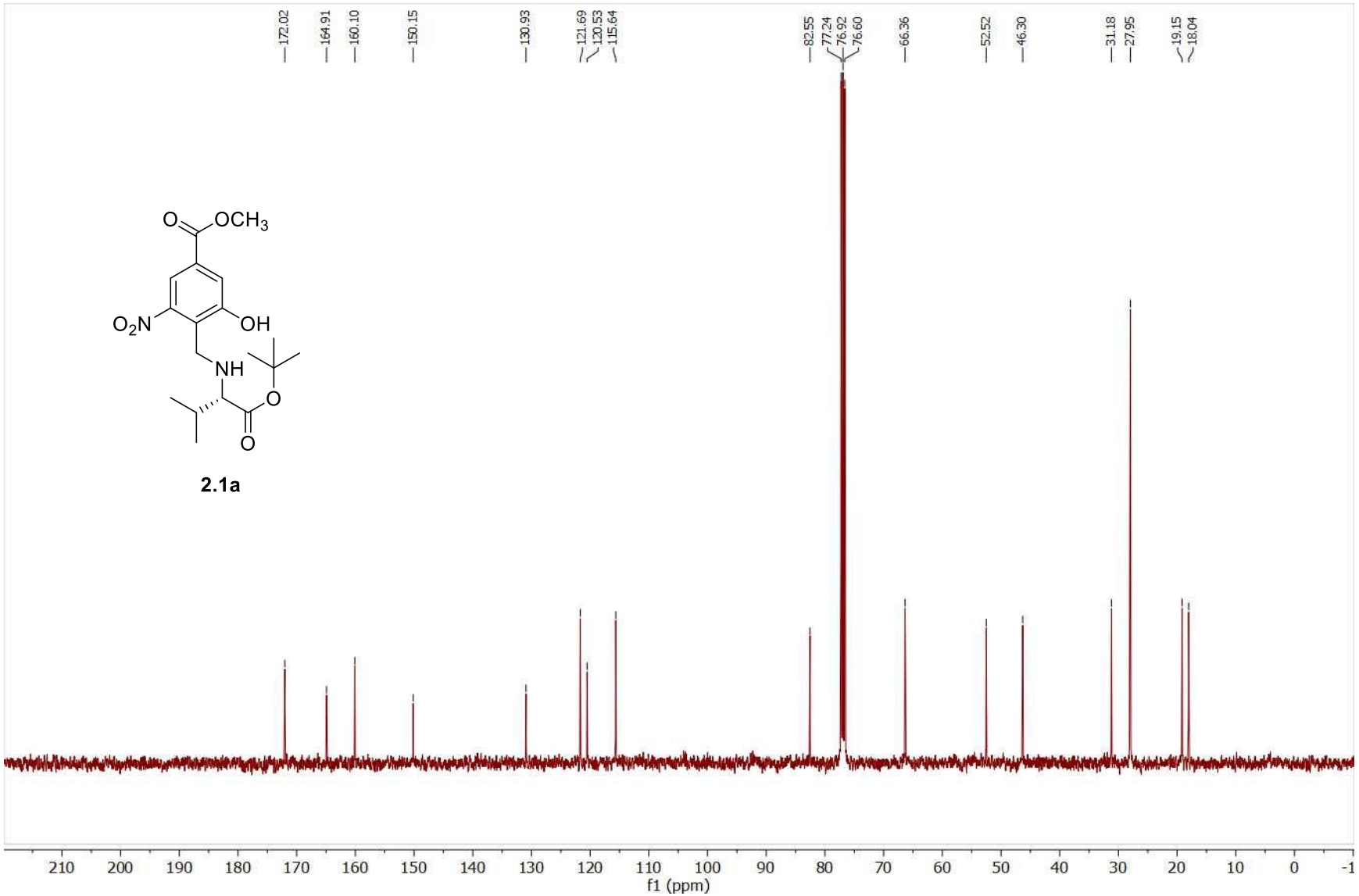

Figure B6: ^{13}C NMR of compound **2.1a**.

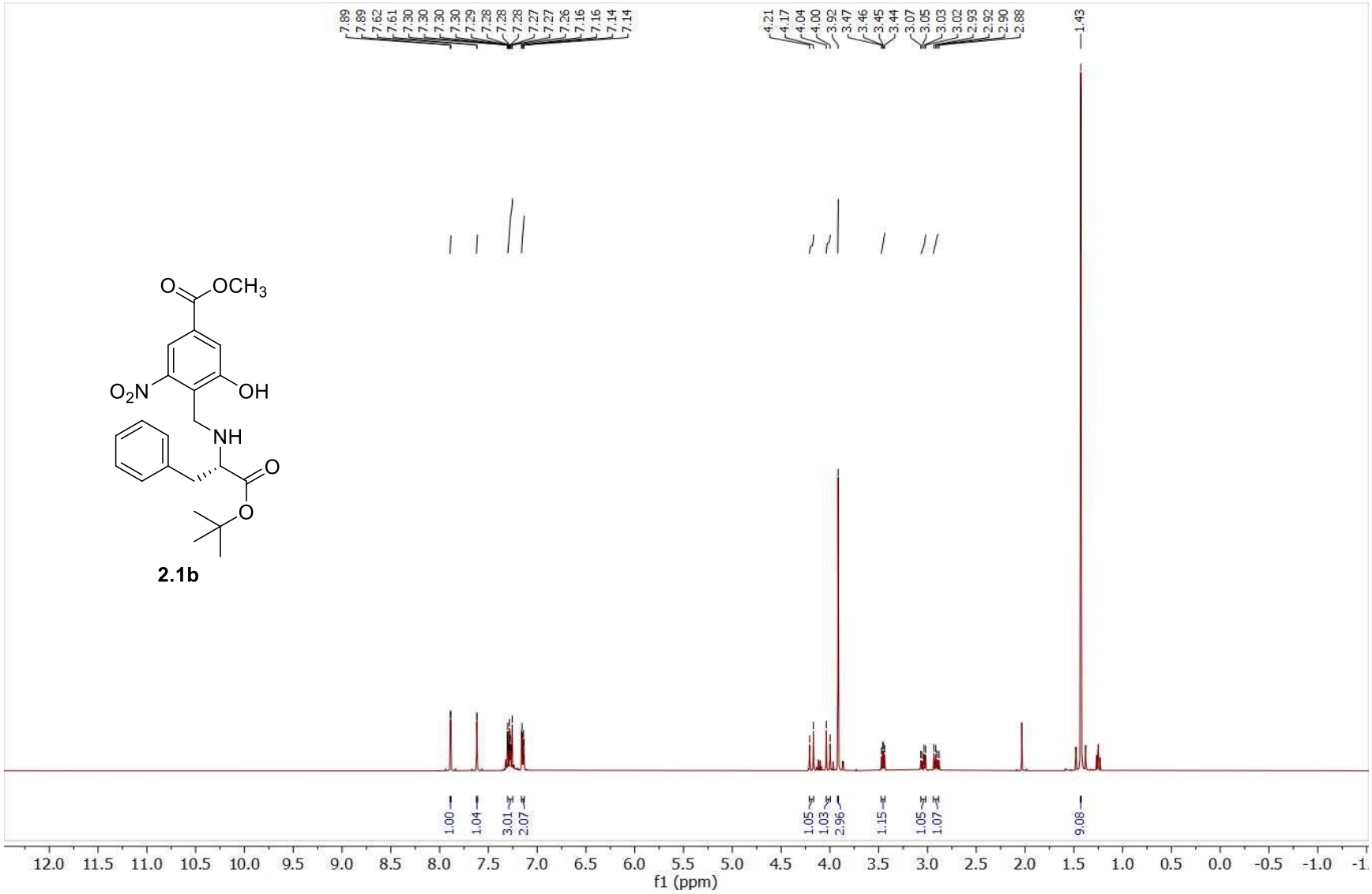

Figure B7: ^{1}H NMR of compound **2.1b**.

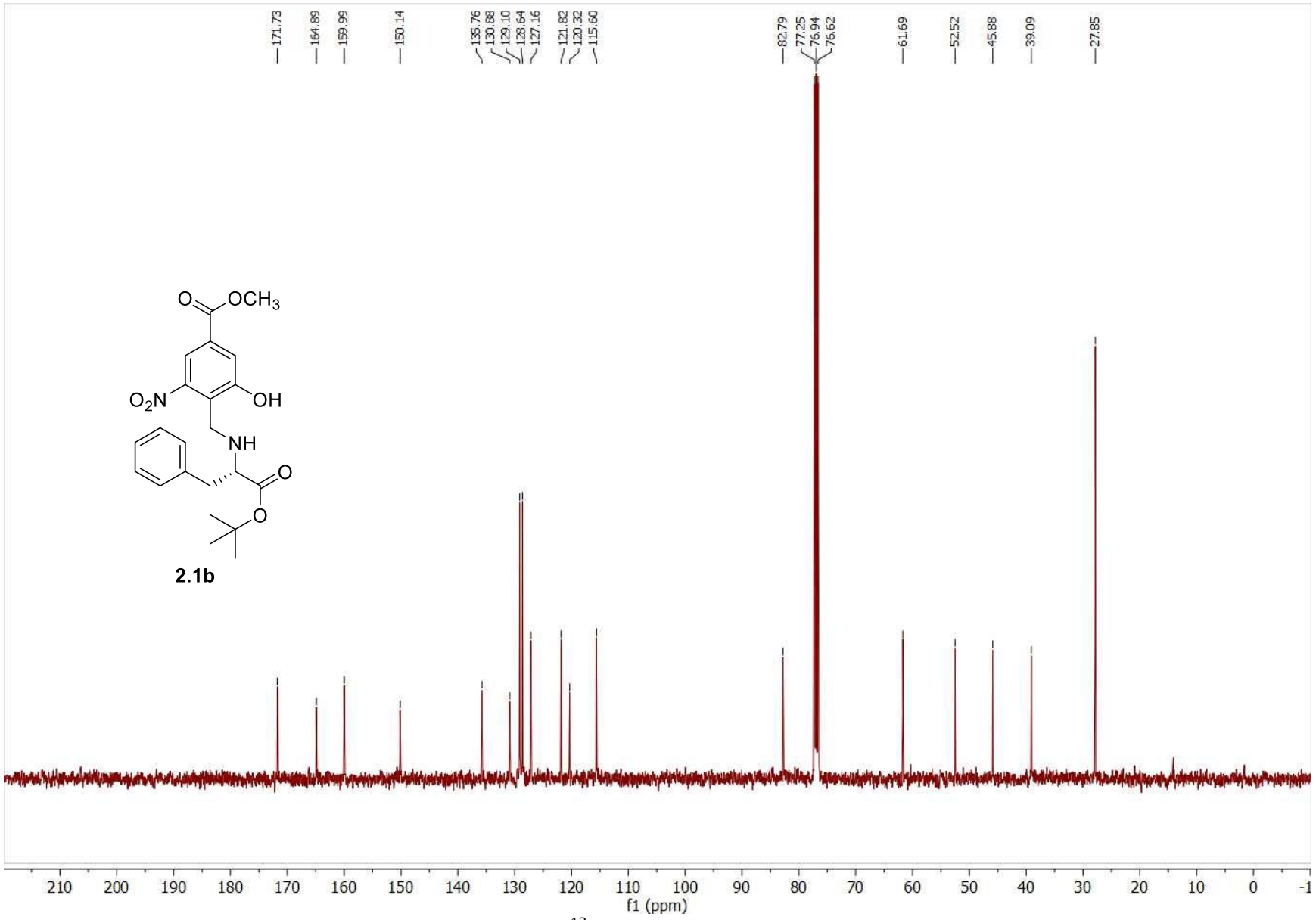

Figure B8: ^{13}C NMR of compound **2.1b**.

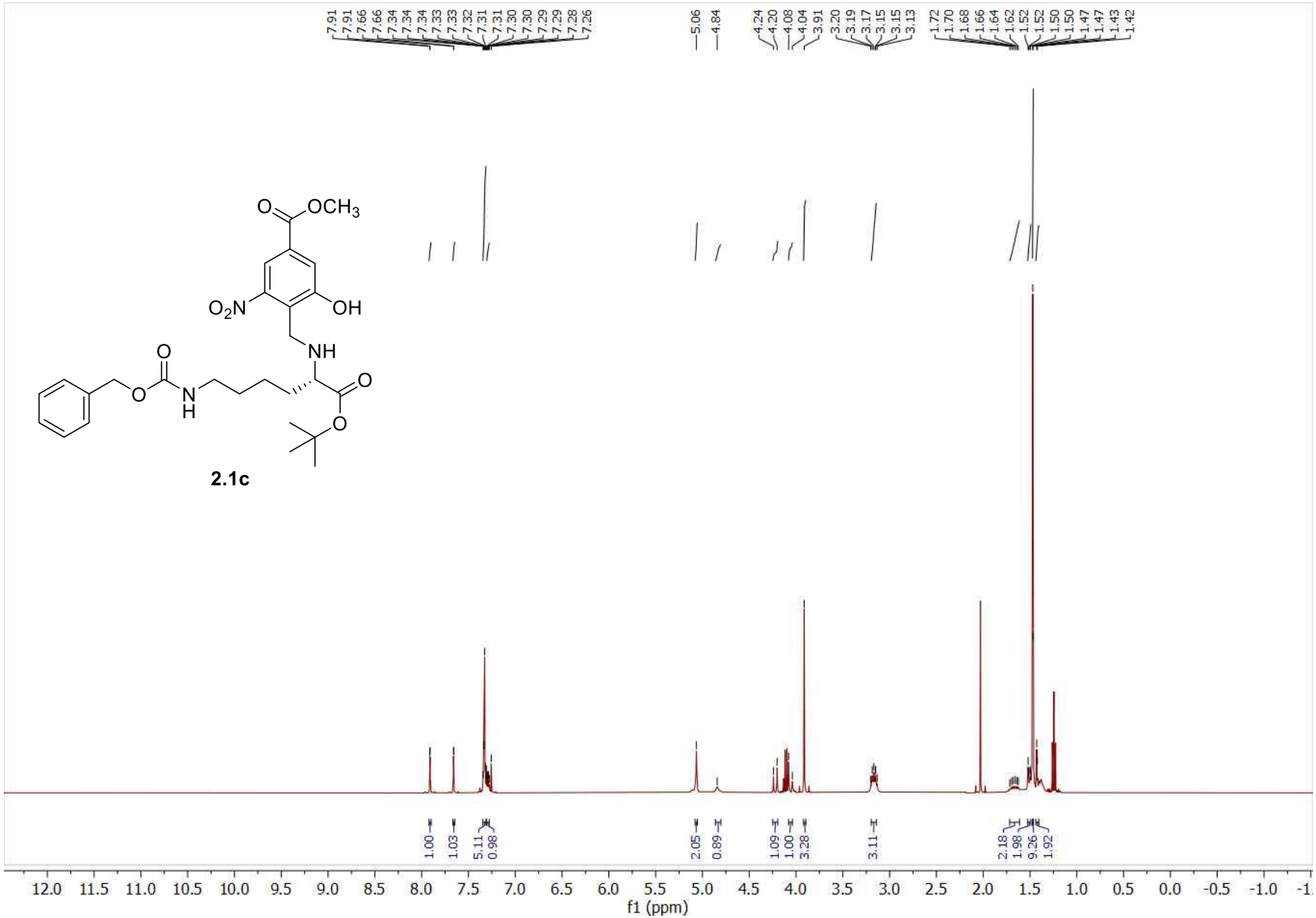

Figure B9: ^{1}H NMR of compound **2.1c**.

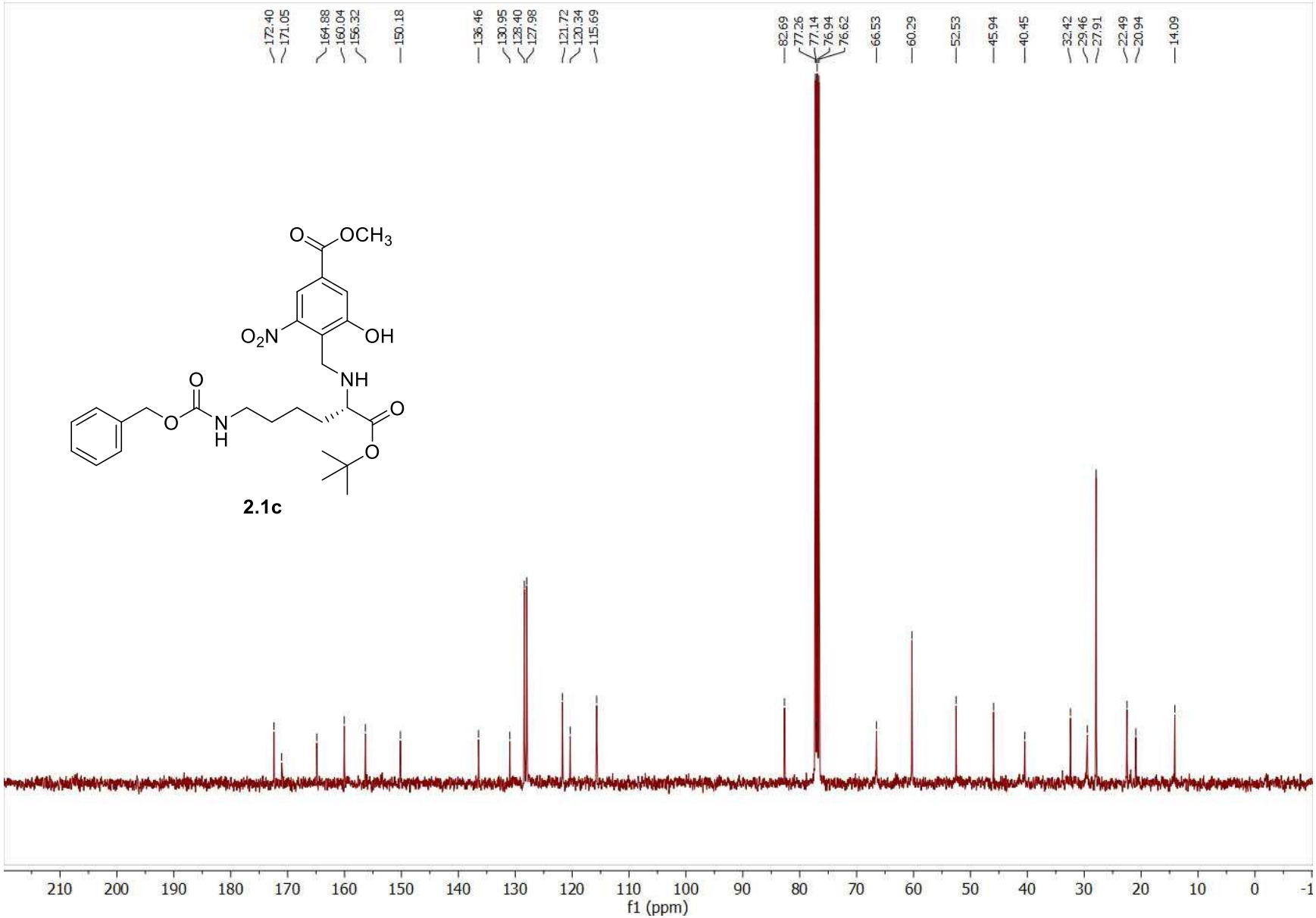

Figure B10: ^{13}C NMR of compound **2.1c**.

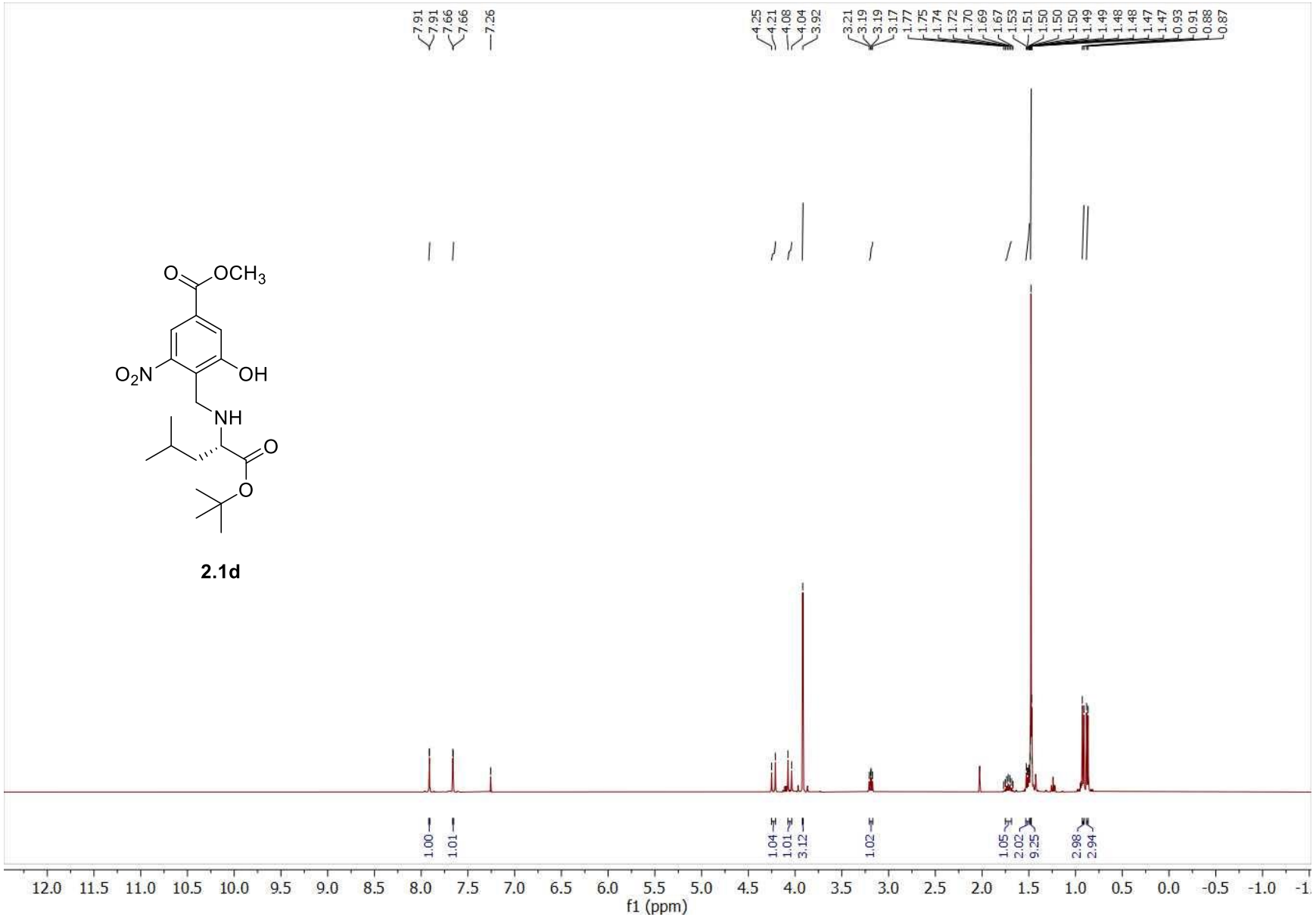

Figure B11: ^{1}H NMR of compound **2.1d**.

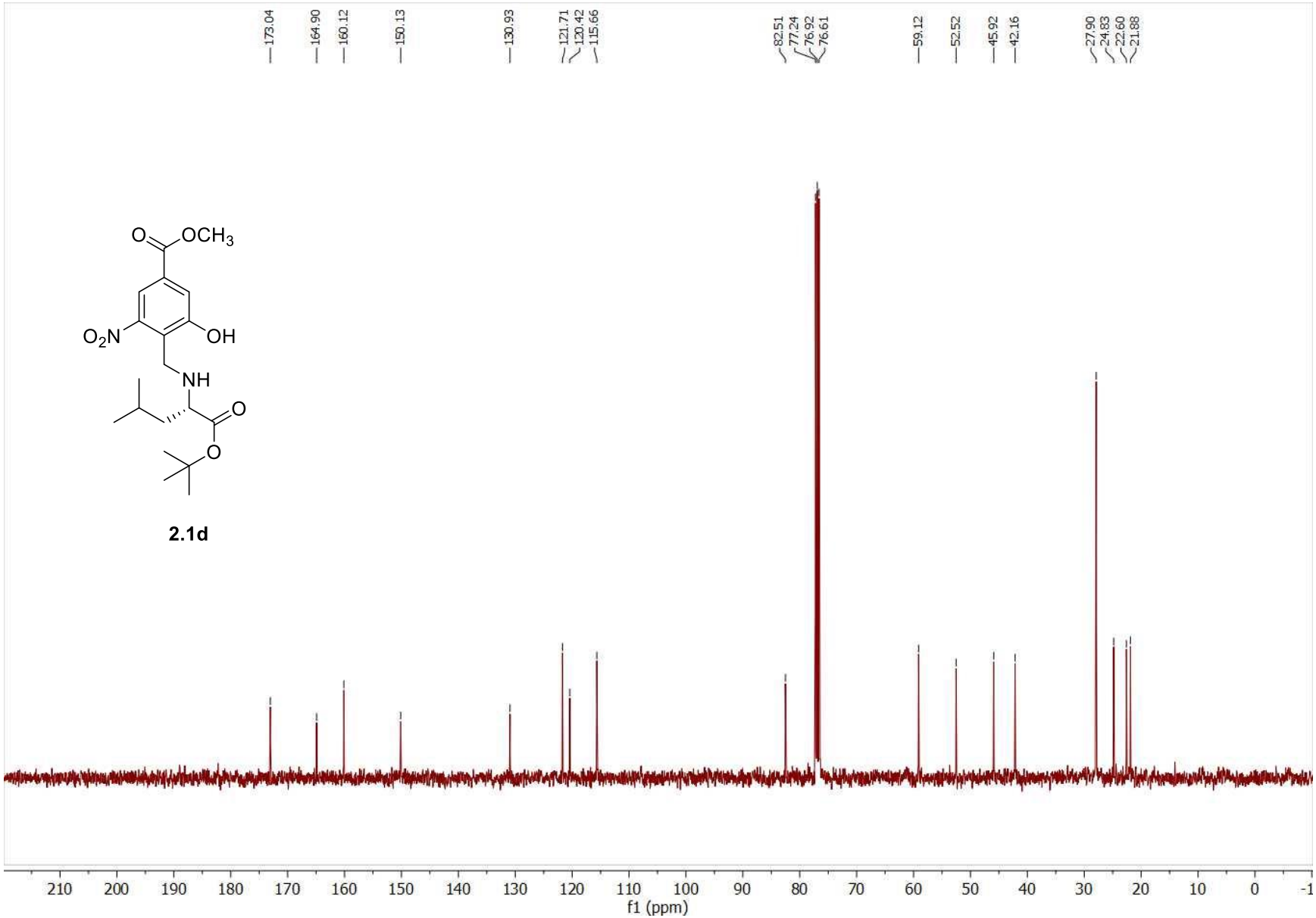

Figure B12: ^{13}C NMR of compound **2.1d**.

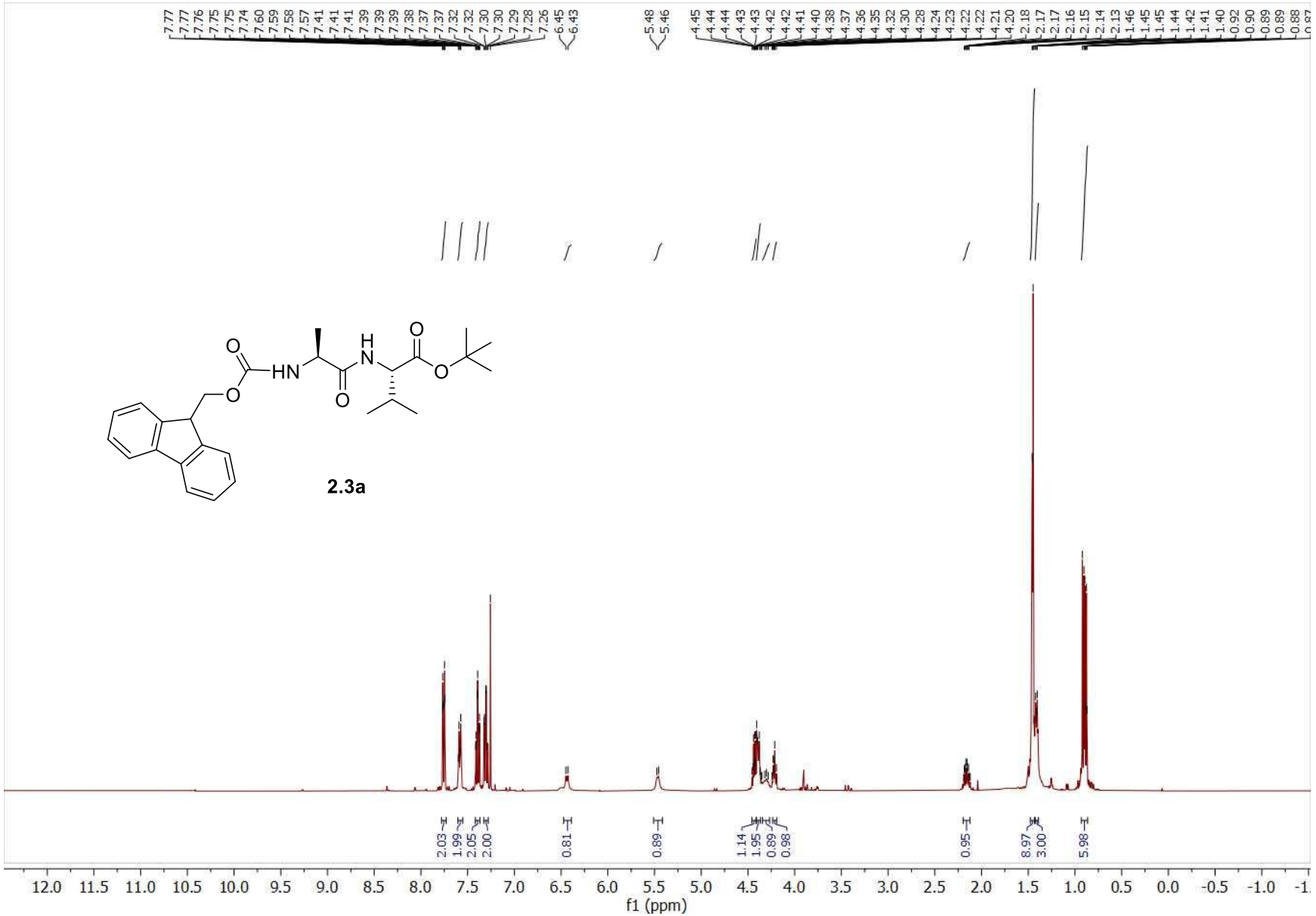

Figure B13: ^{1}H NMR of compound **2.3a**.

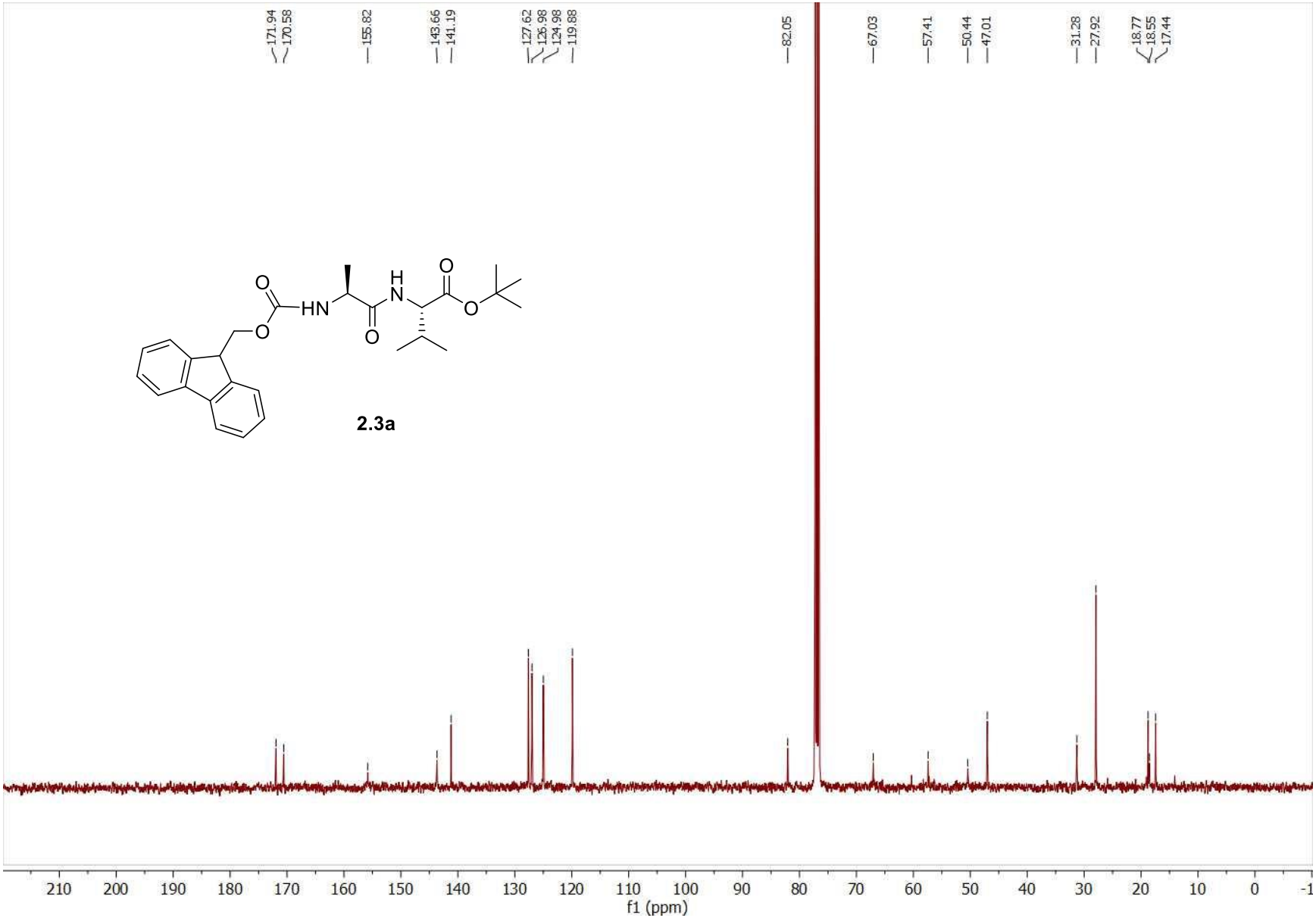

Figure B14: ^{13}C NMR of compound **2.3a**.

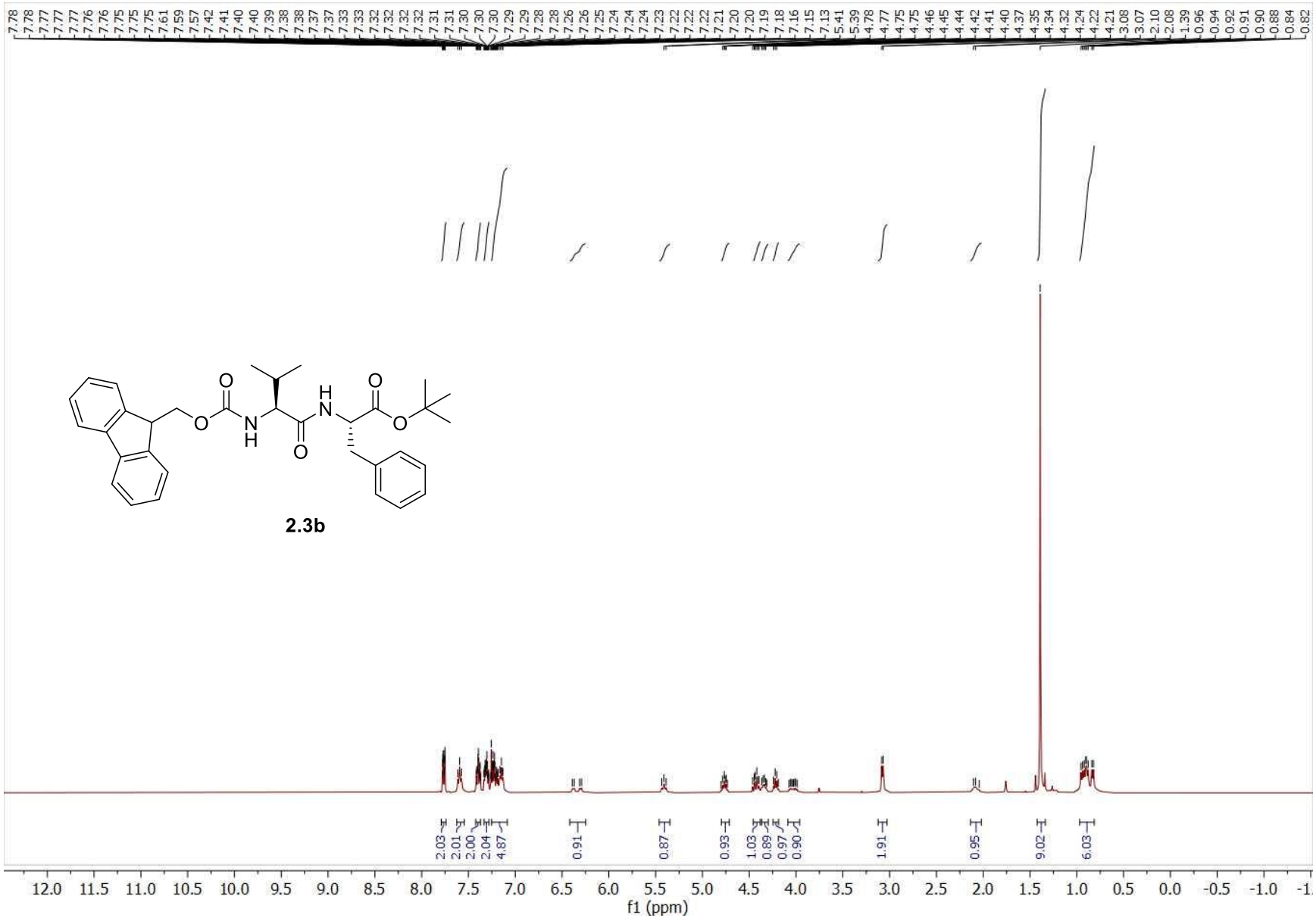

Figure B15: ^{1}H NMR of compound **2.3b**.

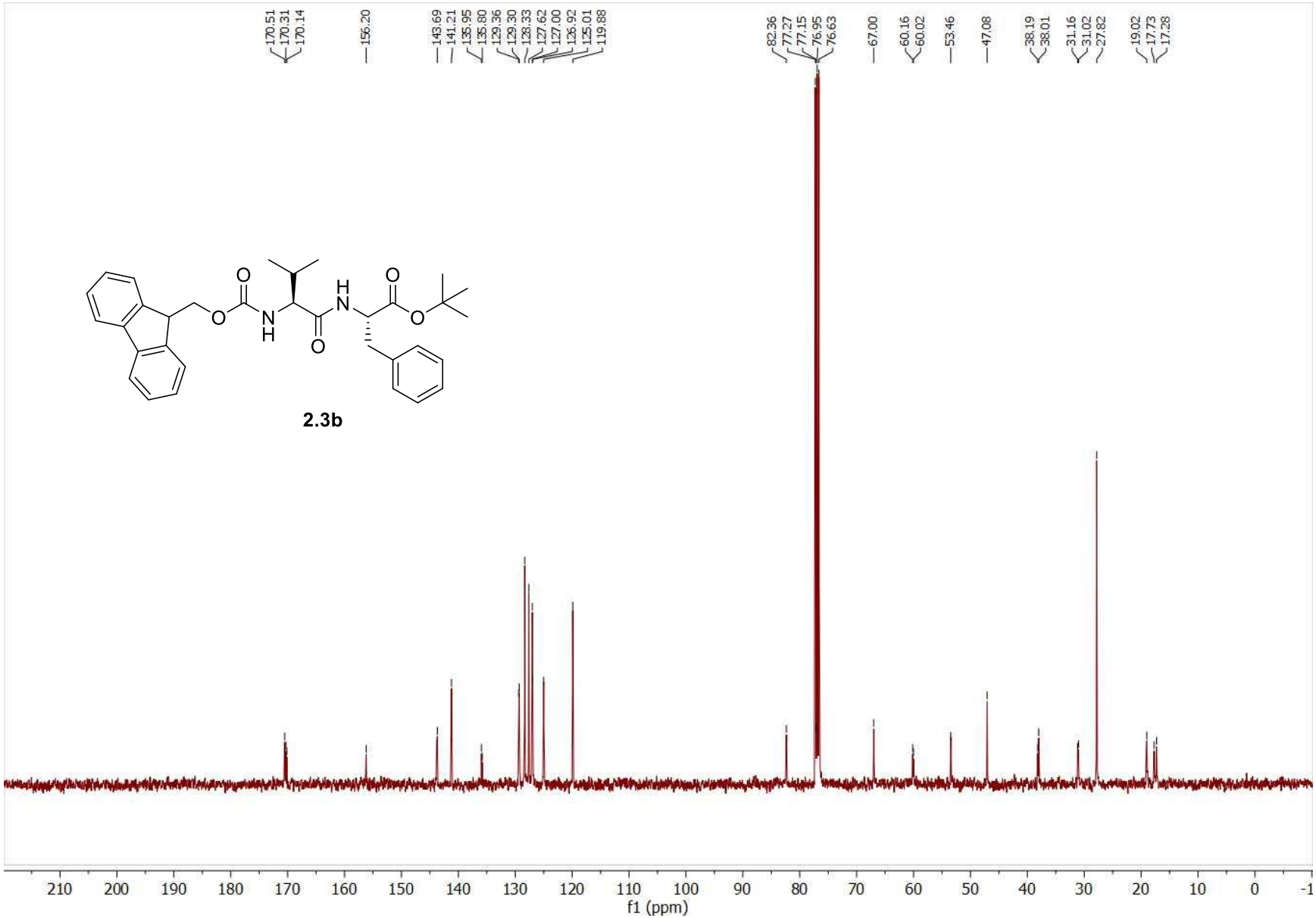

Figure B16: ^{13}C NMR of compound **2.3b**.

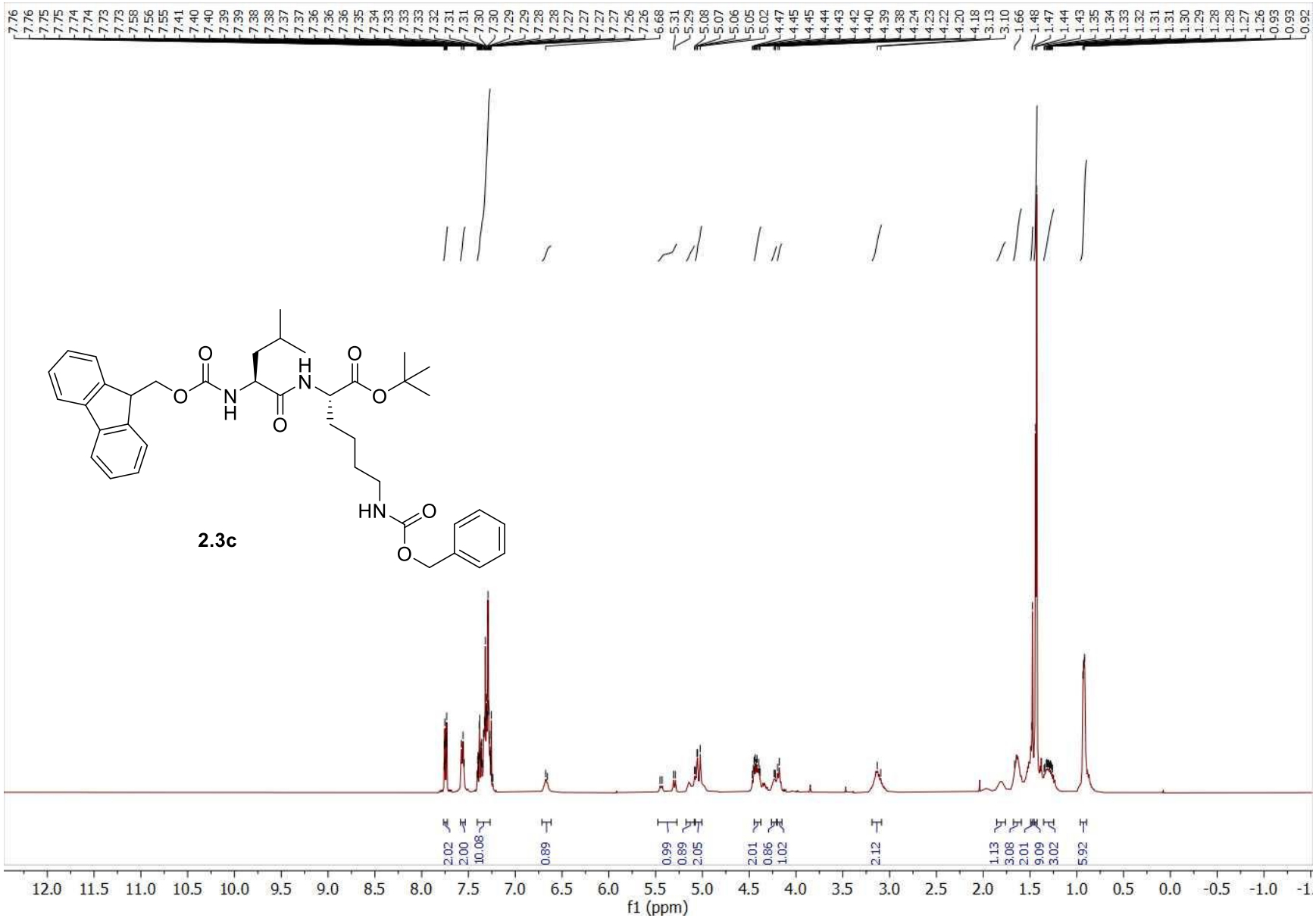

Figure B17: ^{1}H NMR of compound **2.3c**.

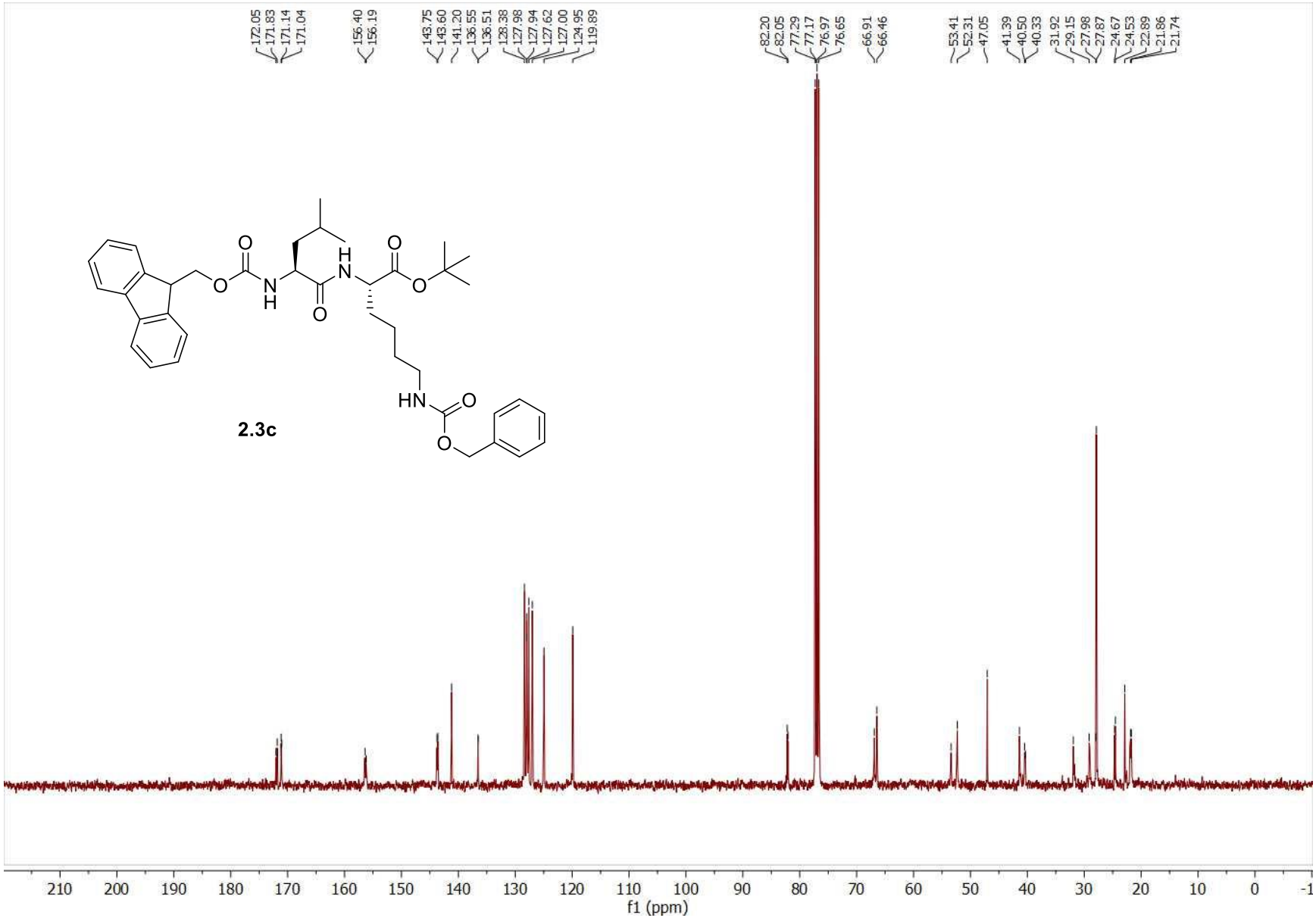

Figure B18: ^{13}C NMR of compound **2.3c**.

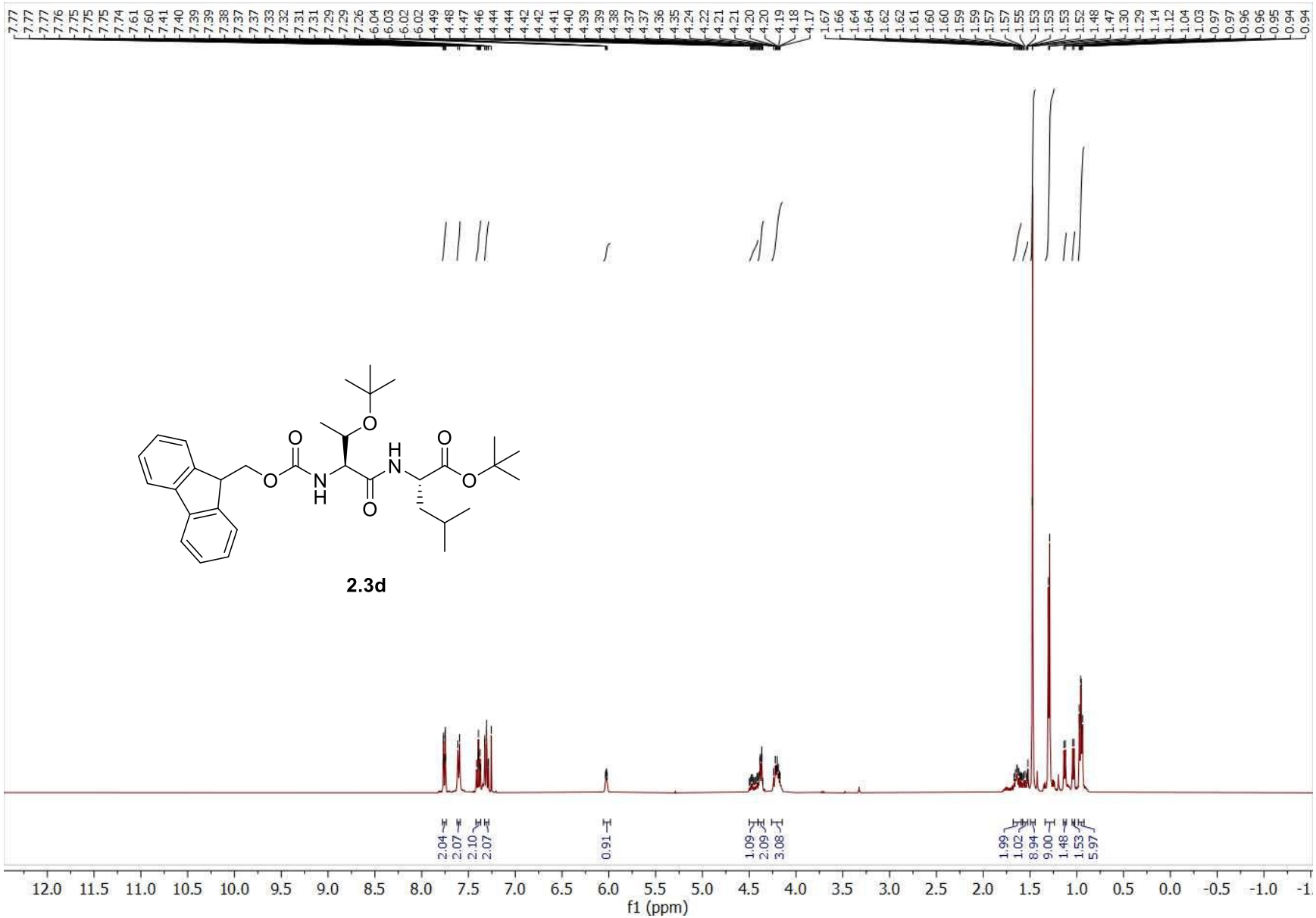

Figure B19: ^{1}H NMR of compound **2.3d**.

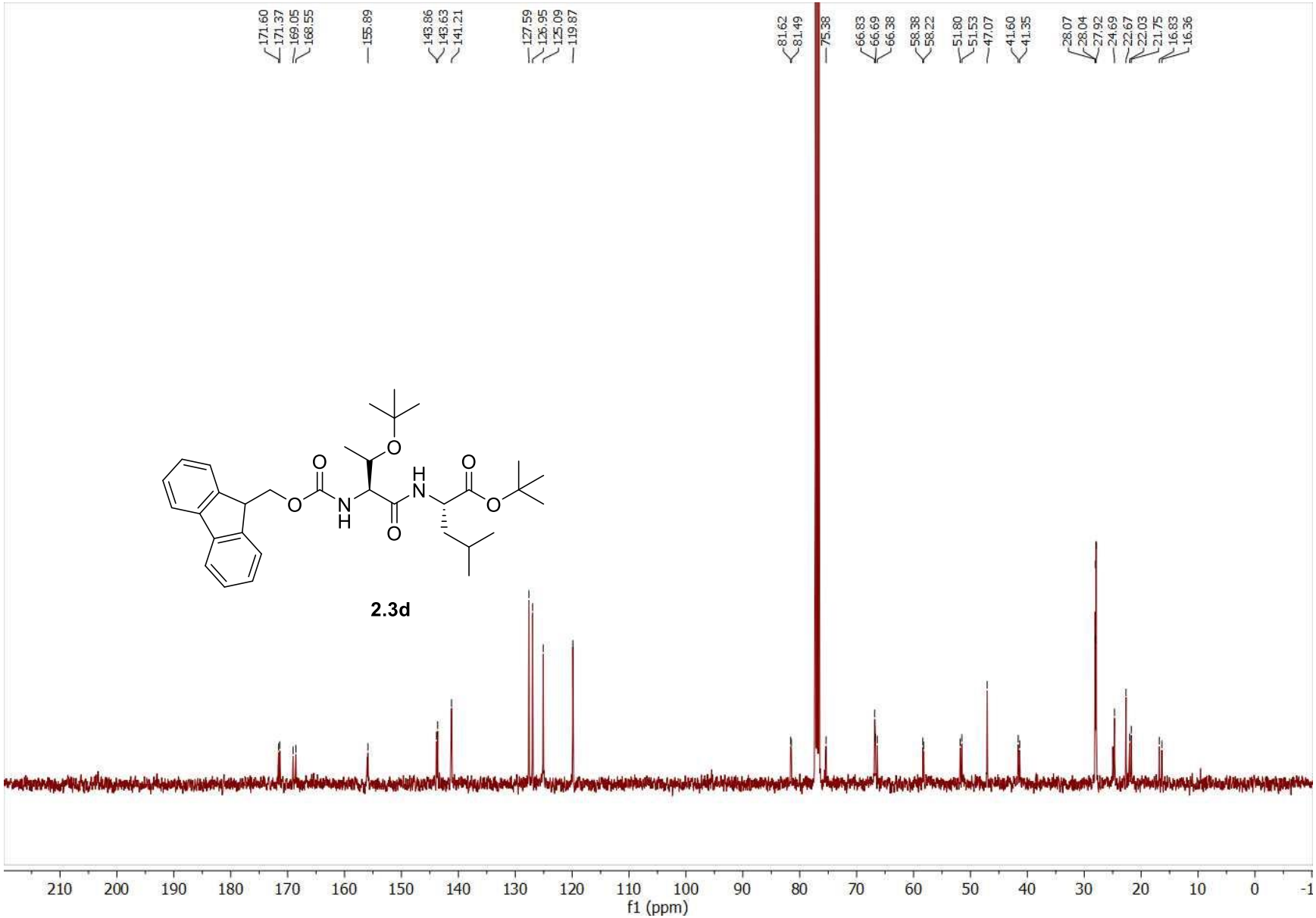

Figure B20: ^{13}C NMR of compound **2.3d**.

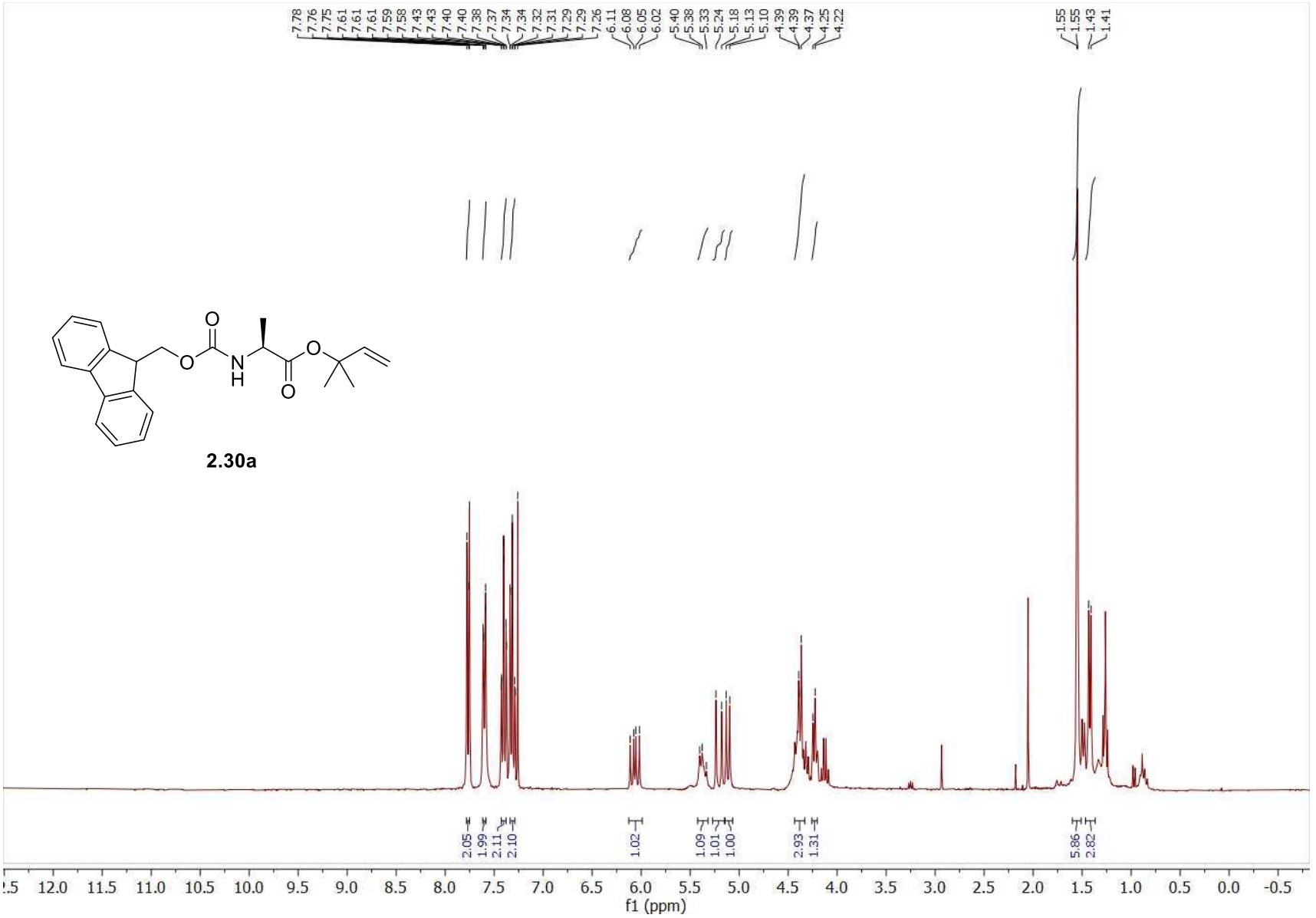

Figure B21: ^{1}H NMR of compound **2.3a**

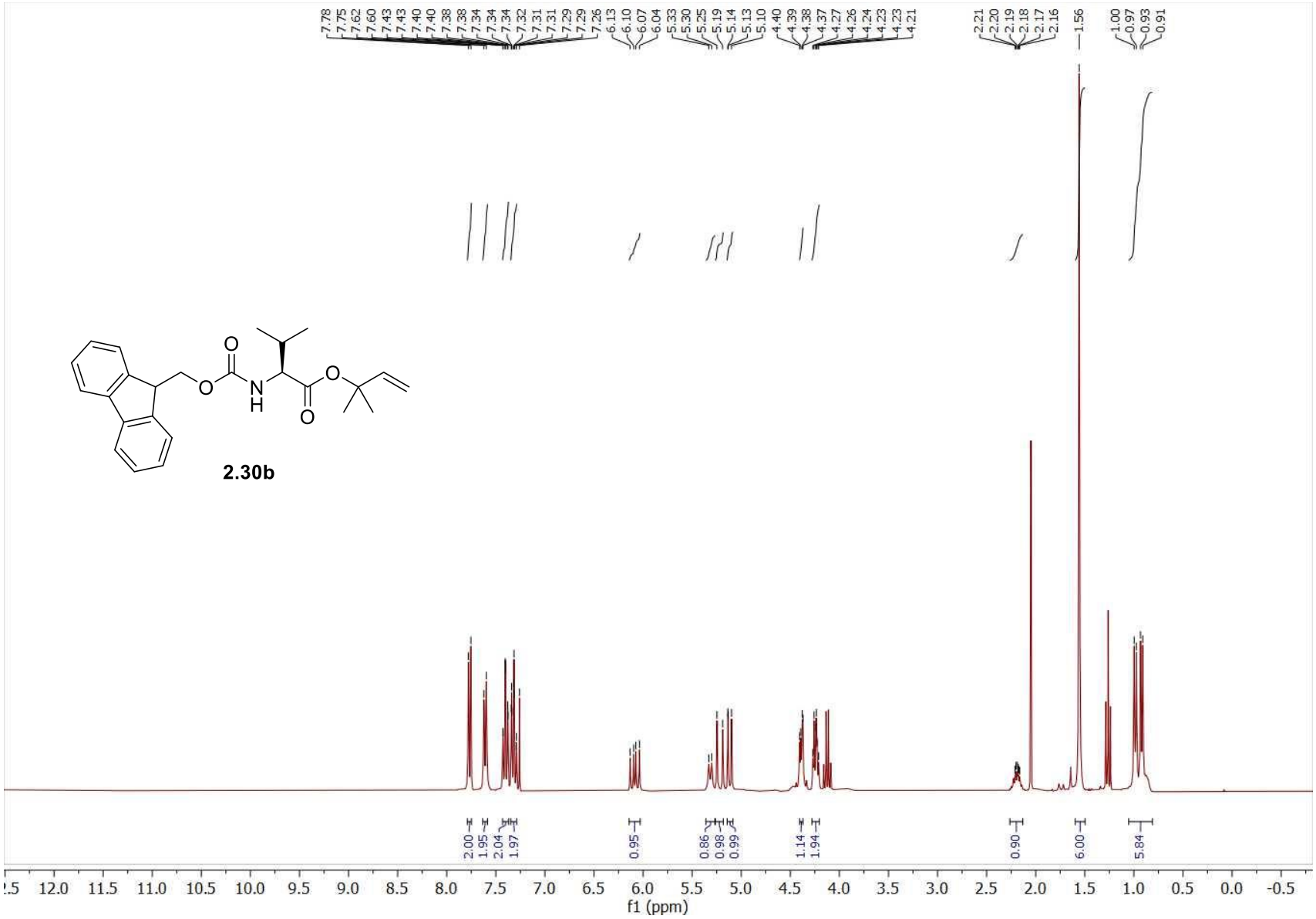

Figure B22: ^{1}H NMR of compound **2.30b**

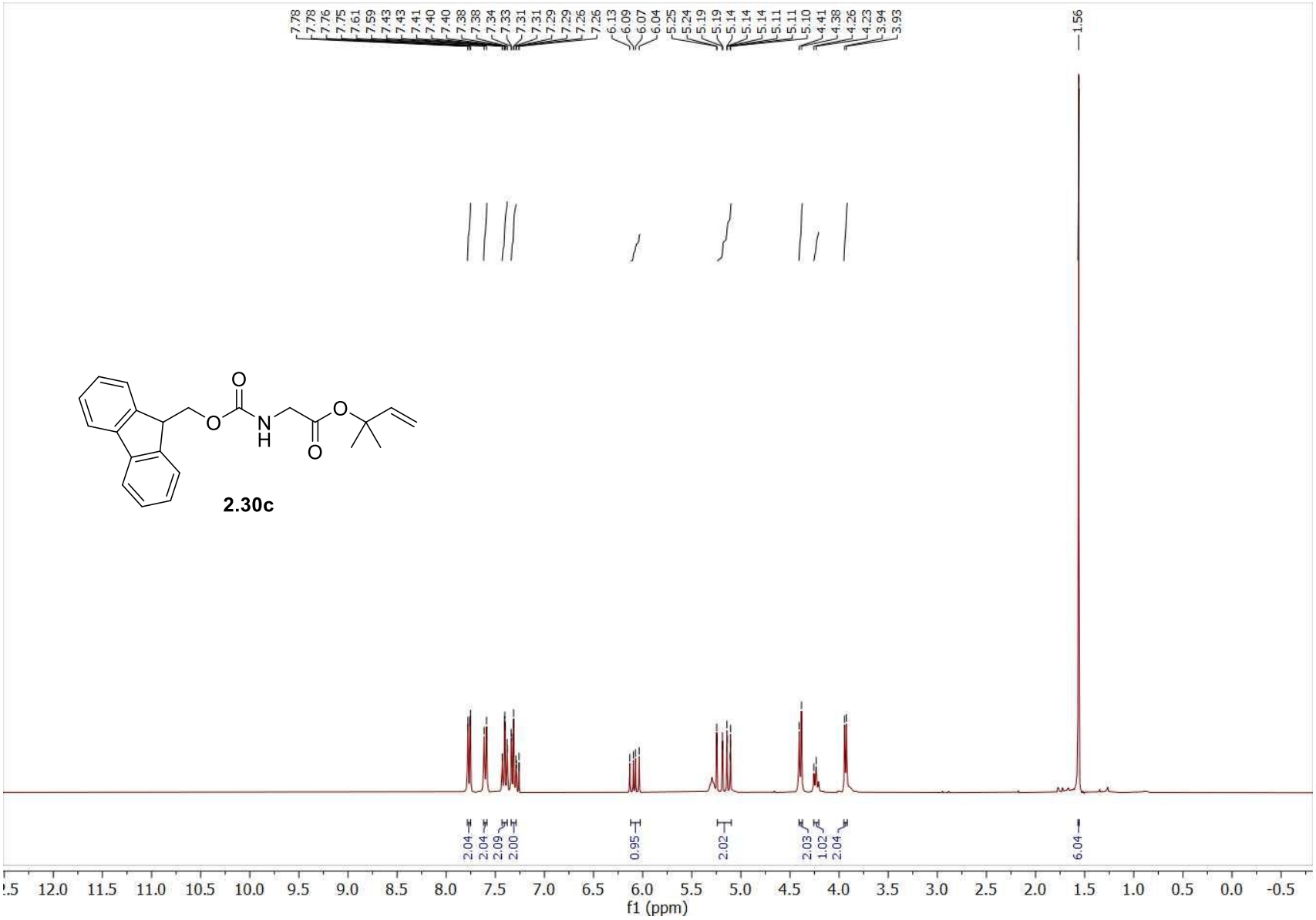

Figure B23: ^{1}H NMR of compound **2.30c**

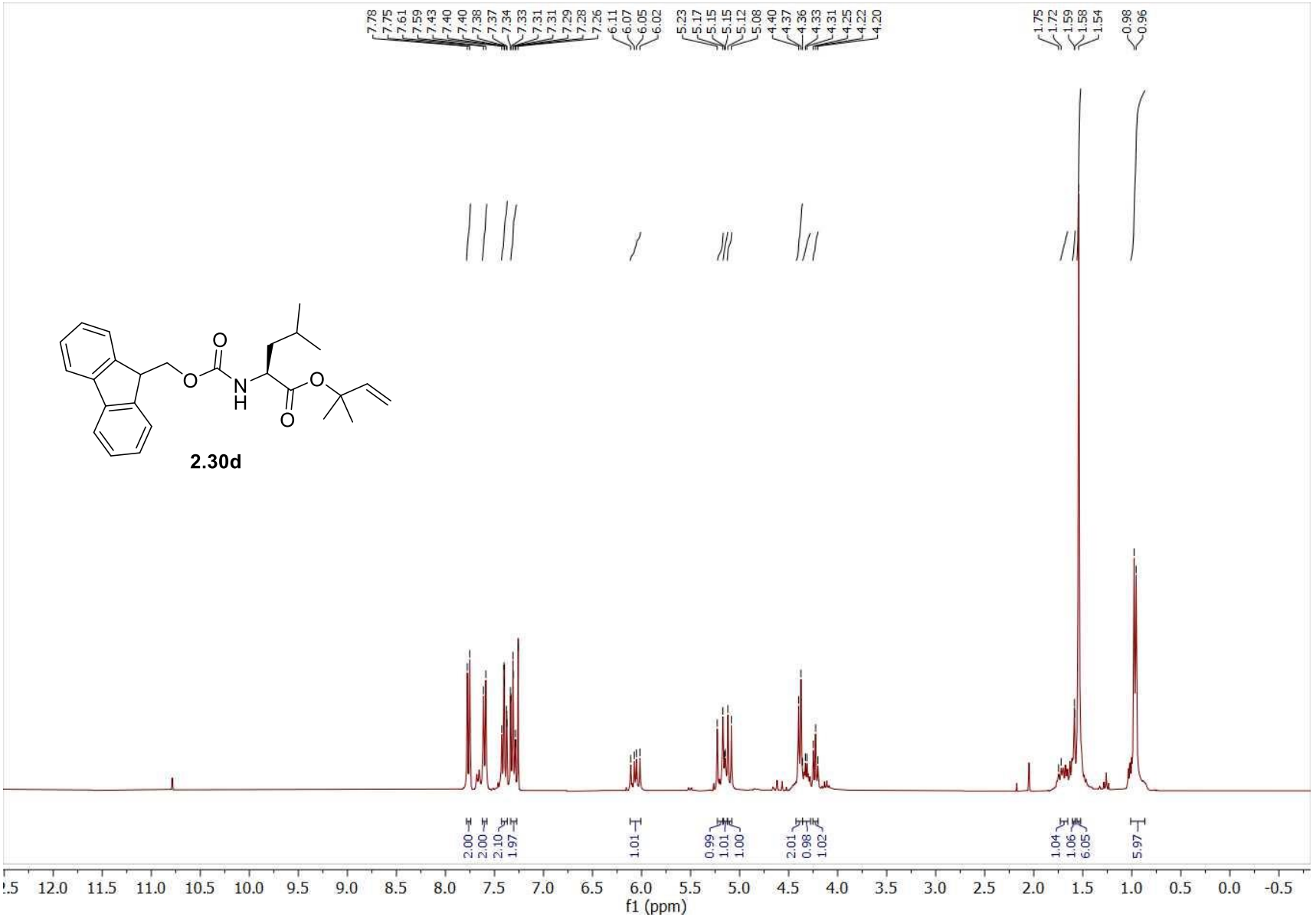

Figure B24: ^{1}H NMR of compound **2.30d**

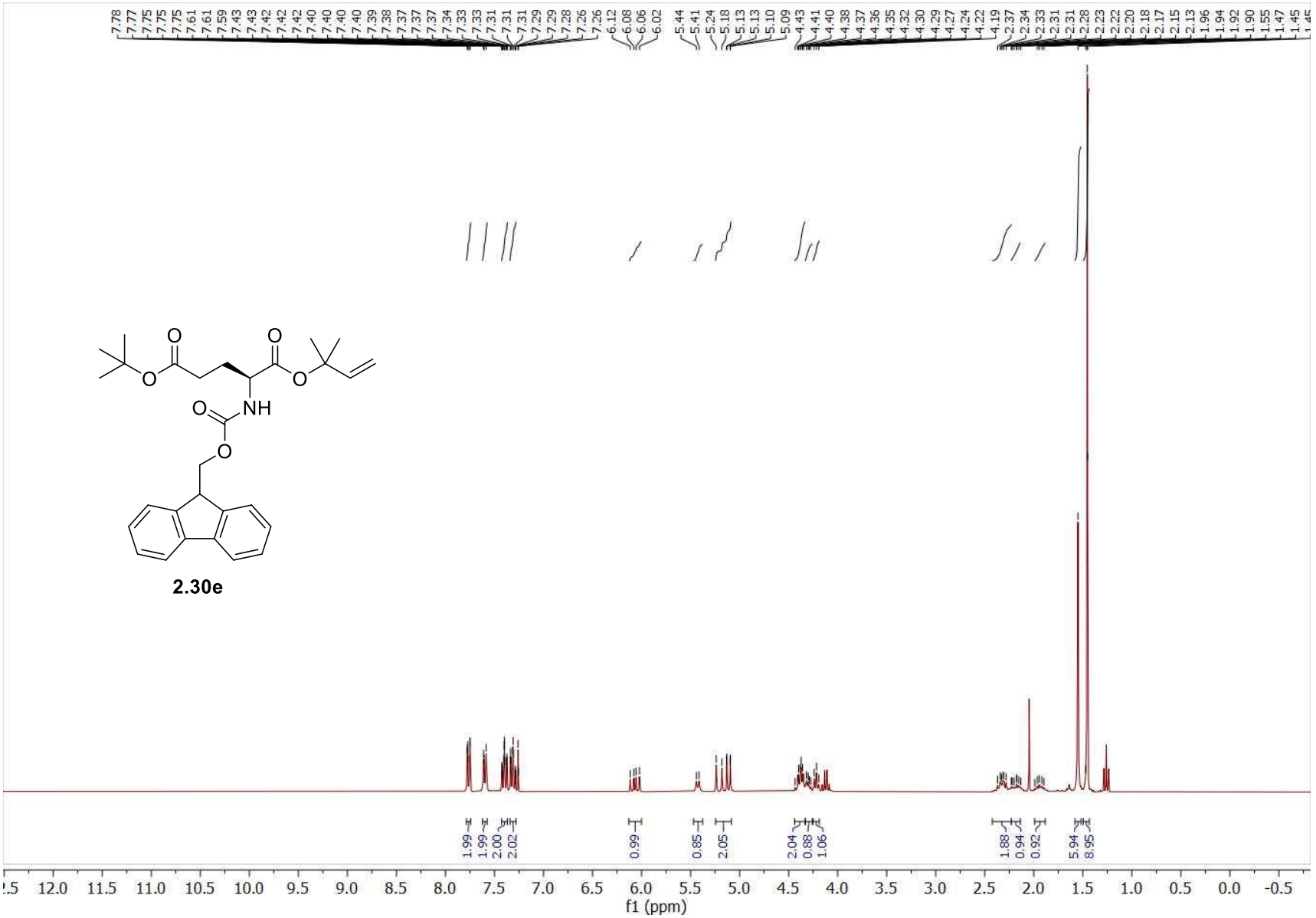

Figure B25: ^{1}H NMR of compound **2.30e**

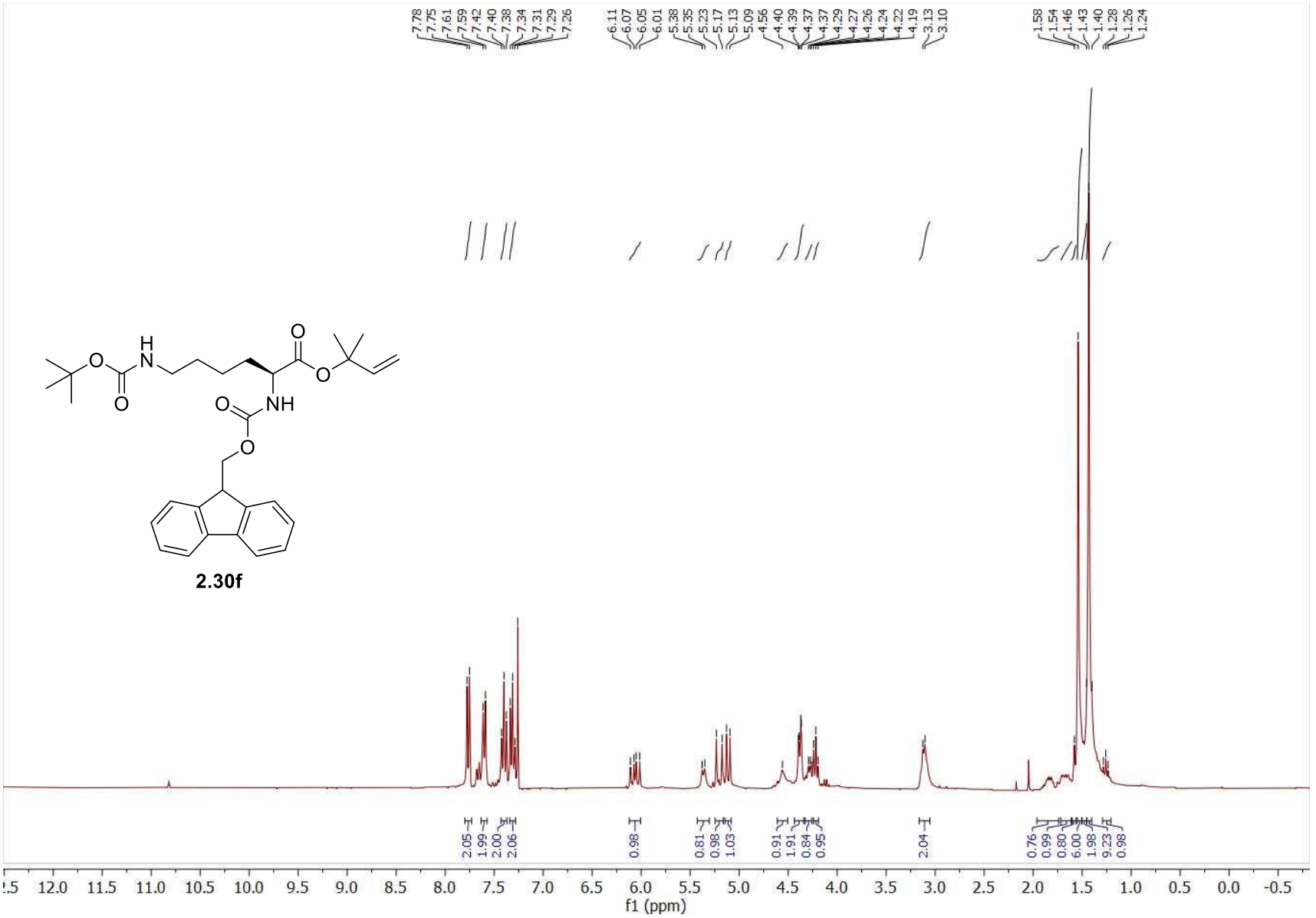

Figure B26: ^{1}H NMR of compound **2.30f**

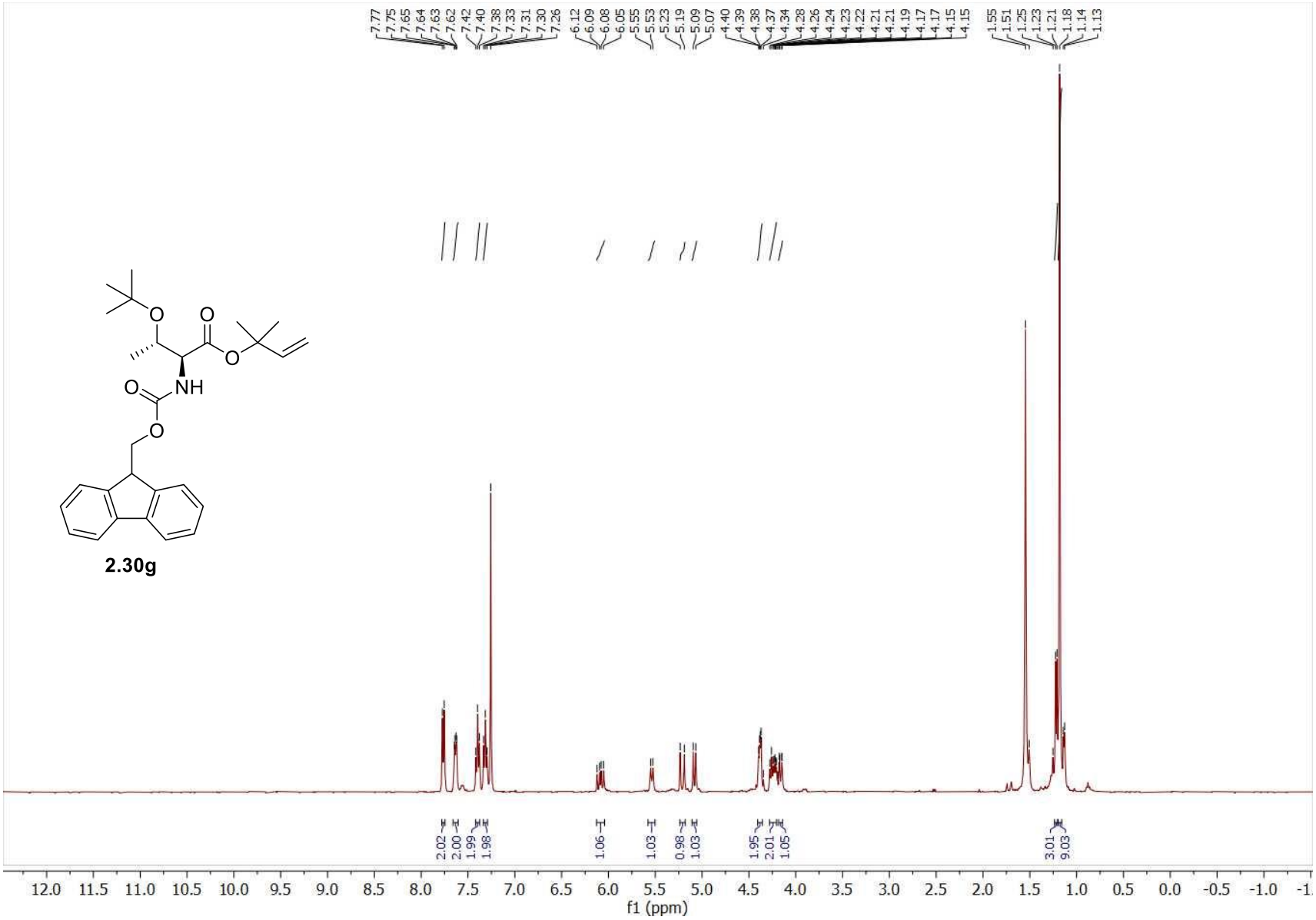

Figure B27: ^{1}H NMR of compound **2.30g**

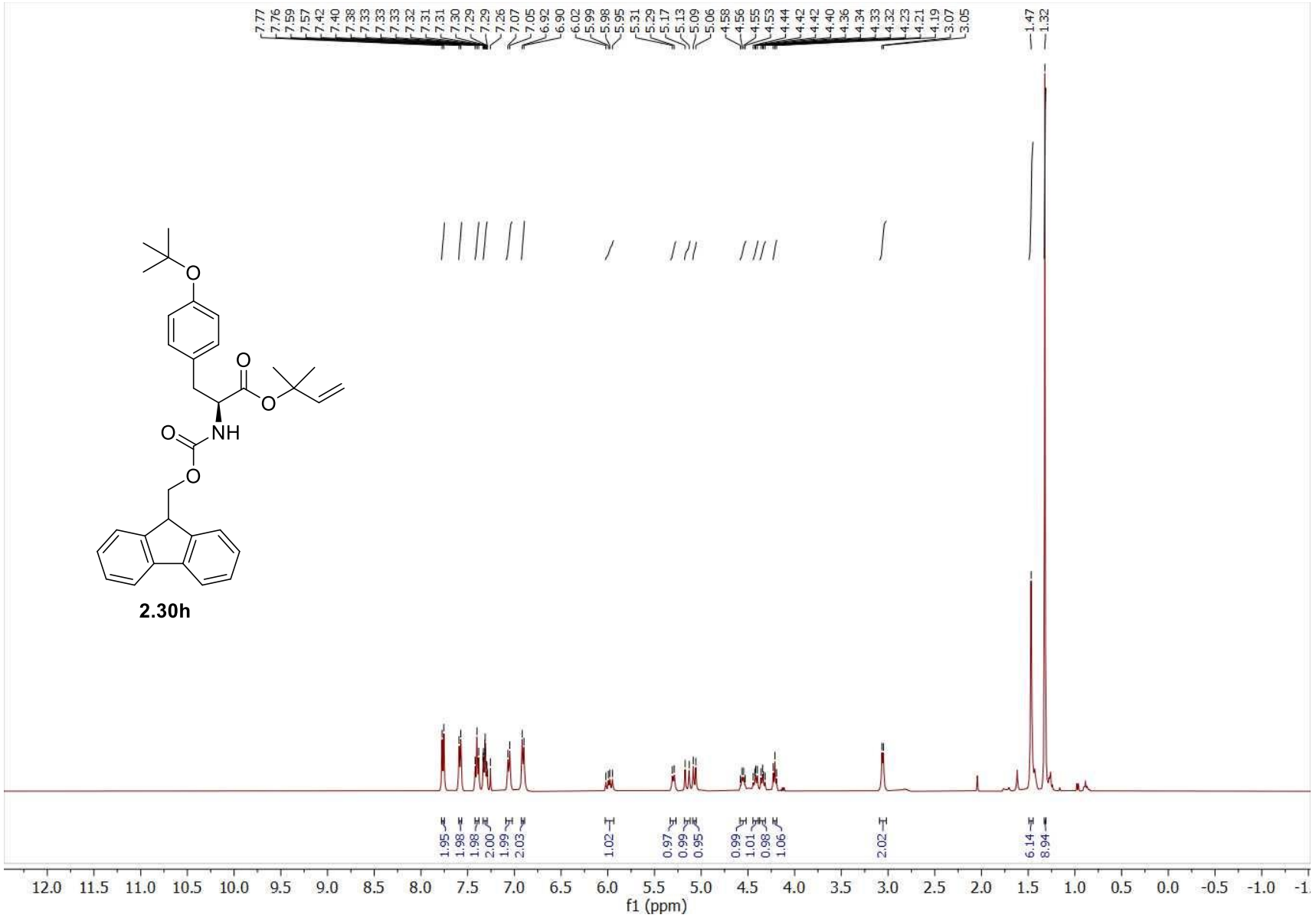

Figure B28: ^{1}H NMR of compound **2.30h**

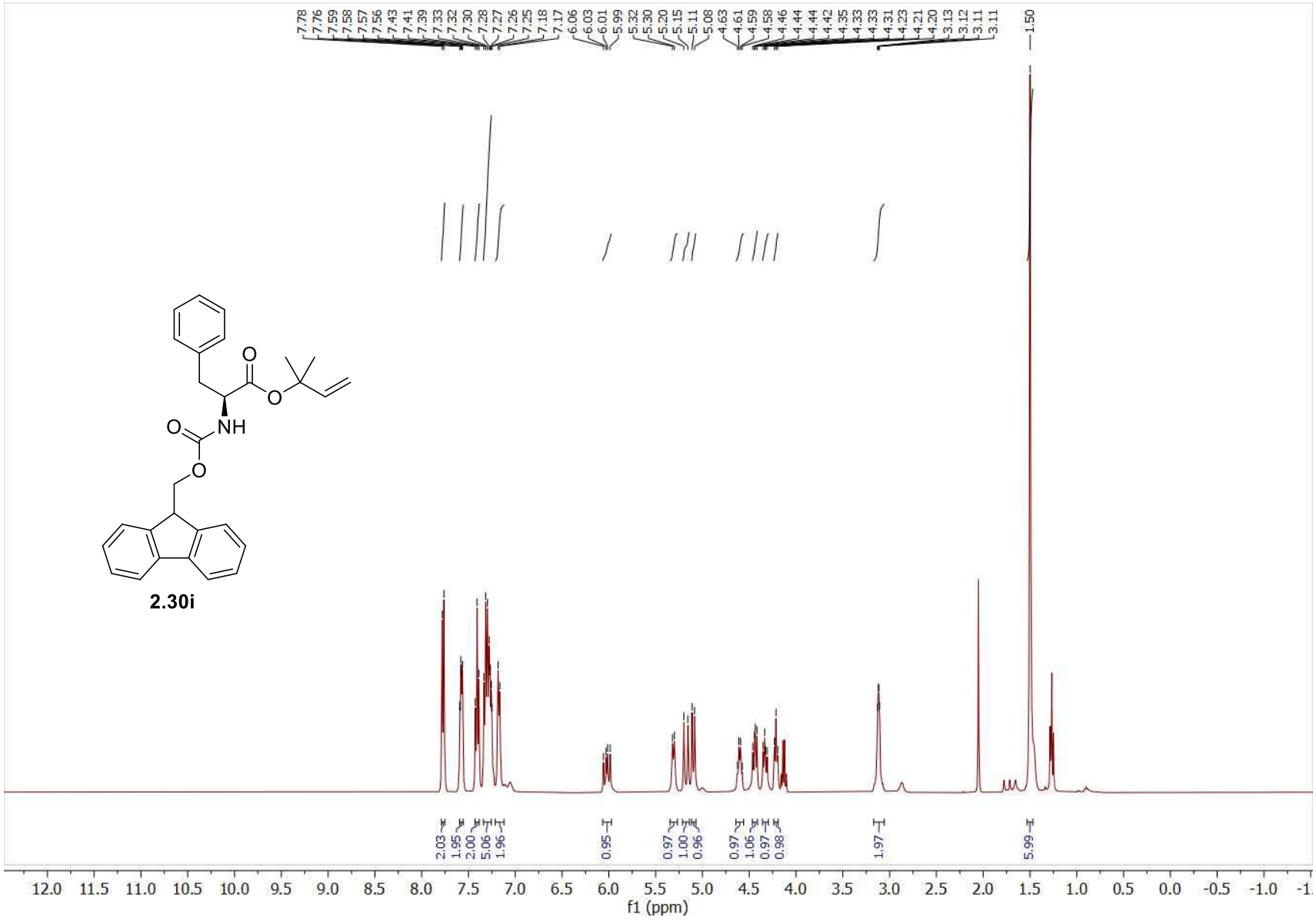

Figure B29: ^{1}H NMR of compound **2.30i**

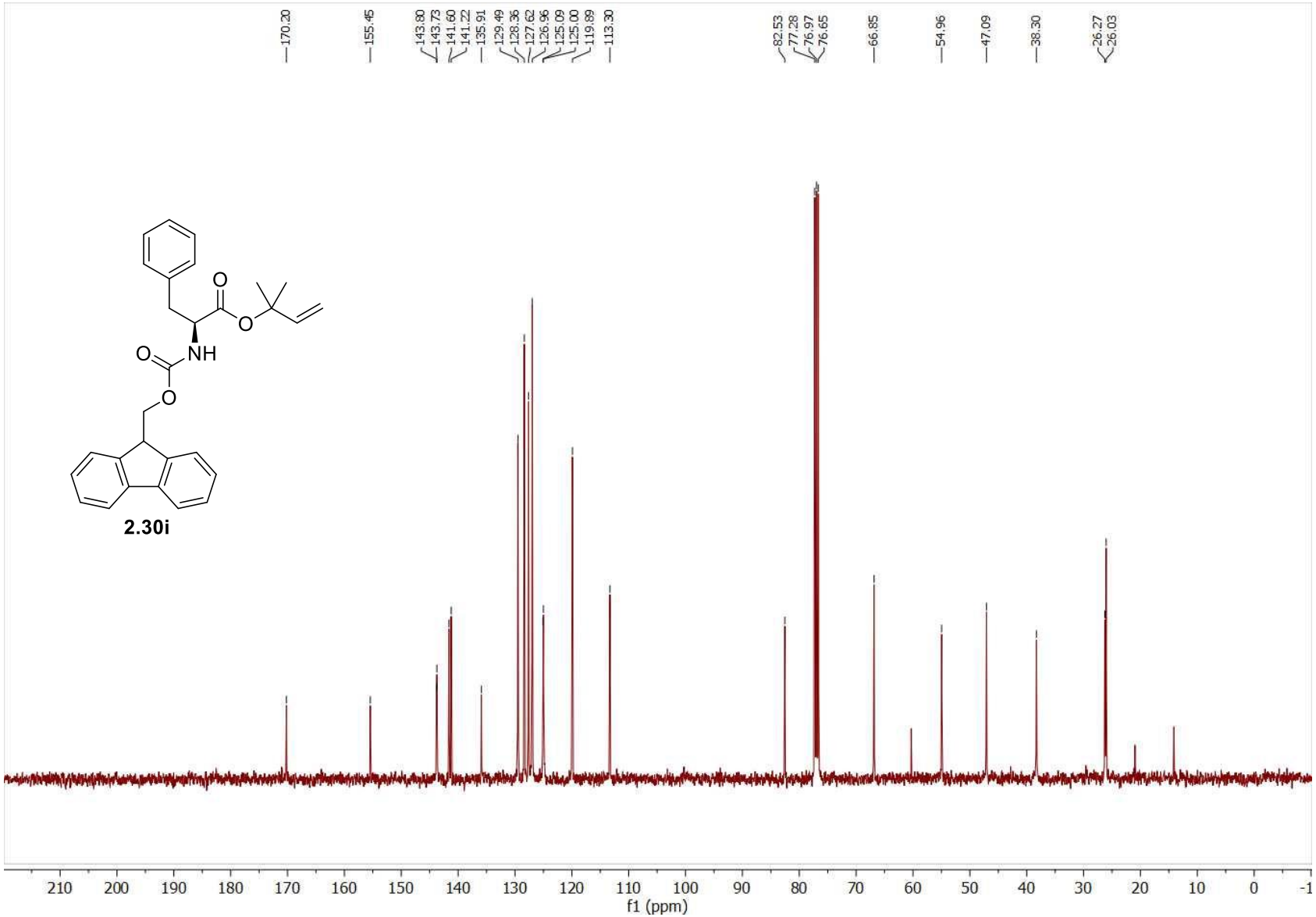

Figure B30: ^{13}C NMR of compound **2.30i**

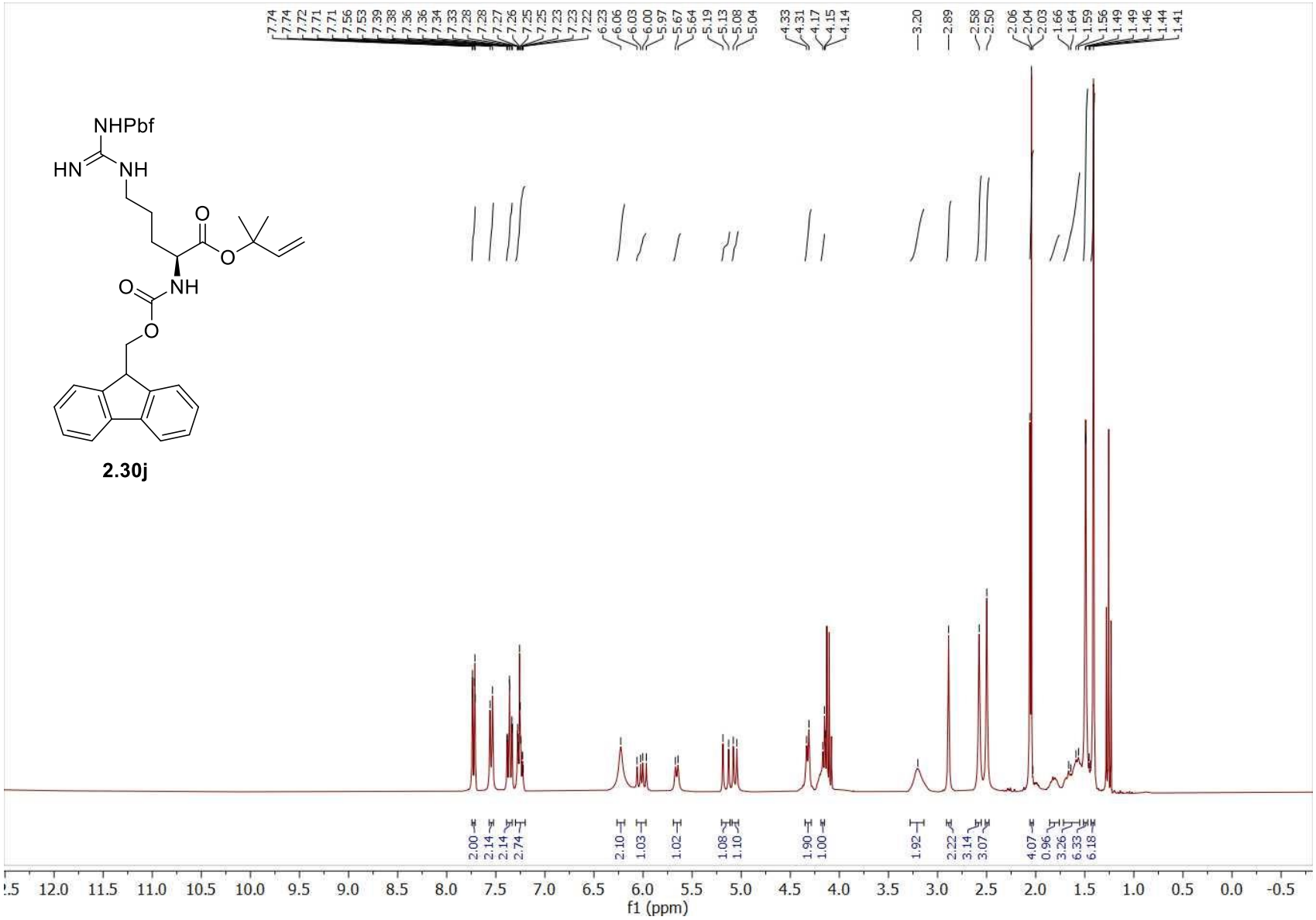

Figure B31: ^{1}H NMR of compound **2.30j**

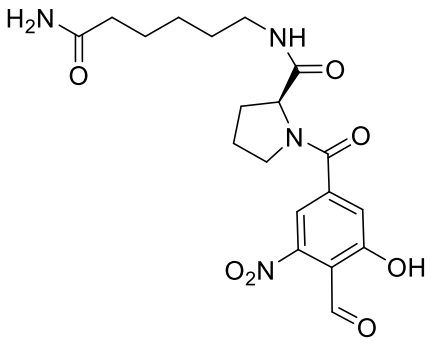

2.13

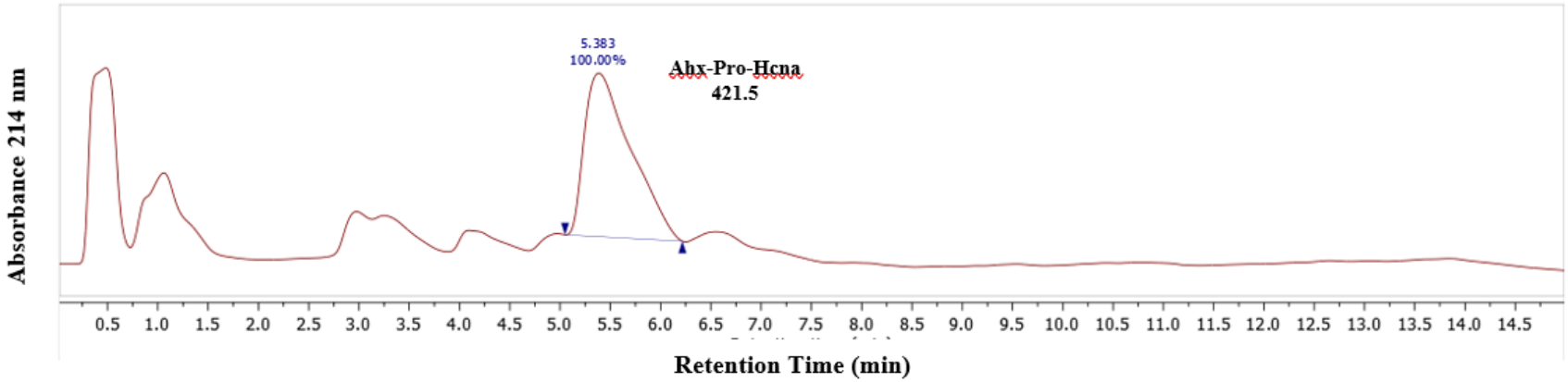

Figure B32: UPLC-MS chromatogram of Ahx-Pro-Hcna (5-30)

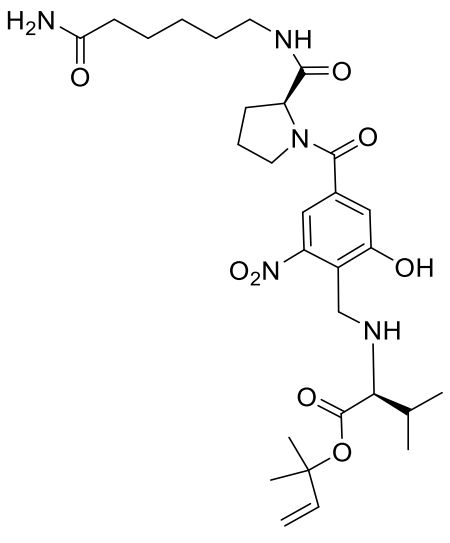

2.5

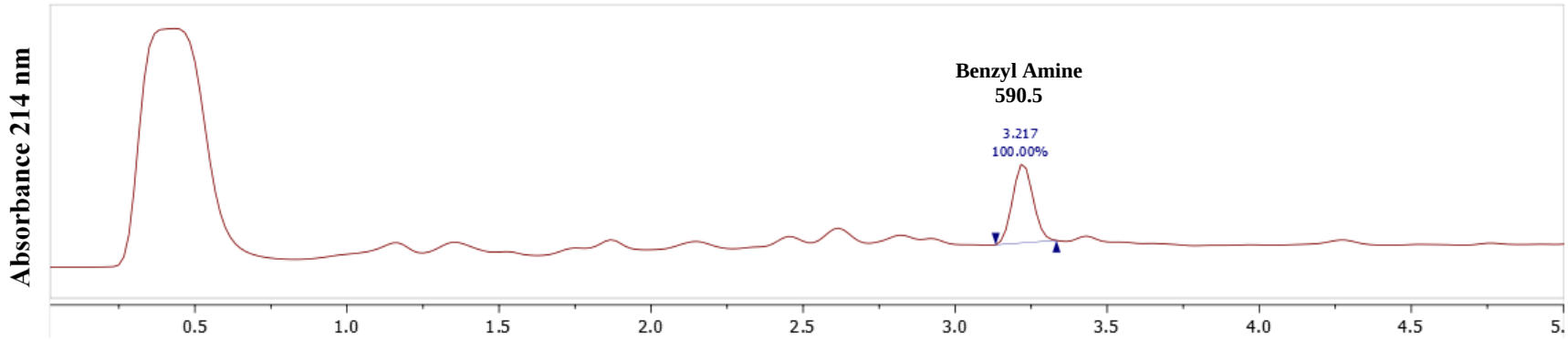

Figure B33: UPLC-MS chromatogram of H-Val-DMA (5-60)

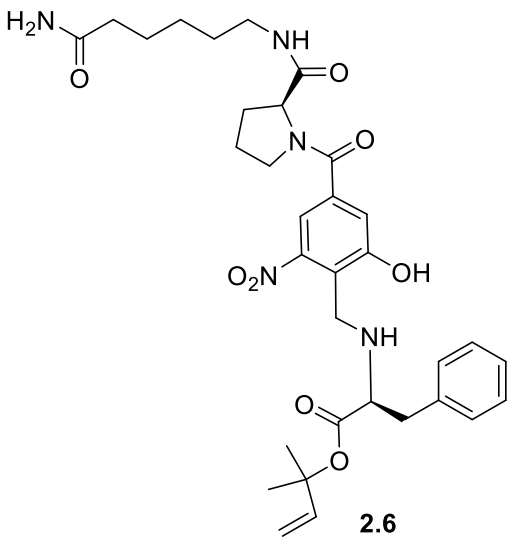

2.6

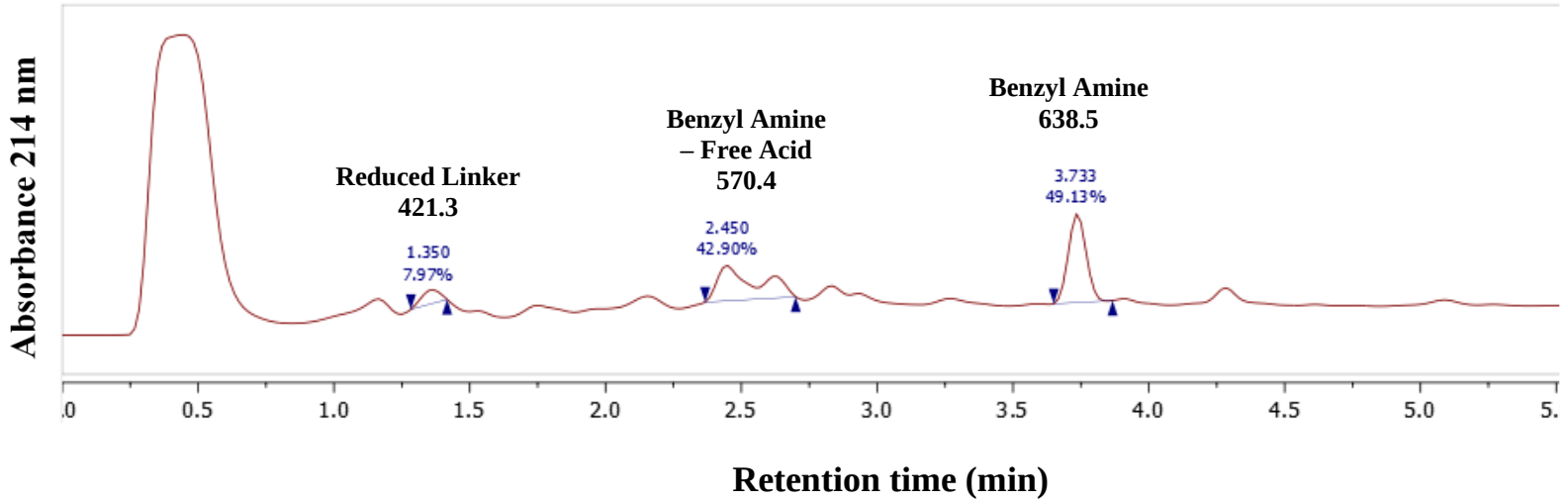

Figure B34: UPLC-MS chromatogram of H-Phe-DMA (5-60)

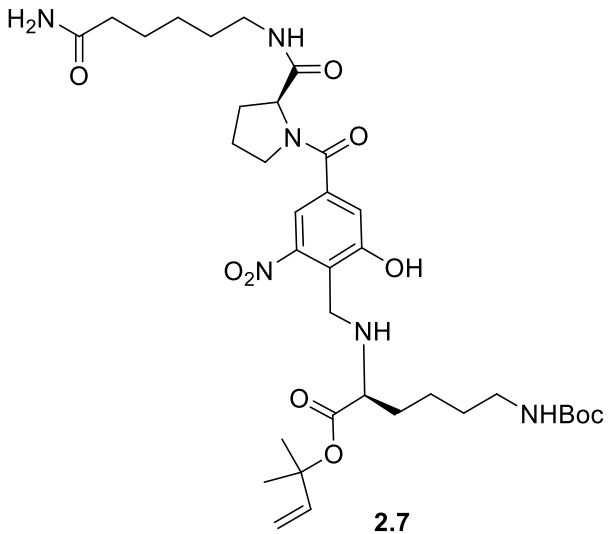

2.7

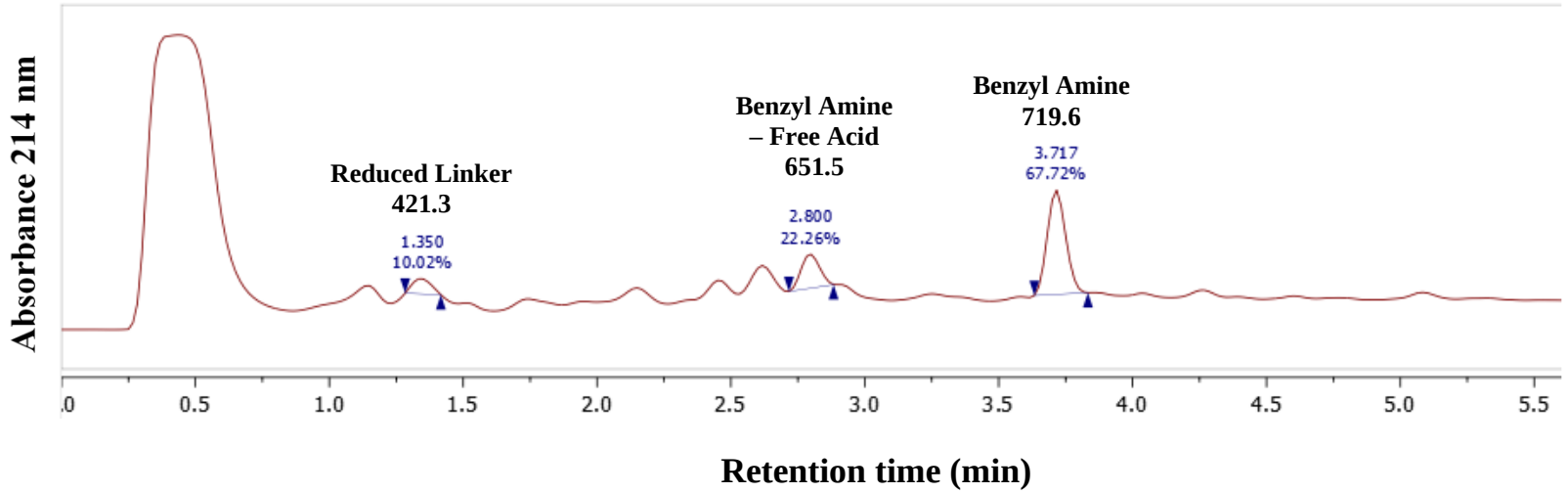

Figure B35: UPLC-MS chromatogram of H-Lys(Boc)-DMA (5-60)

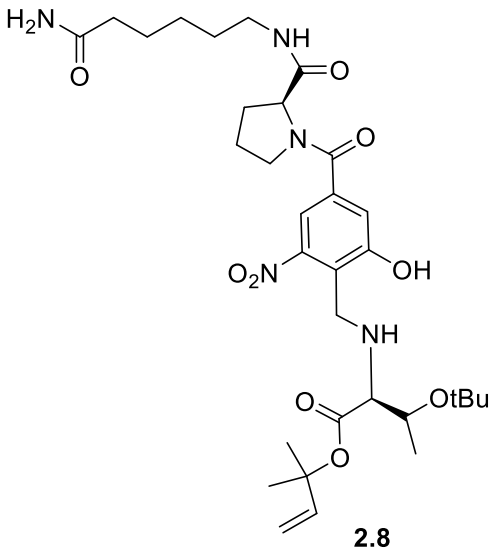

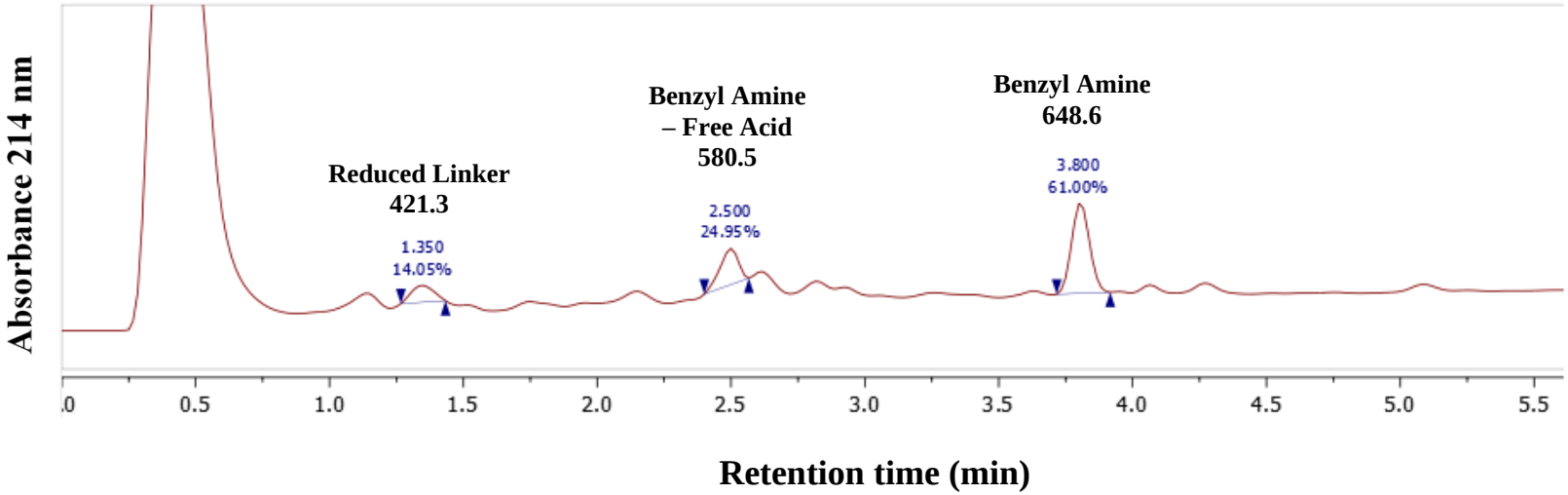

Figure B36: UPLC-MS chromatogram of H-Thr(tBu)-DMA (5-60)

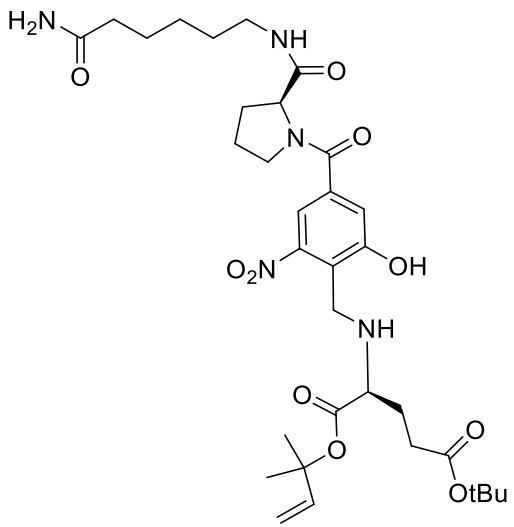

2.9

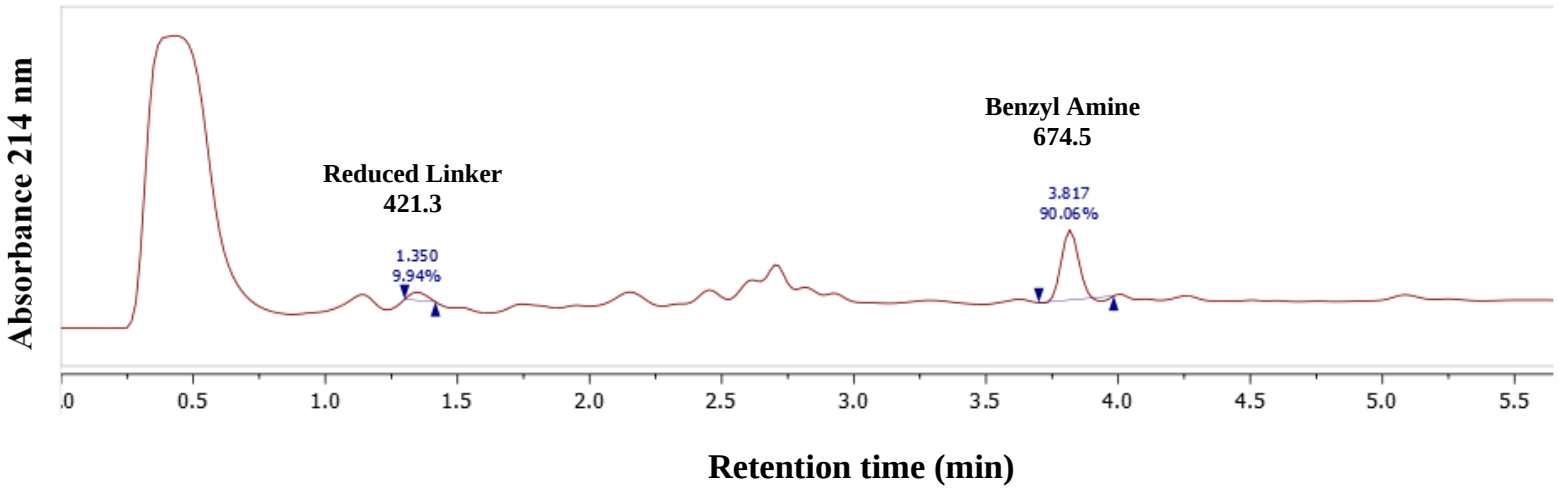

Figure B37: UPLC-MS chromatogram of H-Glu(tBu)-DMA (5-60)

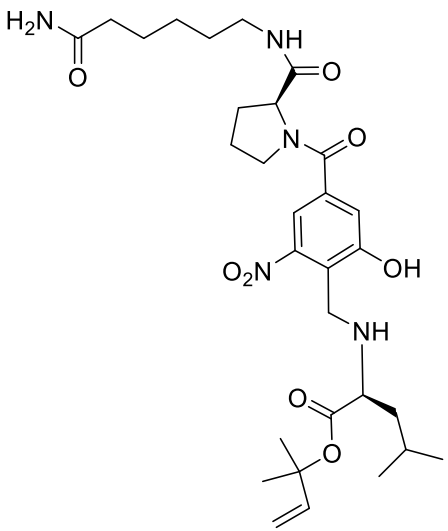

2.10

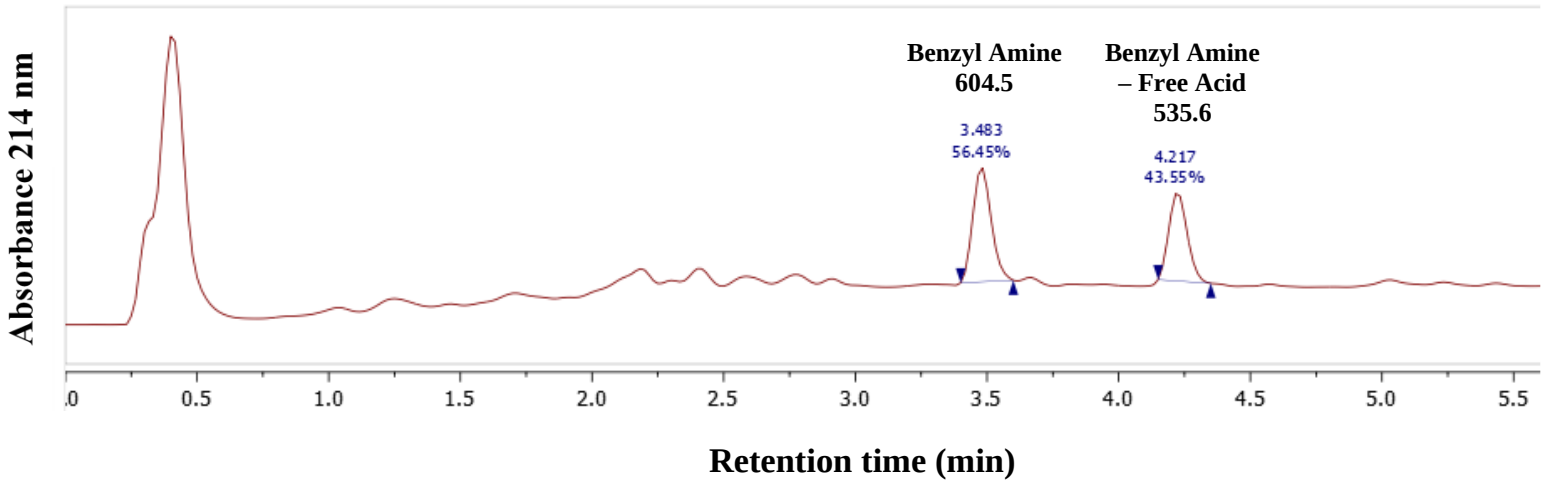

Figure B38: UPLC-MS chromatogram of H-Leu-DMA (5-60)

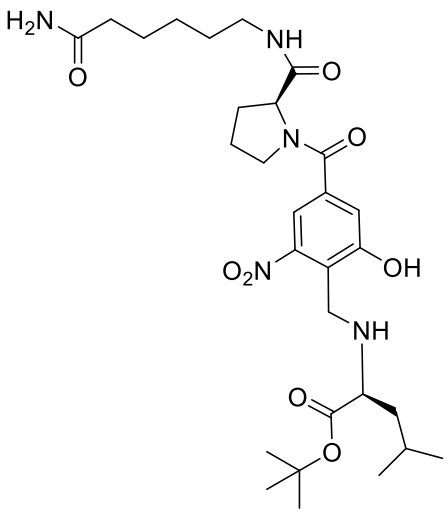

2.11

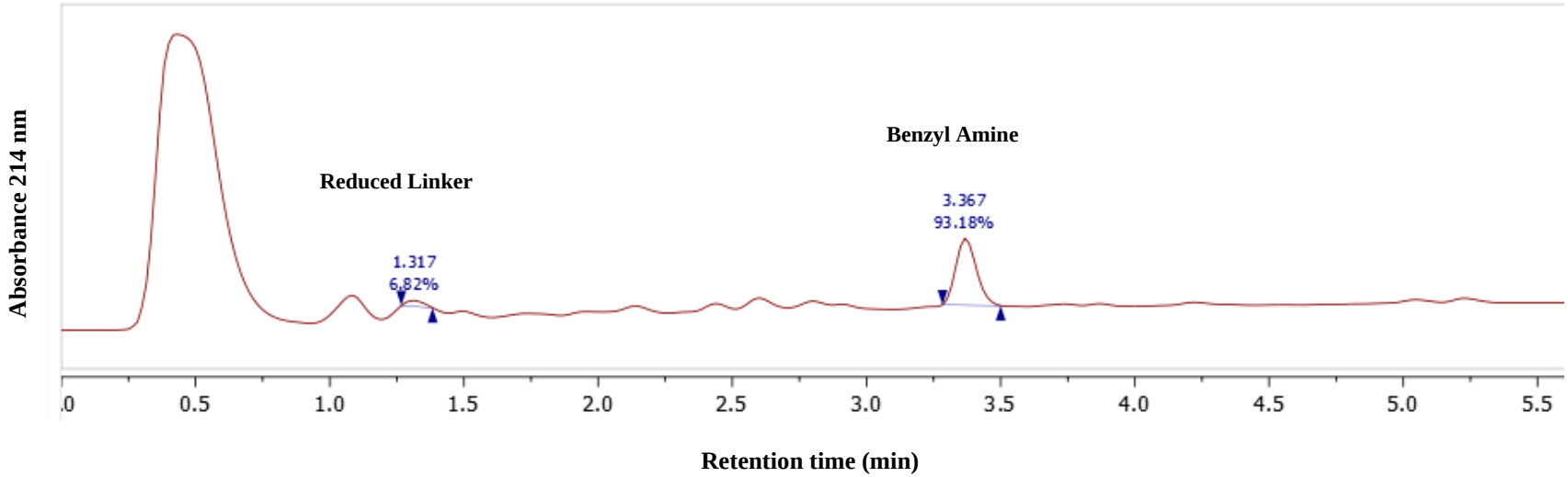

Figure B39: UPLC-MS chromatogram of HCl-Leu-tBu (5-60)

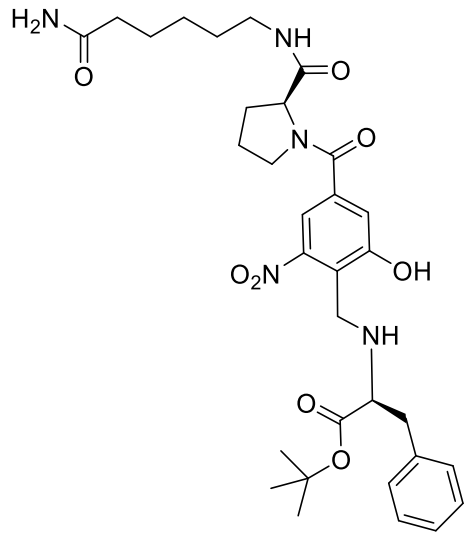

2.12

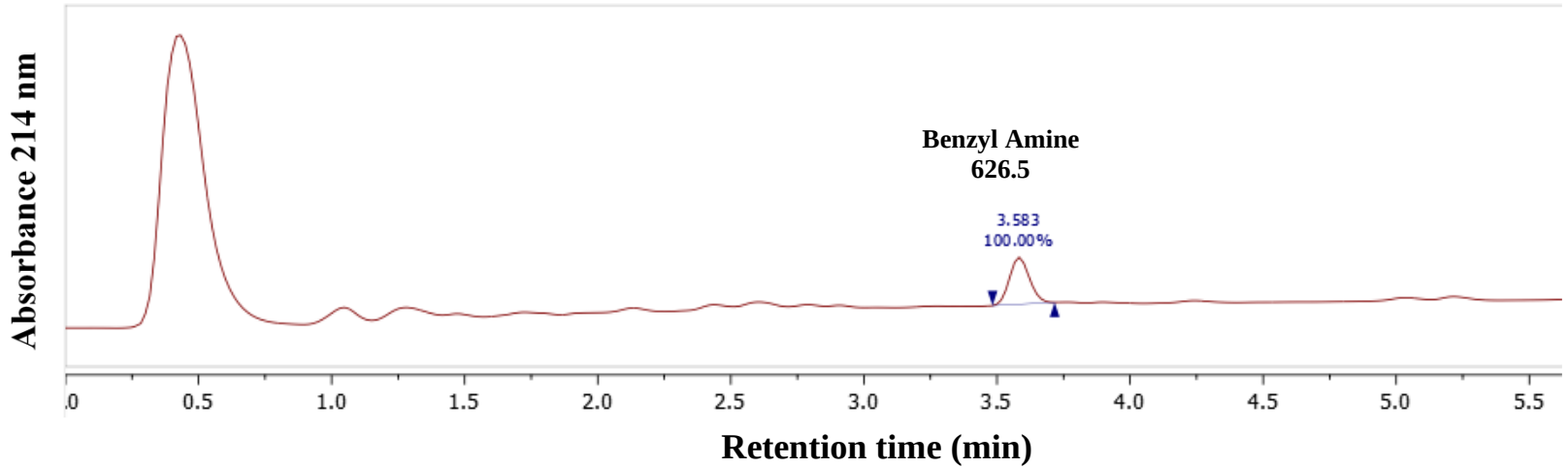

Figure B40: UPLC-MS chromatogram of HCl-Phe-tBu (5-60)

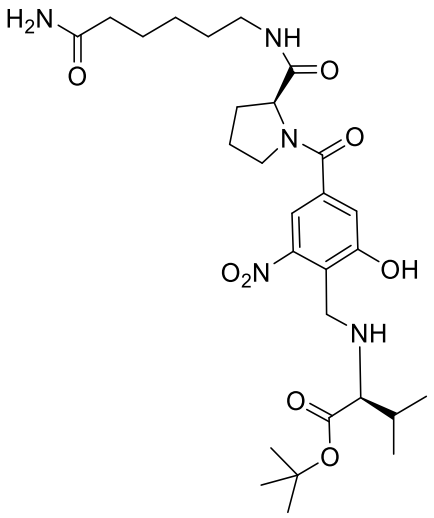

2.13

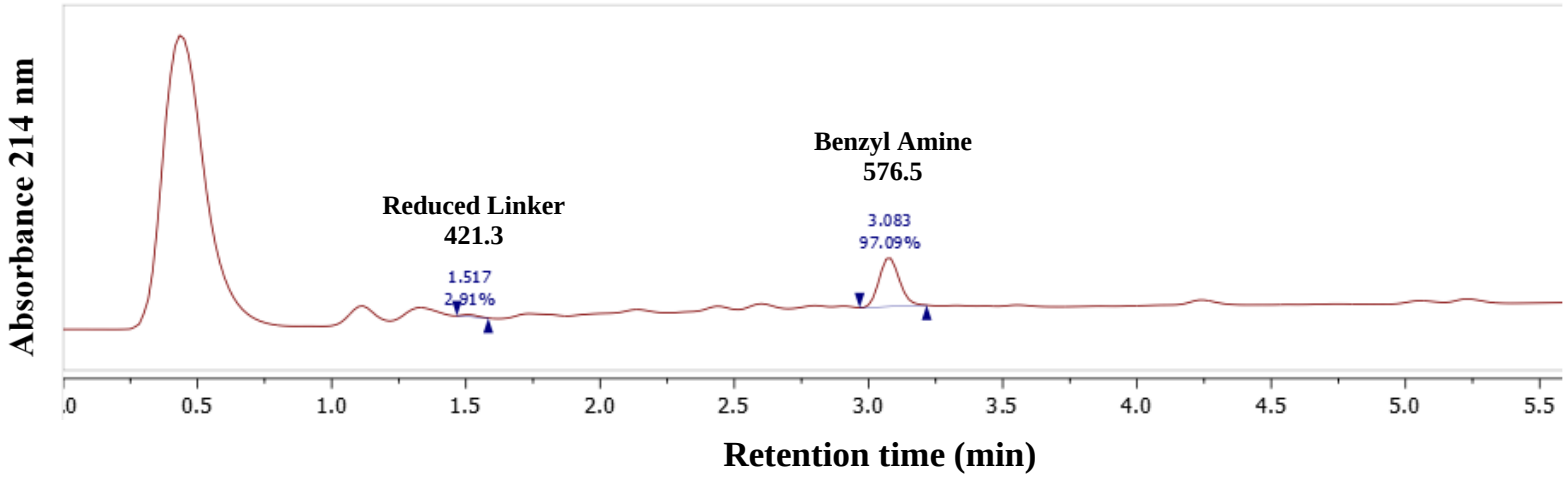

Figure B41: UPLC-MS chromatogram of HCl-Val-tBu (5-60)

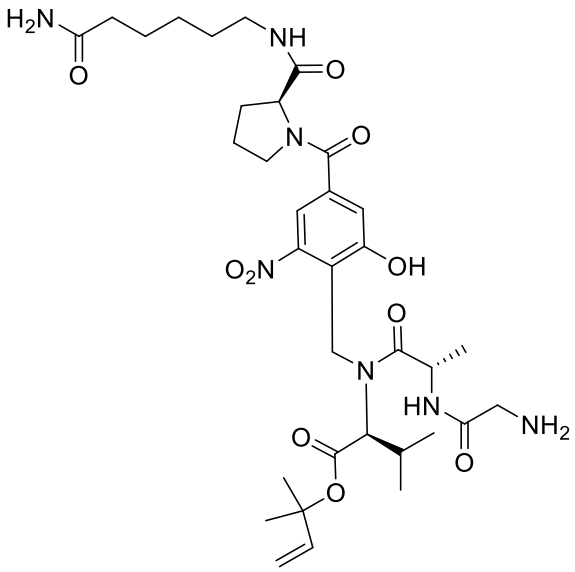

2.19

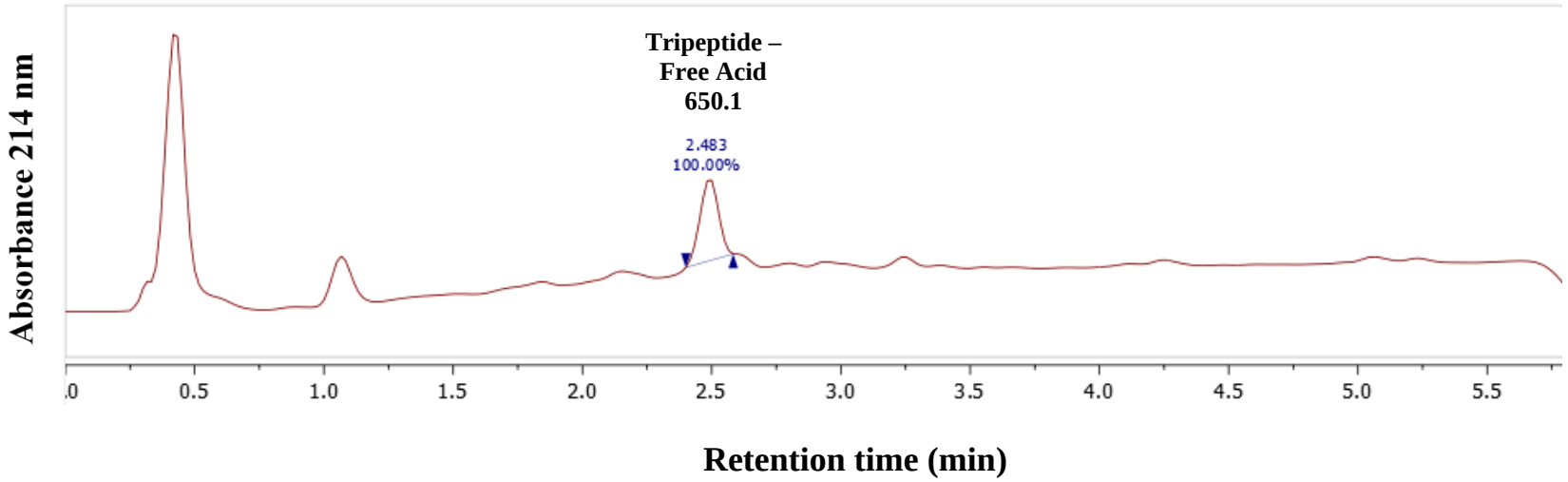

Figure B42: UPLC-MS chromatogram of H-Gly-Ala-Val-DMA (5-60)

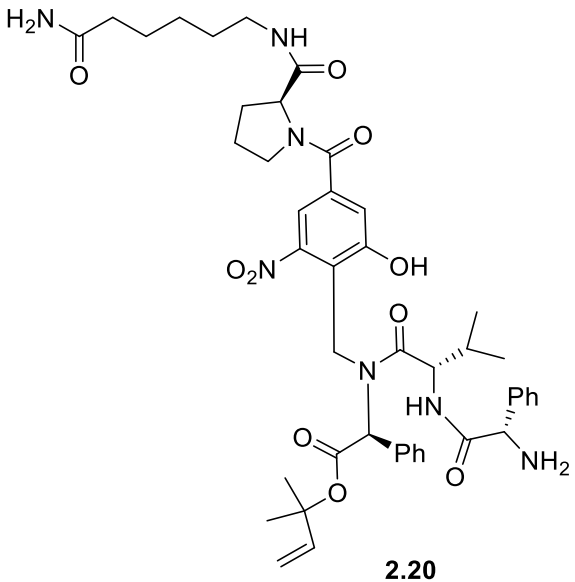

2.20

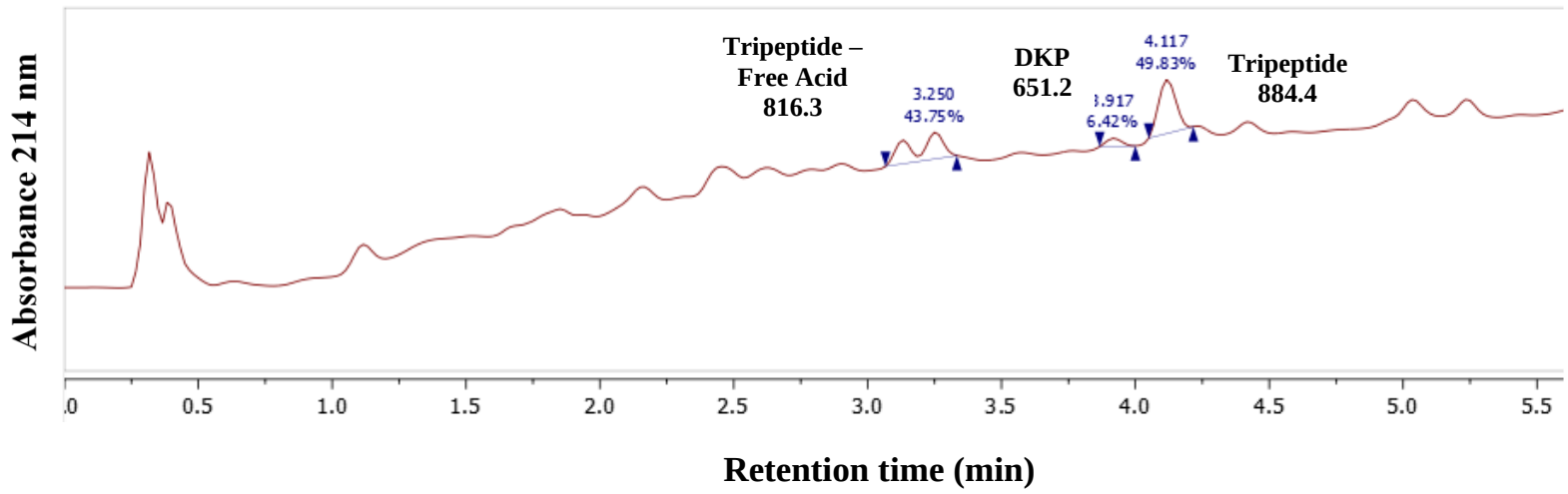

Figure B43: UPLC-MS chromatogram of H-Phe-Val-Phe-DMA (5-60)

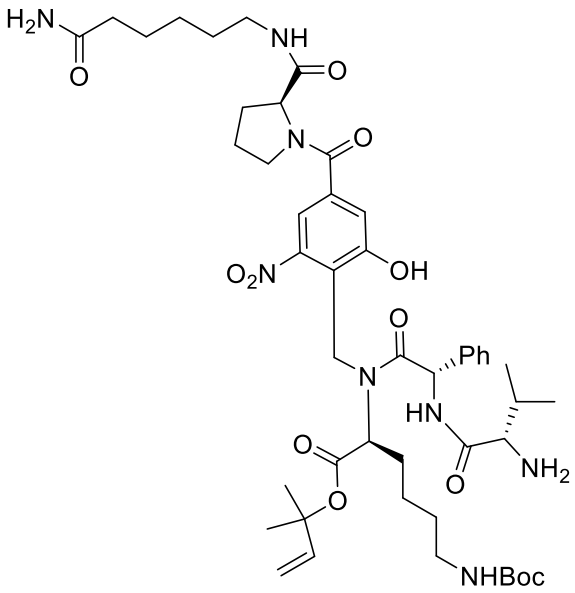

2.21

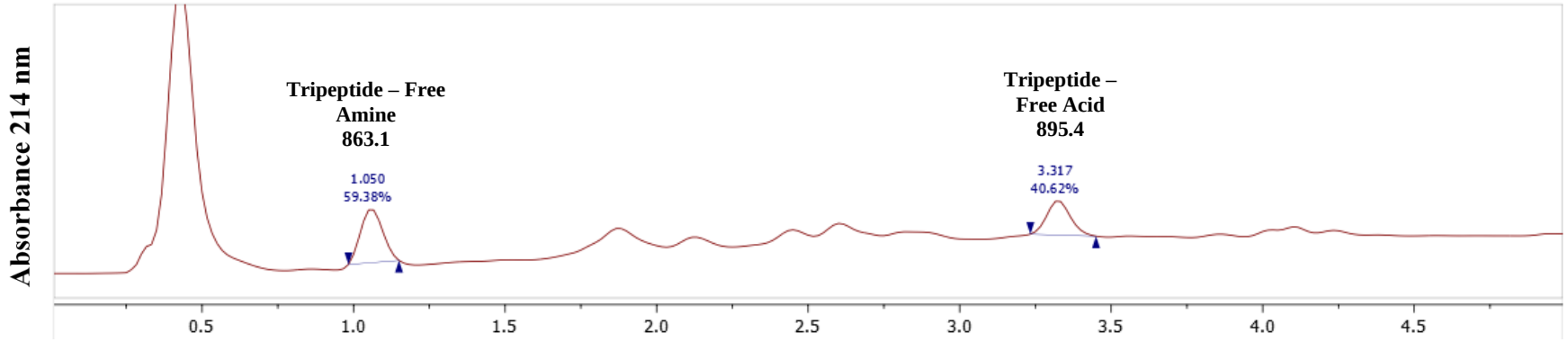

Figure B44: UPLC-MS chromatogram of H-Val-Phe-Lys(Boc)-DMA (5-60)

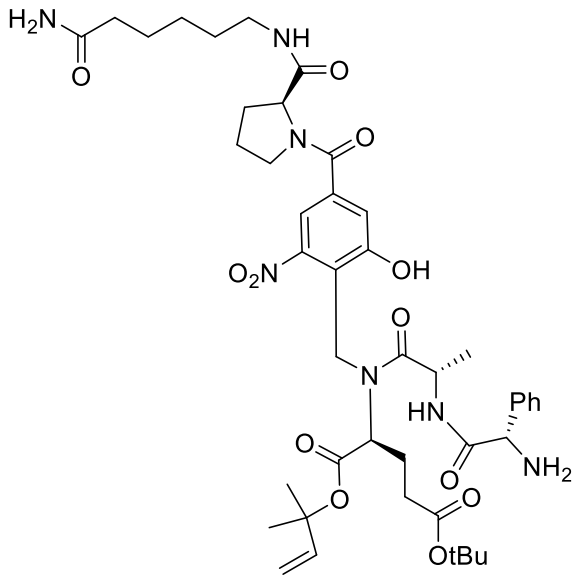

2.22

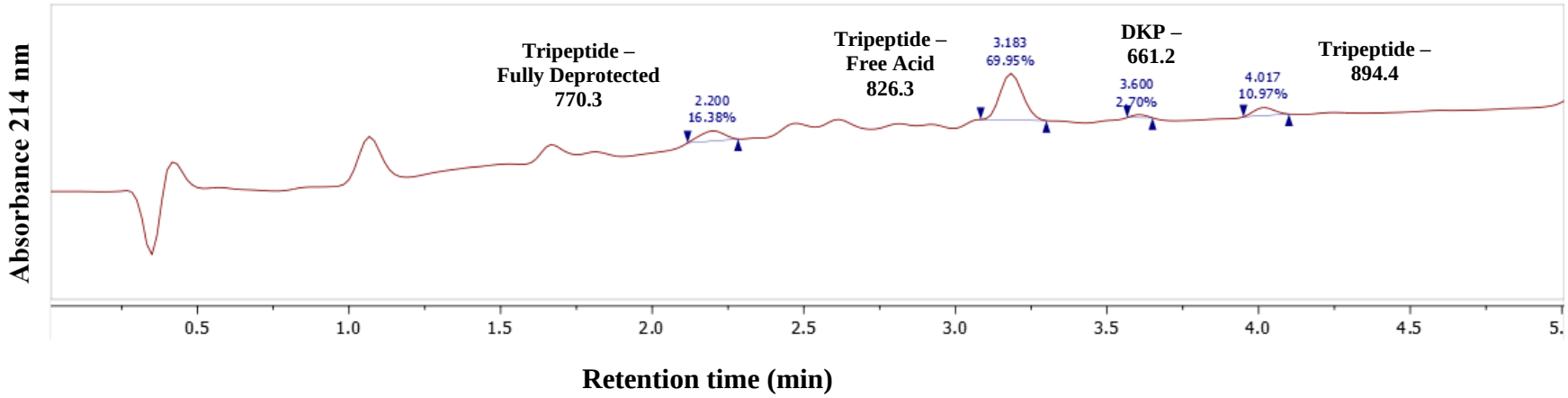

Figure B45: UPLC-MS chromatogram of H-Phe-Ala-Glu(tBu)-DMA (5-60)

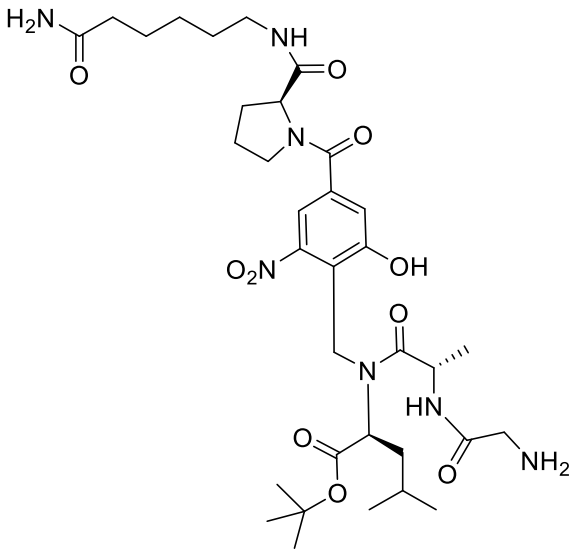

2.23

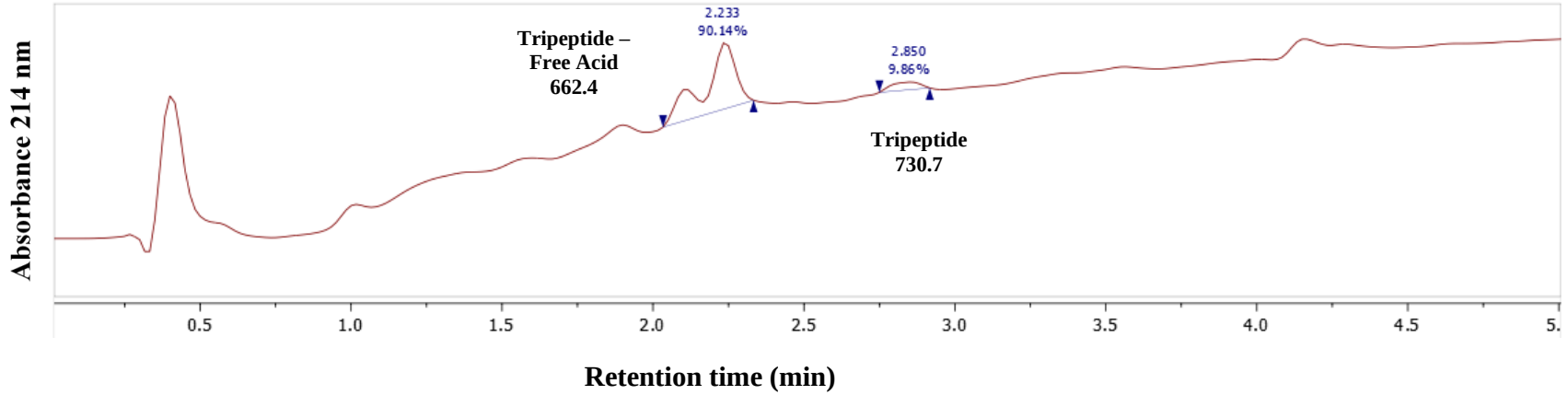

Figure B46: UPLC-MS chromatogram of H-Gly-Ala-Leu-tBu (5-80)

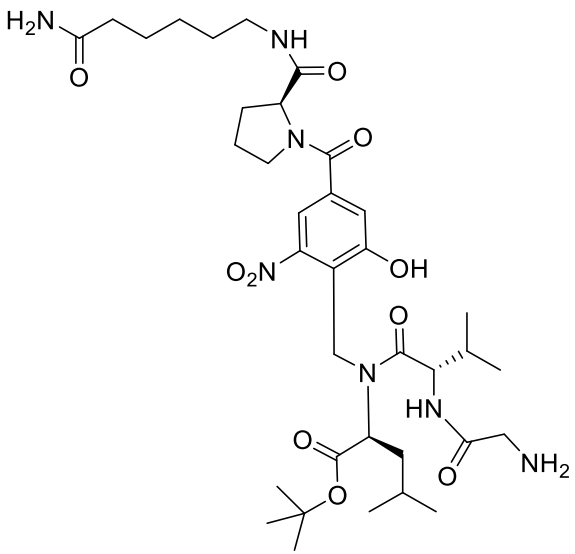

2.24

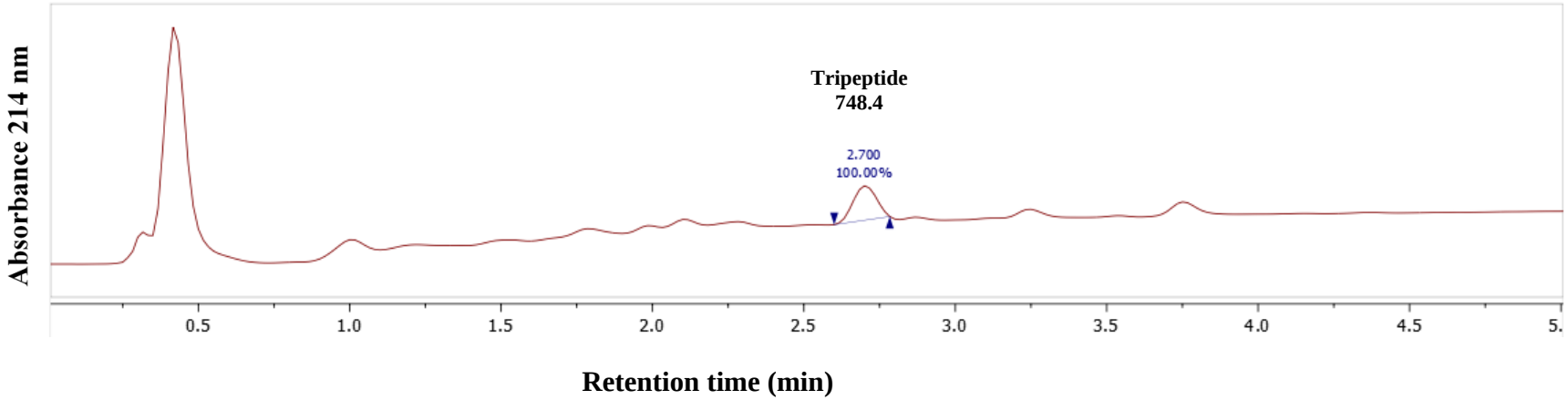

Figure B47: UPLC-MS chromatogram of H-Gly-Val-Leu-tBu (5-60)

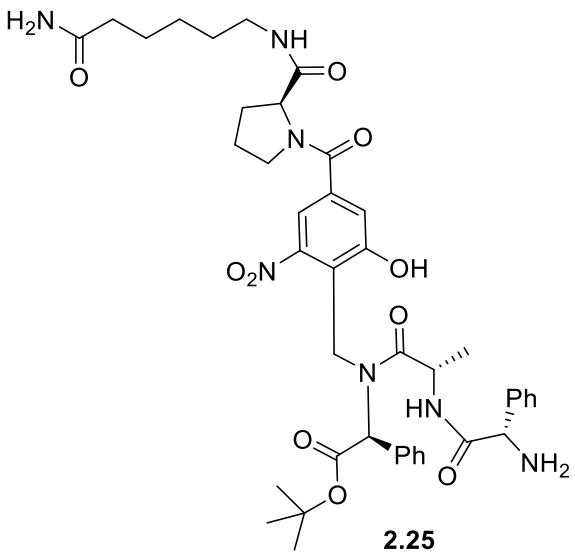

2.25

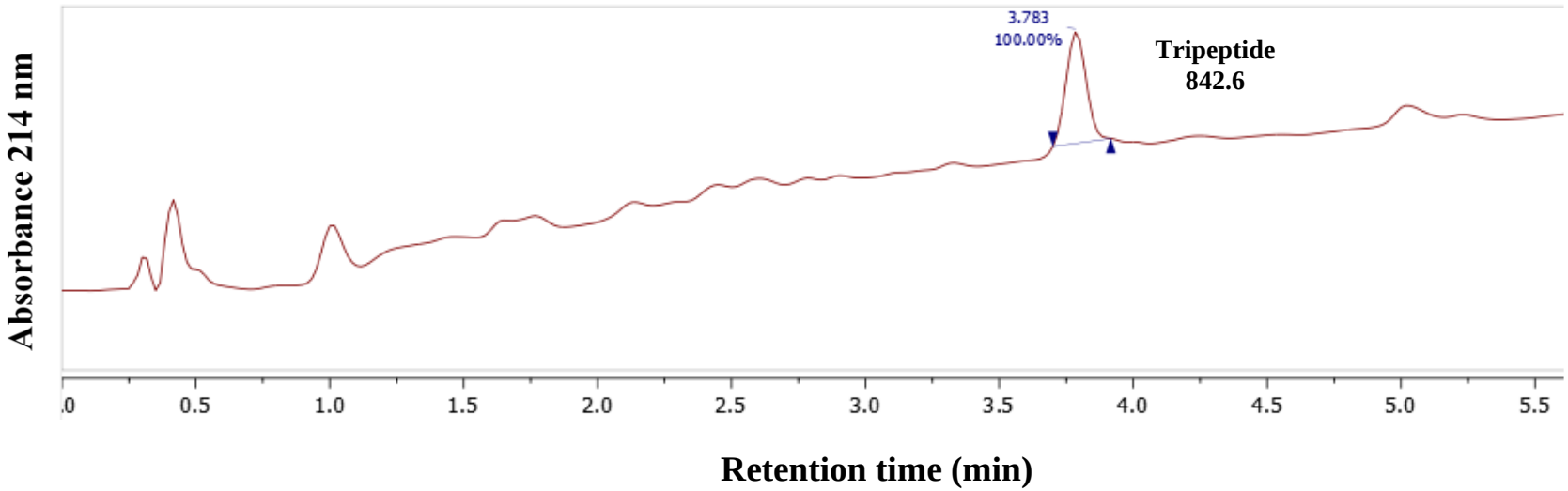

Figure B48: UPLC-MS chromatogram of H-Phe-Ala-Phe-tBu (5-60)

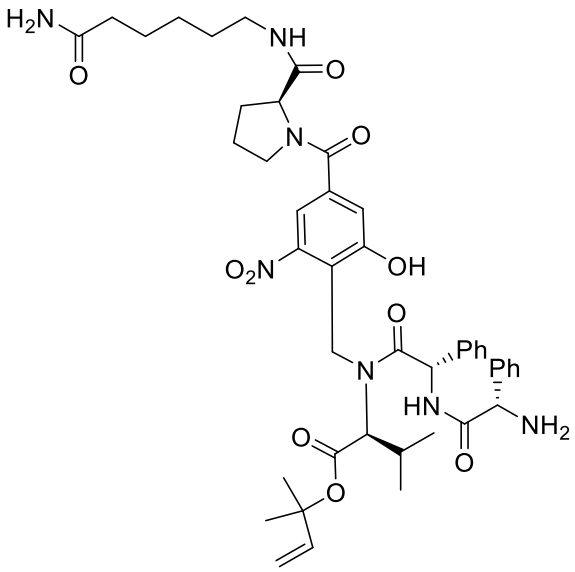

2.26

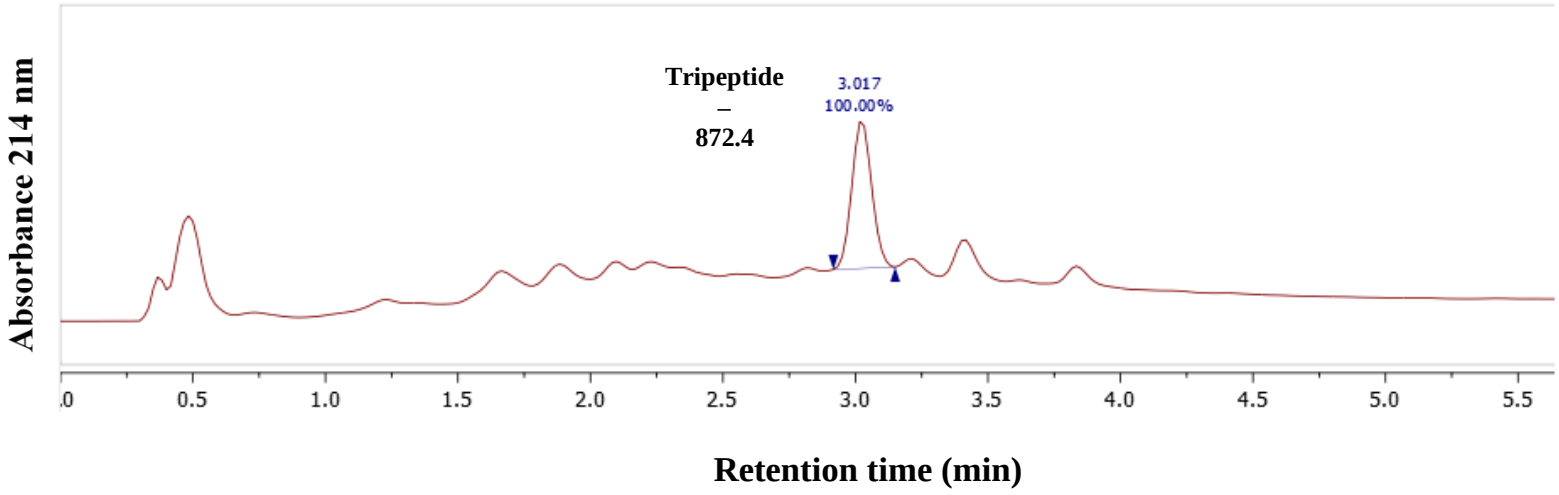

Figure B49: UPLC-MS chromatogram of H-Phe-Phe-Val-tBu (5-60)

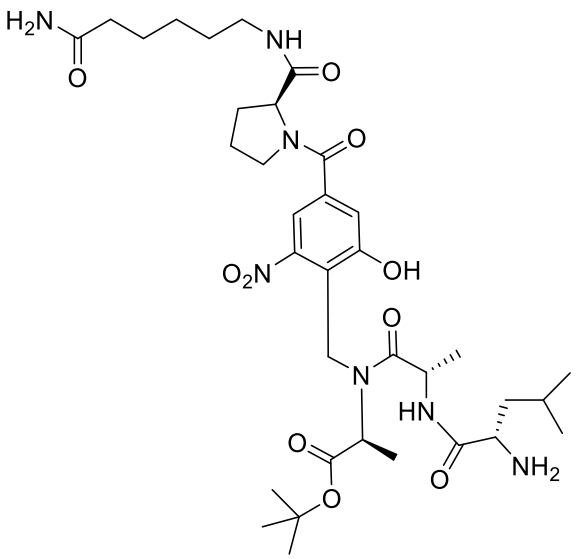

2.18i

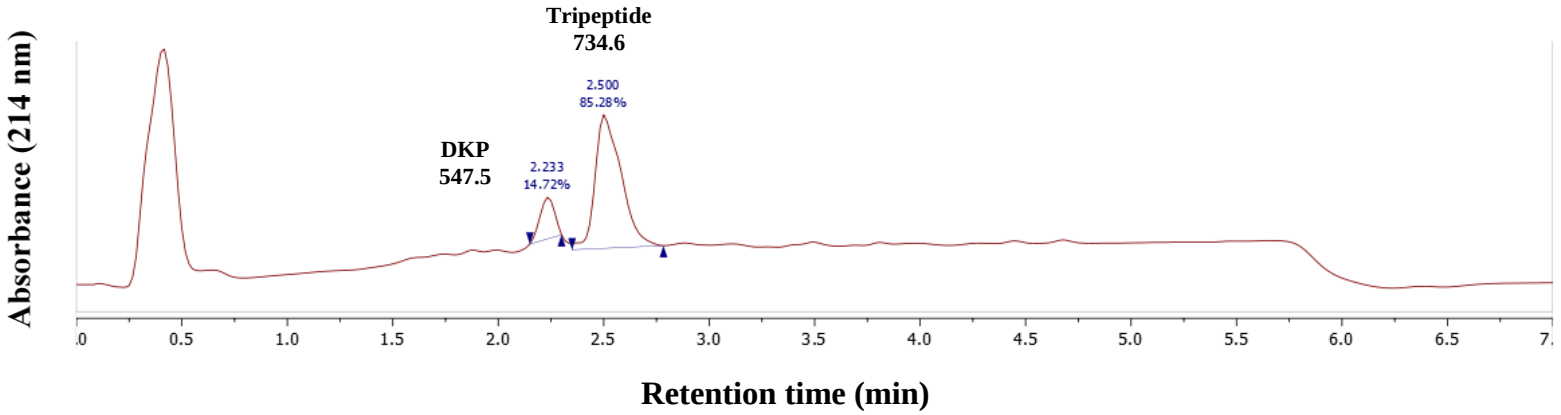

Figure B50: UPLC-MS chromatogram of H-Leu-Ala-Ala-tBu (5-95)

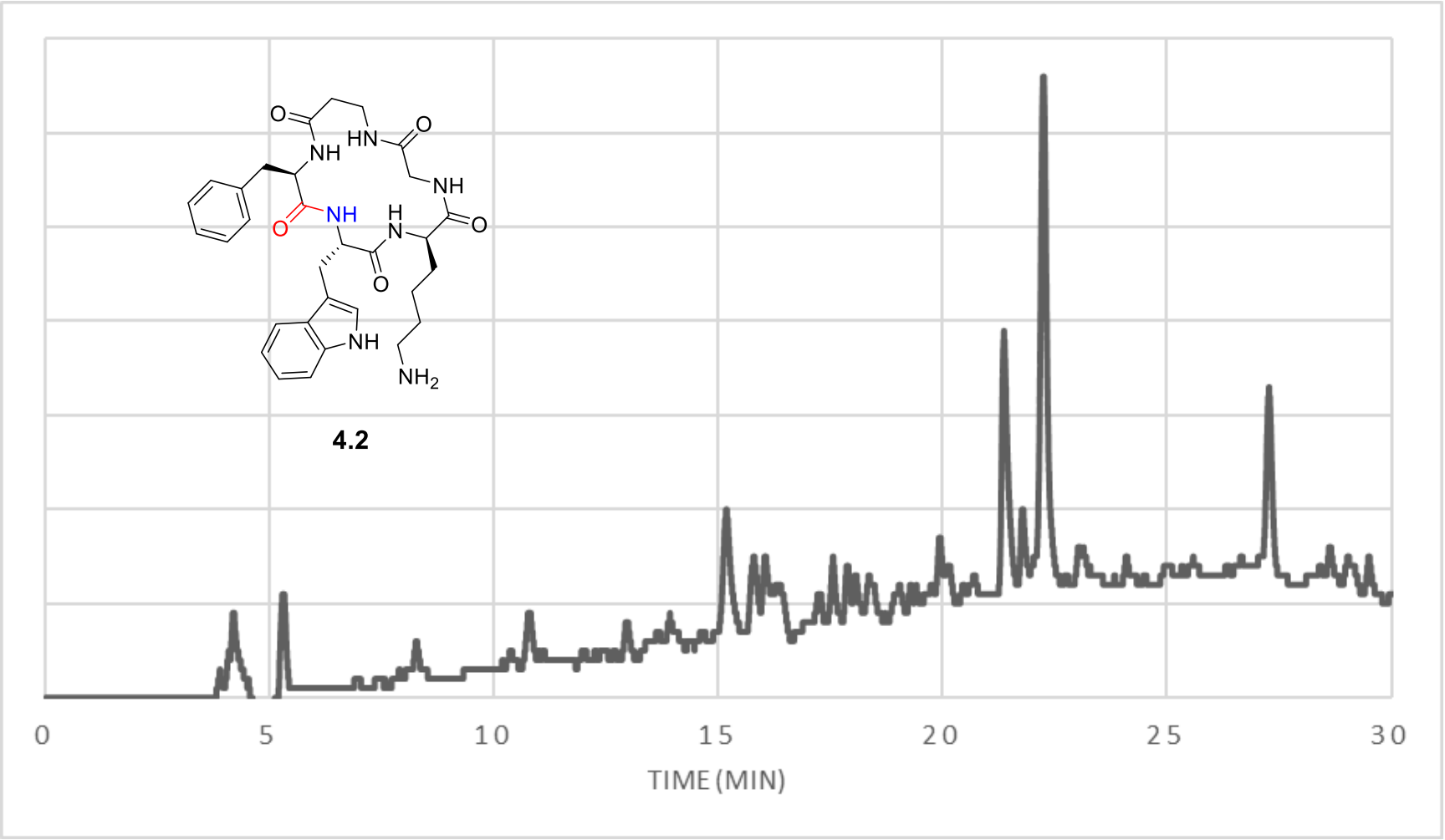

Figure B51: c-[(D)-Trp-Lys-Gly-(β)-Ala-Phe] (4.2). Gradient 5 to 50.

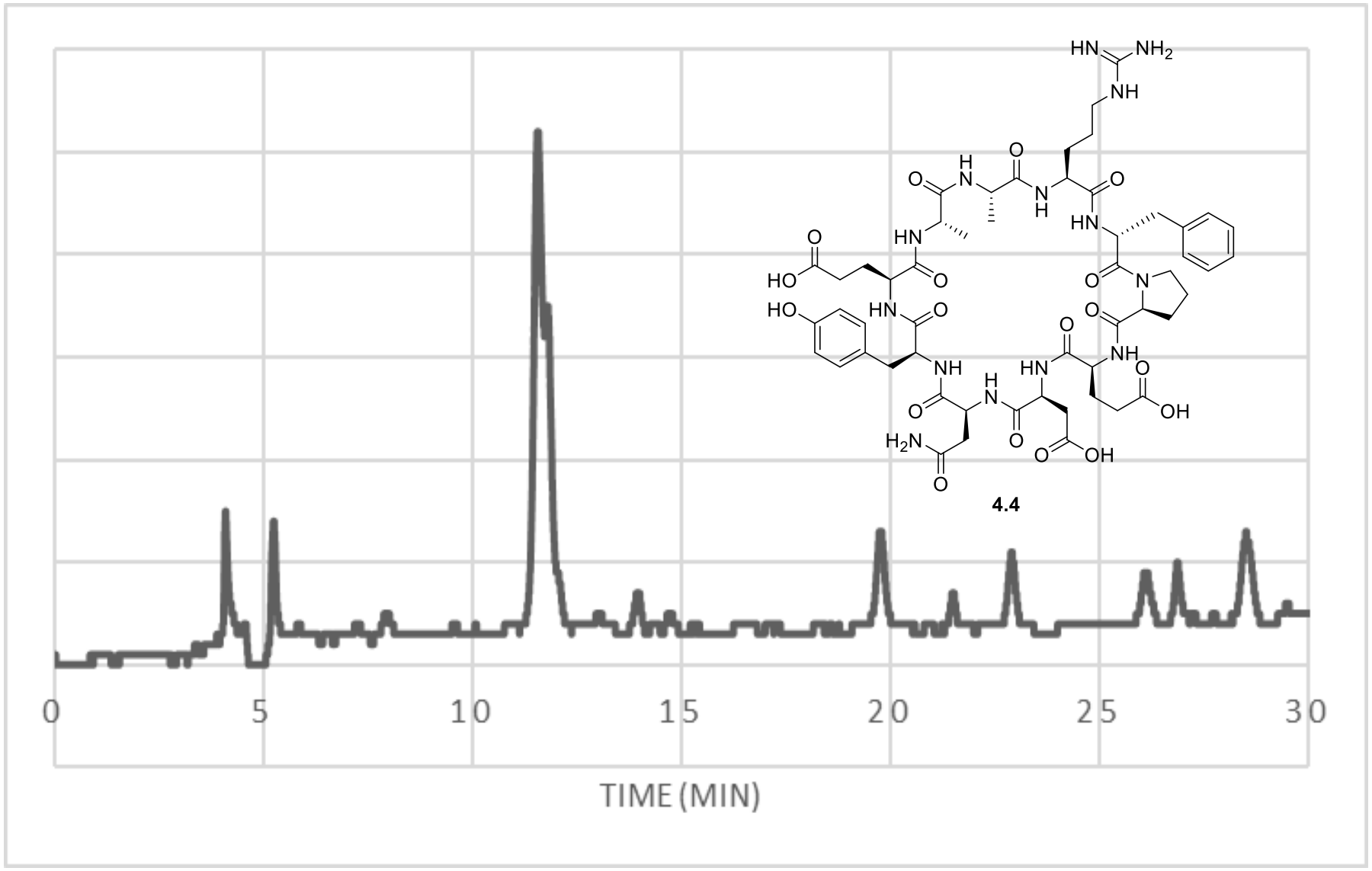

Figure B52: cyclo[Arg-(D)-Phe-Pro-Glu-Asp-Asn-Tyr-Glu-Ala-Ala]. Gradient 5 to 20

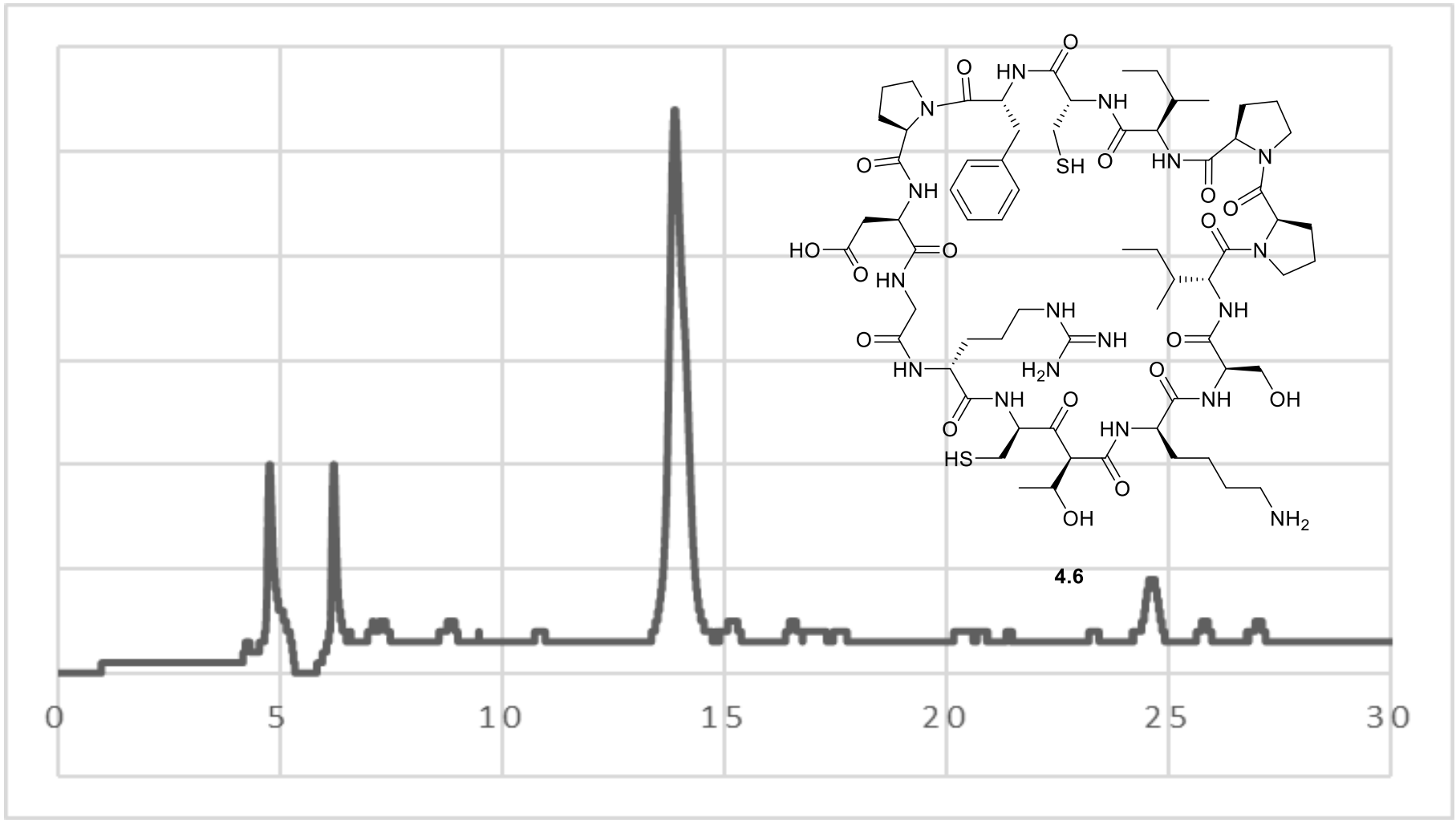

Figure B53: cyclo[Pro-Asp-Gly-Arg-Cys-Thr-Lys-Ser-Ile-Pro-Pro-Ile-Cys-Phe]. Gradient 5 to 15.

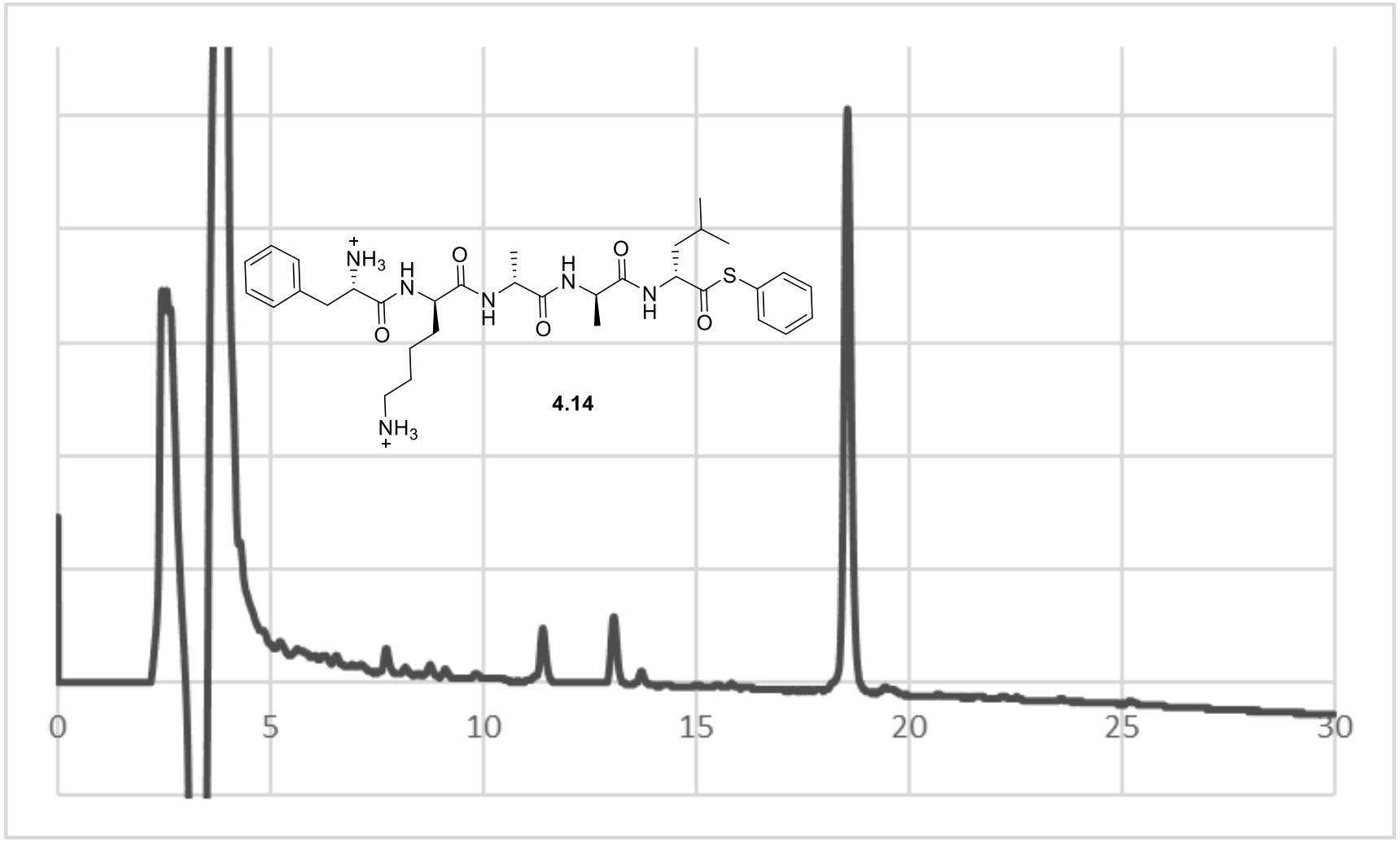

Figure B54: Leu Thioester

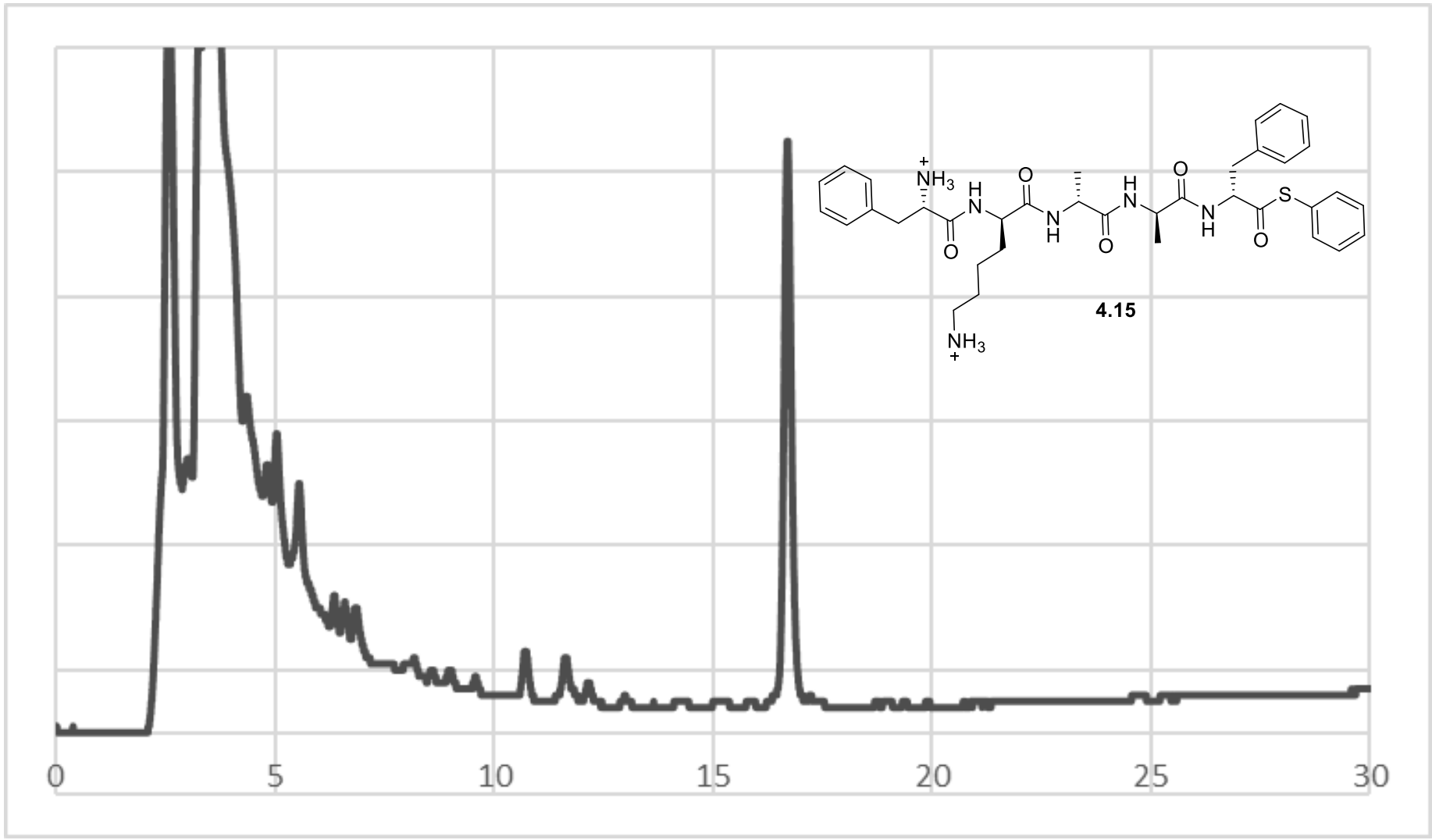

Figure B55: Phe Thioester

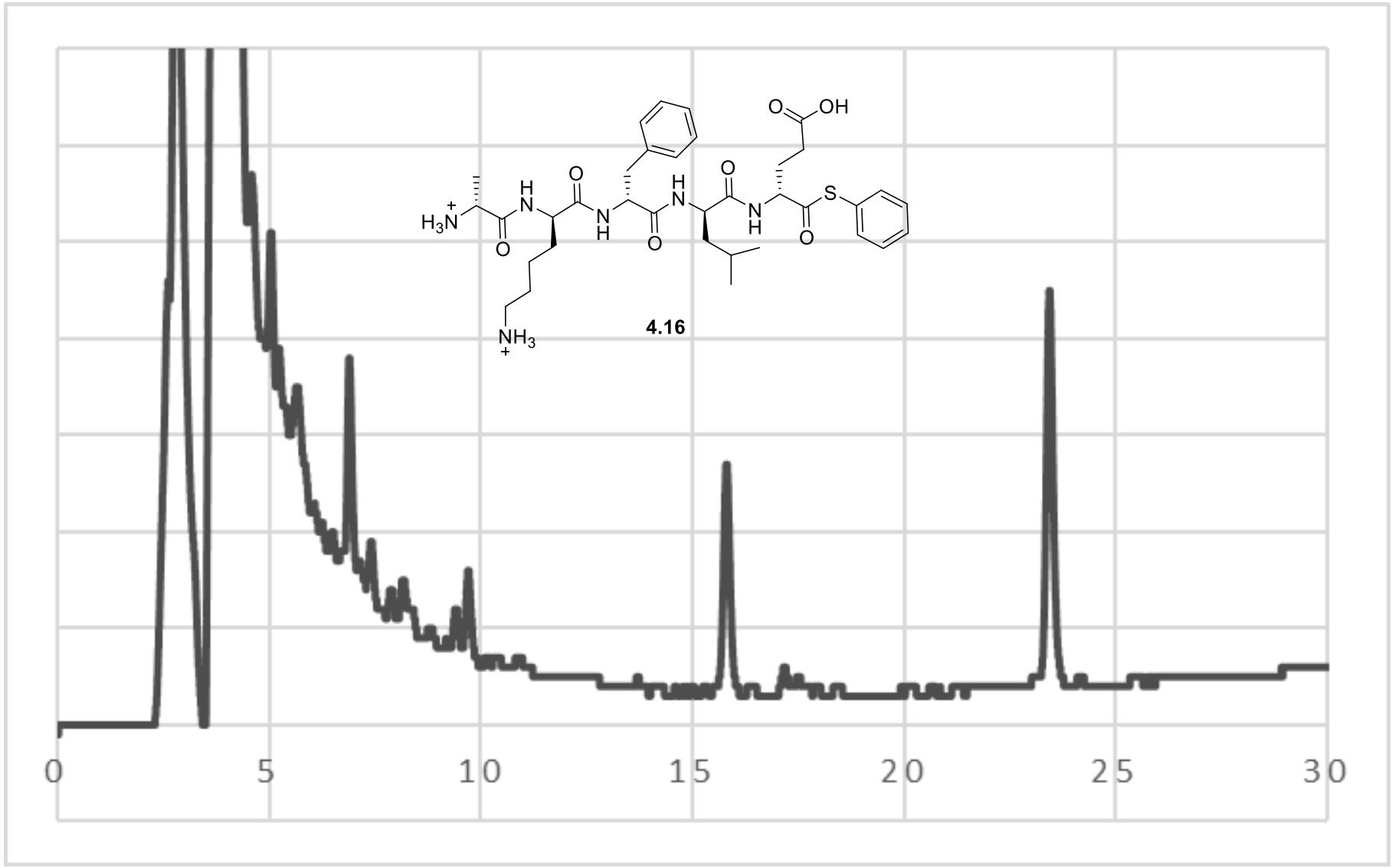

Figure B56: Glu Thioester. Gradient 50 to 75.

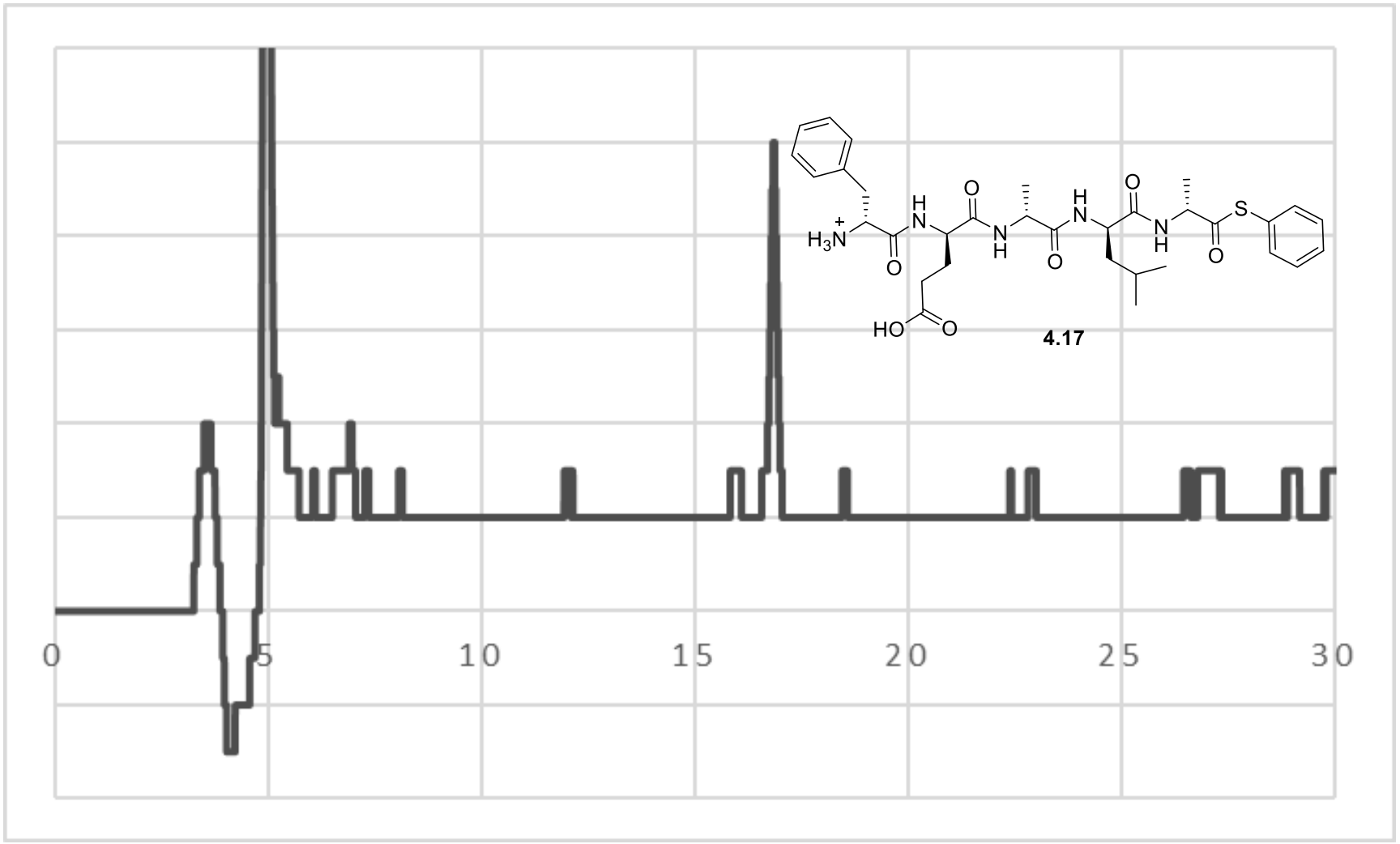

Figure B57: Ala Thioester. Gradient 30 to 50.

NMR and LC-MS Data: Part 2

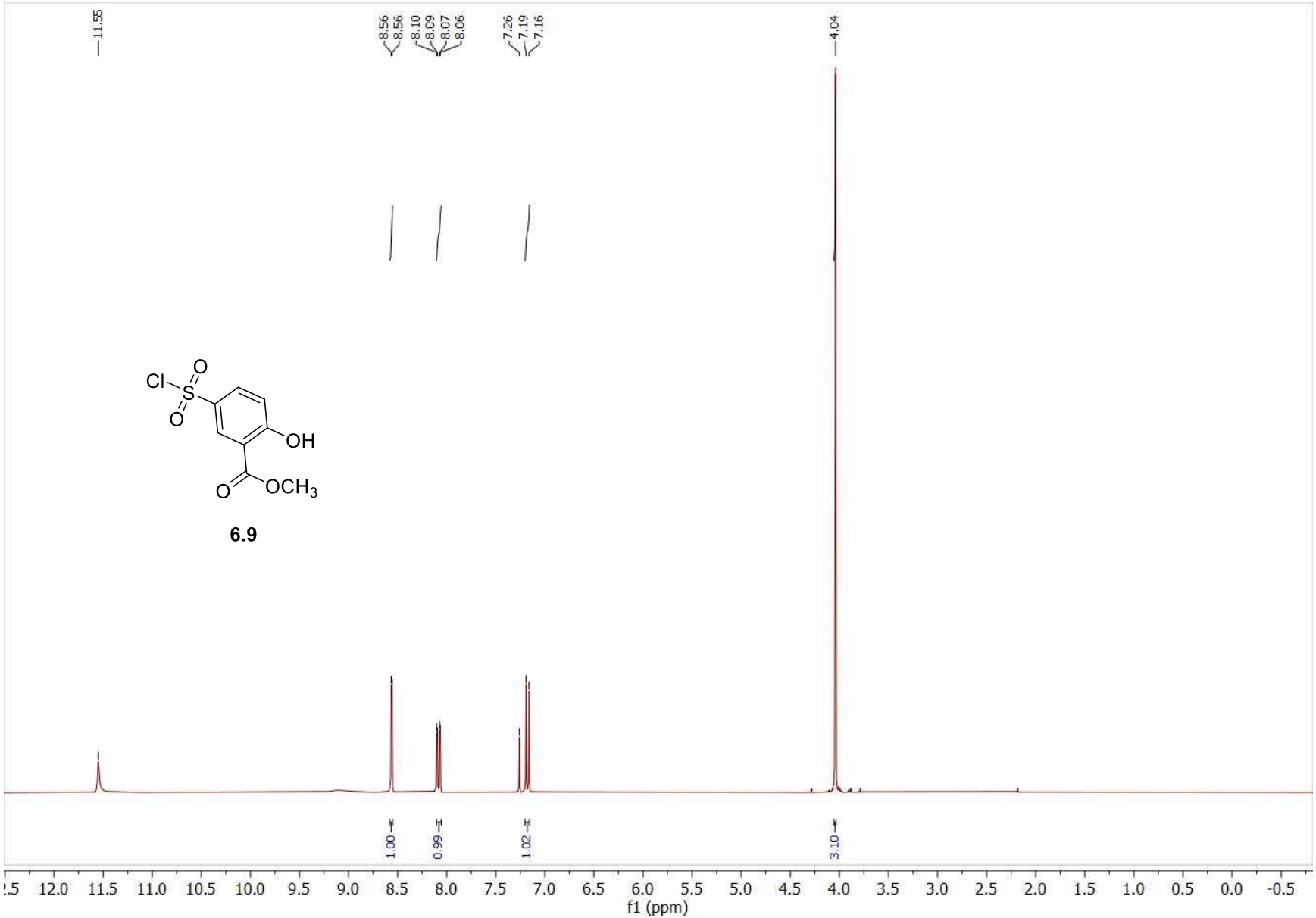

Figure B58: ^{1}H NMR of compound **6.9**.

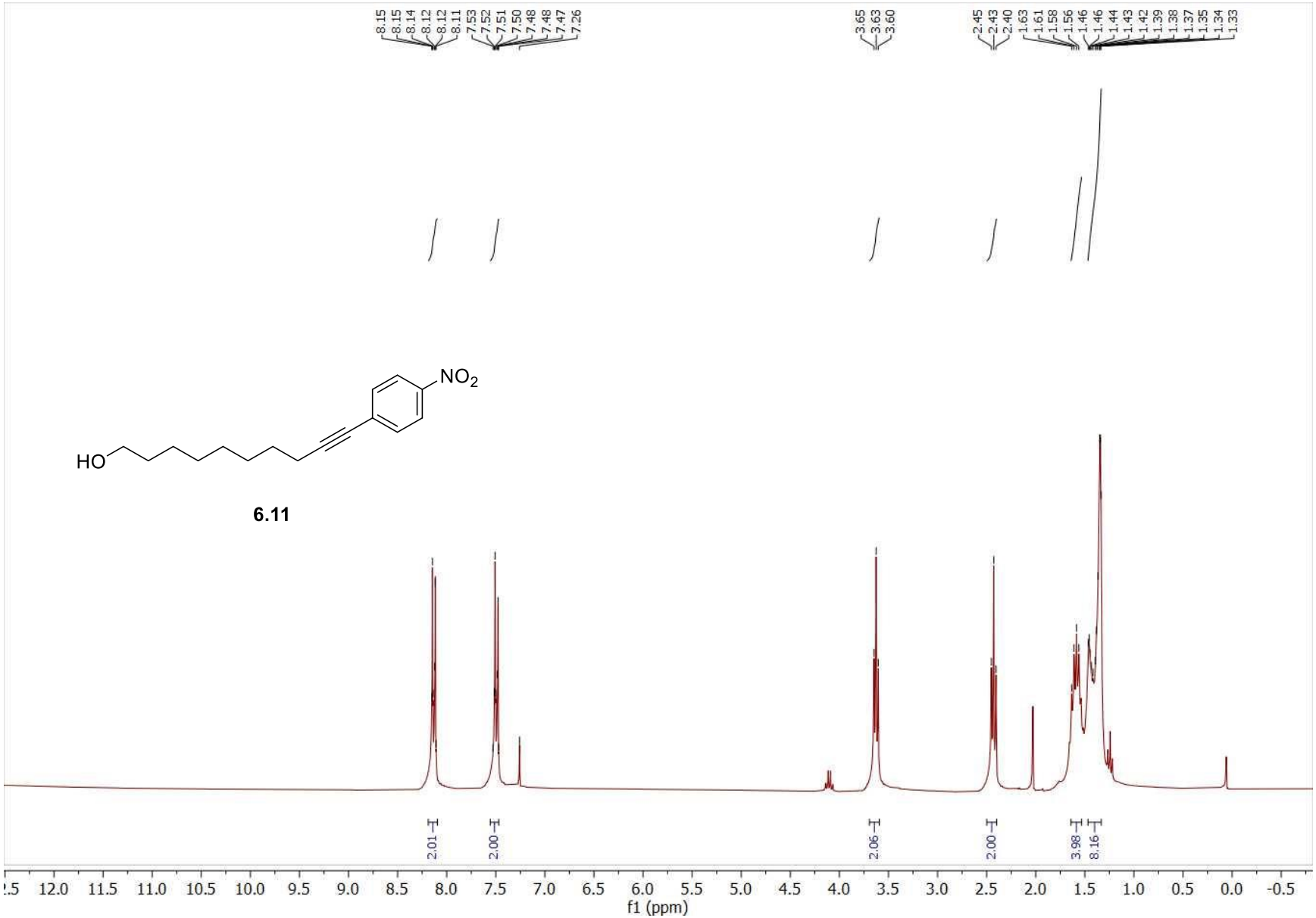

Figure B59: ^{1}H NMR of compound **6.11**.

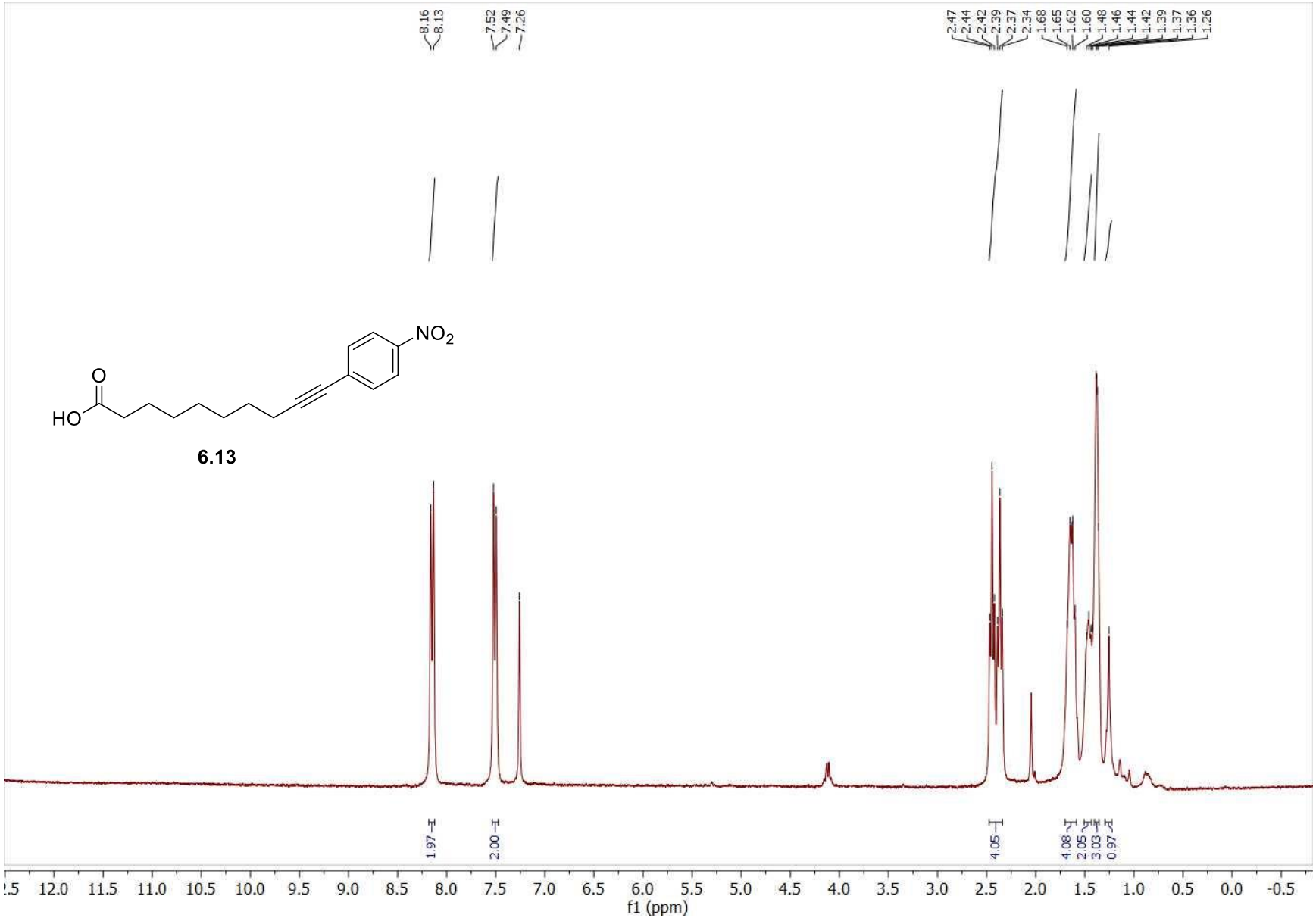

Figure B60: ^{1}H NMR of compound **6.13**.

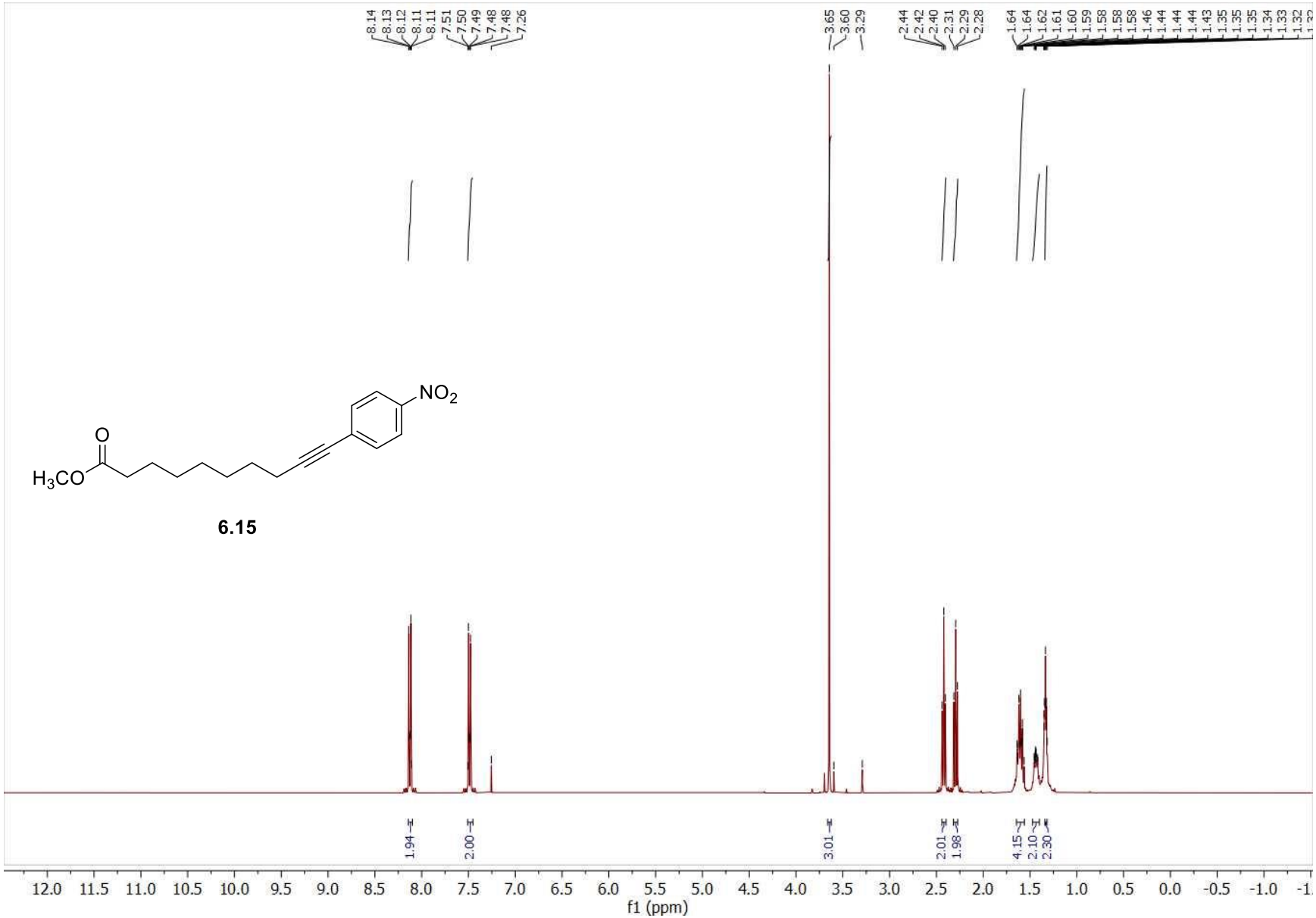

Figure B61: ^{1}H NMR of compound **6.15**.

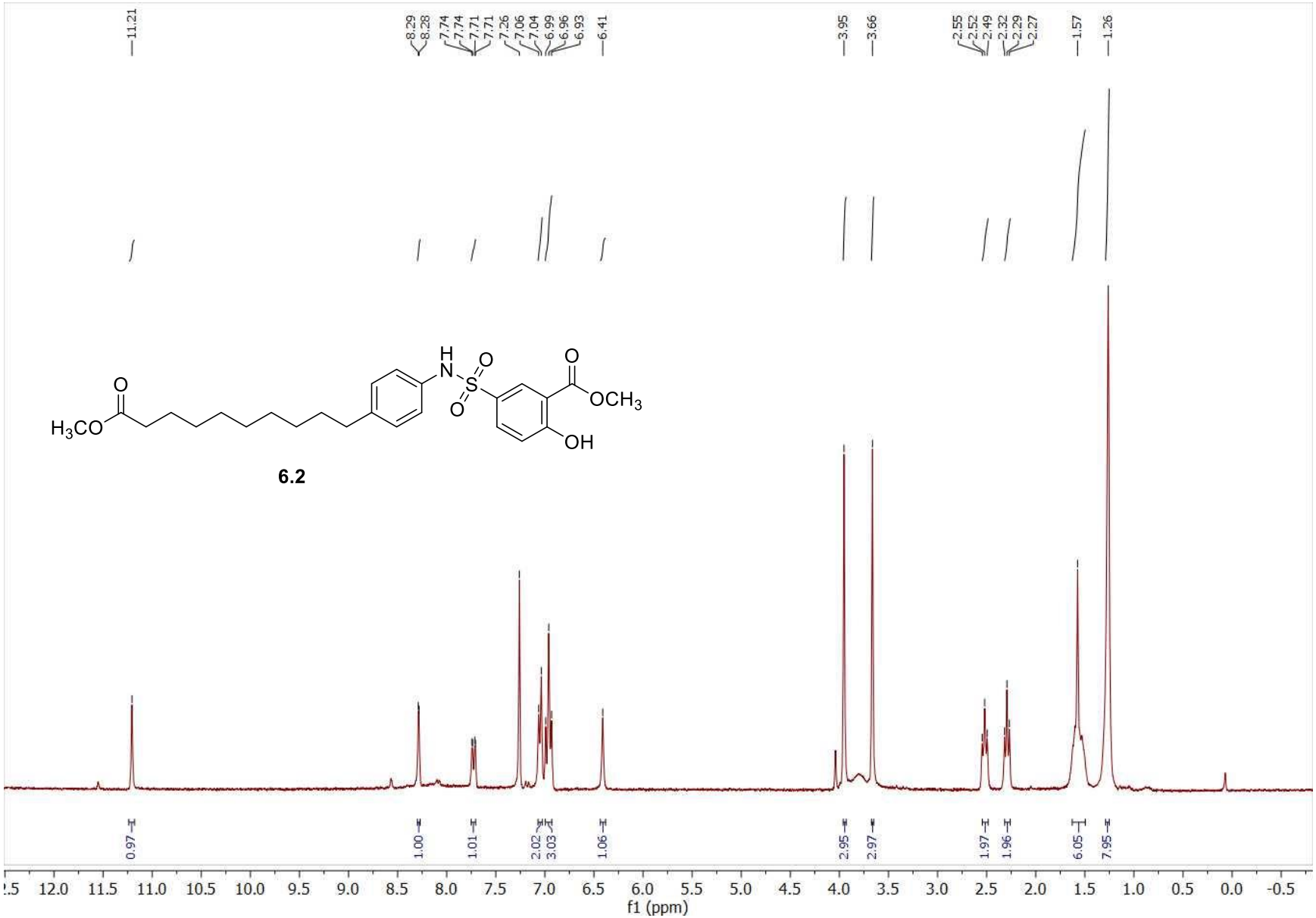

Figure B62: ^{1}H NMR of compound **6.2**.

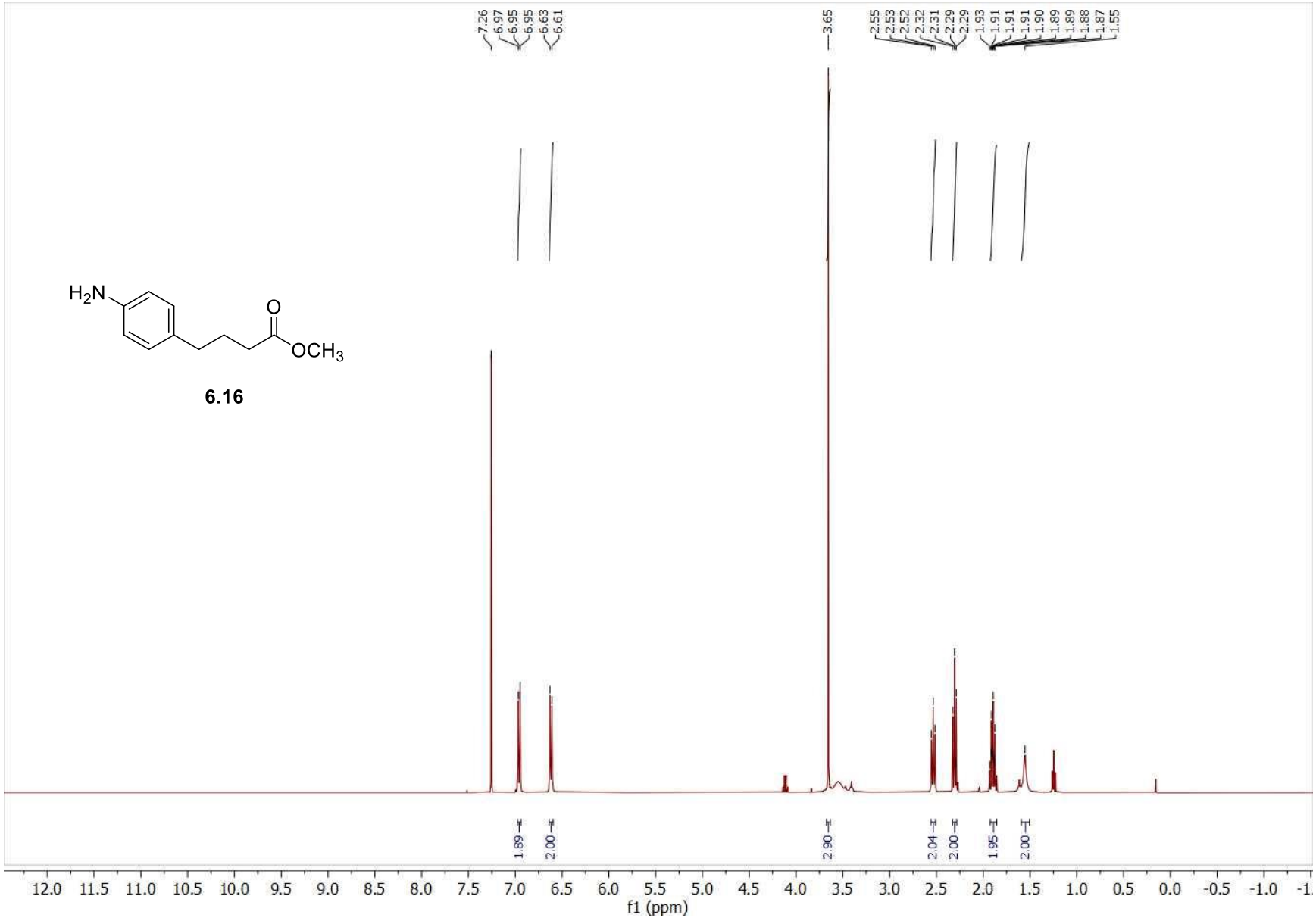

Figure B63: ^{1}H NMR of compound **6.16**.

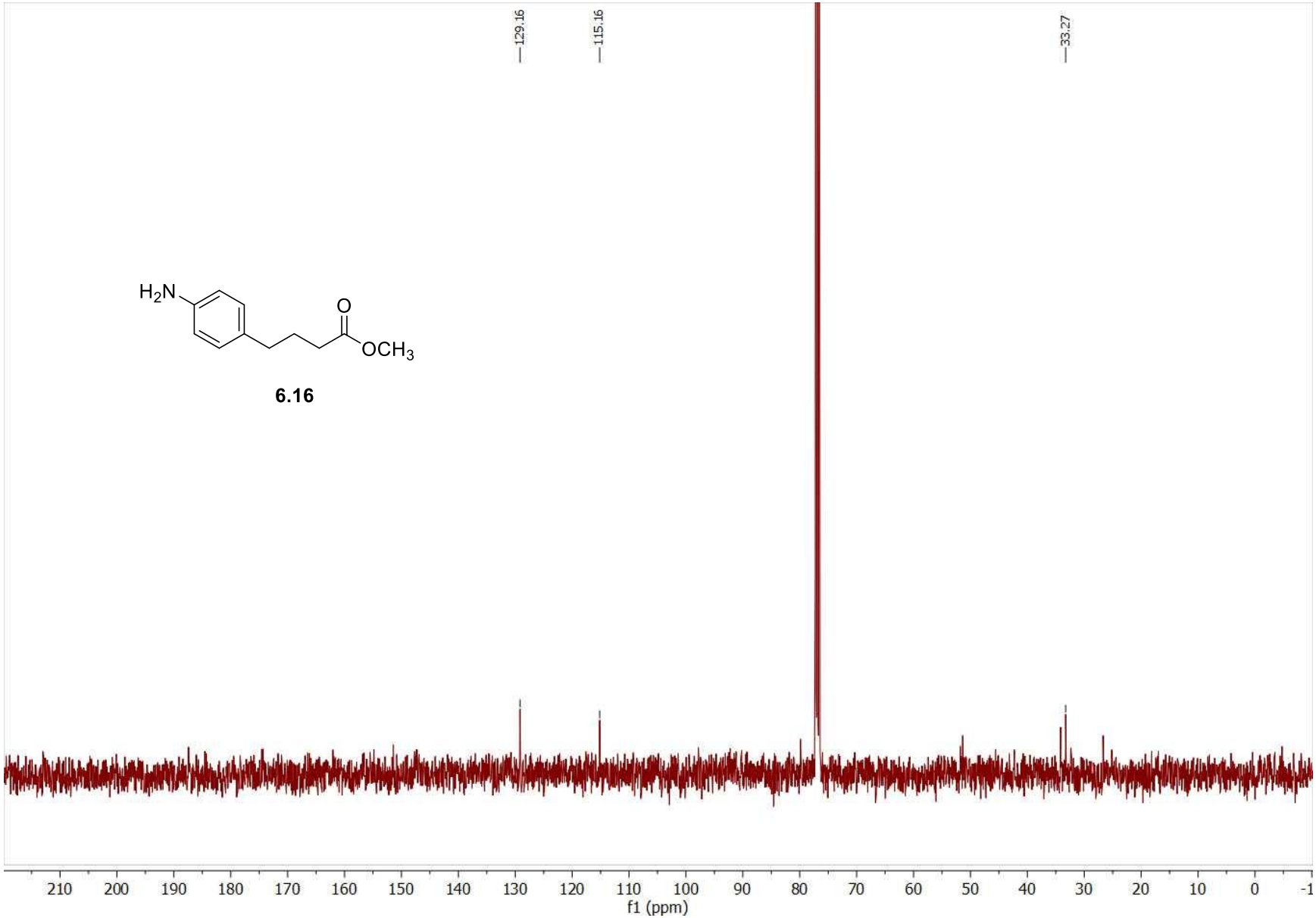

Figure B64: ^{13}C NMR of compound **6.16**.

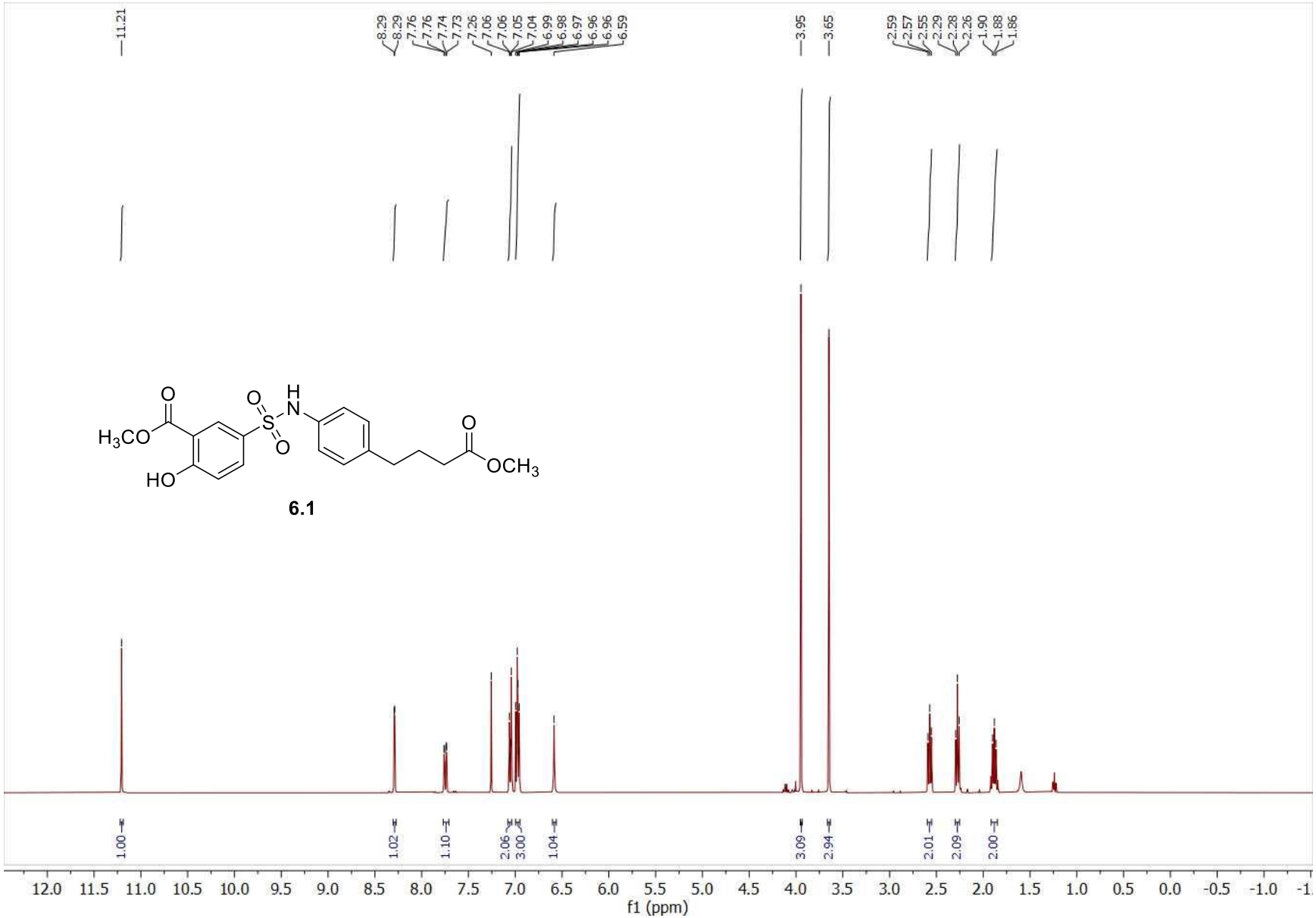

Figure B65: ^{1}H NMR of compound **6.1**

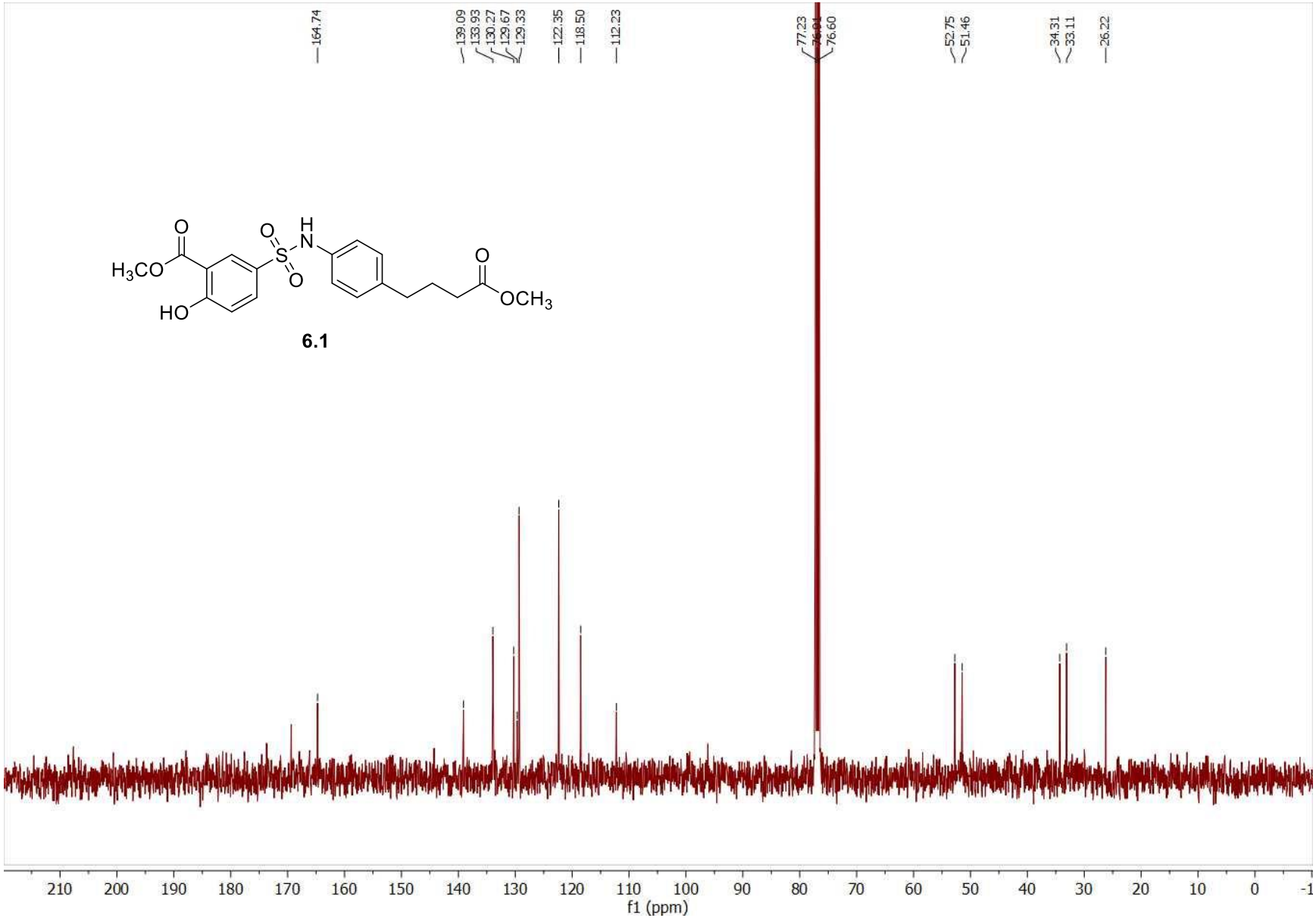

Figure B66: ^{13}C NMR of compound **6.1**.

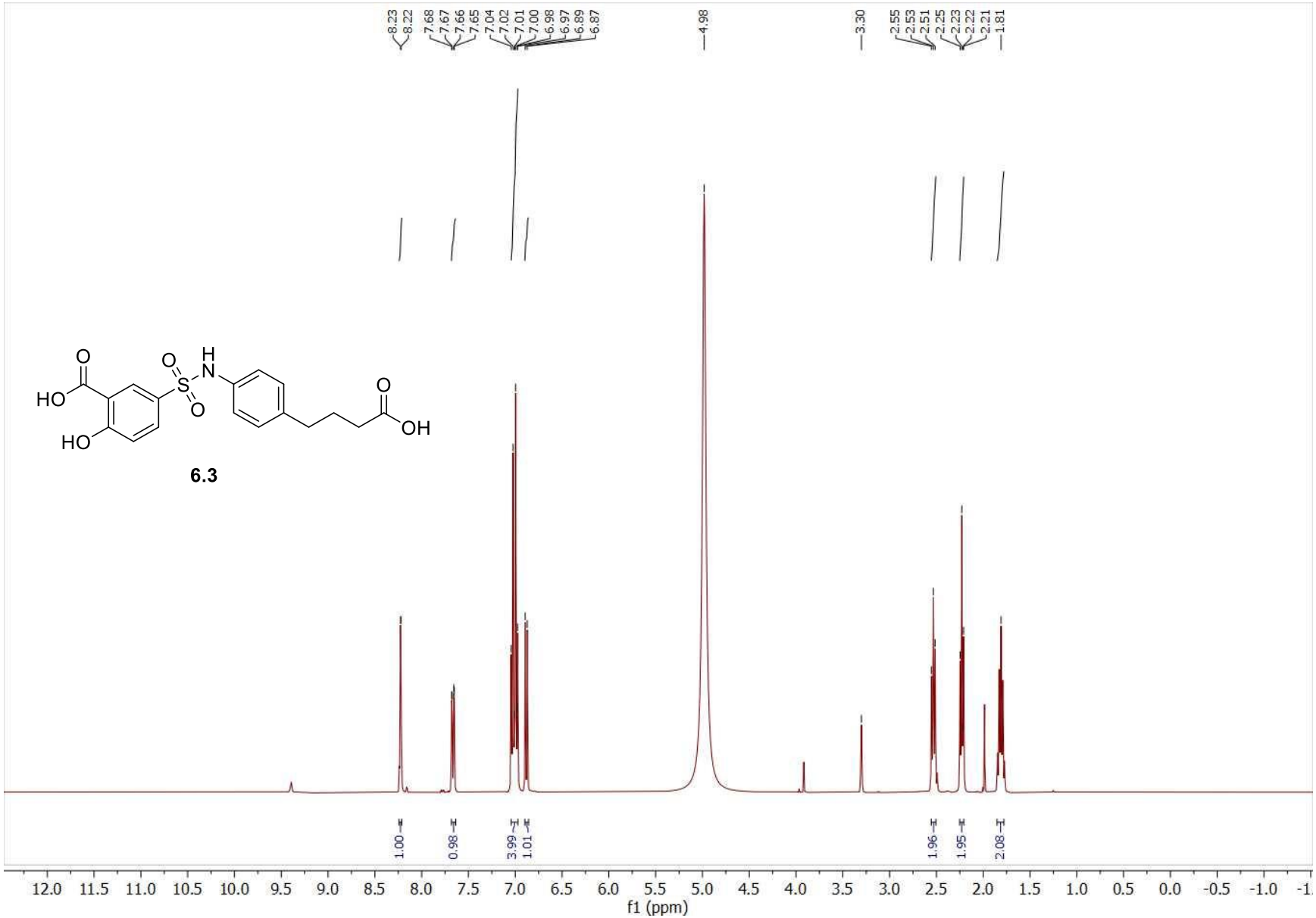

Figure B67: ^{1}H NMR of compound **6.3**.

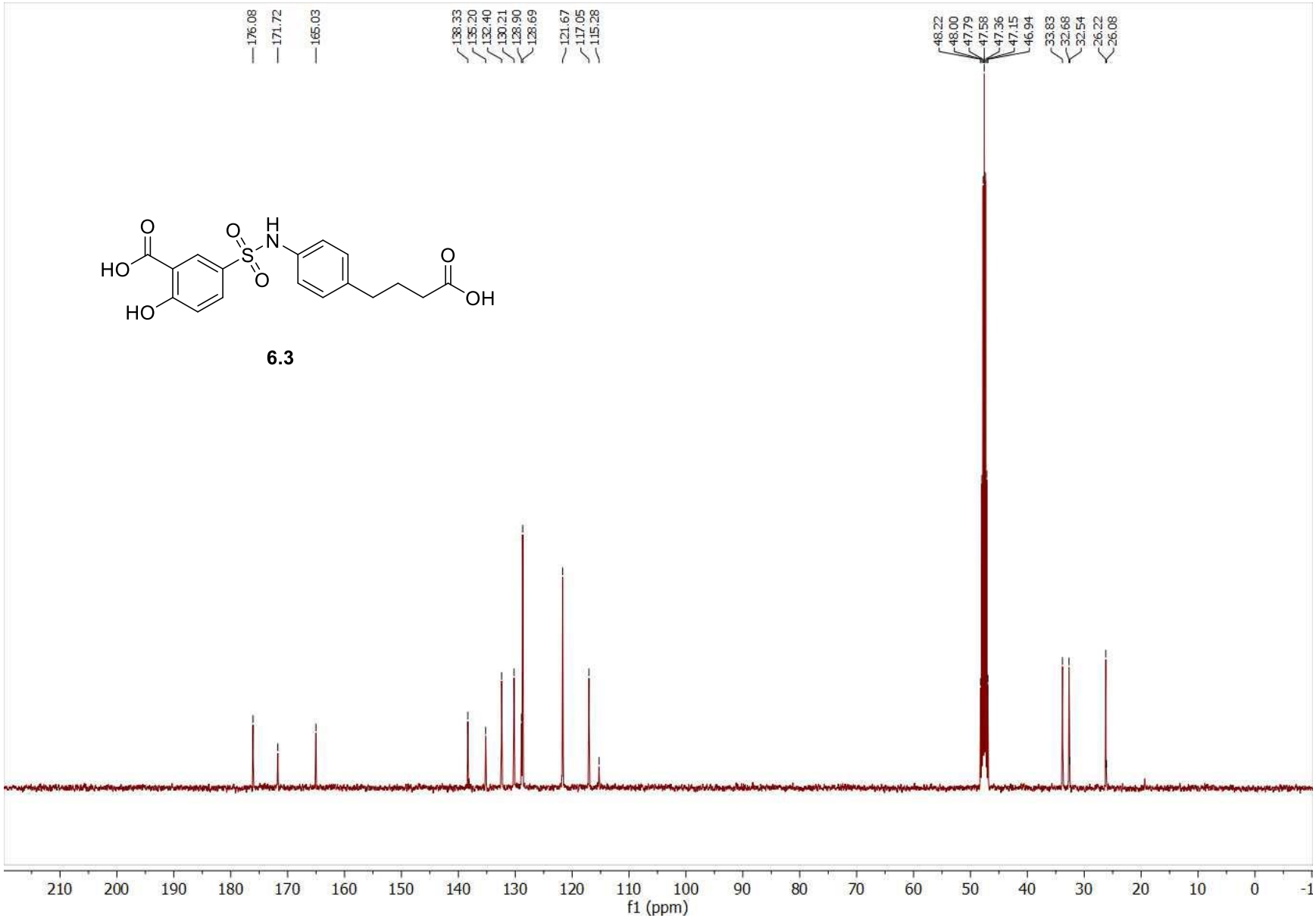

Figure B68: ^{13}C NMR of compound **6.3**.

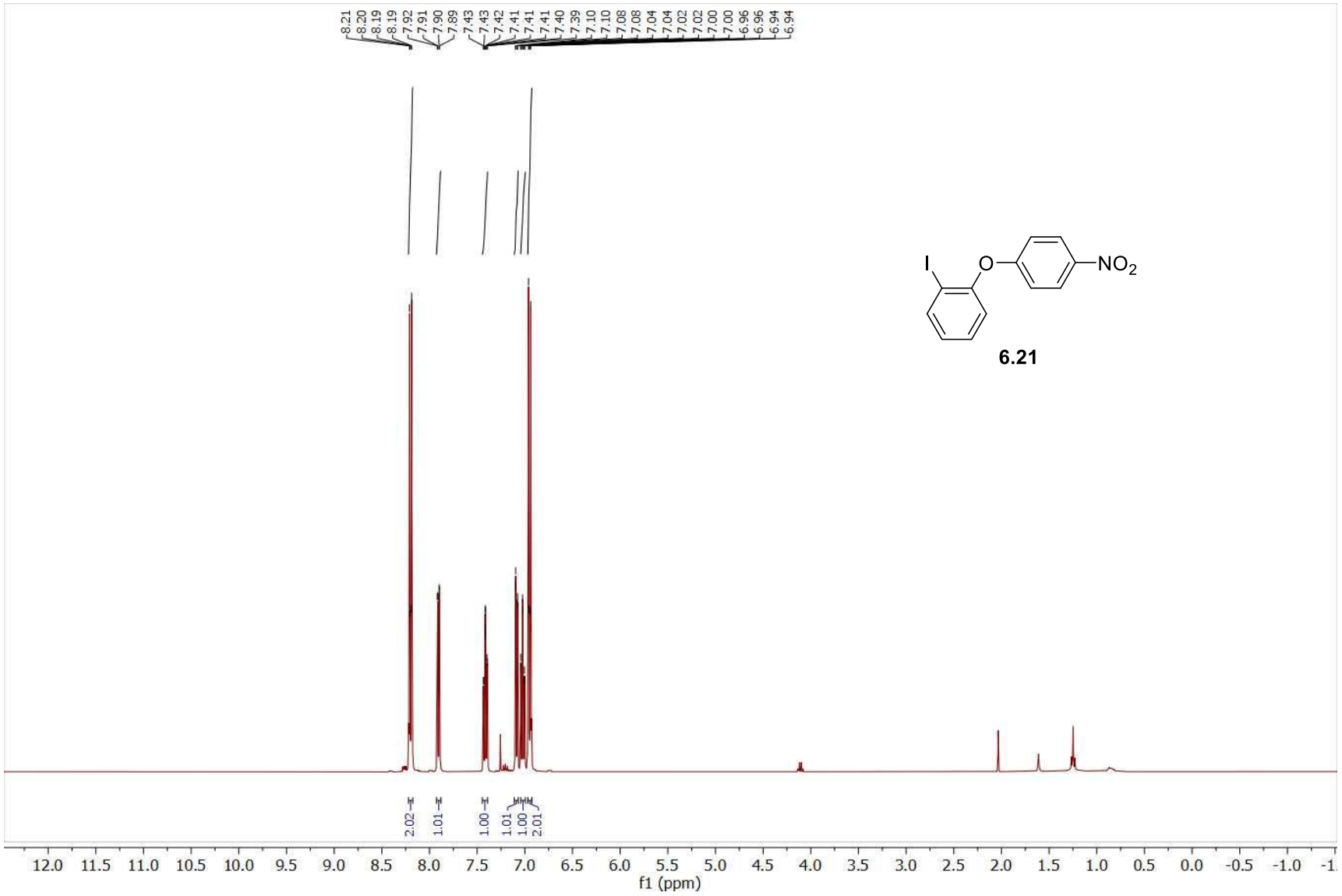

Figure B69: ^{1}H NMR of compound **6.21**.

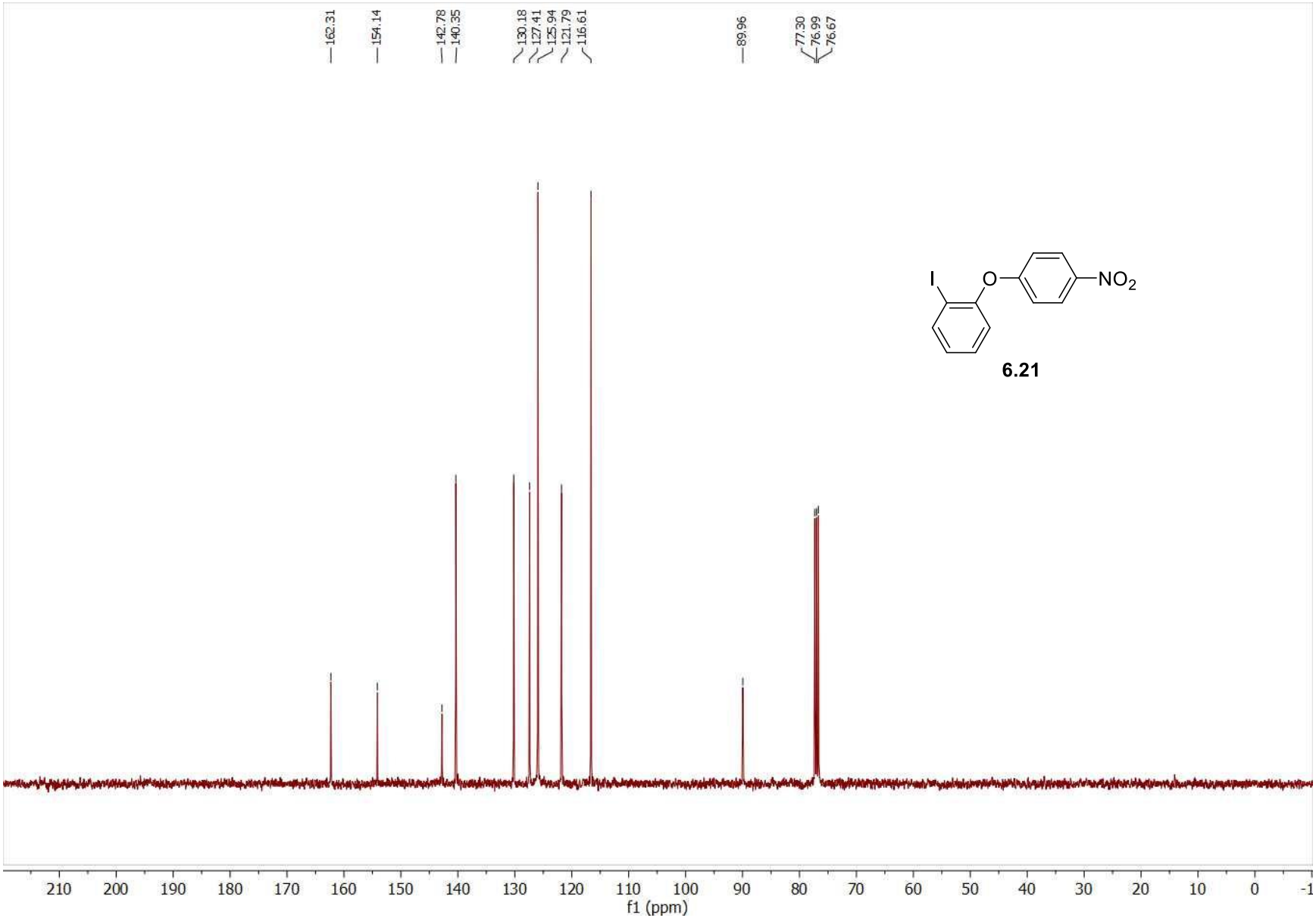

Figure B70: ^{13}C NMR of compound **6.21**.

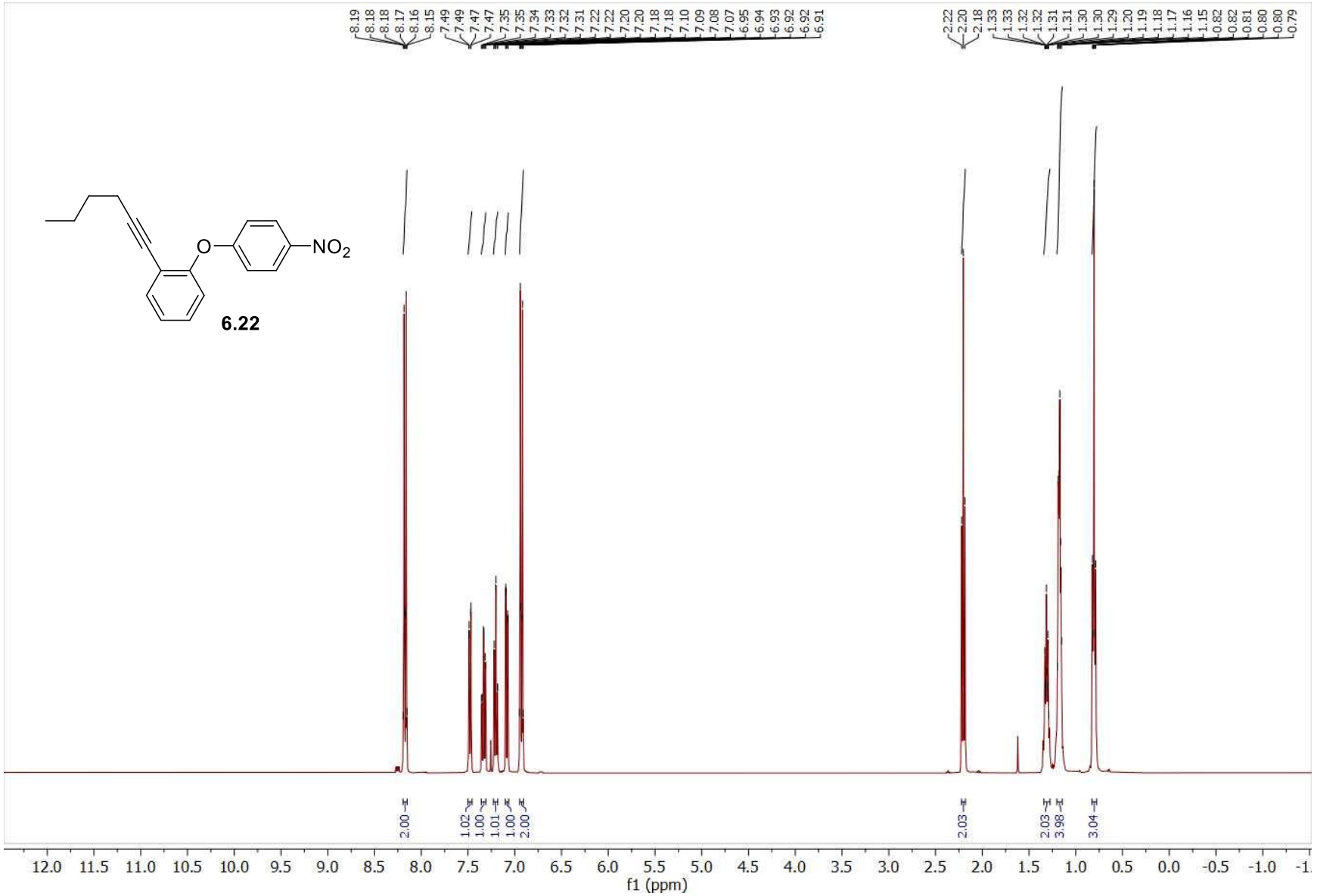

Figure B71: ^{1}H NMR of compound **6.22**.

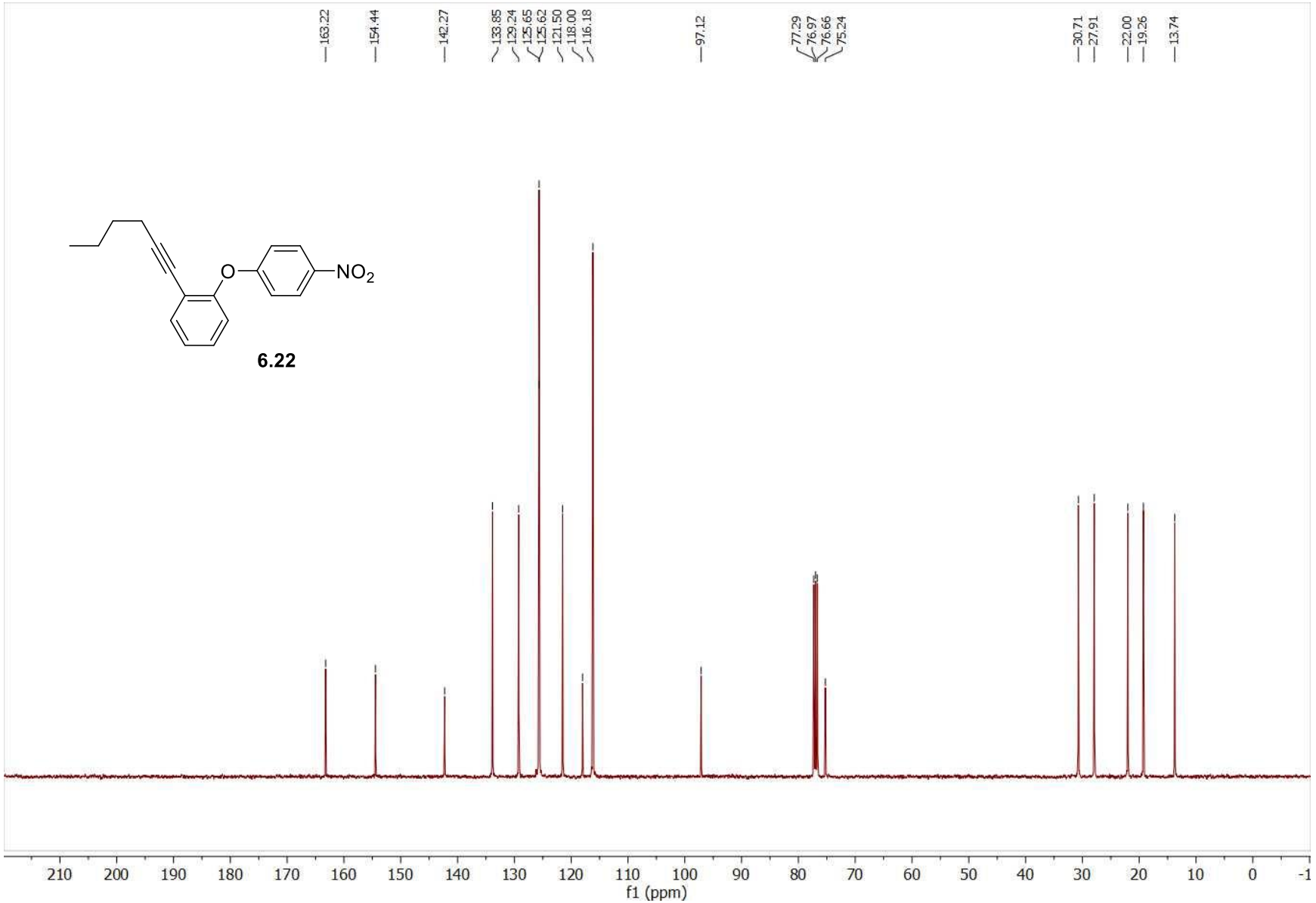

Figure B72: ^{13}C NMR of compound **6.22**.

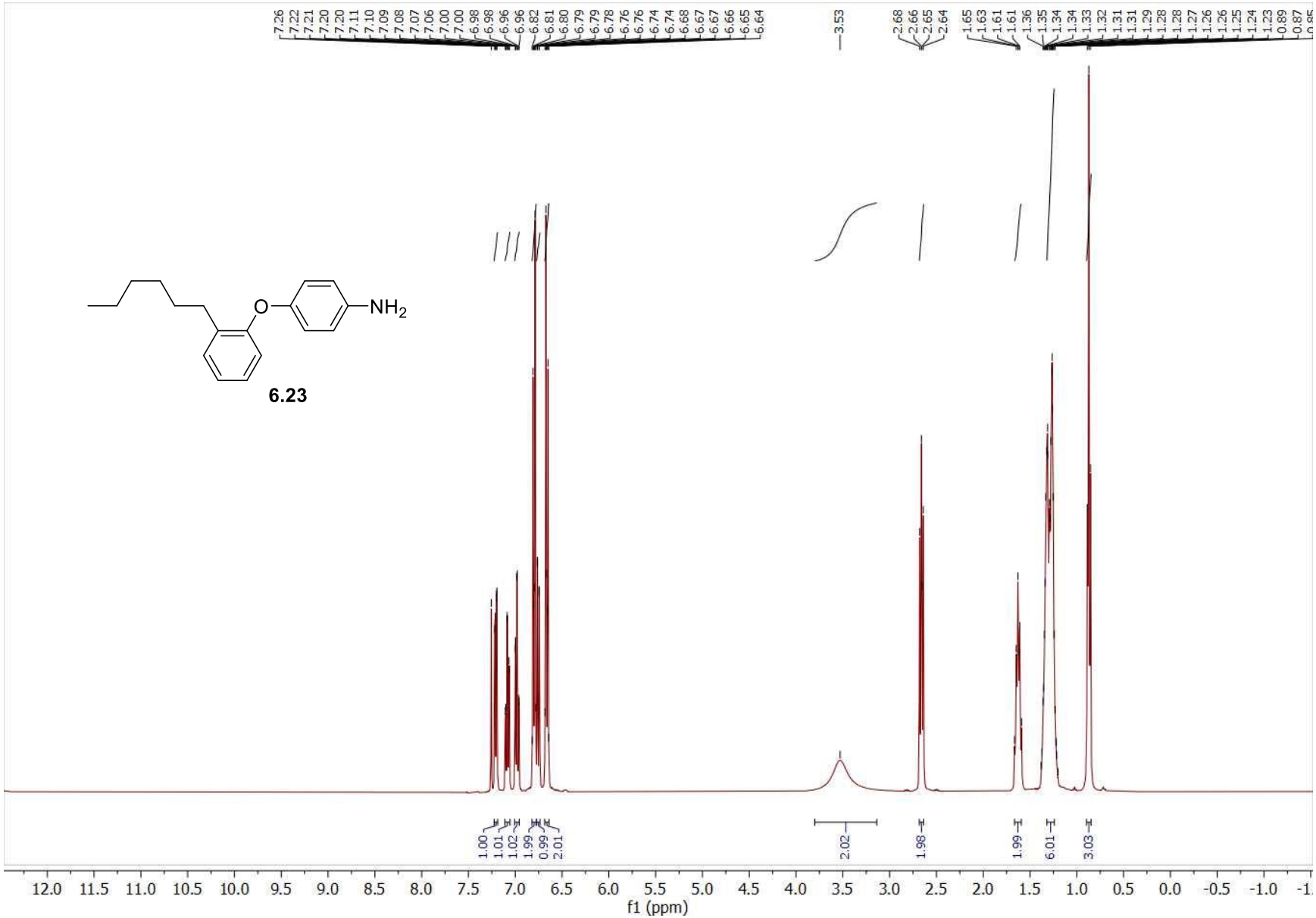

Figure B73: ^{1}H NMR of compound **6.23**.

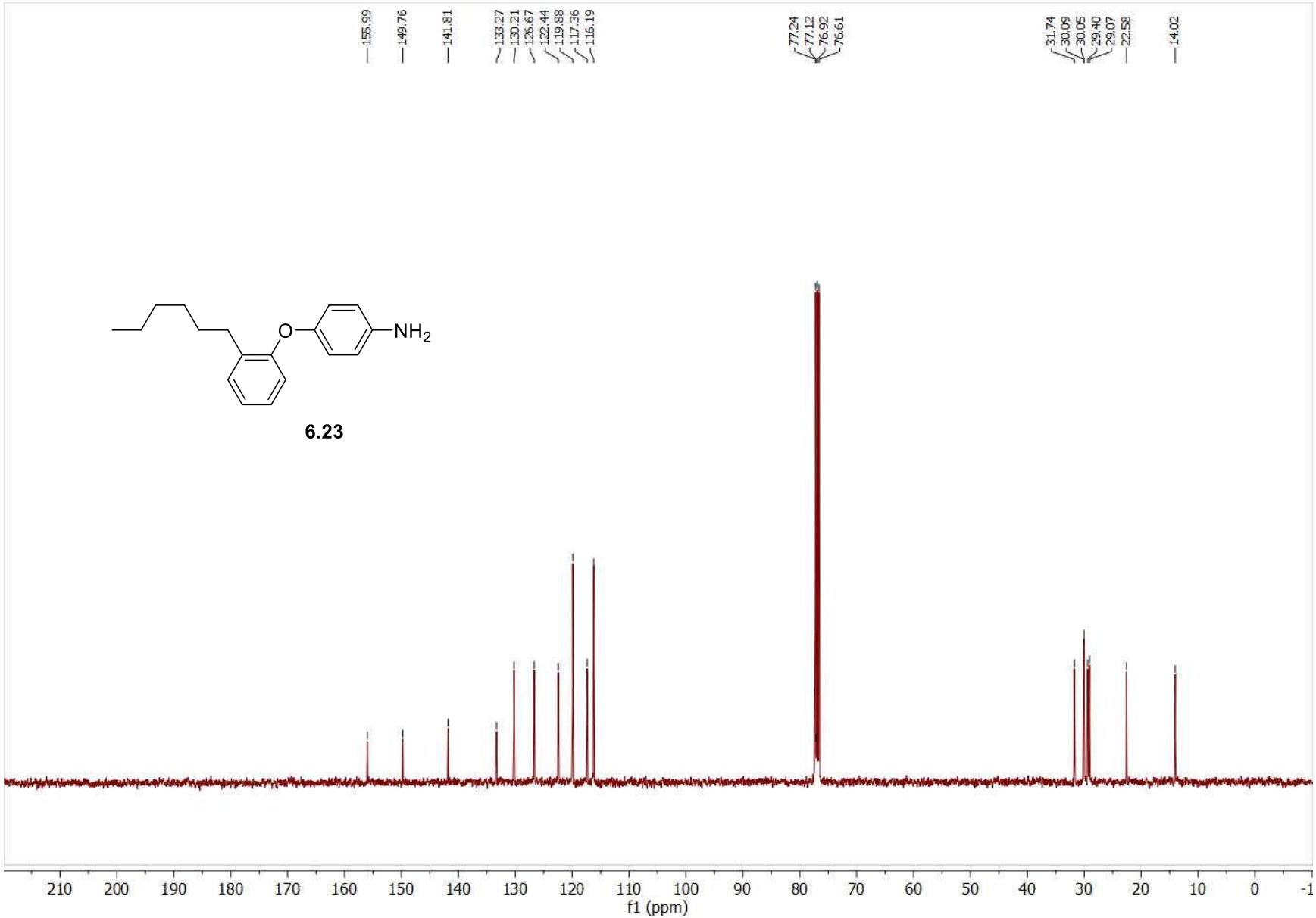

Figure B74: ^{13}C NMR of compound **6.23**.

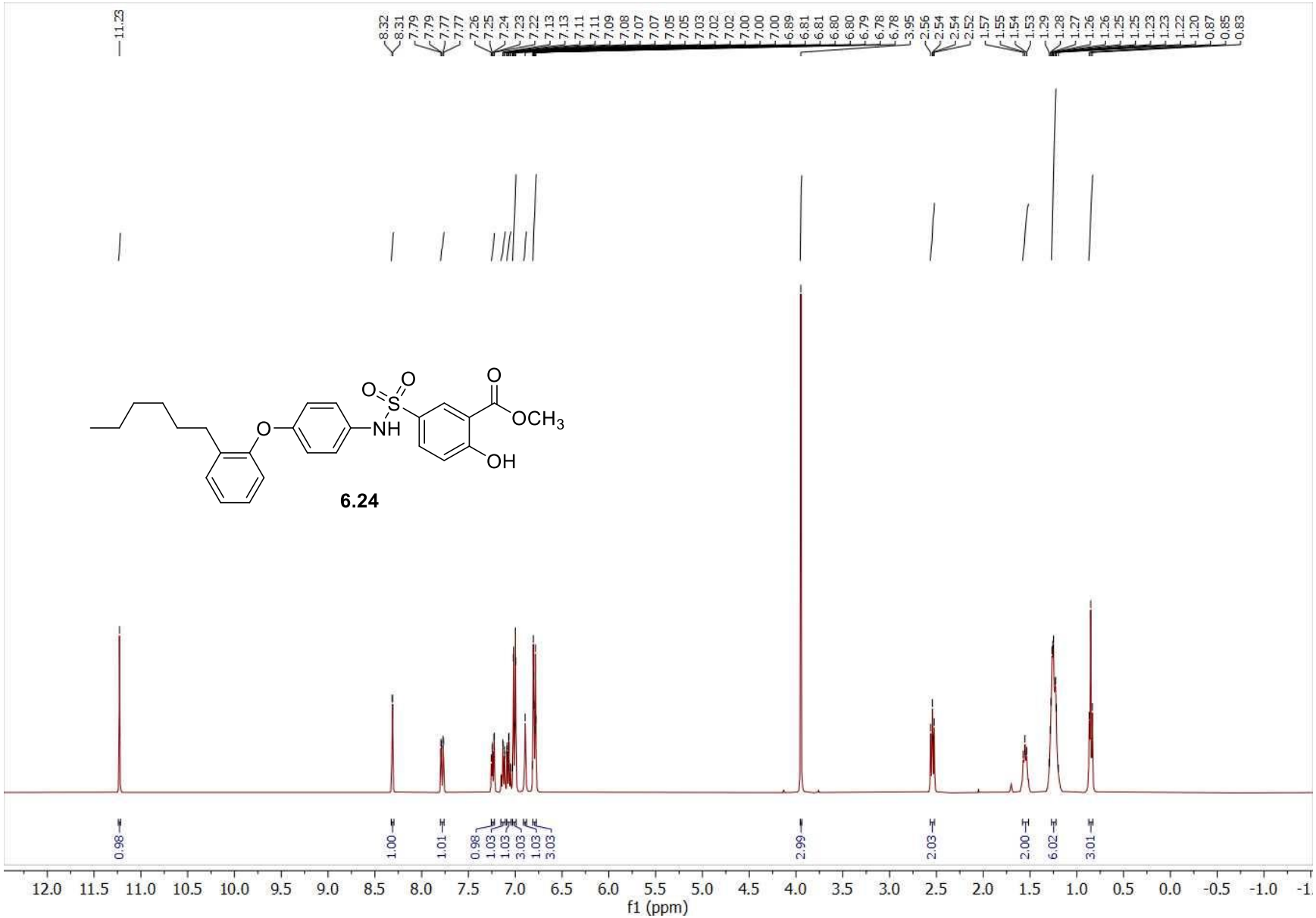

Figure B75: ^{1}H NMR of compound **6.24**.

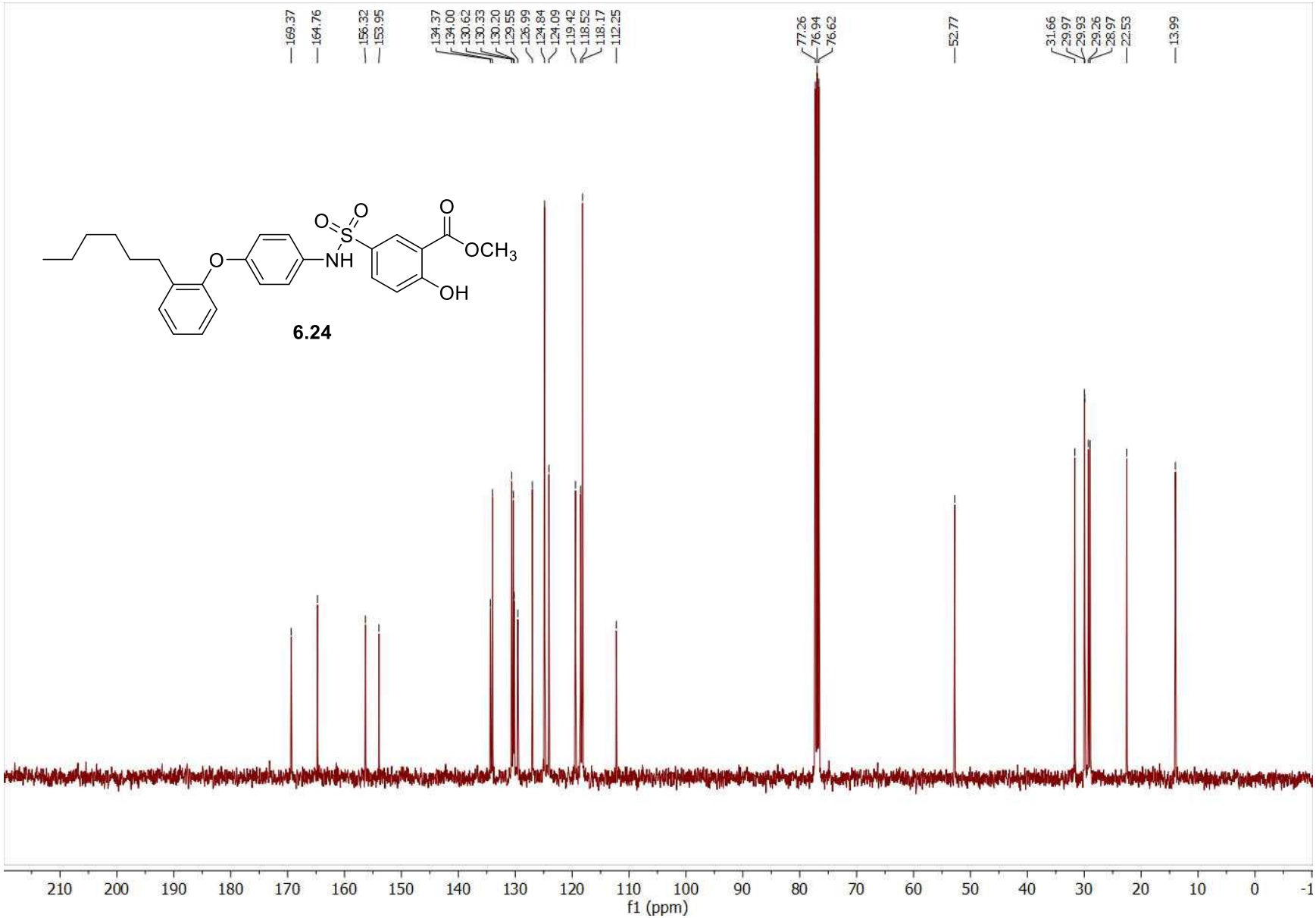

Figure B76: ^{13}C NMR of compound **6.24**.

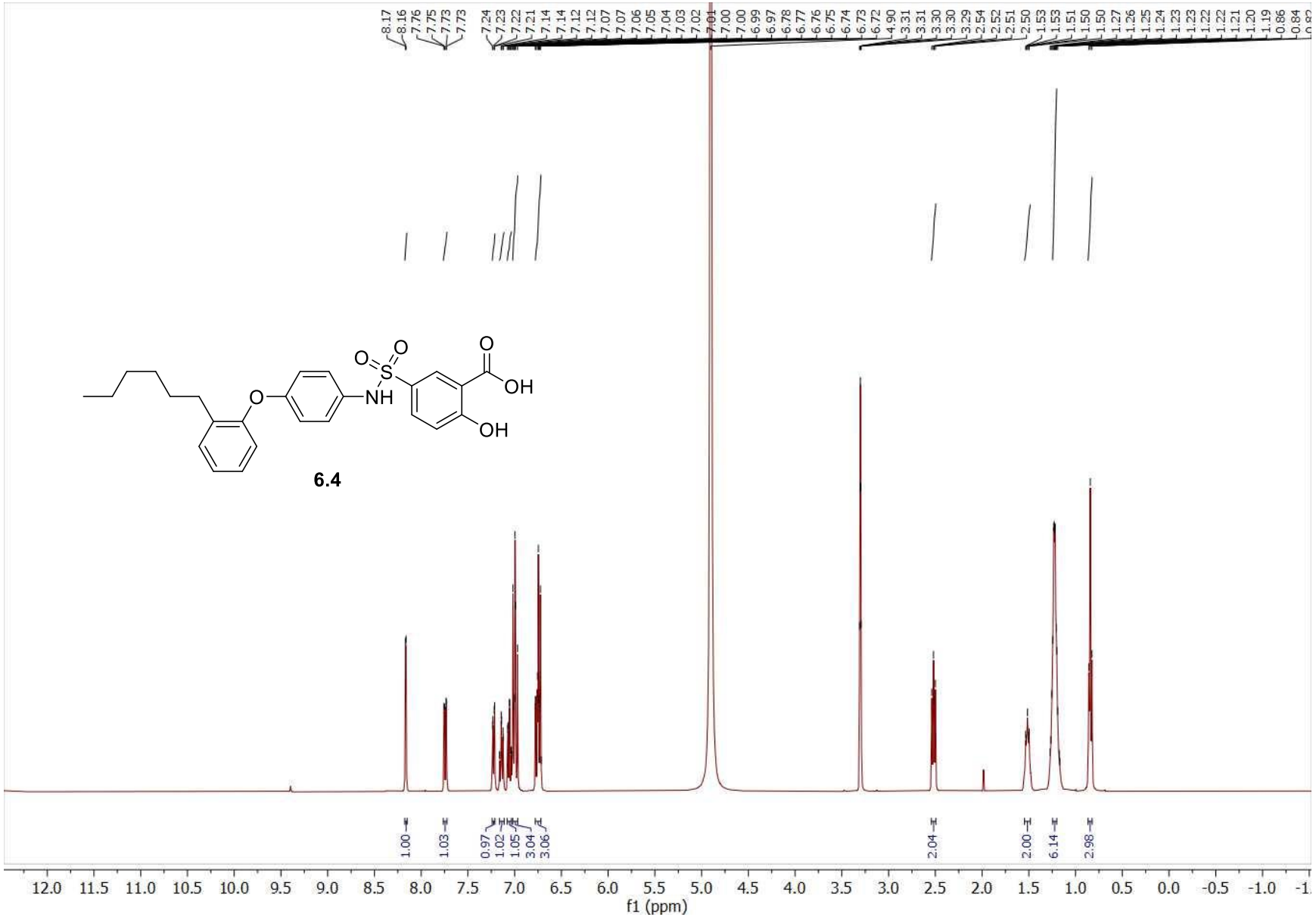

Figure B77: ^{1}H NMR of compound **6.4**.

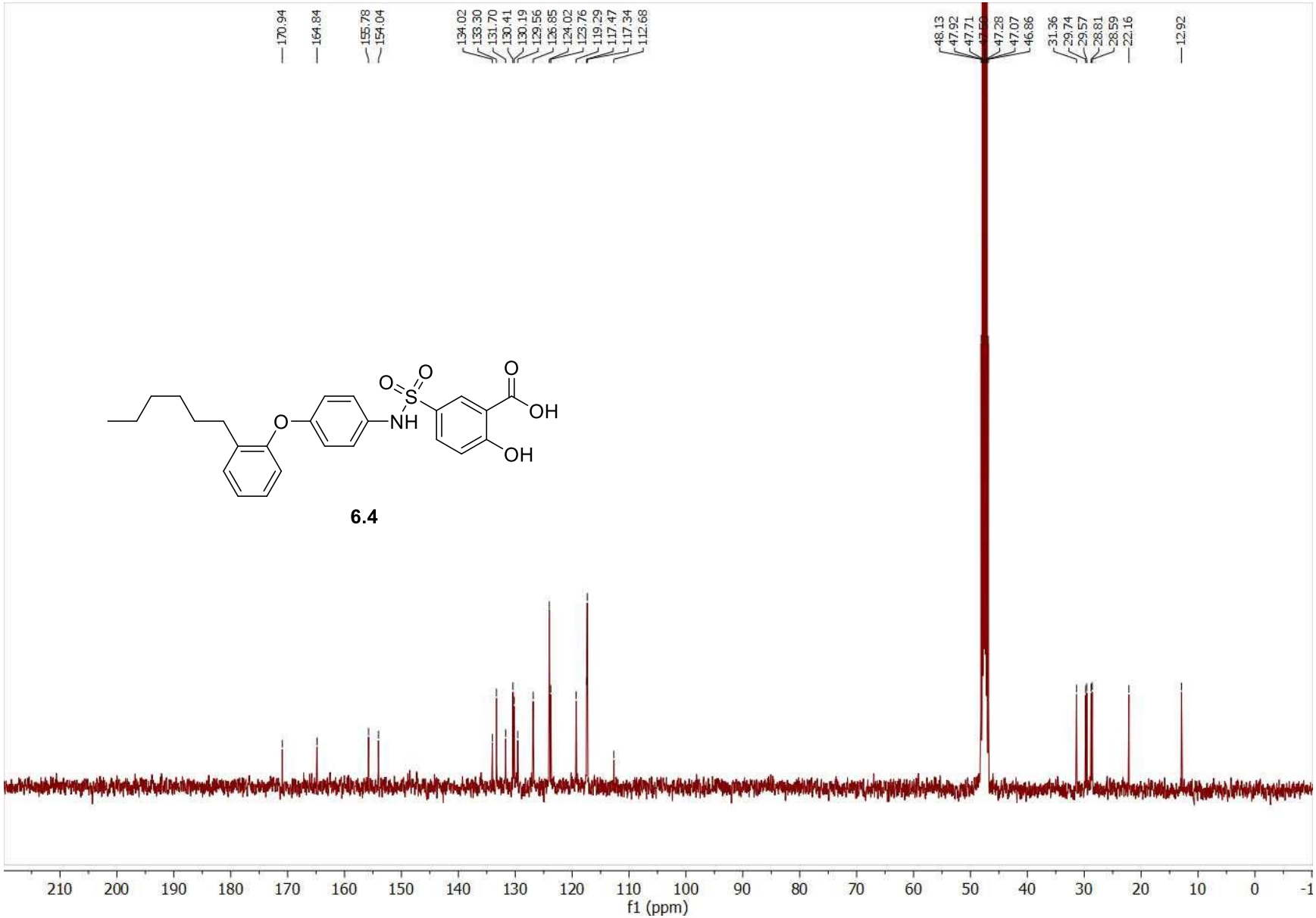

Figure B78: ^{13}C NMR of compound **6.5**.

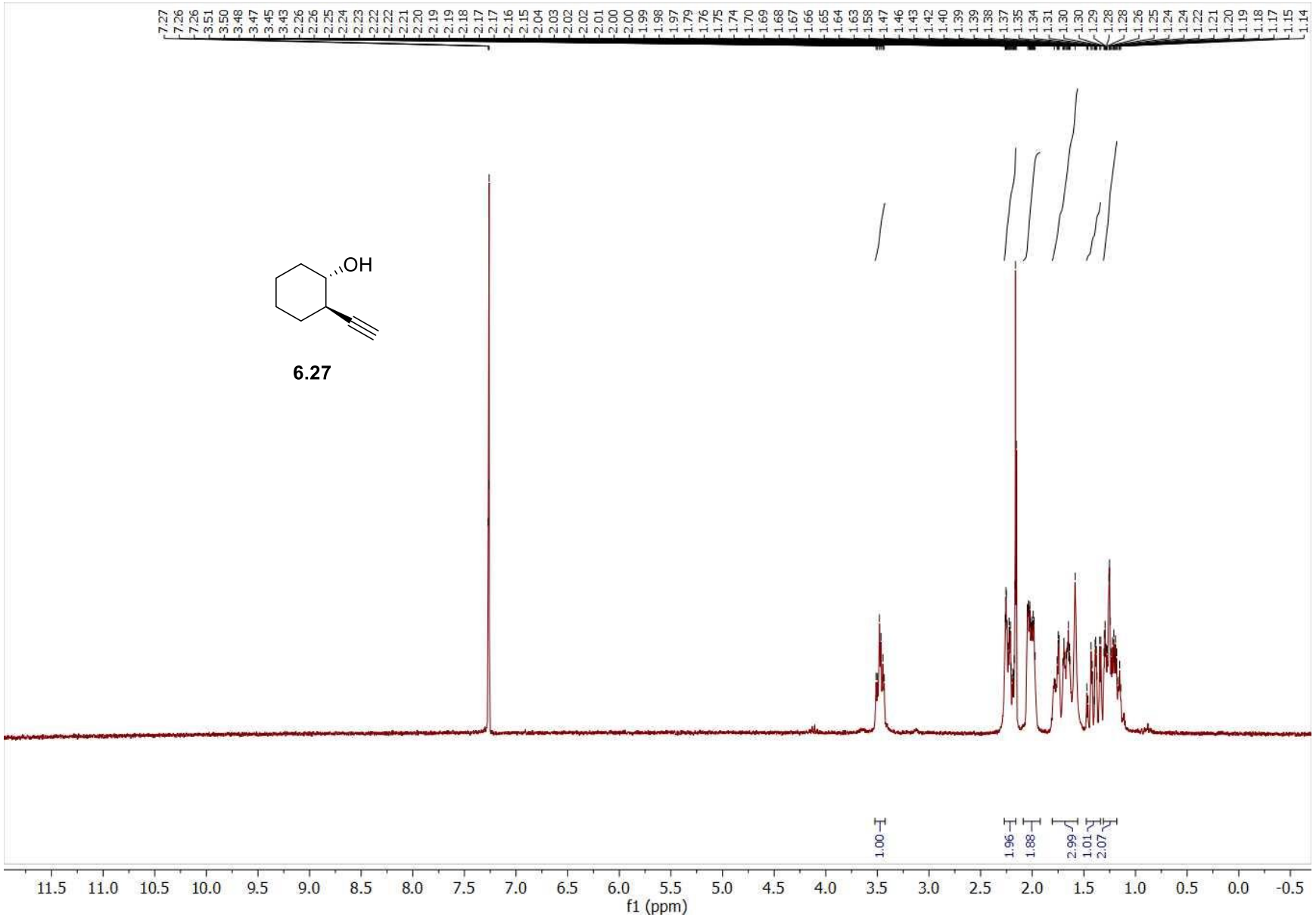

Figure B79: ^{1}H NMR of compound **6.27**.

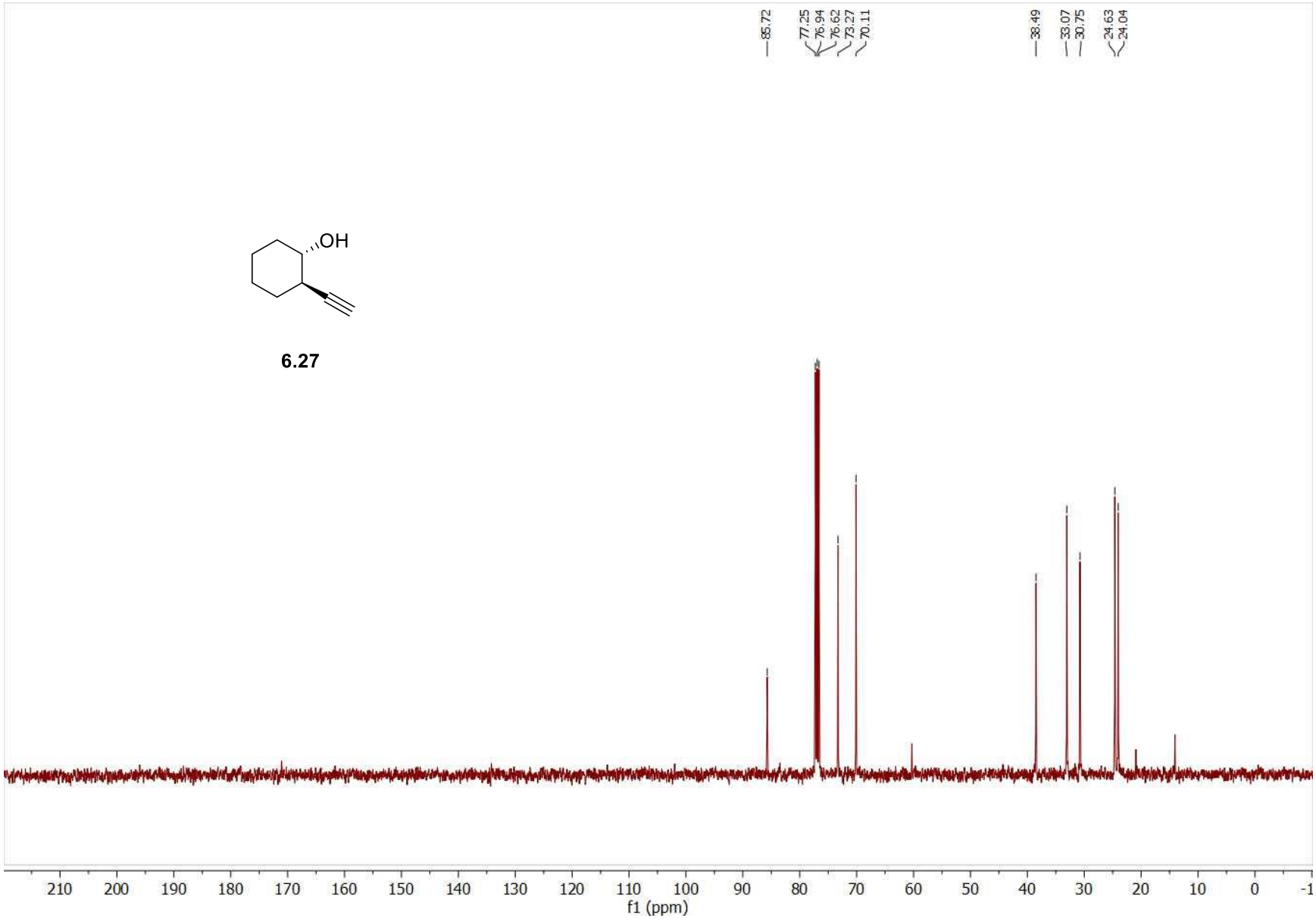

Figure B80: ^{13}C NMR of compound **6.27**.

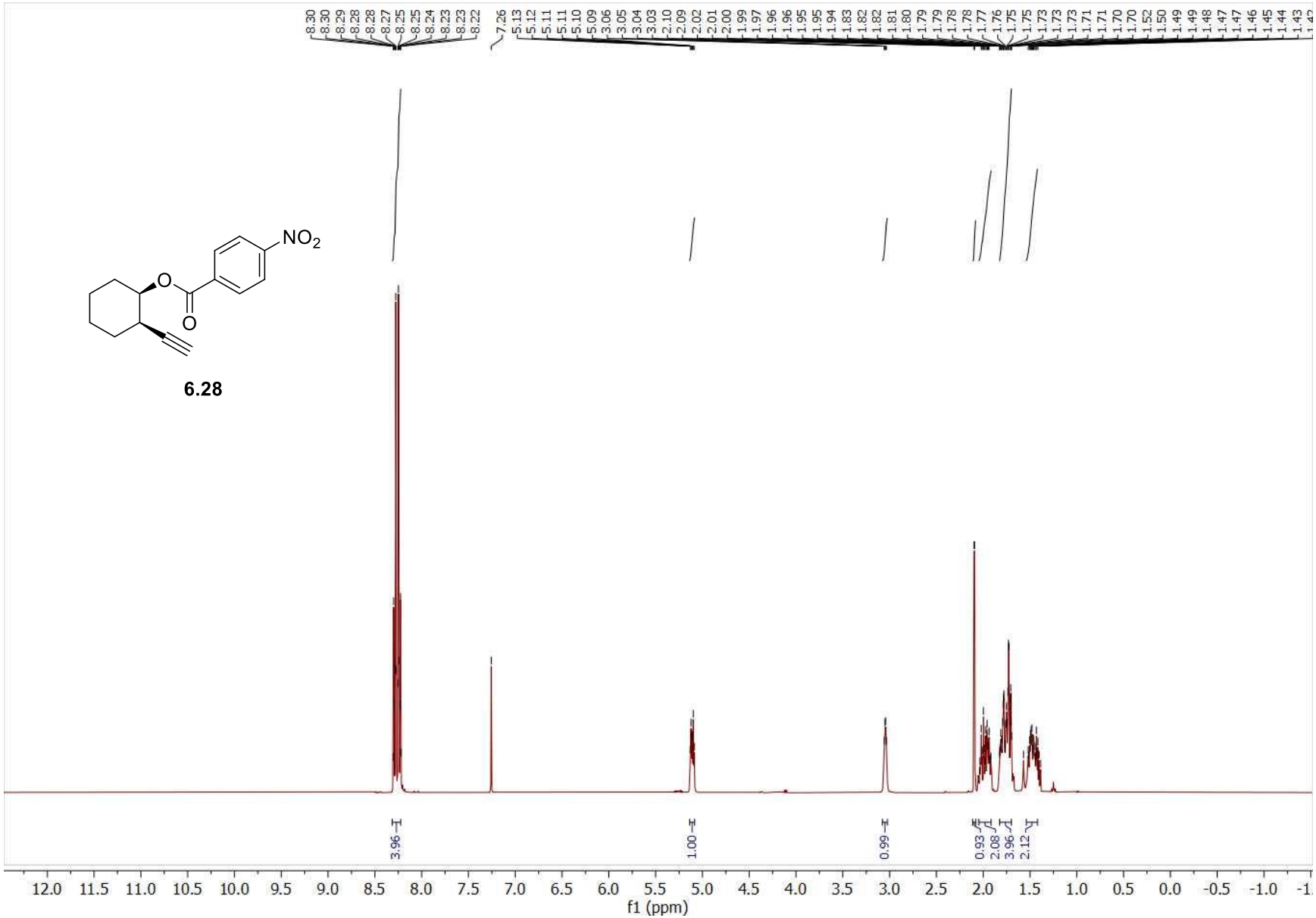

Figure B81: ^{1}H NMR of compound **6.28**.

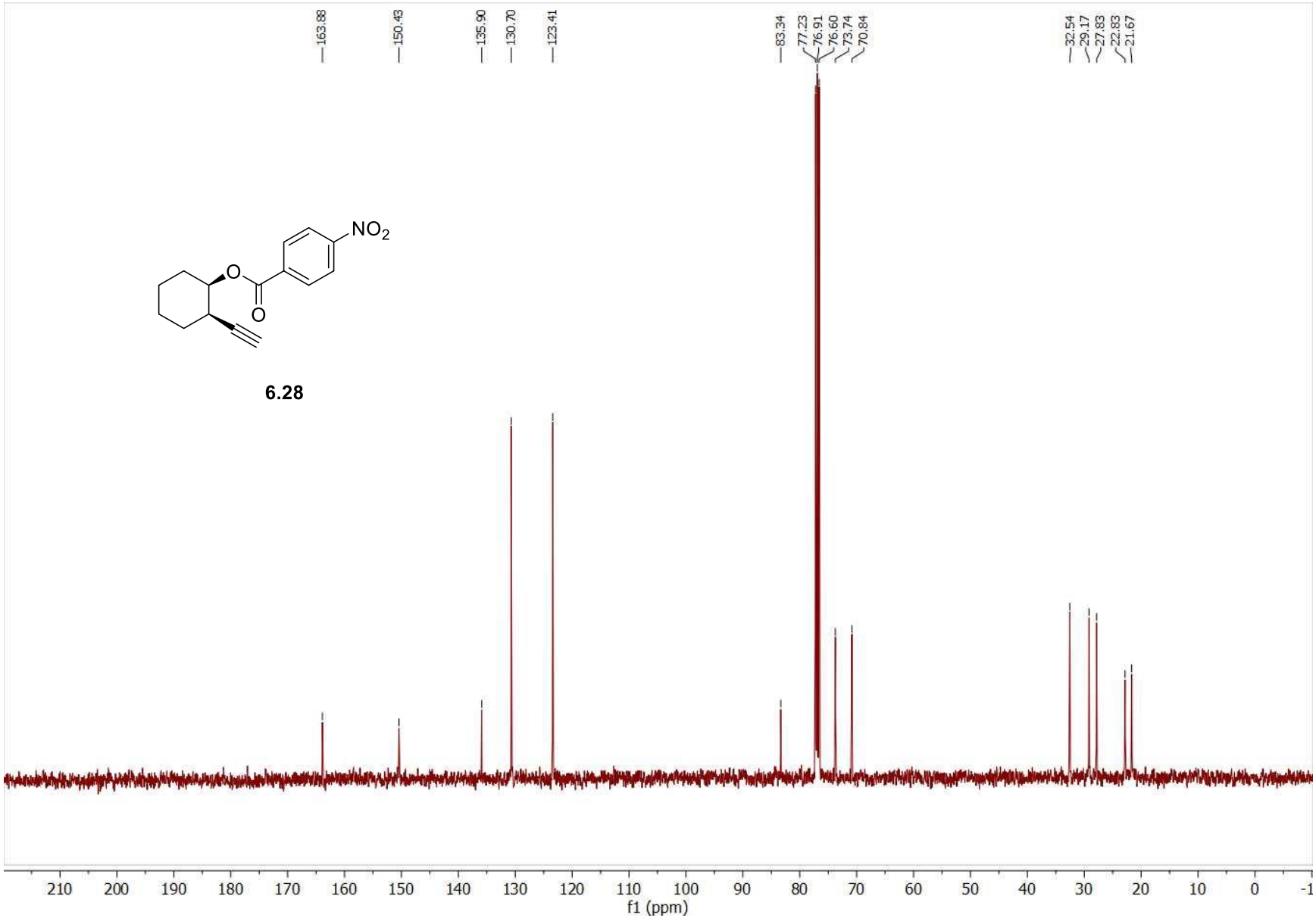

Figure B82: ^{13}C NMR of compound **6.28**.

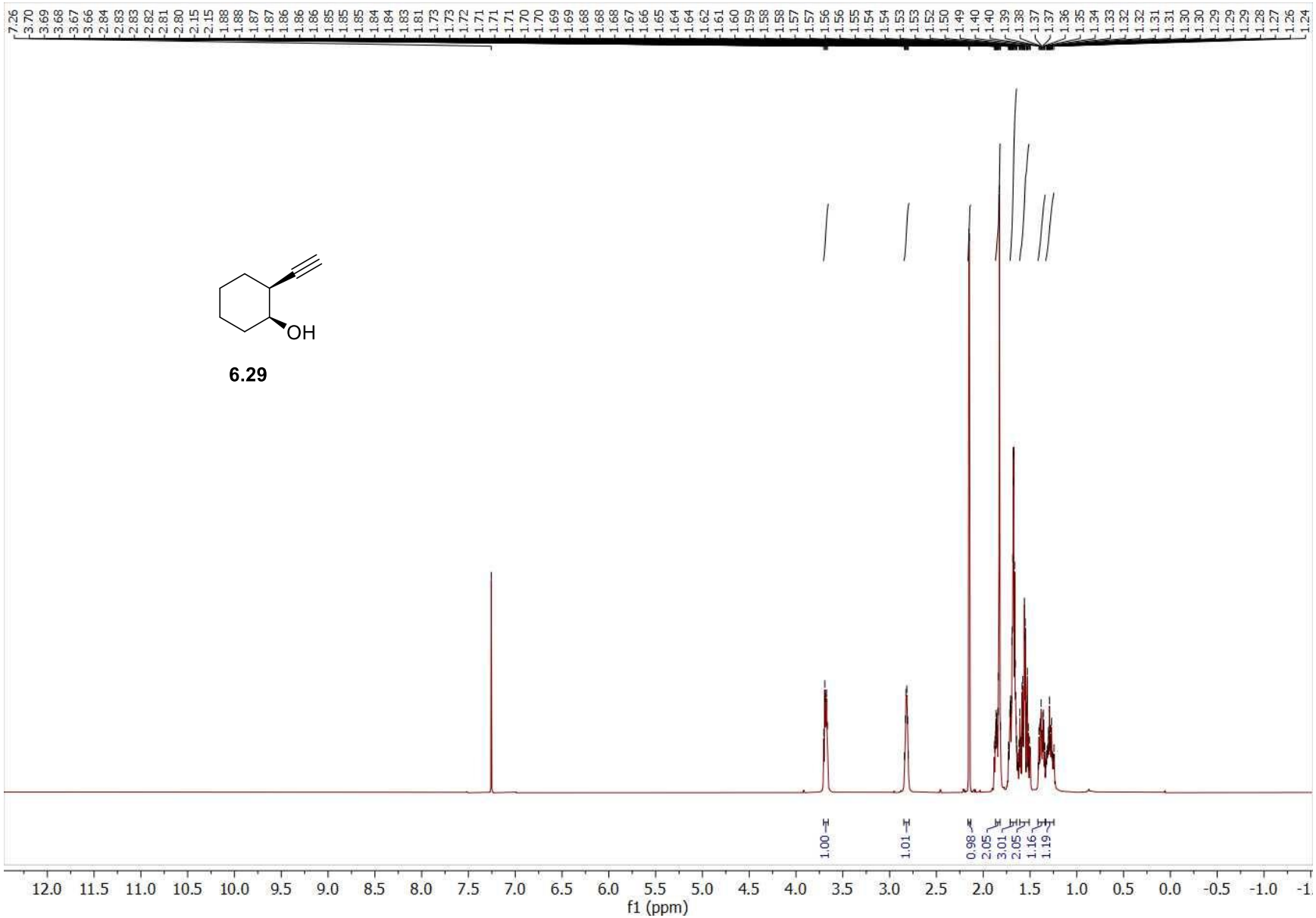

Figure B83: ^{1}H NMR of compound **6.29**.

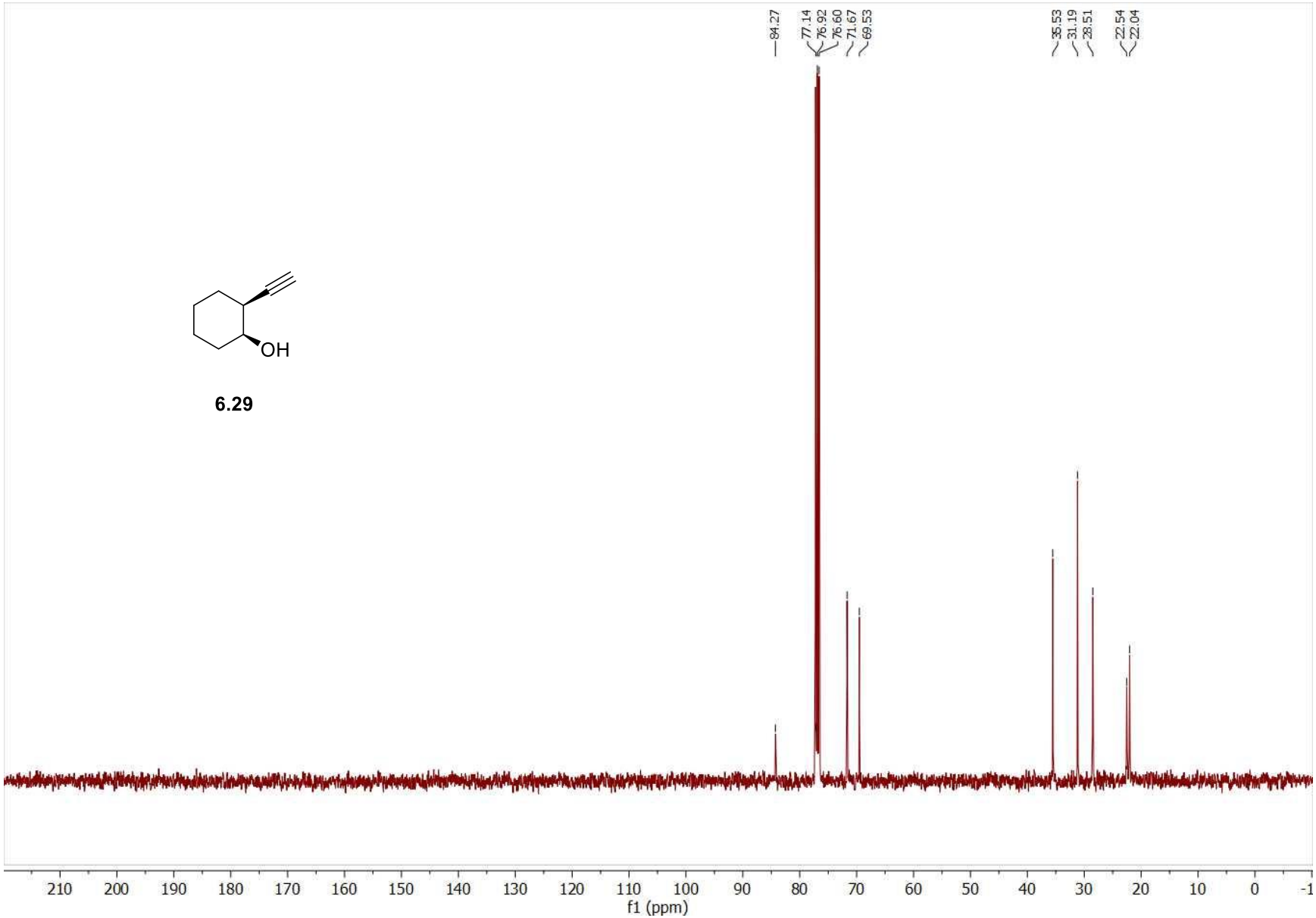

Figure B84: ^{13}C NMR of compound **6.29**.

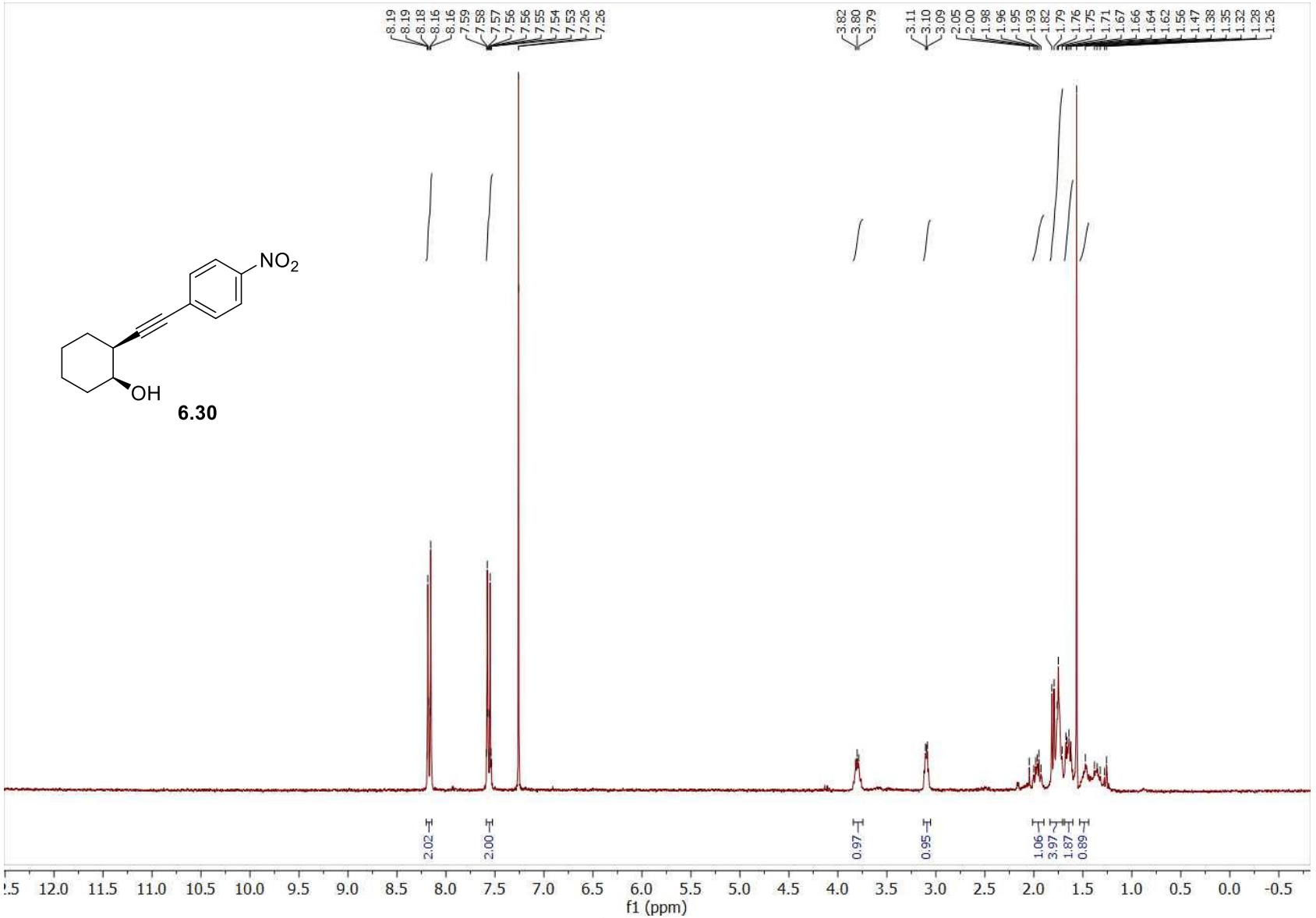

Figure B85: ^{1}H NMR of compound **6.30**.

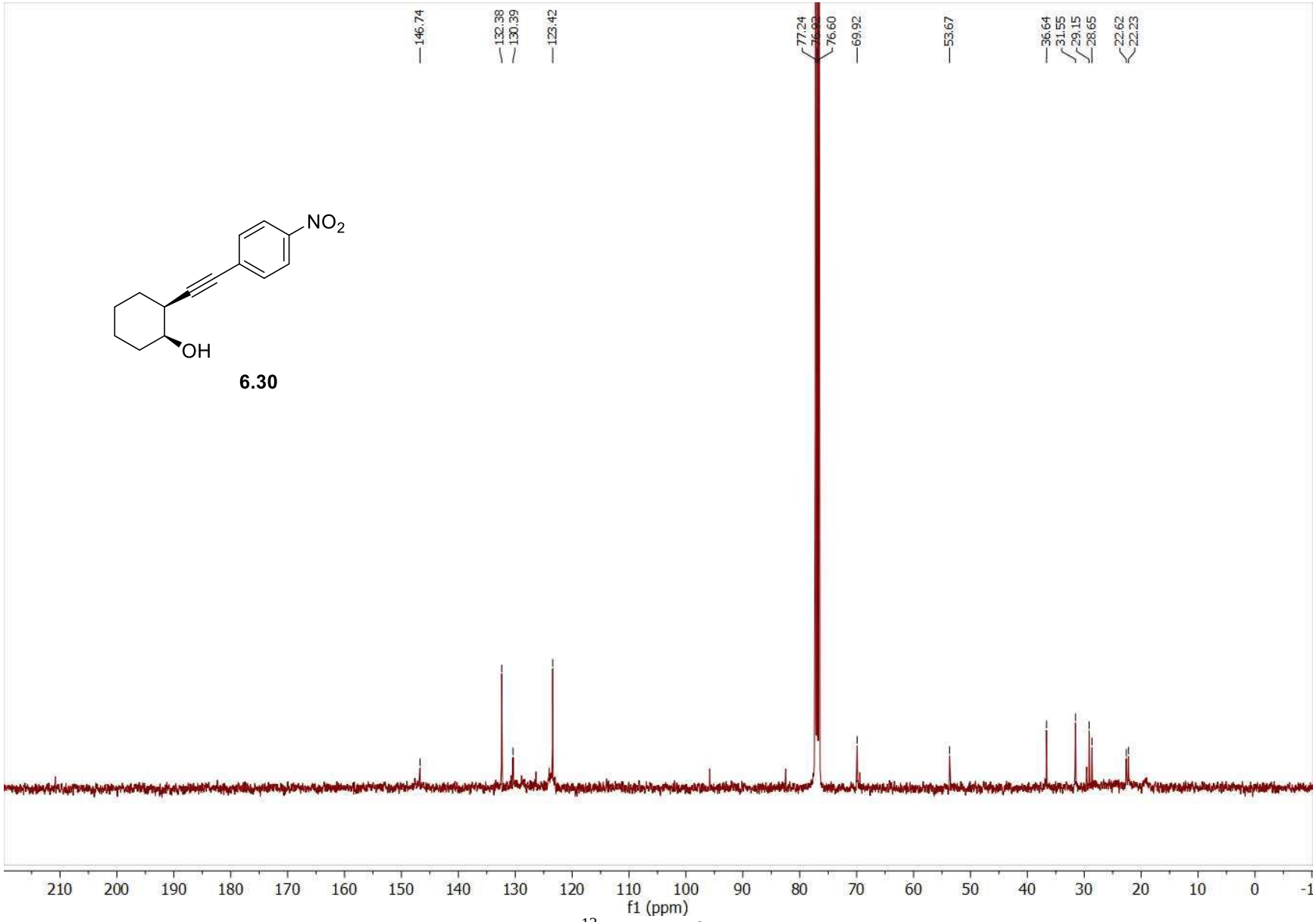

Figure B86: ^{13}C NMR of compound **6.30**

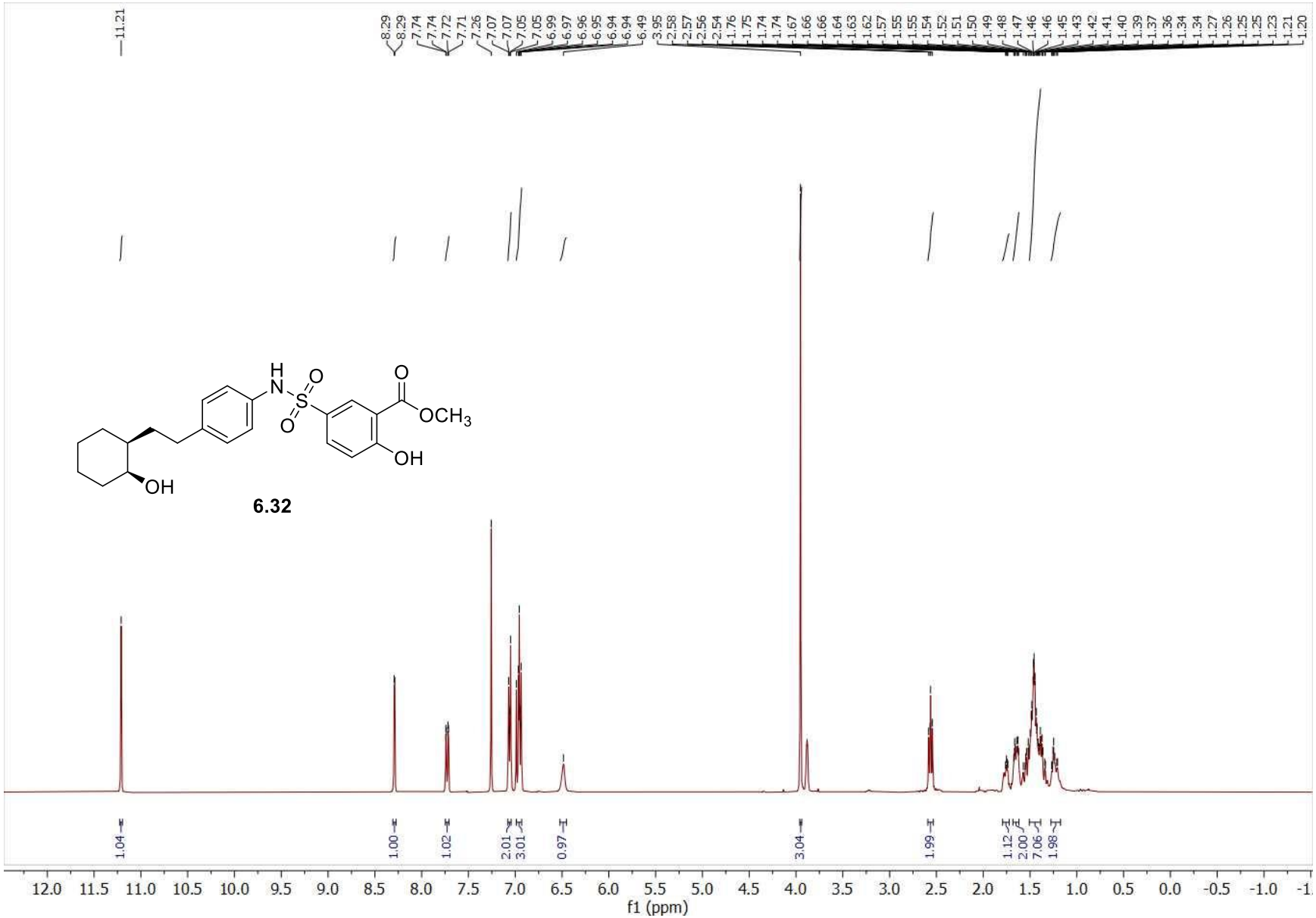

Figure B87: ^{1}H NMR of compound **6.32**.

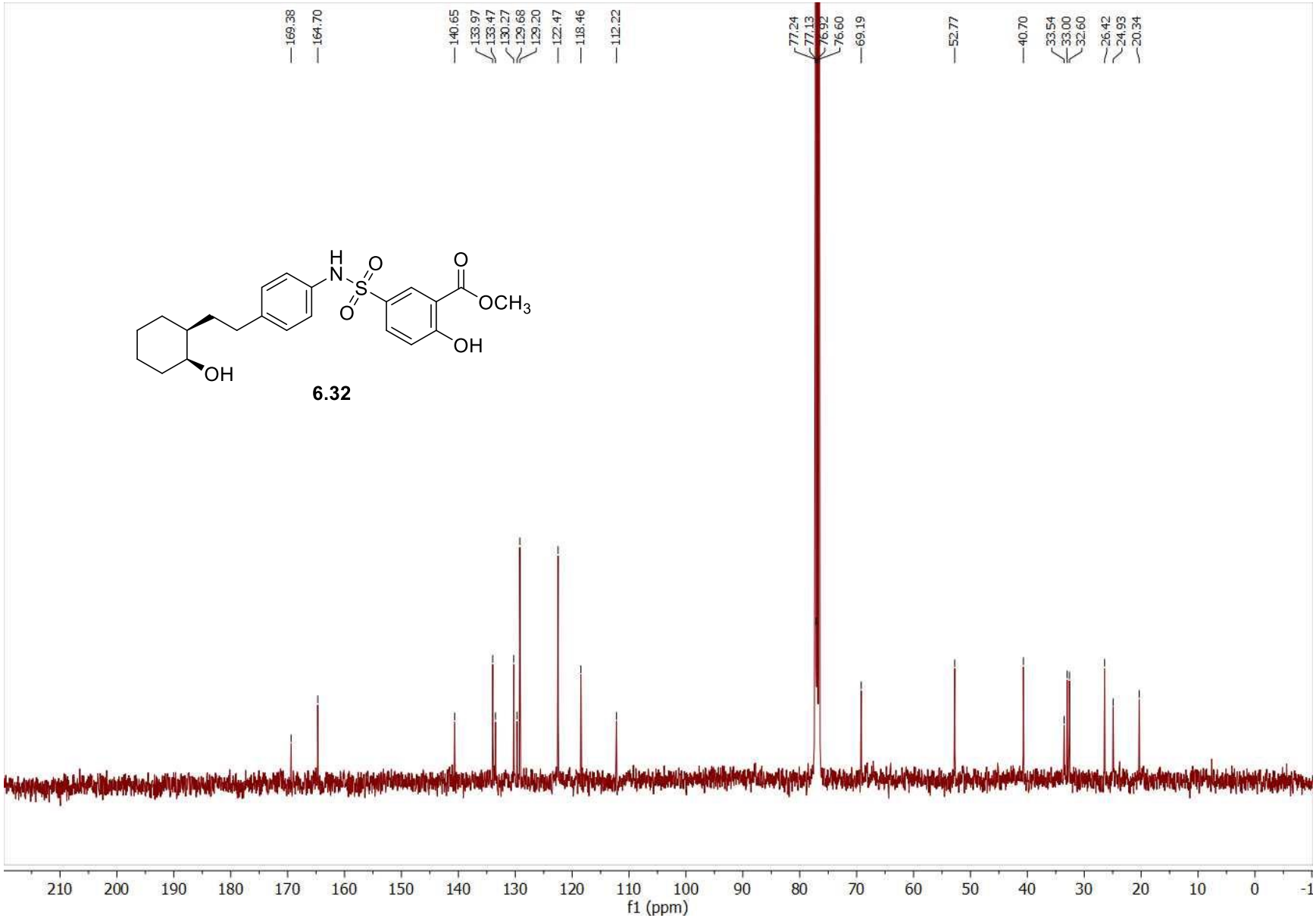

Figure B88: ^{13}C NMR of compound **6.32**.

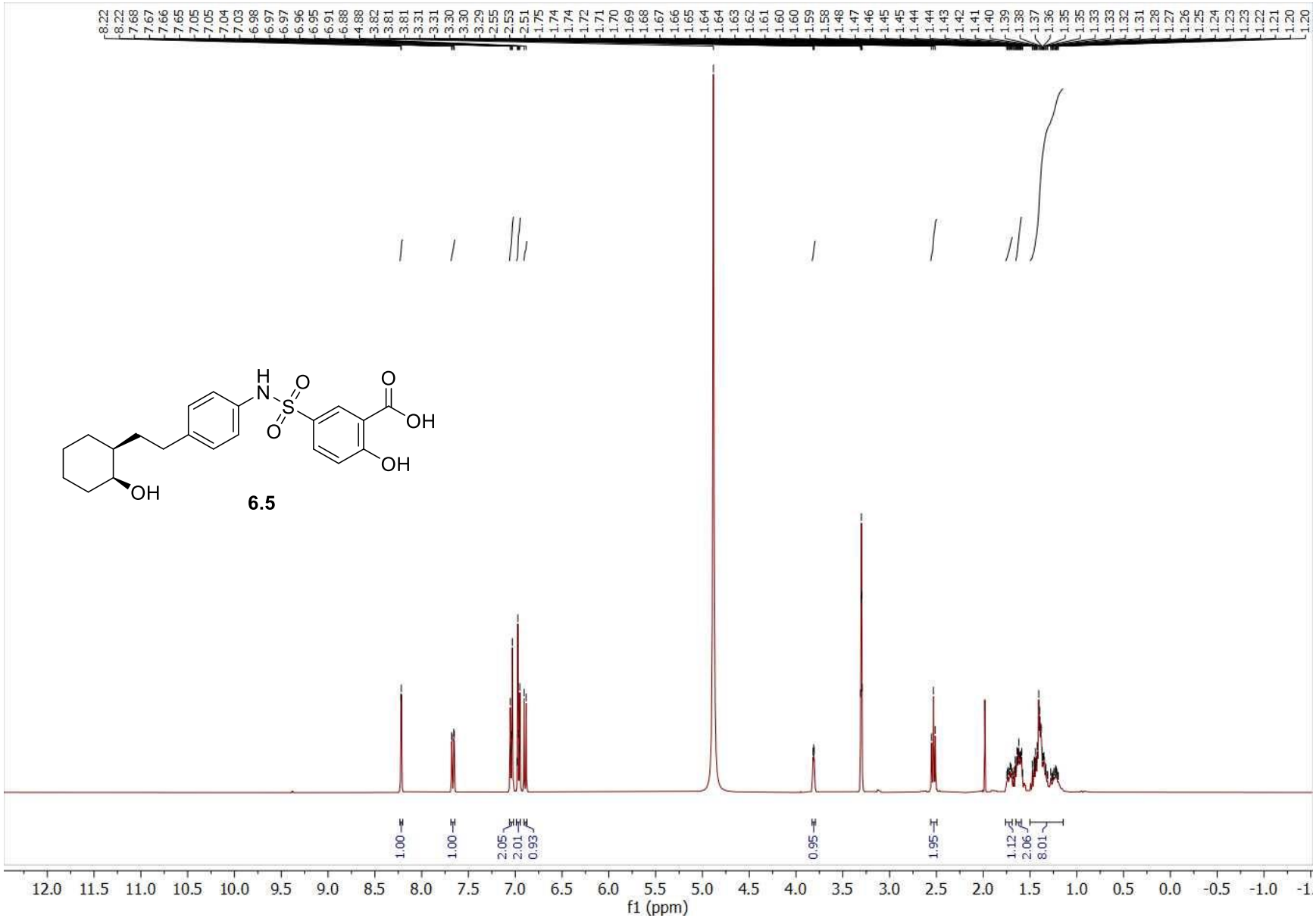

Figure B89: ^{1}H NMR of compound **6.5**.

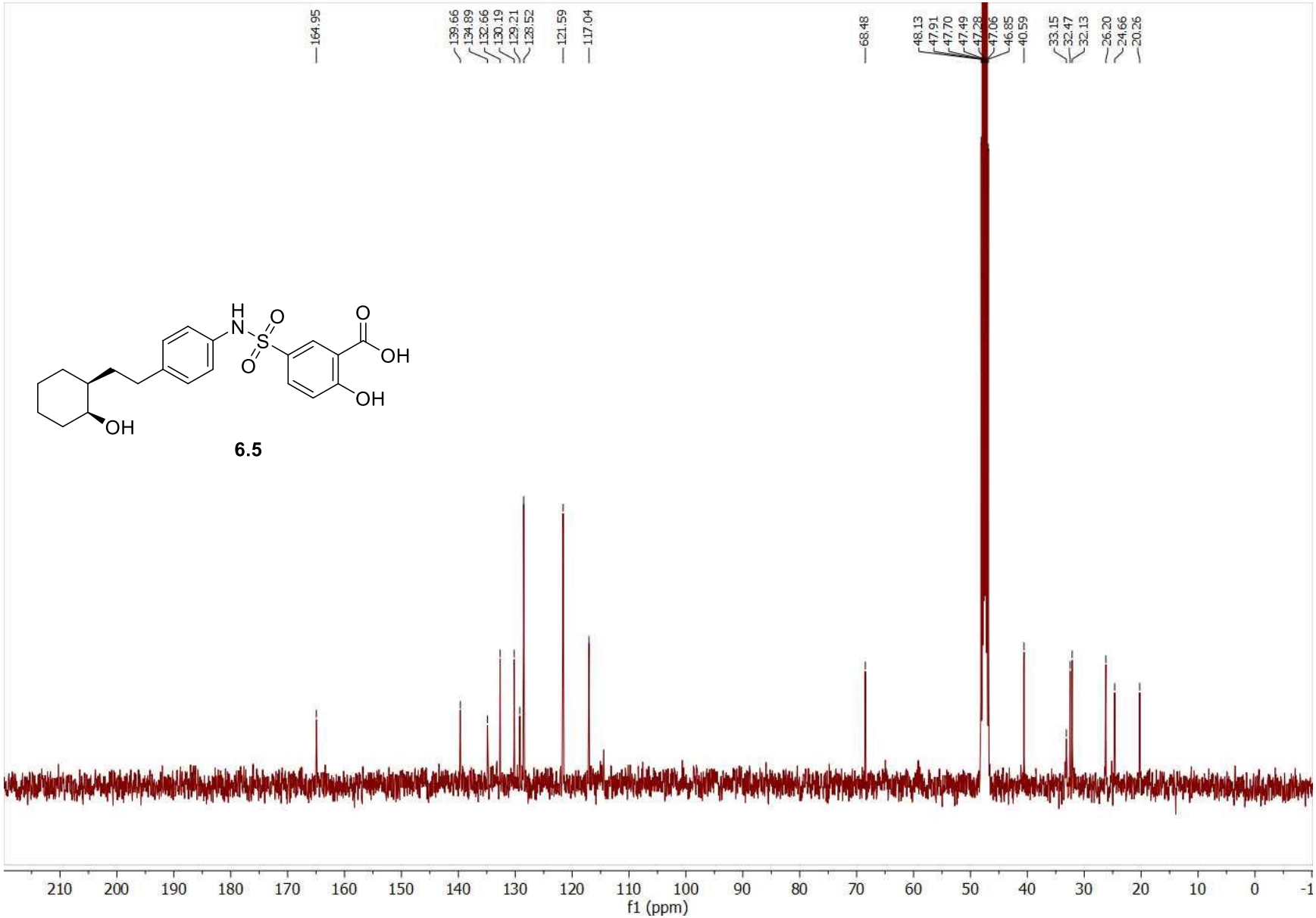

Figure B90: ^{13}C NMR of compound **6.5**.

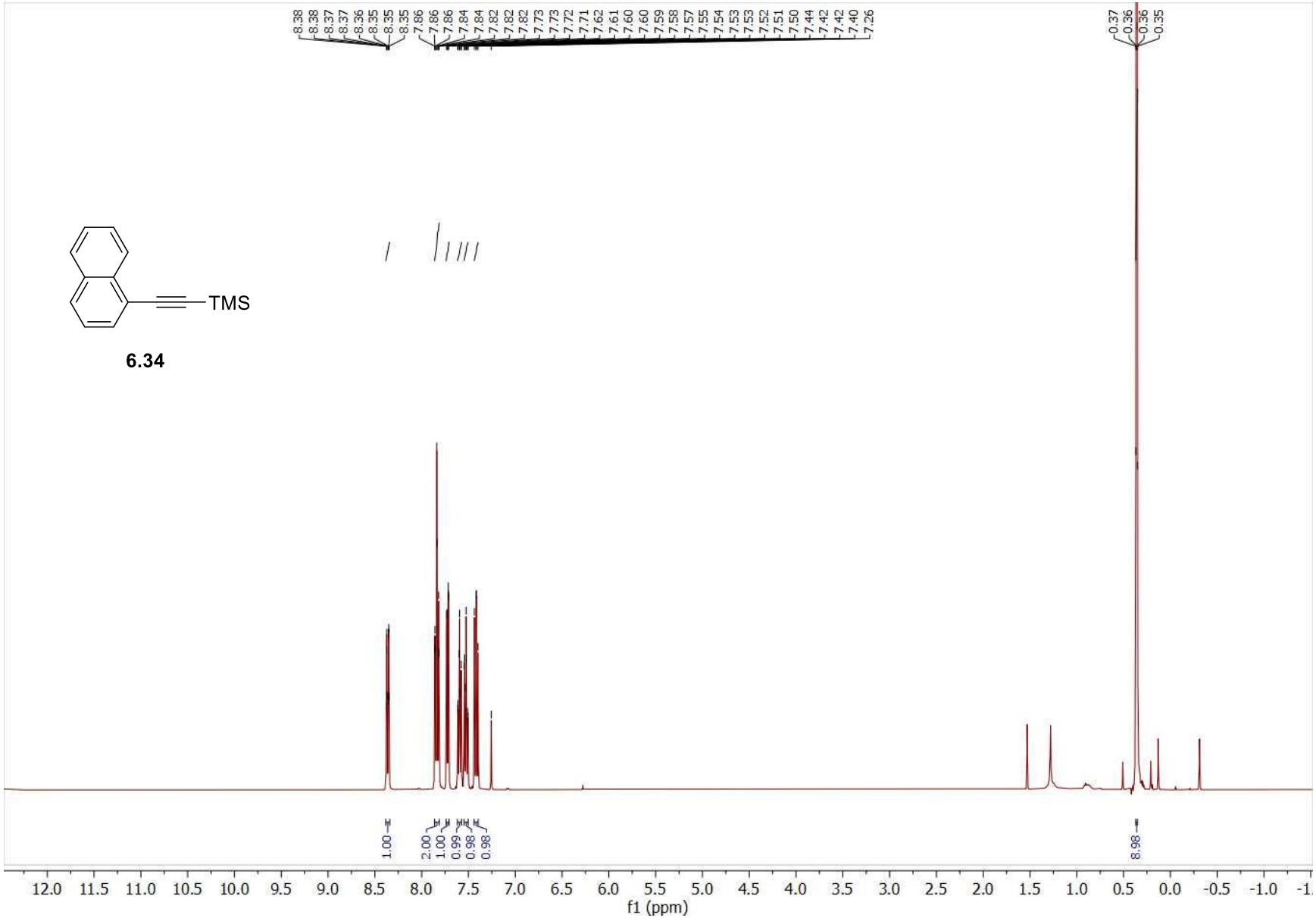

Figure B91: ^{1}H NMR of compound **6.34**.

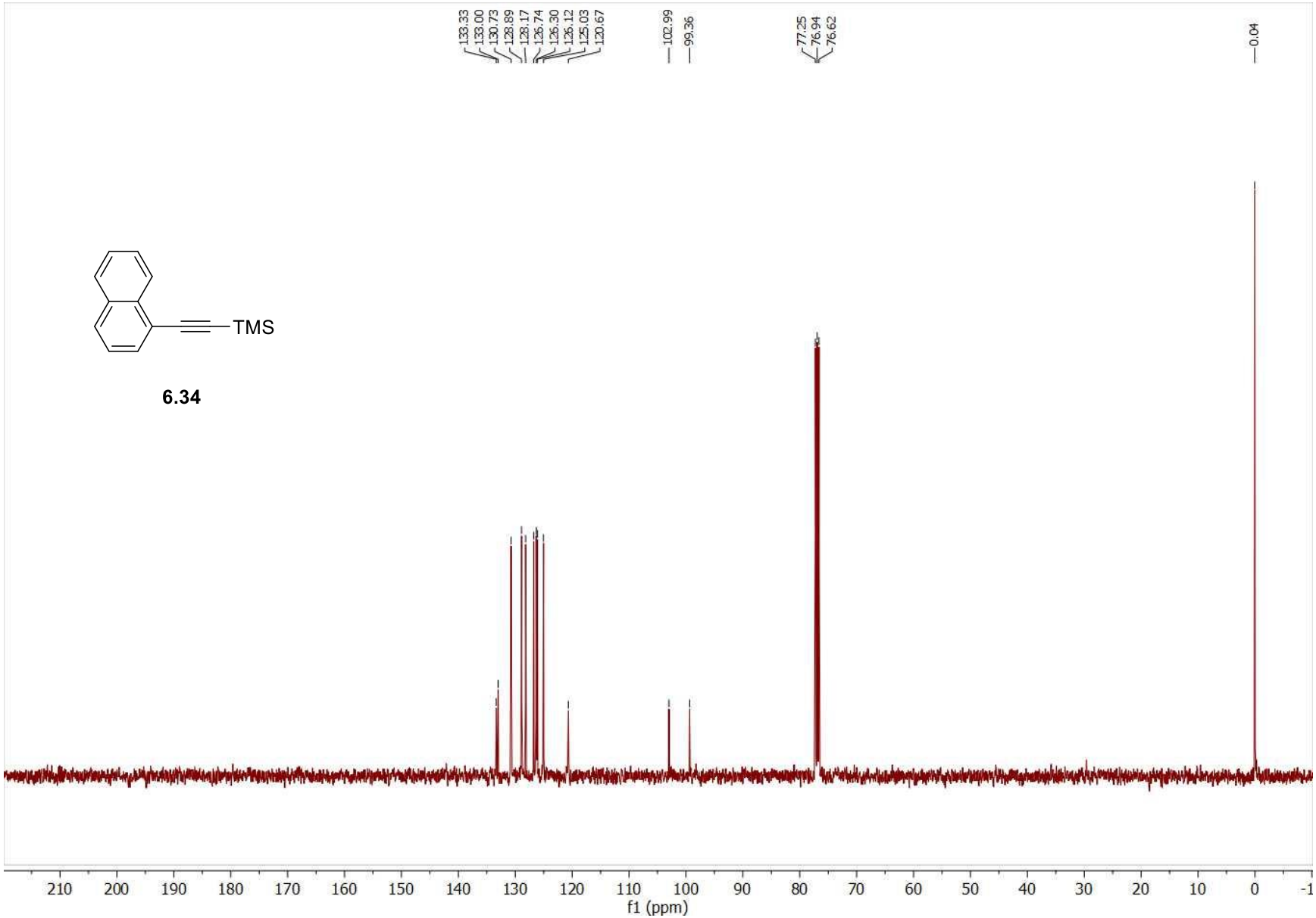

Figure B92: ^{13}C NMR of compound **6.34**.

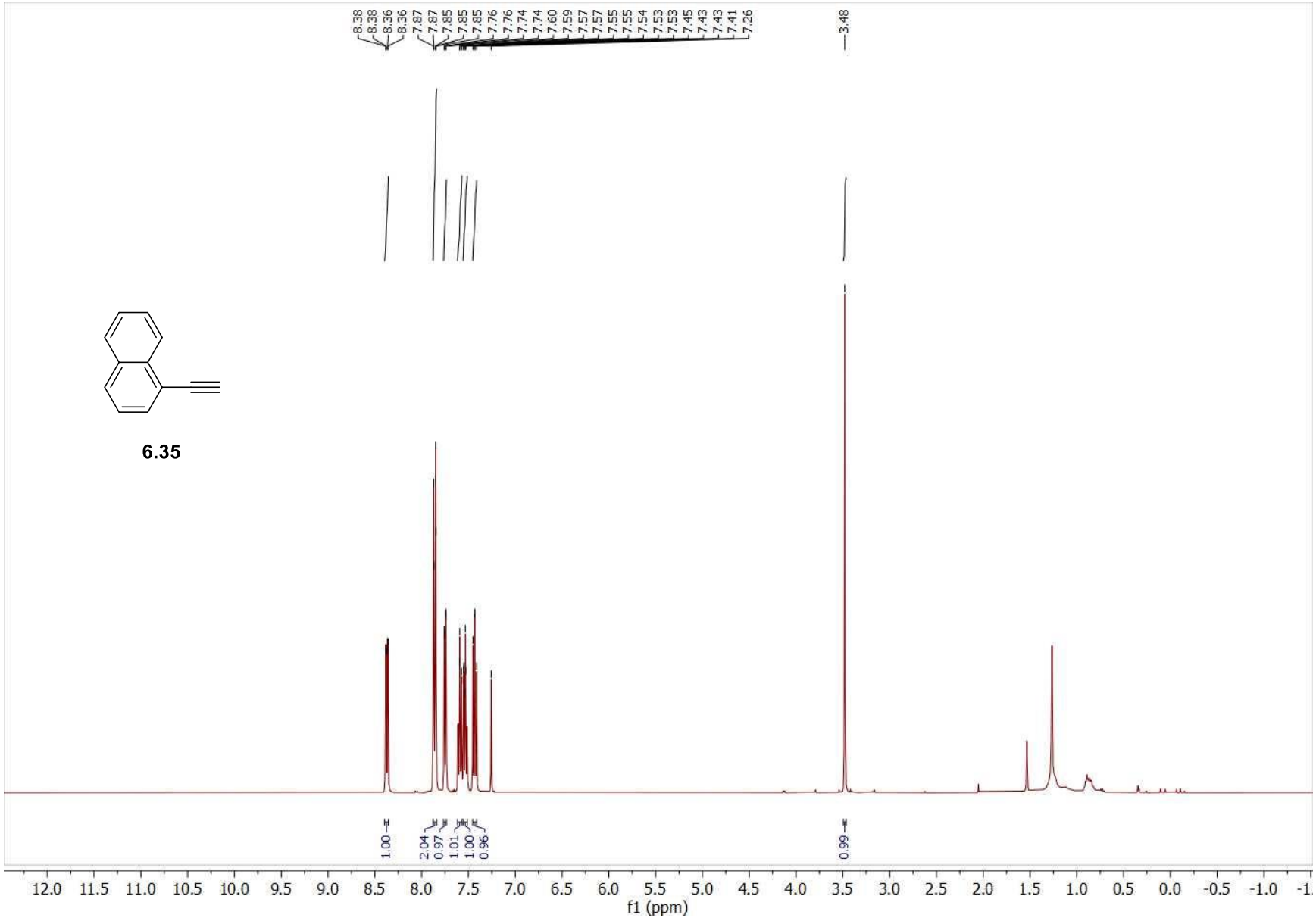

Figure B93: ^{1}H NMR of compound **6.35**.

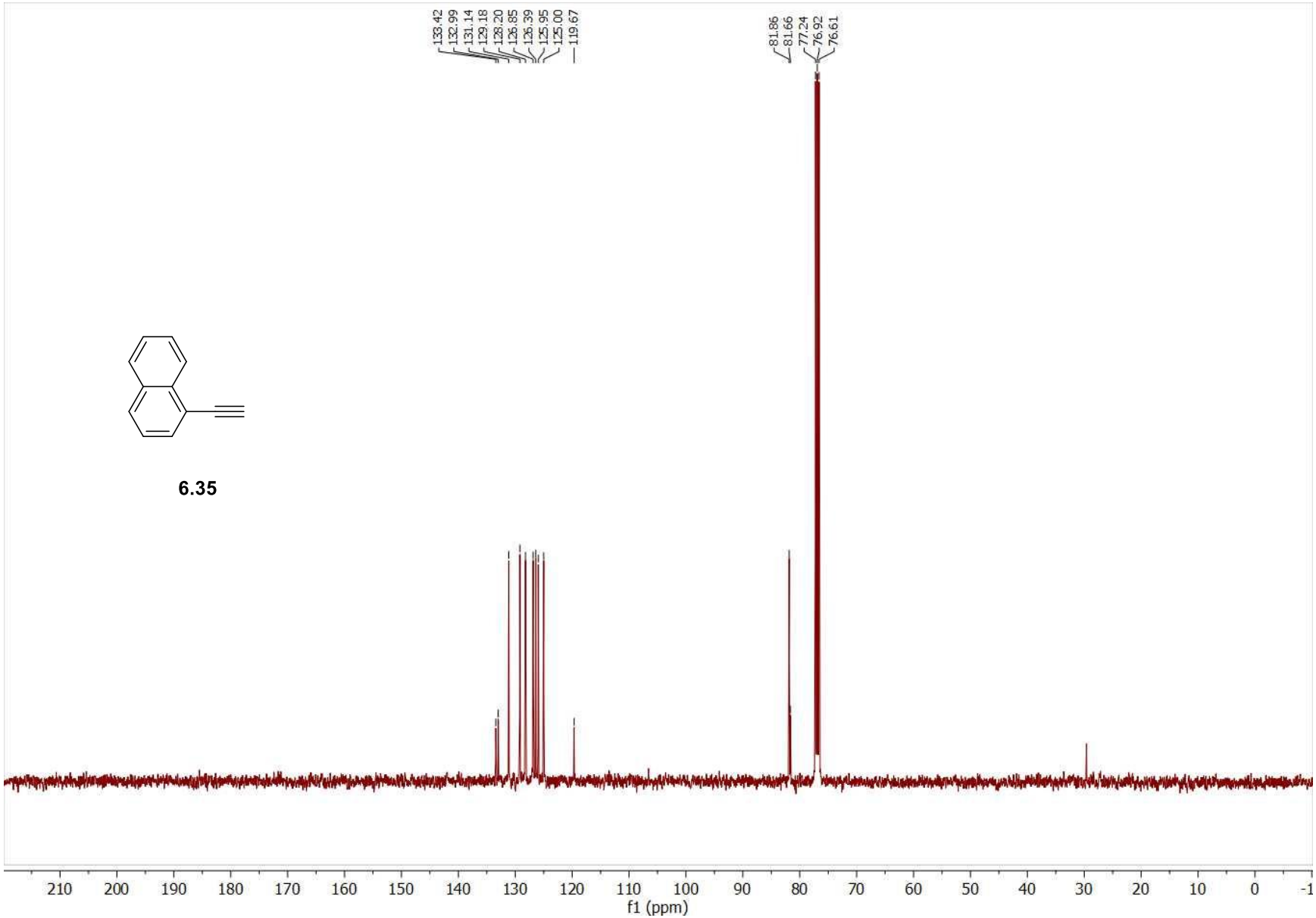

Figure B94: ^{13}C NMR of compound **6.35**.

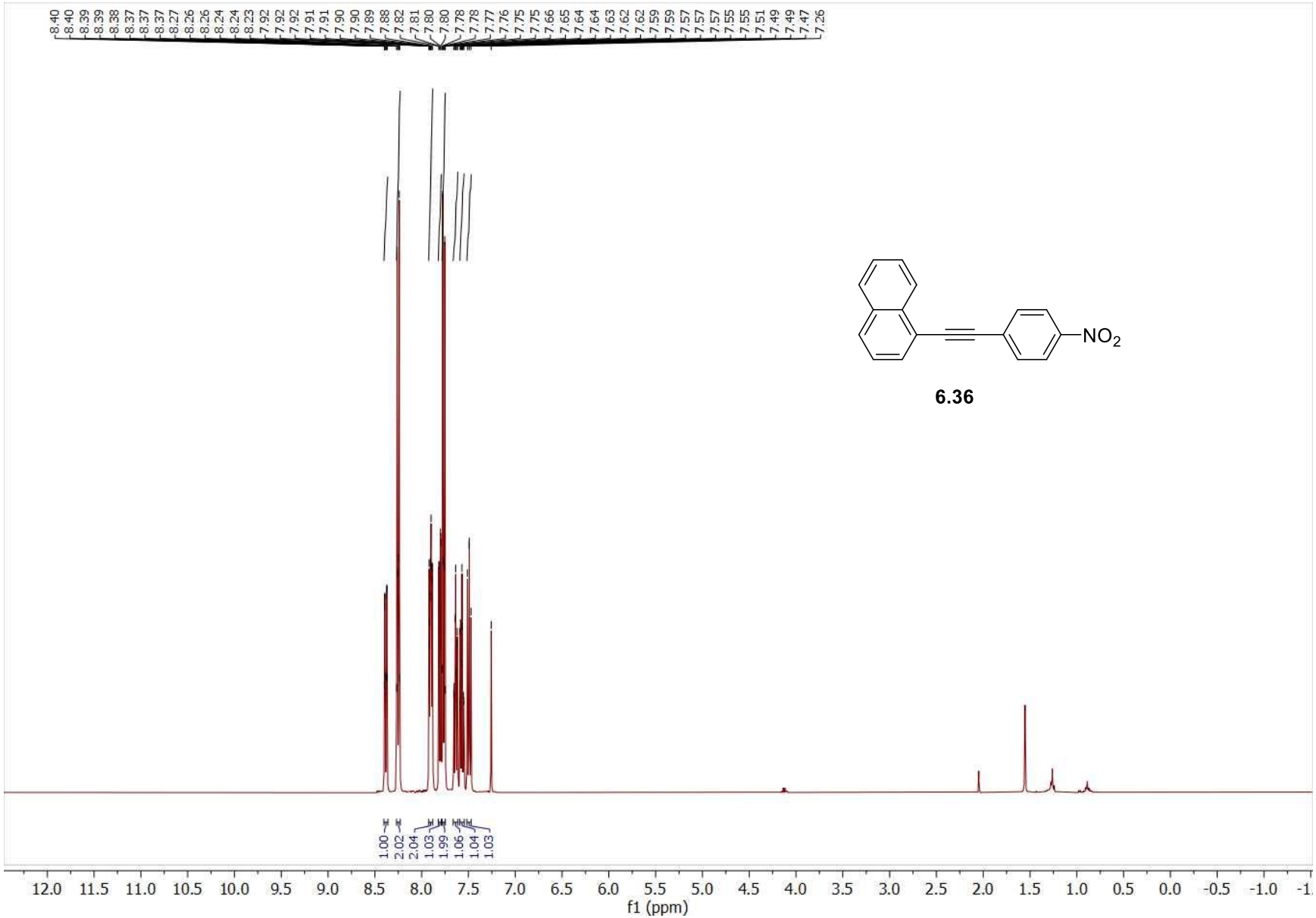

Figure B95: ^{1}H NMR of compound **6.36**.

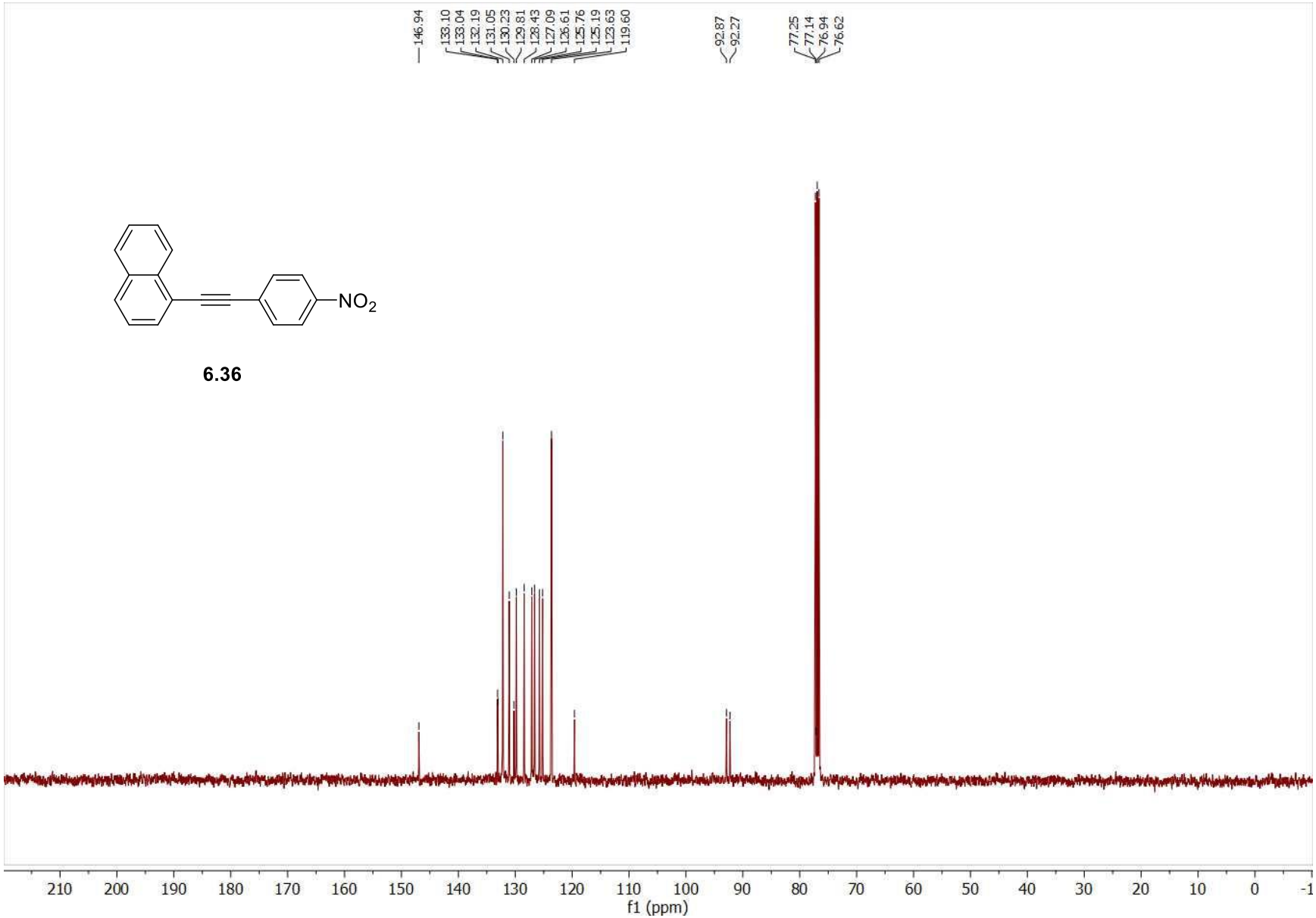

Figure B96: ^{13}C NMR of compound **6.36**.

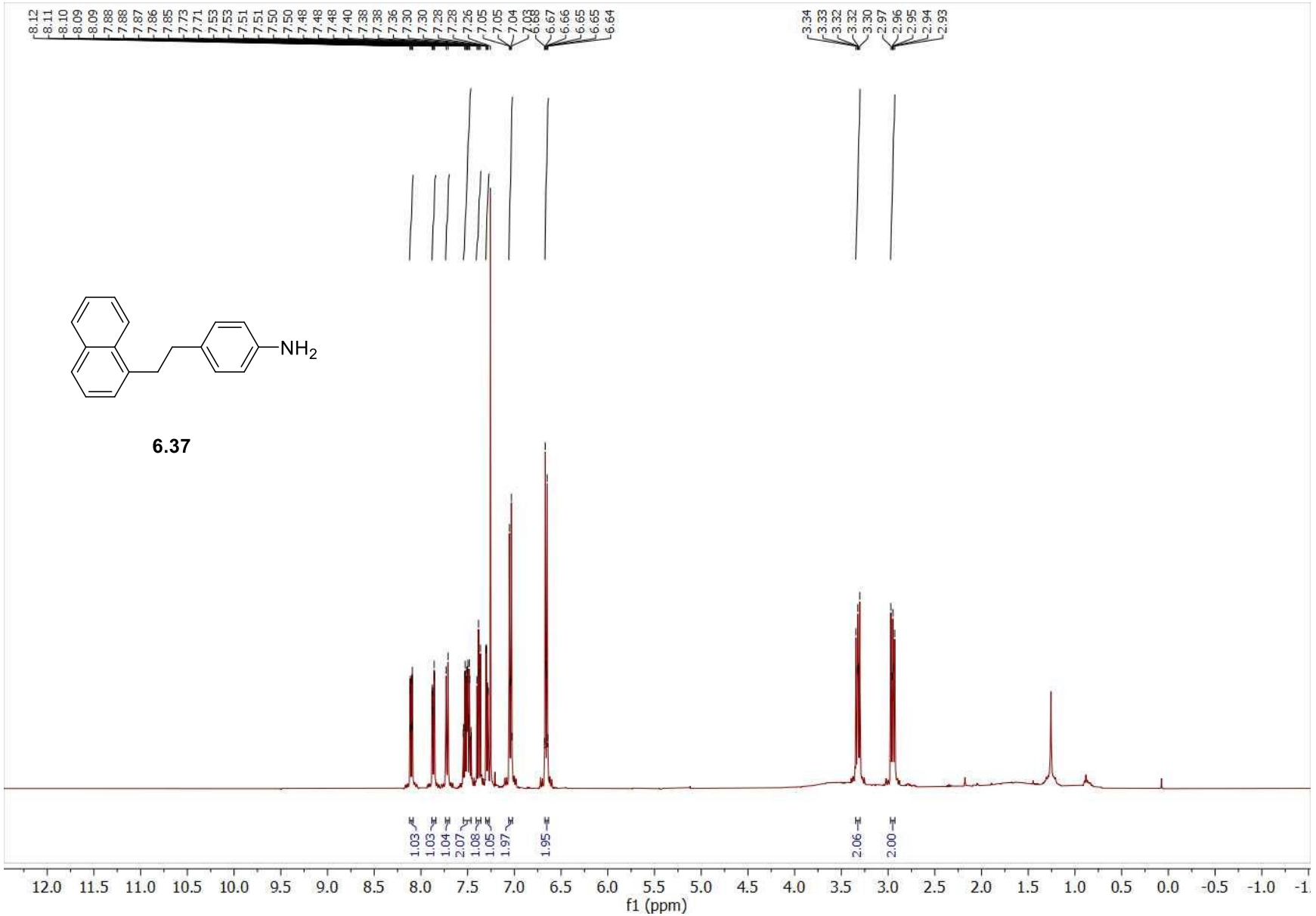

Figure B97: ^{1}H NMR of compound **6.37**.

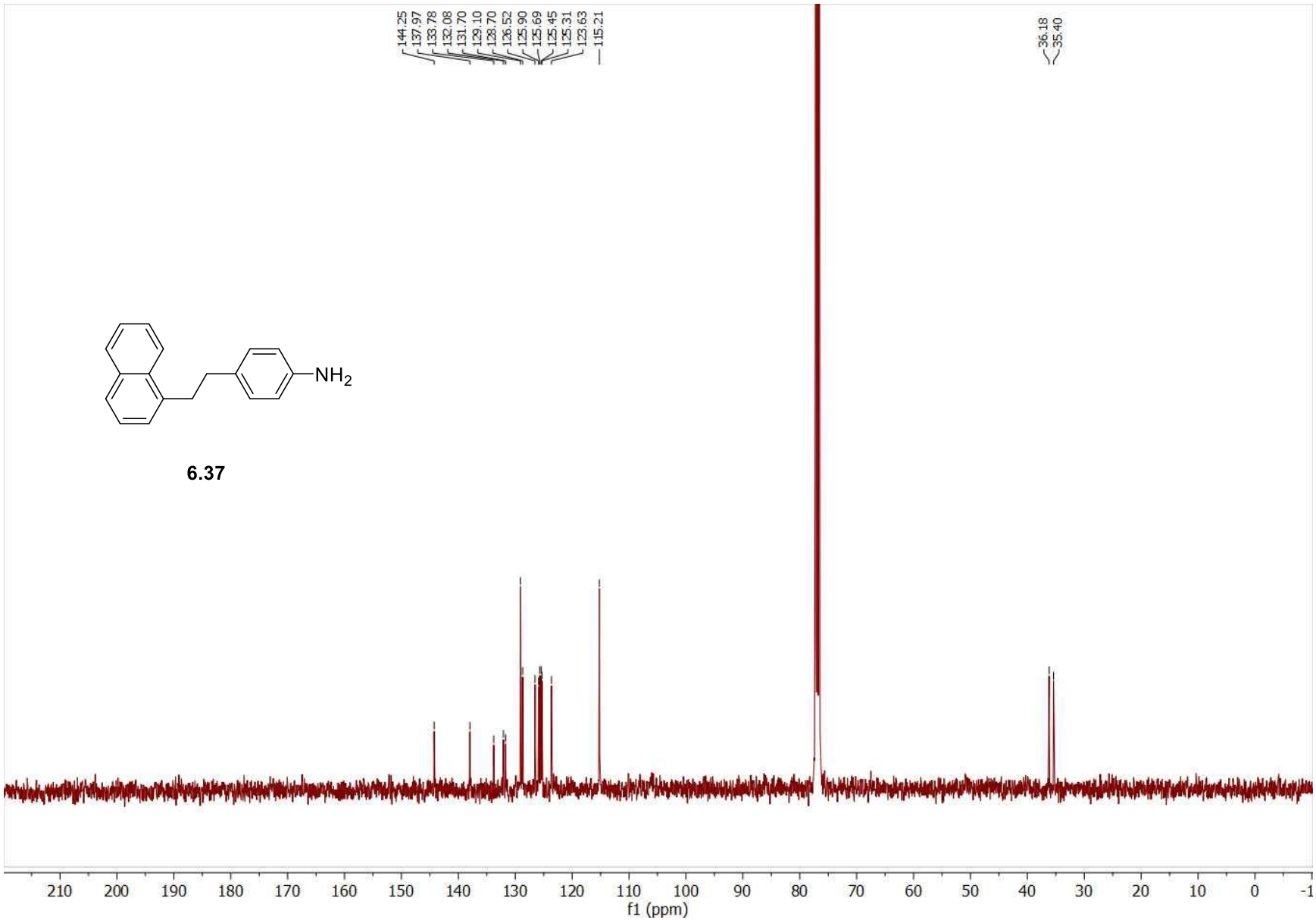

Figure B98: ^{13}C NMR of compound **6.37**.

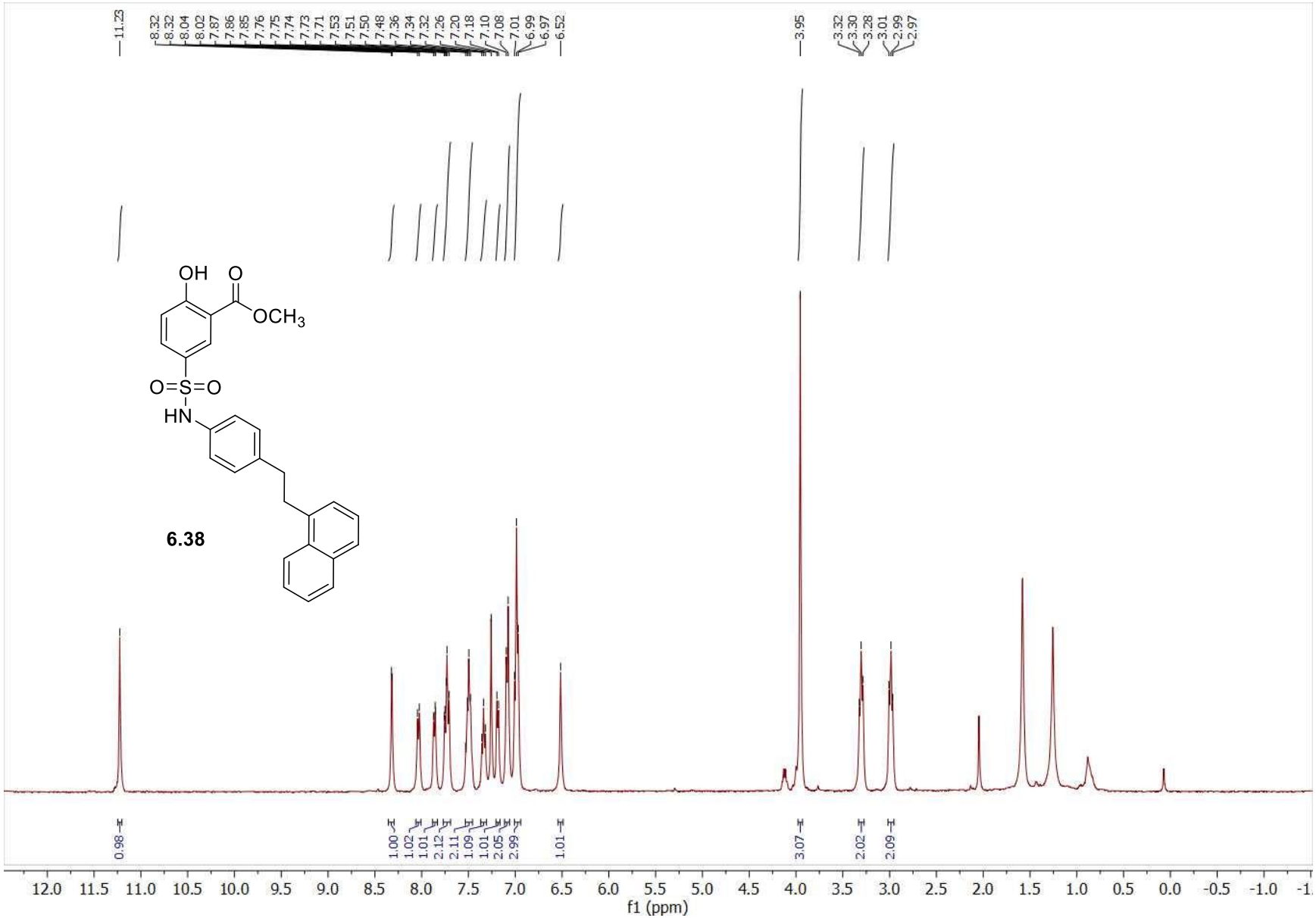

Figure B99: ^{1}H NMR of compound **6.38**.

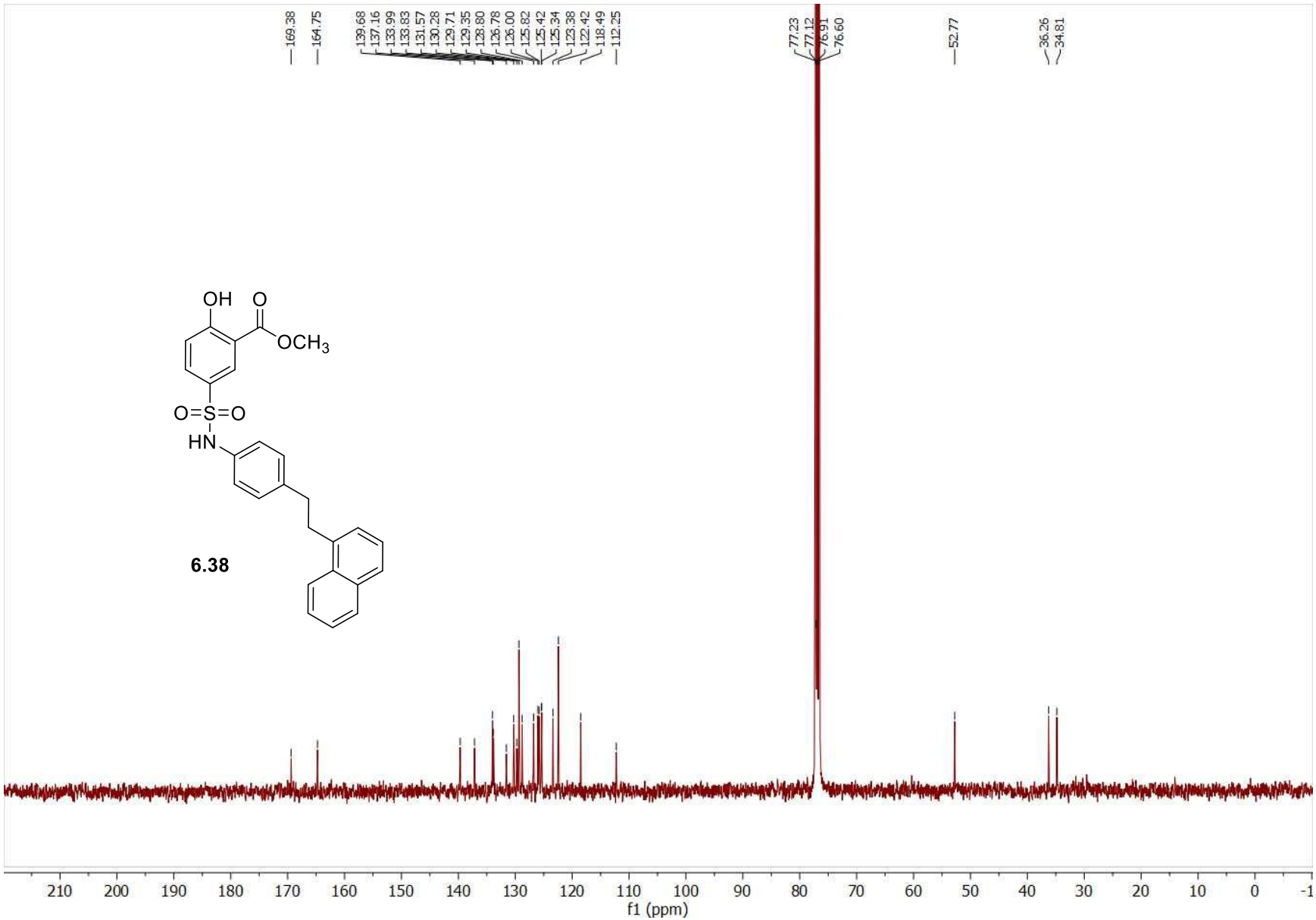

Figure B100: ^{13}C NMR of compound **6.38**.

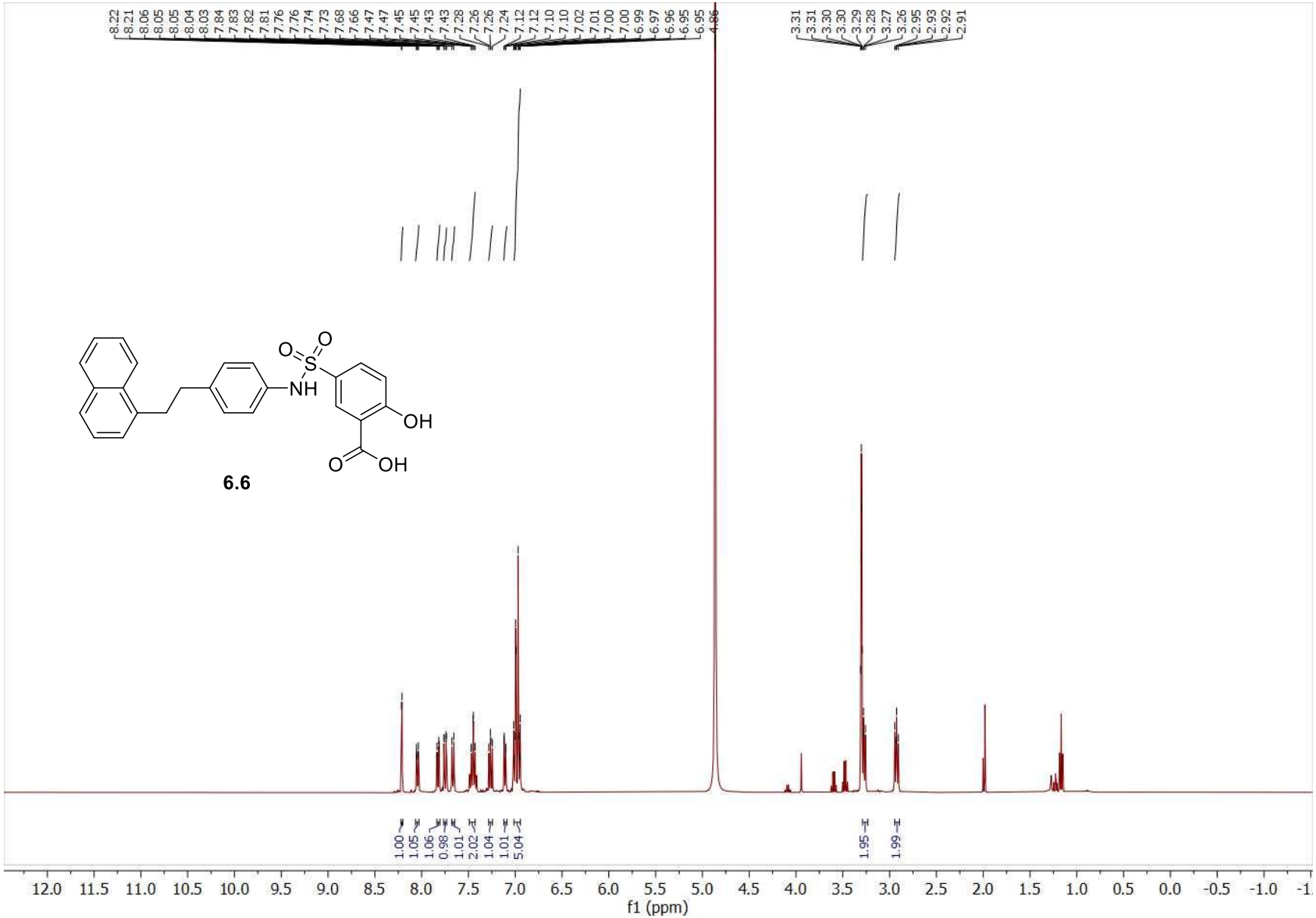

Figure B101: ^{1}H NMR of compound **6.6**.

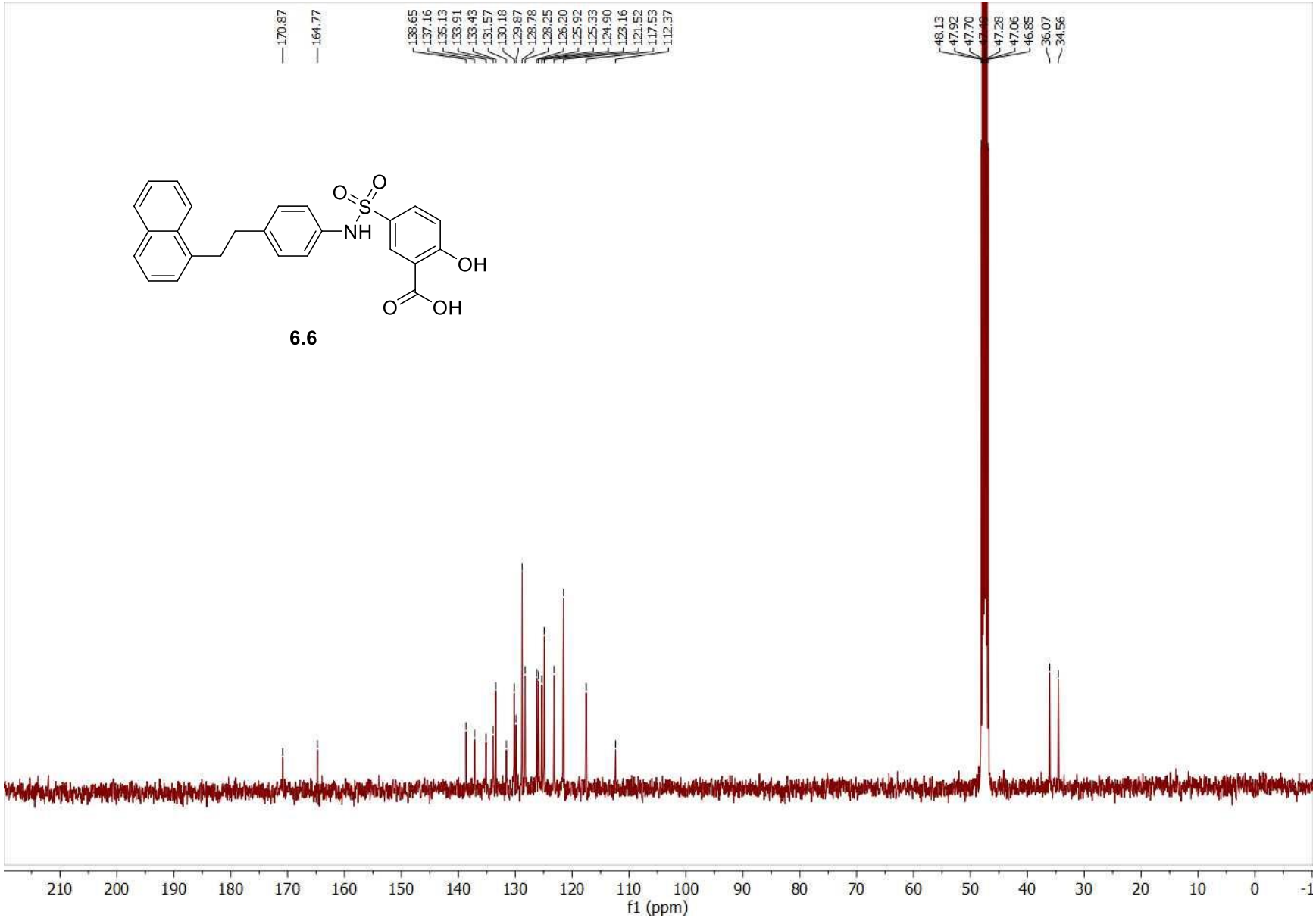

Figure B102: ^{13}C NMR of compound **6.6**.

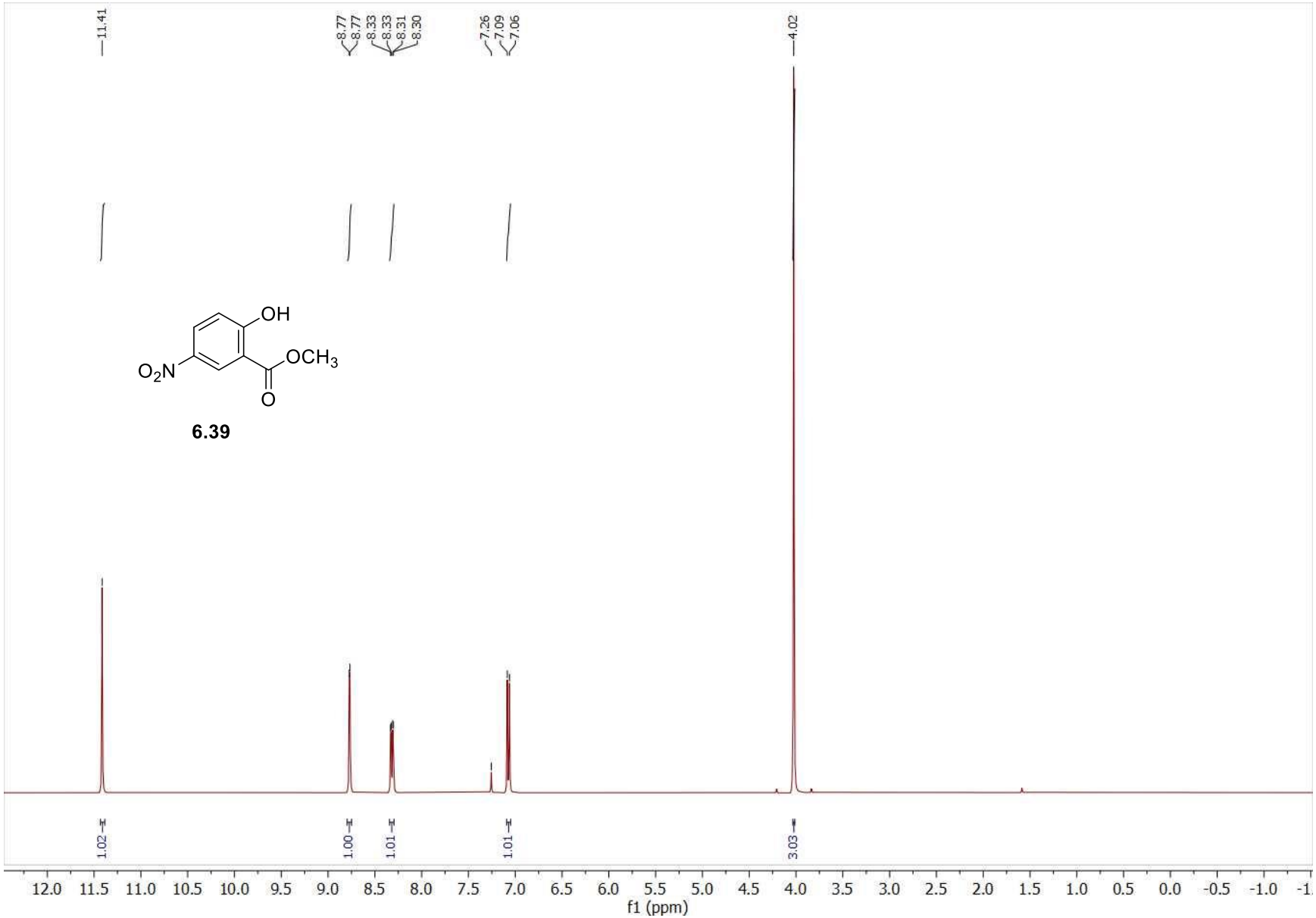

Figure B103: ^{1}H NMR of compound **6.39**.

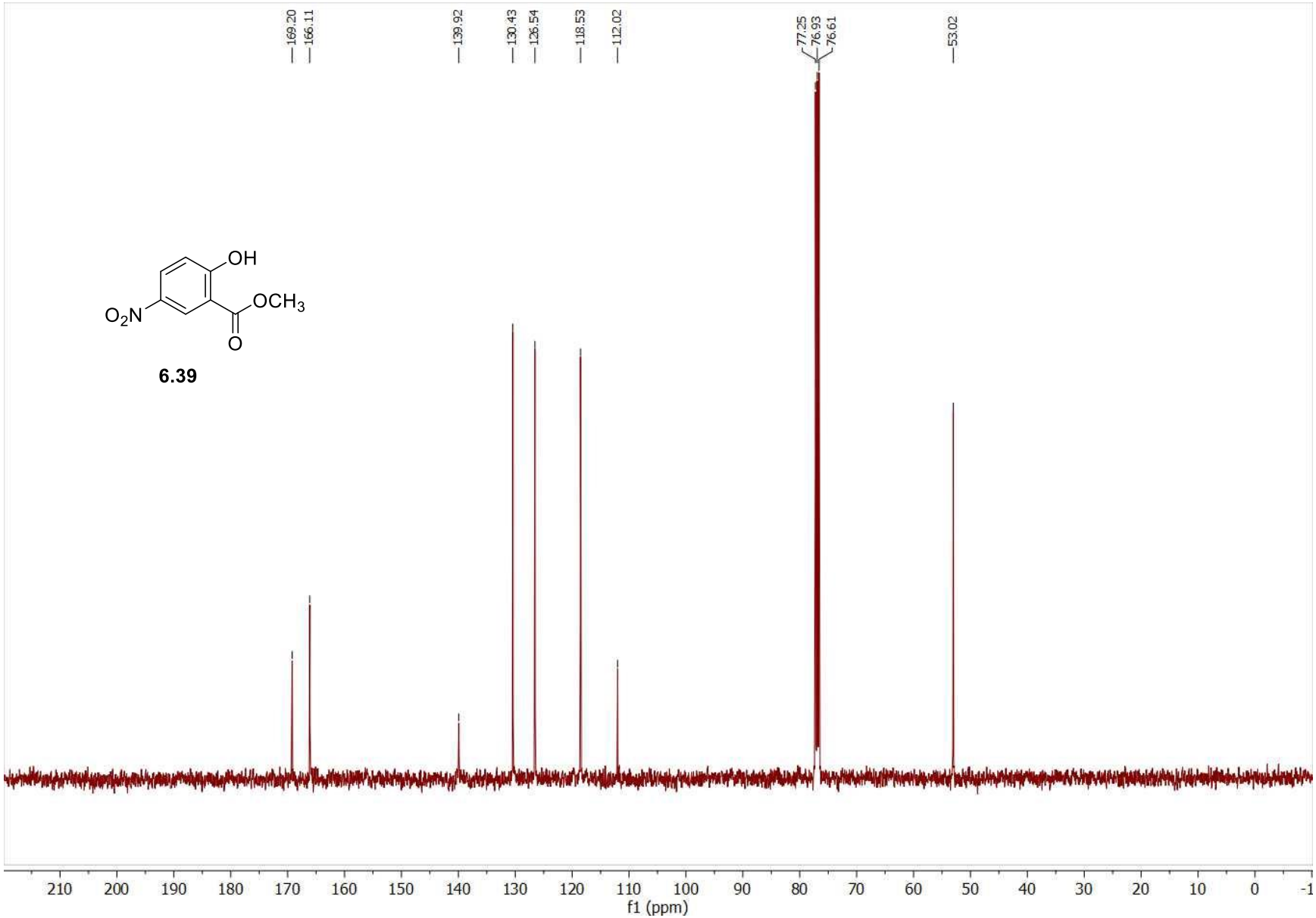

Figure B104: ^{13}C NMR of compound **6.39**.

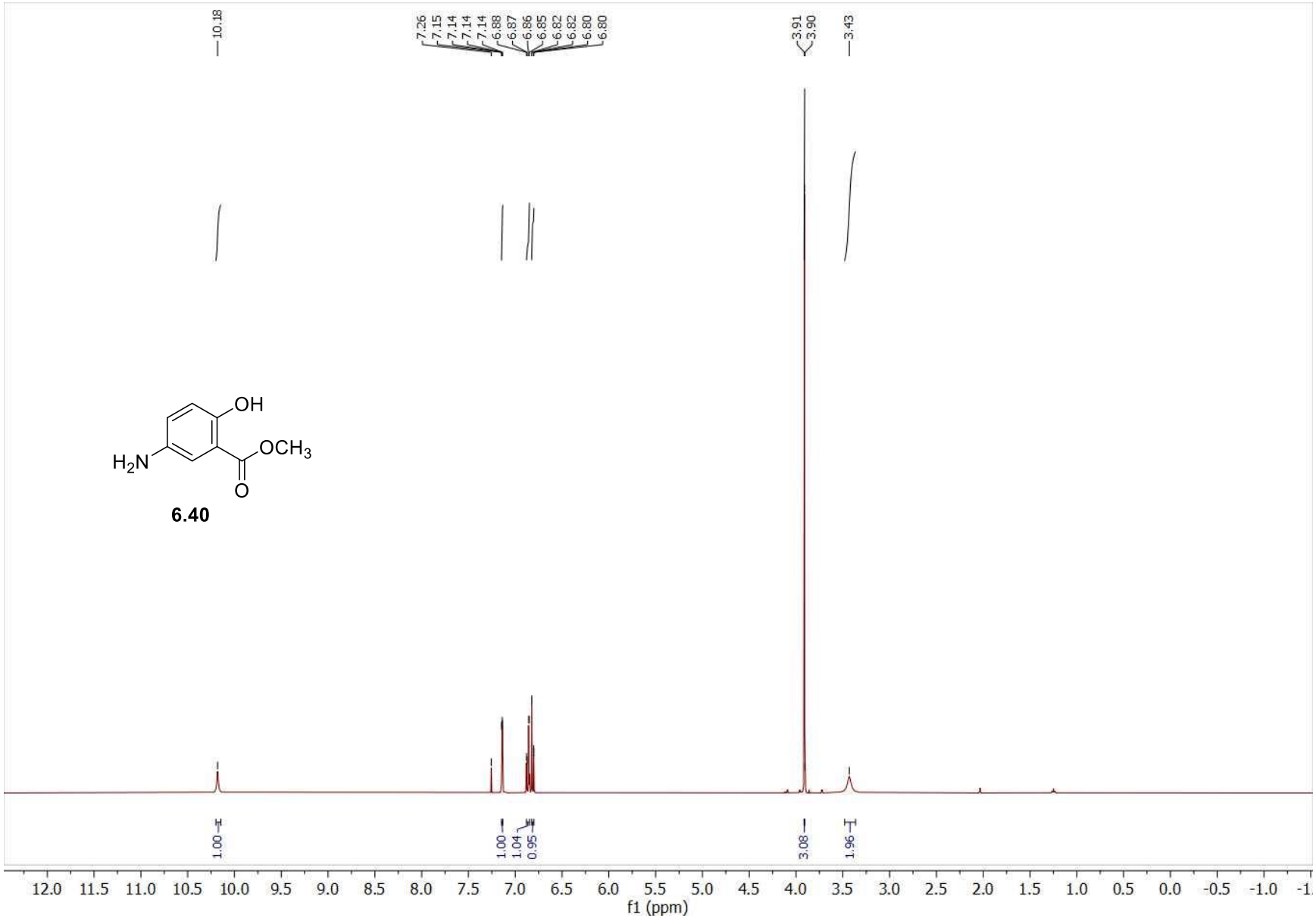

Figure B105: ^{1}H NMR of compound **6.40**.

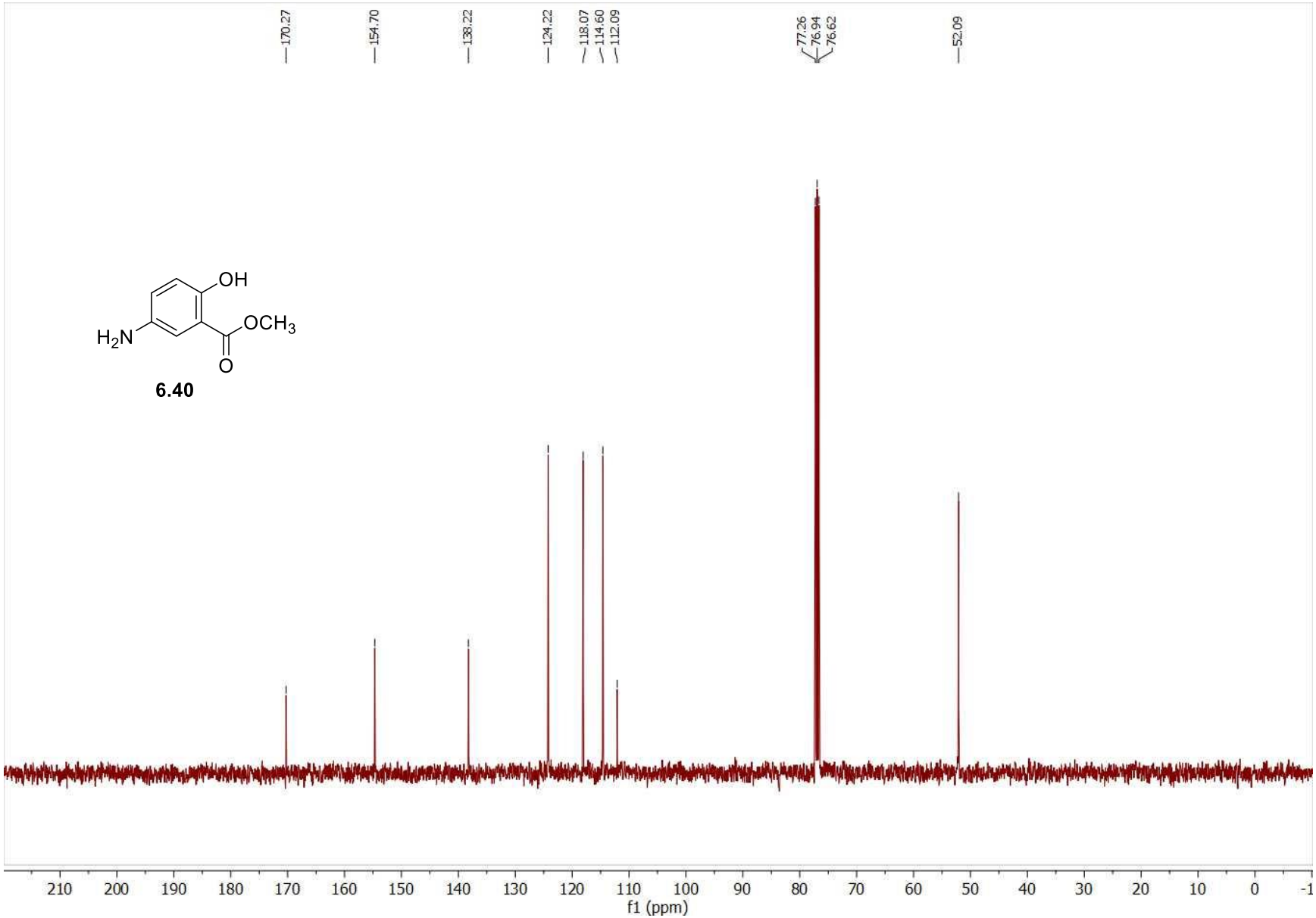

Figure B106: ^{13}C NMR of compound **6.40**.

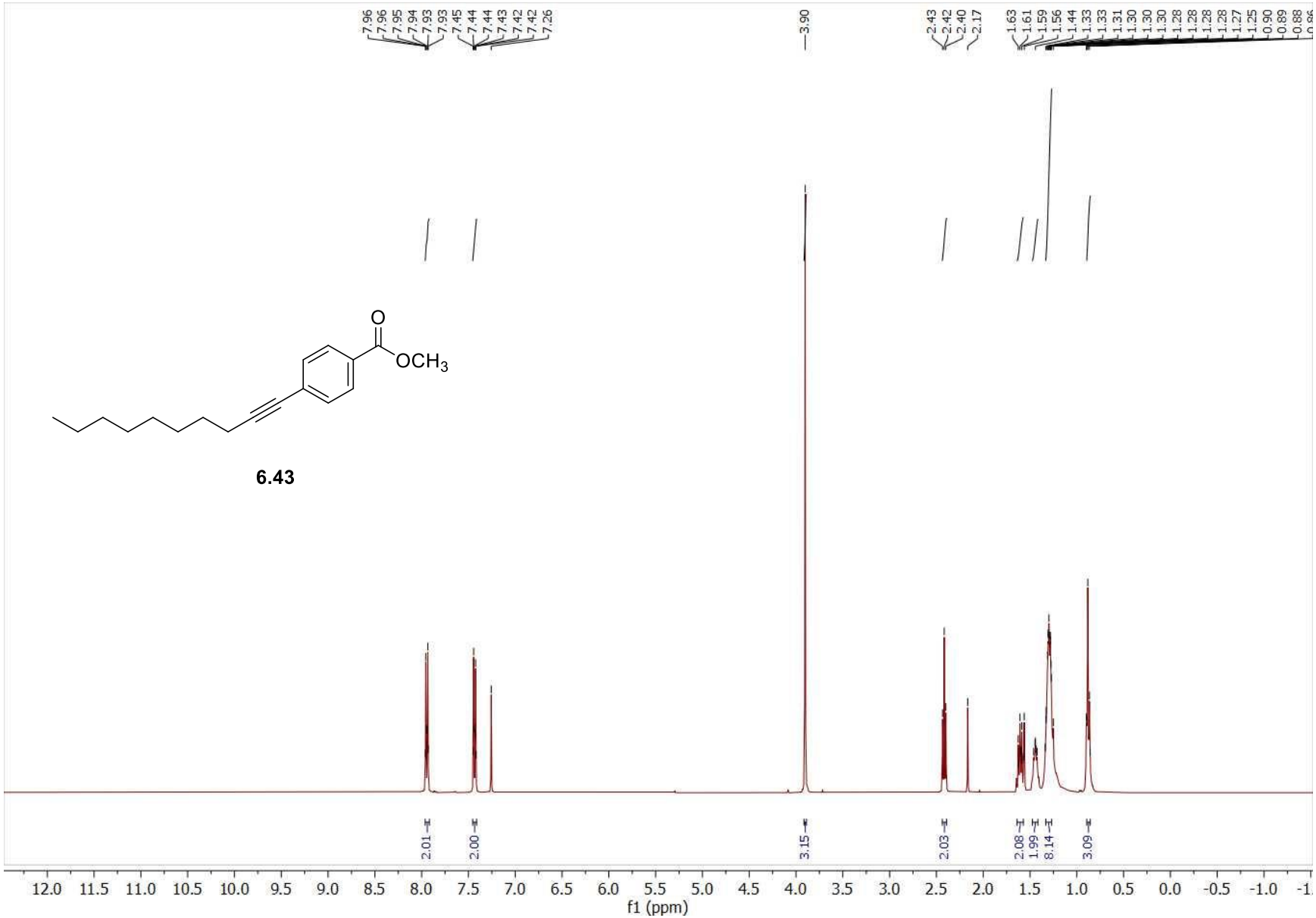

Figure B107: ^{1}H NMR of compound **6.43**.

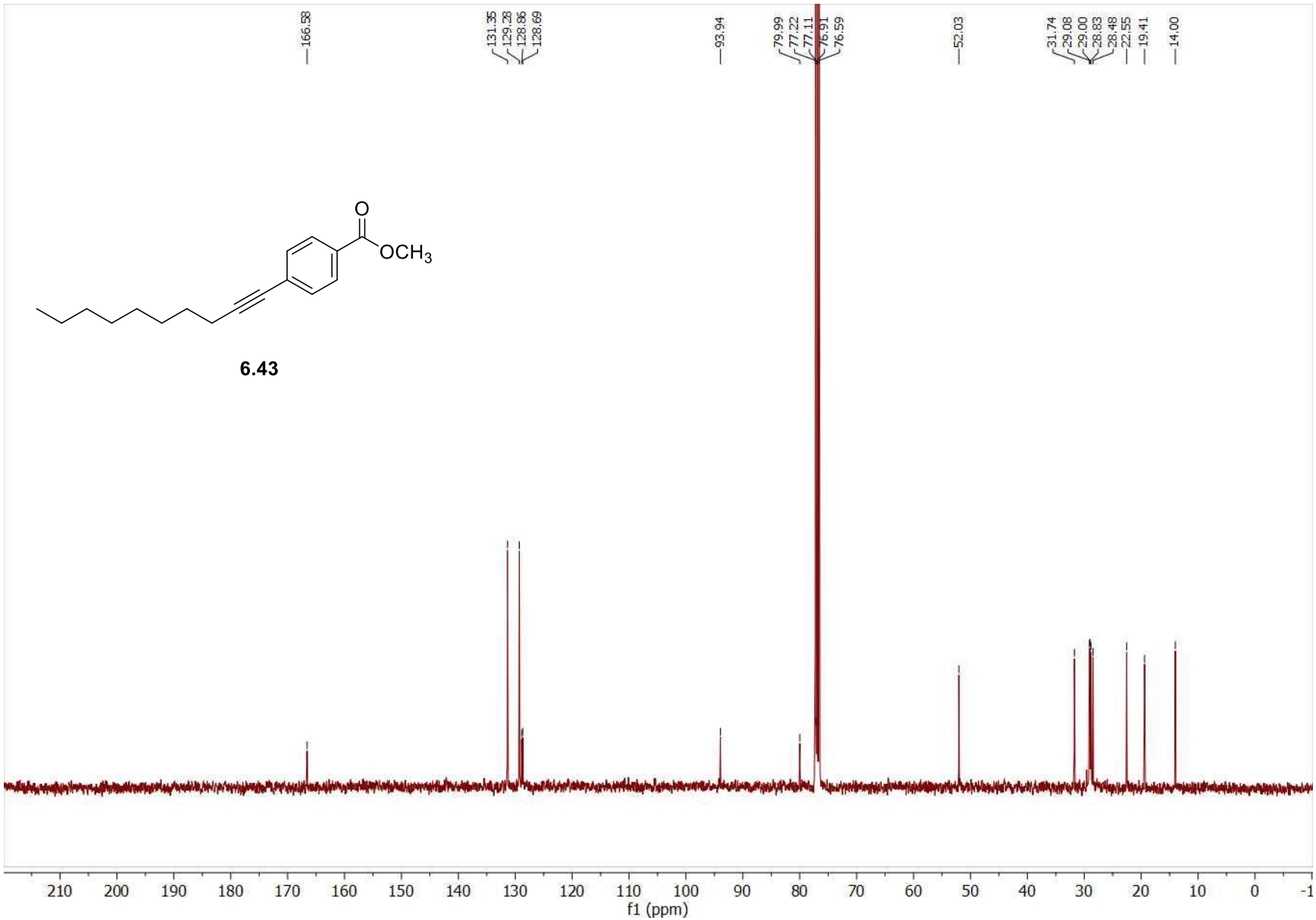

Figure B108: ^{13}C NMR of compound **6.43**.

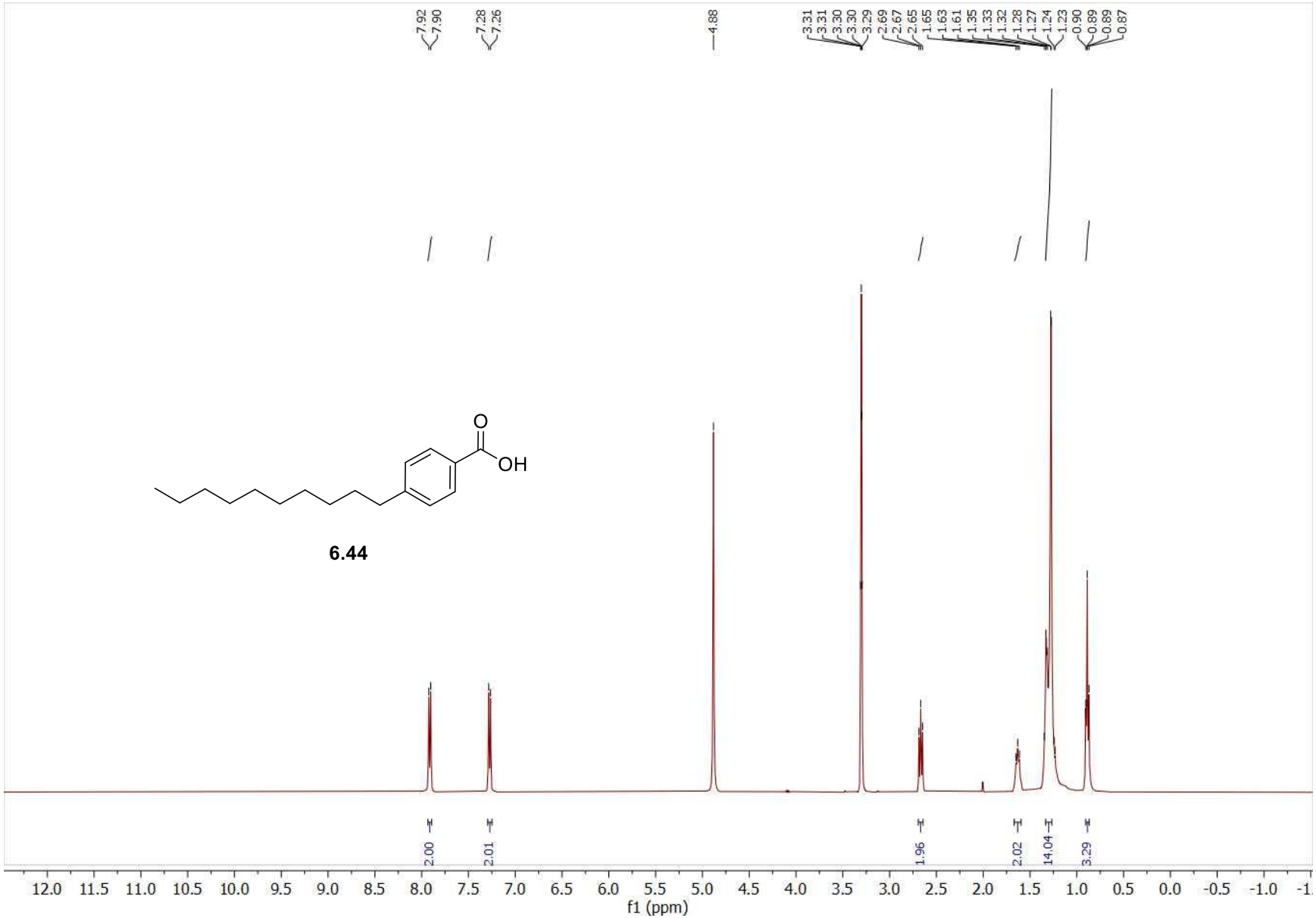

Figure B109: ^{1}H NMR of compound **6.44**.

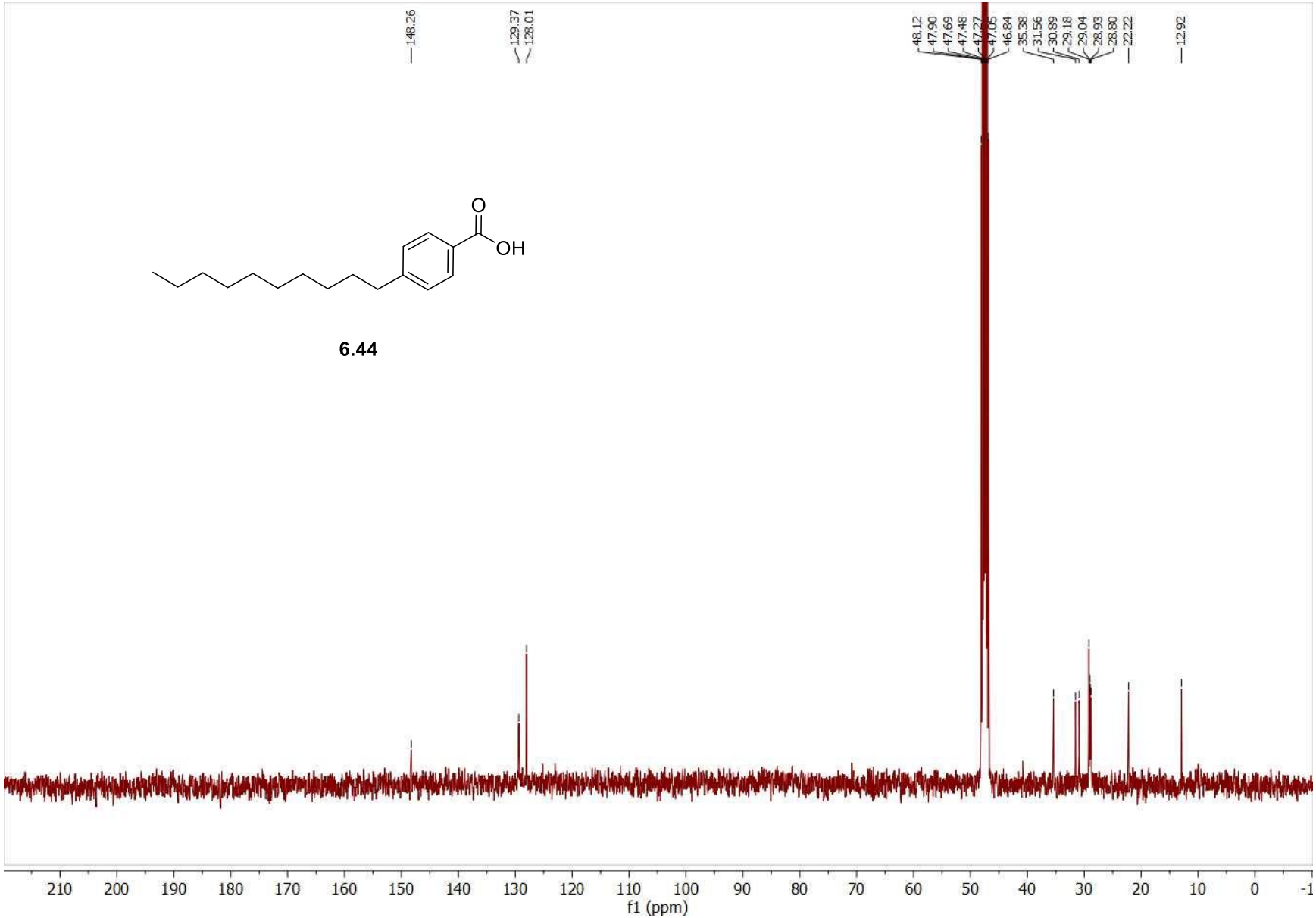

Figure B110: ^{13}C NMR of compound **6.44**.

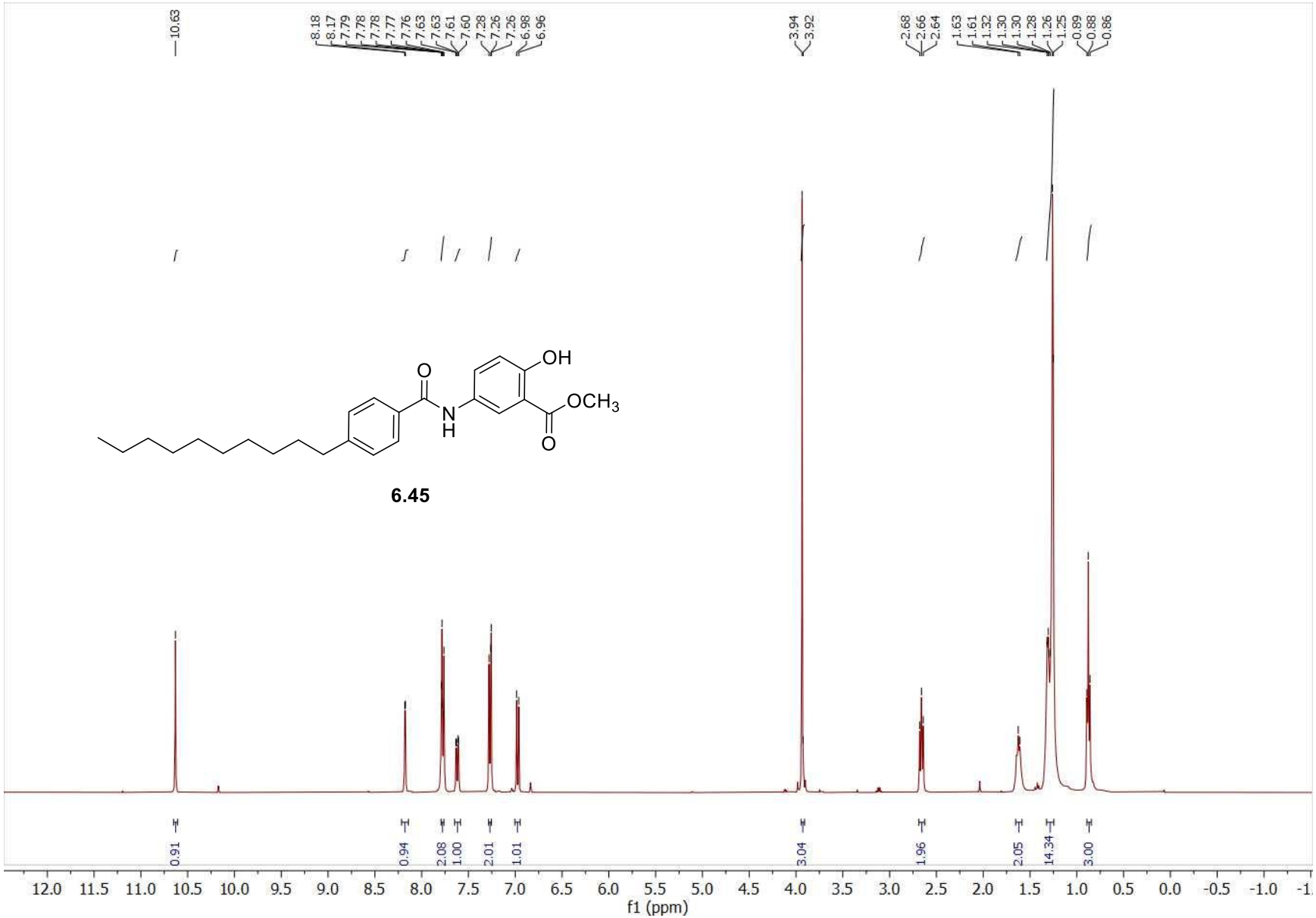

Figure B111: ^{1}H NMR of compound **6.45**.

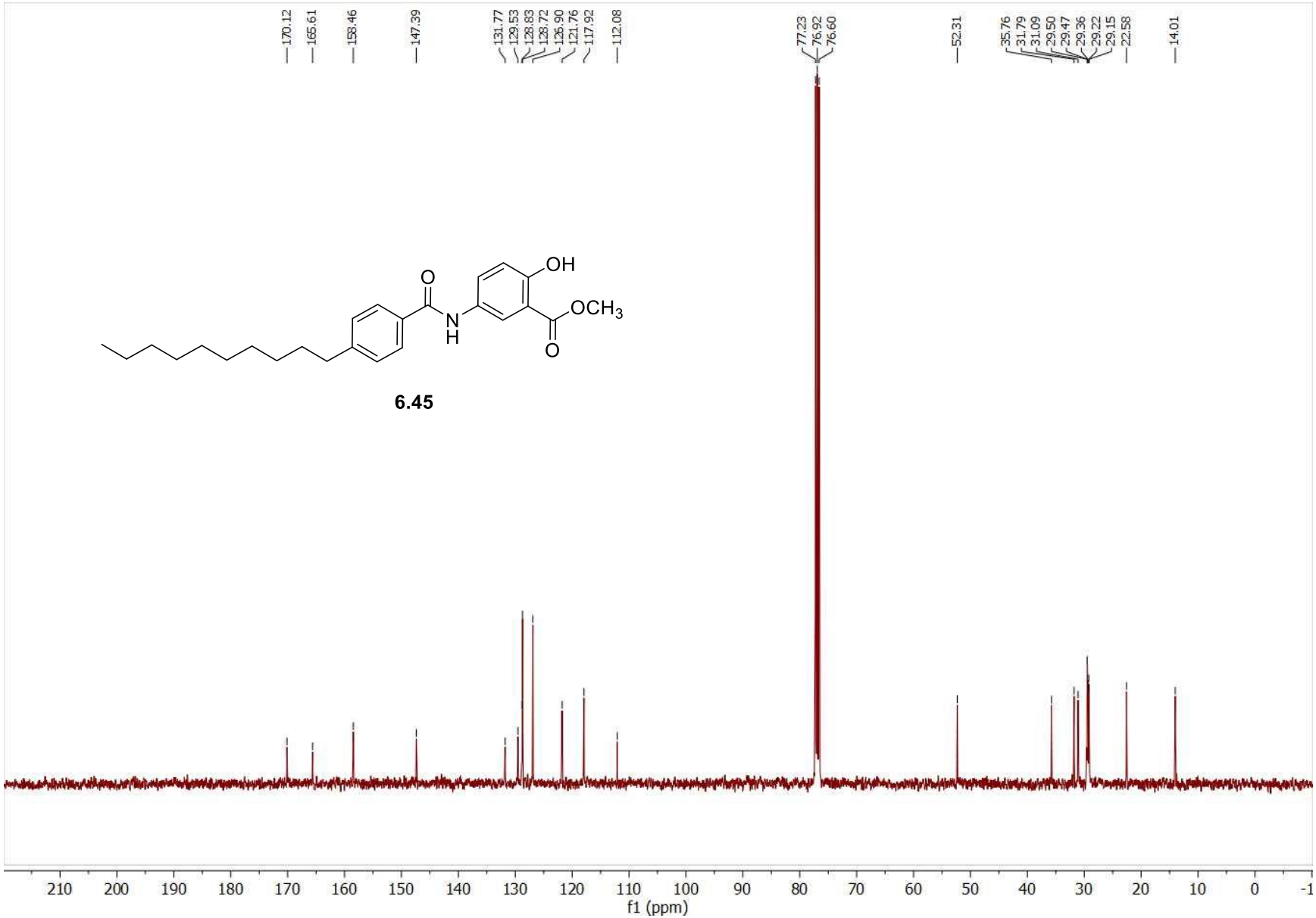

Figure B112: ^{13}C NMR of compound **6.45**.

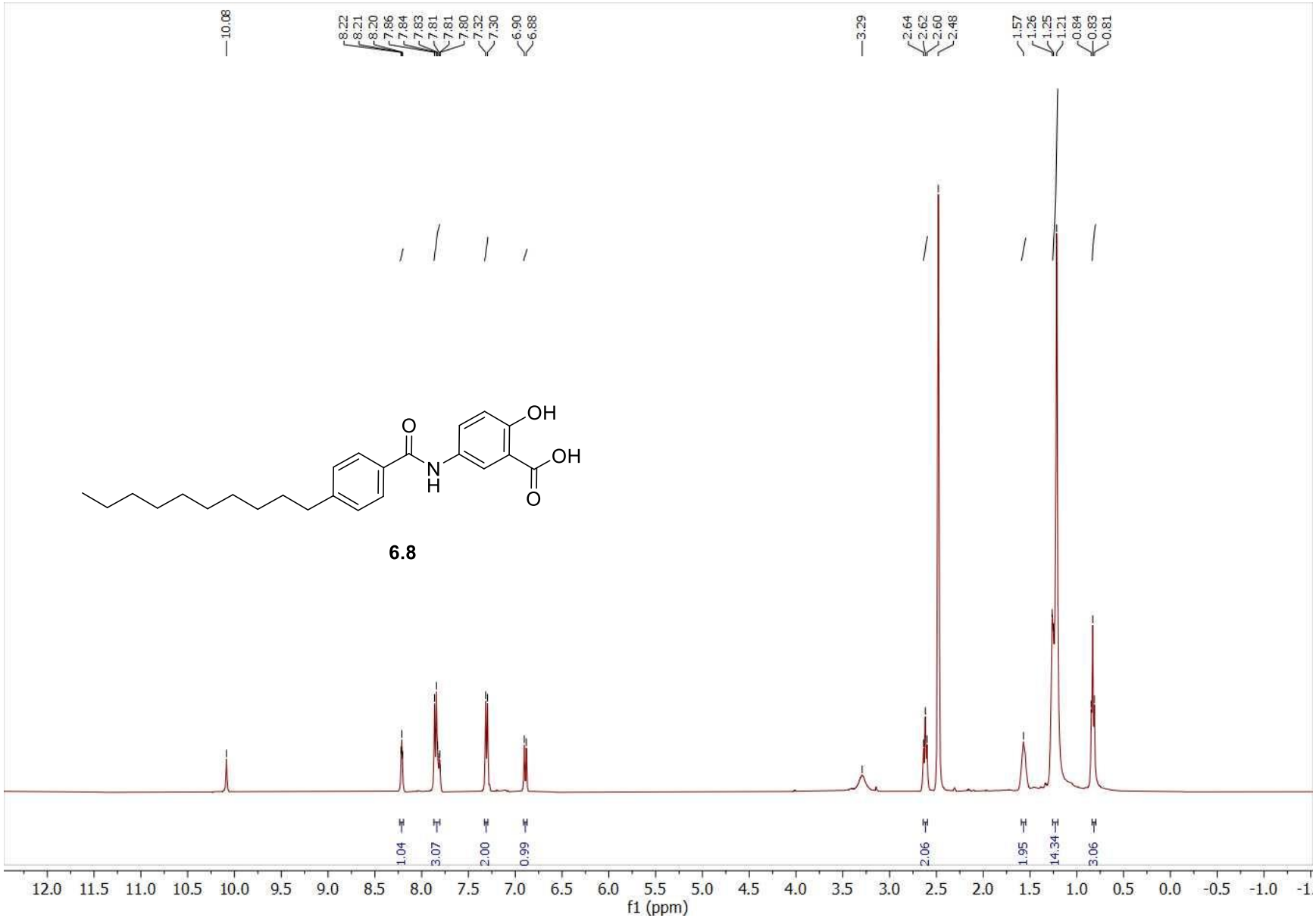

Figure B113: ^{1}H NMR of compound **6.8**.

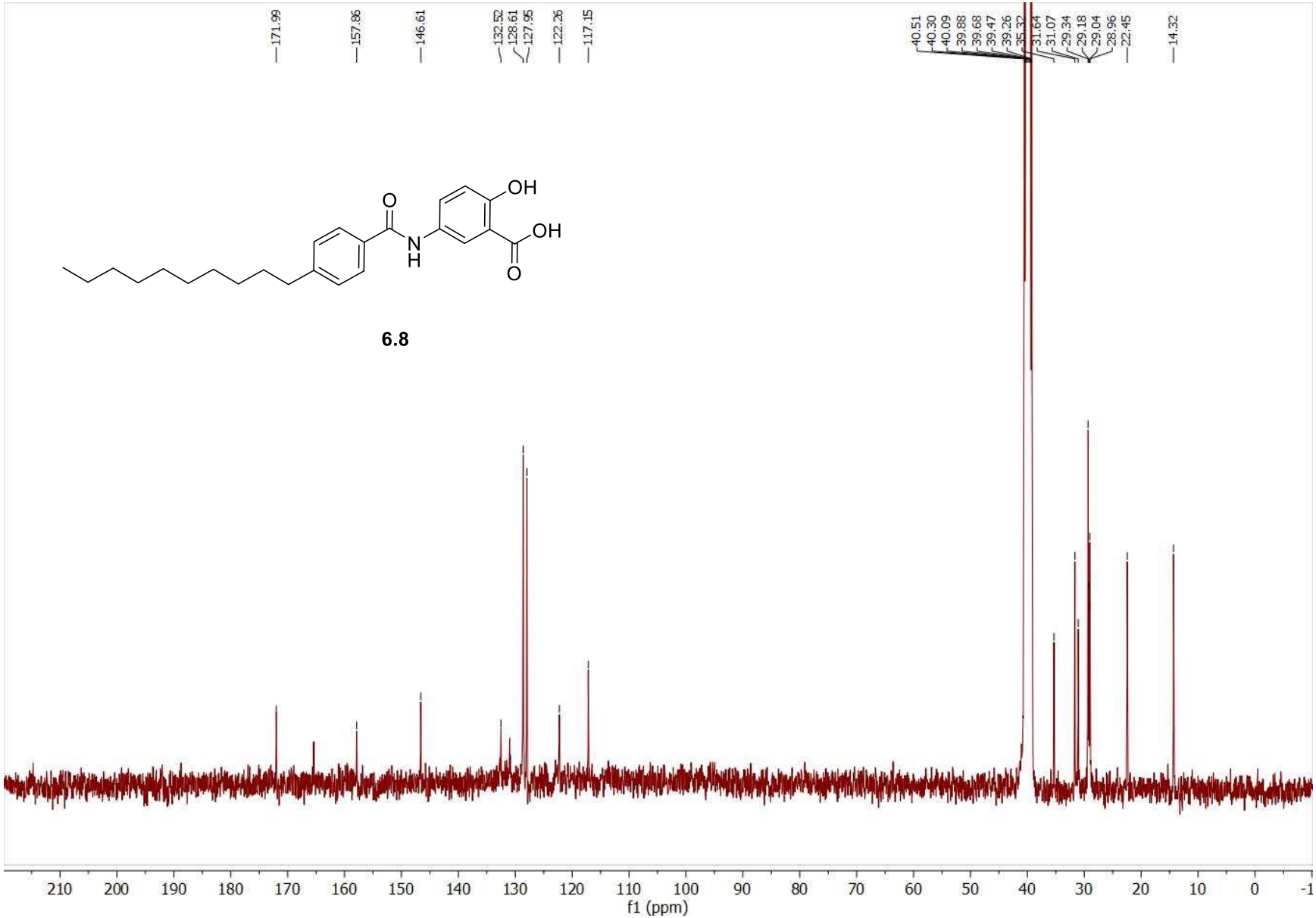

Figure B114: ^{13}C NMR of compound **6.8**.

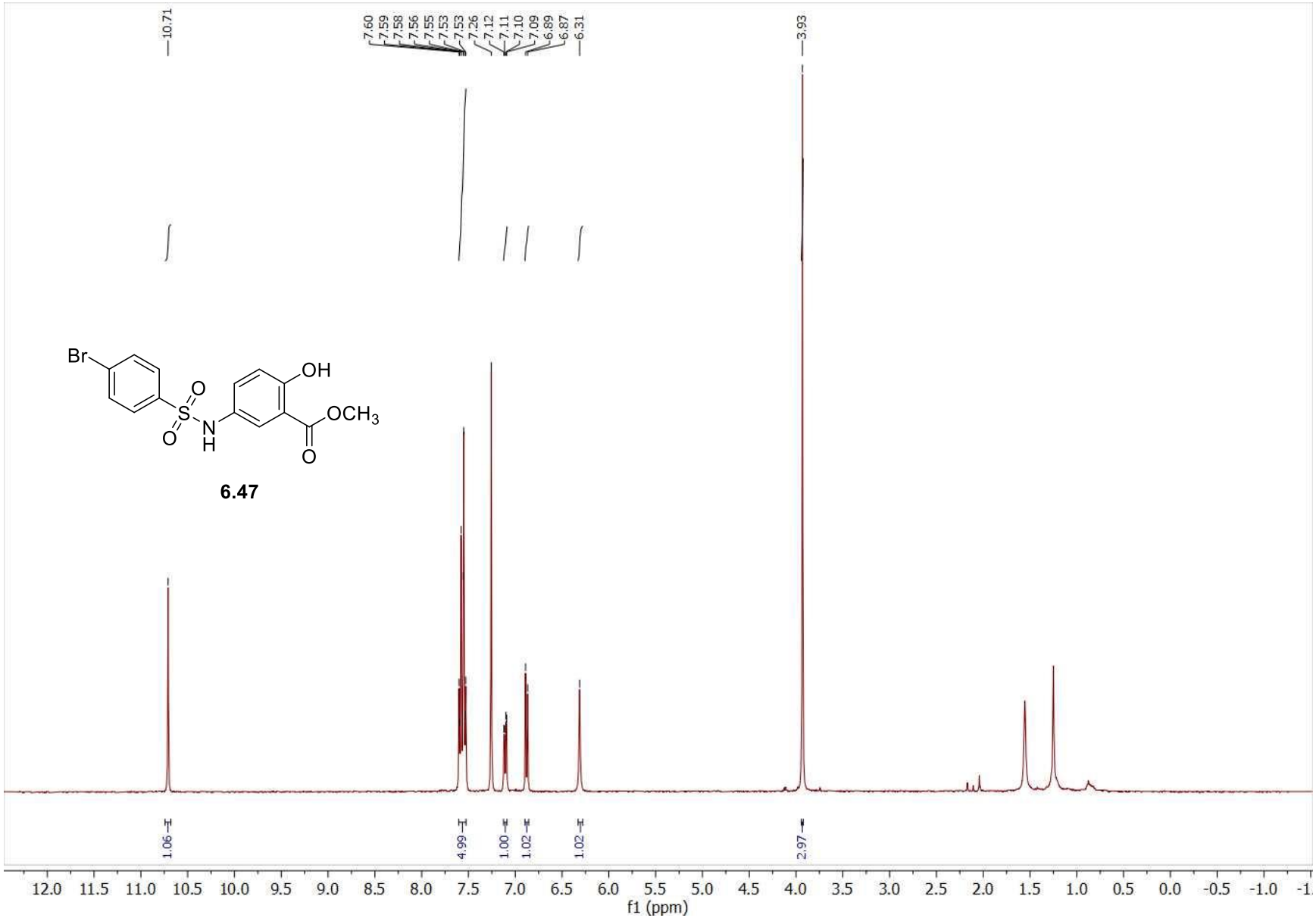

Figure B115: ^{1}H NMR of compound **6.47**.

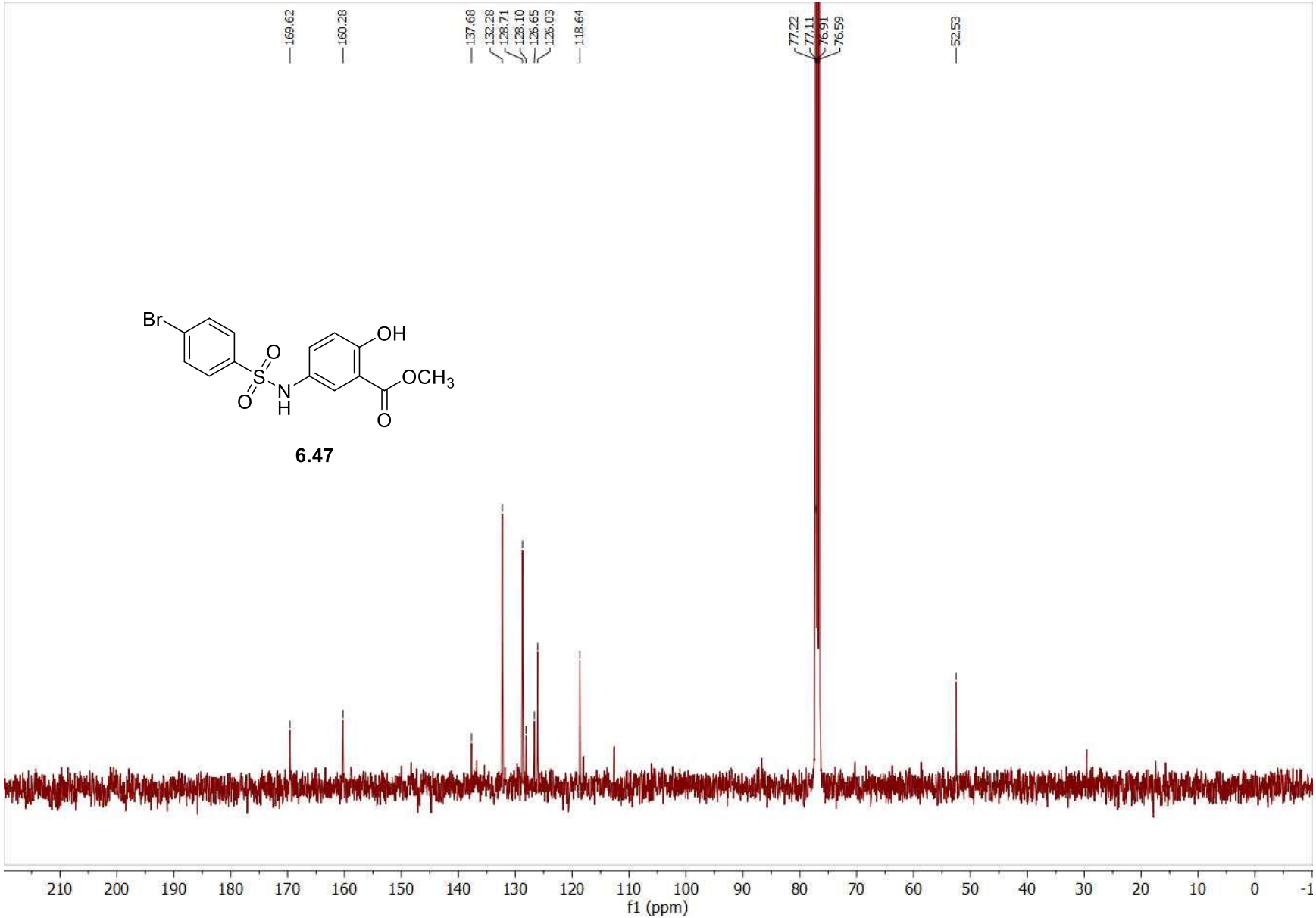

Figure B116: ^{13}C NMR of compound **6.47**.

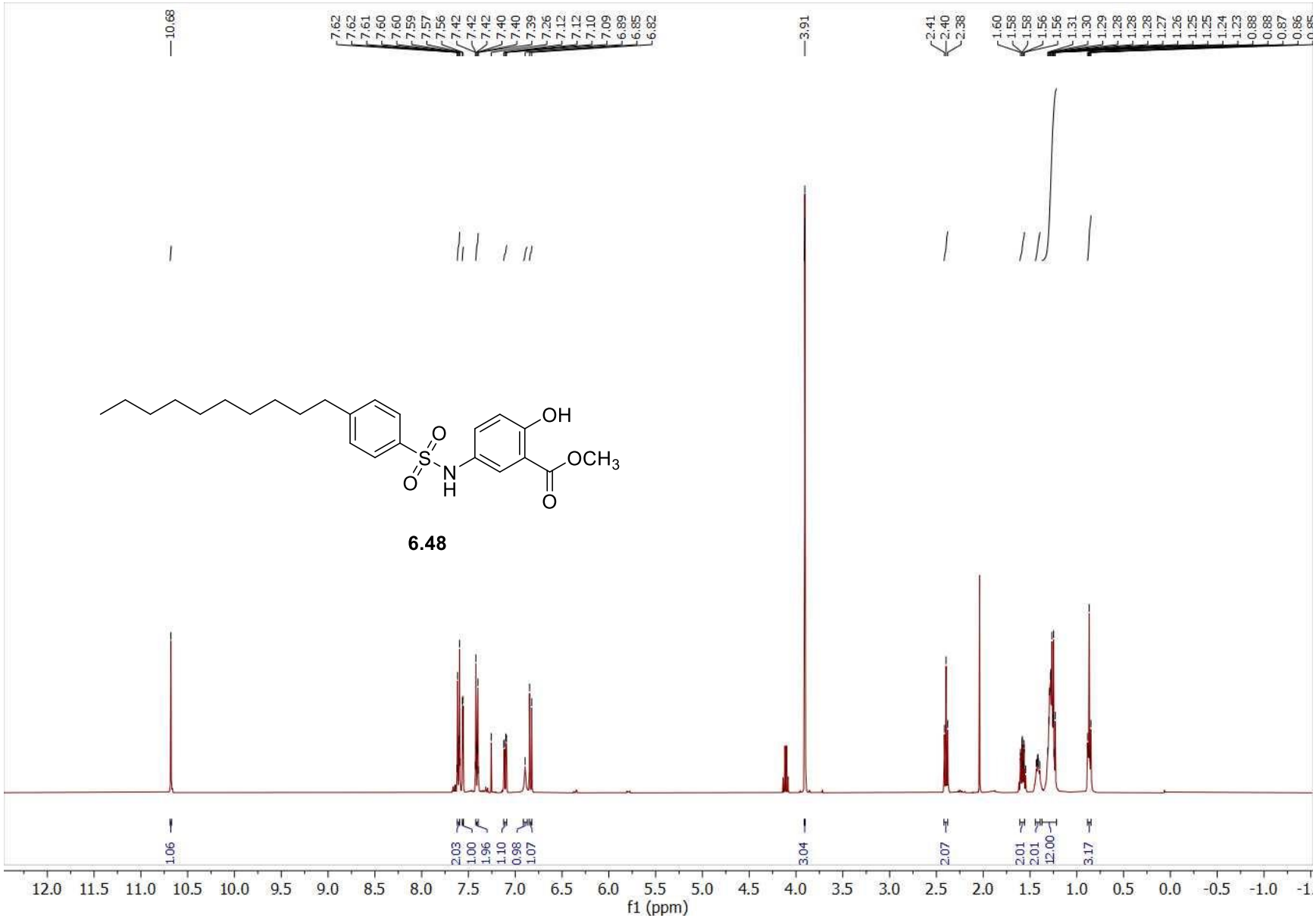

Figure B117: ^{1}H NMR of compound **6.48**.

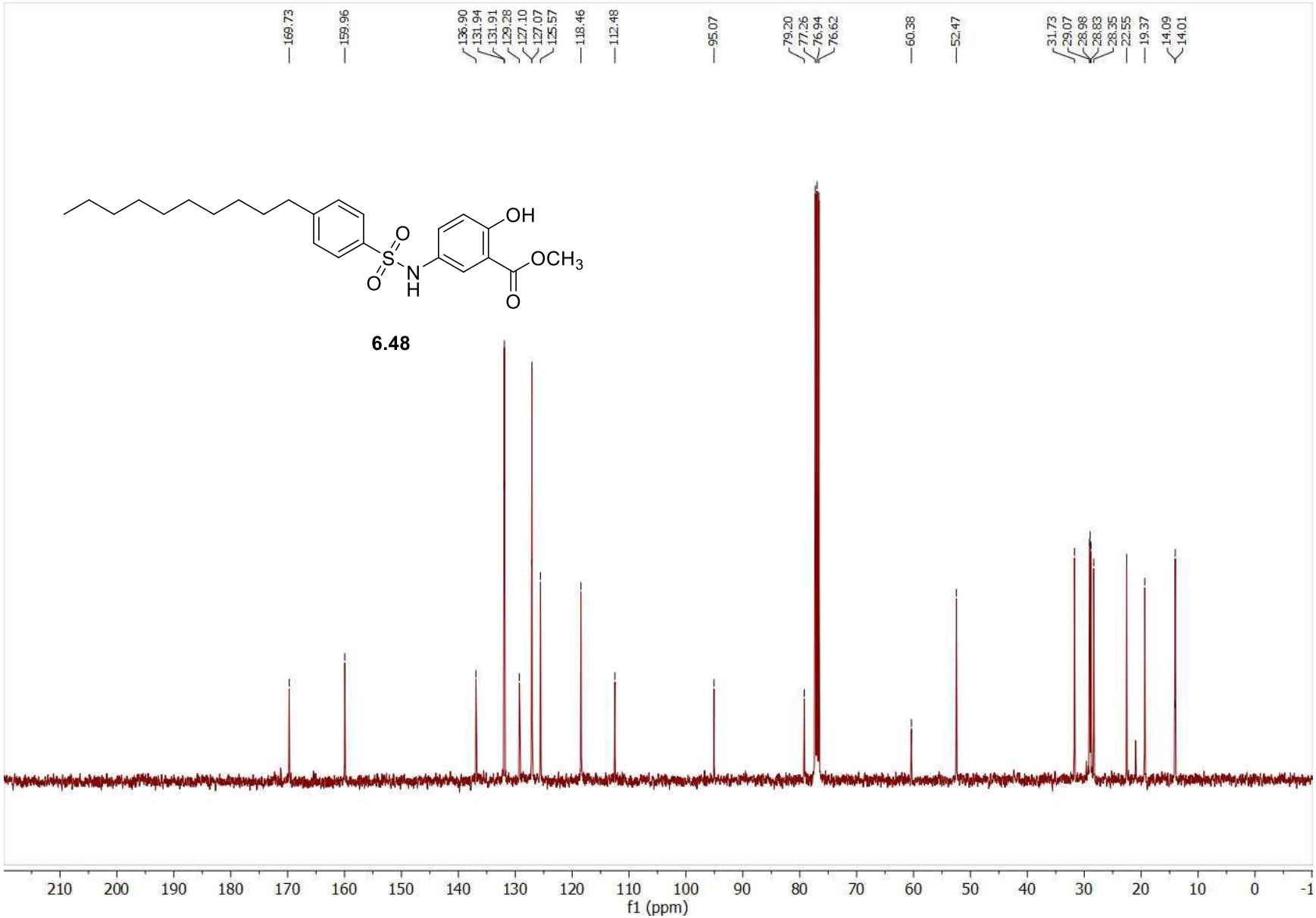

Figure B118: ^{113}C NMR of compound **6.48**.

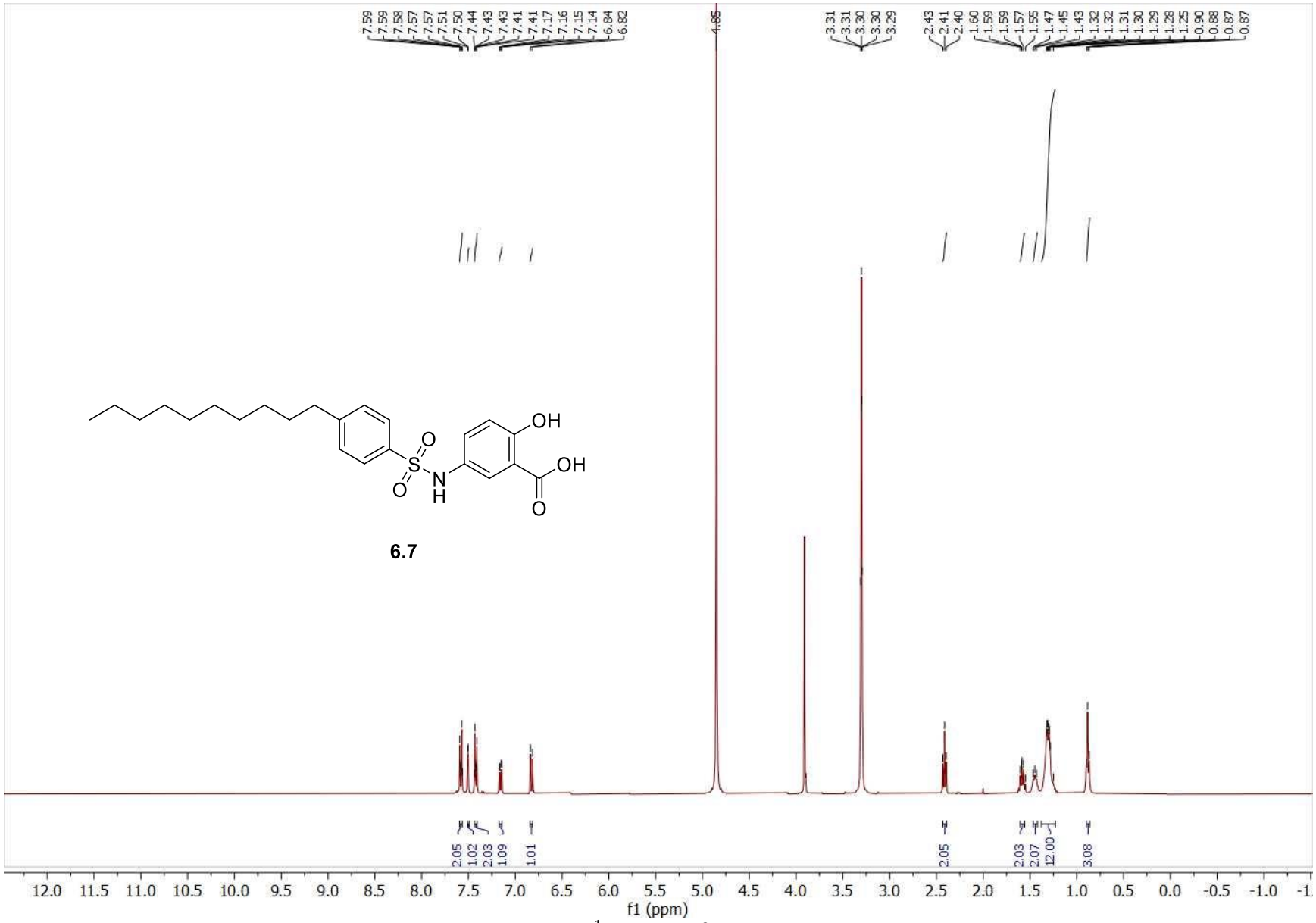

Figure B119: ^{1}H NMR of compound **6.7**.

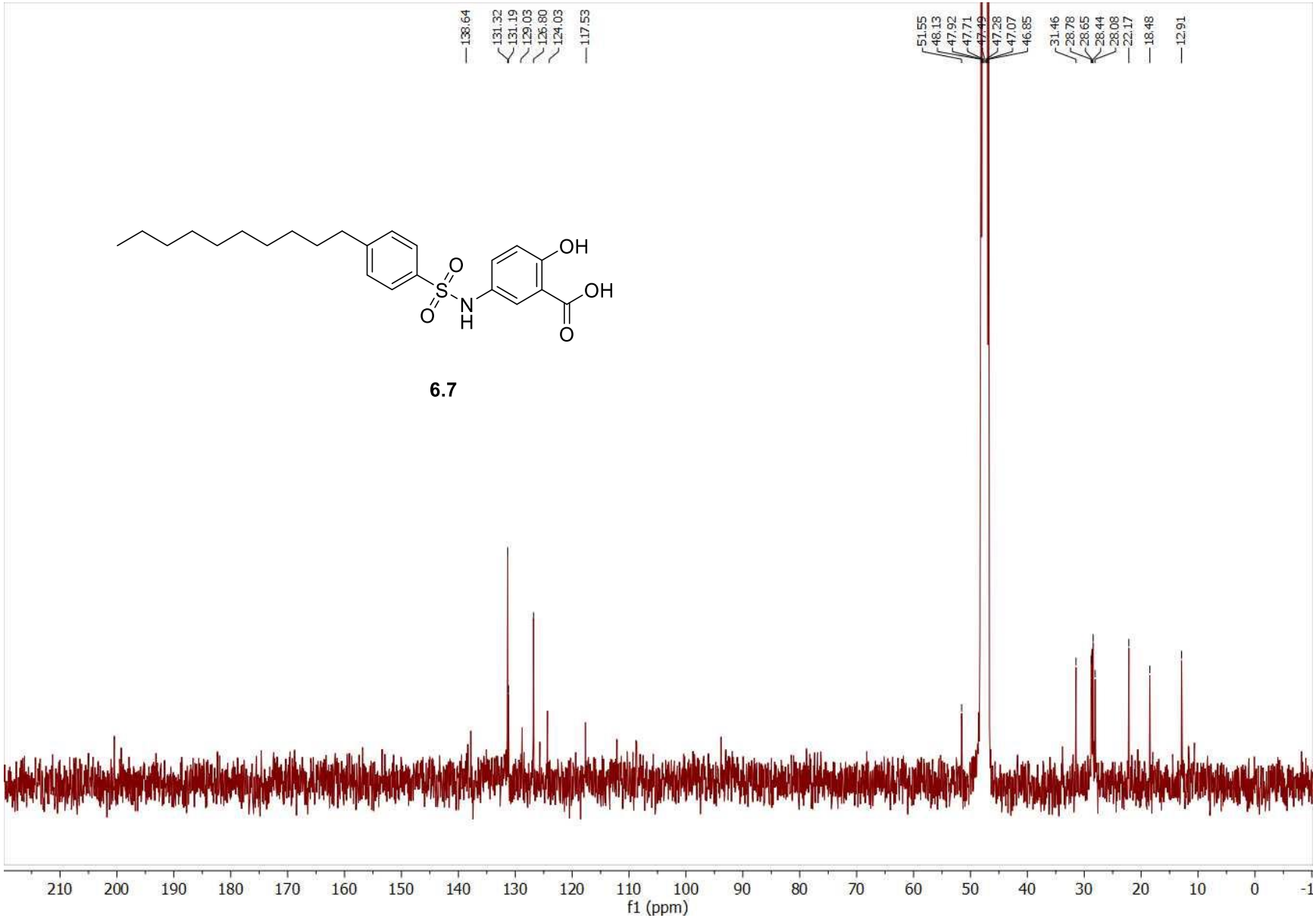

Figure B120: ^{13}C NMR of compound **6.7**.

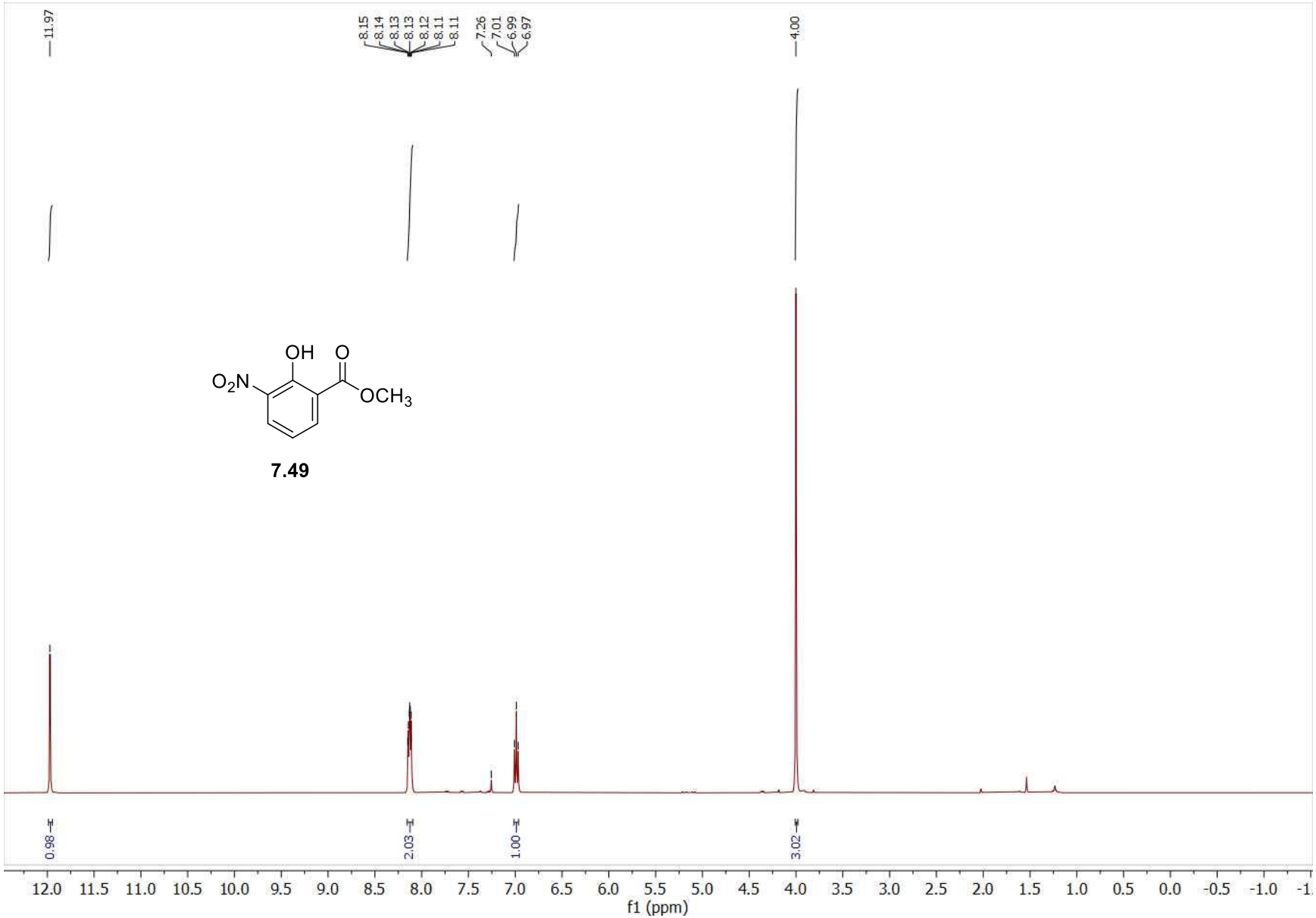

Figure B121: ^{1}H NMR of compound **7.49**.

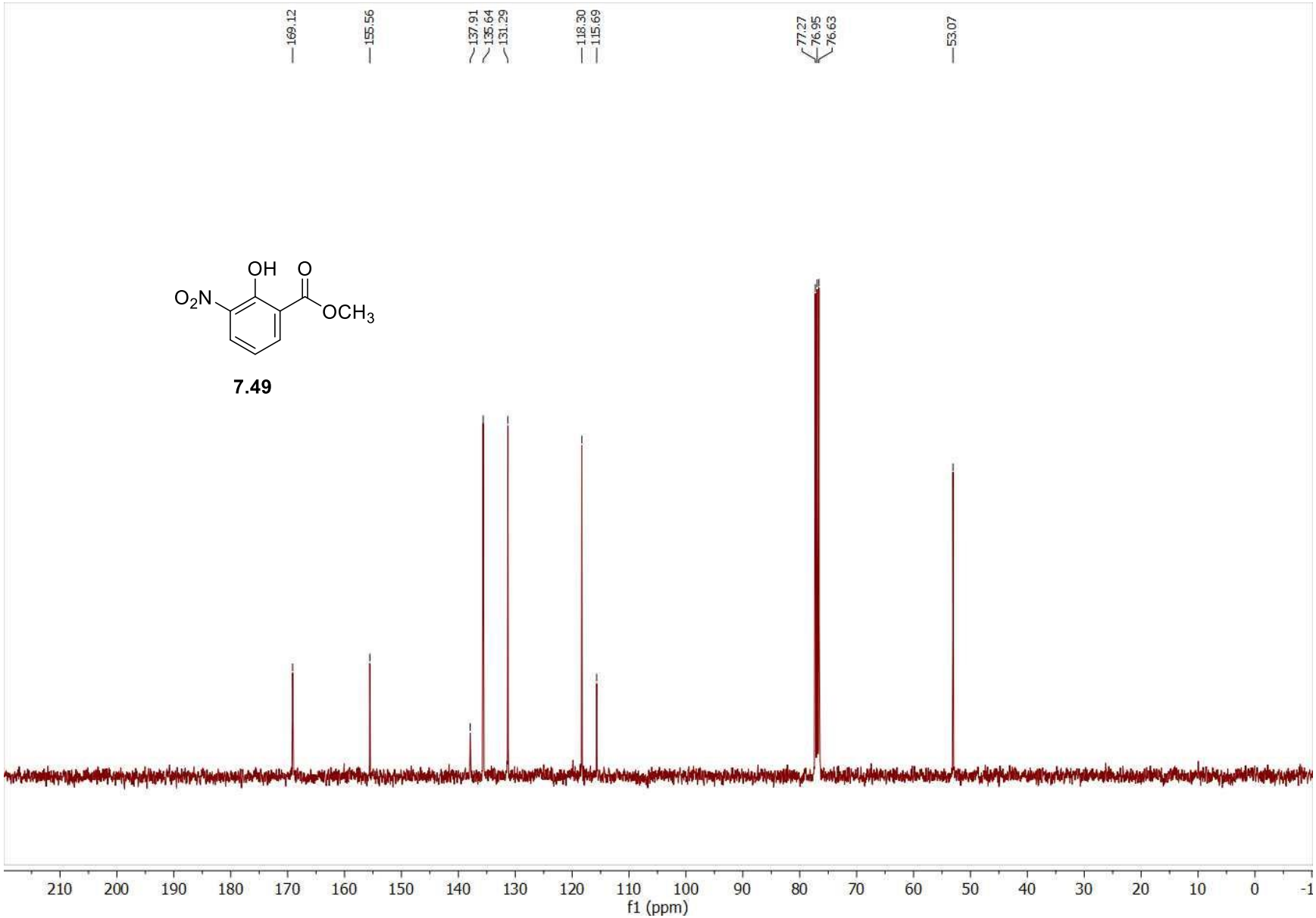

Figure B122: ^{13}C NMR of compound **7.49**.

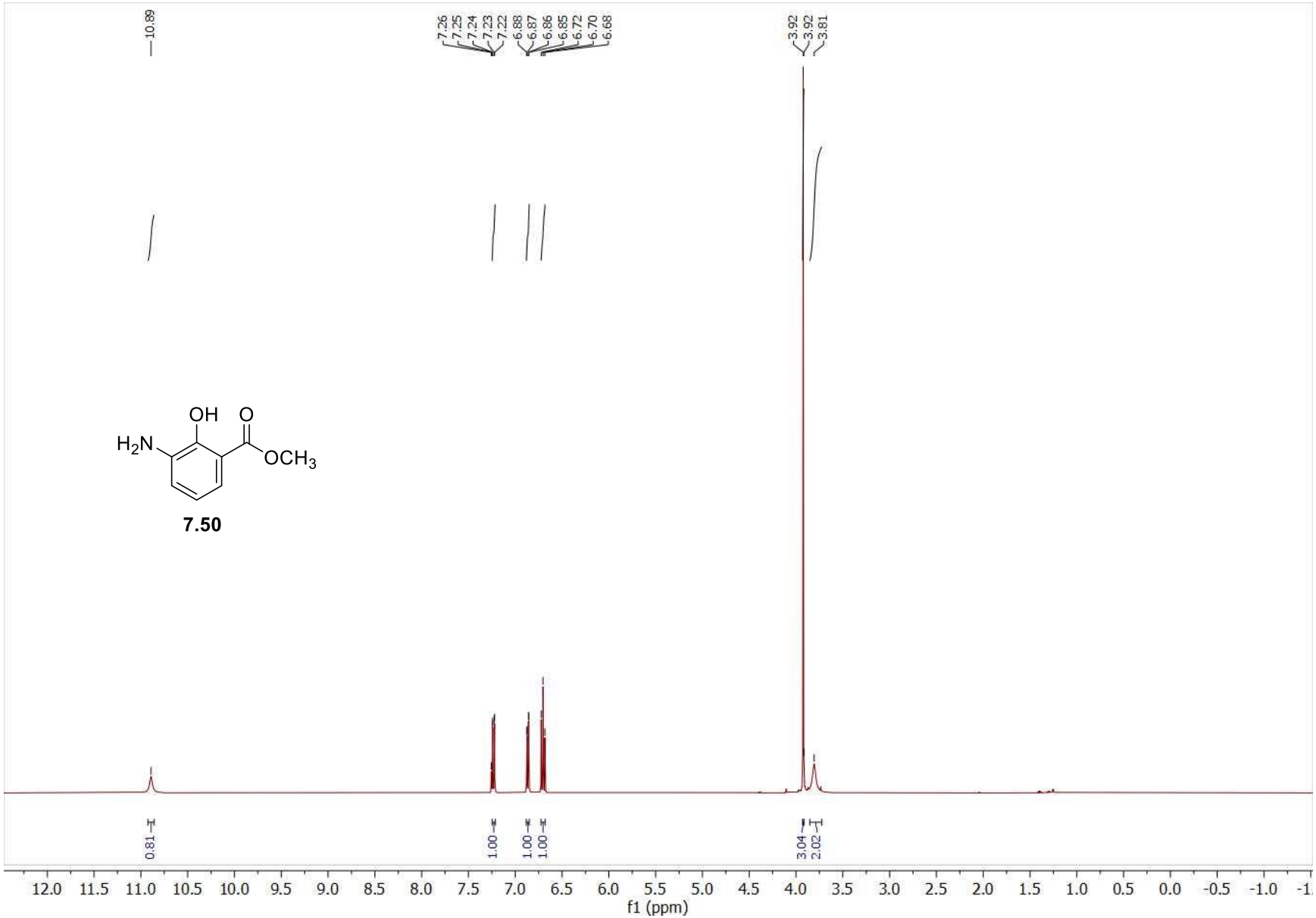

Figure B123: ^{1}H NMR of compound **7.50**.

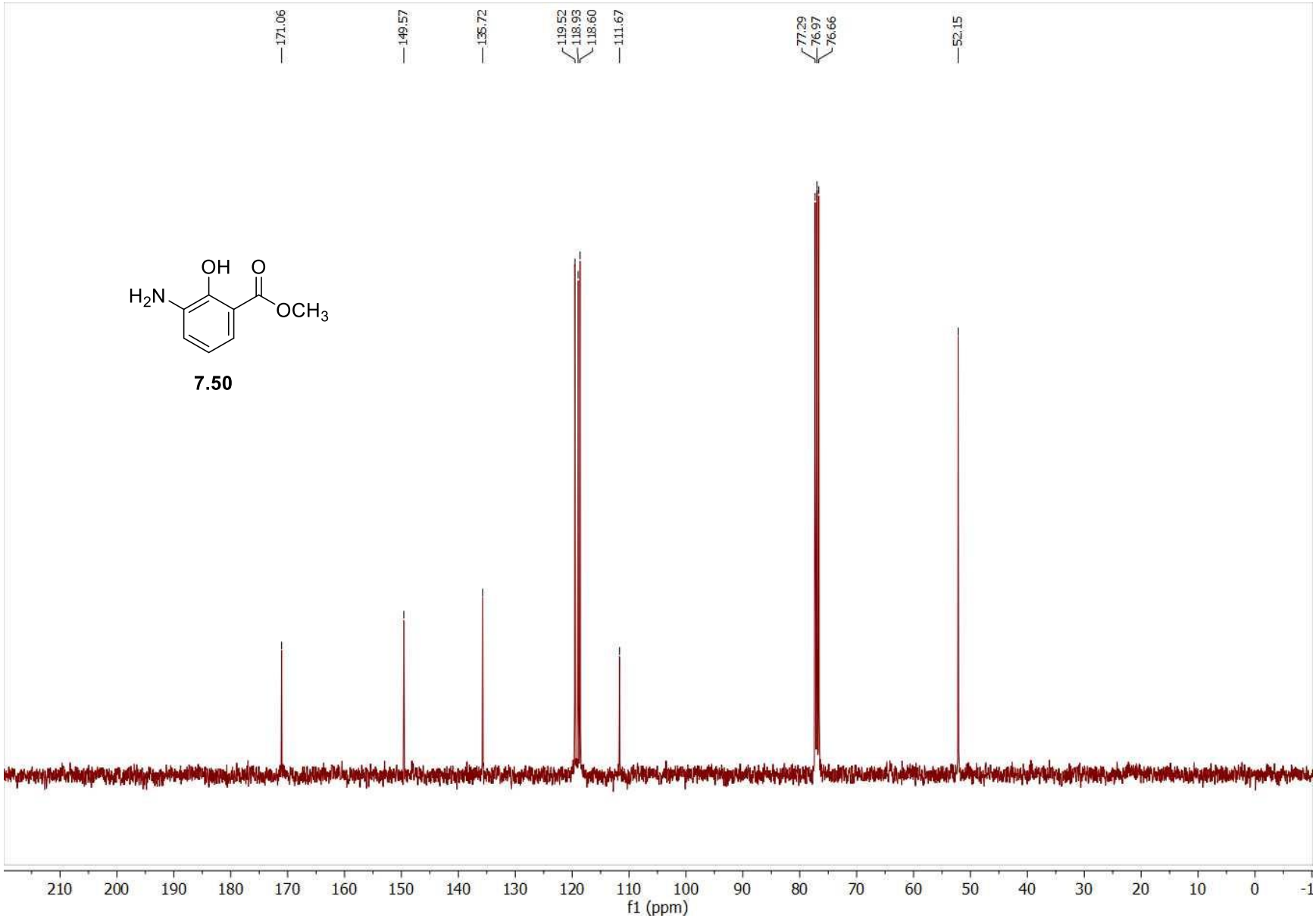

Figure B124: ^{13}C NMR of compound **7.50**.

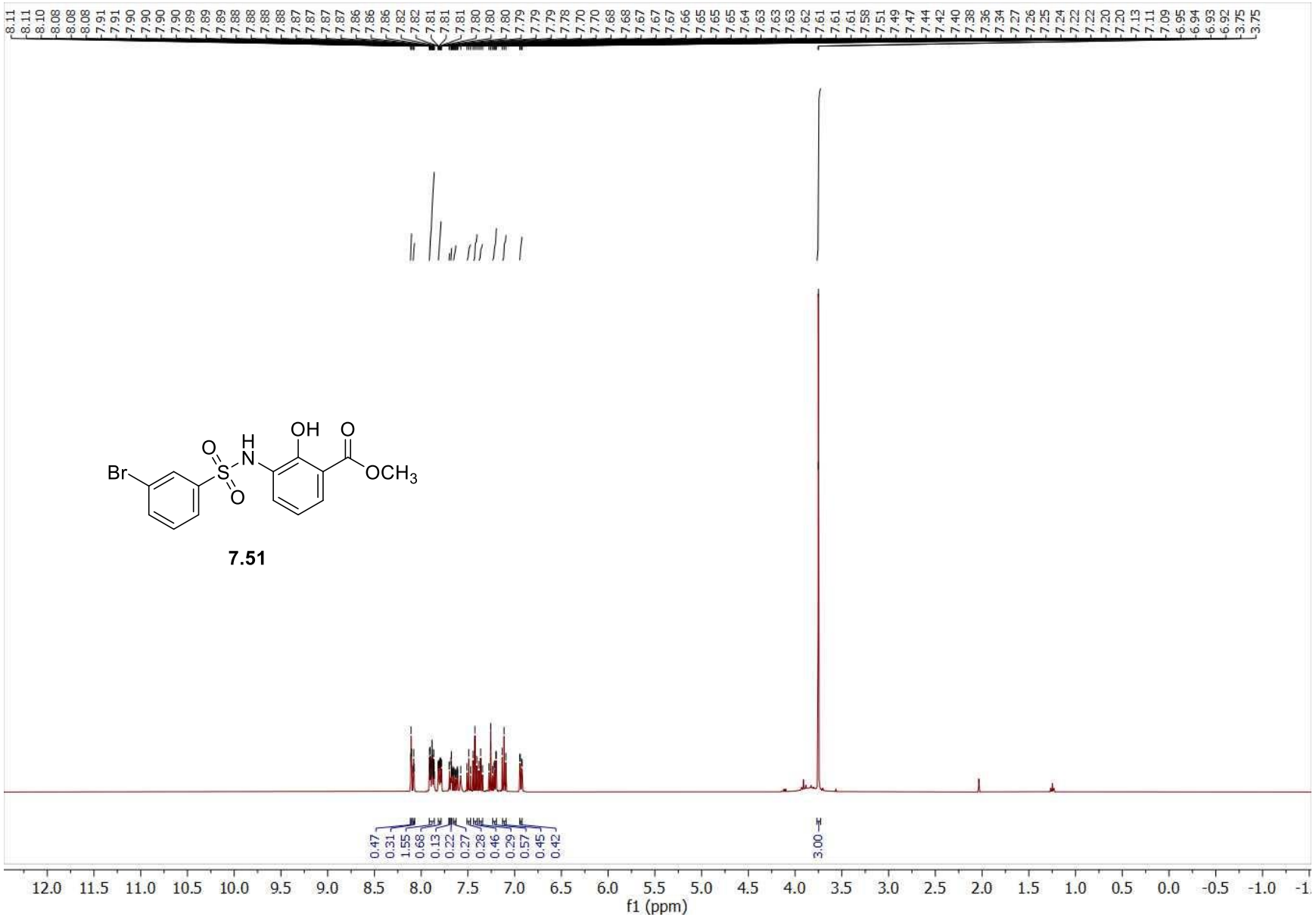

Figure B125: ^{1}H NMR of compound **7.51**.

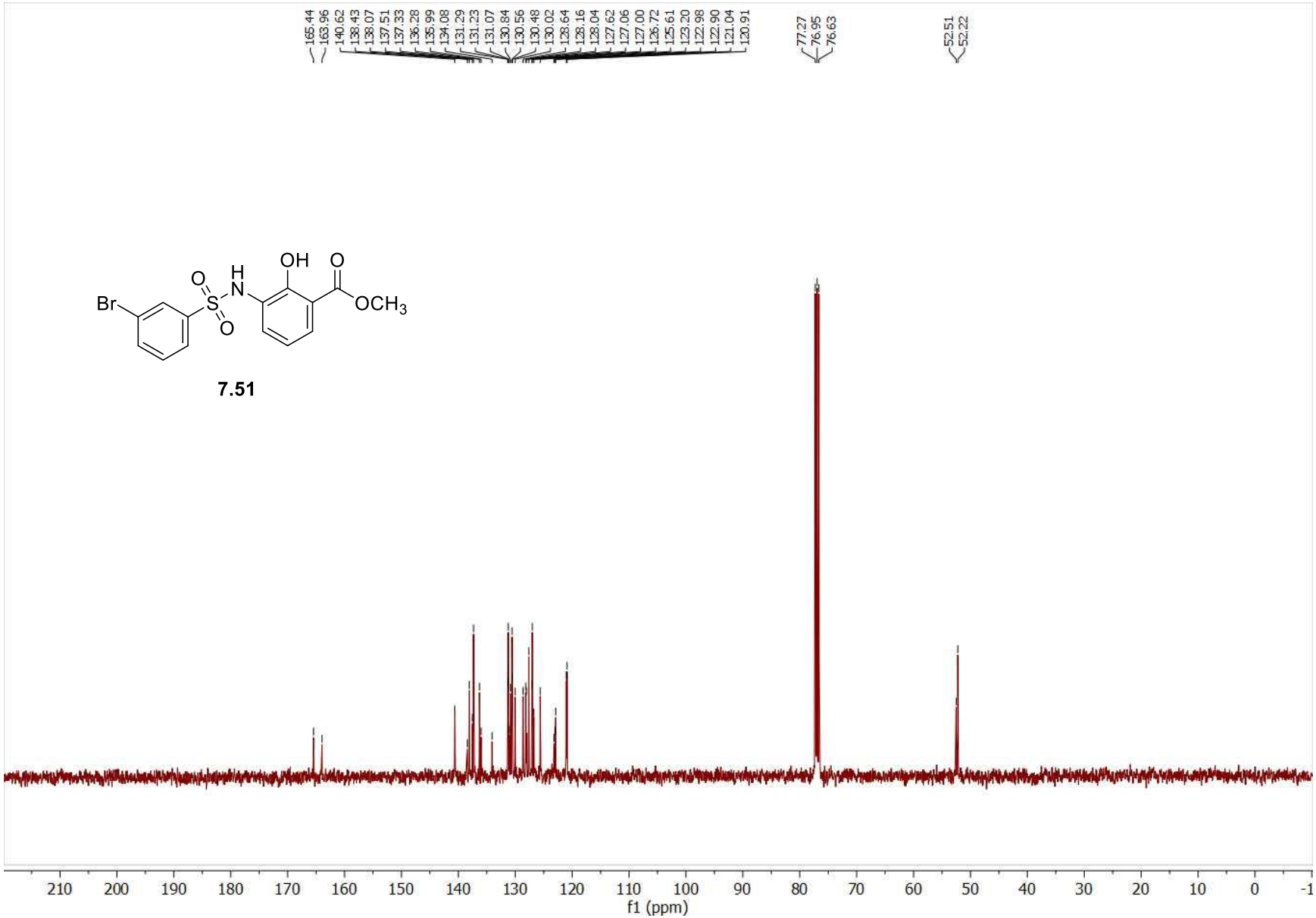

Figure B126: ^{13}C NMR of compound **7.51**.

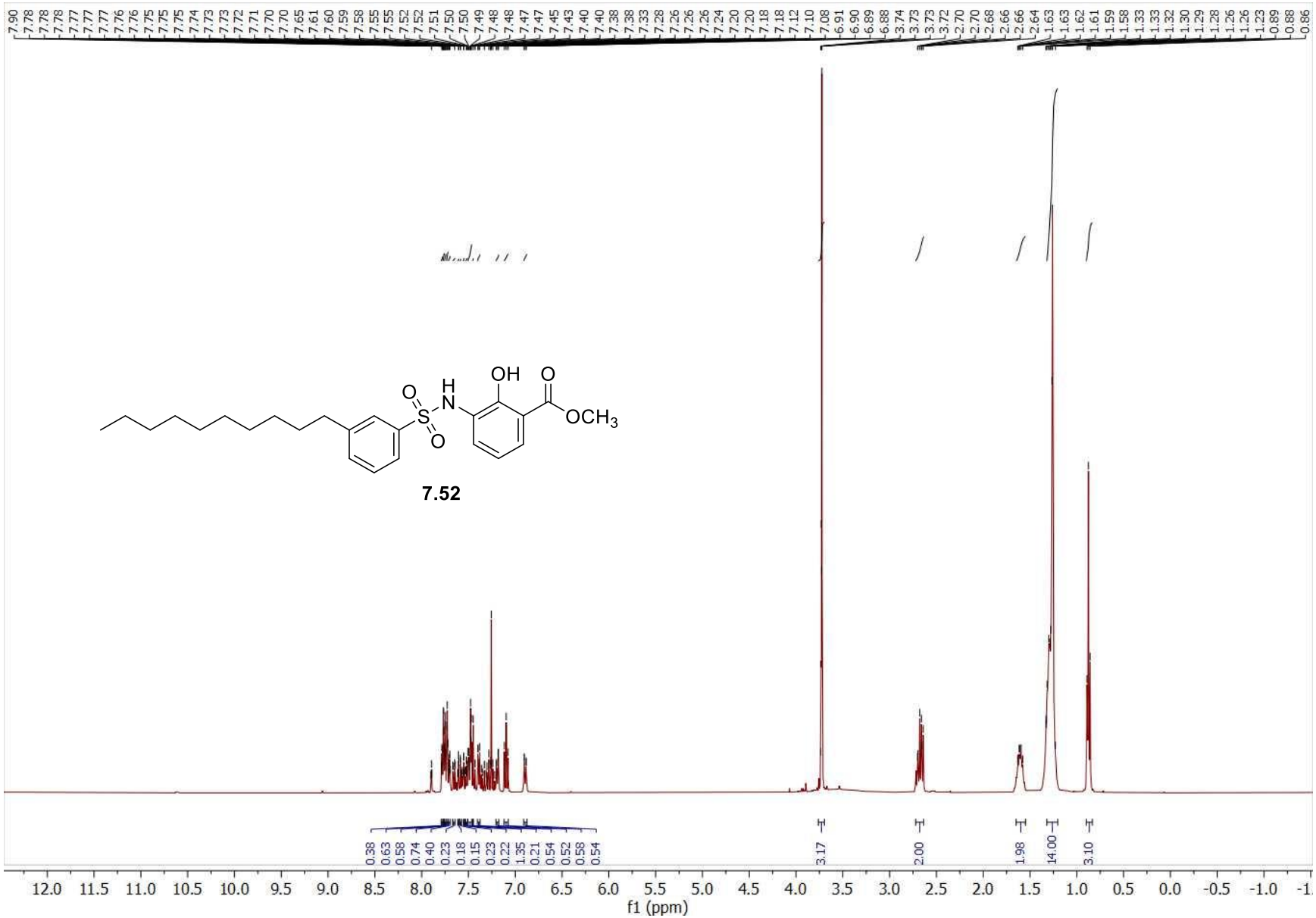

Figure B127: ^{1}H NMR of compound **7.52**.

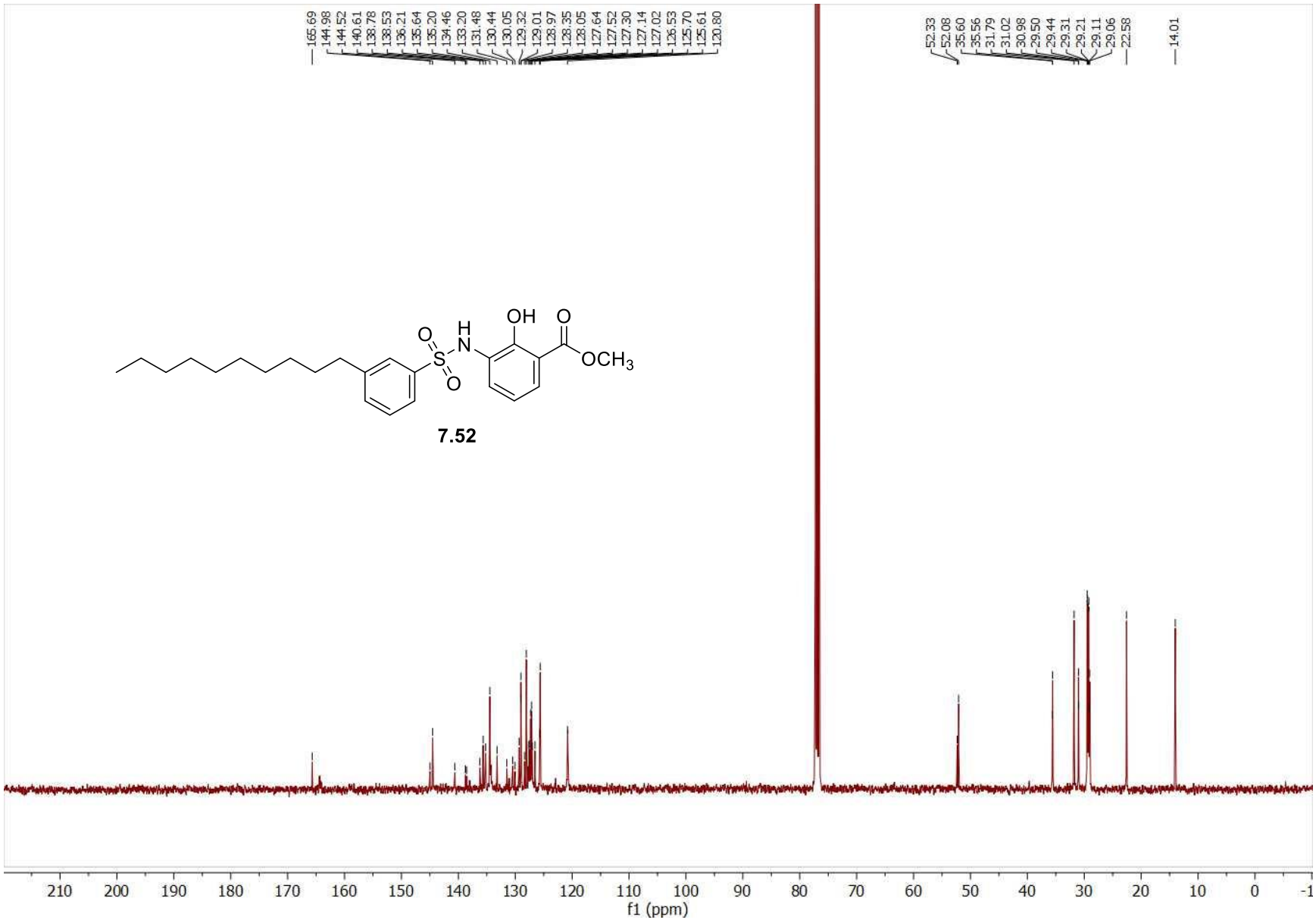

Figure B128: ^{13}C NMR of compound **7.52**.

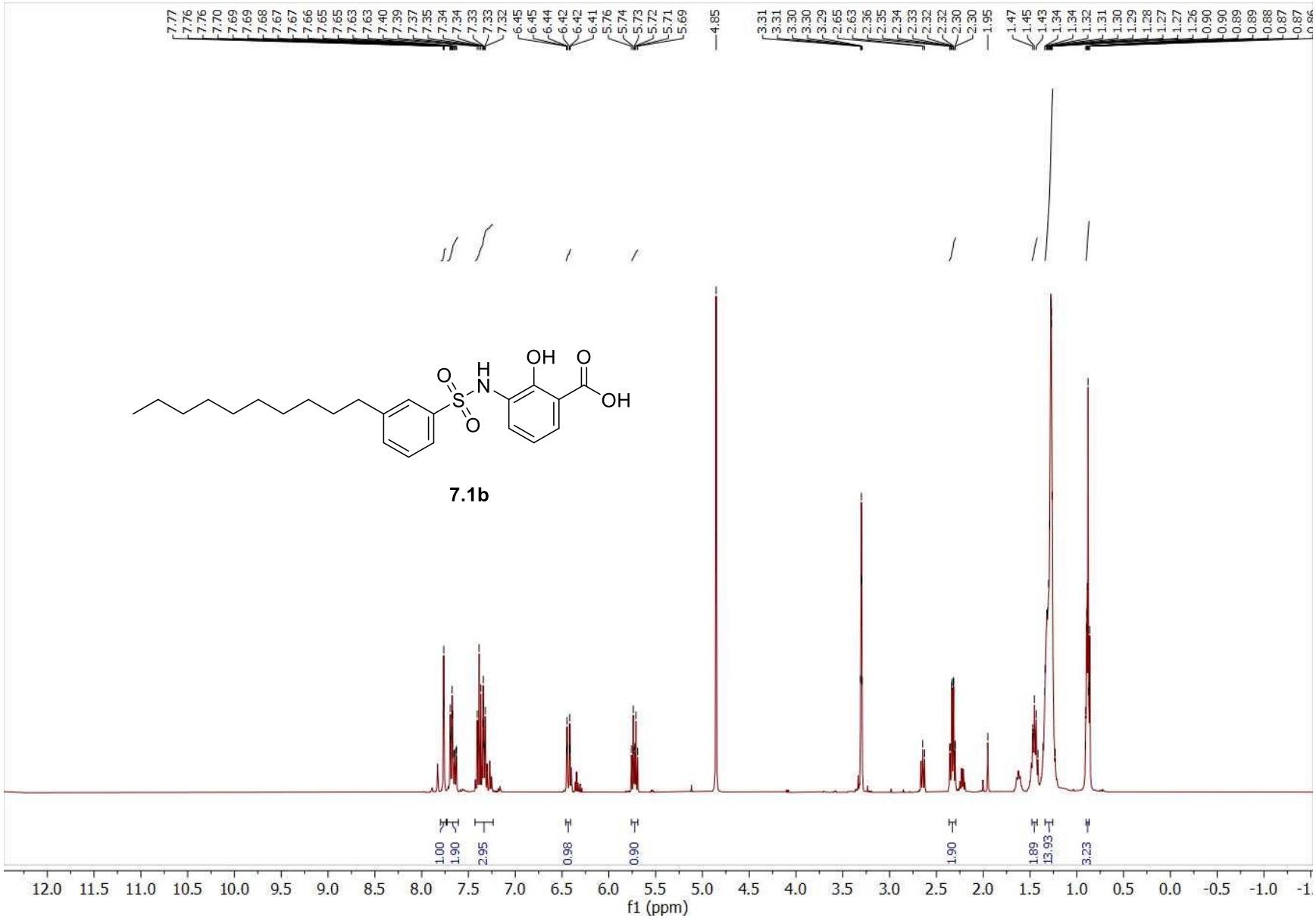

Figure B129: ^{1}H NMR of compound **7.1b**.

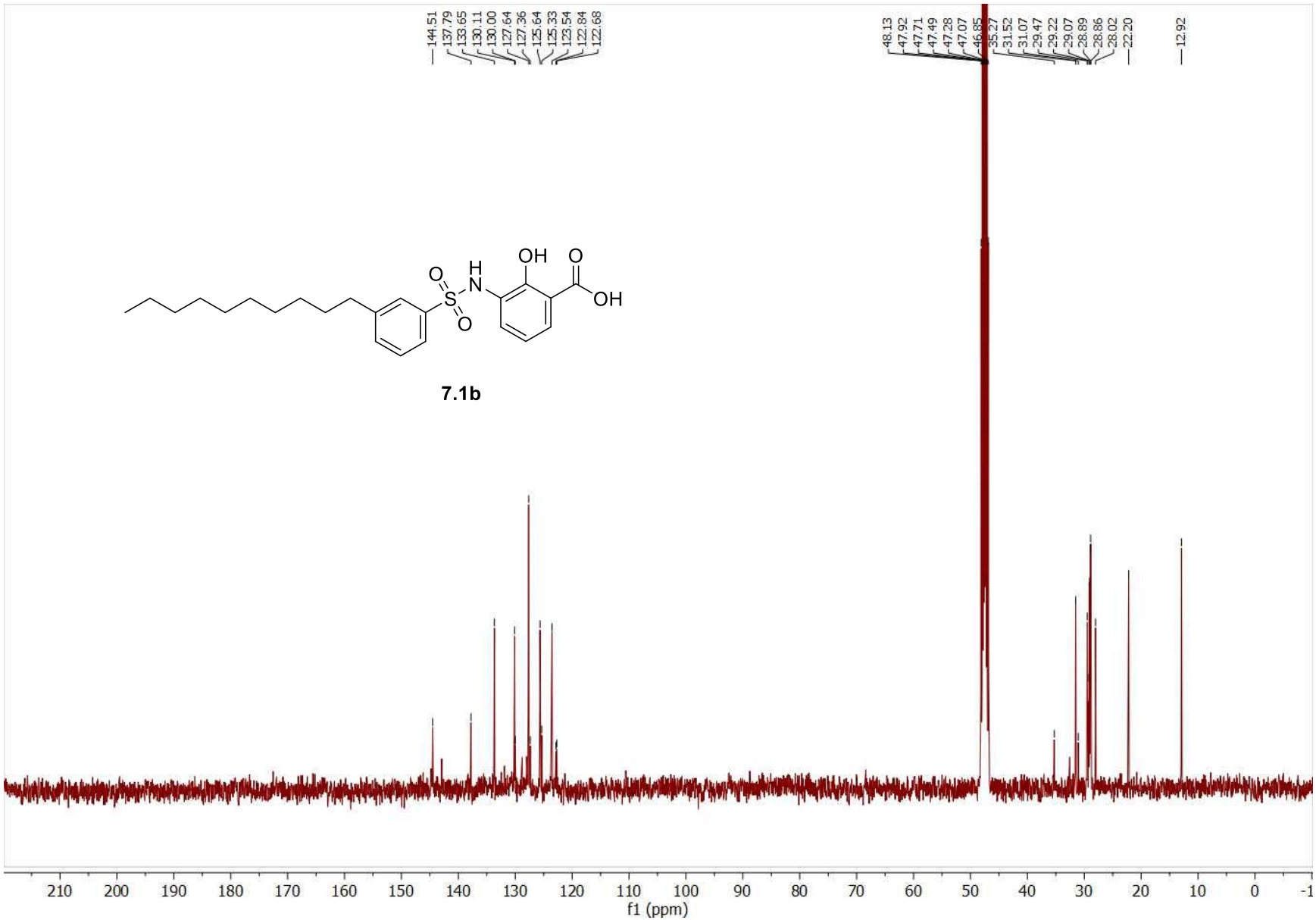

Figure B130: ^{13}C NMR of compound **7.1b**.

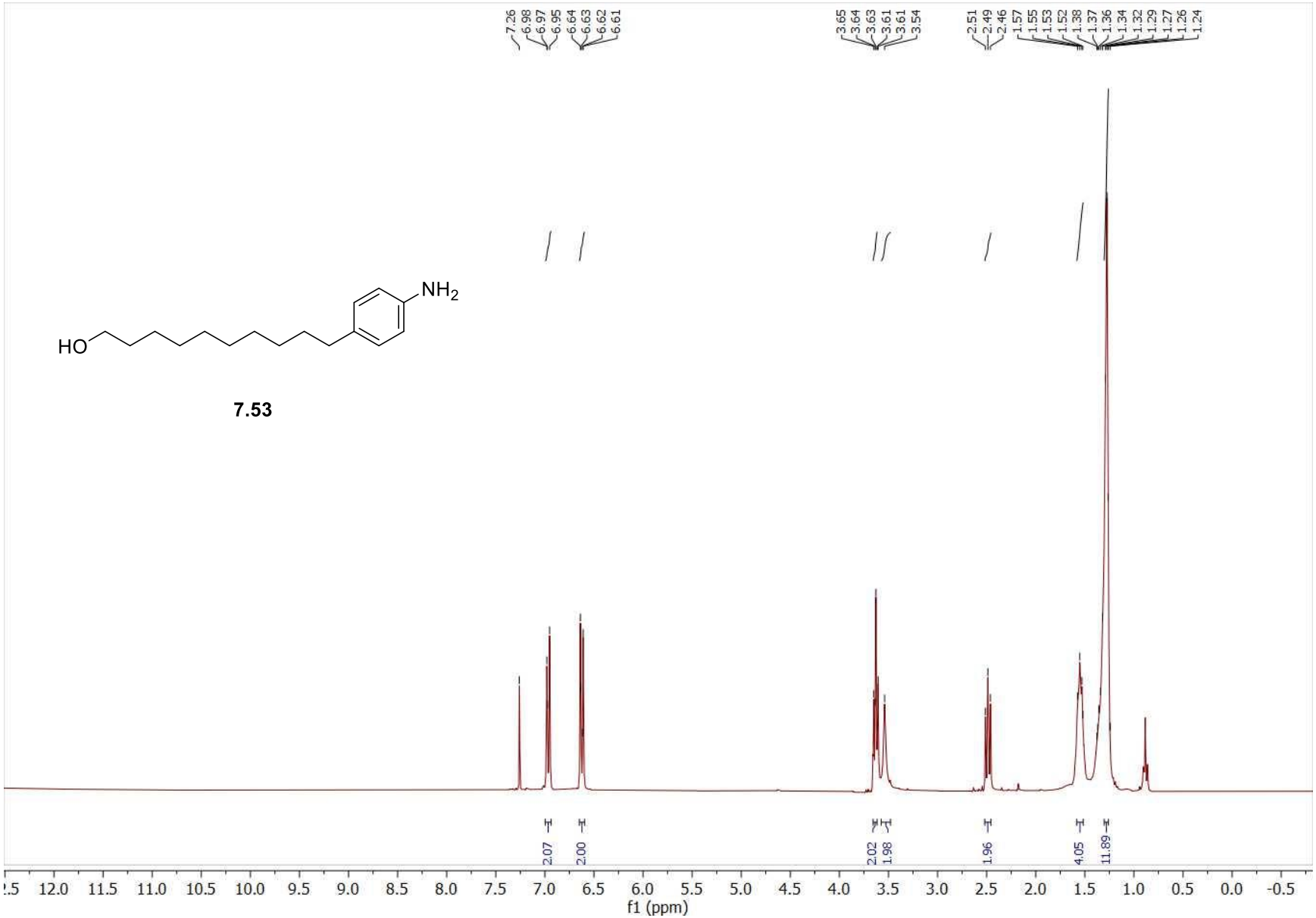

Figure B131: ^{1}H NMR of compound **7.53**.

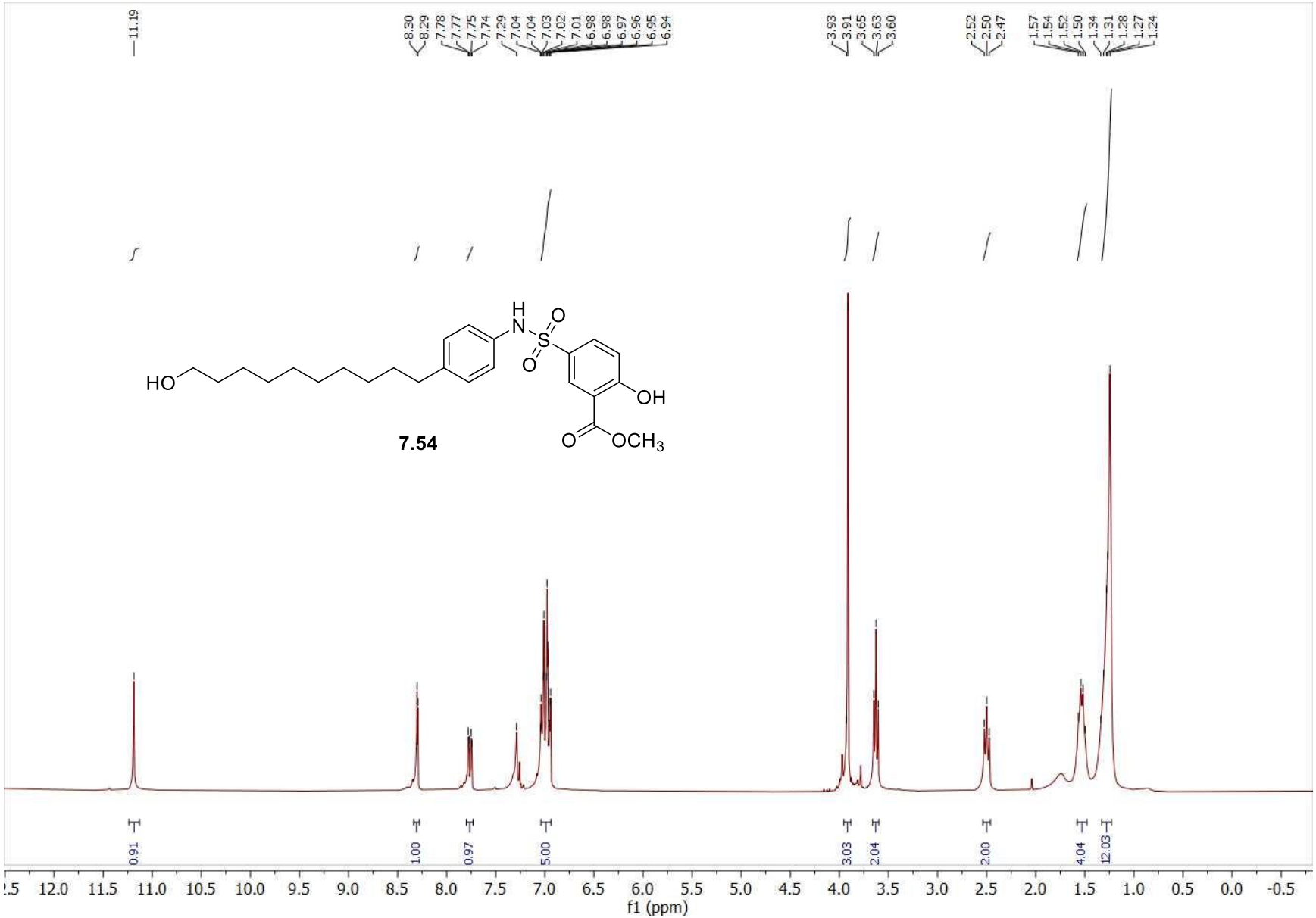

Figure B132: ^{1}H NMR of compound **7.54**.

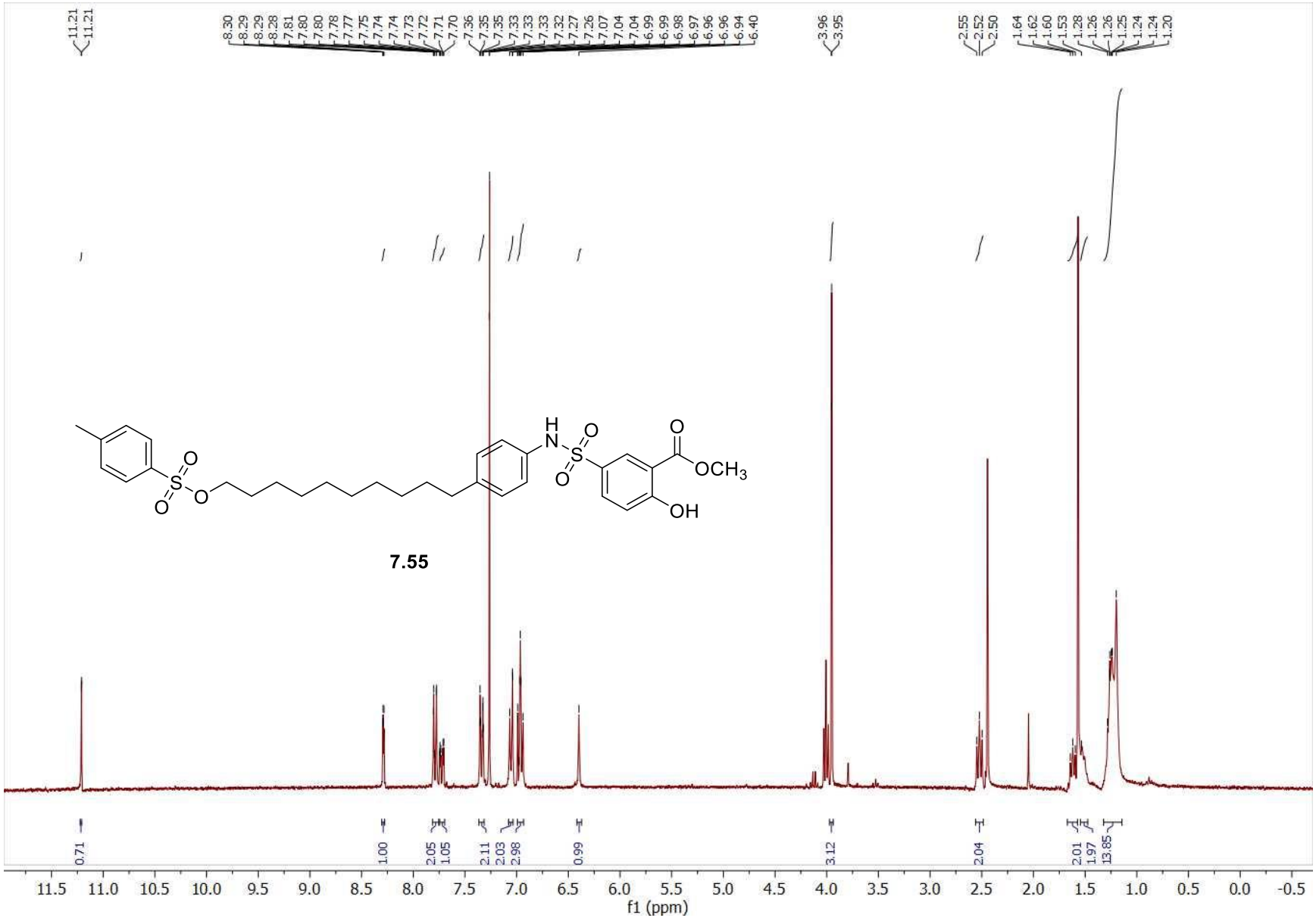

Figure B133: ^{1}H NMR of compound **7.55**.

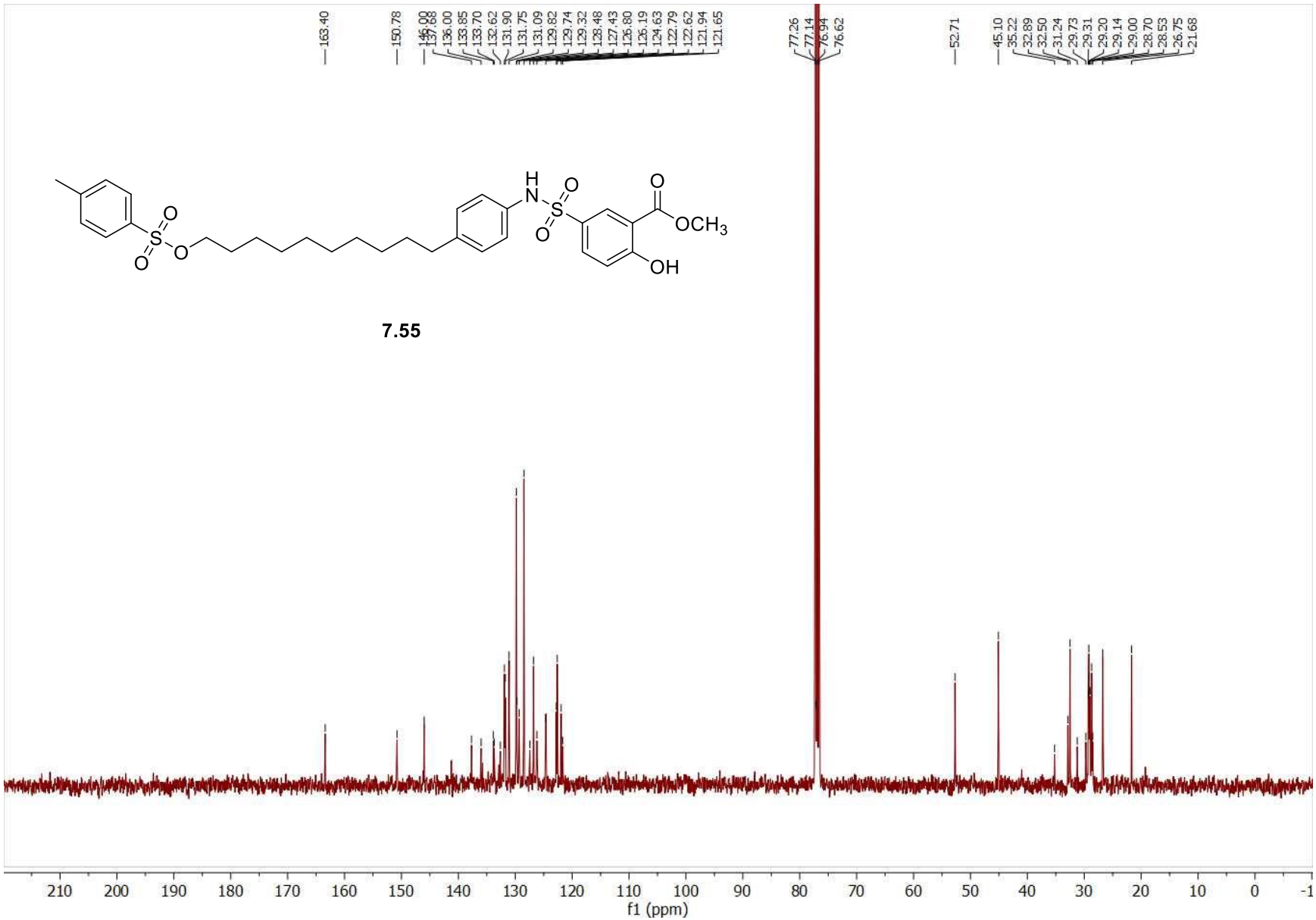

Figure B134: ^{13}C NMR of compound **7.55**.

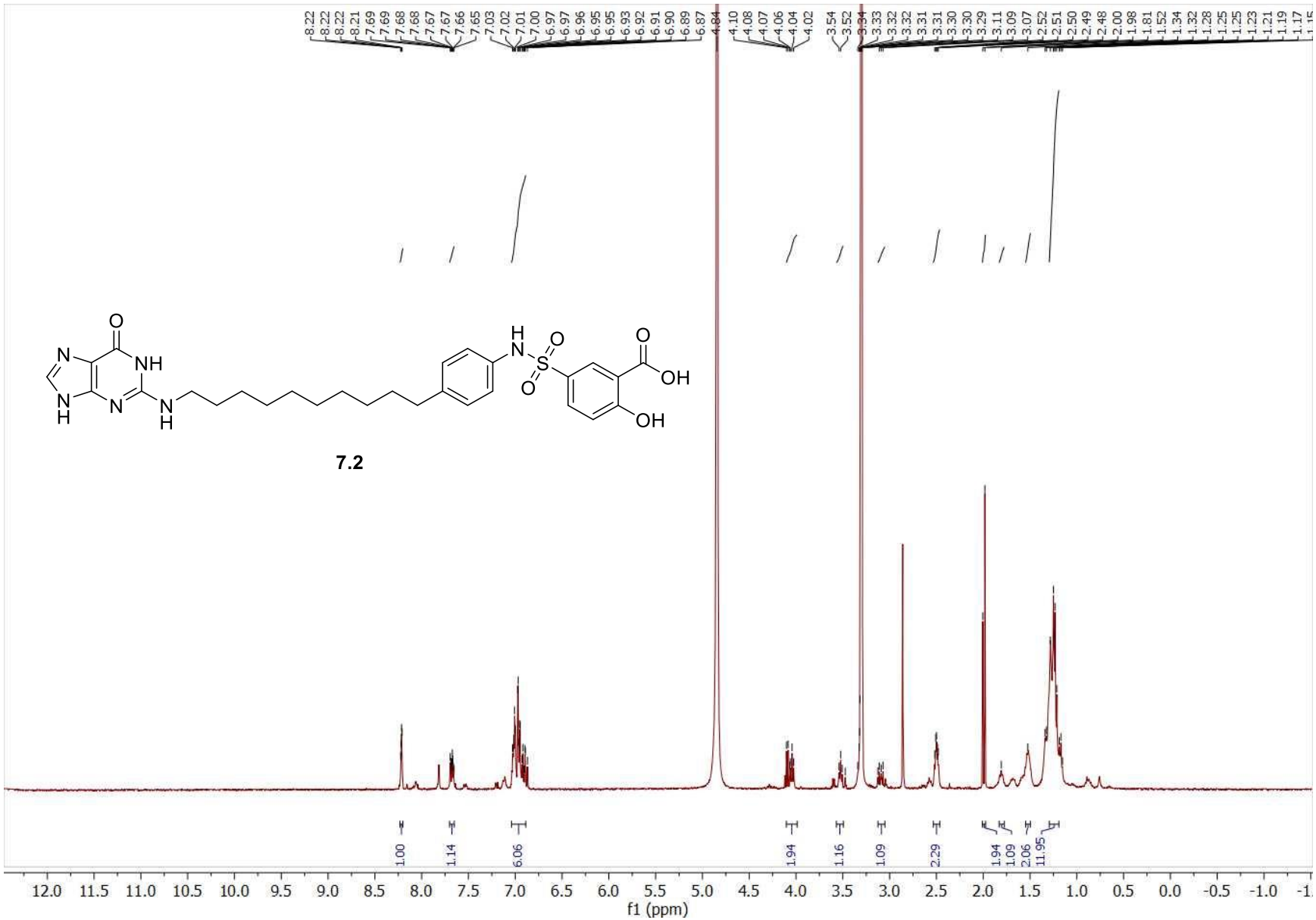

Figure B135: ^{1}H NMR of compound **7.2**.

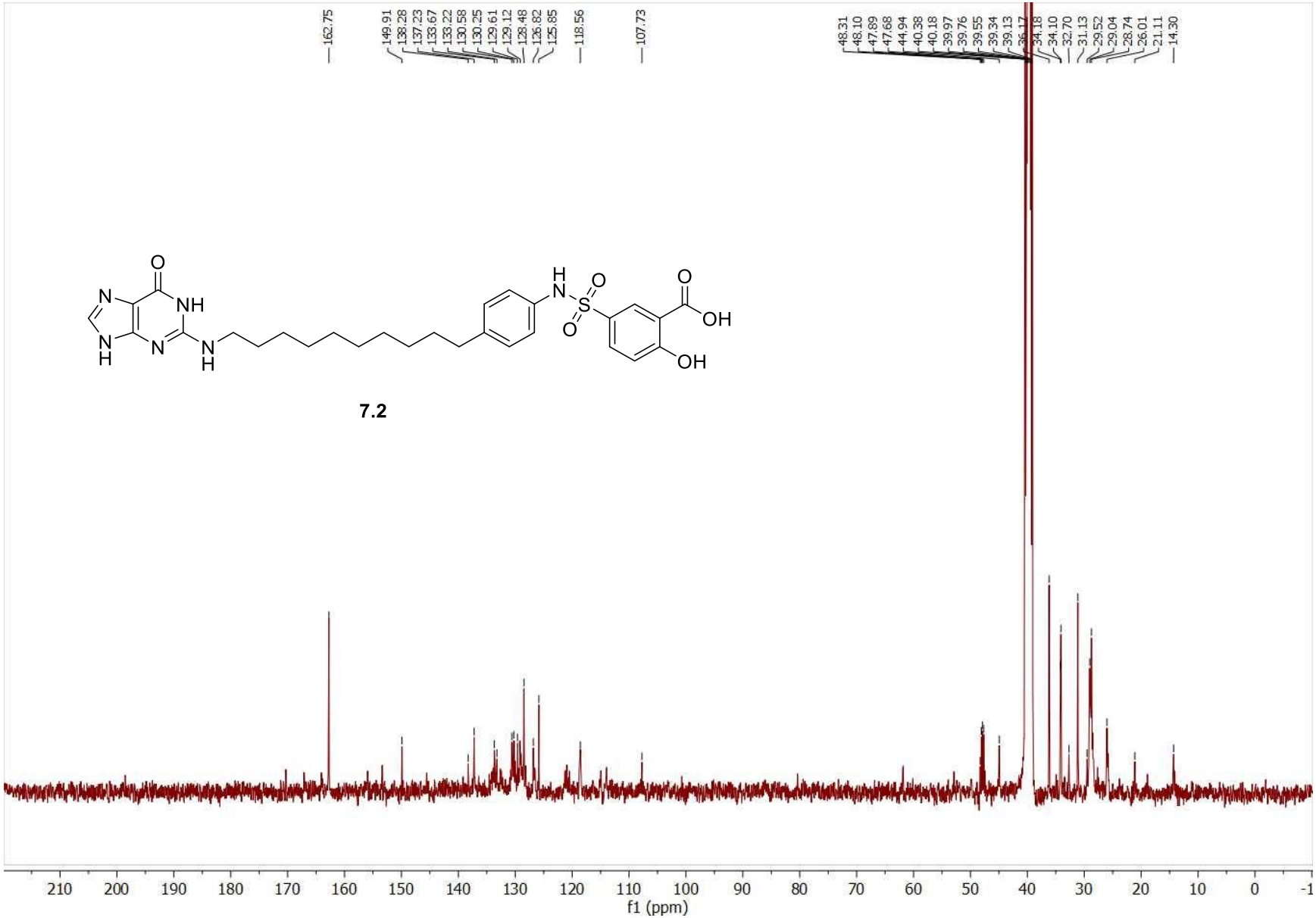

Figure B136: ^{13}C NMR of compound **7.2**.

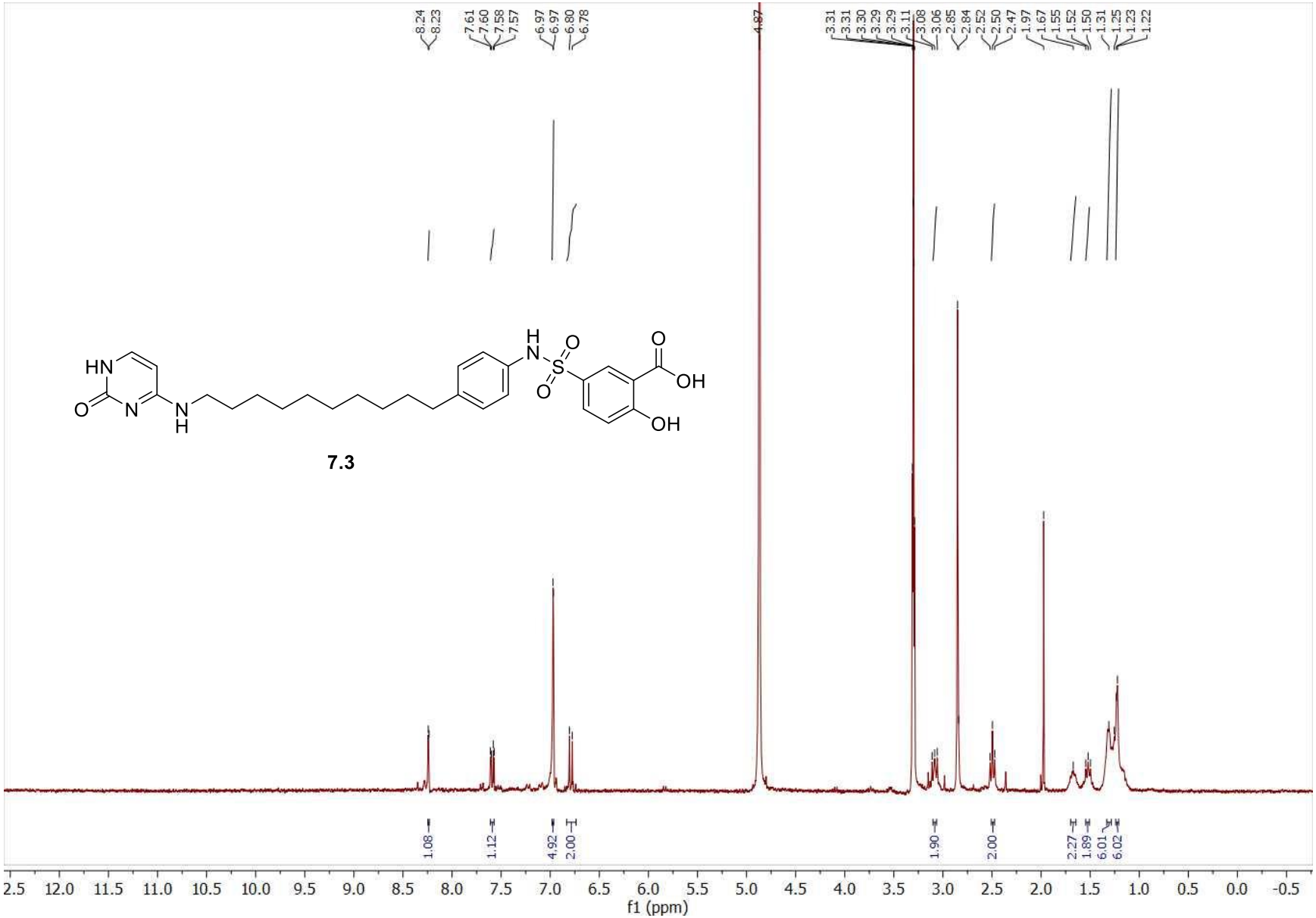

Figure B137: ^{1}H NMR of compound **7.3**.

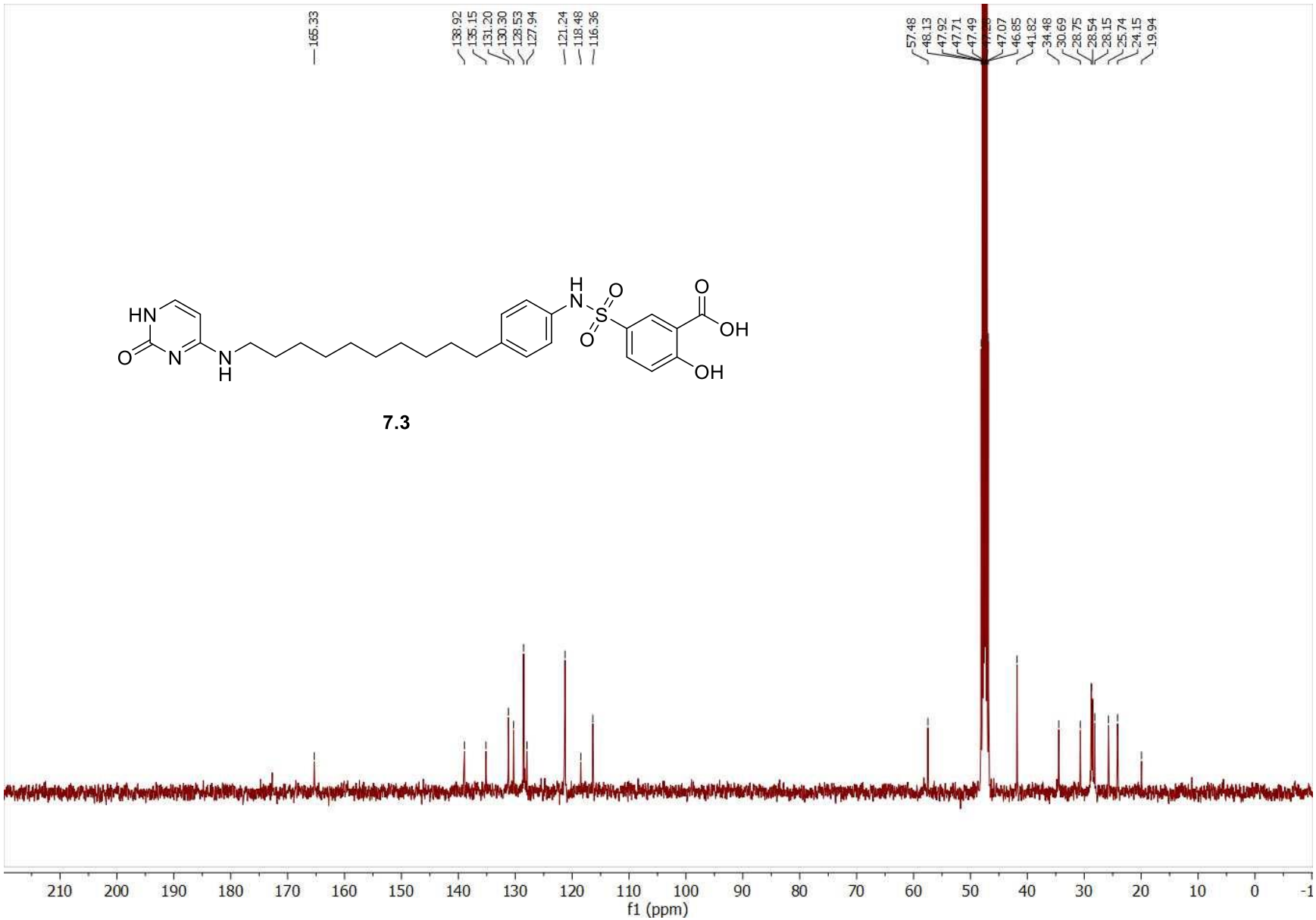

Figure B138: ^{13}C NMR of compound **7.3**.

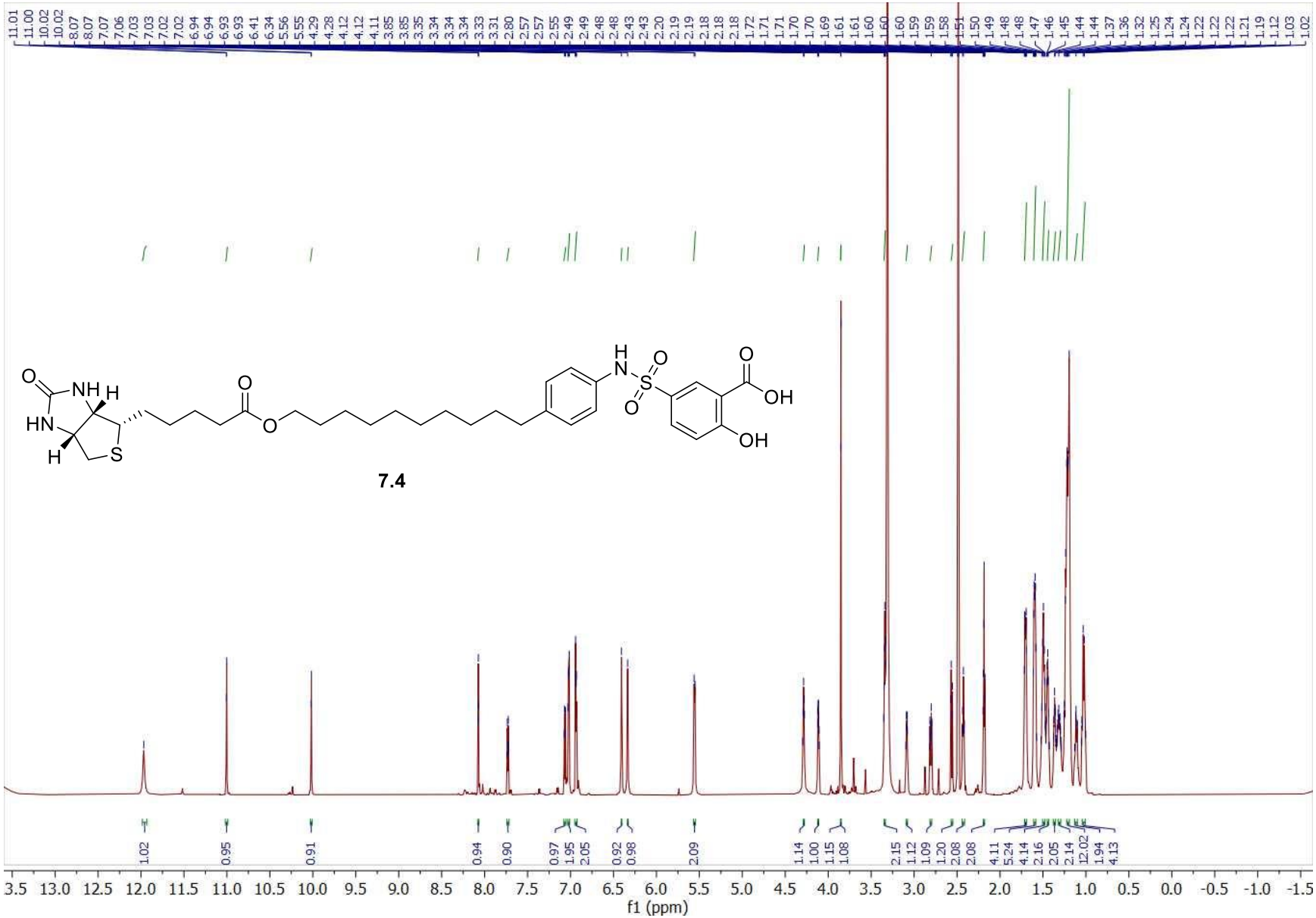

Figure B139: ^{1}H NMR of compound **7.4**.

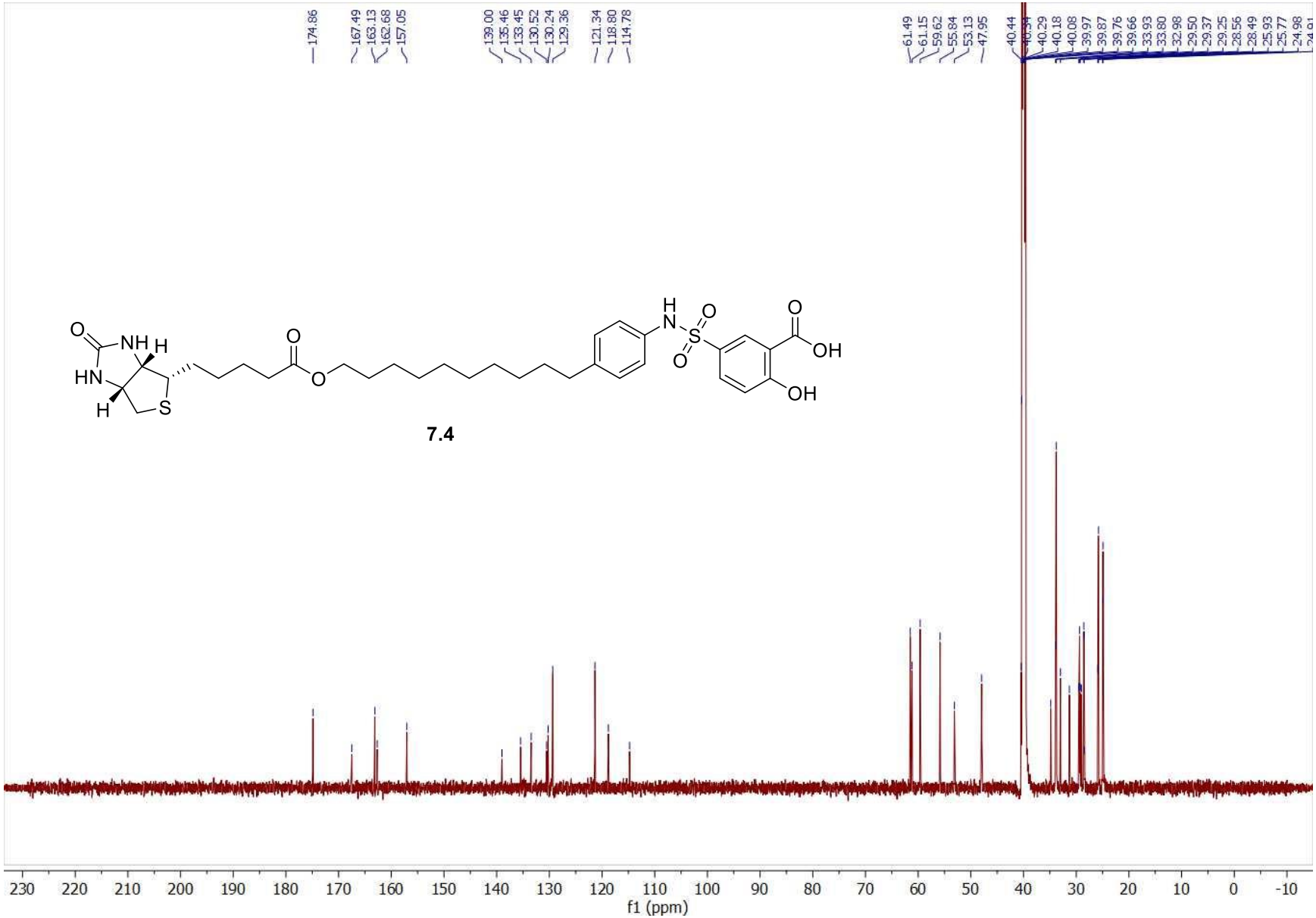

Figure B140: ^{13}C NMR of compound **7.4**.

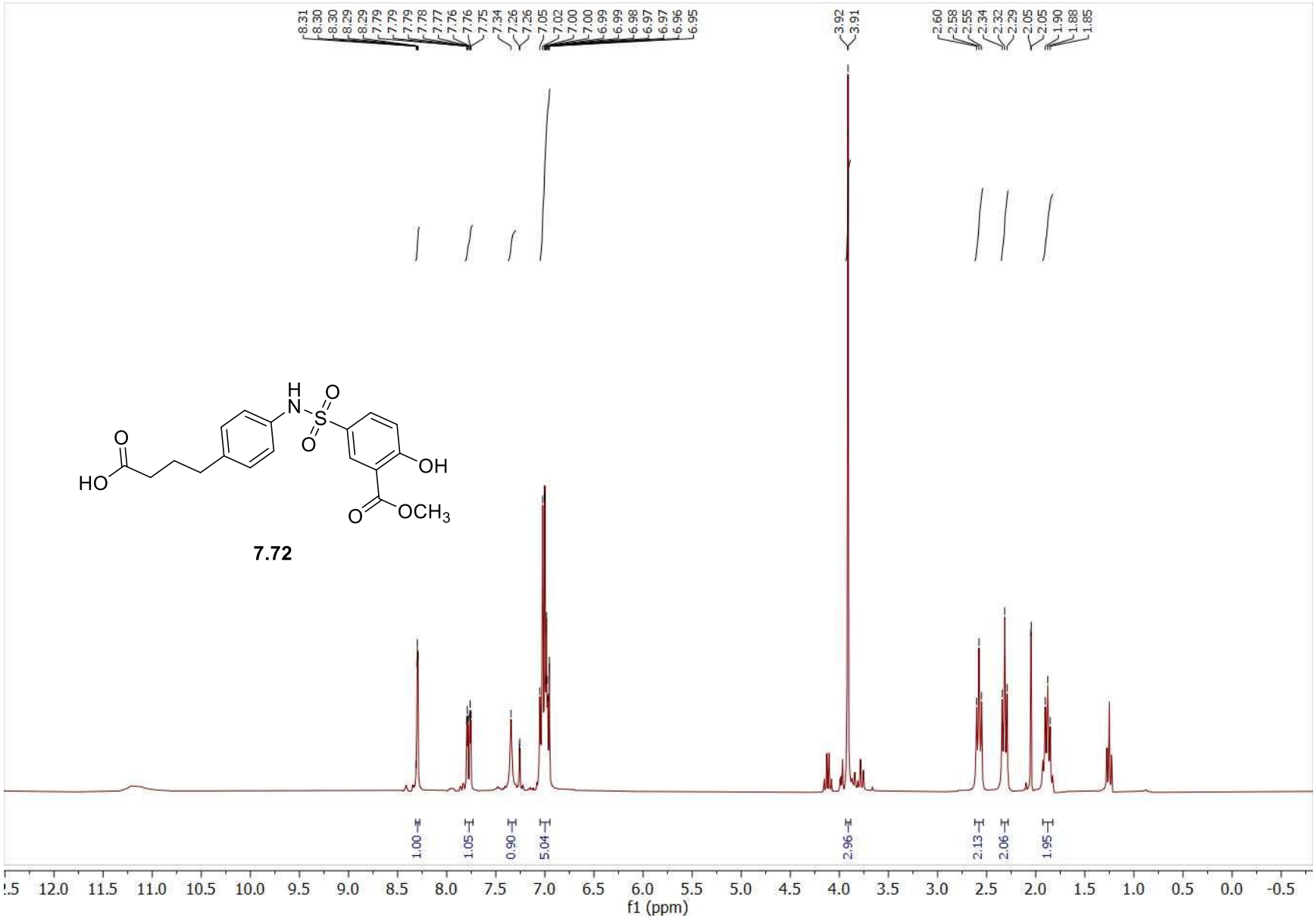

Figure B141: ^{1}H NMR of compound **7.72**.

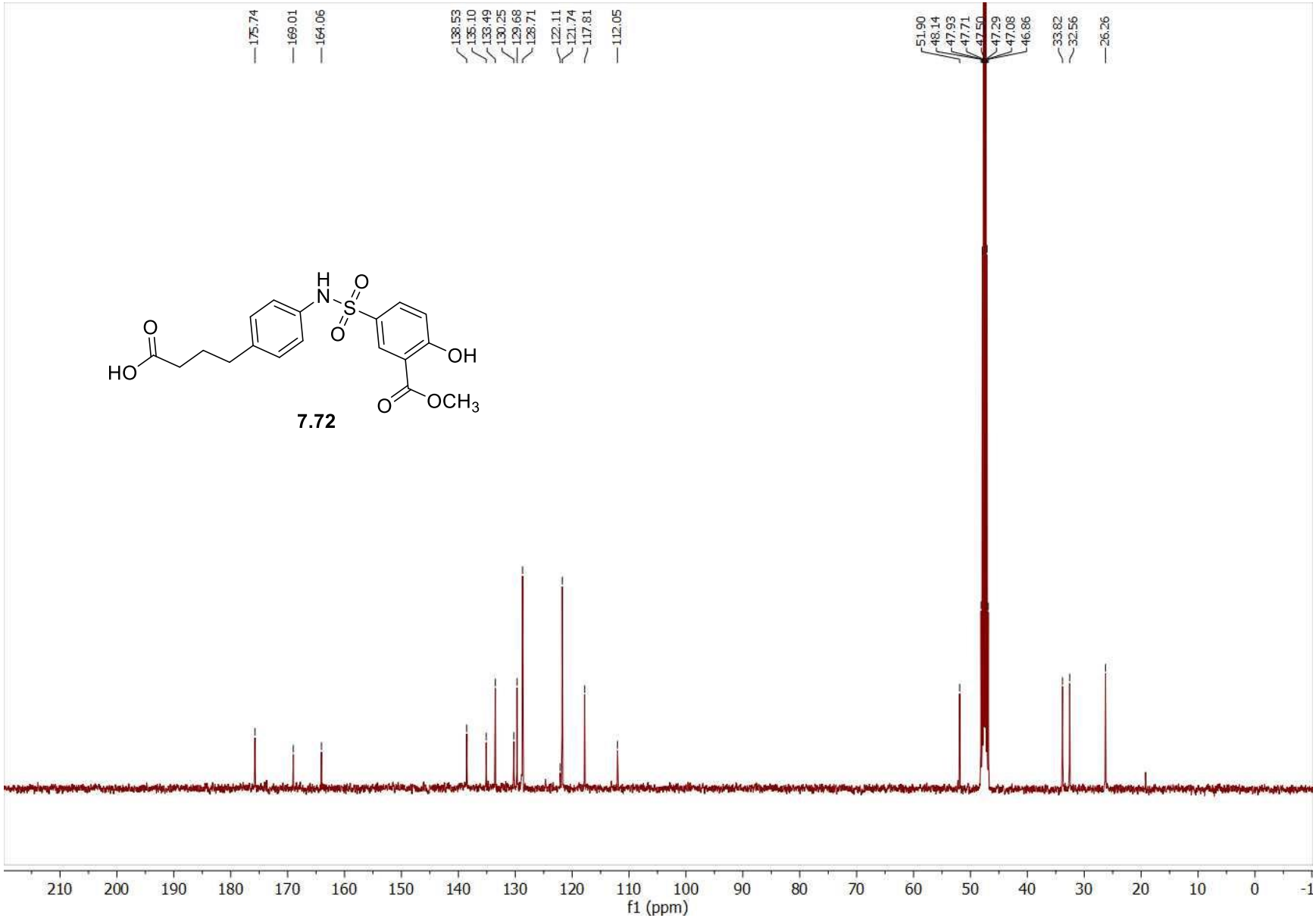

Figure B142: ^{13}C NMR of compound **7.72**.

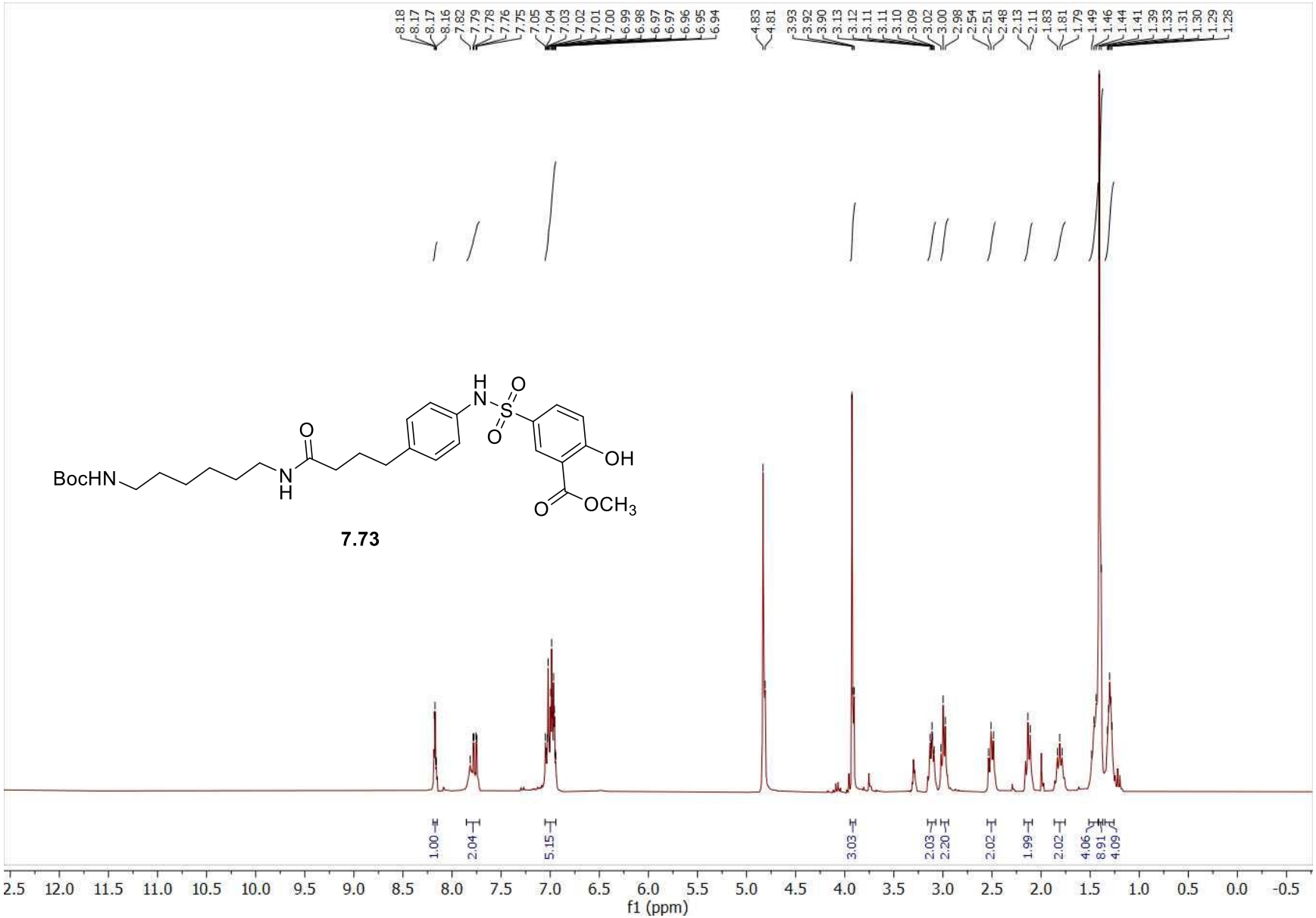

Figure B143: ^{1}H NMR of compound **7.73**.

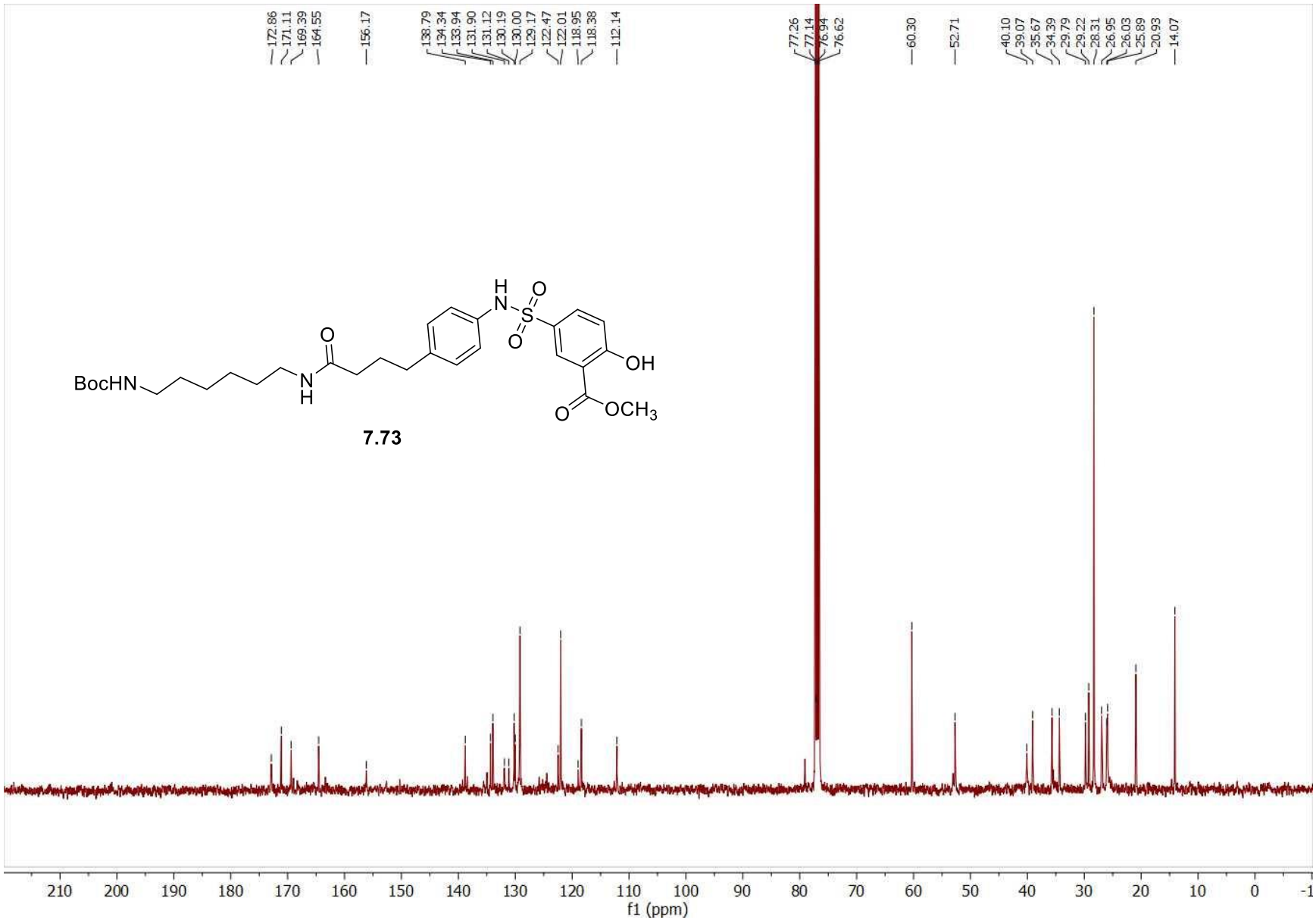

Figure B144: ^{13}C NMR of compound **7.73**.

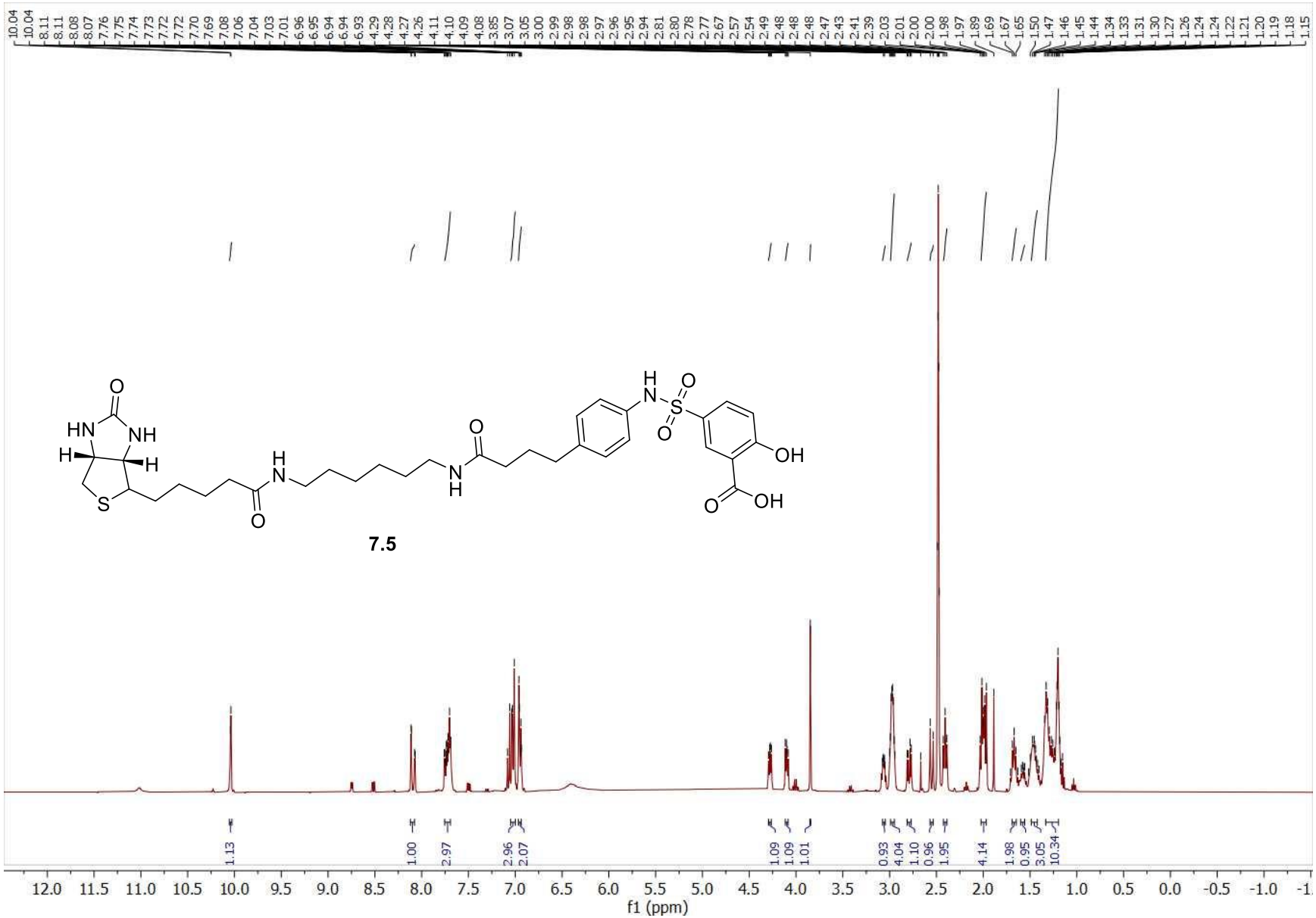

Figure B145: ^{1}H NMR of compound **7.5**.

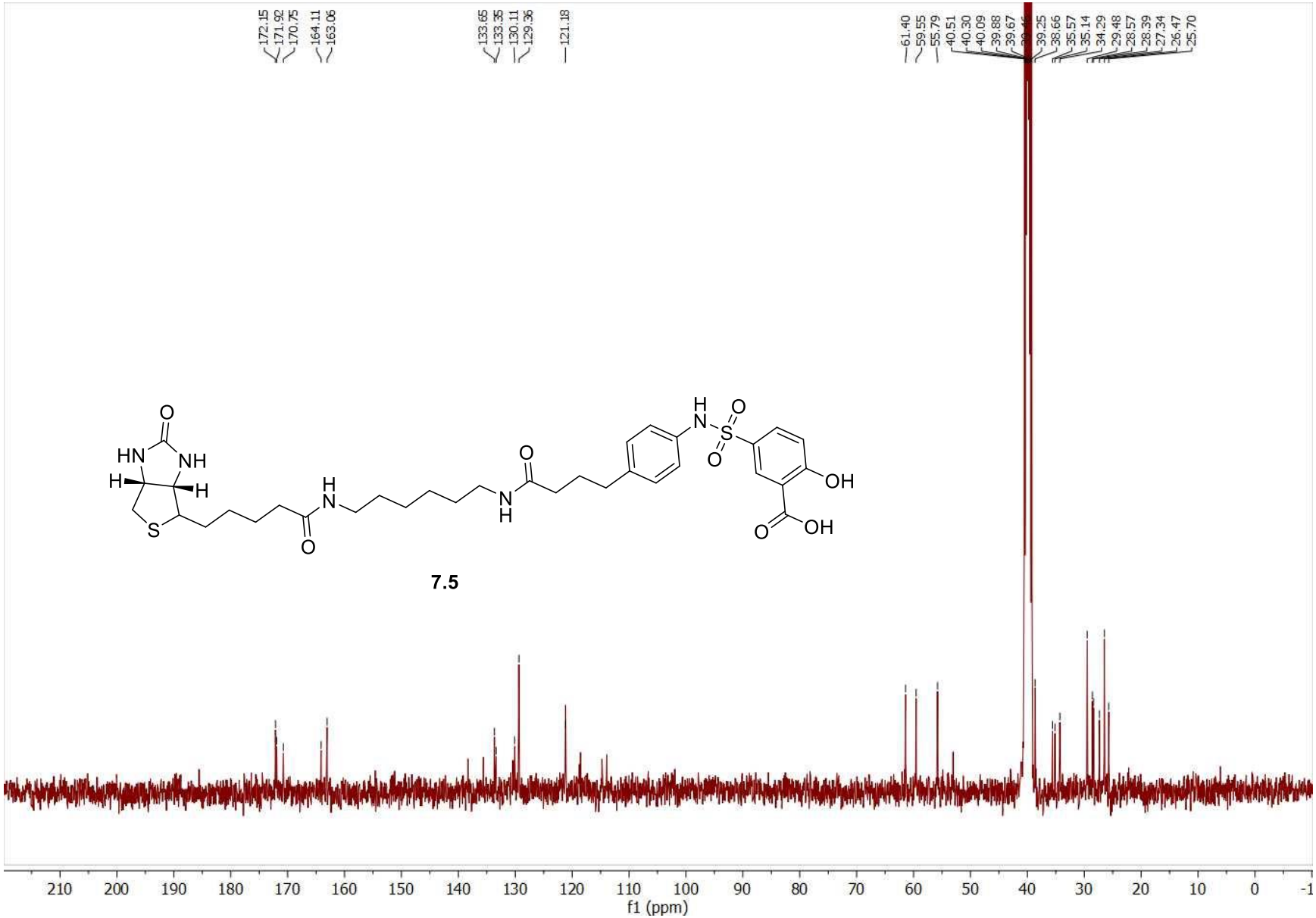

Figure B146: ^{13}C NMR of compound **7.5**

REFERENCES

(1) Goodman, M.; Cai, W.; Smith, N. D. The Bold Legacy of Emil Fischer. *J. Pept. Sci.* **2003**, 9 (9), 594–603.

(2) Fischer, E. Synthese Von Polypeptiden. XVII. *Berichte Dtsch. Chem. Ges.* **1907**, 40 (2), 1754–1767.

(3) Bergmann, M.; Zervas, L. Über Ein Allgemeines Verfahren Der Peptid-Synthese. *Berichte Dtsch. Chem. Ges. B Ser*. **1932**, 65 (7), 1192–1201.

(4) Du Vigneaud, V.; Ressler, C.; Swan, J. M.; Roberts, C. W.; Katsoyannis, P. G. The Synthesis Of Oxytocin1. *J. Am. Chem. Soc*. **1954**, 76 (12), 3115–3121.

(5) Merrifield, R. B. Solid Phase Peptide Synthesis. I. The Synthesis Of A Tetrapeptide. *J. Am. Chem. Soc.* **1963**, 85 (14), 2149–2154

(6) Merrifield, R. B. Solid-Phase Peptide Synthesis. III. An Improved Synthesis Of Bradykinin *. *Biochemistry* **1964**, 3 (9), 1385–1390.

(7) Domagk, G. F. [The 1984 Nobel Prize For Chemistry. Synthetic Hormones And Enzymes With Merrifield's Peptide Synthesizer]. *Dtsch. Med. Wochenschr*. **1984**, 109 (49), 1901–1902.

(8) Albericio, F. Solid-Phase Synthesis: A Practical Guide; CRC Press: New York, NY, **2000.**

(9) Shelton, P. T.; Jensen, K. J. Linkers, Resins, And General Procedures For Solid-Phase Peptide Synthesis. In Peptide Synthesis And Applications; Jensen, K. J., Tofteng Shelton, P., Pedersen, S. L., Eds.; Methods In Molecular Biology; Humana Press: Totowa, NJ, **2013**; Pp 23–.

(10) Góngora-Benítez, M.; Tulla-Puche, J.; Albericio, F. Handles For Fmoc Solid-Phase Synthesis Of Protected Peptides. *ACS Comb. Sci*. **2013**, 15 (5), 217–228.

(11) Dawson, P. E.; Muir, T. W.; Clark-Lewis, I.; Kent, S. B. Synthesis Of Proteins By Native Chemical Ligation. *Science.* **1994**, 266 (5186), 776–779.

(12) Gang, D.; Kim, D.; Park, H.; Cyclic Peptides: Promising Scaffolds For Biopharmaceuticals. *Genes.* **2018**, 9 (11), 557.

(13) Fosgerau, K.; Hoffman, T.; Peptide Therapeutics: Current Status And Future Directions. *Drug Discovery Today.* **2014,** 20 (1), 122-128.

(14) Jing, X.; A Gold Mine For Drug Discovery: Strategies To Develop Cyclic Peptides Into Therapies. *Medicinal Research Reviews.* Https://Onlinelibrary.Wiley.Com/Doi/Abs/10.1002/Med.21639 (Accessed Mar 31, 2020).

(15) Joo, S.; Cyclic Peptides As Therapeutic Agents And Biochemical Tools. *Biomolecules And Therapeutics*. **2012,** 20 (1), 19-26.

(16) Jensen, K. J.; Alsina, J.; Songster, M. F.; Vágner, J.; Albericio, F.; Barany, G. Backbone Amide Linker (BAL) Strategy For Solid-Phase Synthesis Of C-Terminal-Modified And Cyclic Peptides. *J. Am. Chem. Soc*. **1998**, 120 (22), 5441–5452.

(17) Del Fresno, M.; Alsina, J.; Royo, M.; Barany, G.; Albericio, F. Solid-Phase Synthesis Of Diketopiperazines, Useful Scaffolds For Combinatorial Chemistry. *Tetrahedron Lett*. **1998**, 39 (17), 2639–2642.

(18) Kang, S. S. A Photolabile Backbone Amide Linker For The Solid-Phase Synthesis Of Cyclic Peptides. Cysteine-Free Native Chemical Ligation. Synthesis And Biological Evaluation Of A Library Of Resveratrol Analogues. Ph.D., Purdue University, United States -- Indiana, **2009**.

(19) Anderson, J. C.; Reese, C. B. A Photo-Induced Rearrangement Involving Aryl Participation. *Tetrahedron Lett*. **1962,** 3 (1), 1–4.

(20) Sheehan, J. C.; Jr, G. D. D.; Facile Alkyl—Oxygen Ester Cleavage. *J. Org. Chem*. **1964**, 29, 7, 2006–2008.

(21) Chang, J. K.; Shimizu, M.; Wang, S.-Sun. Fully Automated Solid Phase Synthesis Of Protected Peptide Hydrazides On Recycling Hydroxymethyl Resin. *J. Org. Chem*. **1976**, 41 (20), 3255–3258.

(22) Johnson, T.; Quibell, M.; Owen, D.; Sheppard, R. C. A Reversible Protecting Group For The Amide Bond In Peptides. Use In The Synthesis Of 'Difficult Sequences.' *J. Chem. Soc. Chem. Commun*. **1993**, No. 4, 369–372.

(23) Bourne, G. T.; Meutermans, W. D. F.; Alewood, P. F.; Mcgeary, R. P.; Scanlon, M.; Watson, A. A.; Smythe, M. L. A Backbone Linker For BOC-Based Peptide Synthesis And On-Resin Cyclization: Synthesis Of Stylostatin 1. *J. Org. Chem.* **1999**, 64 (9), 3095–3101.

(24) Hostetler, M. A. Part I. The Rational Design, Synthesis, And Evaluation Of Second Generation Class II HMG-COA Reductase Inhibitors Part II. Studies Directed Toward The On-Resin Preparation Of C-Terminal Modified And Cyclic Peptides. Ph.D., Purdue University, United States -- Indiana, **2018**.

(25) Hostetler, M. A.; Lipton, M. A. An Optimized Preparation Of 1,1-Dimethylallyl Esters And Their Application To Solid-Phase Peptide Synthesis. *J. Org. Chem*. **2018**, 83 (15), 7762–7770

(26) Sieber, P. A New Acid-Labile Anchor Group For The Solid-Phase Synthesis Of C-Terminal Peptide Amides By The Fmoc Method. *Tetrahedron Lett*. **1987**, 28 (19), 2107–2110.

(27) Nicolás, E.; Pujades, M.; Bacardit, J.; Giralt, E.; Albericio, F. A New Approach To Hmb-Backbone Protection Of Peptides: Synthesis And Reactivity Of Nα-Fmoc-Nα-(Hmb)Amino Acids. *Tetrahedron Lett*. **1997**, 38 (13), 2317–2320.

(28) Ralhan, K.; Krishnakumar, V. G.; Gupta, S. Piperazine And DBU: A Safer Alternative For Rapid And Efficient Fmoc Deprotection In Solid Phase Peptide Synthesis. *RSC Adv*. **2015**, 5 (126), 104417–104425.

(29) Norrish, R. G. W.; Bamford, C. H. Photo-Decomposition Of Aldehydes And Ketones. *Nature*. **1937**, 140 (3535), 195–196.

(30) Bunin, B. A. 3 - Linkers For Solid-Phase Synthesis. In The Combinatorial Index; Bunin, B. A., Ed.; Academic Press: San Diego, **2012**; p. 9–76.

(31) Tentagel® XV RAM Resins: Http://Www.Rapp-Polymere.Com/Index.Php?Id=1252 (Accessed Jun 26, 2020).

(32) Next Generation LED Lighting | Waveform Lighting Https://Www.Waveformlighting.Com/ (Accessed Jun 26, 2020).

(33) Eakins G.; Niedrauer, M.; Lipton, M.; Photochemical Reactor For Solid Phase Synthesis. U.S. Patent Application No. 63029491, **2020**.

(34) Bourne, G. T.; Golding, S. W.; Meutermans, W. D. F.; Smythe, M. L. Synthesis Of A Cyclic Peptide Library Based On The Somatostatin Sequence Using The Backbone Amide Linker Approach. *Lett. Pept. Sci*. **2000**, 7 (6), 311–316.

(35) Long, Y.-Q.; Lee, S.-L.; Lin, C.-Y.; Enyedy, I. J.; Wang, S.; Li, P.; Dickson, R. B.; Roller, P. P. Synthesis And Evaluation Of The Sunflower Derived Trypsin Inhibitor As A Potent Inhibitor Of The Type II Transmembrane Serine Protease, Matriptase. *Bioorg. Med. Chem. Lett*. **2001**, 11 (18), 2515–2519.

(36) Łęgowska, A.; Bulak, E.; Wysocka, M.; Jaśkiewicz, A.; Lesner, A.; Dębowski, D.; Rolka, K. Peptomeric Analogues Of Trypsin Inhibitor SFTI-1 Isolated From Sunflower Seeds. *Bioorganic Amp Med. Chem*. **2008**, 16 (10), 5644–5652.

(37) Rink Amide Resin, Peptide Synthesis, Peptide Reagents, Custom Peptide - Chempep Inc. Https://Www.Chempep.Com/Chempep_Products2_Resins_For_Peptide_Synthesis_Rink_Amide_Resin.Htm (Accessed Jun 30, 2020).

(38) Otten, H.; Domagk And The Development Of The Sulphonamides. *Journal Of Antimicrobial Chemotherapy*. **1986**, 17 (6), 689–690

(39) Hager, T. The Demon Under The Microscope: From Battlefield Hospitals To Nazi Labs, One Doctor's Heroic Search For The World's First Miracle Drug; Crown, **2006**.

(40) Alexander Fleming Discovery And Development Of Penicillin - Landmark - American Chemical Society Https://Www.Acs.Org/Content/Acs/En/Education/Whatischemistry/Landmarks/Flemingpenicillin.Html (Accessed Jul 1, 2020).

(41) Aminov, R. I. A Brief History Of The Antibiotic Era: Lessons Learned And Challenges For The Future. *Front. Microbiol.* **2010**, 1.

(42) Bax, R,; Antibiotic Resistance: A View From The Pharmaceutical Industry. *Clinical Infectious Disease***. 1997**, 24, 151.

(43) Ventola, C.; The Antibiotic Resistance Crisis. *Pharmacy & Therapeutics*. **2015**, 40 (4), 277-283.

(44) Golkar, Z.; Bagasra, O.; Pace, D. G. Bacteriophage Therapy: A Potential Solution For The Antibiotic Resistance Crisis. *J. Infect. Dev. Ctries*. **2014**, 8 (2), 129–136.

(45) Sarkar, P.; Yarlagadda, V.; Ghosh, C.; Haldar, J.; A Review On Cell Wall Synthesis Inhibitors With An Emphasis On Glycopeptide Antibiotics. *Med. Chem. Comm*. **2017**, 8 (3), 516-533.

(46) Ory, E.; Yow, E. The Use And Abuse Of The Broad Spectrum Antibiotics. *JAMA*. **1963**, 185 (4). 273-279.

(47) Bush, K. Antimicrobial Agents Targeting Bacterial Cell Walls And Cell Membranes. *Rev. Sci. Tech. Int. Off. Epizoot*. **2012**, 31 (1), 43–56.

(48) Biggest Threats And Data | Antibiotic/Antimicrobial Resistance | CDC Https://Www.Cdc.Gov/Drugresistance/Biggest-Threats.Html (Accessed Jul 2, 2020).

(49) Klevens, R. M.; Edwards, J. R.; Chesley L. Richards, J.; Horan, T. C.; Gaynes, R. P.; Pollock, D. A.; Cardo, D. M. Estimating Health Care-Associated Infections And Deaths In U.S. Hospitals, 2002: *Public Health Rep*. **2016**.

(50) Current HAI Progress Report | CDC Https://Www.Cdc.Gov/Hai/Data/Portal/Progress-Report.Html (Accessed Jul 2, 2020).

(51) Monegro, A. F.; Regunath, H. Hospital Acquired Infections. In Statpearls; Statpearls Publishing: Treasure Island (FL), **2020**.

(52) Hedl, M.; Tabernero, L.; Stauffacher, C. V.; Rodwell, V. W. Class II 3-Hydroxy-3-Methylglutaryl Coenzyme A Reductases. *J. Bacteriol*. **2004**, 186 (7), 1927–1932.

(53) Li, D.; Gui, J.; Li, Y.; Feng, L.; Han, X.; Sun, Y.; Sun, T.; Chen, Z.; Cao, Y.; Zhang, Y.; Zhou, L.; Hu, X.; Ren, Y.; Wan, J. Structure-Based Design And Screen Of Novel Inhibitors For Class II 3-Hydroxy-3-Methylglutaryl Coenzyme A Reductase From Streptococcus Pneumoniae. *J. Chem. Inf. Model*. **2012**, 52 (7), 1833–1841.

(54) Bischoff, K. M.; Rodwell, V. W. 3-Hydroxy-3-Methylglutaryl-Coenzyme A Reductase From Haloferax Volcanii: Purification, Characterization, And Expression In Escherichia Coli. *J. Bacteriol*. **1996**, 178 (1), 19–23.

(55) Lopez-Perez, D. Design And Synthesis Of Novel Antibacterials. Ph.D., Purdue University, United States -- Indiana, **2013**.

(56) Heck, R. F.; Nolley, J. P. Palladium-Catalyzed Vinylic Hydrogen Substitution Reactions With Aryl, Benzyl, And Styryl Halides. *J. Org. Chem*. **1972**, 37 (14), 2320–2322.

(57) Epp, J.; Widlanski, T. S.; Facile Preparation Of Nucleoside-5‘-Carboxylic Acids. *J. Org. Chem*. **1999**, 64 (1), 293-295.

(58) Fernandez, E.; Et. Al.; Membrane Microdomain Disassembly Inhibits MRSA Antibiotic Resistance. *Cell*. **2017**, 171 (6), 1354-1367.

(59) Boneca, I. G.; Chiosis, G. Vancomycin Resistance: Occurrence, Mechanisms And Strategies To Combat It. Expert Opin. *Ther. Targets*. **2003**, 7 (3), 311–328.

(60) Martens, E.; Demain, A.; Platensimycin And Platencin: Promising Antibiotics For Future Application In Human Medicine. *The Journal Of Antibiotics.* **2011**, 64, 705-710.

(61) Brezden, A. M. The Design, Synthesis, And Investigation Of Functional Cationic Amphiphilic Polyproline Helices (Caphs). Ph.D., Purdue University, United States -- Indiana, **2016**.

(62) Ghosh, A. K.; Sarkar, A.; Brindisi, M. The Curtius Rearrangement: Mechanistic Insight And Recent Applications In Natural Product Syntheses. *Org. Biomol. Chem*. **2018**, 16 (12), 2006–2027.

(63) Neises, B.; Steglich, W. Simple Method For The Esterification Of Carboxylic Acids. *Angew. Chem. Int. Ed. Engl*. **1978**, 17 (7), 522–524.

(64) Thirumurugan, P.; Matosiuk, D.; Jozwiak, K. Click Chemistry For Drug Development And Diverse Chemical–Biology Applications. *Chem. Rev.* **2013**, 113 (7), 4905-4979.

VITA

Mary Lynn Niedrauer was born on December 29th, 1994. She grew up on a dairy farm in rural Texas, receiving no formal education. At age 15, she enrolled at the University of Texas at Tyler. She graduated from the University Honors Program with a B.S. in Chemistry and a minor in Mathematics in August 2014. She also earned the distinction of Physical Chemistry Student of the Year during her senior year of college. Mary enlisted as an engineer in the Army National Guard in 2012. Following college graduation, she volunteerd for a year-long deployment in Iraq as a Corporal in the U.S. Army, where she earned two Army Achievement Medals for meritorious service. In January 2016, Mary began graduate studies in the Department of Chemistry at Purdue University. She joined the laboratory of Professor Mark A. Lipton, where she conducted research in organic synthesis, methods development, solid-phase peptide synthesis, and drug design. She was awarded the H.C. Brown Student Seminar Award for her work. While enrolled in the PhD program, Mary concurrently completed her Master of Business Administration (MBA) from Purdue University Global. Mary earned her PhD in Organic Chemistry in August 2020. She accepted a position as a Research Scientist at Novosteo, a Biotechnology company. Mary is also a member of the USA Wrestling World Team, and has competed and medalled internationally in grappling.

PUBLICATIONS

PHOTOCHEMICAL REACTOR FOR SOLID PHASE SYNTHESIS

STATEMENT REGARDING GOVERNMENT FUNDING

[0001] The innovation of the present disclosure was not made with government support.

TECHNICAL FIELD

[0002] The present disclosure generally relates to chemical reactions, and in particular, to a reactor for photochemical transformations in solid-phase synthesis.

BACKGROUND

[0003] This section introduces aspects that may help facilitate a better understanding of the disclosure. Accordingly, these statements are to be read in this light and are not to be understood as admissions about what is or is not prior art.

[0004] Solid-phase synthesis is commonplace in chemical arts. A conventional laboratory approach to carrying out solid phase synthesis is based on two types of vessels in which reactions can take place. One class is column-type glass structure, e.g., sintered glass funnels. Another class is the glass shaker funnels. However, limitations exist in each of these types.

[0005] Generally, solid-phase synthesis is an iterative procedure that is widely used in organic and biochemistry for rapid and high purity synthesis of macromolecules with repeating units such as peptides/proteins, oligonucleotides, and complex carbohydrates The first unit of the macromolecule is covalently linked to an insoluble polymeric solid support, typically composed

of polyethylene glycol or polystyrene. A linker molecule is then used to allow for release of the final product from the solid-support, generally under strongly acidic conditions.

[0006] Peptides and proteins are made up of repeating amino acid units, most of which contain highly reactive side chain functional groups. Various protecting group strategies have been developed to effectively 'block' these reactive groups while coupling the amino acid sequence in the C to N direction. The most commonly used approach is to employ the base-labile 9fluorenylmethyloxycarbonyl (Fmoc) protecting group on the N-terminus of each amino acid residue while using acid-labile side chain protecting groups such as tert-butyl (t-Bu) or tbutoxycarbonyl (Boc) groups. Thus the deprotection step at each iteration can be completed under basic conditions to expose the free N-terminus without affecting any other functional groups present.

[0007] For the synthesis of C-terminally modified peptides, a method is employed to link the first residue to the solid-support through a backbone amide, allowing free access to the Cterminus for chemical transformations. This group must also be protected, generally using the acid-labile t-Bu, or palladium-labile allyl or 1,1-dimethylallyl (DMA) protecting groups. This approach faces limitations when there is a need to differentiate between any combination of the resin linkage, the acid-labile side-chain protecting groups, or the protected C-terminus. **[0008]** To achieve such transformation, chemical transformations induced by irradiation with light are common in the field of organic synthesis. A wavelength must be selected which is absorbed by the material of interest. Upon absorbing photons from the light source an electron will then undergo a photoexcitation. The excited electron then goes on to react in various manners, depending on the surrounding system. The use of photochemical reactions to complete transformations in solid-phase peptide synthesis (SPPS) has grown extensively in recent years.

The incorporation of photoreactive functional groups provides an added degree of chemoselectivity, allowing for selective reactions in the presence of acid- and base- reactive groups. Additionally, using light as an activator removes the need for reagents for a given chemical transformation, reducing not only the cost and waste associated with a transformation but also often eliminating the purification that typically follows standard chemical reactions. Photoreactive linkages are typically used in SPPS as either protecting groups or as linkers to the solid-support.

[0009] The equipment required to perform photochemical transformations on molecules attached to solid-support as opposed to in solution continues to pose several challenges. While the commonly used wavelengths are widely available as fluorescent bulbs, the intensity of light output is often low, resulting in long reaction times. These lamps also generate a broad range of wavelengths, further lowering the intensity of light generated at the precise wavelength needed. The lamps generally used in photochemical reactors generate high quantities of heat, even with built in convection systems. This can pose a challenge for organic synthesis, where reactions are often carried out in solvents with low boiling points. Many organic and bioorganic molecules also contain functional groups that are heat-sensitive, limiting the scope of molecules that are compatible with photochemical reactions using the currently available technology. **[0010]** Furthermore, another challenge of conducting synthesis on a solid support is providing sufficient agitation to the system to ensure complete transformation with reasonable reaction times. This is due to the tendency of the insoluble resin beads to coagulate in solvent, limiting the penetration of reagents throughout the sample. The use of magnetic stirring as in traditional organic synthesis cannot be used, as the mechanical force has a tendency to mechanically degrade the polymeric resin beads. Instead, a synthesis vessel is employed consisting of a glass reaction chamber fitted

with a fritted filter across the bottom. The chamber is circularly spun at low speeds, causing constant mixing of the resin slurry. Upon reaction completion, the solvent and excess reagents can be removed by filtration, leaving the resin-bound peptide behind on the filter. The need for agitation poses a challenge when conducting photochemical transformations on the solid support, as the standard solid-phase synthesis vessels are made of glass and thus partly opaque to UV radiation. Additionally, the chamber of commercially available photochemical reactors is sufficiently small to exclude the possibility of inserting a spinning mechanism to permit sample agitation during irradiation.

[0011] Therefore, there is an unmet need for a novel approach for photochemical transformations in solid-phase synthesis that overcomes the aforementioned shortcomings.

DETAILED DESCRIPTION

[0012] For the purposes of promoting an understanding of the principles of the present disclosure, reference will now be made to the embodiments illustrated in the drawings, and specific language will be used to describe the same. It will nevertheless be understood that no limitation of the scope of this disclosure is thereby intended.

[0013] In the present disclosure, the term "about" can allow for a degree of variability in a value or range, for example, within 10%, within 5%, or within 1% of a stated value or of a stated limit of a range.

[0014] In the present disclosure, the term "substantially" can allow for a degree of variability in a value or range, for example, within 90%, within 95%, or within 99% of a stated value or of a stated limit of a range.

[0015] A novel approach is described in the present disclosure for photochemical transformations in solid-phase synthesis. To this end, referring to FIG. 1, a photochemical reactor 1 is shown for conducting photochemical transformations on photosensitive reactants. The reactor 1 includes a vial holder which can hold a sealed vial 16 containing a sample, including a solvent and desired photosensitive reactants. The chosen vial material is optically transparent to the required wavelength of the chemical reaction. The reactor 1 further includes Printed Circuit Boards (PCBs) 11 designed to mount Light Emitting Diodes (LEDs) (see LEDs 25 in FIG. 2) selected to coincide with the required wavelength of the reaction. PCBs 11 are designed to transport heat away from the inner chamber by conduction to prevent sample heating. The reactor 1 also includes a chamber frame 12. The PCBs 11 are mounted to the chamber frame 12. The chamber frame 12 is constructed of a thermally conductive material such as copper, aluminum or steel to provide a thermal reservoir that sinks heat away from the PCBs 11 and radiates it to the surrounding environment.

[0016] Each PCB 11 is mounted on an arc normal to the center of the chamber frame 12, the center of the chamber frame 12 is where the vial 16 is held in place. This orientation serves to maximize light intensity on the sample since LED luminous intensity peaks orthogonal to the mounting surface of the LEDs (see LEDs 25 in FIG. 2).

[0017] The reactor 1 also includes a continuous duty agitator unit 14 capable of rotating the base of the sample vial at a rate fast enough to agitate the sample into a homogeneous mixture that can be evenly irradiated in the reactor 1.

[0018] The reactor 1 further includes a frame 15 that provides support for the remainder of components of the reactor 1. The frame 15 is produced, e.g., through injection molding, extrusion, subtractive machining, or additive manufacturing or a combination thereof into a rigid

configuration. The frame 15 may optionally be constructed of a material that is reflective to the wavelength of light used in the photoreaction chamber frame 12 if reduced temperatures are desired.

[0019] The reactor 1 may also include a sample cap 13 which allows for the vial 16 to be loaded and unloaded from the reactor 1 as needed. Design of the sample cap 13 conforms to the contours of the vial 16 while leaving sufficient room for movement of the vial 16 in the reactor 1 for agitation.

[0020] Referring to FIG. 2, a perspective view of a PCB holder 2 is shown. The PCB holder 2 includes a plurality of PCBs 24 each having a plurality of LEDs 25. Each LED 25 or groups of LEDs 25 are coupled to a current limiting resistor 26 in order to properly operate the LEDs 25.

The current limiting resistors 26 can be positioned between a high-side voltage source 22 and the LEDs 25 or between the LEDs 25 and a low-side source (not shown), e.g., ground. The PCB holder 2 includes a frame with slots 21 therein which includes mounting holes 23 for mounting the PCBs 24. The slots allow for heat generated by the current limiting resistors 26 to escape.

[0021] The PCB holder 2 and the aforementioned components constitute the reaction chamber of the present disclosure.

[0022] Referring to FIG. 3, a top view of the PCB holder 2 is shown. As discussed above, the

PCB holder 2 includes a frame 32 which holds a plurality of PCBs 33 each having a plurality of LEDs 34. A vial 31 is shown in the middle of the PCB holder 2. The frame 32 can be made of a thermally conductive material such as aluminum, copper, or steel to which the PCBs 33 can be mounted.

[0023] Referring to FIGs. 4 and 5, a cross sectional view and a top view of the PCB holder 2 are shown, respectively. Focusing of the radiation generated by LEDs on the sample by use of flat surfaces for mounting standard rigid PCBs 43 such that a line normal to the surface 42 intersects with the sample location 41.

[0024] Each PCB has mounting pads allowing for LEDs of the desired wavelength to be mounted (see FIG. 2). These commonly output in the ultraviolet region of the electromagnetic spectrum (wavelength < 400nm), but may optionally be selected to output in the visible or infrared range. Light intensity scales linearly with the number of LEDs mounted in the design. **[0025]** The PCBs may optionally be equipped with a temperature sensor or thermocouple to provide feedback on chamber temperatures. This feedback can be used to provide temperature control about a fixed setpoint, or a temperature shutoff if the temperature rises above a desired threshold.

[0026] The photoreactor PCBs incorporate a thermal scavenging design that utilizes PCB manufacturing and design features to keep temperatures on the inside surface of the PCB and therefore the inside of the reactor 1 to a minimum. Heat generated by the LEDs flows into the copper pad at the cathode of each LED then through the PCB using metal filled holes (vias) 47. The heat is diffused over a bare copper surface 44 on the back of the PCB and is then conducted to a metal frame 46 through an optional thermally conductive paste 45. Electrically, voltage is applied on the back side 60 of the PCB 54 which is mounted on the frame 53 (see FIG. 5) where it flows through a current limiting resistor 58 (see FIG. 5), then through a via to the anode of the LED 51 (see FIG. 5). The return current flows out of the cathode of the LED into a copper pad 52, through a via 57, and out to a ground plane on the back side of the PCB 54. The heat conductive frame 59 (shown in FIG. 5) is designed with a cutout to allow heat to flow from the current limiting resistors to the surrounding ambient air.

[0027] Thus, according to the present disclosure, a new photolabile backbone amide linker, 2hydroxyl-4-carboxy-6-nitrobenzene (Hcnb) has been described which is stable to strongly acidic conditions and instead releases the completed peptide through photolytic cleavage at 350-365 nm wavelength. The photocleavable Hcnb linker was employed to test the ability of this invention to efficiently complete photochemical transformations when compared with commercially available instruments. The photocleavable linker was used in conjunction with the acid-labile Sieber Amide linker to test the degree of completion for the photocleavage (table 1). The conditions used were as follows: polyethylene glycol or polystyrene resin with 3-10 assorted amino acid residues attached, suspended in 5 mL of solvent consisting of 90% methylene chloride and 10% methanol in a fused-quartz tube. The photochemical reactor used for comparison purposes was a Rayonet fitted with 350 nm lamps. Only trace quantities of product were detected following 24 hours of irradiation. Additionally, measured reaction chamber temperatures reached up to 80 °C, causing rapid evaporation of the solvent when a completely airtight system was not utilized. In contrast, 100% cleavage and 90% overall synthetic yield were achieved with up to 230 mg of resin (largest quantity tested) in under 1 hour with the LED-UV reactor design disclosed herein, fitted with 365 nm LEDs.

TABLE 1: Comparison of cleavage times with commercially available Rayonet photochemical reactor

	Rayonet Reactor	LED Reactor	LED Reactor
Wavelength	350 nm	365 nm	365 nm
Irradiation Time	24 hours	1 h	1 h

Resin Quantity	70 mg	42 mg	230 mg
% Peptide Cleavage	Trace	100%	100%
Peptide	H-Phe-Ala-Ala-OtBu	H-Phe-Leu-Ala-OtBu	Cyclo[Arg-(D)-Phe-Pro-Glu-Asp-Asn-Tyr-Glu-Ala-Ala]

[0028] Those having ordinary skill in the art will recognize that numerous modifications can be made to the specific implementations described above. The implementations should not be limited to the particular limitations described. Other implementations may be possible.

Claims:

1. A photochemical reactor, comprising:

   a reaction chamber, including:

      a frame;

      one or more circuit boards each coupled to the frame and each carrying a plurality of light sources; a power source coupling, adapted to power the one or more circuit boards; a vial receiver centrally disposed about the one or more circuit boards; and an agitator configured to rotate the vial receiver.

2. The photochemical reactor of claim 1, wherein the light sources are light emitting diodes (LEDs).

3. The photochemical reactor of claim 2, wherein the LEDs are configured to output light having a wavelength of between about 300 nm and about 400 nm.
4. The photochemical reactor of claim 2, wherein one or more LEDs are coupled to a current limiting resistor.
5. The photochemical reactor of claim 1, wherein the reaction chamber is structured to conduct heat away from the reaction chamber to ambient air.
6. The photochemical reactor of claim 5, wherein the frame is a metallic structure.
7. The photochemical reactor of claim 6, wherein material of the metallic structure is selected from the group consisting of copper, aluminum, steel, and alloys thereof.
8. The photochemical reactor of claim 1, wherein the one or more circuit boards are disposed in a circular (cylindrical) configuration, wherein the light sources are pointing inwardly towards the vial receiver.
9. The photochemical reactor of claim 4, wherein each of the current limiting resistors are disposed adjacent an opening thermally coupled to ambient air.
10. The photochemical reactor of claim 9, wherein the openings adjacent to each of the one or more circuit boards forms an elongated opening in the frame.

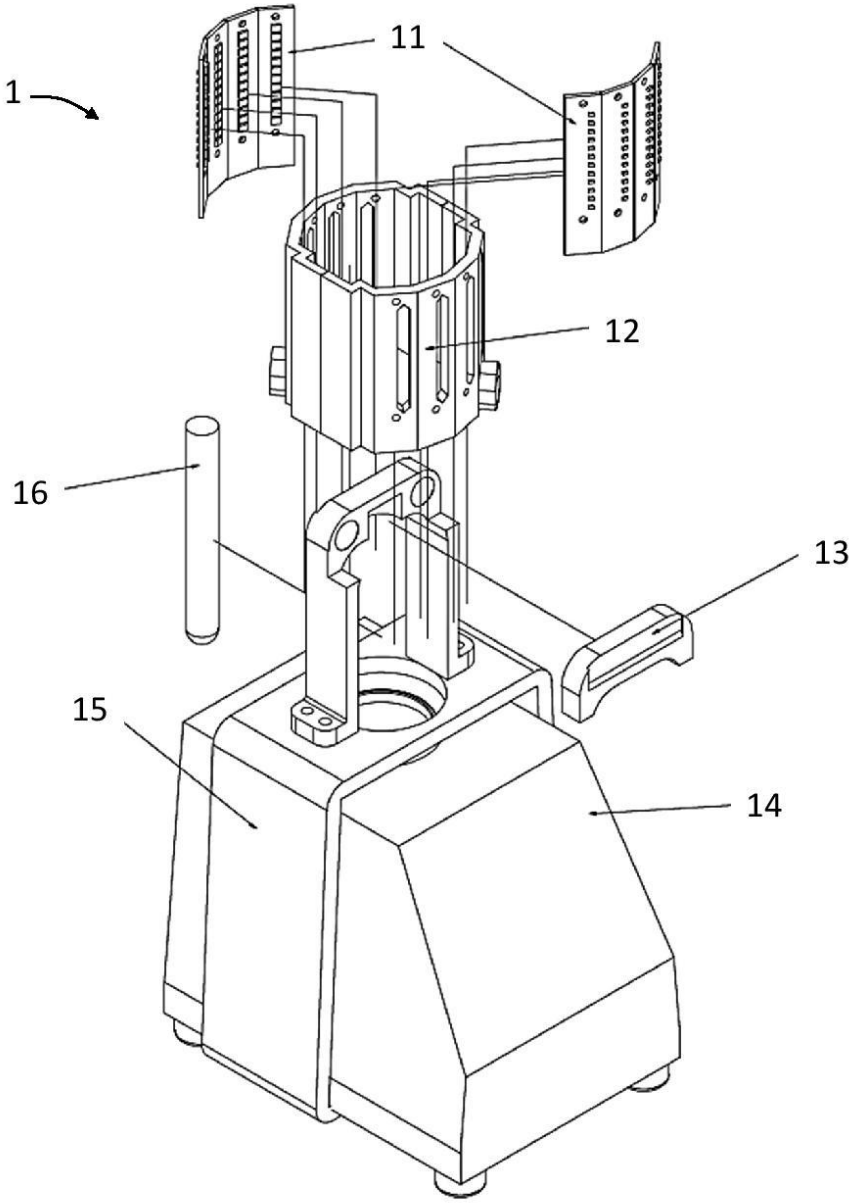

FIG. 1

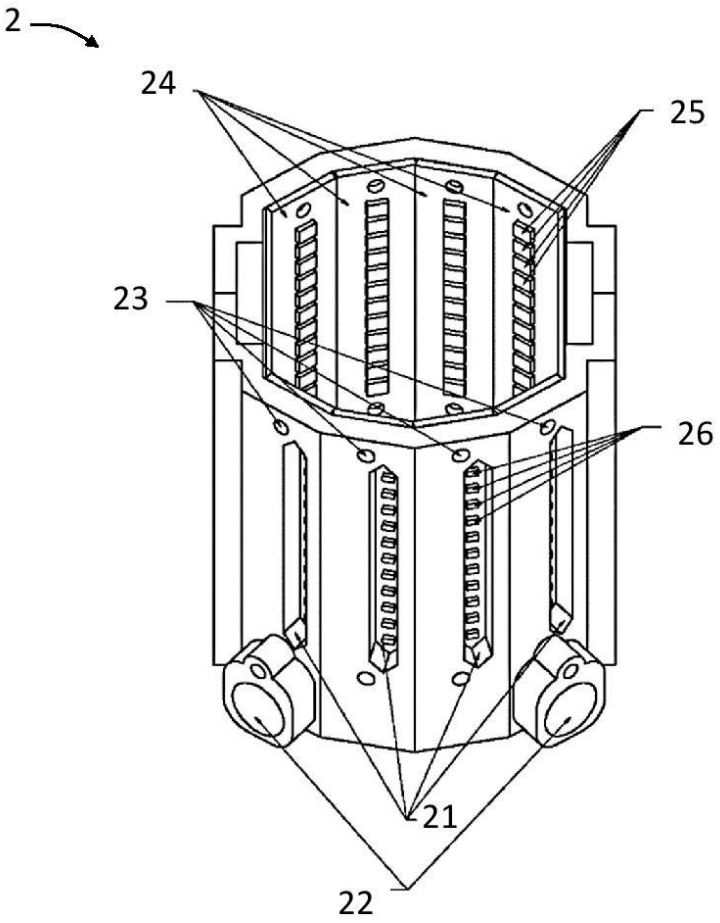

FIG. 2

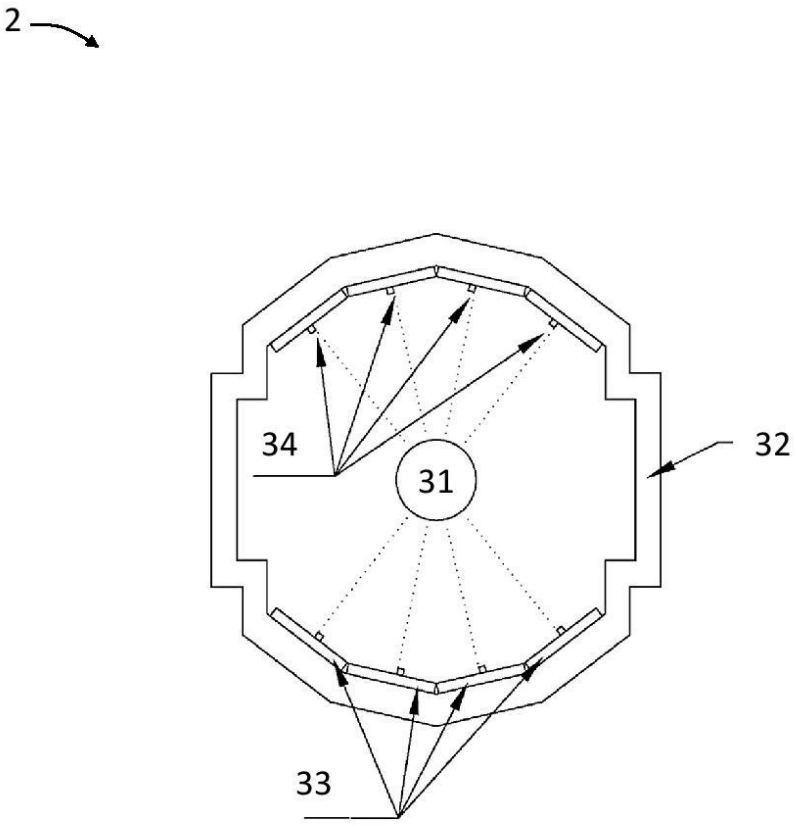

FIG. 3

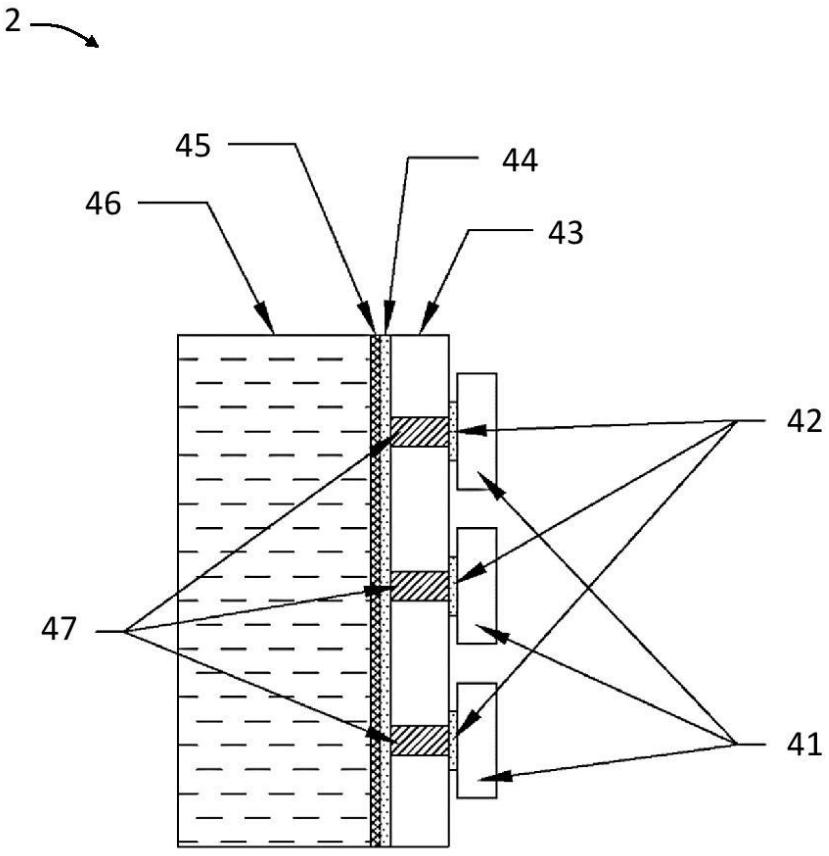

FIG. 4

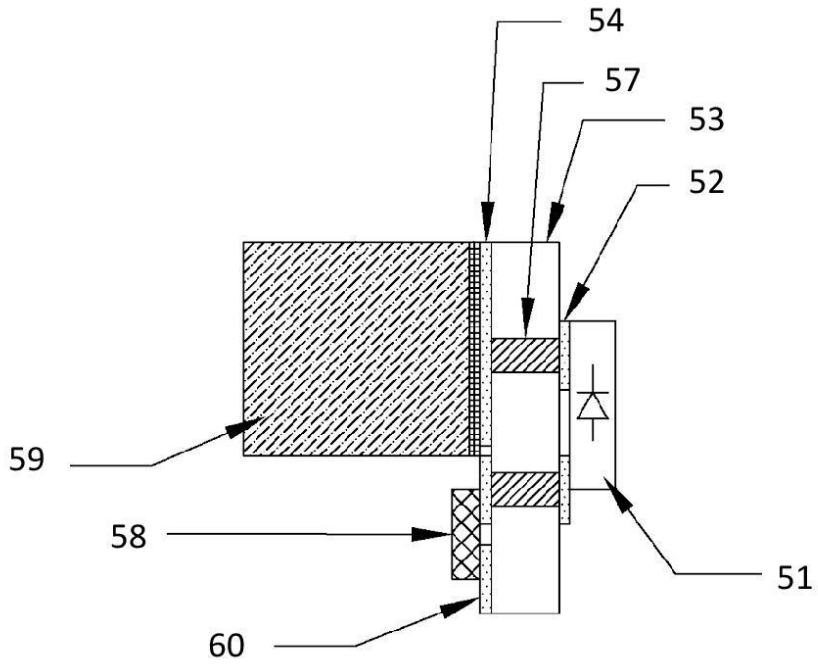

FIG. 5

Submitted to the Journal of Organic Chemistry

A Photolabile Backbone Amide Linker for the Solid-Phase Synthesis of Cyclic Peptides and Peptide Thioesters

Mary L. Niedrauer[a], Matthew A. Hostetler[a,b], Soo Sung Kang[c], and Mark A. Lipton*

Department of Chemistry, Purdue University, 560 Oval Drive, West Lafayette, Indiana, 47907

lipton@purdue.edu

RECEIVED DATE

ABSTRACT: A new backbone amide linker has been developed for the synthesis of cyclic and C-terminally modified peptides that permits photochemical detachment of the synthesized peptide from the solid support, thus avoiding problems associated with acid deprotection conditions. An initial survey of known photolabile motifs for their ability to produce a linker-bound model dipeptide in high yield and their ability to undergo efficient photochemical detachment of the model dipeptide found that the 6-nitroveratryl (Nve) motif afforded the most efficient release of dipeptide. The problematic acylation of Nve-bound amino esters was solved through the development of the 2-hydroxy-4-carboxy-6-nitrobenzyl (Hcnb) linker, which utilizes an O-to-N transacylation to afford efficient acylation of even sterically hindered, linker-bound amino esters. The Hcnb linker was found to afford high yields of amino acid loading, acylation and photolytic cleavage of model tripeptides. Attachment of the Hcnb linker to the aminomethyl TG resin permitted the solid phase synthesis of representative cyclic peptides and C-terminal thioesters in high overall yield and purity.

INTRODUCTION

The head-to-tail cyclization of peptides[i] is a common and important strategy, employed both in nature and in synthetic applications, for improving the bioavailability and conformational rigidity of polypeptides.[ii] The lack of either an N- or C-terminus increases proteolytic stability while internal hydrogen bonding and a more compact structure improve the membrane permeability of cyclic peptides.[iii] These advantages are reflected in the prominence of cyclic peptides among peptidic therapeutic agents,[iv] such as gramicidin S[v] and cyclosporine A.[vi] The chemical synthesis of cyclic peptides, however, has been complicated by the traditional approach to solid-phase peptide synthesis using the C-terminal carboxylate to covalently attach the growing peptide to a polymeric support. The most straightforward approach involving detachment of a fully protected linear peptide precursor from the resin followed by macrocyclization in solution is complicated by oligomerization and C-terminal epimerization reactions. To avoid the problems associated with head-to-tail cyclization in solution, various approaches have been devised for on-resin cyclization of peptides, including Kaiser's Oxime[vii] resin, Richter's thioester[viii] linker, Waldmann's hydrazide[ix] linker, Kenner's sulfonamide[x] linker and side-chain attachment[xi] of the linear peptide to the resin. An important general strategy for the on-resin, head-to-tail cyclization of peptides was introduced by the "backbone amide linker" (BAL) strategy of Albericio and Barany.[xii] In this approach, the nitrogen atom of an internal amide bond is used to tether the growing peptide to the polymeric resin, thereby liberating both N- and C-termini for modification. It is noteworthy that this strategy also addresses the more general problem of C-terminal modification of the resin-bound peptide. Since its introduction, the BAL strategy has been employed by a number of researchers and several modifications have been developed.[xiii,xiv,xv] Despite its manifest appeal, however, the BAL strategy is limited in practice by two problems: the strongly acidic conditions needed to cleave the peptide from the linker and the unwanted cyclization of resin-bound dipeptide intermediates to diketopiperazine (DKP) side products.[xvi] As a result, many of the applications of the BAL strategy involve the synthesis of C-terminal modifications, such as trithioorthoesters,[xvii] aldehydes,[xviii] or functionalized amides[xix]

Another application of the C-terminal modification of peptides was revealed by the discovery of the native chemical ligation of peptide bonds by Kent, Muir and Dawson.[xx] Their use of peptide thioesters to couple with N-terminal cysteine residues has necessitated the development

[a] Contributed equally to this work

[b] Current address: Department of Chemistry, Marshall University, Huntington, WV

[c] Current address: Department of Pharmacy, Ewha Womans University, Seoul, South Korea

of various methods for the solid-phase synthesis of peptide thioesters. [xxi] Since that landmark discovery, related processes such as Staudinger ligation [xxii] have been developed that likewise depend on the availability of peptide thioesters. Despite this, there remains the need for a general and convenient synthesis of peptide thioesters compatible with standard, Fmoc-based solid-phase peptide synthesis (SPPS) conditions.

To avoid the problems associated with acidic deprotection conditions in peptide synthesis, other methodologies have been explored and developed.[xxiii] One of the most appealing ideas has been to use photochemical detachment from the resin as an extra dimension of protecting group orthogonality in solid phase peptide synthesis. Photolabile linkers[xxiv], in which long-wave UV radiation (300 ~ 360 nm) is used to detach an organic functional group – usually a carboxylic acid, a carbamate (a latent amine), an alcohol, or a phosphate – from a polymer or glass surface, provide an alternative to the classic acidic or basic cleavage protocols used in solid-phase organic synthesis. Ideally, photochemical deprotection should proceed with high functional group selectivity, low amounts of side reactions and involve no separation of product from reactants. Photochemical deprotection has also found favor with applications in the parallel synthesis of compound libraries[xxv].

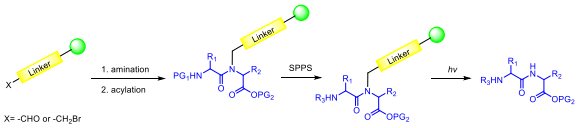

Scheme 1. **General concept of amino acid anchoring and photolytic deprotection.**

Herein we describe studies directed toward the development of a photolabile BAL linker (Scheme 1) to address the problems associated with the BAL strategy as a general method for the synthesis of cyclic and C-terminally modified peptides. Our studies began with a survey of several known photolabile motifs for their applicability to BAL linker design (Figure 1). The candidate photolabile motifs studied were the *p*-oxyphenacyl (Op), [xxvi] α-methyl-*p*-oxyphenacyl (Mop), [xxvii] *p*-oxybenzoin (Obz), [xxviii] α,*o*-dimethyl phenacyl[xxix] (Dmp) and 6-nitroveratryl (NVe). [xxx] All of these photolabile groups undergo facile n-π* or π-π* excitation at 300-360 nm and release oxygen-based substituents with few side reactions. Appropriate synthetic precursors **1**-**5** were chosen for each of the motifs, as shown in Figure 1.

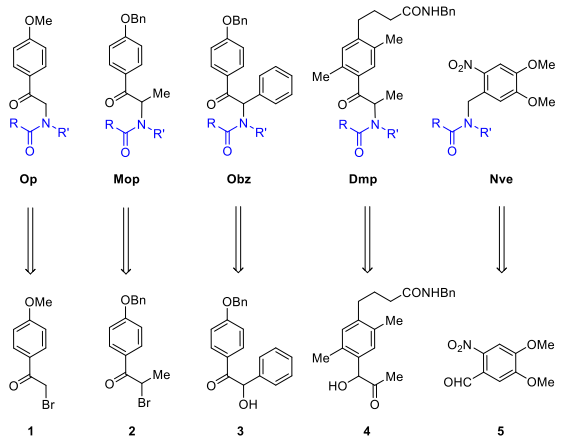

Figure 1. Candidate photolabile backbone amide linkers and their synthetic precursors

Consequently, our preliminary survey focused on the Op, Mop, Obz, Dmp, and Nve motifs, their preparation and photolysis. Of specific interest were a) the ease of anchoring amino acids to the linker, b) the rate and efficiency of photo-cleavage, and c) the suppression of side reactions during photolytic deprotection. To assess these questions, the dipeptide Boc-Phe-Gly-OMe (**8**) was chosen as a model system. After the photolabile motif was chosen, effort was directed toward its attachment to a solid support compatible with the solvents and reagents common to peptide synthesis. Finally, the problems of diketopiperazine formation, photocleavage optimization, and maximization of cyclization yields were addressed.

RESULTS AND DISCUSSION

Synthesis of linker-anchored dipeptides. Using the precursor molecules **1**-**5** (Figure 1), each linker was covalently attached to glycine methyl ester to afford an anchored glycine residue (**6a**-**e**), which was then acylated with Boc-L-phenylalanine to afford an anchored dipeptide **7a**-**e** (Table 1). Each anchored dipeptide was photolyzed at 300 nm to afford Boc-Phe-Gly-OMe (**8**).

Table 1. Photolabile linker candidate and their performance in amination, acylation and photolysis.

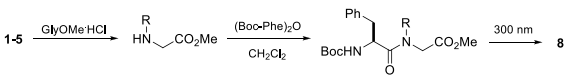

6a, R = Op
6b, R = Mop
6c, R = Obz
6d, R = Dmp
6e, R = Nve

7a, R = Op
7b, R = Mop
7c, R = Obz
7d, R = Dmp
7e, R = Nve

Starting material[a]	Amination (yield, %)	Acylation (yield, %)	Photolysis (yield, %)
1	**6a** (63)[b]	**7a** (81)	5[c]
2	**6b** (78)[b,d]	**7b** (75)	23[c]
3	**6c** (74)[c,e]	**7c** (50)	12[f]
4	**6d** (85)[g]	**7d** (81)	75[f]
5	**6e** (82)[h]	**7e** (77)	80[c]

[a] Details of the preparation of **1**-**5** are given in the Supporting Information. [b] CH_3CN used as solvent. [c] MeOH used as solvent. [d] Reaction run at 82°C. [e] Reaction run at 65°C. [f] $CHCl_3$ used as solvent. [g] Reaction run at 110° in $PhCH_3$. [h] $NaBH_4$ added to the reaction.

The linker precursors **1**-**5** were either commercially available or prepared using literature procedures.[xxxi] Linkers **1** and **2** were anchored to methyl glycinate via nucleophilic displacement, whereas **3** and **4** employed the Amadori rearrangement [xxxii] of an □-hydroxyketone, and **5** was attached to methyl glycinate through reductive amination. In all cases, acylation with the symmetric anhydride of Boc-L-Phe was found to afford the highest yield of anchored dipeptide. A survey of conditions for photolytic cleavage of the dipeptide found that photoexcitation at 300 nm in either methanol or chloroform, depending on the motif, afforded the fastest and cleanest reactions, but only the Dmp (**7d**) and Nve-linked dipeptides showed acceptable photolytic reactivity. Problems arose, however, when amino acids larger than glycine were anchored to Dmp and Nve. Both the initial attachment and subsequent acylation of those anchored amino acids proved to be quite problematic and afforded anchored dipeptides in modest yields at best.

In summary, Op, Mop, and Obz failed to release the dipeptide product efficiently, regardless of solvent and wavelength used, and so were discarded as linker candidates**.** Both the Nve and Dmp motifs displayed acceptable photolytic product release with the appropriate choices of solvent and irradiation wavelength; however, in both cases the modest yields for amino acid anchoring and acylation were insufficient for our needs, necessitating further modification to improve both steps of the reaction sequence.

Development of a Second Generation Photolabile Linker. On the basis of both acylation and photocleavage yields the □-nitrobenzyl motif of the Nve linker was chosen as the basic skeleton for a second generation linker, and the transacylation motif of the 6-hydroxy-4-methoxybenzyl[xxxiii] (Hmb) and 6-hydroxynitrobenzyl[xxxiv] (Hnb) auxiliaries was incorporated into the linker design to improve acylation efficiency. The acid-labile Hmb auxiliary was devised by Sheppard[xxxiiixxxiii] for the protection of peptide amide backbones during the synthesis of 'difficult' peptide sequences. The related, photolabile Hnb auxiliary was developed by Smythe[xxxiv] for the covalent modification of 'difficult' peptide sequences to facilitate their cyclization. Both the Hmb and Hnb auxiliaries employ an *ortho*-hydroxyl group to acylate bulky amino acids via esterification and subsequent O-to-N transacylation.

It was reasoned that the addition of an *o*-hydroxy substituent to the *o*-nitrobenzyl skeleton would assist both the acylation of the first amino acid and later photolytic cleavage. Attachment of a *para*-carboxylate to the *o*-nitrobenzyl skeleton provides a tether for covalent attachment of the linker to a spacer or resin and affords additional electron withdrawal to assist both the transacylation and photolysis reactions. Thus, the 2-hydroxy-4-carboxy-6-nitrobenzyl (Hcnb) linker emerged as a second-generation candidate for a photolabile BAL linker, as exemplified by the Hcnb-glycine adduct **9** (Scheme 2), derived from reductive amination of the aldehyde precursor 2-hydroxy-4-carboxy-6-nitrobenzaldehyde (Hcna) with glycine methyl ester. Treatment of **9** with a symmetric anhydride (Scheme 2) can result in the formation of the desired dipeptide **11** either through direct N-acylation or via initial acylation of the less hindered phenol followed by subsequent O-to-N acyl transfer. This alternate pathway was envisaged as a means to overcome the limitations of the Nve motif when attached to sterically hindered amino acids.

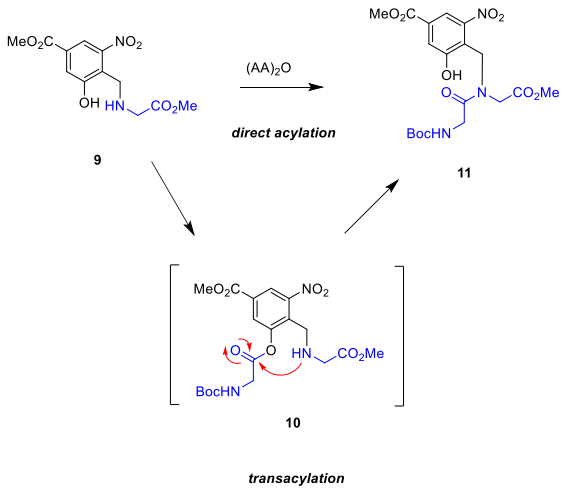

Scheme 2. Transacylation motif in the Hcnb linker.

Synthesis of Hcna linker. 4-formyl-3-hydroxy-5-nitrobenzoic acid (**16**) was prepared from commercially available 4-Methyl-3,5-dinitrobenzoic acid (**12**) (Scheme 3). A condensation reaction between **12** and DMF-DMA afforded the previously reported [xxxv] enamine **13** in 72% yield. Ruthenium (III) chloride-catalyzed oxidative cleavage of the enamine using sodium metaperiodate generated the aldehyde **14** in 61% yield. Unilateral nucleophilic aromatic substitution of a single nitro- group using acetaldoxime to install the *ortho*-phenol group afforded ester-protected linker precursor **15** in 68% yield, which was used for solution-phase studies. Finally, hydrolysis of the methyl ester group using barium hydroxide afforded the free carboxylic acid **16** in 90% yield.

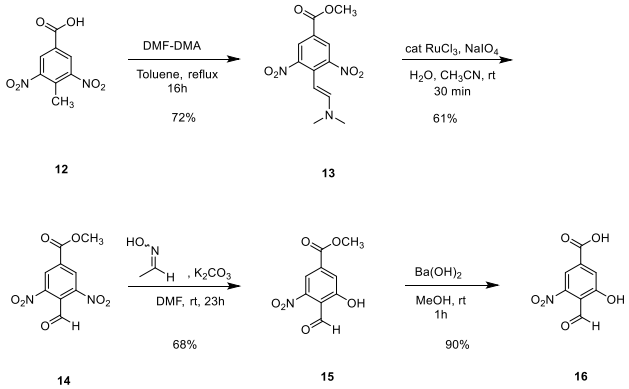

Scheme 3. Preparation of Hnca linker **15**

Solution-Phase Synthesis of Dipeptides using Hcnb

We envisioned linking the peptide to the linker via a reductive amination between the primary amine of the first amino acid and the aldehyde precursor, in similar fashion to the loading protocol for the original BAL Linker. The resulting secondary amine can then be acylated with the next amino acid in sequence, forming a tertiary amide linkage between the peptide and linker. The presence of the *ortho*-phenol in Hcnb is essential for complete acylation of the secondary amine, especially when utilizing amino acids with bulky side chains. Finally, photolysis in the short-wave UV range should cause a clean release of the dipeptide from the linker.

A series of dipeptides was synthesized in solution on the methyl ester-protected Hcna linker precursor **15** (Table 2). In solution, addition of the desired C-terminally protected amino acid to the aldehyde handle in the presence of DIEA in CH_3CN forms the imine intermediate. Reduction of this intermediate by sodium borohydride in methanol yields the Hcnb-linked amino acids **17a-d**. Acylation of the secondary amine with a pre-formed symmetric anhydride of the second amino acid resulted in acylation to give Hcnb-linked dipeptides, even in the case of bulky side-chains such as Thr. Photolysis at 365 nm in MeOH releases the desired dipeptides from the linker to give **18a-d.** Due to rotomeric impurities present in peptides attached to Hcnb, yields were reported over 2 steps.

Table 2: Solution-phase synthesis of dipeptides using Hcnb

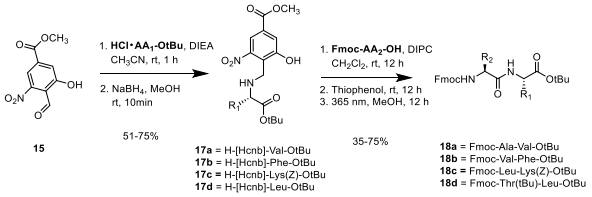

AA_1	Amine (Yield, %)	AA_2	Dipeptide (Yield, %)
Val-OtBu	**16a** (51)	Ala	**18a** (38)
Phe-OtBu	**16b** (63)	Val	**18b** (35)
Lys(Z)-OtBu	**16c** (69)	Leu	**18c** (54)
Leu-OtBu	**16d** (75)	Thr(tBu)	**18d** (53)

Preparation of resin-bound Hcna linker. The free acid form of the Hcna linker, **16** (Scheme 3), was covalently anchored to aminomethyl-functionalized Tentagel resin **21a**, or Sieber TG resin **21b** via acylation of a resin-bound amine. A 6-aminohexanoic acid (Ahx) spacer was employed with both solid supports to improve reactivity. Additionally, a proline residue was introduced to reduce cross-linking between the amine and the aldehyde of the Hcna linker. In both cases, acylation of resin-bound amines was accomplished by coupling **16** to the free amine using PyBOP. Subsequent reactions of **22a** were monitored by photolytic cleavage from the linker and analysis of the crude product, whereas reactions of **22b** were monitored by cleavage using dilute acid and analysis of the crude product. Because of the time required for photolysis of Hcnb-linked peptides (1-2 h), reaction conditions were optimized using **22b** and then applied to **22a**.

Scheme 5. Preparation of resin-bound Hcna linkers 22a-b.

Loading dipeptide by reductive amination and acylation. The first residue was anchored to the resin-bound Hcna linker via a 2-step reductive amination under acidic conditions. (Scheme 6). Quantitative acylation of the resin-bound amine was accomplished using a symmetric anhydride of the second residue (4 eq, 2 x 2h) as determined by LC-MS analysis.

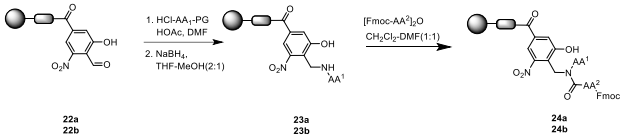

Scheme 6. **Addition of first and second amino acid residues to the Hcna linker.**

Loading of third amino acid. One of the major challenges with the Backbone Amide Linker concept is the formation of a diketopiperazine byproduct upon deprotection at the dipeptide stage. The most common method for overcoming this problem is to employ a sterically hindered C-terminal protecting group such as *t*-butyl or 1,1-dimethylallyl (DMA), [xxxvi] thereby minimizing the formation of this undesired byproduct. However, it was found that quantitative DKP formation was still obtained when using the Hcnb linker, regardless of the C-terminal protecting groups used. It was hypothesized that this results from Brønsted acid activation of the C-terminus by the nearby phenol proton, thereby catalyzing the formation of DKP. It was reasoned that this effect could be eliminated through removal of the phenol proton, thus avoiding Brønsted acid activation. The phenol group is required for efficient loading of the second amino acid residue, as well as for photocleavage of the final peptide, and so a method for only temporarily blocking this group is required. Following the loading of the secondary amine, the phenol remains acylated with excess of the second amino acid, until it is cleared off by the strongly nucleophilic piperidine upon deprotection of the dipeptide. We theorized that replacing piperidine with DBU, a non-nucleophilic alternative for Fmoc deprotection, would leave the acylated phenol intact and minimize formation of DKP. However, it was found that rapid, quantitative DKP formation was still obtained even when using DBU. Other methods were considered for blocking the phenol from interacting with the C-terminus, including silylation. However, due to the electronics of the ring, silylation of the phenol results in an exceedingly unstable transient product. Even attempts to observe the presence of a silyl group by LC-MS analysis were unsuccessful. To monitor the effectiveness of various silylation conditions,

the dipeptide N-terminus was deprotected for 3 min using a cocktail of 2% v/v DBU and 2% v/v 1-Octanethiol in DMF, followed by immediate introduction of the third amino acid as a pre-formed symmetric anhydride. The most successful conditions found were TIPS-OTf and 2,6-Lutidine for introduction of a TIPS protected phenol on the Linker. A variety of tripeptide sequences were tested to determine the efficiency of the TIPS group for blocking DKP formation (table 4). In most cases, only trace amounts of DKP were observed by LC-MS, if any. The worst sequence tested was the Ala-Ala dipeptide, resulting in 12% DKP formation.

Table 3. DKP formation during third amino acid coupling (**27a-g)**

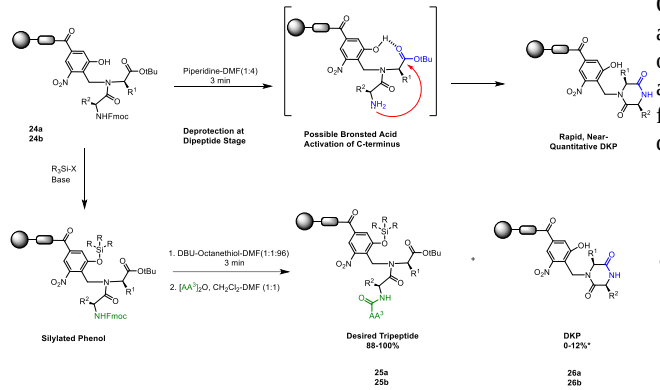

Dipeptide	Tripeptide	tripeptide/ DKP
Fmoc-Ala-*Val-ODMA	Fmoc-Gly-Ala-*Val-ODMA **(27a)**	100 / 0
Fmoc-Val-*Phe-ODMA	Fmoc-Phe-Val-*Phe-ODMA **(27b)**	96 / 6
Fmoc-Phe-*Lys(Boc)-ODMA	Fmoc-Val-Phe-*Lys(Boc)-ODMA **(27c)**	100 / 0
Fmoc-Ala-*Glu(tBu)-ODMA	Fmoc-Phe-Ala-*Glu(tBu)-ODMA **(27d)**	98 / 2
Fmoc-Val-*Leu-O*t*Bu	Fmoc-Gly-Val-*Leu-O*t*Bu **(27e)**	100 / 0
Fmoc-Ala-*Phe-O*t*Bu	Fmoc-Phe-Ala-*Phe-O*t*Bu **(27f)**	100 / 0
Fmoc-Ala-*Ala-O*t*Bu	Fmoc-Leu-Ala-*Ala-O*t*Bu **(27g)**	88 / 12

*residue anchored to Hncb linker.

The choice of model cyclic peptides. Two previously synthesized cyclic peptides were chosen to model the head to tail cyclized peptides to demonstrate the performance of the Hcnb linker on solid support. The 14-residue cyclic peptide c-[Pro-Asp-Gly-Arg-Cys-Thr-Lys-Ser-Ile-Pro-Pro-Ile-Cys-Phe], also known as the Sunflower Trypsin Inhibitor, is a well-known natural product. The cyclic decapeptide c-[Arg-(D)-Phe-Pro-Glu-Asp-Asn-Tyr-Glu-Ala-Ala] was synthesized to demonstrate the efficacy of the original Backbone Amide Linker, published by Albericio and Barany. The 14-mer cyclic Sunflower Trypsin Inhibitor poses some interesting synthetic challenges due to the high prevalence of β-branched amino acids and proline residues, which make selection of a cyclization point difficult. After several attempts, it was found that reductive amination of Phe onto the linker as the first residue, followed by cyclization at Pro yielded the best results. Cyclization and subsequent photocleavage from the resin yielded the final peptide in 90% purity and 80% cleavage yield. The synthesis of the cyclic decapeptide was accomplished through reductive amination of Ala as the first residue and the subsequent linear synthesis. Following cyclization and photocleavage from the resin, the peptide was obtained in 95% purity and 90% cleavage yield. The first peptide chosen was a short-chain analogue of the natural product somatostatin, cyclo[(D)-Trp-Lys-Gly-(β)-Ala-Phe]. The synthesis was carried out according to the procedures mentioned previously. The first residue H-Phe-ODMA was loaded onto the prepared resin **22a** via reductive amination. The subsequent linear synthesis was then carried out as previously discussed. The head-to-tail cyclization was accomplished on the resin using PyBOP. Photocleavage from the resin at 365 nm for 1 h yielded the final cyclic decapeptide **29** in 50% purity and 96% cleavage yield.

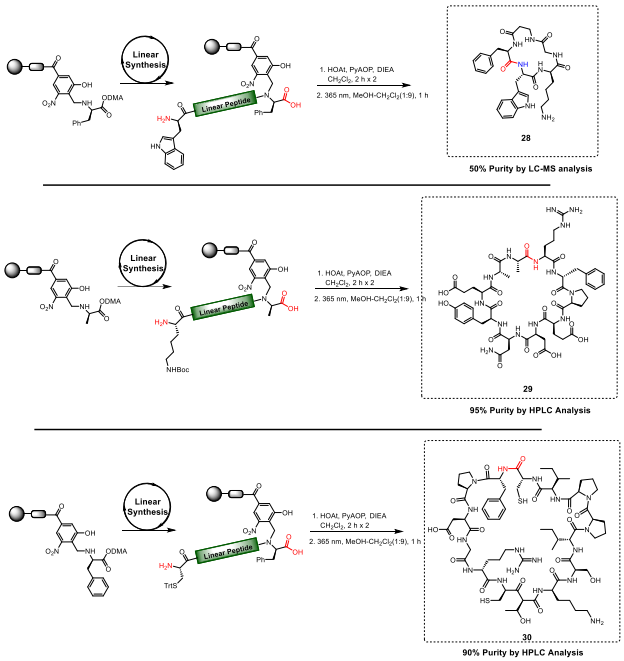

Scheme 8. Cyclization of 5-, 10-, and 14- residue cyclic peptides

Synthesis of C-terminal Thioesters. The synthesis of C-terminal thioesters is an area of interest for their use in native chemical ligation (NCL) reactions.[xx] The Hcnb linker was used to demonstrate the on-resin synthesis of thioesters in high purities. It was established by solution-phase studies that the presence of a free phenol on the linker was problematic for synthesis of C-terminal thioesters, and so the phenol was TIPS protected prior to optimizing the coupling conditions for thioester formation. Use of carbodiimides as a coupling reagent yielded low conversions (0-30%). However, switching to HATU as a coupling reagent and preactivating the carboxylic acid for 5 min prior to addition of the thiol yielded complete conversion to the desired thioester in 2 h. A series of pentapeptides were synthesized to examine the scope of C-terminal residue compatibility with thioester synthesis. It was found that β-branched amino

acids yield poor conversion to the thioester. However, it was reported by Kent[xx] that these sterically hindered amino acids are not amenable to NCL due to the steric hindrance of the carbonyl required for the transthioesterification and subsequent acyl transfer. The linear sequences were synthesized according to the standard procedure outlined previously. The final amino acid in the sequence was coupled as an N-Boc-protected residue. The C-terminal DMA protecting group was removed using Pd(0) and phenylsilane. Following TIPS protection of the linker phenol, the C-terminus was pre-activated for 5 min with HATU and Hunig's base in DMF. Addition of thiophenol resulted in 95 - 100% conversion of carboxylic acid to thioester in 2 h. The thioester peptides were then globally deprotected using 5% H_2O in TFA for 1 h and cleaved from the resin using 365 nm UV irradiation for 1 h. Depending on the identity of the first amino acid residue, peptide thioesters were obtained in 75-99% purity and 66-92% cleavage yield (Table 4). No epimerization of the C-terminal residue was observed.

Table 4. Yields of C-Terminal Thioester peptides

Structure	Purity	Cleavage Yield
H-Phe-Lys-Ala-Ala-Leu-S-Ph **(31a)**	99%	83%
H-Ala-Glu-Phe-Leu-Phe-S-Ph **(31b)**	99%	66%
H-Ala-Lys-Phe-Leu-Glu-S-Ph **(31c)**	75%	71%
H-Phe-Glu-Ala-Leu-Ala-S-Ph **(31d)**	95%	92%

CONCLUSIONS

In a quest for a photolabile backbone amide linker for the solid-phase synthesis of cyclic and C-terminally modified peptides, a survey of various photolabile motifs was conducted, establishing the *o*-nitrobenzyl motif as the best candidate. Problems associated with many of the candidate motifs including the nitroveratryl linker led to the development of the 2-hydroxy-4-carboxy-6-nitrobenzyl (Hcnb**)** linker. A convenient and scalable synthesis of a benzaldehyde precursor (**16**) was developed, and general conditions were found for the anchoring of various amino esters to the linker and their acylation to form anchored dipeptides in good yield. Photolysis of the various Hcnb-linked dipeptides (**18a-d)** at 365 nm cleanly deprotected them in good yield in all cases. The linker can be attached to a wide variety of amino acids, can be selectively removed in the presence of most commonly used protecting groups and tolerates treatment with acid, base and Pd^0. It was found that the Hcnb linker could be conveniently attached to an aminoethyl TG resin using a 6-aminohexanoic acid spacer and proline residue, permitting its use in solid phase peptide synthesis. The ability of the Hcnb linker to facilitate on-resin, head-to-tail cyclization of peptides was demonstrated through the synthesis of three cyclic peptides. The utility of Hcnb to synthesize C-terminal thioesters was also demonstrated. We believe that this new photolabile linker should provide a valuable tool for the synthesis of cyclic and modified peptides, depsipeptides and peptidomimetics such as oligoureas.[xxxvii]

EXPERIMENTAL SECTION

General. Reagents were purchased from Sigma-Aldrich, Alfa-Aesar, and TCI America and used without further purification. Protected amino acids were purchased from Novabiochem, Advanced ChemTech, and Acros. Solvents were purified by passage through a solvent column[xxxviii] composed of activated alumina and a supported copper redox catalyst. Flash chromatography was performed using 230-400 mesh silica gel. NMR spectra were recorded at 500 and 125.74 MHz for proton and carbon nuclei, respectively, on a Bruker DRX500 spectrometer . Infrared spectra were recorded using a Perkin-Elmer instrument. UV-visible spectra were recorded using a HP-8453 Spectrophotometer. Photolyses were carried out in a 5 mL fused-quartz tube, fitted in a laboratory vortexer. The reaction chamber was fitted with 365 nm LEDs as described in U.S Patent Application no 63029491.[xxxix] Analytical HPLC was performed on a Gilson instrument with HPLC grade acetonitrile (CH_3CN) and deionized water (H_2O) and 0.1% (v/v) of trifluoroacetic acid. Usually a C8 reverse phase column was used to analyze small peptide units using a 5-100% CH_3CN/H_2O gradient over 30 min with 214 nm lamp.

1-(2,5-dimethyl-4-alkylphenyl)-propanone (4b) To a mixture of propionyl chloride (0.51 mL, 5.88 mmol) and $AlCl_3$ (780 mg, 5.88 mmol) in CH_2Cl_2 (25 mL) was added a solution of 4-(2,5-dimethylphenyl)butanoic acid (**4a,** 377 mg, 1.96 mmol) in CH_2Cl_2 (5 ml) at 0°C. The reaction mixture was stirred for 1 h at the same temperature and poured into cold HCl solution (40 g ice and 10 mL of conc. HCl). The organic material was extracted by addition of CH_2Cl_2 (25 mL) and the aqueous layer was extracted with another portion of CH_2Cl_2 (50 mL). The combined organic layer was washed with brine (50 mL), dried with anhydrous $MgSO_4$, passed through 3 cm silica gel pad, and evaporated under reduced pressure. The crude product was dissolved in oxalyl chloride (3 mL) and stirred overnight. After removal extra oxalyl chloride by evaporation under reduced pressure, the organic material was dissolved in CH_2Cl_2 (30 mL). To this solution, benzyl amine (0.257 mL, 2.35 mmol) and DIEA (1.7 mL, 9.8 mmol) were added and stirred 3 h. The organic layer was washed with brine (30 mL), dried with anhydrous $MgSO_4$, evaporated under reduced pressure and purified by flash column chromatography using 33% EtOAc in Hexanes to give **4b** as a pale yellow solid (600 mg, 90%). **^{1}H NMR** (300 MHz, $CDCl_3$) δ 7.49 (s, 1H), 7.33 (m, 5H), 7.04 (s, 1H), 5.96 (s, 1H), 4.50 (d, 2H, *J* = 5.7 Hz), 3.00 (q, 2H, *J* = 7.8 Hz), 2.70 (m, 2H), 2.50 (s, 3H), 2.37 (s, 3H), 2.33 (m, 2H), 2.03 (m, 2H), 1.24 (t, 3H, *J* = 7.8 Hz); **^{13}C NMR** (75 MHz, $CDCl_3$) δ 204.7, 172.4, 143.4, 138.4, 135.7, 133.2, 132.8, 130.7, 128.8, 127.9, 127.6, 43.7, 36.1, 34.5, 32.6, 25.8, 21.1, 18.9, 8.5.

1-(2,5-dimethyl-4-alkylphenyl)-1-hydroxypropan-2-one oxime (4c) To a solution of **4b** (0.51g, 1.50 mmol) and isoamyl nitrite (0.24 mL, 1.80 mmol) in MeOH (10 mL) at 45°C was added dropwise to concentrated HC1 (0.25 mL) and the resulting mixture was stirred for 3 h at the same temperature. After cooling to room temperature, the organic material was partitioned into EtOAc (40 mL) and H_2O (40

mL). The organic layer was washed with brine (40 mL), dried with anhydrous $MgSO_4$, passed through 3cm silica gel pad, and evaporated under reduced pressure. The residue was dissolved in MeOH (15 mL) and $NaBH_4$ (50 mg) was added under ice bath. After stirring for 30 min, the organic material was partitioned into EtOAc (40 mL) and HCl solution (0.1 M, 30 mL). The organic layer was washed with saturated $NaHCO_3$ (30 mL) and with brine (30 mL), dried over anhydrous $MgSO_4$, and evaporated under reduced pressure. The residue was purified by flash column chromatography using 66% EtOAc in hexanes to give **4c** as a white solid (347 mg, 63%). **^{1}H NMR** (300 MHz, $CDCl_3$) δ 9.11 (s, 1H), 7.36 (m, 5H), 7.17 (s, 1H), 6.93 (s, 1H), 6.18 (m, 1H), 5.39 (s, 1H), 4.47 (d, 2H, *J* = 5.7 Hz), 3.88 (s, 1H), 2.57 (m, 2H), 2.29 (m, 8H), 1.89 (m, 2H), 1.77 (s, 3H); **^{13}C NMR** (75 MHz, $CDCl_3$) δ 173.1, 158.1, 139.5, 138.3, 135.4, 133.8, 133.5, 131.5, 128.8, 127.9, 127.6, 72.4, 43.7, 36.1, 32.3, 26.0, 19.0, 18.7, 11.0.

1-(2,5-dimethyl-4-alkylphenyl)-1-hydroxypropan-2-one (4) To a solution of **4c** (0.30 g, 0.81 mmol) in DMF (2 mL) was added glyoxylic acid (60 % water solution, 5 mL). After stirring for 5 h, the organic material was partitioned into EtOAc (40 mL) and H_2O (40 mL). The organic layer was washed with brine (2 X 30 mL), dried with anhydrous $MgSO_4$, evaporated under reduced pressure, and the residue was purified by flash column chromatography using 50% EtOAc in hexanes to give **4** as a pale yellow oil (94%, 269 mg). **^{1}H NMR** (300 MHz, $CDCl_3$) δ 7.24 (m, 5H), 7.01 (m, 1H), 6.94 (s, 1H), 6.92 (s, 1H), 5.17 (s, 1H), 4.36 (d, 2H, *J* = 6.0 Hz), 2.54 (m, 2H), 2.31 (s, 3H), 2.31 (m, 2H), 2.26 (s, 3H), 2.04 (s, 3H), 1.89 (m, 2H); **^{13}C NMR** (75 MHz, $CDCl_3$) δ 208.2, 173.3, 140.4, 138.6, 134.1, 133.7, 131.9, 129.9, 128.6, 127.7, 127.3, 77.6, 43.4, 35.9, 32.3, 26.1, 25.5, 18.8.

H-[Op]-Gly-OMe (6a). To a solution of **1**, (150 mg, 0.66 mmol) in anhydrous CH_3CN (5 mL) were added GlyOMe·HCl (248 mg, 1.98 mmol), and DIEA (0.52 mL, 2.97 mmol). The reaction mixture was stirred overnight at room temperature, evaporated under reduced pressure and partitioned into CH_2Cl_2 (20 mL) and H_2O (20 mL). The organic layer was washed with brine (20 mL), dried with anhydrous $MgSO_4$, evaporated under reduced pressure, and purified by flash column chromatography using 33% EtOAc in hexanes to give **6a** as a pale yellow oil (99 mg, 63%). **^{1}H NMR** (300 MHz, $CDCl_3$) δ 7.90 (d, 2H, *J* = 9.0 Hz), 6.92 (d, 2H, *J* = 9.0 Hz), 4.13 (s, 2H), 3.85 (s, 3H), 3.72 (s, 3H), 3.54 (s, 2H), 2.54 (s, 1H); **^{13}C NMR** (75 MHz, $CDCl_3$) δ 195.6, 172.5, 163.8, 130.0, 128.3, 113.9, 55.5, 54.6, 51.8, 50.2; **IR** (NaCl, cm^{-1}) 2925, 1739, 1600.

H-[Mop]-Gly-OMe (6b). To a solution of **2**, (200 mg, 0.63 mmol) in anhydrous CH_3CN (8 mL) were added GlyOMe·HCl (237 mg, 1.89 mmol), DIEA (0.49 mL, 2.84 mmol) and tetrabutylammonium iodide (25 mg). The reaction mixture was refluxed for overnight, cooled to room temperature, evaporated under reduced pressure, and partitioned into CH_2Cl_2 (20 mL) and H_2O (20 mL). The organic layer was washed with brine (20 mL), dried with anhydrous $MgSO_4$, evaporated under reduced pressure, and purified by flash column chromatography using 33% EtOAc in hexanes to give **6b** as a colorless oil (161 mg, 78%). **^{1}H NMR** (300 MHz, $CDCl_3$) δ 8.01 (d, 2H, *J* = 8.7 Hz), 7.46 (m, 5H), 7.08 (d, 2H, *J* = 8.7 Hz), 5.18 (s, 2H), 4.39 (q, 1H, *J* = 7.2 Hz), 3.74 (s, 3H), 3.44 (dd, 2H, *J* = 17.1, 40.5 Hz), 2.47 (s, 1H), 1.39 (d, 3H, *J* = 7.2 Hz); **^{13}C NMR** (75 MHz, $CDCl_3$) δ 200.8, 172.4, 163.0, 136.1, 130.7, 128.8, 128.4, 128.4, 127.5, 114.9, 70.2, 57.1, 51.9, 49.0, 20.1; **IR** (NaCl, cm^{-1}) 2951, 1741, 1675, 1602.

H-[Obz]-Gly-OMe (6c). To a solution of **3**, (123 mg, 0.39 mmol) in anhydrous MeOH (20 mL) was added GlyOMe·HCl (242 mg, 1.93 mmol). The reaction mixture was refluxed for 24 h, cooled to room temperature, evaporated under reduced pressure, and partitioned into CH_2Cl_2 (20 mL) and H_2O (20 mL). The organic layer was washed with brine (20 mL), dried with anhydrous $MgSO_4$, evaporated under reduced pressure, and purified by flash column chromatography using 33% EtOAc in hexanes to give **6c** as a pale yellow oil (111 mg, 74%). **^{1}H NMR** (300 MHz, $CDCl_3$) δ 8.00 (d, 2H, *J* = 9.3 Hz), 7.39 (m, 10H), 6.99 (d, 2H, *J* = 9.3 Hz), 5.46 (s, 1H), 5.13 (s, 2H), 3.76 (s, 3H), 3.47 (s, 2H); **^{13}C NMR** (75 MHz, $CDCl_3$) δ 196.2, 172.5, 162.8, 138.0, 136.1, 131.2, 131.0, 129.7, 129.2, 128.8, 128.4, 128.3, 127.5, 114.7, 70.2, 66.3, 51.9, 48.1; **IR** (NaCl, cm^{-1}) 2924, 1740, 1599.

H-[Dmp]-Gly-OMe (6d). To a solution of **4**, (200 mg, 0.57 mmol) in anhydrous toluene (20 mL) was added GlyOMe·HCl (215 mg, 1.71 mmol). The reaction mixture was refluxed for 5 h, cooled to room temperature, and partitioned into EtOAc (20 mL) and H_2O (40 mL). The organic layer was washed with brine (40 mL), dried with anhydrous $MgSO_4$, evaporated under reduced pressure, and purified by flash column chromatography using 33% EtOAc in hexanes to give **6d** as a colorless oil (204 mg, 85%). **^{1}H NMR** (300 MHz, $CDCl_3$) δ 7.40 (m, 5H), 7.07 (s, 1H), 5.77 (m, 1H), 4.51 (d, 2H, *J* = 5.7 Hz), 4.27 (q, 1H, *J* = 7.2 Hz), 3.50 (dd, 2H, *J* = 17.1, 31.5 Hz), 2.71 (t, 2H, *J* = 7.5 Hz), 2.45 (s, 3H), 2.37 (s, 3H), 2.33 (t, 2H, *J* = 6.9 Hz), 2.01 (m, 2H), 1.30 (d, 3H, *J* = 7.2 Hz); **^{13}C NMR** (75 MHz, $CDCl_3$) δ 205.8, 172.5, 172.4, 144.0, 138.5, 136.1, 134.3, 133.4, 132.7, 130.0, 128.7, 127.8, 127.5, 59.4, 51.9, 48.9, 43.6, 36.0, 32.6, 25.7, 20.5, 19.0, 18.9; **IR** (NaCl, cm^{-1}) 2954, 1744, 1649, 1556.

H-[Nve]-Gly-OMe (6e). To a solution of **5** (515 mg, 2.44 mmol) in MeOH (20 mL), were added GlyOMe·HCl (459 mg, 3.66 mmol), sodium bicarbonate (348 mg, 4.15 mmol). The reaction mixture was stirred for 4 h, cooled to 0°C. After portionwise addition of $NaBH_4$ (6.0 mmol, 227 mg), the mixture was stirred for 30 min and poured into HCl solution (0.1N, 50 mL). The pH of water layer was adjusted to 4~6 by dropwise addition of NaOH (1 M), and the organic material was extracted with CH_2Cl_2 (50 mL). The aqueous layer was extracted with another portion of CH_2Cl_2 (50 mL). The combined organic layer was dried with anhydrous $MgSO_4$, evaporated under reduced pressure and purified by flash column chromatography using 50% EtOAc in hexanes to give **6e** as a colorless oil (568 mg, 82%). **^{1}H NMR** (300 MHz, $CDCl_3$) δ 7.55 (s, 1H), 7.08 (s, 1H), 4.02 (s, 2H), 3.92 (s, 3H), 3.87 (s, 3H), 3.65 (s, 3H), 3.41 (s, 2H); **^{13}C NMR** (75 MHz, $CDCl_3$) δ 172.6, 153.3, 147.7, 140.9, 130.6, 112.1, 108.2, 56.5, 56.3, 51.9, 50.6, 50.4; **IR** (NaCl, cm^{-1}) 2952, 1740, 1520, 1274.

General procedure for acylation of 6a-e with symmetric anhydrides 7a-e. The symmetric anhydride of Boc-Phe was prepared *in situ* by mixing Boc-Phe (860 mg, 4 mmol) with

EDCI (0.422 g, 2.2 mmol) in CH_2Cl_2 (10 ml, 0.2 M) for 5 min. To the solution of symmetric anhydride was added **6a-e** (1 mmol), and the reaction mixture was stirred for 24 h at room temperature. After dilution with CH_2Cl_2 (50 ml), the organic layer was washed with brine (50 mL), dried with anhydrous $MgSO_4$, and evaporated under reduced pressure. The residue was purified by flash column chromatography to obtain an Hcnb-linked dipeptide (**7a-e**).

Boc-Phe-[Op]-Gly-OMe (7a). **^{1}H NMR** (300 MHz, $CDCl_3$) δ 8.00 (d, 1H, *J* = 8.7 Hz), 7.89 (d, 1H, *J* = 8.7 Hz), 7.30 (m, 5H), 6.99 (d, 2H, *J* = 8.7 Hz), 5.09-4.67 (m, 3H), 4.26 (dd, 2H, *J* = 16.8, 59.4 Hz), 3.93 (s, 3H), 3.78 (s, 3H), 3.24-2.92 (m, 2H), 1.43 (s, 4H), 1.34 (s, 5H); **^{13}C NMR** (75 MHz, $CDCl_3$) δ 191.7, 172.7, 169.8, 164.3, 155.0, 136.7, 130.4, 129.7, 128.4, 127.4, 126.8, 114.1, 79.8, 55.7, 54.1, 51.9, 49.6, 48.5, 39.4, 28.3; **IR** (NaCl, cm^{-1}) 2933, 1748, 1693, 1657, 1601.

Boc-Phe-[Mop]-Gly-OMe (7b). Mixture of diastereomers; **^{1}H NMR** (300 MHz, $CDCl_3$) δ 8.09-7.88 (m, 2H), 7.50-7.03 (m, 12H), 6.33 (m, 1H), 5.50 (m, 1H), 5.20 (m, 2H), 4.60 (m, 1H), 4.52-4.05 (m, 2H), 3.69 (m, 3H), 3.29-2.83 (m, 2H), 1.49-1.26 (m, 12H); **^{13}C NMR** (75 MHz, $CDCl_3$) δ 196.9, 173.1, 169.9, 163.3, 155.1, 137.0, 136.5, 136.1, 131.3, 129.8, 129.4, 128.8, 128.5, 127.6, 126.9, 114.9, 79.7, 70.2, 52.6, 52.2, 51.0, 44.9, 39.8, 28.3, 14.3; **IR** (NaCl, cm^{-1}) 2978, 1750, 1702, 1648, 1600.

Boc-Phe-[Obz]-Gly-OMe (7c). Mixture of diastereomers; **^{1}H NMR** (300 MHz, $CDCl_3$) δ 7.99 (m, 2H), 7.38 (m, 16H), 7.00 (m, 2H), 5.15 (m, 2H), 4.84-4.51 (m, 1H), 4.37-3.90 (m, 2H), 3.57-3.52 (m, 3H), 3.29-2.88 (m, 2H), 1.44 (s, 9H); **^{13}C NMR** (75 MHz, $CDCl_3$) δ 194.8, 173.8, 169.9, 163.0, 155.1, 137.0, 136.6, 136.1, 133.8, 131.3, 130.5, 130.2, 129.7, 129.6, 129.1, 128.8, 128.5, 127.5, 126.8, 126.7, 114.8, 79.9, 70.2, 62.3, 52.4, 52.2, 47.2, 39.6, 28.3; **IR** (NaCl, cm^{-1}) 2926, 1747, 1694, 1651, 1600.

Boc-Phe-[Dmp]-Gly-OMe (7d). Mixture of diastereomers; **^{1}H NMR** (300 MHz, $CDCl_3$) δ 7.78-7.02(m, 12H), 6.42-5.75 (m, 2H), 5.47-4.87 (m, 1H), 4.60 (m, 1H), 4.47 (m, 2H), 4.32-4.13 (m, 1H), 3.93-3.72 (m, 4H), 3.16-2.78 (m, 2H), 2.68 (m, 2H), 2.44-2.29 (m, 8H), 1.98 (m, 2H), 1.49-0.96 (m, 12H); **^{13}C NMR** (75 MHz, $CDCl_3$) δ 201.8, 173.1, 172.4, 169.8, 155.1, 144.5, 138.5, 136.9, 136.7, 133.5, 133.3, 132.7, 131.0, 129.5, 128.8, 128.5, 127.9, 127.5, 126.8, 79.8, 68.2, 55.1, 52.7, 52.2, 45.7, 43.6, 35.9, 32.6, 28.3, 25.8, 20.7, 18.9, 13.9; **IR** (NaCl, cm^{-1}) 2929, 1748, 1697, 1649.

Boc-Phe-[Nve]-Gly-OMe (7e). **^{1}H NMR** (300 MHz, $CDCl_3$) δ 7.76 (s, 1H), 7.34 (m, 5H), 7.18 (s, 1H), 5.27 (m, 1H), 4.81 (dd, 2H, *J* = 17.7, 18.6, 49.4 Hz), 4.72 (m, 1H), 4.23 (m, 1H), 4.00 (s, 3H), 3.98 (s, 3H), 3.80 (s, 3H), 3.22-2.92 (m, 2H), 1.42 (s, 9H); **^{13}C NMR** (75 MHz, $CDCl_3$) δ 173.6, 168.9, 155.0, 154.1, 148.2, 140.0, 136.0, 129.4, 128.8, 128.6, 127.2, 110.1, 108.6, 80.0, 56.7, 56.5, 52.8, 52.2, 50.2, 48.9, 39.4, 28.3; **IR** (NaCl, cm^{-1}) 2977, 1749, 1706, 1654, 1520.

methyl(E)-4-(2-(dimethylamino)vinyl)-3,5-dinitrobenzoate (13). To a stirred mixture of 4-Methyl-3,5-dinitrobenzoic acid (2.0 g, 8.8 mmol) in anhydrous toluene (29 mL) was added DMF-DMA (3.2 mL, 24 mmol) dropwise at rt. The resulting mixture was heated reflux and became dark red in color. After 16 h, the reaction was cooled to rt and the solvent removed under reduced pressure by co-evaporation with MeOH. The crude residue was recrystallized from hot ethanol to afford enamine **13** (1.88 g, 72%) as a reflective green solid which became red upon grinding. **R_f** = 0.37 (25% EA/Hex); **mp** 128-130 °C (lit.14 128-130 °C); **^{1}H NMR** (500 MHz, CDCl3) δ 8.31 (s, 2H), 6.70 (d, J = 13.4 Hz, 1H), 5.49 (d, J = 13.4 Hz, 1H), 3.93 (s, 3H), 2.95 (s, 6H); **^{13}C NMR** (125 MHz, $CDCl_3$) δ 163.90, 148.75, 147.61, 132.89, 128.19, 122.57, 83.78, 52.73; **IR** (neat, cm^{-1}) 3091, 2955, 2161, 2034, 1715, 1632, 1580, 1522, 1438, 1414, 1395, 1372, 1352, 1289, 1263, 1149, 1096, 986, 962, 922, 912, 871; **HRMS** (nESI-TOF) m/z: [M+Na]+ Calcd for $C_{12}H_{13}N_3O_6Na$ 318.07021, Found 318.07074.

methyl 4-formyl-3,5-dinitrobenzoate (14). To a mixture of **13** (1.08 g, 3.66 mmol) and $RuCl_3$ stock solution (0.1 M in H_2O, 1.2 mL, 0.13 mmol) in CH_3CN-H_2O (6:1, 37 mL) was added $NaIO_4$ (2.0 g, 9.1 mmol) in portions at rt. The color quickly dissipated, and solids formed. Note: it is important to wait for TLC to show clean product spot before workup so as to ensure facile separation (typically 10-30 min). After stirring for 30 min, the solids were removed by vacuum filtration and washed with CH_2Cl_2. The filtrate was partitioned between H_2O and CH_2Cl_2, and the organic layer was removed. The resulting aqueous layer was extracted twice more with CH_2Cl_2 and the combined organic extracts were washed with brine then sat. aq. $Na_2S_2O_4$. The organic extracts were dried over Na_2SO_4, filtered and concentrated under reduced pressure. The resulting crude residue was purified by flash column chromatography (30% EA/Hex) to afford **14** (571 mg, 61%) as an off-white solid. **R_f** = 0.33 (30% EA/Hex); **mp** 103.5-104 °C; **^{1}H NMR** (500 MHz, CDCl3) δ 10.63 (s, 1H), 9.08 (s, 2H), 4.08 (s, 3H); **^{13}C NMR** (125 MHz, CDCl3) δ 184.91, 162.25, 147.85, 134.67, 133.98, 130.25, 53.82; **IR** (neat, cm^{-1}) 3096, 2967, 2162, 1979, 1729, 1705, 1573, 1535, 1470, 1437, 1382, 1348, 1317, 1297, 1201, 1177, 1161, 1087, 974, 931, 924, 898, 835; **HRMS** (nESI-TOF) m/z: [M+Na]+ Calcd for $C_9H_6N_2O_7Na$ 277.00727, Found 277.00686.

methyl 4-formy-3-hydroxyl-5-nitrobenzoate (15). A solution of **14** (678 mg, 2.67 mmol) in anhydrous DMF (5.1 mL) was added dropwise to a mixture of acetaldoxime [mixture of isomers] (325 µL, 5.33 mmol) and K_2CO_3 (811 mg, 5.87 mmol) in anhydrous DMF (5.1 mL) dropwise at rt. The reaction mixture immediately turned bright red-purple upon mixing, then brown-green after overnight. After 21 h, ~10 mL of H_2O was added to the reaction and the resulting solution extracted 5x with Et_2O. The aqueous layer was then acidified to pH ~1-2 with concentrated HCl and extracted 4x with CH_2Cl_2. The combined organic extracts were dried over Na_2SO_4, filtered and concentrated under reduced pressure. The crude residue was purified by flash chromatography (25% EA/Hex) to afford **15** (407 mg, 68%) as a bright yellow solid. **R_f** = 0.34 (25% EA/Hex); **mp** = 101-101.5 °C; **^{1}H NMR** (500 MHz, $CDCl_3$) δ 12.05 (s, 1H), 10.37 (s, 1H), 8.15 (d, J = 1.6 Hz, 1H), 7.93 (d, J = 1.4 Hz, 1H), 4.00 (s, 3H); **^{13}C NMR** (125 MHz, $CDCl_3$) δ 193.57, 163.59, 163.14, 151.28, 136.80, 125.25, 116.29, 114.27, 53.29. **IR** (neat, cm^{-1}) 3093, 2959, 2161, 1979, 1728, 1719, 1666, 1649, 1561, 1535, 1483, 1433, 1386, 1350, 1307, 1241, 1185, 1160, 1091, 1010, 972, 931, 901; **HRMS** (nESI-TOF) m/z: [M+Na]+ Calcd for $C_9H_7NO_6Na$ 248.01711, Found 248.01593.

4-formyl-3-hydroxy-5-nitrobenzoic acid (16). Solid $Ba(OH)_2 \cdot 8\ H_2O$ (1.97 g, 6.24 mmol) was added in portions to a solution of **15** (468 mg, 2.08 mmol) in MeOH (23 mL) at rt. Following reaction completion (TLC), the mixture was concentrated under reduced pressure and the crude residue was partitioned between EtOAc and H_2O. The organic layer was removed and the aqueous layer was extracted twice more with EtOAc. The resulting aqueous layer was acidified to pH ~1-2 with concentrated HCl and extracted 3x with EtOAc. The combined organic extracts were washed with brine, dried over Na_2SO_4, filtered and concentrated under reduced pressure to afford **16** (379 mg, 86%) as a brown solid. $\mathbf{R_f}$ = 0.31 (20% MeOH/CH_2Cl_2); **mp** = 187-189 °C; **^{1}H** NMR (300 MHz, DMSO-d6) δ 11.73 (s, 1H), 10.28 (s, 1H), 7.77 (d, J = 1.3 Hz, 1H), 7.75 (s, 1H); **^{1}H NMR** (300 MHz, CD_3OD) δ 10.30 (s, 1H), 7.95 (d, J = 1.4 Hz, 1H), 7.83 (d, J = 1.4 Hz, 1H), 7.71 (d, J = 1.6 Hz, 1H), 7.63 (d, J = 1.6 Hz, 1H), 6.07 (s, 1H); **^{13}C NMR** (125 MHz, DMSO-d6) δ 189.09, 165.24, 160.03, 149.11, 136.52, 122.26, 119.82, 114.52; **IR** (neat, cm^{-1}) 3103, 2161, 2034, 1710, 1660, 1566, 1528, 1493, 1413, 1393, 1352, 1294, 1242, 1199, 1165, 1098, 1007, 929, 916, 902, 867; MS (ESI-) m/z: [M-H]- Calcd for $C_8H_4NO_6$ 210.0, Found 443.3 [2M+Na-2H]-

General Procedure for Solution-Phase Reductive Amination (17a-d). HCl-AA-OtBu (0.666 mmol) was added to a solution of **15** (200.0 mg, 0.666 mmol) and DIEA (244 µL, 1.40 mmol) in CH_3CN (9.5 mL). The reaction was stirred at rt for 45 min. Volatiles were removed and the residue was dissolved in MeOH (3.3 m). $NaBH_4$ (75.6 mg, 2.00 mmol) was added and the reaction was stirred for 15 min. Volatiles were removed and the residue was purified by flash column chromatography (20-45% EA/Hex) to yield **17a-d** in 51-75% yield.

H-[Hcnb]-Val-OtBu (17a). Yellow Oil; **Yield** = 51%; $\mathbf{R_f}$ = 0.32 (20% EA/Hex); **^{1}H NMR** (500 MHz, CD_3OD) δ 8.21 (d, J = 1.6 Hz, 1H), 7.90 (d, J = 1.6 Hz, 1H), 4.71 (d, J = 13.3 Hz, 1H), 4.55 (d, J = 13.3 Hz, 1H), 3.97 (s, 3H), 3.96 (s, 1H), 2.42 (ddq, J = 10.6, 7.0, 3.5 Hz, 1H), 1.55 (s, 9H), 1.18 (d, J = 7.0 Hz, 3H), 1.08 (d, J = 6.9 Hz, 3H); **^{13}C NMR** (125 MHz, CD_3OD) δ 166.41, 164.17, 158.21, 150.49, 133.03, 120.34, 116.24, 84.49, 66.08, 51.95, 41.31, 29.22, 26.70, 18.42, 15.73; **IR** (neat, cm-1) 2978, 2948, 2162, 1734, 1718, 1624, 1582, 1538, 1457, 1420, 1437, 1395, 1372, 1344, 1300, 1242, 1200, 1161, 1104, 1031, 1006, 982, 931, 902, 888, 837.

H-[Hcnb]-Phe-OtBu (17b). Yellow Oil; **Yield** = 63%; $\mathbf{R_f}$ = 0.26 (20% EA/Hex); **^{1}H NMR** (500 MHz, CD_3OD) δ 8.21 (d, J = 1.6 Hz, 1H), 7.89 (d, J = 1.6 Hz, 1H), 7.39 – 7.28 (m, 5H), 4.68 (d, J = 13.4 Hz, 1H), 4.57 (d, J = 13.4 Hz, 1H), 4.32 (dd, J = 9.8, 5.6 Hz, 1H), 3.97 (s, 3H), 3.49 – 3.43 (m, 1H), 3.14 (dd, J = 13.8, 9.9 Hz, 1H), 1.31 (s, 9H); **^{13}C NMR** (125 MHz, CD_3OD) δ 166.88, 164.18, 158.15, 150.36, 133.88, 133.01, 129.07, 128.43, 127.31, 120.35, 116.54, 116.18, 84.12, 61.63, 51.95, 40.74, 35.66, 26.37; **IR** (neat, cm-1) 2986, 2257, 2096, 1721, 1620, 1580, 1532, 1458, 1448, 1430, 1395, 1370, 1314, 1258, 1240, 1196, 1156, 1131, 1099, 1065, 1034, 1010, 999, 900, 839.

H-[Hcnb]-Lys(Z)-OtBu (17c). Yellow Oil; **Yield** = 69%; $\mathbf{R_f}$ = 0.23 (40% EA/Hex); **^{1}H NMR** (500 MHz, CD3OD) δ 8.20 (d, J = 1.6 Hz, 1H), 7.89 (d, J = 1.6 Hz, 1H), 7.33 (d, J = 4.3 Hz, 4H), 7.32 – 7.26 (m, 1H), 5.04 (s, 2H), 4.66 (d, J = 13.3 Hz, 1H), 4.52 (d, J = 13.2 Hz, 1H), 4.05 (dd, J = 7.4, 5.1 Hz, 1H), 3.96 (s, 3H), 3.15 (t, J = 6.3 Hz, 2H), 2.02 (ddd, J = 12.0, 9.0, 6.0 Hz, 2H), 1.61 – 1.55 (m, 3H), 1.53 (s, 9H), 1.49 – 1.41 (m, 1H); **^{13}C NMR** (125 MHz, CD3OD) δ 167.32, 164.19, 158.18, 157.49, 150.37, 136.81, 132.96, 127.92, 127.45, 127.23, 120.33, 116.62, 116.15, 84.33, 65.83, 60.75, 51.95, 40.71, 39.48, 28.94, 28.88, 26.63, 21.64; **IR** (neat, cm-1) 3371, 2943, 2162, 1979, 1722, 1684, 1621, 1586, 1531, 1457, 1435, 1396, 1365, 1316, 1290, 1236, 1262, 1212, 1196, 1152, 1116, 1098, 1063, 1028, 1010, 955, 912, 901, 854, 838.

H-[Hcnb]-Leu-OtBu (17d). Yellow Oil; **Yield** = 75%; $\mathbf{R_f}$ = 0.40 (20% EA/Hex); **^{1}H NMR** (400 MHz, $CDCl_3$) δ 7.91 (d, *J* = 1.7 Hz, 1H), 7.66 (d, *J* = 1.7 Hz, 1H), 4.23 (d, *J* = 15.7 Hz, 1H), 4.06 (d, *J* = 15.7 Hz, 1H), 3.92 (s, 3H), 3.21 – 3.17 (m, 1H), 1.75 – 1.69 (m, 1H), 1.53 – 1.49 (m, 2H), 1.48 (s, 9H), 0.92 (d, *J* = 6.6 Hz, 3H), 0.87 (d, *J* = 6.6 Hz, 3H); **^{13}C NMR** (101 MHz, $CDCl_3$) δ 173.04, 164.90, 160.12, 150.13, 130.93, 121.71, 120.42, 115.66, 82.51, 59.12, 52.52, 45.92, 42.16, 27.90, 24.83, 22.60, 21.88; **IR** (neat, cm-1) 3295, 2958, 1724, 1656, 1574, 1531, 1435, 1391, 1366, 1298, 1231, 1145, 1096, 1017, 905, 843.

General Procedure for Solution-Phase Acylation and Photolysis (18a-d). A mixture of Fmoc-AA-OH (1.10 mmol) and DIPC (85 µL, 0.550 mmol) was preactivated in dry CH_2Cl_2 (0.88 mL) for 5 min. **17a-d** (0.500 mmol) as a solution in CH_2Cl_2 (0.85 mL) was added and the reaction was stirred for 2 h. 1-octanethiol (433 µL, 2.5 mmol) was added and the reaction was stirred overnight. Volatiles were removed and the residues were purified by flash column chromatography (20-45% EA/Hex) and used directly in the next reaction. A solution of Hcnb-linked dipeptides in MeOH (3 mL) were subject to 365 nm light for 12 h. Volatiles were removed and the residues were purified by flash column chromatography (15-35% EA/Hex) to give dipeptides **18a-d** in 35-53% yield.

Fmoc-Ala-Val-OtBu (18a). Yellow Oil; **Yield** = 38%; **^{1}H NMR** (400 MHz, $CDCl_3$) δ 7.76 (dt, *J* = 7.6, 0.9 Hz, 2H), 7.59 (dd, *J* = 7.3, 2.9 Hz, 2H), 7.39 (tt, *J* = 7.5, 0.9 Hz, 2H), 7.30 (td, *J* = 7.5, 1.2 Hz, 2H), 6.44 (d, *J* = 8.8 Hz, 1H), 5.47 (d, *J* = 7.6 Hz, 1H), 4.46 – 4.41 (m, 1H), 4.41 – 4.37 (m, 2H), 4.30 (t, *J* = 7.1 Hz, 1H), 4.21 (t, *J* = 7.1 Hz, 1H), 2.20 – 2.12 (m, 1H), 1.48 – 1.43 (m, 9H), 1.43 – 1.39 (m, 3H), 0.93 – 0.86 (m, 6H); **^{13}C NMR** (101 MHz, $CDCl_3$) δ 171.94, 170.58, 155.62, 143.66, 141.19, 127.62, 126.98, 124.98, 119.88, 67.03, 57.41, 50.44, 47.01, 31.28, 27.92, 18.77, 18.55, 17.44; **IR** (neat, cm-1) 3292, 2968, 1727, 1688, 1655, 1530, 1477, 1449, 1390, 1367, 1292, 1243, 1149, 1103, 1079, 1029, 916, 844.

Fmoc-Val-Phe-OtBu (18b). Yellow Waxy Solid; **Yield** = 35%; **^{1}H NMR** (400 MHz, $CDCl_3$) δ 7.76 (ddt, *J* = 7.6, 2.2, 1.2 Hz, 2H), 7.59 (t, *J* = 7.7 Hz, 2H), 7.39 (td, *J* = 7.6, 6.7, 2.7 Hz, 2H), 7.31 (dddd, *J* = 8.4, 5.9, 2.9, 1.8 Hz, 2H), 7.25 – 7.08 (m, 5H), 6.34 (dd, *J* = 31.4, 7.9 Hz, 1H), 5.41 (t, *J* = 9.2 Hz, 1H), 4.80 – 4.71 (m, 1H), 4.46 – 4.38 (m, 1H), 4.34 (q, *J* = 6.4 Hz, 1H), 4.22 (q, *J* = 7.1 Hz, 1H), 4.03 (ddd, *J* = 20.3, 8.8, 5.9 Hz, 1H), 3.08 (d, *J* = 6.2 Hz, 2H), 2.06 (d, *J* = 15.9 Hz, 1H), 1.39 (s, 9H), 0.90 (ddd, *J* = 29.6, 18.2, 6.8 Hz, 6H); **^{13}C NMR** (101 MHz, $CDCl_3$) δ 170.51, 170.31, 170.14, 156.20, 143.69, 141.21, 135.95, 135.80, 129.36, 129.30, 128.33, 127.62, 127.00, 126.92, 125.01, 119.88, 82.36, 67.00, 60.16, 60.02, 53.46, 47.08, 38.19, 38.01, 31.16, 31.02,

27.82, 19.02, 17.73, 17.28; **IR** (neat, cm-1) 3290, 3064, 2956, 1729, 1688, 1650, 1531, 1498, 1477, 1449, 1390, 1465, 1367, 1293, 1244, 1151, 1101, 1080, 1028, 910, 845.

Fmoc-Leu-Lys(Z)-OtBu (18c). Yellow Oil; **Yield** = 54%; **^{1}H NMR** (400 MHz, $CDCl_3$) δ 7.75 (dq, *J* = 7.6, 1.3 Hz, 2H), 7.57 (d, *J* = 7.4 Hz, 2H), 7.41 – 7.27 (m, 10H), 6.67 (d, *J* = 7.6 Hz, 1H), 5.37 (dd, *J* = 56.8, 8.3 Hz, 1H), 5.15 (t, *J* = 5.7 Hz, 1H), 5.05 (dd, *J* = 11.1, 8.5 Hz, 2H), 4.45 – 4.38 (m, 2H), 4.23 (d, *J* = 3.8 Hz, 1H), 4.19 (d, *J* = 7.3 Hz, 1H), 3.11 (d, *J* = 14.9 Hz, 2H), 1.86 – 1.76 (m, 1H), 1.66 (s, 3H), 1.47 (s, 2H), 1.43 (d, *J* = 4.3 Hz, 9H), 1.35 – 1.25 (m, 3H), 0.96 – 0.90 (m, 6H); **^{13}C NMR** (101 MHz, $CDCl_3$) δ 172.05, 171.83, 171.14, 171.04, 156.40, 156.19, 143.75, 143.60, 141.20, 136.55, 136.51, 128.38, 127.98, 127.94, 127.62, 127.00, 124.95, 119.89, 82.20, 82.05, 66.91, 66.46, 53.41, 52.31, 47.05, 41.39, 40.50, 40.33, 31.92, 29.15, 27.98, 27.87, 24.67, 24.53, 22.89, 21.86, 21.74; **IR** (neat, cm-1) 3314, 2953, 1703, 1660, 1517, 1449, 1367, 1236, 1153, 1042, 910, 844.

Fmoc-Thr(tBu)-Leu-OtBu (18d). Yellow Oil; **Yield** = 53%; **^{1}H NMR** (400 MHz, $CDCl_3$) δ 7.76 (dq, *J* = 7.6, 1.1 Hz, 2H), 7.61 (d, *J* = 7.5 Hz, 2H), 7.42 – 7.37 (m, 2H), 7.33 – 7.28 (m, 2H), 6.03 (dd, *J* = 5.1, 2.5 Hz, 1H), 4.50 – 4.41 (m, 1H), 4.41 – 4.34 (m, 2H), 4.26 – 4.15 (m, 3H), 1.68 – 1.59 (m, 2H), 1.58 – 1.52 (m, 1H), 1.47 (d, *J* = 1.4 Hz, 9H), 1.30 (d, *J* = 5.2 Hz, 9H), 1.13 (d, *J* = 6.3 Hz, 1H), 1.04 (d, *J* = 6.3 Hz, 2H), 0.96 (td, *J* = 6.4, 2.0 Hz, 6H); **^{13}C NMR** (101 MHz, $CDCl_3$) δ 171.60, 171.37, 169.05, 168.55, 155.89, 143.86, 143.63, 141.21, 127.59, 126.95, 125.09, 119.87, 81.62, 81.49, 66.83, 66.69, 66.38, 58.38, 58.22, 51.80, 51.53, 47.07, 41.60, 41.35, 28.07, 28.04, 27.92, 24.69, 22.67, 22.03, 21.75, 16.83, 16.36; **IR** (neat, cm-1) 3326, 2973, 1726, 1669, 1487, 1449, 1391, 1366, 1235, 1210, 1189, 1144, 1077, 1041, 990, 917, 868, 844.

General Solid-Phase Procedures

Cleavage condition A (Sieber Amide cleavage). An aliquot (~1 mg) of resin-bound peptide was treated with 200 µL TFA/H_2O/CH_2Cl_2 (2:1:97) and the mixture agitated for 5 min at rt. Following this time period, volatiles were removed by N_2 stream. The resulting residue was dissolved in 200 µL MeOH-H_2O (1:1), filtered and analyzed by UPLC-MS. Note: Product / DKP ratio was determined by integrating 214 and 254 nm peaks and are reported as relative percentages.

Cleavage condition B (photocleavage). The resin-bound peptide was suspended in a 5 mL solution of 1:10 MeOH:CH_2Cl_2 in a fused quartz tube and agitated under 365 nm UV light for 1 h. The solvent was filtered to remove the resin and removed under reduced pressure. The resulting residue was dissolved in MeOH-H2O (1:1), filtered and analyzed by UPLC-MS and HPLC.

Standard wash protocol. DMF (3 x 1 mL), CH_2Cl_2 (3 x 1 mL), MeOH (3 x 1 mL), CH_2Cl_2 (3 x 1 mL), then DMF (3 x 1 mL).

Preparation of Hcna-loaded resin (22a-b).

Fmoc-Sieber Amide PS Resin (0.6 mmol/g) or TentaGel S NH_2 (0.26 mmol/g) was swelled in DMF for 15 min, drained, and treated with piperidine-DMF (1:4, 1 x 2 mL, 30 min). The mixture was drained and washed with standard wash protocol to afford a positive Kaiser ninhydrin test. To a mixture of Fmoc-Ahx-OH (4 eq) and HATU (3.9 eq) in DMF (0.03 M) was added DIEA (8 eq) and this mixture was added to the resin (pre-washed with DMF) after a 5 min pre-activation period. After 2 h, the mixture was drained and washed with the standard wash protocol to afford a negative Kaiser ninhydrin test. The resin was then agitated with piperidine-DMF (1:4, 1 x 2 mL, 30 min). The mixture was drained, and the resin washed with standard wash protocol to afford a positive Kaiser ninhydrin test. To a mixture of Fmoc-Pro-OH (4 eq), HATU (3.9 eq) and HOAt (4 eq) in DMF (0.03 M) was added DIEA (8 eq) and this mixture was added to the resin (pre-washed with DMF) after a 5 min pre-activation period. After 2 h, the mixture was drained and washed with the standard wash protocol to afford a negative Kaiser ninhydrin test. The resin was then treated with piperidine-DMF (1:4, 1 x 2 mL, 30 min). The mixture was drained, and resin washed with standard wash protocol to afford a positive chloranil test. To a mixture of **16** (3 eq) and PyBOP in DMF (0.03 M) was added DIEA (6 eq) and this mixture was added to the resin (pre-washed with DMF) after a 5 min pre-activation period. After 2 h, the mixture was drained and washed with the standard wash protocol to afford a negative chloranil test.

General procedure for solid-phase reductive amination. The prepared resin **22a** or **22b** was swelled in DMF for 15 min then treated with a mixture of H-AA-ODMA or HCl-AA-O*t*Bu (10 eq) and AcOH (10 eq) in CH_2Cl_2 (0.03 M). After 3 h, the mixture was drained and washed briefly with standard wash protocol then THF-MeOH (2:1). The resin was then taken up in THF-MeOH (2:1, 0.03 M) and treated with solid $NaBH_4$ (5 eq). After 2 h, the mixture was drained and washed with H_2O, standard wash protocol, then piperidine-DMF (1:4, 5 min). The resin was washed once more with standard wash protocol to afford a positive chloranil test.

General procedure for loading of second amino acid residue. A flame-dried flask was charged with the 2nd Amino Acid residue (4 eq) and dry CH_2Cl_2 (0.05 M), and symmetric anhydride formation was initiated by addition of DIPC (2 eq) dropwise at rt. The mixture was stirred at rt for 12 min and the resulting solution was solubilized by addition of DMF (0.05 M). This solution was added directly to prepared resin **2.14a-j** and mixture was agitated for 2 h, followed by standard wash protocol to afford a slightly positive chloranil test. This procedure was repeated once more to afford resin-bound dipeptide (and a negative chloranil test).

General procedure for coupling of 3rd amino acid residue. A solution of 1-octanthiol (10 eq), DIEA (10 eq), and DMF (0.03 M) was added to the prepared resin **2.16** and the mixture was agitated for 1 h, followed by the standard wash protocol. Next, a mixture of TIPS-OTf (10 eq), 2,6-Lutidine (10 eq), and DMF (0.03 M) was added to the resin and the mixture was agitated for 4 h, followed by the standard wash protocol. A flame-dried flask was charged with the 3rd Amino Acid residue (4 eq) and dry CH_2Cl_2 (0.05 M), and symmetric anhydride formation was initiated by addition of DIPC (2 eq) dropwise at rt. The mixture was stirred at rt for 12 min and the resulting solution was solubilized by addition of DMF (0.05 M). The resin was agitated with a solution of DBU-1-Octanthiol-DMF (2:2:96, 1 x 2 mL, 3 min), washed with the standard wash protocol, and the pre-activated amino acid solution was added, taking care to minimize the time

between deprotection and coupling. The mixture was agitated for 2 h, followed by standard wash protocol to afford a negative chloranil test. The resin was agitated with piperidine-DMF (1:4, 1 x 2 mL, 30 min). The mixture was drained, and the resin washed with standard wash protocol to afford a positive Kaiser ninhydrin test

General procedure for amino acid coupling. To a mixture of Fmoc-AA-OH (4 eq), HATU (3.9 eq) and HOAt (4 eq) in DMF (0.03 M) was added DIEA (8 eq) and this mixture was added to the resin after a 5 min preactivation period. After 2 h (3h following Proline), the mixture was drained and washed with the standard wash protocol to afford a negative Kaiser ninhydrin test. The resin was agitated with piperidine-DMF (1:4, 1 x 2 mL, 30 min). The mixture was drained, and the resin washed with standard wash protocol to afford a positive Kaiser ninhydrin test. The procedure was then repeated as needed.

Peptide cyclization condition A. After complete synthesis of the desired Fmoc or Boc-protected peptide, the C-terminal DMA protecting group was removed using $Pd(PPh_3)_4$ (1 eq) and Phenylsilane (20 eq) in CH_2Cl_2 under N2 for 2 h, after which the resin was drained and washed with DMF (3 x 1 min), sodium N,N-diethyldithiocarbamate (0.03 M in DMF, 3 x 1 min), and CH_2Cl_2 (3 x 1 min). The resin was agitated with piperidine-DMF (1:4, 1 x 2 mL, 30 min). The mixture was drained, and the resin washed with standard wash protocol to afford a positive Kaiser ninhydrin test. A mixture of PyAop (5 eq), HOAt (5 eq), and DIEA (10 eq) in DMF (0.03 M) was added directly to the resin. After 2 h, the mixture was drained and washed with the standard wash protocol to afford a negative Kaiser ninhydrin test.

Peptide cyclization condition B. After complete synthesis of the desired Fmoc or Boc-protected peptide, the C-terminal DMA protecting group was removed using $Pd(PPh_3)_4$ (1 eq) and Phenylsilane (20 eq) in CH_2Cl_2 under N2 for 2 h, after which the resin was drained and washed with DMF (3 x 1 min), sodium N,N-diethyldithiocarbamate (0.03 M in DMF, 3 x 1 min), and CH_2Cl_2 (3 x 1 min). The resin was agitated with piperidine-DMF (1:4, 1 x 2 mL, 30 min). The mixture was drained, and the resin washed with standard wash protocol to afford a positive Kaiser ninhydrin test. A mixture of PyAOP (3 eq), 2,4,6-collidine (6 eq), and DIEA (6 eq) in 9:1 CH_2Cl_2-DMF (0.03 M) was added directly to the resin. After 2 h, the mixture was drained and washed with the standard wash protocol to afford a negative Kaiser ninhydrin test.

General procedure for thioester synthesis. After complete synthesis of the desired Boc-protected peptide, the C-terminal DMA protecting group was removed using $Pd(PPh_3)_4$ (1 eq) and Phenylsilane (20 eq) in CH_2Cl_2 under N2 for 2 h, after which the resin was drained and washed with DMF (3 x 1 min), sodium N,N-diethyldithiocarbamate (0.03 M in DMF, 3 x 1 min), and CH_2Cl_2 (3 x 1 min). A mixture of PyAOP (5 eq), HOAt (5 eq), and DIEA (10 eq) in DMF (0.03 M) was added directly to the resin. After 2 h, the mixture was drained and washed with the standard wash protocol to afford a negative Kaiser ninhydrin test. A solution of 1-octanthiol (10 eq), DIEA (10 eq), and DMF (0.03 M) was added to the resin and the mixture was agitated for 1 h, followed by the standard wash protocol. Next, a mixture of TIPS-OTf (10 eq), 2,6-Lutidine (10 eq), and DMF (0.03 M) was added to the resin and the mixture was agitated for 4 h, followed by the standard wash protocol. A solution of HATU (5 eq) and DIEA (20 eq) in DMF (0.03 M) was added to the resin and agitated for a 5 min period. Without draining, thiophenol (10 eq) was added to the mixture. After 2 h, the mixture was drained and washed with the standard wash protocol to afford a negative Kaiser ninhydrin test

General procedure for global deprotection A. The resin was agitated with a solution of CH_2Cl_2-H_2O (95:5). After 2 h, the mixture was drained and washed with the standard wash protocol.

General procedure for global deprotection B. The resin was agitated with a solution of TFA-TIPS-CH_2Cl_2 (50:2:48). After 6 h, the mixture was drained and washed with the standard wash protocol.

H-Gly-Ala-Val-ODMA (27a). Fmoc-Sieber Amide PS Resin (16.7 mg, 0.01 mmol) was prepared according to the *general procedure for preparation of resin-loaded tripeptide.* Resin cleavage was achieved using *cleavage condition A* (Sieber Amide cleavage) to afford **27a**. **UPLC-MS** (5→60, CH_3CN-H_2O, 5 min gradient): $\mathbf{R_t}$ 2.48 min, 0% DKP

H-Phe-Val-Phe-ODMA (27b). Fmoc-Sieber Amide PS Resin (16.7 mg, 0.01 mmol) was prepared according to the *general procedure for preparation of resin-loaded tripeptide.* Resin cleavage was achieved using *cleavage condition A* (Sieber Amide cleavage) to afford **27b**. **UPLC-MS** (5→60, CH_3CN-H_2O, 5 min gradient): $\mathbf{R_t}$ 4.12 min, 6% DKP.

H-Val-Phe-Lys(Boc)-ODMA (27c). Fmoc-Sieber Amide PS Resin (16.7 mg, 0.01 mmol) was prepared according to the *general procedure for preparation of resin-loaded tripeptide.* Resin cleavage was achieved using *cleavage condition A* (Sieber Amide cleavage) to afford **27c**. **UPLC-MS** (5→60, CH_3CN-H_2O, 5 min gradient): $\mathbf{R_t}$ 3.32 min, 0% DKP.

H-Phe-Ala-Glu(tBu)-ODMA (27d). Fmoc-Sieber Amide PS Resin (16.7 mg, 0.01 mmol) was prepared according to the *general procedure for preparation of resin-loaded tripeptide.* Resin cleavage was achieved using *cleavage condition A* (Sieber Amide cleavage) to afford **27d**. **UPLC-MS** (5→60, CH_3CN-H_2O, 5 min gradient): $\mathbf{R_t}$ 3.18 min, 3% DKP.

H-Gly-Val-Leu-O*t*Bu (27e). Fmoc-Sieber Amide PS Resin (16.7 mg, 0.01 mmol) was prepared according to the *general procedure for preparation of resin-loaded tripeptide.* Resin cleavage was achieved using *cleavage condition A* (Sieber Amide cleavage) to afford **27e**. **UPLC-MS** (5→60, CH_3CN-H_2O, 5 min gradient): $\mathbf{R_t}$ 2.70 min, 0% DKP.

H-Phe-Ala-Phe-O*t*Bu (27f). Fmoc-Sieber Amide PS Resin (16.7 mg, 0.01 mmol) was prepared according to the *general procedure for preparation of resin-loaded tripeptide.* Resin cleavage was achieved using *cleavage condition A* (Sieber Amide cleavage) to afford **27f**. **UPLC-MS** (5→60, CH_3CN-H_2O, 5 min gradient): $\mathbf{R_t}$ 3.78 min, 0% DKP.

H-Leu-Ala-Ala-O*t*Bu (27g). Fmoc-Sieber Amide PS Resin (16.7 mg, 0.01 mmol) was prepared according to the *general procedure for preparation of resin-loaded tripeptide.* Resin cleavage was achieved using *cleavage condition A* (Sieber Amide cleavage) to afford **2.18i**. **UPLC-MS** (5→95, CH_3CN-H_2O, 5 min gradient): $\mathbf{R_t}$ 2.50 min, 12% DKP.

c-[(D)-Trp-Lys-Gly-(β)-Ala-Phe] (28). TentaGel S NH_2 (230.8 mg, 0.06 mmol) was prepared according to the *general procedure for preparation of resin-loaded tripeptide.* The remaining amino acid residues were coupling using the *general procedure for amino acid coupling.* Cyclization of the peptide was achieved using the *peptide cyclization condition B* followed by *global deprotection condition A.* Resin cleavage was achieved using *cleavage condition B* (photocleavage) to afford **28**. **Cleavage yield** = 96% ; **HPLC** (5→50, CH_3CN-H_2O, 30 min gradient): $\mathbf{R_t}$ 22.3 min; 50% purity.

c-[Arg-(D)-Phe-Pro-Glu-Asp-Asn-Tyr-Glu-Ala-Ala] (29). TentaGel S NH_2 (230.8 mg, 0.06 mmol) was prepared according to the *general procedure for preparation of resin-loaded tripeptide.* The remaining amino acid residues were coupling using the *general procedure for amino acid coupling.* Cyclization of the peptide was achieved using the *peptide cyclization condition A*, followed by *global deprotection condition B.* Resin cleavage was achieved using *cleavage condition B* (photocleavage) to afford **29**. **Cleavage yield =** 90%; **HPLC** (5→20 CH_3CN-H_2O, 30 min gradient): $\mathbf{R_t}$ 11 min; 95% purity.

c-[Pro-Asp-Gly-Arg-Cys-Thr-Lys-Ser-Ile-Pro-Pro-Ile-Cys-Phe] (30). TentaGel S NH_2 (230.8 mg, 0.06 mmol) was prepared according to the *general procedure for preparation of resin-loaded tripeptide.* The remaining amino acid residues were coupling using the *general procedure for amino acid coupling.* Cyclization of the peptide was achieved using the *peptide cyclization condition A*, followed by *global deprotection condition B.* Resin cleavage was achieved using *cleavage condition B* (photocleavage) to afford **30**. **Cleavage yield =** 80%; **HPLC** (5→15 CH_3CN-H_2O, 30 min gradient):$\mathbf{R_t}$ 14 min; 90% purity.

H-Phe-Lys-Ala-Ala-Leu-S-C_6H_5 (31a). TentaGel S NH_2 (115.4 mg, 0.03 mmol) was prepared according to the *general procedure for preparation of resin-loaded tripeptide.* The remaining amino acid residues were coupling using the *general procedure for amino acid coupling*, using a Boc-Phe-OH as the final residue. Thioester formation was achieved using the *general procedure for thioester synthesis* followed by *global deprotection condition A.* Resin cleavage was achieved using *cleavage condition B* (photocleavage) to afford **31a**. **Cleavage yield =** 83%; **HPLC** (30→50 CH_3CN-H_2O, 30 min gradient): $\mathbf{R_t}$ 18 min; 99% purity.

H-Ala-Glu-Phe-Leu-Phe-S-C_6H_5 (31b). TentaGel S NH_2 (115.4 mg, 0.03 mmol) was prepared according to the *general procedure for preparation of resin-loaded tripeptide.* The remaining amino acid residues were coupling using the *general procedure for amino acid coupling*, using a Boc-Ala-OH as the final residue. Thioester formation was achieved using the *general procedure for thioester synthesis* followed by *global deprotection condition A.* Resin cleavage was achieved using *cleavage condition B* (photocleavage) to afford **31b**. **Cleavage yield =** 66%; **HPLC** (30→50 CH_3CN-H_2O, 30 min gradient): $\mathbf{R_t}$ 17 min; 99% purity.

H-Ala-Lys-Phe-Leu-Glu-S-C_6H_5 (31c). TentaGel S NH_2 (115.4 mg, 0.03 mmol) was prepared according to the *general procedure for preparation of resin-loaded tripeptide.* The remaining amino acid residues were coupling using the *general procedure for amino acid coupling*, using a Boc-Ala-OH as the final residue. Thioester formation was achieved using the *general procedure for thioester synthesis* followed by *global deprotection condition A.* Resin cleavage was achieved using *cleavage condition B* (photocleavage) to afford **31c**. **Cleavage yield =** 71%; **HPLC** (50→75 CH_3CN-H_2O, 30 min gradient): $\mathbf{R_t}$ 23 min; 75% purity.

H-Phe-Glu-Ala-Leu-Ala-S-C_6H_5 (31d). TentaGel S NH_2 (115.4 mg, 0.03 mmol) was prepared according to the *general procedure for preparation of resin-loaded tripeptide.* The remaining amino acid residues were coupling using the *general procedure for amino acid coupling*, using a Boc-Ala-OH as the final residue. Thioester formation was achieved using the *general procedure for thioester synthesis* followed by *global deprotection condition A.* Resin cleavage was achieved using *cleavage condition B* (photocleavage) to afford **31d**. **Cleavage yield =** 92%; **HPLC** (30→50 CH_3CN-H_2O, 30 min gradient): $\mathbf{R_t}$ 16 min; 95% purity.

ACKNOWLEDGMENT**:** S. S. K. thanks Dr. Cristina Acevedo for DKP study on Nve

Supporting Information Available: Preparation of linkers, amination and acylation experimental details, photolabile linker's UV spectrum, photolysis kinetic studies, and characterization of the intermediates and final products including full ^1H and ^{13}C NMR spectra. This material is available free of charge via the Internet at http://pubs.acs.org.

REFERENCES

[i]For a general review of cyclic peptides: (a) Katsara, M.; Tselios, T.; Deraos, S.; Deraos, G.; Matsoukas, M.; Lazoura, E.; Matsoukas, J.; Apostolopoulos V. Round and round we go: cyclic peptides in disease. *Current Med. Chem.* **2006**, *13*, 2221. (b) Fusetani, N; Matsunaga, S. Bioactive sponge peptides. *Chem. Rev*. **1993**, *93*, 1793. (c) Humphrey, J. M.; Chamberlin, A. R. Chemical Synthesis of Natural Product Peptides: Coupling Methods for the Incorporation of Noncoded Amino Acids into Peptides. *Chem. Rev*. **1997**, *97*, 2243.

[ii] (a) Samanen, J.; Ali, F.; Romoff, T.; Calvo, R.; Sorenson, E.; Vasko, J.; Storer, B.; Berry, D.; Bennett, D.; Strohsacker, M.; Powers, D.; Stadel, J.; Nichols, A. Development of a small RGD peptide fibrinogen receptor antagonist with potent antiaggregatory activity in vitro. *J. Med. Chem.* **1991**, *34*, 3114. (b) Biron, E.; Chatterjee, J.; Ovadia, O.; Langenegger, D.; Brueggen, J.; Hoyer, D. Schmid, H. A.; Jelinek, R.; Gilon, C.; Hoffman, A.; Kessler, H. Improving oral bioavailability of peptides by multiple N-methylation: somatostatin analogues. *Angew. Chem. Int. Ed.* **2008**, *47*, 2595. (c) Kessler, H. Conformation and Biological Activity of Cyclic Peptides. *Angew. Chem. Int. Ed.* **1982**, *21*, 512.

[iii] (a) White, T. R.; Renzelman, C. M.; Rand, A. C.; Rezai, T.; McEwen, C. M.; Gelev, V. M.; Turner, R. A.; Linington, R. G.; Leung, S. S.; Kalgutkar, A. S.; Bauman, J. N.; Zhang, Y.; Liras, S.; Price, D. A.; Mathiowetz, A. M.; Jacobson, M. P.; Lokey, R. S. On-resin N-methylation of cyclic peptides for discovery of orally bioavailable scaffolds. *Nat Chem Biol.* **2011,** *7*, 810. (b)

Dougherty, P. G.; Sahni, A.; Pei, D. Understanding Cell Penetration of Cyclic Peptides. *Chem. Rev.* **2019**, *119*, 10241.

[iv] (a) **Urotensin analogues**: Coulouarn, Y.; Lihrmann, I.; Jegou, S.; Anouar, Y.; Tostivint, H.; Beauvillain, J. C.; Conlon, J. M.; Bern, H. A.; Vaudry, A. Cloning of the cDNA encoding the urotensin II precursor in frog and human reveals intense expression of the urotensin II gene in motoneurons of the spinal cord. *Proc. Natl. Acad. Sci.* **1998**, *95*, 15803.; Foister, S.; Taylor, L. L.; Feng, J.; Chen, W.; Lin, A.; Cheng, F.; Smith III, A. B.; Hirschmann, Design and Synthesis of Potent Cystine-Free Cyclic Hexapeptide Agonists at the Human Urotensin Receptor. R. *Org Lett.* **2006**, *8*, 1799. (b) **Somatostatin analogues**: Veber, D. F.; Freidinger, R. M.; Perlow, D. S.; Paleveda, W. J.; Holly, F. W.; Strachan, R. G.; Nutt, R. F.; Arison, B. H.; Homnick, C.; Randall, W. C.; Glitzer, M. S.; Saperstein, R.; Hirschmann, R. A potent cyclic hexapeptide analogue of somatostatin. *Nature* **1981**, *292*, 55.; Kessler, H.; Anders, U.; Schudok, M. An Unexpected Cis Peptide Bond in the Minor Conformation of a Cyclic Hexapeptide Containing Only Secondary Amide Bonds . J. Am. Chem. Soc. 1990, 112, 5908. (c) **cyclic RGD peptide**: see ref. 2a JMC 1991 Samanen) (d) **Apicidin**: Darkin-Rattray, S. J.; Gurnett, A. M.; Myers, R. W.; Dulski, P. M.; Crumley, T. M.; Allocco, J. J.; Cannova, C.; Meinke, P. T.; Colletti, S. L.; Bednarek, M. A.; Singh, S. B.; Goetz, M. A.; Dombrowski, A. W.; Polishook, J. D.; Schmatz, D. M. Apicidin: a novel antiprotozoal agent that inhibits parasite histone deacetylase. *Proc. Natl. Acad. Sci.* **1996**, *93*, 13143.

[v] Gause, G. F.; Brazhnikova, M. G. Antimicrobial peptide gramicidin S is accumulated in granules of producer cells for storage of bacterial phosphagens. *Nature* **1944**, *154*, 703.

[vi] Shevach, E. M. The Effects of Cyclosporin A on the Immune System. *Ann. Rev. Immuno1.* **1985**, *3*, 397.

[vii] Mihara, H.; Yamabe, S.; Nildome, T.; Aoyagi, H.; Kumagai, H. Evaluation of the oxime resin based segment synthesis-condensation approach using RNase T1 as a model synthetic target. *Tetrahedron Lett*. **1995**, 36, 4837.

[viii] Richter, L. S.; Tom, J. Y. K.; Brunier, J. P. Peptide-Cyclizations on solid support: A fast and efficient route to small cyclopeptides. *Tetrahedron Lett*. **1994**, *35*, 5547.

[ix] Rosenbaum, C.; Waldmann, H. Solid phase synthesis of cyclic peptides by oxidative cyclative cleavage of an aryl hydrazide linker—Synthesis of stylostatin 1. *Tetrahedron Lett*. **2001**, *42*, 5677.

[x] Kenner, G. W.; McDermott, J. R.; Sheppard, R. C. The safety catch principle in solid phase peptide synthesis. *J. Chem. Soc. Chem. Comm.* **1971**,636.

[xi] Krishnamoorthy, R.; Vazquez-Serrano, L. D.; Turk, J. A.; Kowalski, J. A.; Benson, A. G.; Breaux, N. T.; Lipton, M. A. Solid-Phase Total Synthesis and Structure Proof of Callipeltin B. *J. Am. Chem. Soc*. **2006,** *128*, 15392.

[xii] Jensen, K. J.; Alsina, J.; Songster, M. F.; Vagner J.; Albericio, F.; Barany, G. Backbone Amide Linker (BAL) Strategy for Solid-Phase Synthesis of C-Terminal-Modified and Cyclic Peptides. *J. Am. Chem. Soc*. **1998**, *120*, 5441.

[xiii] Liley, M. J.; Johnson, T.; Gilson, S. E. An Improved Aldehyde Linker for the Solid Phase Synthesis of Hindered Amides. *J. Org. Chem.* **2006**, *71*, 1322.

[xiv] (a) Bourne, G. T.; Meutermans, W. D. F.; Smythe, M. L. The development of solid phase protocols for a backbone amide linker and its application to the Boc-based assembly of linear peptides. *Tetrahedron Lett.* **1999**, *40*, 7271. (b) Bourne, G. T.; Golding, S. W.; Meutermans, W. D. F.; Smythe, M. L. Synthesis of a cyclic peptide library based on the somatostatin sequence using the backbone amide linker approach. *Letters in Peptide Science*, **2001**, *7*, 311.

[xv] (a) Boas, U.; Brask, J.; Christensen, J. B.; Jensen, K. J. The Ortho Backbone Amide Linker (o-BAL) Is an Easily Prepared and Highly Acid-Labile Handle for Solid-Phase Synthesis. *J. Comb. Chem.* **2002**, *4*, 223. (b) Boas, U.; Christensen, J. B.; Jensen, K. J. Two Dialkoxynaphthalene Aldehydes as Backbone Amide Linkers for Solid-Phase Synthesis. *J. Comb. Chem.* **2004**, *6*, 497. (c) Pittelkow, M.; Boas, U.; Jessing, M.; Jensen, K. J.; Christensen, J. B. Role of the peri-effect in synthesis and reactivity of highly substituted naphthaldehydes: a novel backbone amide linker for solid-phase synthesis. *Org. Biomol. Chem.* **2005**, *3*, 508. (d) Pittelkow, M.; Boas, U.; Christensen, J. B. Carbocations in Action. Design, Synthesis, and Evaluation of a Highly Acid-Sensitive Naphthalene-Based Backbone Amide Linker for Solid-Phase Synthesis. *Org. Lett.* **2006**, *8*, 5817. (e) Jessing, M.; Brandt, M.; Jensen, K. J.; Christensen, J. B.; Boas, U. Thiophene Backbone Amide Linkers, a New Class of Easily Prepared and Highly Acid-Labile Linkers for Solid-Phase Synthesis. *J. Org. Chem.* **2006**, *71*, 6734.

[xvi] (a) Fresno, M.; Alsina, J.; Royo, M.; Barany, G.; Albericio, F. Exploring privileged structures: The combinatorial synthesis of cyclic peptides. *Tetrahedron. Lett.* **1998**, *39*, 2639. (b) Alsina, J.; Jensen, K. J.; Albericio, F.; Barany, G. Solid-Phase Synthesis with Tris(alkoxy)benzyl Backbone Amide Linkage (BAL). *Chem. Eur. J.* **1999**, *5*, 2787.

[xvii] (a) Brask, J.; Albericio, F.; Jensen, K. Fmoc Solid-Phase Synthesis of Peptide Thioesters by Masking as Trithioortho Esters. J. *Org. Lett*. **2003**, *5*, 2951.

[xviii] (a) Guillaumie, F.; Kappel, J. C.; Kelly, N. M.; Barany, G.; Jensen, K. J. Solid-phase synthesis of C-terminal peptide aldehydes from amino acetals anchored to a backbone amide linker (BAL) handle. *Tetrahedron Lett.* **2000**, *41*, 6131. (b) Kappel, J. C.; Barany, G. *J.* Backbone amide linker (BAL) strategy for Nalpha-9-fluorenylmethoxycarbonyl (Fmoc) solid-phase synthesis of peptide aldehydes. *Peptide Sci.* **2005**, *11*, 525.

[xix] (a) Springer, J.; de Cuba, K. R.; Calvet-Vitale, S.; Geenevasen, J. A. J.; Hermkens, P. H. H.; Hiemstra, H.; van Maarseveen, J. H. Backbone Amide Linker Strategy for the Synthesis of 1,4-Triazole-Containing Cyclic Tetra- and Pentapeptides, *Eur. J. Org. Chem*. **2008**, *15*, 2592. (b) Mori, A.; Akahoshi, I.; Hashimoto, M.; Doi, T.; Takahashi T. Solid-phase combinatorial syntheses of mesomorphic 4-alkoxyphenyl 4-alkoxybenzoylaminobenzoates. *Tetrahedron Lett.* **2004**, *45*, 813. (c) Soural, M.; Krchnak, V. Efficient Solid-Phase Synthesis of 2-Substituted-3-Hydroxy-4(1H)-Quinolinone-7-Carboxamides with Two Diversity Positions. *J. Comb. Chem.* **2007**, *9*, 793.

[xx] Dawson, P. E.; Muir, T. W.; Clark-Lewis, I.; Kent, S. B. Synthesis of proteins by native chemical ligation. *Science* **1994**, *266*, 776.

[xxi] (a) Mende, F.; Seitz, O. 9-Fluorenylmethoxycarbonyl-Based Solid-Phase Synthesis of Peptide α-Thioesters. *Angew. Chem. Int. Ed.* **2011**, *50*, 1232. (b) Li, H.; Dong, S. Recent advances in the preparation of Fmoc-SPPS-based peptide thioester and its surrogates for NCL-type reactions. *Sci. China Chem.* **2017**, *60*, 201.

[xxii] Nilsson, B. L.; Kiessling, L. L.; Raines, R. T. Staudinger Ligation: A Peptide from a Thioester and Azide. *Org. Lett.* **2000**, *2*, 1939.

[xxiii] For a general review (a) Guillier F.; Orain, D.; Bradley, M. Linkers and Cleavage Strategies in Solid-Phase Organic Synthesis and Combinatorial Chemistry, *Chem. Rev.* **2000**, *100*, 2091. (b) Scott, P.; Steel, P., Diversity Linker Units for Solid-Phase Organic Synthesis. *Eur. J. Org. Chem.* **2006**, 2251. (c) Heidler, P.; Link, A. N-acyl-N-alkyl-sulfonamide anchors derived from Kenner's safety-catch linker: powerful tools in bioorganic and medicinal chemistry. *Bioorg. Med. Chem.* **2005**, *13*, 585. (d) McAllister, L. A.; McCormick, R. A.; Procter, D. J. Sulfide- and selenide-based

linkers in phase tag-assisted synthesis. *Tetrahedron* **2005**, *61*, 11527. (e) Lloyd-Williams, P.; Albericio, F.; Giralt, E. Convergent solid-phase peptide synthesis. *Tetrahedron* **1993**, *49*, 11065.

[xxiv] (a) Kang, S S. and Lipton, M. A. *Chap.17 Photolabile and Miscellaneous Linkers/Resins* in 'The Power of Functional Resins in Organic Synthesis'; Editor: Albericio, F.; Wiley-VCH; ISBN: 978-3527319367, 2008. (b) Bochet, C. G. J. *Chem. Soc, Perkin Trans. 1*, **2002**, 125.

[xxv] Gallop, M. A.; Barrett, R. W.; Dower, W. J.; Fodor, S. P. A.; Gordon. E. M. Applications of Combinatorial Technologies to Drug Discovery. 1. Background and Peptide Combinatorial Libraries. *J. Med. Chem*, **1994**, *37*, 1233.

[xxvi] Sheehan, J. C.; Umezawa, K. Phenacyl photosensitive blocking groups. *J. Org. Chem.* **1973**, *38*, 3771.

[xxvii] Bellof, D.; Mutter, M. A new phenacyl-type handle for polymer supported peptide-synthesis. *Chimia* **1985**, *39*, 317.

[xxviii] (a) Sheehan, J. C.; Davies, G. D. Facile Alkyl—Oxygen Ester Cleavage. *J. Org. Chem.* **1964**, *29(7)*, 2006. (b) Peach, J. M.; Pratt, A. J.; Snaith, J. S. Photolabile benzoin and furoin esters of a biologically active peptide. *Tetrahedron* **1995**, *51*, 10013.

[xxix] Bergmark, W. R.; Barnes, C.; Clark, J.; Paparian, S.; Marynowski, S. Photoenolization with .alpha.-chloro substituents. *J. Org. Chem.* **1985**, *50*, 5612.

[xxx] Patchornik, A.; Amit, B.; Woodward, R. B. Photosensitive protecting groups. *J. Am. Chem. Soc.* **1970**, *92*, 6333.

[xxxi] Linker 1 & 5 were purchased from Sigma-Aldrich. Linker 2 was prepared by Viswanathan's described method (Synthesis and evaluation of uterine relaxant activity for a novel series of substituted p-hydroxyphenylethanolamines, *Bioorg. Med. Chem.* **2006**, *14*, 6581). Linker 3 was prepared by Stowell's described method (Efficient synthesis of photolabile alkoxy benzoin protecting groups. *Tetrahedron Lett.* **1996**, *37*, 307). The preparation of Linker 4 is in the Supplementary Information.

[xxxii] (a) Amadori, W. The Amadori Rearrangement. *Atti. Reale Accad. Nazl. Lincei*, **1925**, *2*, 337. (b) Isbell, H. S.; Frush, H. L. Mutarotation, Hydrolysis, and Rearrangement Reactions of Glycosylamines. *J. Org. Chem*. **1958**, *23*, 1309

[xxxiii] Sheppard, R. C.; Johnson, T.; Quibell, M.; Owen, D., A reversible protecting group for the amide bond in peptides. Use in the synthesis of 'difficult sequences'. *J. Chem. Soc., Chem. Commun*. **1993**, 369.

[xxxiv] Smythe, M.; Meutermans, W.; Golding, S.; Bourne, G.; Miranda, L.; Dooley, M.; Alewood, P. Synthesis of Difficult Cyclic Peptides by Inclusion of a Novel Photolabile Auxiliary in a Ring Contraction Strategy. *J. Am. Chem. Soc.* **1999**, *121*, 9790.

[xxxv] Starosotnikov, A. M.; Lobach, A. V.; Shevelev, S. A. An Efficient One-Step Method for the Conversion of β-(Dimethylamino)Sty-renes into Arylacetonitriles. Synthesis 2005, 2005 (17), 2830–2832.

[xxxvi] Hostetler, M. A.; Lipton, M. A. An Optimized Preparation of 1,1-Dimethylallyl Esters and Their Application to Solid-Phase Peptide Synthesis. *J. Org. Chem.* **2018**, *83* (15), 7762–7770.

[xxxvii] (a) Boeijen, A.; Liskamp, R. M. J. Solid-Phase Synthesis of Oligourea Peptidomimetics. *Eur. J. Org. Chem*. **1999**, 2127. (b) Boeijen, A.; van Ameijde, J.; Liskamp, R. M. J. Solid-Phase Synthesis of Oligourea Peptidomimetics Employing the Fmoc Protection Strategy. *J. Org. Chem*, **2001**, *66*, 8454.

[xxxviii] The solvent columns are composed of activated alumina and supported copper redox catalyst. See: Pangaborn, A. B.; Girardello, M. A.; Grubbs, R. H.; Rosen, R. K.; Timmers, F. Safe and Convenient Procedure for Solvent Purification. *J. Organometallics* **1996**, *15*, 1518.

[xxxix] Eakins G.; Niedrauer, M.; Lipton, M.; Photochemical Reactor for Solid Phase Synthesis. *U.S. Patent Application No. 63029491*, **2020**.